MICROBIAL COMMUNITIES OF POLAR AND ALPINE SOILS

EDITED BY: Laura Zucconi and Pietro Buzzini

PUBLISHED IN: Frontiers in Microbiology

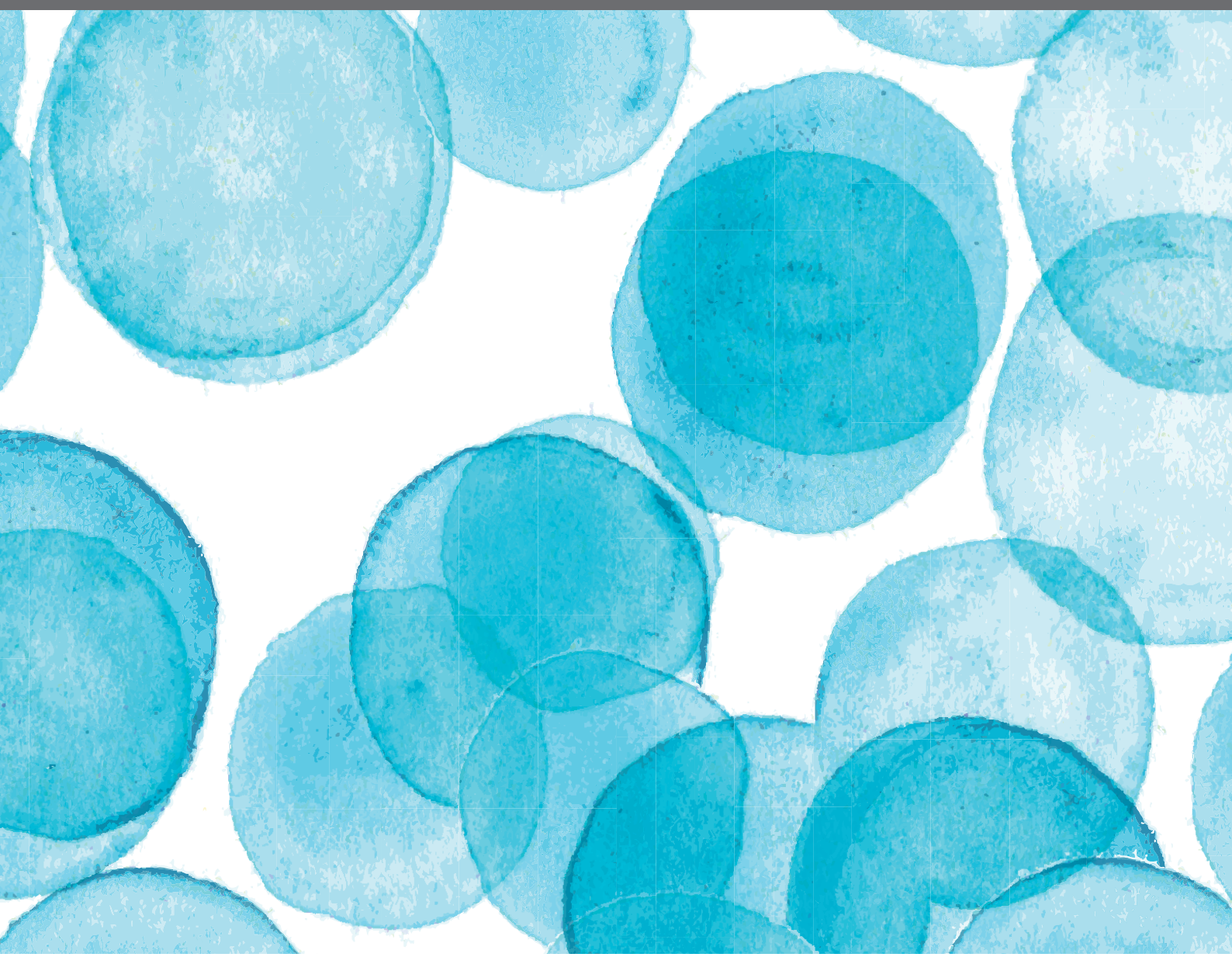

frontiers Research Topics

frontiers

ISSN 1664-8714
ISBN 978-2-88971-618-0
DOI 10.3389/978-2-88971-618-0

About Frontiers

Frontiers is more than just an open-access publisher of scholarly articles: it is a pioneering approach to the world of academia, radically improving the way scholarly research is managed. The grand vision of Frontiers is a world where all people have an equal opportunity to seek, share and generate knowledge. Frontiers provides immediate and permanent online open access to all its publications, but this alone is not enough to realize our grand goals.

Frontiers Journal Series

The Frontiers Journal Series is a multi-tier and interdisciplinary set of open-access, online journals, promising a paradigm shift from the current review, selection and dissemination processes in academic publishing. All Frontiers journals are driven by researchers for researchers; therefore, they constitute a service to the scholarly community. At the same time, the Frontiers Journal Series operates on a revolutionary invention, the tiered publishing system, initially addressing specific communities of scholars, and gradually climbing up to broader public understanding, thus serving the interests of the lay society, too.

Dedication to Quality

Each Frontiers article is a landmark of the highest quality, thanks to genuinely collaborative interactions between authors and review editors, who include some of the world's best academicians. Research must be certified by peers before entering a stream of knowledge that may eventually reach the public - and shape society; therefore, Frontiers only applies the most rigorous and unbiased reviews.
Frontiers revolutionizes research publishing by freely delivering the most outstanding research, evaluated with no bias from both the academic and social point of view. By applying the most advanced information technologies, Frontiers is catapulting scholarly publishing into a new generation.

What are Frontiers Research Topics?

Frontiers Research Topics are very popular trademarks of the Frontiers Journals Series: they are collections of at least ten articles, all centered on a particular subject. With their unique mix of varied contributions from Original Research to Review Articles, Frontiers Research Topics unify the most influential researchers, the latest key findings and historical advances in a hot research area! Find out more on how to host your own Frontiers Research Topic or contribute to one as an author by contacting the Frontiers Editorial Office: frontiersin.org/about/contact

MICROBIAL COMMUNITIES OF POLAR AND ALPINE SOILS

Topic Editors:
Laura Zucconi, University of Tuscia, Italy
Pietro Buzzini, University of Perugia, Italy

Citation: Zucconi, L., Buzzini, P., eds. (2021). Microbial Communities of Polar and Alpine Soils. Lausanne: Frontiers Media SA. doi: 10.3389/978-2-88971-618-0

Table of Contents

frontiers in Microbiology

EDITORIAL
published: 23 September 2021
doi: 10.3389/fmicb.2021.713067

Editorial: Microbial Communities of Polar and Alpine Soils

Laura Zucconi[1]* *and Pietro Buzzini*[2]

[1] Department of Ecological and Biological Sciences, University of Tuscia, Viterbo, Italy, [2] Department of Agricultural, Food and Environmental Sciences - Industrial Yeasts Collection DBVPG, University of Perugia, Perugia, Italy

Keywords: soil microorganisms, polar regions, Alpine environments, climate change, microbial communities

Editorial on the Research Topic

Microbial Communities of Polar and Alpine Soils

THE THREE POLES AND THE CHALLENGES OF CLIMATE CHANGE

In recent years Arctic, Antarctic, and Alpine regions have experienced the highest rates of warming worldwide (Zemp et al., 2006; Anisimov et al., 2007). In Arctic and Alpine environments these phenomena are resulting in an increase of the duration of ice-free periods and an overall greening of terrestrial areas. The effects of warming on microbial decomposition of vast carbon pools in permafrost soils have the potential to cause a significant positive feedback to global climate change (Cavicchioli et al., 2019). Climate change in Antarctica, is firstly feared to result in the loss of unique and highly adapted ecosystems, mainly because of shifts in temperature and precipitation regimes, as well as longer term changes in edaphic profiles and the invasion of allochthonous, more competitive species (Convey and Peck, 2019).

Soil microorganisms play a crucial role in mediating carbon and nitrogen balance and other biogeochemical cycles of global importance. Therefore, understanding the soil microbial diversity and ecology, including the ecological drivers that shape microbial communities, may be a key for understanding how biogeochemical cycles will respond to large-scale environmental and climatic changes. Given the key role of microorganisms in maintaining the balance of these environments, they could be viewed both as sentinels and amplifiers of global change (Maloy et al., 2016).

In this framework, the e-book *Microbial Communities of Polar and Alpine Soils* aimed to collect original and noticeable research papers about diversity and functionality of soil microbial communities, their interactions with the other biotic components, including the aboveground plant coverage, and the abiotic factors determinant for the colonization of these habitats, as well their adaptation and resilience abilities to stressing conditions and environmental changes.

COLD-LIVING MICROORGANISMS AND THEIR ROLE IN POLAR AND ALPINE ENVIRONMENTS

This brief editorial summarizes and highlights experimental researches carried out in different environments, ranging from the Qinghai-Tibetan Plateau, to the Arctic, to maritime and continental Antarctica, or spreading across the poles. Different types of soils were studied, from oligotrophic to nitrogen rich soils, from soils underneath plants to thawed permafrost, dry soils, moraines, gullies, polygon soils, or soils around rocks. Some papers dealt with fungi, others with bacteria, others to actinomycetes and/or other organisms.

Ray et al. wanted to define the spread of the "atmospheric chemosynthesis," a microbial carbon fixation process supporting primary production in dry and nutrient-poor environments. Those

OPEN ACCESS

Edited by:
Thulani Peter Makhalanyane, University of Pretoria, South Africa

Reviewed by:
José A. Siles, University of California, Berkeley, United States
Beat Frey, Swiss Federal Institute for Forest, Snow and Landscape Research (WSL), Switzerland

***Correspondence:**
Laura Zucconi
zucconi@unitus.it

Specialty section:
This article was submitted to Extreme Microbiology, a section of the journal Frontiers in Microbiology

Received: *21 May 2021*
Accepted: *31 August 2021*
Published: *23 September 2021*

Citation:
Zucconi L and Buzzini P (2021) Editorial: Microbial Communities of Polar and Alpine Soils. Front. Microbiol. 12:713067. doi: 10.3389/fmicb.2021.713067

genes associated to this process were reported as widespread across cold desert soils, spanning the Tibetan Plateau, and both Antarctic and high Arctic sites.

Otherwise, in some coastal sites of maritime Antarctica, seabirds and marine mammal colonies exert, through the accumulation of their feces and urine, a strong influence on the edaphic N content. Nitrogen cycle in Antarctic tundra ecosystems has also been investigated by Dai et al. and Acuña-Rodríguez et al. The former recorded differences in the denitrification rates and the denitrifier community structures between nitrogen rich soils and animal-lacking tundra soils. The latter observed as fungal symbionts (root endophytes), associated to the only two Antarctic vascular plants *Colobanthus quitensis* and *Deschampsia antarctica*, actively participate in the plants N-uptake, even in non-N limited soils, with positive impacts on plant biomass.

Two contributions by Newsham et al. dealt with the effects of climate change on a single fungal species and the whole communities of soils from maritime Antarctica, respectively. An undescribed member of the order Helotiales was recorded to be superabundant in Antarctic Islands soils under *D. antarctica* (Newsham, Cox et al.). A range of its physiological and morphological features were reported, and an increase of its growth rate was suggested with the rising temperatures that are expected to occur in maritime Antarctica at the end of this century, with the potential loss of ancient C from soils.

Three fungal guilds and growth forms—lichenized and saprotrophic fungi and yeasts—of barren fellfield soils sampled from along a transect encompassing almost the entire maritime Antarctica were studied, in order to define the main environmental factors affecting their richness, relative abundance and taxonomic structure. Air temperature and edaphic factors were reported as main drivers, and discussed in view of the expected future climate changes of the region (Newsham, Davey et al.).

Glacier retreats expose new ice-free barren soils. Some areas have been only recently deglaciated, while others have been mostly deglaciated for millennia. The bacterial communities of these soils have been studied by Almela et al. Those of older soils seemed to be significantly different along the soil profiles, while they were similar in recently (from decades) deglaciated soils. A high degree of heterogeneity was also observed among microbial communities of soils at different sampling locations.

Water tracks, that seasonally flow on the ice-free soils of the McMurdo Dry Valleys in continental Antarctica, are expected to increase with ongoing climate change. They select for bacterial taxa able to cope with challenging environmental conditions. Significant differences in microbial community assembly between on- and off-water track samples, and across two distinct locations were recorded, mainly driven by soil salinity (George et al.). Heterogeneous microbial communities have been found to characterize four different habitats present in higher elevations of Taylor Valley, where biological soil crusts were reported in a gully and moraine next to Canada Glacier, accounted as islands of biodiversity, able to spread organisms and nutrients in the surrounding landscape (Solon et al.).

The Northern high latitudes are a preferential open-air laboratory to study the impact of climate change on soil microbial communities, as they are warming twice as fast as the global average. Four out of 13 contributing articles of the Topic report studies carried out in the Arctic.

Arctic permafrost has become particularly vulnerable to thaw, with consequences on microbial communities that are not yet perfectly known. The bacterial community assembly during permafrost thaw was studied using *in situ* observations and a laboratory incubation of soils in sub-Arctic Sweden, where permafrost thaw has occurred over the past decade. It showed to be driven by randomness (i.e., stochastic processes) immediately after thaw, while environmentally driven (i.e., deterministic) processes became increasingly important in structuring them in post-thaw successions (Doherty et al.). Geospatial differences in hydrology in polygon soils causing gradients in biogeochemistry, soil C storage potential, and thermal properties influencing the distribution of microbial CO_2 and CH_4 release, has been studied by Roy Chowdhury et al. by laboratory incubation at increasing temperatures of frozen soil cores collected in the Arctic coastal tundra in Alaska.

A comparison between the microbial community structure of rocks (and surrounding soils) in a high Arctic polar desert (Svalbard) showed significant differences between these substrates. Differences were also reported between rock sandstones and limestones, due to the determinant role of rock physiochemical properties in determining the successful establishment of lichens in lithic environments (Choe et al.).

Shifts in vegetation and soil fungal communities have been recorded in the Arctic tundra as a response to warming temperatures. In this context, fungal community composition in long-term experimental plots simulating the expected increase in summer warming and winter snow depth, were compared using DNA metabarcoding data, and dry and moist tundra appeared to have different trajectories in response to climate change (Geml et al.).

Cultivable actinomycetes isolated from soils near roots of different plants from the Qinghai-Tibetan Plateau were investigated for their enzymatic activity, and for the production of diffusible pigments and organic acids (Ma et al.).

This volume brings together the scientific community to cover all aspects of cold-adapted microorganisms and their role in Polar and Alpine environments. It gives a significant contribution to the long-standing debate on the multiple ecological roles of microorganisms in cold soil ecosystems. We hope that this range of articles will be highly attractive to worldwide researchers involved in the study of soil microbial communities.

AUTHOR CONTRIBUTIONS

The authors have equally contributed to the Editorial, and approved it for publication.

ACKNOWLEDGMENTS

The editors would like to thank all reviewers who evaluated manuscripts for this Research Topic. Their contribution in improving the manuscripts has been greatly appreciated.

REFERENCES

Anisimov, O. A., Vaughan, D. G., Callaghan, T. V., Furgal, C., Marchant, H., Prowse, T. D., et al. (2007). "Polar regions (arctic and antarctic)," in *Climate Change 2007: Impacts, Adaptation and Vulnerability. Contribution of Working Group II to the Fourth Assessment Report of the Intergovernmental Panel on Climate Change*, eds M. L. Parry, O. F. Canziani, J. P. Palutikof, P. J. van der Linden, and C. E. Hanson (Cambridge: Cambridge University Press), 653–685. Available online at: https://www.ipcc.ch/site/assets/uploads/2018/02/ar4-wg2-chapter15-1.pdf

Cavicchioli, R., Ripple, W. J., Timmis, K. N., Azam, F., Bakken, L. R., Baylis, M., et al. (2019). Scientists' warning to humanity: microorganisms and climate change. *Nat. Rev. Microbiol.* 17, 569–586. doi: 10.1038/s41579-019-0222-5

Convey, P., and Peck, L. S. (2019). Antarctic environmental change and biological responses. *Sci. Adv.* 5:eaaz0888. doi: 10.1126/sciadv.aaz0888

Maloy, S., Moran, M. A., Mulholland, M. R., Sosik, H. M., and Spear, J. R. (2016). *FAQ: Microbes and Climate Change: Report on an American Academy of Microbiology and American Geophysical Union Colloquium held in Washington, DC, in* March *2016* (Washington, DC).

Zemp, M., Haeberli, W., Hoelzle, M., and Paul, F. (2006). Alpine glaciers to disappear within decades? *Geophys. Res. Lett.* 33:L13504. doi: 10.1029/2006GL026319

Conflict of Interest: The authors declare that the research was conducted in the absence of any commercial or financial relationships that could be construed as a potential conflict of interest.

Publisher's Note: All claims expressed in this article are solely those of the authors and do not necessarily represent those of their affiliated organizations, or those of the publisher, the editors and the reviewers. Any product that may be evaluated in this article, or claim that may be made by its manufacturer, is not guaranteed or endorsed by the publisher.

frontiers in Microbiology

ORIGINAL RESEARCH
published: 12 August 2020
doi: 10.3389/fmicb.2020.01936

Soil Microbiomes With the Genetic Capacity for Atmospheric Chemosynthesis Are Widespread Across the Poles and Are Associated With Moisture, Carbon, and Nitrogen Limitation

*Angelique E. Ray[1], Eden Zhang[1], Aleks Terauds[2], Mukan Ji[3], Weidong Kong[3] and Belinda C. Ferrari[1]**

[1]School of Biotechnology and Biomolecular Sciences, University of New South Wales, Sydney, NSW, Australia, [2]Australian Antarctic Division, Department of Environment, Antarctic Conservation and Management, Kingston, TAS, Australia, [3]Key Laboratory of Alpine Ecology and Biodiversity, Institute of Tibetan Plateau Research, Chinese Academy of Sciences, Beijing, China

OPEN ACCESS

Edited by:
Laura Zucconi,
University of Tuscia, Italy

Reviewed by:
Claudia Coleine,
University of Tuscia, Italy
Marcelo Baeza,
University of Chile, Chile

***Correspondence:**
Belinda C. Ferrari
b.ferrari@unsw.edu.au

Specialty section:
This article was submitted to Extreme Microbiology, a section of the journal Frontiers in Microbiology

Received: 12 June 2020
Accepted: 22 July 2020
Published: 12 August 2020

Citation:
Ray AE, Zhang E, Terauds A, Ji M, Kong W and Ferrari BC (2020) Soil Microbiomes With the Genetic Capacity for Atmospheric Chemosynthesis Are Widespread Across the Poles and Are Associated With Moisture, Carbon, and Nitrogen Limitation. Front. Microbiol. 11:1936. doi: 10.3389/fmicb.2020.01936

Soil microbiomes within oligotrophic cold deserts are extraordinarily diverse. Increasingly, oligotrophic sites with low levels of phototrophic primary producers are reported, leading researchers to question their carbon and energy sources. A novel microbial carbon fixation process termed atmospheric chemosynthesis recently filled this gap as it was shown to be supporting primary production at two Eastern Antarctic deserts. Atmospheric chemosynthesis uses energy liberated from the oxidation of atmospheric hydrogen to drive the Calvin-Benson-Bassham (CBB) cycle through a new chemotrophic form of ribulose-1,5-bisphosphate carboxylase/oxygenase (RuBisCO), designated IE. Here, we propose that the genetic determinants of this process; RuBisCO type IE (*rbcL1E*) and high affinity group 1h-[NiFe]-hydrogenase (*hhyL*) are widespread across cold desert soils and that this process is linked to dry and nutrient-poor environments. We used quantitative PCR (qPCR) to quantify these genes in 122 soil microbiomes across the three poles; spanning the Tibetan Plateau, 10 Antarctic and three high Arctic sites. Both genes were ubiquitous, being present at variable abundances in all 122 soils examined (*rbcL1E*, 6.25×10^3–1.66×10^9 copies/g soil; *hhyL*, 6.84×10^3–5.07×10^8 copies/g soil). For the Antarctic and Arctic sites, random forest and correlation analysis against 26 measured soil physicochemical parameters revealed that *rbcL1E* and *hhyL* genes were associated with lower soil moisture, carbon and nitrogen content. While further studies are required to quantify the rates of trace gas carbon fixation and the organisms involved, we highlight the global potential of desert soil microbiomes to be supported by this new minimalistic mode of carbon fixation, particularly throughout dry oligotrophic environments, which encompass more than 35% of the Earth's surface.

Keywords: carbon fixation, atmospheric chemosynthesis, trace gases, photosynthesis, environmental drivers, quantitative PCR

INTRODUCTION

Dry oligotrophic environments encompass more than 35% of the Earth's surface (Mares and History, 1999). Due to global warming, dry environments are expected to expand to cover up to 56% of the Earth's surface by the end of the 21st century (Cherlet et al., 2018). Despite their exposure to frequent freeze-thaw cycles, intense UV radiation, and limited carbon, nitrogen, and moisture availability (Wynn-Williams, 1990; Yergeau et al., 2006; Margesin and Miteva, 2011; Pearce, 2012; Cowan et al., 2014), polar soil microbiomes are diverse and abundant, driving important ecological processes (Yergeau et al., 2006; Cowan et al., 2014; Kleinteich et al., 2017). Such cold desert soil microbiomes are often dominated by *Actinobacteria*, *Proteobacteria*, and *Bacteroidetes* (Tindall, 2004; Cary et al., 2010; Bottos et al., 2014; Tytgat et al., 2014; Zhang et al., 2020), with a high abundance of phototrophic primary producers, particularly *Cyanobacteria* and algae (Friedmann, 1982; Elster, 2002; Namsaraev et al., 2010; Jansson and Taş, 2014). However, in ice-free polar deserts, these phototrophs are often restricted to lithic niches that protect them from intense UV radiation and desiccation (Walker and Pace, 2007; Pointing et al., 2009; Wierzchos et al., 2012; Cowan et al., 2014; McKay, 2016; Goordial et al., 2017). Oligotrophic deserts comprising little to no detectable photoautotrophs are distributed worldwide, leading researchers to question what carbon and energy sources support the microbial communities functioning in these harsh ecosystems (Warren-Rhodes et al., 2006; Albertsen et al., 2013; Ferrari et al., 2015; Ji et al., 2015; Tebo et al., 2015; Zhang et al., 2020).

In a recent study by Ji et al. (2017), a novel form of light-independent autotrophy termed atmospheric chemosynthesis was discovered in soils across two oligotrophic East Antarctic deserts; the arid Robinson Ridge (average organic carbon 0.17%, moisture 4.4%) in the Windmill Islands and the hyper-arid Adams Flat (average organic carbon 0.09%, moisture 0.42%) in the Vestfold Hills region. At these sites, H_2-oxidizing bacteria were proposed to employ high-affinity type 1h-[NiFe]-hydrogenases to scavenge and oxidize hydrogen gas that has diffused into the subsurface soil from the atmosphere. The energy liberated from this oxidation process was proposed to support cell maintenance as well as carbon fixation *via* the Calvin-Benson-Bassham (CBB) cycle, and was linked to a novel chemotrophic form of ribulose-1,5-bisphosphate carboxylase/oxygenase (RuBisCO), type IE (Grostern and Alvarez-Cohen, 2013; Tebo et al., 2015; Ji et al., 2017). RuBisCO type IE (*rbcL1E*) is phylogenetically distinct from the photoautotrophic RuBisCO types IA and IB and is notably also distinct from the other chemoautotrophic RuBisCO red-types IC and ID, diverging from these clades prior to their own separation (Park et al., 2009; Tebo et al., 2015). Despite this discovery, the broader ecological role and significance of this novel RuBisCO has still not been determined.

Here, we propose that terrestrial microbiomes inhabiting cold oligotrophic deserts throughout the world may be genetically capable of supporting cell growth through atmospheric chemosynthesis, particularly in environments where photoautotrophs are limited. We used quantitative PCR (qPCR) targeting the *rbcL1E* and the 1h-[NiFe]-hydrogenase large subunit (*hhyL*) genes to survey 122 desert soils spanning the Tibetan Plateau and 13 Antarctic and high Arctic sites. The taxonomic composition of each soil was analyzed using amplicon sequencing. We also aimed to identify the abiotic parameters associated with the genetic capacity for atmospheric chemosynthesis within each region, by correlating the relative abundances of *rbcL1E* and *hhyL* against 26 measured soil physicochemical parameters. We hypothesize that atmospheric chemosynthesis, as a new form of chemoautotrophy, is associated with low moisture and nutrient limitation in cold desert soils, under the general exclusion of phototrophs.

MATERIALS AND METHODS

Site Descriptions

Sampling was conducted across 14 cold desert sites spanning Antarctica (the Windmill Islands and Vestfold Hills), the high Arctic and the Tibetan Plateau (**Figure 1**). The Windmill Islands is an ice-free region located in Wilkes land, Eastern Antarctica (Gasparon et al., 2007). Centered at 110°30′E and 66°22′S, the region covers an area of 75 km^2 (Goodwin, 1993), has an elevation of below 100 m and includes five major peninsulas and multiple rocky islands (Siciliano et al., 2014; Bissett et al., 2016). Five sites from the Windmill Islands were sampled in this study; Mitchell Peninsula (MP; 66°31′S, 110°59′E), Robinson Ridge (RR; 66°22′S, 110°35′E), Browning Peninsula (BP; 66°27′S, 110°32′E), Herring Island (HI; 66°24′S, 110°39′E), and Casey station (CST; 66°16′S, 110°31′E).

Soil samples were also obtained from five sites near Davis station (68°35′S, 77°58′E), the most southerly research station in Eastern Antarctica; Old Wallow (OW; 68°36'S, 77°57′E), Heidemann Valley (HV; 68°35'S, 78°0′E), Adams Flat (AF; 68°33'S, 78°1′E), Rookery Lake (RL; 68°30'S, 78°7′E), and The Ridge (TR; 68°54′S, 78°07′E). These sites are in the low-lying Vestfold Hills region of Eastern Antarctica, a region consisting of numerous deep-sea inlets and lakes (Zhang et al., 2020). High Arctic surface soils were previously collected from a Canadian site, Alexandra Fjord Highlands (AFH; 78°51′N, 75°54′W), and two Norwegian sites; Spitsbergen Slijeringa (SS; 78°14′N, 15°30′W) and Spitsbergen Vestpynten (SV; 78°14′N, 15°20′W). Soil samples were also collected from the cold, high-altitude Qinghai-Tibet Plateau in Western China (TP; 32°27′N, 80°4′E), which has been previously referred to as Earth's third pole (Gao et al., 2018).

Soil Sampling

Soil samples were obtained from the 13 high Arctic and Antarctic sites by Australian Antarctic Program (AAP) expeditioners, while the Tibetan Plateau soil samples were obtained by expeditioners from the Chinese Academy of Sciences. In total, 122 samples were collected from the top 10 cm of soil, as previously described (Siciliano et al., 2014; Ji et al., 2020; Zhang et al., 2020). All soil samples were stored at −80°C until downstream analysis.

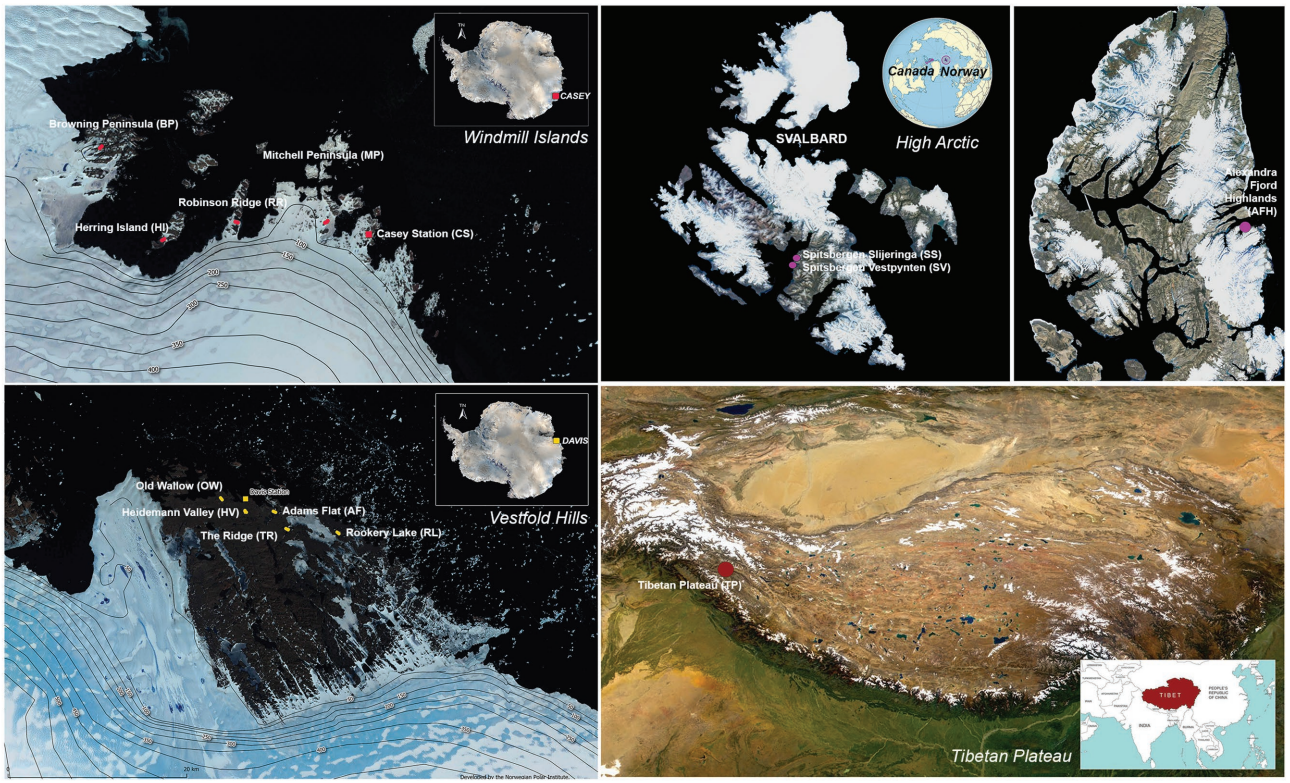

FIGURE 1 | Map of the 14 sites studied with approximate sampling locations across the Vestfold Hills and Windmill Island regions of Eastern Antarctica, as well as the high Arctic and the Tibetan Plateau. Satellite image (Quantarctica v3 GIS package in QGIS 3.4.7).

Soil Physicochemical Analysis

For all the Antarctic and high Arctic soil samples (n = 117), physicochemical parameters (n = 26) were quantified using standard procedures described previously by Siciliano et al. (2014) and van Dorst et al. (2014b) (**Supplementary Materials 1–3**). Briefly, chemical parameters included those obtained by X-Ray fluorescence elemental analysis (SiO_2, TiO_2, Al_2O_3, Fe_2O_3, MnO, MgO, CaO, Na_2O, K_2O, and P_2O_5) and water extraction (Cl^-, Br^-, NO_3^-, NO_2^-, PO_4^{3-}, and SO_4^{2-}). Laser scatter was used to quantify soil particle size, while pH and conductivity were measured using a 1:5 soil to distilled water suspension. Global positioning system (GPS), geographic information system (GIS), and digital elevation models (DEMs) were implemented to measure physical parameters, including location, elevation, and aspect. Combustion and nondispersive infrared (NDIR) gas analysis were used to quantify total carbon (TC), total phosphorus (TP), and total nitrogen (TN) content (Rayment and Lyons, 2011). As comprehensive soil physicochemical analysis was not performed on the Tibetan Plateau soils, these samples were excluded from downstream correlation analysis.

Community Genomic DNA (gDNA) Extraction

DNA was extracted in triplicate from 0.25 to 0.3 g of each soil sample using the FastDNA SPIN kit for soil (MP Biomedicals, NSW, Australia) as per the manufacturer's instructions. DNA was quantified with Picogreen (Life Technologies, Vic, Australia) and fluorescence measured on a fluorescence plate reader (SpectraMax M3 Multi-Mode Microplate Reader; Molecular Devices, CA), prior to being stored at −80°C until used.

Bacterial 16S rRNA Gene Sequencing and Data Analysis

Barcode tag amplification of the bacterial 16S ribosomal RNA (rRNA) gene was previously performed on soil gDNA using primers 28F and 519R (Bissett et al., 2016; Ji et al., 2020; Zhang et al., 2020). ARISA analysis confirmed that each set of triplicate gDNA extractions were significantly correlated (data not shown; van Dorst et al., 2014b; Ferrari et al., 2015). Therefore, 16S rRNA sequencing and all downstream analysis was performed using a single gDNA extract from each of the soil samples. Paired-end amplicon sequencing was performed using the Illumina MiSeq platform (Illumina, 312 California, US) in accordance with protocols from the Biome of Australia Soil Environments (BASE) project by Bioplatforms Australia (Bissett et al., 2016). The Antarctic and high Arctic data were downloaded together from the Australian Antarctic Datacentre[1], and the BASE repository[2]. Amplicon sequencing data for the Tibetan Plateau soils was obtained from Ji et al. (2020) and analyzed separately. Open operational taxonomic unit (OTU) picking, assignment

[1]http://dx.doi.org/10.4225/15/526F42ADA05B1
[2]https://data.bioplatforms.com/organization/about/australian-microbiome

and classification were performed according to previously described methods (Zhang et al., 2020). In brief, USEARCH v10.0.240 (Edgar et al., 2011) and VSEARCH v2.8.0 (Torbjørn et al., 2016) were employed according to the UPARSE-OTU algorithm (Edgar, 2013). Sequences were quality filtered, trimmed, and clustered *de novo* to classify OTUs at 97% identity, and assigned to separate sample-by-OTU matrices where singletons were discarded manually. Sequences were then taxonomically classified against the SILVA v3.2.1323 SSU rRNA database (Quast et al., 2013).

Validation of the RuBisCO Type IE qPCR Primer Set

The RuBisCO type IE qPCR primer set (rbcL1Ef/rbcL1Er) designed in Ji et al. (2017) was validated for use in polar soils by amplicon sequencing DNA lysates. PCR was performed in reaction mixtures composed of 2 µl template gDNA, 5 µl GoTaq Flexi Buffer; pH 8.5 (Promega Corporation, USA), 1 µl 25 mM MgCl2, 0.5 µl 10 mM dNTPs (Bioline), 13.75 µl UltraPure DNase/RNase-free distilled water (Invitrogen, Scotland), 0.312 µl of each 40 µM primer (rbcL1Ef/rbcL1Er; **Table 1**; Integrated DNA Technologies), 0.126 µl GoTaq polymerase (Promega Corporation, USA), and 2 µl of 1 mg/µl Bovine Serum Albumin (BSA). Amplifications were conducted using a Mastercycler nexus X2 (Eppendorf, NSW, Australia) under the following conditions; 95°C for 5 min, 35 cycles of denaturing at 95°C for 30 s, annealing at 55°C for 30 s and extension at 72°C for 30 s, and a final extension of 72°C for 5 min. PCR products underwent amplicon sequencing using the Illumina platform at the Australian Centre for Ecogenomics (University of Queensland). Sequences that lacked both the forward and reverse primer binding sites were discarded, as were those with average quality scores <35. The remaining sequences were matched to reference RuBisCO subtype sequences using the National Centre for Biotechnology Information (NCBI) Basic Local Alignment Search Tool (BLAST; Ye et al., 2012).

qPCR Analysis of *rbcL1E* and *hhyL* Genes

qPCR was performed on all 122 gDNA extracts using previously published qPCR primers targeting *rbcL1E* (rbcL1Ef/rbcL1Er; Ji et al., 2017), *hhyL* (NiFe-244f/NiFe-568r; Constant et al., 2010, 2011), and the 16S rRNA gene (Eub1048f/Eub1194r; Maeda et al., 2003; **Table 1**). Positive controls were synthetically designed gene fragments (gBlocks; Integrated DNA Technologies, VIC, Australia) composed of representative *rbcL1E* (JX458468.1), *hhyL* (AB894417.1), and 16S rRNA (MF689012.1) gene sequences. Standard curves were generated over 5–7 orders of magnitude.

qPCR reaction mixtures for *rbcL1E* and the *hhyL* target genes were prepared using 10 µl QuantiFast SYBR Green PCR Master Mix (Qiagen, VIC, Australia), 0.5 µl of each 40 µM primer (Integrated DNA Technologies), 8 µl UltraPure DNase/RNase-free distilled water (Invitrogen), and 1 µl diluted (1:10) gDNA. The reaction mix for the 16S rRNA gene was identical, except that 7 µl molecular water and 1 µl of 5 ng/µl T4gene32 Protein (Sigma-Aldrich, NSW, Australia) were added to reduce non-specific amplification (Baugh et al., 2001; Villalva et al., 2001). Thermocycling reactions was completed using a CFX96 Touch™ Real-Time PCR Detection System (Bio-Rad Laboratories, NSW, Australia) under standard two-step conditions; 94°C for 5 min, 45 cycles of 94°C for 20 s, and 54°C for 50 s, followed by a melt-curve step from 50 to 95°C. The quantitative fluorescence data were spectrophotometrically collected during the 54°C step.

qPCR Data Analysis

CFX manager software (Bio-Rad Laboratories) was used for data analysis. Melt peak analysis confirmed amplification specificity. Amplification within the most dilute standard was detected at least 5 C_t before the negative template controls. The average C_t values across replicates were determined, and then standard curve efficiencies and copy numbers were converted into copies/g of soil. Here, the average efficiencies for the 16S rRNA, *rbcL1E* and *hhyL* genes qPCR reactions were 86.9% (±3.55), 91.1% (±1.48), and 89.9% (±3.06), respectively. The R^2 value for each qPCR was equal to or greater than 0.99. In accordance with Jones and Hallin (2019), the genetic copy numbers of *rbcL1E* quantified were corrected against the proportion of *rbcL1E* target reads observed during site-specific primer validation [section "Validation of the RuBisCO Type IE qPCR Primer Set"]. Next, *rbcL1E* and *hhyL* copy numbers normalized against 16S rRNA gene copy numbers and expressed as a percentage. Beanplots comparing the relative abundances of *rbcL1E* and the *hhyL* gene were produced using BoxPlotR (Kampstra, 2008; RStudio and Inc, 2013; R Core Team, 2018).

Multivariate Data Analysis

Skewness was eliminated from the 26 measured physicochemical factors using log or square root transformations within the PRIMER v7 + PERMANOVA package (Clarke and Warwick, 2001), and normalized (mean/standard deviation; van Dorst et al., 2014a). Subsequent multivariate data analysis of the physicochemical, 16S rRNA amplicon and qPCR data was carried out in the R v3.5.1 environment (R Core Team, 2018).

TABLE 1 | Quantitative PCR (qPCR) primer sets used in this study.

Target gene	Primer name and sequence (5'-3')		Target size (bp)	Reference
	Forward	Reverse		
1h-[NiFe]-hydrogenase large subunit gene (*hhyL*)	NiFe-244f; GGGATCTGCGGGGACAACCA	NiFe-568r; TCTCCCGGGTGTAGCGGCTC	324	(Constant et al., 2010)
RuBisCO type IE (*rbcL1E*)	rbcL1Ef; GGACBGTSGTVTGGACSGA	rbcL1Er; TTGAABCCRAAVACRTTGC	187	(Ji et al., 2017)
16S rRNA gene	Eub1048f; GTGSTGCAYGGYTGTCGTCA	Eub1194r; ACGTCRTCCMCACCTTCCTC	146	(Maeda et al., 2003)

Non-metric multi-dimensional scaling (NMDS) ordination plots were generated using the R package "vegan" (Oksanen et al., 2015) to visualize the ordering of samples in reduced two-dimensional space. Euclidean dissimilarity index was applied to the physicochemical parameters, while the Bray–Curtis dissimilarity index was applied to the bacterial taxonomic abundance dataset. Ellipse paths were calculated using the "veganCovEllipse" function developed by Torondel et al. (2016). The veg.dist() and anosim() function from the "vegan" R package was used to conduct one-way analysis of similarity (ANOSIM) on dissimilarity matrices on our OTU and physicochemical datasets, grouped on a regional and site level (permutations = 999, $\alpha = 0.05$). Subsequently, the qPCR data was analyzed against the 26 measured physicochemical factors. To identify the most appropriate correlation method to apply to this analysis, the linearity between the genetic abundance of *rbcL1E* and *hhyL* with each physicochemical parameter was tested through the generation of scatterplots using the "ggscatter" function from the "ggplot2" R package (Wickham, 2016). Spearman correlations between *rbcL1E* and *hhyL* genetic abundances and each physicochemical condition were displayed using the R package "corrplot" (Wei et al., 2017) to determine the direction of correlations observed. Multivariate random forest regression analysis was subsequently conducted using the "rfPermute" package (Archer, 2013) under the R-environment[3]. The relative importance and the significance of environmental factors in explaining the relative abundance of *rbcL1E*, *hhyL*, and the total bacterial abundance were determined.

RESULTS

Validation of the *rbcL1E* qPCR Primer Set

Following quality control, amplicon sequencing using the *rbcL1E* primer set resulted in a total of 760, 855 sequence reads. In these polar soils, the primers were on average 73.8% specific toward *rbcL1E* (**Supplementary Material 4**). The specificity of the *rbcL1E* primer pair ranged between 61.5 and 86.9% with most non-target sequences retrieved classified as RuBisCO type 1C. Genetic copies of *rbcL1E* obtained during later qPCR analysis were corrected against the site-specific primer specificities obtained here.

Relative Abundances of *rbcL1E* and *hhyL* Genes in Cold Desert Soils

The genetic determinants for atmospheric chemosynthesis were detected in high abundances across all 122 polar soils analyzed (**Figure 2**). As a percentage of 16S rRNA gene copies/g soil, average relative abundances of *rbcL1E* were highest within the Vestfold Hills (58.1%), followed by the Tibetan Plateau (42.1%), the Windmill Islands (31.0%), and the high Arctic (10.0%). The relative abundances of the *hhyL* gene were also variable, with the highest relative abundance observed in the Vestfold Hills (7.73%), followed by the Windmill Islands (3.95%), the high Arctic (3.86%), and Tibetan Plateau (1.21%).

[3]http://cran.r-project.org/

The average copy numbers of *rbcL1E* and *hhyL* genes per site were highest within the Vestfold Hills at 3.42×10^8 and 6.05×10^7 copies/g soil, respectively. Within the Vestfold Hills, Adams Flat exhibited the highest relative abundance of both target genes (*rbcL1E* 7.24×10^8 and *hhyL* 1.33×10^8), while the lowest abundances were found at The Ridge (*rbcL1E* 5.68×10^7 and *hhyL* 4.61×10^6). In comparison to the Vestfold Hills, the relative abundances of *rbcL1E* and *hhyL* were lower on average within the Windmill Islands with 1.11×10^8 and 1.20×10^7 copies, respectively. Within the Windmill Islands, the *rbcL1E* gene abundances ranged between 2.32×10^7 copies/g soil at Browning Peninsula and 2.72×10^8 copies/g soil at Mitchell Peninsula. The lowest *hhyL* gene abundances in the Windmill Islands were observed for soils from the human impacted Casey station (4.18×10^6 copies/g soil), with the highest numbers detected at Herring Island (3.39×10^7 copies/g soil).

Bacterial Communities Across the Poles

Soil bacterial communities were dominated by *Actinobacteria* at most sites, with relative abundances ranging from 23.57% at the Ridge to 58.63% at Herring Island (**Figure 3, Supplementary Material 5**). While *Proteobacteria*, *Chloroflexi*, *Bacteroidetes*, and *Acidobacteria* were also highly abundant, *Cyanobacteria* were present in low relative abundances (<1%) at 8 of the 13 sites (Spitsbergen Vestpynten, Spitsbergen Slijeringa, Heidemann Valley, Old Wallow, Adams Flat, Mitchell Peninsula, Robinson Ridge, and the Tibetan Plateau). In contrast, the relative abundances of *Cyanobacteria* were higher at 5–9% within the Alexandra Fjord Highlands, Rookery Lake, Casey station, and Browning Peninsula. Candidate phyla accounted for substantial proportions of the bacterial communities particularly within the Windmill Islands, dominating microbial communities at Mitchell Peninsula (12.71%), Robinson Ridge (8.71%), and Casey station (4.52%). Of the candidate phyla residing in the Windmill Islands, *Candidatus Eremiobacterota* (WPS-2) was the most abundant comprising 7.42% relative abundances on average at Mitchell Peninsula, followed by *Candidatus Dormibacterota* (AD3) at an average relative abundance of 4.06% at Mitchell Peninsula.

Soil Physicochemistry and Bacterial Community Similarity Across East Antarctica and the High Arctic

At the global scale, the bacterial communities were more similar within, rather than between regions as indicated by the distinct formation of regional clusters when viewed using an NMDS plot (**Figure 4B**). Accordingly, ANOSIM results indicated that bacterial community composition varied significantly between the Antarctic and the high Arctic samples (ANOSIM $R = 0.520$, $p = 0.001$), with significant differences also observed on regional level between Norway, Canada, the Windmill Islands, and Vestfold Hills (ANOSIM $R = 0.872$, $p = 0.001$). Site-level bacterial community similarities have also been visualized, with the greatest variations occurring within Mitchell Peninsula and Alexandra Fjord Highlands (**Figure 4D**). Bacterial communities

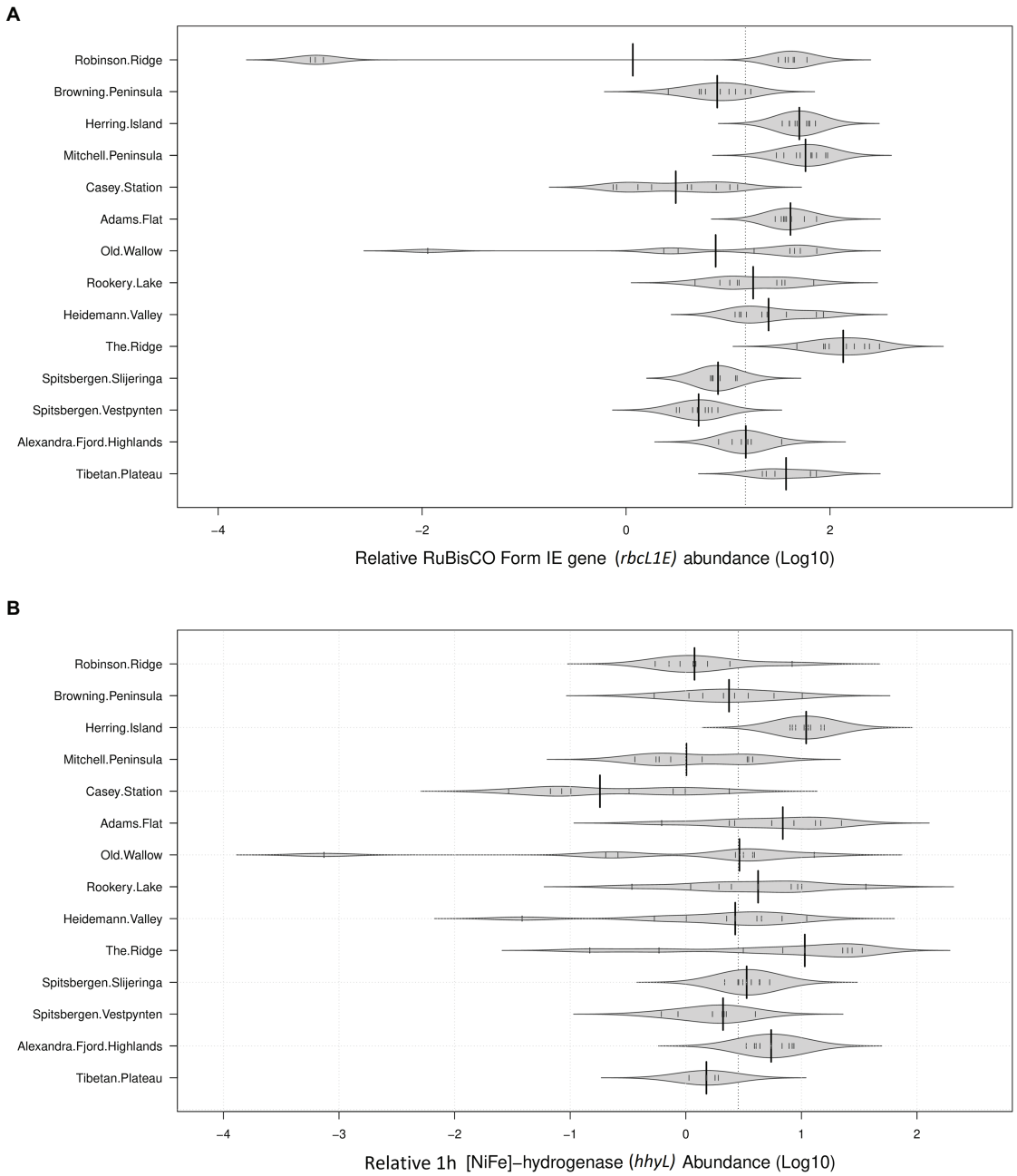

FIGURE 2 | Relative abundances of target genes associated with atmospheric chemosynthesis within polar desert soils. The proposed genetic determinants of this process were widely distributed across all 14 sites spanning Antarctica, the high Arctic, and Tibetan Plateau **(A)**. Ribulose-1,5-bisphosphate carboxylase/oxygenase (RuBisCO) type IE (*rbcL1E*; **B**). 1h-[NiFe]-hydrogenase large subunit gene (*hhyL*). Large solid black lines indicate average relative abundances per site; the dotted black line indicates the mean relative abundance of all 14 sites (36.68% for *rbcL1E* and 5.22% for *hhyL*); the small, solid black lines represent individual data points; polygons represent the estimated density of the data.

within soils from the three high Arctic sites were significantly similar to each other (ANOSIM $R = 0.328$, $p = 0.002$), as were soils sampled from within the Vestfold Hills (ANOSIM $R = 0.276$, $p = 0.001$). Comparatively, a significant and more substantial variation in bacterial composition was observed within the Windmill Island sites (ANOSIM $R = 0.476$, $p = 0.001$).

The measured soil physicochemical properties mirrored the bacterial community data, with distinct regional clusters showing that soils were more similar within than between regions (**Figure 4A**). The associated ANOSIM results indicated that physicochemical conditions varied significantly between the Antarctic and the high Arctic samples (ANOSIM $R = 0.626$, $p = 0.001$), with differences also observed on a regional level

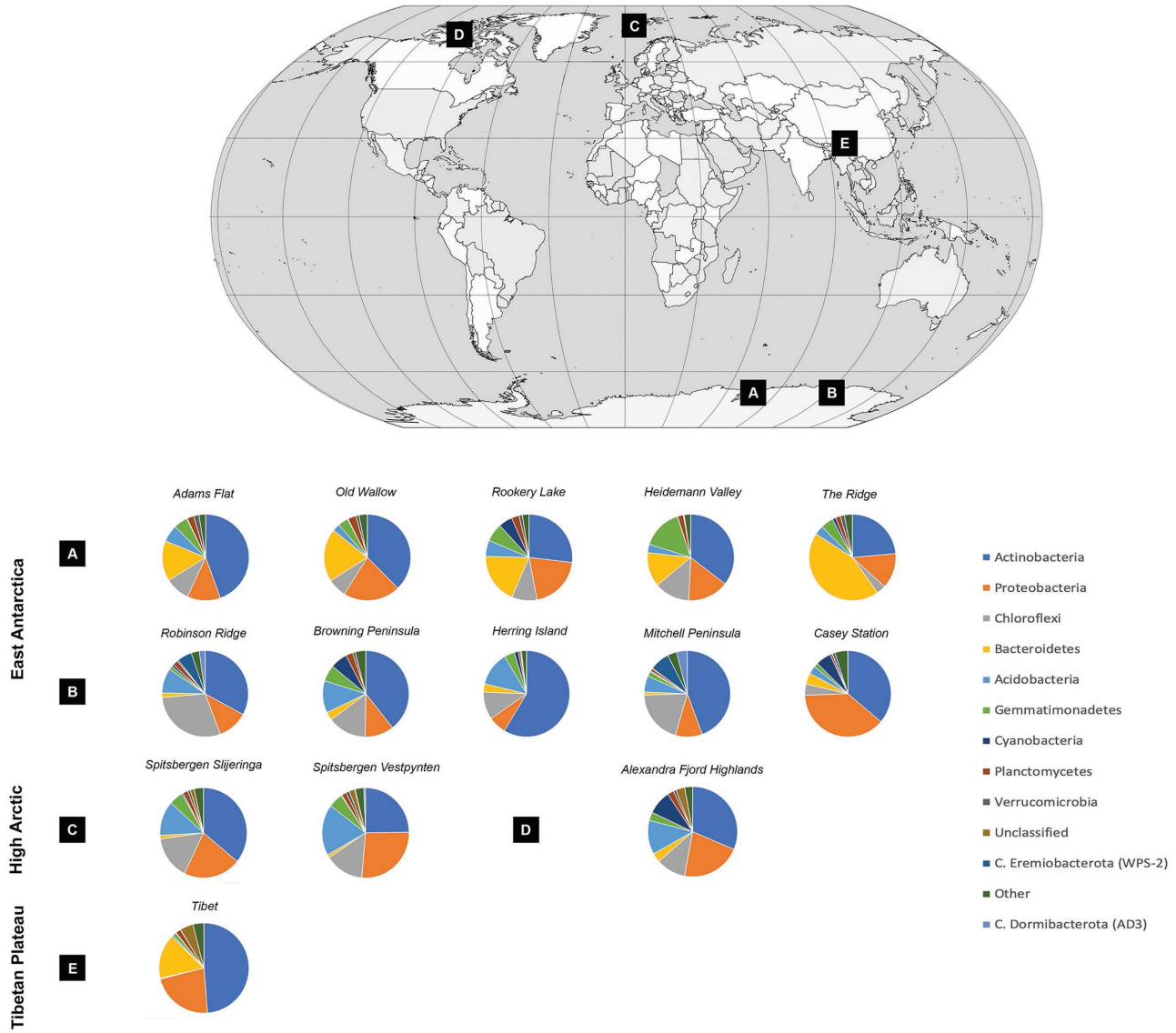

FIGURE 3 | Soil bacterial community diversity at a phylum level across all 14 cold desert sites, and their locations throughout the **(A)** Vestfold Hills, **(B)** Windmill Islands, **(C)** Norway, **(D)** Canada, and **(E)** Tibetan Plateau. *Actinobacteria* dominated all soils, with average site-level relative abundances ranging from 23.6% at The Ridge to 58.6% at Herring Island. *Proteobacteria*, *Chloroflexi*, *Bacteroidetes*, and *Acidobacteria* were also highly abundant. In contrast, *Cyanobacteria* were present in low relative abundances accounting for <1% of the bacterial communities in eight sites, increasing to 5–9% within the Alexandra Fjord Highlands, Rookery Lake, Casey station, and Browning Peninsula. Within the Windmill Islands region, *Candidatus Eremiobacterota* was present in high relative abundances, with site-level averages ranging between 0.02% at Herring Island and 7.42% at Mitchell Peninsula. Similarly, *Candidatus Dormibacterota* was also present in high relative abundances in the Windmill Islands only.

between Norway, Canada, the Windmill Islands, and Vestfold Hills (ANOSIM R = 0.730, p = 0.001). Site-level variations in physicochemical conditions have also been visualized (**Figure 4C**). On this more localized level, soil samples from within the Vestfold Hills demonstrated a high degree of physicochemical similarity to each other compared to those from other regions (ANOSIM R = 0.302, p = 0.001). High Arctic soils were also more physicochemically like each other than soils from other regions (ANOSIM R = 0.302, p = 0.001). In contrast, the Windmill Island soil samples demonstrated greater dissimilarity within sites (ANOSIM R = 0.617, p = 0.001).

The East Antarctic soils (n = 90) analyzed in this study were low in moisture (0.0023–0.26%) and nutrients, particularly TC (0.008–2.58%), TN (0.0065–0.22%), and TP (0.027–0.23%; **Supplementary Materials 1, 2**). Within the high Arctic (n = 27), these values were higher (TN was 0.022–0.080% in Canada and 0.073–0.43% in Norway; TC was 0.29–6.89% in Canada and 1.15–6.55% in Norway; Moisture was 0.042–0.11% in Canada and 0.11–0.42% in Norway; **Supplementary Material 3**). Soils obtained from the Windmill Islands and Norway were acidic (average pH 6.08 and 5.97, respectively), while soils from the Vestfold

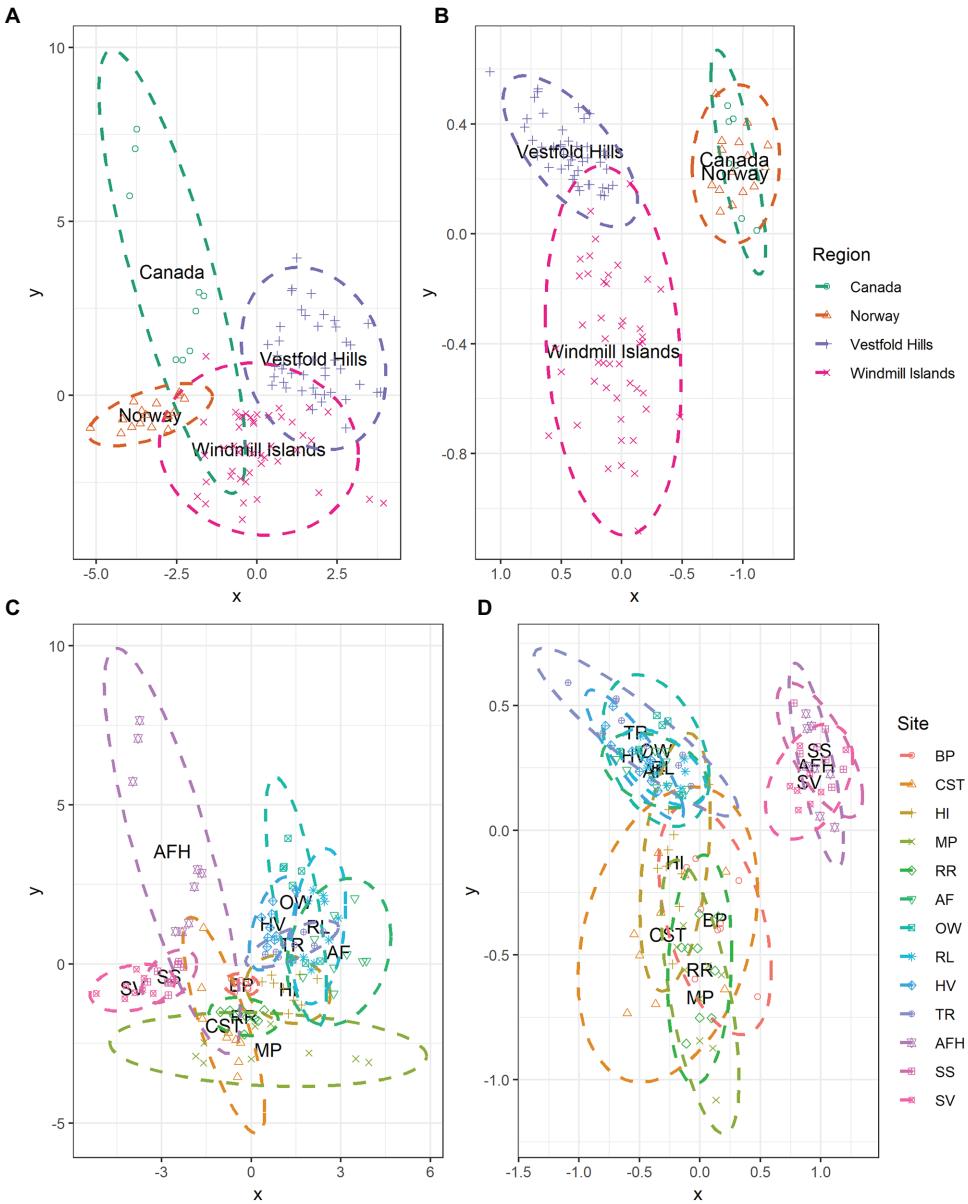

FIGURE 4 | NMDS plots showing the relationships among samples on a regional and local scale for **(A,C)** measured soil physicochemical parameters and **(B,D)** bacterial community composition at phylum level. Soil samples displayed greater environmental and bacterial community similarities within rather than between regions, as indicated by the formation of regional-level clustering. Bacterial communities within the high Arctic samples (Norway and Canada) were highly similar to each other with the clusters overlapping. Soil samples clustered according to site, indicating that soils from the same location share similar environmental conditions and bacterial community structures. For both environmental and bacterial communities, the greatest dissimilarity was observed within the Windmill Islands although variation in physicochemical parameters was also observed across the high Arctic sites, predominantly Alexandra Fjord Highlands.

Hills and Canada were more alkaline (average pH 8.49 and 7.81, respectively; **Supplementary Materials 1–3**).

Multivariate random forest analysis revealed strong and significant relationships between the genetic abundances of *rbcL1E*, *hhyL*, and multiple environmental parameters, while Spearman correlations showed the direction of these relationships. The relative abundances of *rbcL1E* and *hhyL* were most significantly explained by soil moisture (IncMSE = 69.35 and 24.38, respectively), TC (IncMSE = 16.45 and 17.48, respectively), and mud composition (IncMSE = 28.73 and 15.61, respectively), with significantly greater ($p < 0.05$; **Table 2**) abundances of both genes occurring under low moisture, carbon and mud composition (**Figure 5**). Additionally, *rbcL1E* was significantly explained by various oxides including NO_3 (IncMSE = 32.83), Na_2O (IncMSE = 24.40), MgO (IncMSE = 19.47), CaO (IncMSE = 26.44), and MnO (IncMSE = 16.09; $p < 0.05$; **Table 2**). Spearman analysis revealed that in these cases, greater *rbcL1E* was associated with lower NO_3 content and greater

levels of the other oxides (**Figure 5**). Random forest analysis revealed that multiple environmental factors significantly influenced microbial community structure, including pH (IncMSE = 31.35), conductivity (IncMSE = 23.86), TN (IncMSE = 26.91), K_2O (IncMSE = 27.04), Al_2O_3 (IncMSE = 20.59), SiO_2 (IncMSE = 16.87), PO_4 (IncMSE = 17.23), and NO_2 (IncMSE = 12.83; $p < 0.05$), however, these factors did not significantly explain either genetic determinant of atmospheric chemosynthesis (**Table 2**).

DISCUSSION

Atmospheric hydrogen oxidation has only recently been identified as an energetic driver of microbial autotrophic CO_2 fixation through the CBB cycle (Ji et al., 2017). Until now, atmospheric chemosynthesis has been overlooked as a niche process with unknown global significance. Here, we confirm that the genetic determinants of this new form of chemoautotrophy (*rbcL1E* and *hhyL*) are widespread and abundant throughout soil microbiomes of geographically distinct polar regions throughout Antarctica, the high Arctic, and the Tibetan Plateau. These findings support the hypothesis that this minimalistic carbon fixation strategy may be considered a globally occurring phenomenon and an important widespread survival adaptation in oligotrophic desert soil ecosystems.

While the role of hydrogen oxidation in contributing to microbial primary production is newly discovered, the role of high affinity hydrogenases (*hyyL*) in fulfilling the energy requirements of dormant soil bacteria is well established (Constant et al., 2008, 2010, 2011; Berney and Cook, 2010; Berney et al., 2014; Greening et al., 2015; Islam et al., 2019; Piche-Choquette and Constant, 2019). During periods of extreme environmental stress, H_2-oxidizers can reversibly lower their metabolic activity and thereby, their energy requirements (Lennon and Jones, 2011). Under these conditions, the aerobic oxidation of atmospheric hydrogen provides bacteria with a ubiquitous and reliable source of energy (Morita, 1999; Smith-Downey et al., 2008; Constant et al., 2011). The process is indeed widespread, with *hyyL* reported at abundances of 10^6–10^8 genetic copies per gram of soil in both oligotrophic and copiotrophic ecosystems (Constant et al., 2011). Moreover, greater *hhyL* expression and hydrogen oxidizing activity have been linked to environments with lower organic carbon content (King, 2003; Greening et al., 2015), with H_2-oxidizers reported to be among the earliest colonizers of volcanic deposits, despite the negligible amounts of organic matter present (King, 2003; Sato et al., 2004). Here, we also revealed the presence of high numbers of *hhyL* genes (4.18×10^6–3.39×10^7 copies/g soil) in cold desert soils from across the three poles, many of which contained extremely low levels of carbon and nitrogen. We note here that although the qPCR primer are widely implemented (Constant et al., 2010, 2011;

TABLE 2 | Random forest analysis of the genetic abundances of *hhyL* and *rbcL1E*, relative to 16S rRNA genes, and 16S rRNA genes against 26 physicochemical parameters.

	***hyyL*/16S rRNA**		***rbcL1E*/16S rRNA**		**16S rRNA**	
	%IncMSE	**%IncMSE.pval**	**%IncMSE**	**%IncMSE.pval**	**%IncMSE**	**%IncMSE.pval**
Moisture	24.38	**0.002**	69.35	**0.001**	26.19	**0.003**
Mud	15.61	**0.034**	28.73	**0.003**	40.45	**0.001**
TC	17.48	**0.019**	16.45	**0.023**	27.47	**0.004**
pH	11.64	0.077	14.7	0.052	31.35	**0.002**
Elevation	13.12	**0.046**	9.49	0.105	31.81	**0.001**
NO_3	6	0.266	32.83	**0.002**	15.28	**0.033**
Na_2O	–2.71	0.981	24.4	**0.004**	17.63	**0.026**
MgO	10.71	0.135	19.47	**0.013**	21.33	**0.008**
CaO	10.87	0.130	26.44	**0.005**	11.92	0.139
TN	7.48	0.323	11.84	0.075	26.91	**0.003**
Aspect	3.96	0.421	18.61	**0.025**	19.25	**0.028**
K_2O	5.6	0.459	8.55	0.145	27.04	**0.001**
MnO	6.39	0.392	16.09	**0.037**	17.99	**0.033**
Al_2O_3	7.65	0.218	11.33	0.070	20.59	**0.013**
Cl	15.37	**0.031**	14.5	**0.045**	8.84	0.199
Conductivity	8.61	0.218	5.74	0.282	23.86	**0.006**
Sand	2.67	0.686	22.82	**0.009**	9.06	0.261
Fe_2O_3	4.04	0.690	12.49	0.080	12.94	0.121
SiO_2	4.82	0.601	6.94	0.251	16.87	**0.037**
TiO_2	6.35	0.375	8.32	0.170	13.63	0.078
PO_4	5.06	0.327	5.88	0.215	17.23	**0.025**
NO_2	4.44	0.182	8.29	0.087	12.83	**0.040**
SO_4	7.78	0.202	7.18	0.202	10.09	0.175
P_2O_5	5.58	0.472	7.56	0.221	10.59	0.186
Br	3.62	0.411	3.71	0.337	15.53	**0.017**
TP	2.49	0.724	4.11	0.398	12.79	0.089

Bold text = significant p values (<0.05).

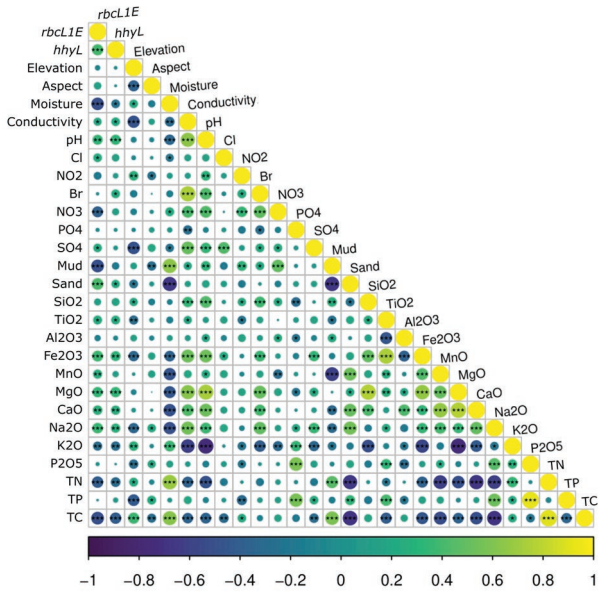

FIGURE 5 | Spearman correlations between the relative abundance of the two target genes, *rbcL1E* and *hhyL*, against all 26 measured physicochemical parameters for the 117 Antarctic and high Arctic soils. *rbcL1E* and *hhyL* each produced positive correlations with soil conductivity, pH, and sand composition as well as with greater abundances of various oxides. *rbcL1E* and *hhyL* both occurred in higher abundance within samples of low moisture, total carbon (TC), and total nitrogen (TN). *rbcL1E* also occurred in higher abundance within samples of low NO_3^- and mud composition.

Meredith et al., 2014; Khdhiri et al., 2015; Piché-Choquette et al., 2016), the discovery of high-affinity hydrogenases beyond group 1 h (D. Cowan, personal communication; Greening et al., 2014; Islam et al., 2020) suggests that the high-affinity hydrogenase gene abundances quantified here are underestimations.

Despite the widespread and abundant distribution of *hhyL*, the global co-occurrence of *hhyL* and *rbcL1E* has been unknown. The high and widespread co-occurrence of *hhyL* and *rbcL1E* across all 122 soils analyzed here indicates that the energy liberated from atmospheric hydrogen oxidation may be directed toward bacterial cell growth and primary production more pervasively than anticipated. Previous studies have indicated that trace gas chemosynthetic bacteria belong to the phyla *Actinobacteria*, *C. Eremiobacterota*, and *C. Dormibacterota* phyla (Park et al., 2009; Ji et al., 2017). The *rbcL1E* gene has also been detected within *Chloroflexota*, *Firmicutes*, and *Verrucomicrobiota* (Tebo et al., 2015). In this study, these taxa dominated soil communities from across the three poles, together accounting for up to 76.2% of the microbial community composition (**Figure 3**; **Supplementary Material 5**). Thus, in cold nutrient-starved deserts, trace gas chemoautotrophs appear to have a selective advantage for survival.

It has been proposed that atmospheric chemosynthesis and photosynthesis are both contributors to microbial primary production in oligotrophic environments, with contributions likely to vary along an aridity gradient (Ji et al., 2017; Bay et al., 2018). Indeed, variability in photo and chemoautotrophic potential was observed here with abundances of *rbcL1E* being particularly low in the high Arctic (10.0%), Casey station (4.8%), and Browning Peninsula (9.0%) soils (**Figure 2**). Each of these sites also contained greater photosynthetic potential than the other sites due to higher abundances of *Cyanobacteria* (5.7–8.6%; Kleinteich et al., 2017; Pudasaini et al., 2017; Zhang et al., 2020). *rbcL1E* gene abundances were also more variable than *hhyL*, reflecting the more widespread role of the high affinity hydrogenases in supplying maintenance energy to dormant microbial communities (Berney and Cook, 2010; Constant et al., 2010, 2011; Berney et al., 2014; Greening et al., 2015), as well as for reproduction.

It has been proposed that atmospheric chemosynthesis occurs increasingly within drier, more nutrient-starved soils (Ji et al., 2017; Bay et al., 2018), in part due to the exclusion of phototrophic microorganisms under moisture limitation (Warren-Rhodes et al., 2006; McKay, 2016). We found that the genetic capacity for atmospheric chemosynthesis was associated with increasingly drier, more nutrient-limited soils (Ji et al., 2017; Bay et al., 2018). Random forest and Pearson correlations revealed that *rbcL1E* and *hhyL*, relative to 16S rRNA, increased significantly across Antarctic and high Arctic soils that were increasingly limited in moisture and TC (**Table 2** and **Figure 5**). Additionally, the relative abundance of *rbcL1E* also significantly increased in soils limited in NO_3^- (**Table 2** and **Figure 5**). Neither genetic determinant formed a significant positive correlation with bioavailable substances that are widely utilized by geothermal chemoautotrophic bacteria such as NO_2^- and PO_4^- (**Figure 5**; Engel, 2012). This lack of correlative data supports our current understanding that *rbcL1E* catalyzed primary production is not driven by geochemical energy sources. As a result, atmospheric chemosynthesis may occur within environments where soil nutrients are limited. Positive correlations were detected between *rbcL1E* and multiple trace oxides measured by X-Ray fluorescence elemental analysis (MnO, MgO, CaO, and Na_2O; **Table 2**; **Figure 5**), suggesting a potential metabolic significance that requires further investigation.

It is recommended that additional studies are conducted to focus upon the isolation and characterization of trace gas chemosynthetic bacteria. Additionally, metagenomic and biochemical studies, including hydrogen oxidation and $^{14}CO_2$ assimilation assays should be performed on a broader range of environments where atmospheric chemosynthesis is likely to occur. We suggest that sites should be targeted where organic carbon, water, and photoautotrophs are limited and the utilization of atmospheric gases by microbial communities is well documented (King, 2003; Lynch et al., 2012, 2014). This includes volcanic deposits as well as additional cold and hot deserts, such as the McMurdo Dry Valleys (Babalola et al., 2009; Van Goethem et al., 2016), Namib (van der Walt et al., 2016; Gunnigle et al., 2017), Thar (Rao et al., 2016), and Atacama (Lynch et al., 2014; Schulze-Makuch et al., 2018). Finally, this study highlights the genetic potential of microbial communities residing in cold oligotrophic deserts across the globe to conduct atmospheric chemosynthesis and

their propensity for survival in regions with highly limited water and nutrient availability.

DATA AVAILABILITY STATEMENT

The datasets presented in this study can be found in online repositories described in the article. Original sequencing data is publicly available through NCBI under the accession number PRJNA645753. All other original contributions presented are included in the article/**Supplementary Material**.

AUTHOR CONTRIBUTIONS

BF determined the research objective with input from AR, MJ, and AT. AR conducted tag sequencing and qPCR. Soil parameter data for the Vestfold Hills was led by AT. Tag sequencing analysis was performed by AR and MJ. MJ and WK provided the Tibetan Plateau soil samples. AR, EZ, and MJ conducted multivariate data analysis, with input from BF. AR and BF wrote the manuscript with input from remaining authors. All authors contributed to the article and approved the submitted version.

FUNDING

This work was supported by the Australian Government Research Training Program (RTP) Scholarship (awarded to AR and EZ), the Australian Research Council Future Fellowship (FT170100341; awarded to BF), the Australian Antarctic Program Project 5097, and the Australian Antarctic Science project grant (4406; awarded to BF).

ACKNOWLEDGMENTS

We thank the Australian Antarctic Program expedition teams between 2005 and 2018 for sampling of the Antarctic and Arctic soils used in this study. We thank J. Gao and G. Guo for assisting soil sampling of the Tibetan Plateau. We thank A. Palmer for physicochemical analysis.

SUPPLEMENTARY MATERIAL

The Supplementary Material for this article can be found online at: https://www.frontiersin.org/articles/10.3389/fmicb.2020.01936/full#supplementary-material.

REFERENCES

Albertsen, M., Hugenholtz, P., Skarshewski, A., Nielsen, K., Tyson, G., and Nielsen, P. (2013). Genome sequences of rare, uncultured bacteria obtained by differential coverage binning of multiple metagenomes. *Nat. Biotechnol.* 31, 533–538. doi: 10.1038/nbt.2579

Archer, E. (2013). Estimate permutation p-values for importance metrics. R package version 1.5.2.

Babalola, O. O., Kirby, B. M., Le Roes-Hill, M., Cook, A. E., Cary, S. C., Burton, S. G., et al. (2009). Phylogenetic analysis of actinobacterial populations associated with Antarctic dry valley mineral soils. *Environ. Microbiol.* 11, 566–576. doi: 10.1111/j.1462-2920.2008.01809.x

Baugh, L. R., Hill, A. A., Brown, E. L., and Hunter, C. P. (2001). Quantitative analysis of mRNA amplification by in vitro transcription. *Nucleic Acids Res.* 29:E29. doi: 10.1093/nar/29.5.e29

Bay, S., Ferrari, B., and Greening, C. (2018). Life without water: how do bacteria generate biomass in desert ecosystems? *Microbiol. Aust.* 39, 28–32. doi: 10.1071/MA18008

Berney, M., and Cook, G. M. (2010). Unique flexibility in energy metabolism allows mycobacteria to combat starvation and hypoxia. *PLoS One* 5:e8614. doi: 10.1371/journal.pone.0008614

Berney, M., Greening, C., Conrad, R., Jacobs, W. R., and Cook, G. M. (2014). An obligately aerobic soil bacterium activates fermentative hydrogen production to survive reductive stress during hypoxia. *Proc. Natl. Acad. Sci. U. S. A.* 111, 11479–11484. doi: 10.1073/pnas.1407034111

Bissett, A., Fitzgerald, A., Meintjes, T., Mele, P. M., Reith, F., Dennis, P. G., et al. (2016). Introducing BASE: the biomes of Australian soil environments soil microbial diversity database. *Gigascience* 5:21. doi: 10.1186/s13742-016-0126-5

Bottos, E., Scarrow, J., Archer, S., McDonald, I., and Cary, S. (2014). "Bacterial community structures of Antarctic soils" in *Antarctic terrestrial microbiology*. ed. D. Cowan (Berlin: Springer), 9–33.

Cary, S., McDonald, I., Barrett, J., and Cowan, D. (2010). On the rocks: the microbiology of Antarctic dry valley soils. *Nat. Rev. Microbiol.* 8, 129–138. doi: 10.1038/nrmicro2281

Cherlet, M., Hutchinson, C., Reynolds, J., and Hill, J., S. Sommer, and von Maltitz, G. (eds.) (2018). *World atlas of desertification. 3rd Edn*. Luxembourg: Publication Office of the European Union.

Clarke, K. R., and Warwick, R. M. (2001). *Changes in marine communities: An approach to statistical analysis and interpretation*. Plymouth: PRIMER-E.

Constant, P., Chowdhury, S. P., Hesse, L., Pratscher, J., and Conrad, R. (2011). Genome data mining and soil survey for the novel group 5 [NiFe]-Hydrogenase to explore the diversity and ecological importance of presumptive high-affinity H(2)-oxidizing bacteria. *Appl. Environ. Microbiol.* 77, 6027–6035. doi: 10.1128/AEM.00673-11

Constant, P., Chowdhury, S. P., Pratscher, J., and Conrad, R. (2010). Streptomycetes contributing to atmospheric molecular hydrogen soil uptake are widespread and encode a putative high-affinity [NiFe]-hydrogenase. *Environ. Microbiol.* 12, 821–829. doi: 10.1111/j.1462-2920.2009.02130.x

Constant, P., Poissant, L., and Villemur, R. (2008). Isolation of *Streptomyces* sp. PCB7, the first microorganism demonstrating high-affinity uptake of tropospheric H2. *ISME J.* 2, 1066–1076. doi: 10.1038/ismej.2008.59

Cowan, D., Makhalanyane, T., Dennis, P., and Hopkins, D. (2014). Microbial ecology and biogeochemistry of continental Antarctic soils. *Front. Microbiol.* 5:154. doi: 10.3389/fmicb.2014.00154

Edgar, R. C. (2013). UPARSE: highly accurate OTU sequences from microbial amplicon reads. *Nat. Methods* 10, 996–998. doi: 10.1038/nmeth.2604

Edgar, R. C., Haas, B. J., Clemente, J. C., Quince, C., and Knight, R. (2011). UCHIME improves sensitivity and speed of chimera detection. *Bioinformatics* 27, 2194–2200. doi: 10.1093/bioinformatics/btr381

Elster, J. (2002). "Ecological classification of terrestrial algal communities in polar environments" in *Geoecology of Antarctic ice-free coastal landscapes*. eds. L. Beyer and M. Bölter (Berlin, Heidelberg: Springer Berlin Heidelberg), 303–326.

Engel, A. S. (2012). "Chemoautotrophy" in *Encyclopedia of caves. 2nd Edn*. eds. W. B. White and D. C. Culver (Amsterdam: Academic Press), 125–134.

Ferrari, B., Bissett, A., Snape, I., van Dorst, J., Palmer, A., Ji, M., et al. (2015). Geological connectivity drives microbial community structure and connectivity in polar, terrestrial ecosystems. *Environ. Microbiol.* 18, 1834–1849. doi: 10.1111/1462-2920.13034

Friedmann, E. I. (1982). Endolithic microorganisms in the Antartic cold desert. *Science* 215, 1045–1053. doi: 10.1126/science.215.4536.1045

Gao, Y., Wang, W., Yao, T., Lu, N., and Lu, A. (2018). Hydrological network and classification of lakes on the third pole. *J. Hydrol.* 560, 582–594. doi: 10.1016/j.jhydrol.2018.03.062

Gasparon, M., Ehrler, K., Matschullat, J., and Melles, M. (2007). Temporal and spatial variability of geochemical backgrounds in the Windmill Islands, East Antarctica: implications for climatic changes and human impacts. *Appl. Geochem.* 22, 888–905. doi: 10.1016/j.apgeochem.2006.12.018

Goodwin, I. D. (1993). Holocene deglaciation, sea-level change, and the emergence of the Windmill Islands, Budd coast, Antarctica. *Quat. Res.* 40, 70–80. doi: 10.1006/qres.1993.1057

Goordial, J., Davila, A., Greer, C. W., Cannam, R., Diruggiero, J., McKay, C. P., et al. (2017). Comparative activity and functional ecology of permafrost soils and lithic niches in a hyper-arid polar desert. *Environ. Microbiol.* 19, 443–458. doi: 10.1111/1462-2920.13353

Greening, C., Berney, M., Hards, K., Cook, G. M., and Conrad, R. (2014). A soil actinobacterium scavenges atmospheric H2 using two membrane-associated, oxygen-dependent [NiFe] hydrogenases. *Proc. Natl. Acad. Sci. U. S. A.* 111, 4257–4261. doi: 10.1073/pnas.1320586111

Greening, C., Constant, P., Hards, K., Morales, S. E., Oakeshott, J. G., Russell, R. J., et al. (2015). Atmospheric hydrogen scavenging: from enzymes to ecosystems. *Appl. Environ. Microbiol.* 81, 1190–1199. doi: 10.1128/AEM.03364-14

Grostern, A., and Alvarez-Cohen, L. (2013). RubisCO-based CO2 fixation and C1 metabolism in the actinobacterium *Pseudonocardia* dioxanivorans CB1190. *Environ. Microbiol.* 15, 3040–3053. doi: 10.1111/1462-2920.12144

Gunnigle, E., Frossard, A., Ramond, J. -B., Guerrero, L., Seely, M., and Cowan, D. A. (2017). Diel-scale temporal dynamics recorded for bacterial groups in Namib desert soil. *Sci. Rep.* 7:40189. doi: 10.1038/srep40189

Islam, Z. F., Cordero, P. R. F., Feng, J., Chen, Y. -J., Bay, S. K., Jirapanjawat, T., et al. (2019). Two *Chloroflexi* classes independently evolved the ability to persist on atmospheric hydrogen and carbon monoxide. *ISME J.* 13, 1801–1813. doi: 10.1038/s41396-019-0393-0

Islam, Z. F., Welsh, C., Bayly, K., Grinter, R., Southam, G., Gagen, E. J., et al. (2020). A widely distributed hydrogenase oxidises atmospheric H_2 during bacterial growth. *ISME J.* doi: 10.1038/s41396-020-0713-4 [Epub ahead of print]

Jansson, J. K., and Taş, N. (2014). The microbial ecology of permafrost. *Nat. Rev. Microbiol.* 12, 414–425. doi: 10.1038/nrmicro3262

Ji, M., Greening, C., Vanwonterghem, I., Carere, C. R., Bay, S. K., Steen, J. A., et al. (2017). Atmospheric trace gases support primary production in Antarctic desert surface soil. *Nature* 552, 400–403. doi: 10.1038/nature25014

Ji, M., Kong, W., Stegen, J., Yue, L., Wang, F., Dong, X., et al. (2020). Distinct assembly mechanisms underlie similar biogeographical patterns of rare and abundant bacteria in Tibetan plateau grassland soils. *Environ. Microbiol.* 22, 2261–2272. doi: 10.1111/1462-2920.14993

Ji, M., van Dorst, J., Bissett, A., Brown, M., Palmer, A., Snape, I., et al. (2015). Microbial diversity at Mitchell peninsula, eastern Antarctica: a potential biodiversity "hotspot". *Polar Biol.* 39, 237–249. doi: 10.1007/s00300-015-1776-y

Jones, C. M., and Hallin, S. (2019). Geospatial variation in co-occurrence networks of nitrifying microbial guilds. *Mol. Ecol.* 28, 293–306. doi: 10.1111/mec.14893

Kampstra, P. (2008). Beanplot: a boxplot alternative for visual comparison of distributions. *J. Stat. Softw.* 28, 1–9. doi: 10.18637/jss.v028.c01

Khdhiri, M., Hesse, L., Popa, M. E., Quiza, L., Lalonde, I., Meredith, L. K., et al. (2015). Soil carbon content and relative abundance of high affinity H2-oxidizing bacteria predict atmospheric H2 soil uptake activity better than soil microbial community composition. *Soil Biol. Biochem.* 85, 1–9. doi: 10.1016/j.soilbio.2015.02.030

King, G. M. (2003). Contributions of atmospheric CO and hydrogen uptake to microbial dynamics on recent Hawaiian volcanic deposits. *Appl. Environ. Microbiol.* 69, 4067–4075. doi: 10.1128/AEM.69.7.4067-4075.2003

Kleinteich, J., Hildebrand, F., Bahram, M., Voigt, A. Y., Wood, S. A., Jungblut, A. D., et al. (2017). Pole-to-pole connections: similarities between Arctic and Antarctic microbiomes and their vulnerability to environmental change. *Front. Ecol. Evol.* 5:137, doi: 10.3389/fevo.2017.00137

Lennon, J. T., and Jones, S. E. (2011). Microbial seed banks: the ecological and evolutionary implications of dormancy. *Nat. Rev. Microbiol.* 9, 119–130. doi: 10.1038/nrmicro2504

Lynch, R. C., Darcy, J. L., Kane, N. C., Nemergut, D. R., and Schmidt, S. K. (2014). Metagenomic evidence for metabolism of trace atmospheric gases by high-elevation desert *Actinobacteria*. *Front. Microbiol.* 5:698. doi: 10.3389/fmicb.2014.00698

Lynch, R. C., King, A. J., Farías, M. E., Sowell, P., Vitry, C., and Schmidt, S. K. (2012). The potential for microbial life in the highest-elevation (>6000 m.a.s.l.) mineral soils of the Atacama region. *J. Geophys. Res. Biogeosci.* 117, 1–10. doi: 10.1029/2012JG001961

Maeda, H., Fujimoto, C., Haruki, Y., Maeda, T., Kokeguchi, S., Petelin, M., et al. (2003). Quantitative real-time PCR using TaqMan and SYBR green for *Actinobacillus actinomycetemcomitans*, *Porphyromonas gingivalis*, *Prevotella intermedia*, tetQgene and total bacteria. *FEMS Immunol. Med. Microbiol.* 39, 81–86. doi: 10.1016/s0928-8244(03)00224-4

Mares, M. A., and History, O. M. N. (1999). *Encyclopedia of deserts*. Norman, Oklahoma: University of Oklahoma Press.

Margesin, R., and Miteva, V. (2011). Diversity and ecology of psychrophilic microorganisms. *Res. Microbiol.* 162, 346–361. doi: 10.1016/j.resmic.2010.12.004

McKay, C. P. (2016). Water sources for *Cyanobacteria* below desert rocks in the Negev desert determined by conductivity. *Glob. Ecol. Conserv.* 6, 145–151. doi: 10.1016/j.gecco.2016.02.010

Meredith, L. K., Rao, D., Bosak, T., Klepac-Ceraj, V., Tada, K. R., Hansel, C. M., et al. (2014). Consumption of atmospheric hydrogen during the life cycle of soil-dwelling *Actinobacteria*. *Environ. Microbiol. Rep.* 6, 226–238. doi: 10.1111/1758-2229.12116

Morita, R. Y. (1999). Is H(2) the universal energy source for long-term survival? *Microb. Ecol.* 38, 307–320. doi: 10.1007/s002489901002

Namsaraev, Z., Mano, M. J., Fernandez, R., and Wilmotte, A. (2010). Biogeography of terrestrial cyanobacteria from Antarctic ice-free areas. *Ann. Glaciol.* 51, 171–177. doi: 10.3189/172756411795931930

Oksanen, J., Blanchet, F. G., Friendly, M., Kindt, R., Legendre, P., McGlinn, D., et al. (2015). Vegan: Community ecology packageR package version 2.5–2. Available at: https://CRAN.R-project.org/package=vegan (Accessed November 16, 2018).

Park, S. W., Hwang, E. H., Jang, H. S., Lee, J. H., Kang, B. S., Oh, J. I., et al. (2009). Presence of duplicate genes encoding a phylogenetically new subgroup of form I ribulose 1,5-bisphosphate carboxylase/oxygenase in *Mycobacterium* sp. strain JC1 DSM 3803. *Res. Microbiol.* 160, 159–165. doi: 10.1016/j.resmic.2008.12.002

Pearce, D. A. (2012). "Extremophiles in Antarctica: life at low temperatures" in *Adaption of microbial life to environmental extremes*. eds. H. Stan-Lotter and S. Fendrihan (New York: Springer-Verlag/Wien).

Piche-Choquette, S., and Constant, P. (2019). Molecular hydrogen, a neglected key driver of soil biogeochemical processes. *Appl. Environ. Microbiol.* 85:e02418. doi: 10.1128/AEM.02418-18

Piché-Choquette, S., Tremblay, J., Tringe, S. G., and Constant, P. (2016). H2-saturation of high affinity H2-oxidizing bacteria alters the ecological niche of soil microorganisms unevenly among taxonomic groups. *PeerJ* 4:e1782. doi: 10.7717/peerj.1782

Pointing, S. B., Chan, Y., Lacap, D. C., Lau, M. C. Y., Jurgens, J. A., and Farrell, R. L. (2009). Highly specialized microbial diversity in hyper-arid polar desert. *Proc. Natl. Acad. Sci. U. S. A.* 106, 19964–19969. doi: 10.1073/pnas.0908274106

Pudasaini, S., Wilson, J., Ji, M., van Dorst, J., Snape, I., Palmer, A. S., et al. (2017). Microbial diversity of Browning peninsula, Eastern Antarctica revealed using molecular and cultivation methods. *Front. Microbiol.* 8:591. doi: 10.3389/fmicb.2017.00591

Quast, C., Pruesse, E., Yilmaz, P., Gerken, J., Schweer, T., Yarza, P., et al. (2013). The SILVA ribosomal RNA gene database project: improved data processing and web-based tools. *Nucleic Acids Res.* 41, D590–D596. doi: 10.1093/nar/gks1219

R Core Team (2018). R: A Language and environment for statistical computing. R Foundation for Statistical Computing, Vienna. Available at: https://www.R-project.org (Accessed November 16, 2018).

Rao, S., Chan, Y., Bugler-Lacap, D. C., Bhatnagar, A., Bhatnagar, M., and Pointing, S. B. (2016). Microbial diversity in soil, sand dune and rock substrates of the Thar Monsoon desert, India. *Indian J. Microbiol.* 56, 35–45. doi: 10.1007/s12088-015-0549-1

Rayment, R. E., and Lyons, D. J. (2011). *Soil chemical methods-Australasia*. Collingwood, VIC: CSIRO Publishing.

RStudio and Inc. (2013). Shiny: Web application framework for R. R package version 0.5.0.

Sato, Y., Nishihara, H., Yoshida, M., Watanabe, M., Rondal, J. D., and Ohta, H. (2004). Occurrence of hydrogen-oxidizing *Ralstonia* species as primary microorganisms in the Mt. Pinatubo volcanic mudflow deposits. *Soil Sci. Plant Nutr.* 50, 855–861. doi: 10.1080/00380768.2004.10408546

Schulze-Makuch, D., Wagner, D., Kounaves, S. P., Mangelsdorf, K., Devine, K. G., de Vera, J. -P., et al. (2018). Transitory microbial habitat in the hyperarid Atacama desert. *Proc. Natl. Acad. Sci. U. S. A.* 115, 2670–2675. doi: 10.1073/pnas.1714341115

Siciliano, S. D., Palmer, A. S., Winsley, T., Lamb, E., Bissett, A., Brown, M. V., et al. (2014). Soil fertility is associated with fungal and bacterial richness, whereas pH is associated with community composition in polar soil microbial communities. *Soil Biol. Biochem.* 78, 10–20. doi: 10.1016/j.soilbio.2014.07.005

Smith-Downey, N. V., Randerson, J. T., and Eiler, J. M. (2008). Molecular hydrogen uptake by soils in forest, desert, and marsh ecosystems in California. *J. Geophys. Res. Biogeosci.* 113, 1–11. doi: 10.1029/2008JG000701

Tebo, B., Davis, R., Anitori, R., Connell, L., Schiffman, P., and Staudigel, H. (2015). Microbial communities in dark oligotrophic volcanic ice cave ecosystems of Mt. Erebus, Antarctica. *Front. Microbiol.* 6:179. doi: 10.3389/fmicb.2015.00179

Tindall, B. J. (2004). Prokaryotic diversity in the Antarctic: the tip of the iceberg. *Microb. Ecol.* 47, 271–283. doi: 10.1007/s00248-003-1050-7

Torbjørn, R., Tomáš, F., Ben, N., Christopher, Q., and Frédéric, M. (2016). VSEARCH: a versatile open source tool for metagenomics. *PeerJ* 4:e2584. doi: 10.7717/peerj.2584

Torondel, B., Ensink, J. H. J., Gundogdu, O., Ijaz, U. Z., Parkhill, J., Abdelahi, F., et al. (2016). Assessment of the influence of intrinsic environmental and geographical factors on the bacterial ecology of pit latrines. *Microb. Biotechnol.* 9, 209–223. doi: 10.1111/1751-7915.12334

Tytgat, B., Verleyen, E., Obbels, D., Peeters, K., De Wever, A., D'hondt, S., et al. (2014). Bacterial diversity assessment in Antarctic terrestrial and aquatic microbial mats: a comparison between bidirectional pyrosequencing and cultivation. *PLoS One* 9:e97564. doi: 10.1371/journal.pone.0097564

van der Walt, A. J., Johnson, R. M., Cowan, D. A., Seely, M., and Ramond, J. -B. (2016). Unique microbial phylotypes in Namib desert dune and gravel plain fairy circle soils. *Appl. Environ. Microbiol.* 82, 4592–4601. doi: 10.1128/AEM.00844-16

van Dorst, J., Bissett, A., Palmer, A. S., Brown, M., Snape, I., Stark, J. S., et al. (2014b). Community fingerprinting in a sequencing world. *FEMS Microbiol. Ecol.* 89, 316–330. doi: 10.1111/1574-6941.12308

van Dorst, J., Siciliano, S., Winsley, T., Snape, I., and Ferrari, B. (2014a). Bacterial targets as potential indicators of diesel fuel toxicity in Subantarctic soils. *Appl. Environ. Microbiol.* 80, 4021–4033. doi: 10.1128/aem.03939-13

Van Goethem, M. W., Makhalanyane, T. P., Valverde, A., Cary, S. C., and Cowan, D. A. (2016). Characterization of bacterial communities in lithobionts and soil niches from Victoria valley. *FEMS Microbiol. Ecol.* 92:fiw051. doi: 10.1093/femsec/fiw051

Villalva, C., Touriol, C., Seurat, P., Trempat, P., Delsol, G., and Brousset, P. (2001). Increased yield of PCR products by addition of T4 gene 32 protein to the SMART PCR cDNA synthesis system. *Biotechniques* 31, 81–86. doi: 10.2144/01311st04

Walker, J. J., and Pace, N. R. (2007). Endolithic microbial ecosystems. *Annu. Rev. Microbiol.* 61, 331–347. doi: 10.1146/annurev.micro.61.080706.093302

Warren-Rhodes, K. A., Rhodes, K. L., Pointing, S. B., Ewing, S. A., Lacap, D. C., Gómez-Silva, B., et al. (2006). Hypolithic cyanobacteria, dry limit of photosynthesis, and microbial ecology in the Hyperarid Atacama desert. *Microb. Ecol.* 52, 389–398. doi: 10.1007/s00248-006-9055-7

Wei, T., Simko, V., Levy, M., Xie, Y., Jin, Y., and Zemla, J. (2017). Package 'corrplot'. Statistician 56:e24.

Wickham, H. (2016). *ggplot2: Elegant graphics for data analysis*. Springer International Publishing.

Wierzchos, J., de Los Rios, A., and Ascaso, C. (2012). Microorganisms in desert rocks: the edge of life on earth. *Int. Microbiol.* 15, 172–182. doi: 10.2436/20.1501.01.170

Wynn-Williams, D. D. (1990). "Ecological aspects of Antarctic microbiology" in *Advances in microbial ecology*. ed. K. C. Marshall (Boston, MA: Springer US), 71–146.

Ye, J., Coulouris, G., Zaretskaya, I., Cutcutache, I., Rozen, S., and Madden, T. (2012). Primer-BLAST: a tool to design target-specific primers for polymerase chain reaction. *BMC Bioinformatics* 13:134. doi: 10.1186/1471-2105-13-134

Yergeau, E., Bokhorst, S., Huiskes, A., Boschker, H., Aerts, R., and Kowalchuk, G. (2006). Size and structure of bacterial, fungal and nematode communities along an Antarctic environmental gradient. *FEMS Microbiol. Ecol.* 59, 436–451. doi: 10.1111/j.1574-6941.2006.00200.x

Zhang, E., Thibaut, L. M., Terauds, A., Wong, S., van Dorst, J., Tanaka, M. M., et al. (2020). Lifting the veil on arid-to-hyperarid Antarctic soil microbiomes: a tale of two oases. *Microbiome* 8:37. doi: 10.1186/s40168-020-00809-w

Conflict of Interest: The authors declare that the research was conducted in the absence of any commercial or financial relationships that could be construed as a potential conflict of interest.

frontiers in Microbiology

ORIGINAL RESEARCH
published: 02 October 2020
doi: 10.3389/fmicb.2020.555351

Phylogenetic and Physiological Diversity of Cultivable Actinomycetes Isolated From Alpine Habitats on the Qinghai-Tibetan Plateau

*Aiai Ma[1,2], Xinfang Zhang[1], Kan Jiang[3], Changming Zhao[1], Junlin Liu[2], Mengdan Wu[3], Ying Wang[1], Mingming Wang[2], Jinhui Li[1] and Shijian Xu[1]**

[1] School of Life Sciences, Lanzhou University, Lanzhou, China, [2] Life Science and Engineering College of Northwest University for Nationalities, Lanzhou, China, [3] College of Agronomy, Gansu Agricultural University, Lanzhou, China

Actinomycetes in extreme alpine habitat have attracted much attention due to their unique physiological activities and functions. However, little is known about their ecological distribution and diversity. Here, we explored the phylogenetic relationship and physiological heterogeneity of cultivable actinomycetes from near-root soils of different plant communities in the Laohu Ditch (2200 – 4200 m) and Gaize County area (5018 – 5130 m) on the Qinghai-Tibetan Plateau. A total of 128 actinomycete isolates were obtained, 16S rDNA-sequenced and examined for antimicrobial activities and organic acid, H_2S, diffusible pigments, various extracellular enzymes production. Seventy three isolates of the total seventy eight isolates from the Laohu Ditch, frequently isolated from 2200 to 4200 m, were closely related to *Streptomyces* spp. according to the 16S rDNA sequencing, while four isolates within the genus *Nocardia* spp. were found at 2200, 2800, and 3800 m. In addition, one potential novel isolate with 92% sequence similarity to its nearest match *Micromonospora saelicesensis* from the GenBank database, was obtained at 2200 m. From the Gaize County area, fifty *Streptomyces* isolates varied in diversity at different sites from 5018 to 5130 m. The investigation of phenotypic properties of 128 isolates showed that 94.5, 78.9, 68, 64.8, 53, 51.6, 50, 36.7, 31.2, and 22.7% of the total isolates produced catalase, lipase 2, urease, protease, H_2S, lipase 3, amylase, lipase 1, diffusible pigment and organic acid, respectively. The antimicrobial assays of the total isolates revealed that 5, 28, 19, and 2 isolates from *Streptomyces* spp. exhibited antimicrobial activity against *Escherichia coli*, *Staphylococcus aureus*, *Candida albicans*, and *Pseudomonas aeruginosa*, respectively. This study intends to bring helpful insights in the exploitation and utilization of alpine actinomycetes for novel bioactive compounds discovery.

Keywords: actinomycetes, phylogenetic diversity, physiological activities, alpine habitat, Qinghai-Tibetan Plateau

OPEN ACCESS

Edited by:
Laura Zucconi,
University of Tuscia, Italy

Reviewed by:
Reed M. Stubbendieck,
University of Wisconsin-Madison, United States
Gina Lewin,
Georgia Institute of Technology, United States

***Correspondence:**
Shijian Xu
xushijian@lzu.edu.cn

Specialty section:
This article was submitted to Extreme Microbiology, a section of the journal Frontiers in Microbiology

Received: *24 April 2020*
Accepted: *20 August 2020*
Published: *02 October 2020*

Citation:
Ma A, Zhang X, Jiang K, Zhao C, Liu J, Wu M, Wang Y, Wang M, Li J and Xu S (2020) Phylogenetic and Physiological Diversity of Cultivable Actinomycetes Isolated From Alpine Habitats on the Qinghai-Tibetan Plateau. Front. Microbiol. 11:555351. doi: 10.3389/fmicb.2020.555351

INTRODUCTION

Actinomyces had served as the sources of novel antibiotic and bioactive molecule candidates with application in many fields (Ramesh and Mathivanan, 2009; Genilloud et al., 2011). Today, the exploitation of actinomycetes with bioactive metabolites from unexplored or extreme ecosystems may be an efficient way to satisfy the everlasting demand for novel natural products, which have

antimicrobial and therapeutic properties to combat human and plant pathogens (Intra et al., 2011; Ouyang et al., 2011). During the last decades, the research of actinomycetes in several alpine habitats has gained some remarkable results. For example, the study in the high Arctic permafrost of Spitsbergen has shown that there is a high diversity of actinobacterial communities in this alpine soil and many of the phylotypes identified may represent novel, uncultured species, which might be the sources of genetic diversity and ultimately novel bioactive compounds (Hansen et al., 2007). Ivanova et al. (2009) presented that a large amount of trehalose and glycerol as cryopreservation additives produced by *Streptomyces* spp. from the permafrost in Spitsbergen could be a reason for the strains to survive in cold and dry conditions. Further studies revealed that production of a range of bioactive metabolites including antibiotics, trehalose, lipase and pigment by actinobacteria from alpine cold habitats, could be a strategy for the strains in response to harsh environmental conditions (Fong et al., 2001; Dillon et al., 2003; Zhang et al., 2008; Babalola et al., 2009; Ivanova et al., 2009; Sivalingam et al., 2019). Malviya et al. (2009) documented that some *Streptomyces* isolates from alpine zones of Pindari glacier region in Indian Himalaya exhibited strong antifungal properties. These findings provide evidence that a wide diversity of Actinobacteria can survive in alpine environments, and most of which could yield bioactive compounds. In addition, as pivotal participants in the biogeochemical cycles, actinobacteria were known to possess diverse physiology and metabolic flexibility to survive in unfavorable environments (Shivlata and Satyanarayana, 2015). Thus exploring the phylogenetic and physiological diversity patterns of alpine actinomycetes may provide an opportunity for selecting strains that are under environmental pressures, which may drive adaptions that produce unique biosynthetic or hydrolytic capabilities.

The Qinghai-Tibetan Plateau, as the largest and highest plateau on Earth, possesses unique climate characteristics: alpine hypoxia, less precipitation, low humidity, osmotic stress and high incident radiation, which involves the plants and soil on the plateau in extreme harsh environmental conditions such as low temperature, anoxygenous, prolonged UV radiation and oligotrophic (Zhang et al., 2007a). Accordingly, the actinomycetes living in it may represent novel species and develop unique physiological adaption mechanism, ultimately yield bioactive compounds. However, the cultivable soil actinomycetes in this unique habitat remain relatively unexplored except for the preliminary survey on the *Potentilla fruticosa* L. alpine meadow and reports of novel actinomycetes (Wang et al., 2004; Chen et al., 2011; Zhang et al., 2016a, 2019). Thus, we had isolated and characterized actinomycetes from near-root soils of different plant communities, which distributed in two geographically diverse alpine habitats along an altitudinal gradient (2200 – 4200 m at the Laohu Ditch site; 5018 – 5130 m at the Gaize County area) on the Qinghai-Tibetan Plateau, aiming to explore the phylogenetic and physiological diversity of the cultivable actinomycetes.

MATERIALS AND METHODS

Site Description and Sample Collection

The Laohu Ditch, located in the northeast of the Qinghai-Tibetan Plateau, is characterized by distinct vertical distribution of plant communities, from desert and desertification grassland (2200 m), mountain grassland (2800 m), alpine bushwood (3350 m), alpine meadow (3800 m), to alpine cold-desert (4200 m). The mean annual precipitation (MAP) ranged from 73.3 mm (2200 m) to 279.4 mm (4200 m), and the mean annual temperature (MAT) was from 8.1°C (2200 m) to – 5.3°C (4200 m) (offered by Qilian Mountains Station, State Key Laboratory of Cryospheric Sciences). The area of Gaize County underlain by permafrost in the central Tibetan Plateau, is distinguished by its high elevation (>5000 m) and unique plant communities adapting to this low temperature, anoxia and strong UV habitats. The MAT in the area of Gaize sampling sites was approximately 0°C with monthly mean temperature - 12.1°C in January and 12.8°C in July, and the MAP was approximately 150 mm year^{-1} (Qiao et al., 2015). The detailed information was depicted in **Table 1**.

Near-root soils were sampled from fifteen dominant plants distributing along the altitude gradients in the Laohu Ditch and five distinct dominant plants in the Gaize County area in July. The samples were aseptically processed according to the previous described (Xu et al., 1996; Zhang et al., 2007a,b; Mingma et al., 2014). Briefly, five soil cores, which were 4.5 cm in diameter and 10 cm deep, were collected radially up to ∼10 cm from the base of the plant with ∼20 cm distances, mixed to form one composite soil sample. All the samples were immediately placed in sterilized ice coolers and transported to the laboratory within 24 h.

Isolation of Actinomycetes

Actinomycetes were isolated by spreading dilutions of soil samples on petri dishes using Gao's No. 1 medium (20 g of soluble starch, 1 g of KNO_3, 0.5 g of K_2HPO_4, 0.5 g of $MgSO_4{\cdot}7H_2O$, 0.5 g of NaCl, 0.01 g of $FeSO_4{\cdot}7H_2O$, 20 g of agar, pH 7.2 – 7.4). The media also contained 25 μg/mL potassium dichromate to minimize bacterial and fungal contamination (Xu et al., 1996). All the plates were incubated at 20°C ± 1 for 30 days.

The growth and appearance of actinomycetes were observed every day on the medium plates and the colonies were recognized by their characteristics such as leathery or powdery appearance with concave, convex, crumpled or flate surface etc. Representative isolates of 128 that formed colonies with visually different morphologies were selected from 200 initially recovered colonies and subcultured to obtain pure colonies for further studies.

DNA Extraction, 16S rDNA Amplification, and Sequencing

Total DNA were extracted from subcultures as described by Orsini and Romano-Spica (2001) with minor adjustment. Briefly, fresh biomass (around 50 mg) was suspended in 1 mL washing solution [50 mM Tris–HCl, pH 7.7, 25 mM EDTA, 0.1% sodium dodecyl sulfate (SDS), 0.1% polyvinylpyrrolidone (PVP)]. After centrifuging at 12,000 × *g* for 2 min, the biomass was

TABLE 1 | Detailed description of the sampling sites on the Qinghai-Tibetan Plateau.

Laohu Ditch				Gaize County			
Site/GPS	**Altitude (m)**	**Dominant plant species**	**Vegetation type and cover**	**Site/GPS**	**Altitude (m)**	**Dominant plant species**	**Vegetation type and cover**
96°11.39′; 39°44.71′	2200	*Salsola collina* Pall *Cl* *Stipa glareosa* PA Smirn	DDG, 8%	85°37.694′; 33°23.506′	5130	*Dh*	Desert steppe, 10%
96°24.98′; 39°37.95′	2800	*Al* *Potentilla saudersiana* Royle	Mountain grassland, 15%	85°37.712′; 33°23.251′	5056	*Carex moocroftii* Falc. ex Boott	Alpine meadow, 80%
96°26.10′; 39°35.40′	3350	*Saussurea japonica* Kuntze *Potentilla fruticosa* L. *Ll* *Rq*	Alpine bushwood, 36%	85°37.579′; 33°23.156′	5100	*Kobresia pygmaea* C.B. Clarke	Alpine meadow, 80%
96°30.28′; 39°32.05′	3800	*Au* *Arenaria kansuensis* Maxim *Draba nemorosa* L. *Poa annua* L.	Alpine meadow, 41%	85°37.772′; 33°23.264′	5018	*Stipa capillata* L.	Alpine steppe, 50%
96°31.18′; 39°29.96′	4200	*Al* *Cd*	Alpine cold-desert, 5%	85°07.650′; 33°48.080′	5020	*Stipa purpurea* Griseb.	Alpine steppe, 40%

DDG, desert and desertification grassland; Cl, Ceratoides latens reveal & N. H. Holmgren; Al, Astragalus licentianus Hand.-Mazz.; Ll, Leontopodium leontopodoides beauverd; Rq, Rhodiola quadrifida Fisch. & C.A. Mey; Au, Androsace umbellata (Lour.) Merr.; Cd, Cancrinia discoidea Poljakov ex Tzvelev; Dh, Dracocephalum heterophyllum Benth.

resuspended in 100 μl lysis solution (50 mM Tris–HCl, pH 8.0, 25 mM EDTA, 3% SDS, 1.2% PVP) and heated in a microwave oven at 700 W for 45 s, then added 400 μl preheated (65°C) extraction solution (10 mM Tris–HCl, pH 8.0, 1 mM EDTA, 0.3 M sodium acetate, 1.2% PVP). The DNA pellet was phenol−chloroform extracted, precipitated in isopropyl alcohol, washed with 70% ethanol, air-dried at room temperature then resuspended in deionized distilled water for use. The universal bacterial primers 27F (5′-AGAGTTTGATCCTGGCTCAG-3′) and 1504R (5′-TTAAGGATGGTGATGCCGCA-3′) were used for amplification of 16S rDNA sequences, and the PCR amplication was performed as follows: 5 min at 95°C, followed by 30 cycles of 1 min at 95°C, 1 min at 56°C for annealing and 2 min at 72°C for extension, and a final extension for 8 min at 72°C. The PCR products were confirmed by electrophoresis in a 1% (w/v) agarose gel, stained with ethidium bromide in TAE buffer, then sent to purify and cycle sequencing using an ABI3100 automated sequencer at Beijing Sangon Biotech (Beijing, China).

Nucleotide Sequence Accession Numbers

The 16S rDNA sequences of 128 isolates reported in this study have been submitted to the GenBank nucleotide sequence databases under accession nos. JQ812058-JQ812111 and JQ838073-JQ838150 available at https://www.ncbi.nlm.nih.gov/nucleotide.

Phylogenetic Analysis

For further phylogenetic analysis, the sequenced 16S rDNA of the 128 isolates were matched with those in a public database using the EzBioCloud tool, and the nearest representative gene sequences of related type strains were downloaded then aligned with the isolated sequences using Clustal W program. Phylogenetic trees of the isolates were constructed by using the Maximum Likelihood method and Tamura-Nei model (Tamura and Nei, 1993) with bootstrap analysis of 1,000 replicates (Felsenstein, 1985) performed in the MEGA X package, and then the trees were edited by Evolview[1].

Screening of Soil Actinomycetes for Organic Acid, H_2S and Extracellular Enzymes Production

All the 128 soil actinomycetes were examined qualitatively for the production of organic acid, H_2S and extracellular enzymes including lipase 1, lipase 2, and lipase 3, amylase, protease, urease, catalase. Each isolate was inoculated on the center of the respective substrates such as tween 20 (lipase 1), tween 40 (lipase 2), tween 80 (lipase 3), starch (amylase), gelatin (protease) amended agar plates separately and incubated for 7–14 days at room temperature, the plates directly detected by clearing zones around the colonies were regarded as positive for enzyme activity (Sanchez-Porro et al., 2003; Ramesh and Mathivanan, 2009). The assays of urease, catalase, organic acid and H_2S production were performed as described by Shirling and Gottlieb (1966). In addition, the diffusible pigments were also documented. Each test was conducted in triplicate, and plates or tubes with the same medium but without actinomycete isolates were maintained for controls.

Screening of Soil Actinomycetes for Antimicrobial Activity

All the 128 soil actinomycete isolates were screened for antimicrobial activity by agar overlay method as described by Anand et al. (2006) with minor adjustment. Spore suspensions of actinomycetes were inoculated on Gao's No. 1 medium and cultured at 20°C ± 1 for 7 days, then overlaid with 5 ml of soft nutrient agar (0.6% agar) containing 500 μL of overnight growing culture of the tested microorganisms, including *Escherichia coli* ATCC25922 representing Gram-negative bacteria, *Staphylococcus aureus* ATCC25923 representing Gram-positive bacteria, *Candida albicans* ATCC66415 representing yeast-like fungi and a clinical isolated *Pseudomonas aeruginosa* strain representing freshly pathogenic multi-resistant bacterial strain. The overlaid plates were then incubated at 28°C for 24 h and the clear inhibition zone around each isolate was recorded as positive for antimicrobial activity (Ramesh and Mathivanan, 2009). Plates with the same medium simultaneously inoculated with the tested human pathogens but without actinomycete isolates were maintained for controls.

RESULTS

16S rDNA-Based Phylogenetic Diversity of the Cultivable Actinomycetes

Seventy eight actinomycetes with representative phenotypes were recovered from the Laohu Ditch, and the 16S rDNA sequencing revealed that the predominant genus was *Streptomyces* (73 isolates), followed by *Nocardia* (4 isolates), and one isolate with only 92% sequence similarity to its nearest match *Micromonospora saelicesensis* from the GenBank database, indicating that it may be a potential novel isolate at genus level. The phylogenetic tree demonstrating the relationship between the genera *Streptomyces* spp. (randomly selected representative sequences of *Streptomyces* spp.), *Nocardia* spp., and *Micromonospora* spp. was presented on **Figure 1**.

As the dominant isolates, a phylogenetic tree displaying the relationships between 73 *Streptomyces* isolates in this study, and between them and their nearest relatives from GenBank, was also constructed as shown in **Figure 2**. This allowed the sorting of the sequences into two disparate groups, designed as Groups I and II. In Group I, the single isolate QLS81 from near-root soil of *Potentilla saudersiana* Royle at 2800 m, a putatively new species of *Streptomyces* spp. to be furtherly confirmed by DNA-DNA pairing value, formed a distinct branch with the highest 16S rDNA sequence similarity of 99% to the type strain of *Streptomyces specialis*. Strikingly, it can produce substantial diffusible black pigment which biological significances needed to be furtherly explored (**Supplementary Figure S1**). In Group II, 52 out of the 72 *Streptomyces* isolates formed relatively

[1]http://www.evolgenius.info/evolview

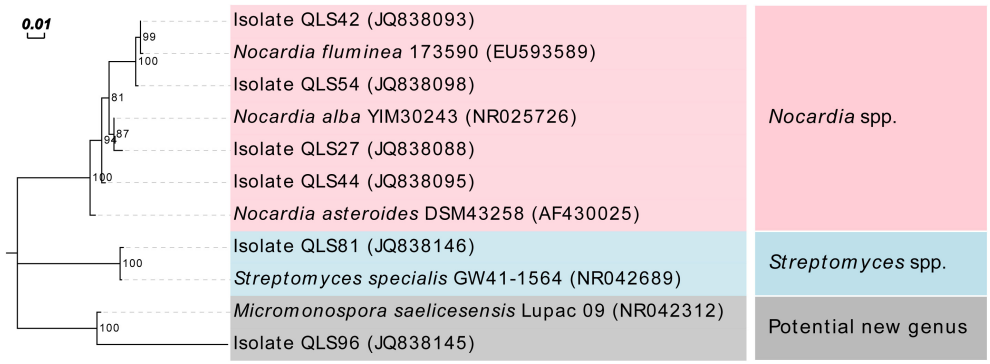

FIGURE 1 | Maximum Likelihood tree based on nearly complete 16S rDNA sequences showing relationship between the isolates from the Laohu Ditch and the genera *Streptomyces* spp., *Nocardia* spp., and *Micromonospora* spp.

distinct phyletic lines with their 16S rDNA sequences showing 99 to 100% similarities to their type strains obtained from the GenBank database. Interestingly, 42 isolates amongst the 52 isolates were sorted into ten clusters, with most of the isolates originating from the same plant assigned to the same cluster. Cluster 1 consisted of 10 isolates showing 99–100% similarity to the sequence of *Streptomyces cavourensis*. One isolate was obtained from *Ceratoides latens* Reveal & N.H. Holmgren at 2200 m, four (QLS40, QLS67, QLS84, and QLS87) from *Astragalus licentianus* Hand.-Mazz. at 2800 m, the other two (QLS02 and QLS09) from *A. licentianus* Hand.-Mazz. at 4200 m, one (QLS85) from *Androsace umbellata* (Lour.) Merr. at 3800 m, and two (QLS18 and QLS22) from *Leontopodium leontopodoides* Beauverd and *Potentilla fruticosa* L. at 3350 m, respectively. Four isolates in Cluster 2 showing 99–100% identity to *Streptomyces anulatus*, were found in *Salsola collina* Pall at 2200 m (QLS04), *A. licentianus* Hand.-Mazz. at 2800 m (QLS31), *P. fruticosa* L. at 3350 m (QLS13) and *A. licentianus* Hand.-Mazz. at 4200 m (QLS29). Cluster 3 consisting of 5 isolates displaying 99–100% identity to *Streptomyces microflavus* could be divided into two sub-clusters. Two isolates, QLS03 and QLS08 from *A. licentianus* Hand.-Mazz. at 4200 m, with brown pigmented aerial mycelium and brown diffusible pigment, respectively, formed a distinct sub-clade; While isolates QLS16 from *Arenaria kansuensis* Maxim at 3800 m, QLS17 from *Saussurea japonica* Kuntze at 3350 m, QLS19 from *Poa annua* L. at 3800 m producing pale yellow, deep yellow and labile yellow diffusible pigments, respectively, formed another sub-clade. Cluster 4 contained 3 isolates from *Saussurea japonica* Kuntze at 3350 m showing 99–100% similarity to *Streptomyces cyaneofuscatus*. And 3 isolates in Cluster 5 showing 99% identity to *Streptomyces aureus* were isolated from *Rhodiola quadrifida* Fisch. & C.A. Mey at 3350 m. Cluster 6 containing three isolates showing 99–100% similarity to *Streptomyces chryseus* were obtained from *R. quadrifida* Fisch. & C.A. Mey at 3350 m. Two isolates in Cluster 7, QLS62, and QLS68 from *A. licentianus* Hand.-Mazz. at 4200, 2800 m, respectively, demonstrated 99% similarity to *Streptomyces enissocaesilis*. Cluster 8 consisted of 4 isolates (QLS10, QLS82, QLS74, and QLS24), obtained from *Ceratoides latens* Reveal & N.H. Holmgren at 2200 m, *A. licentianus* Hand.-Mazz. at 2800 m, *R. quadrifida* Fisch. & C.A. Mey at 3350 m and *A. licentianus* Hand.-Mazz. at 4200 m, respectively, showing 99–100% identity to *Streptomyces agglomeratus*. And Cluster 9 consisted of 5 isolates showing 99–100% identity to *Streptomyces durmitorensis*, isolated from *P. saudersiana* Royle (QLS33) and *A. licentianus* Hand.-Mazz. (QLS45, QLS50, QLS76, and QLS77) at 2800 m. Cluster 10 contained three isolates from *Ceratoides latens* Reveal & N.H. Holmgren (QLS11, QLS80) and *Stipa glareosa* PA Smirn (QLS37) at 2200 m.

From the Gaize County area, fifty isolates with typical colony morphologies were obtained and they all pertained to *Streptomyces* spp. according to the 16S rDNA sequencing. The phylogenetic tree exhibiting the relationships between the fifty isolates, and between them and their closest relatives, was presented in **Figure 3**. As shown in **Figure 3**, isolate QZGYFj1 from *Stipa capillata* L. at 5018 m, solely formed a distinct phyletic branch, although it demonstrated 98% sequence similarity to its nearest match *Streptomyces rimosus*, indicating that it may be a potential new isolate. Isolate QZGYEb4 from *Stipa purpurea* Griseb. at 5020 m, showing 99% identity to *Streptomyces rectiviolaceus*, formed relatively phylogenetically distinct clade. While isolate QZGYEd3 solely formed relatively distinct phyletic line. The 47 remaining isolates were assigned to seven clusters. Cluster I contained 16 isolates distributing in *S. capillata* L. at 5018 m, *Carex moocroftii* Falc. ex Boott at 5056 m, *Kobresia pygmaea* C.B. Clarke at 5100 m and *Dracocephalum heterophyllum* Benth at 5130 m, exhibiting 99–100% similarity to *Streptomyces griseus*. Cluster II containing four isolates at 5056 m demonstrated 99–100% identity to *S. cyaneofuscatus*. Cluster III consisted of 5 isolates distributing at 5020, 5018, 5100, and 5130 m, showing 99–100% identity to *Streptomyces bottropensis*. Cluster IV consisted of three isolates QZGYEb5, QZGYEb2 and QZGYEc1, with isolates QZGYEc1 at 5130 m and QZGYEb2 at 5018 m forming a subclade. And three isolates in Cluster V displayed 99% similarity to *Streptomyces subrutilus*, with QZGYFe2 and QZGYEf1 at 5056 m and QZGYFc8 at 5130 m. Cluster VI contained eight isolates, with four isolates, QZGYFd1 and QZGYFc5 at 5130 m, QZGYFa1 and QZGYFb3 at 5020 m forming a sub-cluster, while another four isolates clustering together showing 99–100% similarity to *Streptomyces*

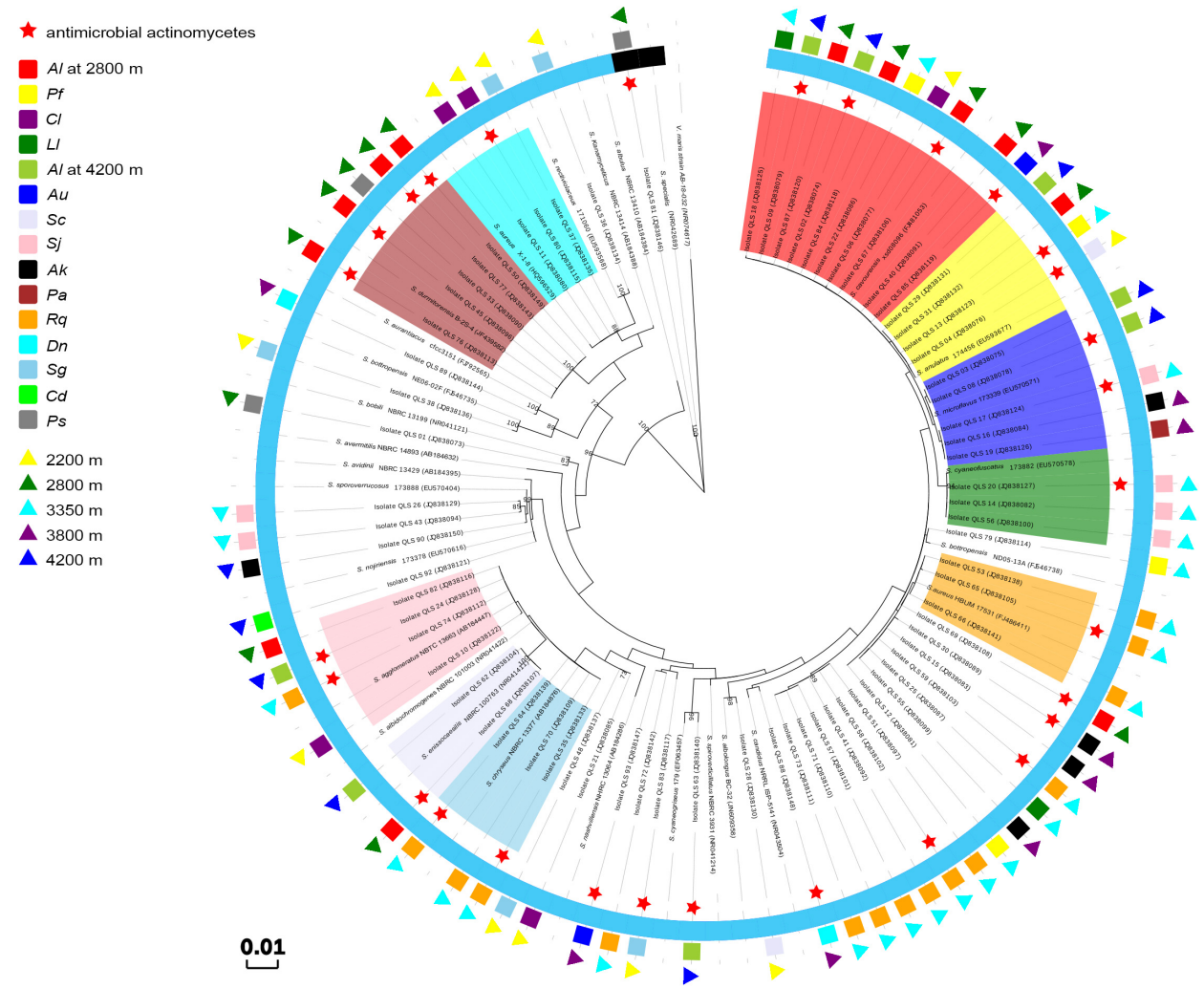

FIGURE 2 | Phylogenetic tree of the *Streptomyces* isolates from the Laohu Ditch and their nearest relatives based on 16S rDNA sequences. The inner ring indicates the relationship of the *Streptomyces* spp., Cluster 1 in shade of red, Cluster 2 in shade of yellow, Cluster 3 in shade of blue, Cluster 4 in shade of green, Cluster 5 in shade of orange, Cluster 6 in shade of lavender, Cluster 7 in shade of skyblue, Cluster 8 in shade of pink, Cluster 9 in shade of brown, Cluster 10 in shade of cyan; the black semi-ring and the light blue semi-ring represent Group I and GroupII, respectively; the middle ring indicates the distribution of the 73 isolates in near-root soils of 15 plant communities. *Al*, *Astragalus licentianus* Hand.-Mazz.; *Ll*, *Leontopodium leontopodoides* Beauverd; *Pf*, *Potentilla fruticosa* L.; *Cl*, *Ceratoides latens* Reveal & N.H. Holmgren; *Au*, *Androsace umbellata* (Lour.) Merr.; *Sc*, *Salsola collina* Pall; *Sj*, *Saussurea japonica* Kuntze; *Ak*, *Arenaria kansuensis* Maxim; *Pa*, *Poa annua* L.; *Rq*, *Rhodiola quadrifida* Fisch. & C.A. Mey; *Dn*, *Draba nemorosa* L.; *Sg*, *Stipa glareosa* PA Smirn; *Cd*, *Cancrinia discoidea* Poljakov ex Tzvelev; *Ps*, *P. saudersiana* Royle; the outer ring indicates the distribution of the 73 isolates in diverse altitudes.

phaeochromogenes. And eight isolates in Cluster VII distributed at 5020, 5056, and 5130 m, with 3 isolates forming a sub-cluster and the other 5 clustering together demonstrating 99–100% identity to *S. chryseus*.

As shown in **Figures 2–4**, isolates with 99–100% 16S rDNA sequence similarity to *S. cavourensis* widely distributed in different plant communities across five altitudes on the Laohu Ditch. While isolates with 99–100% 16S rDNA sequence identity to *S. griseus* predominated among the isolates on the Gaize County area, constituting 32% of the total isolates. In addition, isolates with 99–100% 16S rDNA sequence identities to *S. rectiviolaceus*, *S. chryseus*, *S. cyaneofuscatus* and *S. bottropensis* occurred both in the Laohu Ditch and Gaize County area. However, variances of *Streptomyces* isolates in the Laohu Ditch and Gaize County area were observed. For example, isolates with 99–100% 16S rDNA sequence identities to *S. specialis*, *Streptomyces goshikiensis*, *Streptomyces aurantiacus*, *Streptomyces nojiriensis*, *Streptomyces purpureus* only occurred at 2800, 3350, 3800, 4200, and 5130 m, respectively.

Phenotypic Characteristics of the Cultivable Actinomycetes

The phenotypic properties of the isolates were shown in **Figures 5**, **6**. From the Laohu Ditch, more than half of the 78 isolates produced catalase, lipase 2, urease, gelatinase, lipase

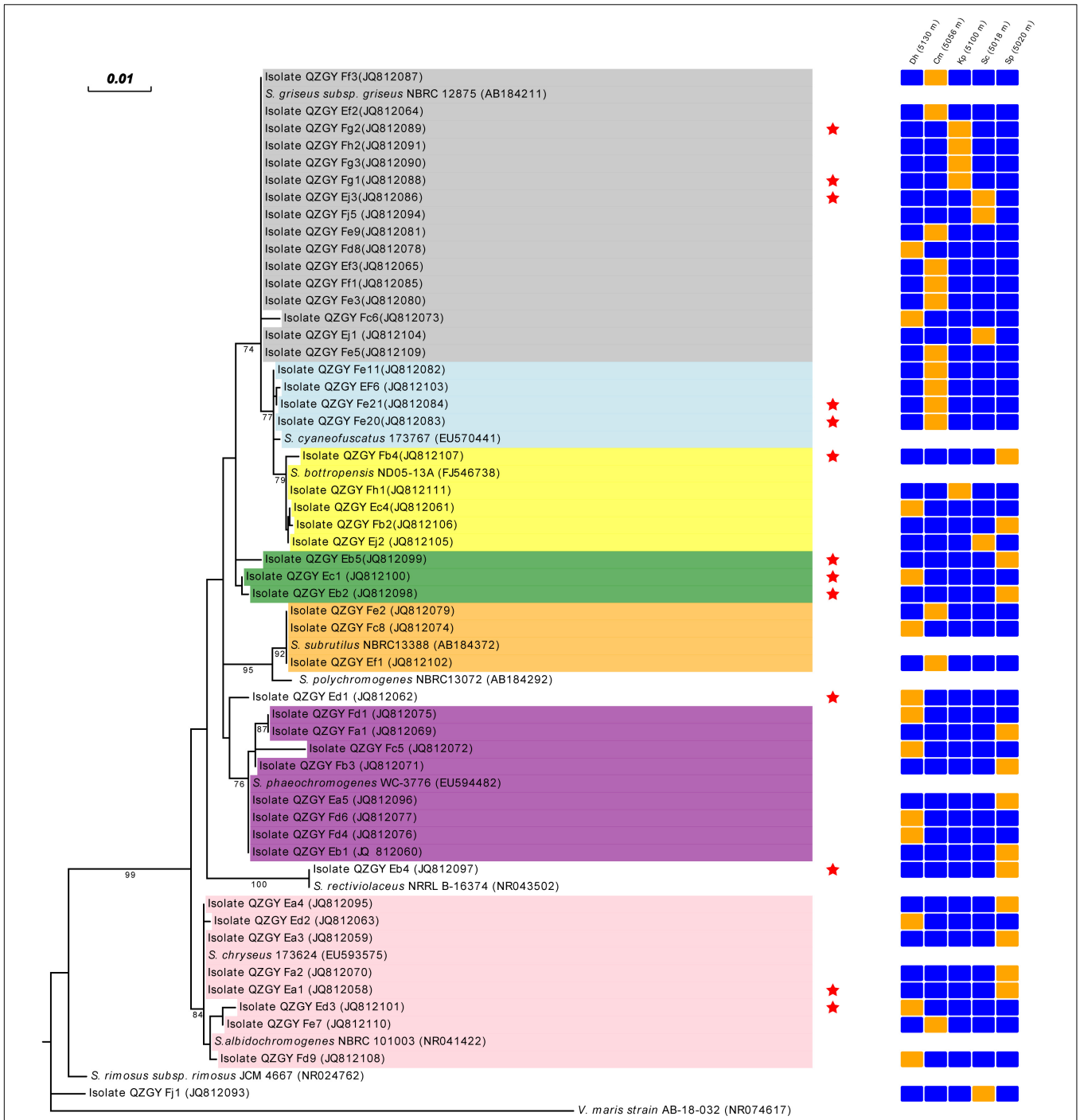

FIGURE 3 | Phylogenetic tree displaying relationships of the *Streptomyces* isolates from the Gaize County area and their nearest relatives based on the 16S rDNA sequences (⋆ indicates antimicrobial actinomycetes). *Dh*, *Dracocephalum heterophyllum* Benth; *Cm*, *Carex moocroftii* Falc. ex Boott; *Kp*, *Kobresia pygmaea* C.B. Clarke; *Sp*, *Stipa purpurea* Griseb.; *Sc*, *Stipa capillata* L.; orange cell, detected; blue cell, not detected; Cluster I in shade of dark gray, Cluster II in shade of light blue; Cluster III in shade of yellow; Cluster IV in shade of green; Cluster V in shade of orange; Cluster VI in shade of purple; Cluster VII in shade of pink.

3 amylase. H_2S, lipase 1, pigment and organic acid producing isolates accounted for 48.7, 44.9, 33.3, and 17.9% of the total isolates, respectively. As shown in **Figure 5**, H_2S, organic acid, diffusible pigment and various extracellular enzymes producing isolates were widely distributed in the five altitudes, with diffusible pigment, urease, H_2S, lipase 1, lipase 3 and protease producing isolates dominating at 2800 m, amylase and lipase 1 producing isolates predominant at 3350 m, organic

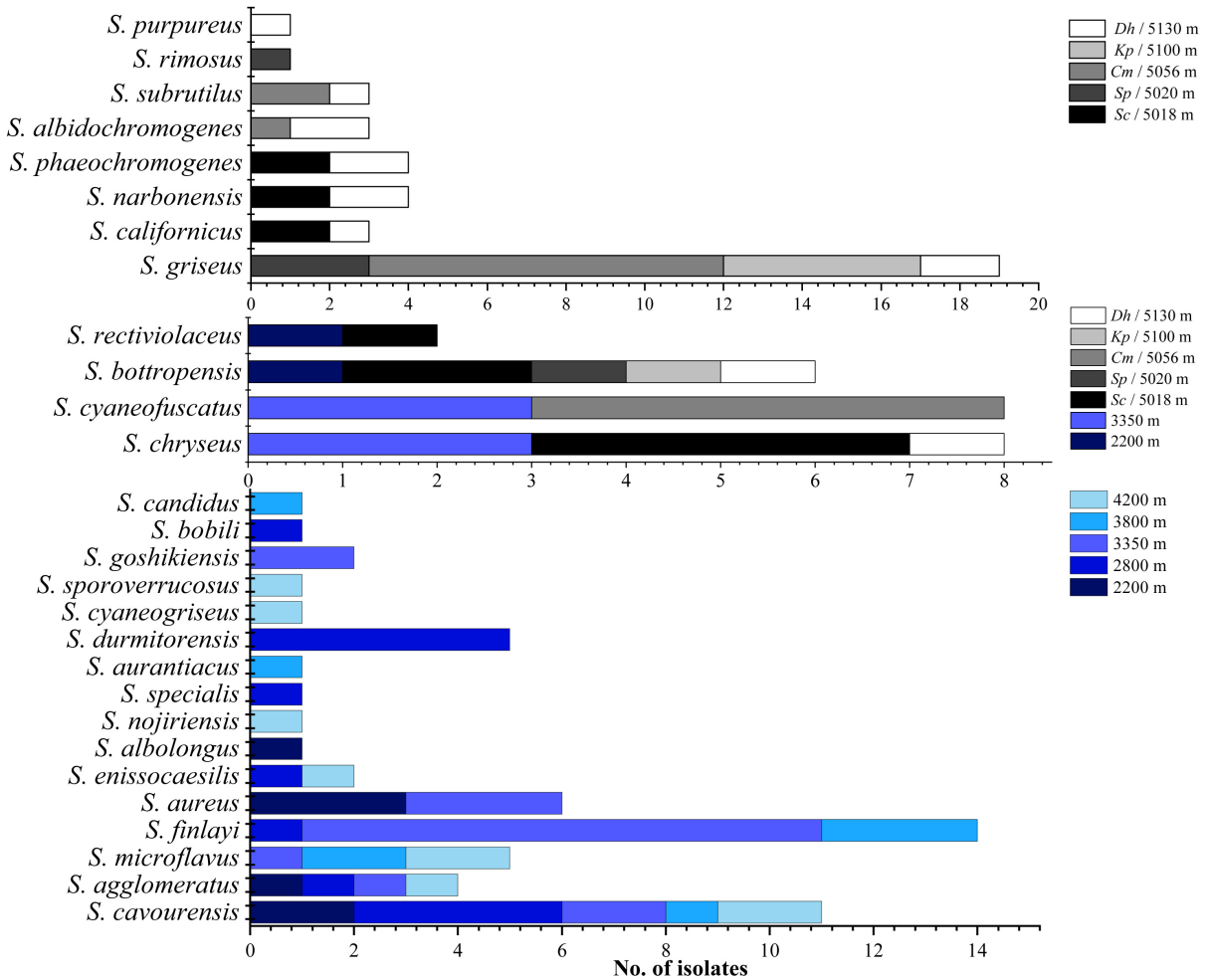

FIGURE 4 | Distribution of isolates related to different *Streptomyces* species on diverse altitudes of the Laohu Ditch and Gaize County area.

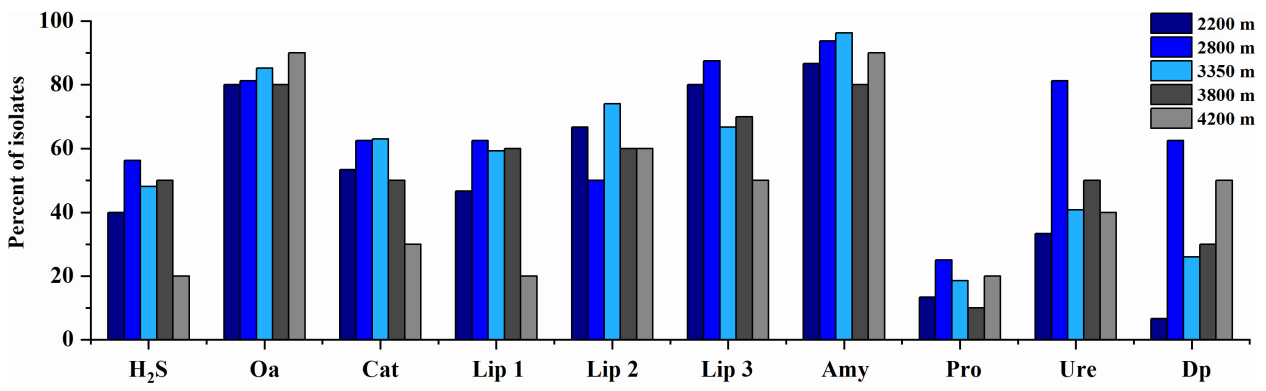

FIGURE 5 | Distribution of H_2S, organic acid, diffusible pigments and various enzymes producing isolates at the increasing altitudes of the Laohu Ditch. Cat, catalase; Lip 2, lipase 2; Ure, urease; Pro., protease; Lip 3, lipase 3; Amy, amylase; Lip 1, lipase 1; Dp, diffusible pigment; Oa, organic acid.

acid producing isolates dominating at 4200 m. However, as displayed in **Figure 6** the proportion of H_2S, organic acid, diffusible pigment and extracellular enzymes producing isolates demonstrated great discrepancy in near-root soils of different plant communities. Catalase and urease producing isolates were distributed across 15 plant communities; lipase 2, protease

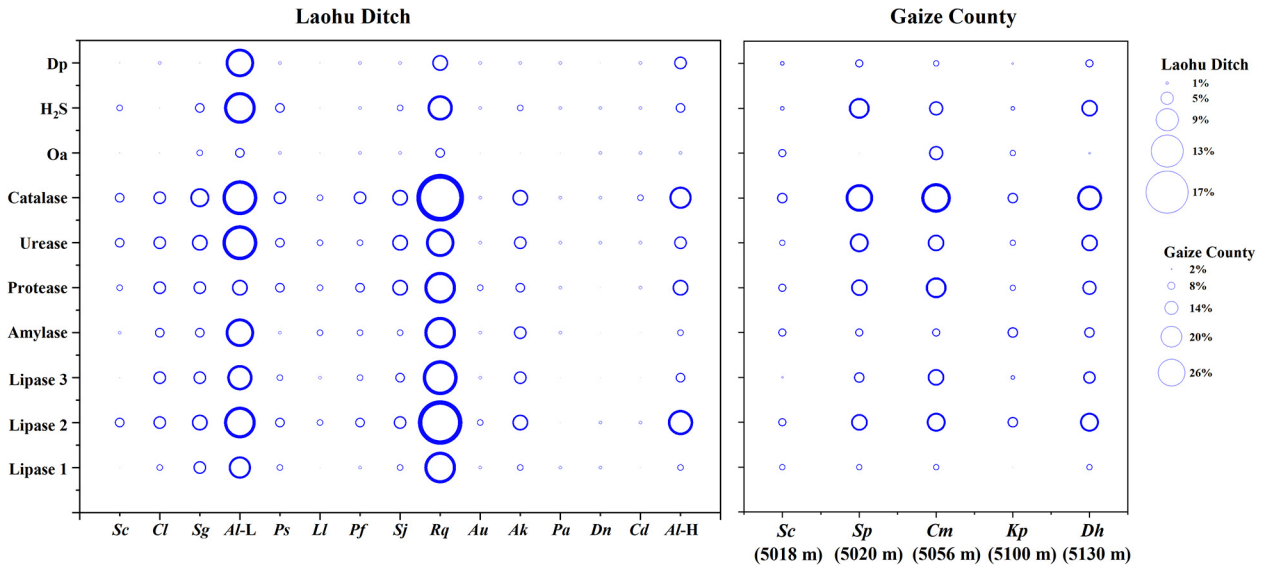

FIGURE 6 | Distribution of H_2S, organic acid, diffusible pigment and various enzymes producing isolates in near-root soils of twenty plant communities on the Tibetan Plateau. (The size of the bubble indicates the proportion of organic acid, H_2S, diffusible pigment and various enzymes producing isolates to the total isolates, respectively). *Al* (L), *Astragalus licentianus* Hand.-Mazz. at 2800 m, *Al* (H), *Astragalus licentianus* Hand.-Mazz. at 4200.

producing isolates occurred in 14 plants; amylase, H_2S, diffusible pigment producing isolates occurred in 13 plants, and lipase 1, lipase 3 in 12 plants, organic acid producing isolates only occurred in 10 plants. In addition, H_2S, organic acid, diffusible pigment and various enzymes producing isolates frequently occurred in two medicinal plants, *A. licentianus* Hand.-Mazz. and *R. quadrifida* Fisch. & C.A. Mey.

Among 50 *Streptomyces* isolates from the Gaize County area, more than half of the isolates produced catalase, lipase 2, urease, protease, H_2S. Amylase, lipase 3, lipase 1, pigment and organic acid producing isolates accounted for 46, 46, 24, 28, and 30% of the total isolates, respectively. As shown in **Figure 6** organic acid and lipase 1 producing isolates occurred across four plant communities except for *Stipa purpurea* Griseb. at 5020 m and *Kobresia pygmaea* C.B. Clarke at 5100 m, respectively. The other eight were found in all of the five plant communities, with discrepancy in proportion and variety.

Antimicrobial Activity of the Cultivable Actinomycetes

The antimicrobial activity varied among the actinomycetes as shown in **Table 2**. Among 78 actinomycete isolates from the Laohu Ditch, 29 isolates (37.2%) exhibited antimicrobial activity against the human pathogens. Of which, 2, 19, 14, 1 isolates demonstrated antimicrobial activity against *E. coli*, *S. aureus*, *C. albicans*, and *P. aeruginosa*, respectively. In addition, 7 isolates showed antimicrobial activity against two of the four human pathogens. And the 29 antagonistic actinomycetes were all screened from *Streptomyces* spp. As shown in **Figure 2**, they were widely spread in distinct phylogenetic clusters from 12 plant communities at different altitudes. Noticeably, 51.4% of the tested isolates (35 in total) from near-root soils of two medicinal plants (*A. licentianus* Hand.-Mazz. and *R. quadrifida* Fisch. & C.A. Mey) demonstrated antimicrobial activity, which comprised 62% of the total antagonistic isolates.

While from the Gaize County area, thirteen of the fifty actinomycete isolates (26.0%) showed growth inhibitory activity against the human pathogens. Among them, 3, 9, 5, 1 isolates displayed antimicrobial activity against *E. coli*, *S. aureus*, *C. albicans*, and *P. aeruginosa*, respectively. Moreover, five isolates showed a broad antimicrobial spectrum against two of the four human pathogens. As shown in **Table 2**, antagonistic actinomycetes were scattered around five plant communities, with the most occurring in *Stipa purpurea* Griseb. at 5020 m.

In this study, the distinct phenotypic characters and antimicrobial activities were detected among isolates with identical 16S rDNA sequences as shown in **Table 3**. Though apparent division of the isolates to different clusters in accordance with the 16S rDNA sequences, there was just as much physiological variation among the isolates within the same clusters obtained from the same area, as among the isolates with identical 16S rDNA sequences but in disparate area, such as isolates with 99–100% 16S rDNA sequence identities to *S. cavourensis*, *S. griseus*, and *S. rectiviolaceus* (**Table 3**), *S. chryseus*, *S. cyaneofuscatus*, and *S. bottropensis* (**Supplementary Tables 1–3**).

DISCUSSION

Actinomycetes remain a mainstream source of antibiotics against constantly emerging multidrug resistant pathogenic microorganisms (Tiwari and Gupta, 2013; Shivlata and Satyanarayana, 2015; Barka et al., 2016). To raise the screening efficiency of valuable strains, knowledge about

TABLE 2 | Antimicrobial activity of the actinomycetes from the alpine habitats on the Tibetan Plateau.

Laohu Ditch							Gaize County					
Altitude (m)	**Plant species**	**Isolate no.**	**Antimicrobial activity**				**Altitude (m)/plant species**	**Isolate no.**	**Antimicrobial activity**			
			E. coli	***S. aureus***	***C. albicans***	***P. aeruginosa***			***E. coli***	***S. aureus***	***C. albicans***	***P. aeruginosa***
2200	*Sc*	QLS04	−	−	−	+	5020/*Sp*	QZGYEa1	+	−	−	−
	Cl	QLS80	−	−	+	−						
	Sg	QLS83	−	−	+	−		QZGYEb2	+	+	−	−
2800	*Al*	QLS50	−	+	+	−						
	Al	QLS76	−	+	−	−		QZGYEb4	−	+	+	−
	Al	QLS77	−	+	+	−						
	Al	QLS68	−	+	−	−		QZGYEb5	−	−	+	−
	Al	QLS67	−	−	+	−						
	Al	QLS69	−	+	−	−		QZGYFb4	−	+	−	−
	Ps	QLS81	+	−	+	−						
3350	*Sj*	QLS17	−	−	+	−	5018/*Sc*	QZGYE j3	−	−	+	−
	Sj	QLS20	−	+	−	−						
	Pf	QLS13	−	+	−	−	5056/*Cm*	QZGYFe20	+	+	−	−
	Rq	QLS35	−	+	−	−						
	Rq	QLS65	−	+	−	−	5100/*Kp*	QZGYFe21	−	+	−	−
	Rq	QLS58	−	+	−	−						
	Rq	QLS59	−	+	−	−		QZGYFg1	−	+	−	−
	Rq	QLS64	−	+	−	−						
	Rq	QLS74	−	+	−	−		QZGYFg2	−	−	−	+
3800	*Au*	QLS85	−	+	+	−						
	Au	QLS93	−	−	+	−	5130/*Dh*	QZGYEc1	−	+	+	−
	Ak	QLS30	−	+	−	−						
	Dn	QLS88	−	+	+	−						
4200	*Al*	QLS02	−	+	+	−		QZGYEd1	−	+	+	−
	Al	QLS09	−	−	+	−						
	Al	QLS08	−	+	+	−						
	Al	QLS24	−	+	−	−		QZGYEd3	−	+	−	−
	Al	QLS45	+	−	−	−						
	Al	QLS63	−	−	+	−						

+, antimicrobial activity; −, no antimicrobial activity; Sc, Salsola collina Pall; Cl, Ceratoides latens Reveal & N.H. Holmgren; Sg, Stipa glareosa PA Smirn; Al, Astragalus licentianus Hand.-Mazz.; Ps, Potentilla saudersiana Royle; Sj, Saussurea japonica Kuntze; Pf, Potentilla fruticosa L.; Rq, Rhodiola quadrifida Fisch. & C.A. Mey; Au, Androsace umbellata (Lour.) Merr.; Ak, Arenaria kansuensis Maxim; Dn, Draba nemorosa L.; Sp, Stipa purpurea Griseb.; Sc (5018 m): Stipa capillata L.; Cm, Carex moocroftii Falc. ex Boott; Kp, Kobresia pygmaea C.B. Clarke; Dh, Dracocephalum heterophyllum Benth.

TABLE 3 | Physiological heterogeneity between different isolates of the same clusters in the same area or disparate area.

Streptomycetes	***Streptomyces cavourensis***					***Streptomyces griseus***				***Streptomyces rectiviolaceus***	
Isolate no.	**QLS06**	**QLS87**	**QLS18**	**QLS85**	**QLS02**	**QZGYEj3**	**QZGYFe9**	**QZGYFg1**	**QZGYFd8**	**QLS36**	**QZGYEb4**
Source of isolates	***Cl* (2200 m)**	***Al* (2800 m)**	***Ll* (3350 m)**	***Au* (3800 m)**	***Al* (4200 m)**	***Sc* (5018 m)**	***Cm* (5056 m)**	***Kp* (5100 m)**	***Dh* (5130 m)**	***Sg* (2200 m)**	***Sp* (5020 m)**
Phenotypic character											
Lipase 1	−	+	−	+	−	+	−	−	+	+	−
Lipase 2	+	+	+	+	+	+	−	+	+	+	+
Lipase 3	+	+	+	+	+	−	−	−	+	+	+
Amylase	+	+	+	+	+	+	+	+	+	+	+
Protease	+	−	+	+	+	+	−	−	−	+	+
Urease	−	+	+	+	+	+	−	−	−	+	+
Catalase	+	+	+	+	+	+	+	+	+	+	+
Organic acid	+	−	−	−	−	+	+	+	+	+	−
H_2S production	+	+	−	+	−	−	+	−	+	+	+
Diffusible pigment	brown	brown	−	brown	yellow	−	−	purple	brown	−	−
Antimicrobial activity											
Escherichia coli	−	−	−	−	−	−	−	−	+	−	−
Staphylococcus aureus	−	−	−	+	+	−	−	+	−	−	+
Candida albicans	−	−	−	+	+	+	−	−	−	−	+
Pseudomonas aeruginosa	−	−	−	−	−	−	−	−	−	−	−

+, positive effect; −, negative effect.

the diversity, physiological activity and ecological distribution of unexploited actinomycete flora is urgently needed (Tiwari and Gupta, 2013). Our study added to this field by displaying the phylogenetic diversity and physiological heterogeneity of the cultivable actinomycetes from near-root soils of different plant communities at the increasing altitudes on the Qinghai-Tibetan Plateau.

It is notable that the 16S rDNA sequence as the sole marker for phylogenetic and taxonomic analysis is limited. In fact, it has been reported that *Streptomyces* isolates with 97% 16S rDNA sequence identities can vary by as much as 30% in core genome divergence with average nucleotide identities ranging from 100–78.3% (Chevrette et al., 2019). However, the 16S rDNA sequence is widely used as an indispensable gene marker in the bacterial taxonomic analysis (Martina et al., 2019). In this study, the 128 isolates were assigned to *Streptomyce* spp., *Nocardia* spp. and one potential new genus based on the 16S rDNA sequences. Moreover, the 97% 16S rDNA sequence identity threshold has been extensively used as a boundary for bacterial species delineation (Meier-Kolthoff et al., 2013), however, this threshold value has been raised to 99% for actinomycetes (Stach et al., 2003; Guo et al., 2015) based on comparative studies between 16S rDNA sequence identities, average nucleotide identity (ANI) values of whole genomes and DNA–DNA hybridization (DDH) (Guo et al., 2015). Accordingly, we empolyed a threshold of 99–100% to assign *Streptomyces* isolates to different clusters. Surely, based on this metric, the isolates identified as potential novel isolates according to the 16S rDNA sequences deserved to be furtherly confirmed by polyphasic taxonomic approach (Zhang et al., 2019).

Streptomyces spp. possess high adaptive capability for surviving in many extreme environmental conditions and their incidence had been documented in diverse extreme habitats including frozen soils, deserts, oceans, Arctic and Antarctic regions (Maldonado et al., 2008; Le Roes-Hill et al., 2009; Malviya et al., 2009; Okoro et al., 2009; Ramesh and Mathivanan, 2009; Verma et al., 2009; Ivanova et al., 2010; Zothanpuia et al., 2018). Studies in frozen soils, Arctic and Antarctic regions had revealed a great diversity of cultivable *Streptomyces* species (Le Roes-Hill et al., 2009; Ivanova et al., 2010; Li et al., 2011; Zhang et al., 2016b; Kamjam et al., 2019), while in marine and deserts, *Streptomyces* spp. had been reported as one of the dominant culturable genera (Okoro et al., 2009; Prieto-Davo et al., 2016). In this study, *Streptomyces* isolates were isolated from near-root soils of the studied plant communities from an altitude of 2200 to 5130 m on the Qinghai-Tibetan Plateau, with variances in diversity on different sites. By contrast, four *Nocardia* isolates and one potential novel genus just detected in *Salsola collina* Pall of 2200 m (QLS27, QLS44), *Stipa glareosa* PA Smirn of 2200 m (QLS96), *P. saudersiana* Royle of 2800 m (QLS42) and *Arenaria kansuensis* Maxim of 3800 m (QLS54) from the Laohu Ditch. This may be attributed to high dependency of the rare actinomycetes (*Nocardia* spp. and the potential new genus) upon their living conditions, with a relatively narrow ecological niche (Horner-Devine et al., 2004). Additionally, differences in the basic nutrients such as energy, carbon and nitrogen sources necessary for actinomycetes supplied by vegetation litter and/or plant root exudates, could cause variation in actinobacterial composition (Rasche et al., 2011; Zhang et al., 2013). For example, isolates with 98–100% 16S rDNA sequence identities to 28 species of *Streptomyces* spp. were detected in 20 plant communities along different altitudes on the Tibetan Plateau. Compared to the frequent occurrence of members related to *S. cavourensis* and *S. griseus* in different plant communities at the increasing altitudes, quite a few *Streptomyces* isolates specifically occurred in near-root soils of diverse plant communities at varying altitudes. This finding implied that a high degree of *Streptomyces* spp. diversity could adapt to the extreme alpine habitats and different plants may be selective to their root-associated *Streptomyces* isolates (Adil et al., 2017; Naylor et al., 2017). Noticeably, isolates with 99–100% 16S rDNA sequence identities to *S. chryseus*, *S. rectiviolaceus*, *S. bottropensis*, and *S. cyaneofuscatus* were detected in both of the studied geographically diverse cold environments. Furthermore, based on the same taxonomy according to the 16S rDNA sequences, the occurrence of some *Streptomyces* isolates in the studied extreme alpine habitats was observed in other extreme environments as well. For example, members related to *S. griseus* and *S. rimosus* had been isolated even from thermophilic environment (Shivlata and Satyanarayana, 2015). Isolate ISP 5300 affiliated to *S. cavourensis* had been reported as an alkaliphilic *Streptomyces* species by Mikami et al. (1982). And two isolates M-169 and M-157 related to *S. cyaneofuscatus* explored in deep-sea were found to produce novel antimicrobial and antitumor compounds (Ortiz-López et al., 2018; Rodríguez et al., 2018).

In this study, almost all of the *Streptomyces* isolates from the alpine habitats produced catalase, which was consistent with the catalase-positive of *Streptomyces* spp. described in Bergey's Manual of Systematic Bacteriology (Ruan, 2013). Colony pigment or diffusible pigment produced by bacteria is a physiological strategy of adaption to low temperature and of resistant to environmental stress (Dillon et al., 2003; Ponder et al., 2005; Zhang et al., 2008). For example, microorganisms in diverse cold habitats would increase carotenoid production to keep membrane stabilization at lower temperature and secrete dark pigment to absorb UV light (Fong et al., 2001; Dillon et al., 2003; Zhang et al., 2008). Marine actinomycetes producing diffusible pigments were able to survive longer than those with no diffusible pigment production (Ramesh and Mathivanan, 2009). In our study, forty *Streptomyces* isolates obtained from the two alpine habitats produced diffusible pigments, which may be of significance for the isolates adapting to the alpine habitats on the Tibetan Plateau. In addition, as saprophytic inhabitants, soil actinomycetes thrive on decomposing organic materials such as lignin, chitin, cellulose, sulfocompounds etc., which is enabled by means of producing diverse extracellular hydrolytic enzymes (Bhatnagar and Kim, 2010; Suela Silva et al., 2013). The result of biochemical assays for the obtained actinomycetes showed that lipase 2, urease, protease, amylase and H_2S producing strains accounted for 82.1, 70.5, 62.8, 52.6, and 48.7% of the total isolates from the Laohu Ditch, while 72, 62, 66, 46, and 60% of the total isolates from the Gaize County area, respectively. This demonstrated that most of the *Streptomyces* isolates possessed the capability of hydrolyzing activity on polyesters, urea, gelatin,

amylum and sulfur-containing amino acids, reflecting that those isolates may associate with the cyclings of carbon, nitrogen and sulfur on the Tibetan Plateau (Shivlata and Satyanarayana, 2015; Barka et al., 2016). However, variances in proportion of H_2S, diffusible pigment, organic acid and enzymes producing isolates in each plant community at increasing altitudes on the Tibetan Plateau were detected, implying the differences in soil ingredient of diverse plant root habitats closely relate to distinct plant litter and/or root exudates (Goodfellow and Williams, 1983; Bais et al., 2006). For example, the enrichment of H_2S, diffusible pigment, organic acid and enzymes producing isolates in near-root soils of two medicinal plants, *A. licentianus* Hand.-Mazz. and *R. quadrifida* Fisch. & C.A. Mey, was observed. Studies have shown that medicinal plant roots are rich in bioactive compounds that could affect the physiological activities of their root-associated actinomycetes (Li et al., 2008; Zhao et al., 2012; Patrycja et al., 2015; Martina et al., 2019).

Moreover, the physiological heterogeneity of some *Streptomyces* isolates was detected on the Tibetan Plateau. For example, 13.7% of the total *Streptomyces* isolates related to *S. cavourensis* frequently occurring at different plant communities across five altitudes on the Laohu Ditch, and 32% of the total isolates in the Gaize County area affiliated with *S. griseus* across four sites, exhibited distinct physiological capabilities. Most notably, with the same taxonomy according to the 16S rDNA sequences, isolate QZGYEb4 from 5020 m on the Gaize County area showed diverse antimicrobial activity and phenotypic traits from its counterpart QLS36 from 2200 m on the Laohu Ditch. The study of marine actinomycetes also found that though nearly or fully identical 16S rDNA sequences to known terrestrial organisms, the actinomycetes still have signs of adaption to their marine environment (Bredholt et al., 2008). Zhang et al. (2008) revealed that physiological variation between strains with close evolutionary relationships suggested the differences in the ecological conditions of bacteria survival habitats.

It has been demonstrated that actinomycetes in extreme environments are capable of yielding antagonistic bioactive compounds (Shivlata and Satyanarayana, 2015; Sivalingam et al., 2019). Twenty nine actinomycetes from the Laohu Ditch and thirteen from the Gaize County area, respectively, exhibiting antimicrobial activity against four kinds of pathogenic microorganisms, were all screened from *Streptomyces* spp., which were widely spread at the increasing altitudes of the studied areas on the Tibetan Plateau. Interestingly, the antagonistic isolates still slightly enriched in the near-root soils of two medicinal plants, *A. licentianus* Hand.-Mazz. (28.6% of the total antagonistic streptomycetes) and *R. quadrifida* Fisch. & C.A. Mey (14.3% of the total antagonistic streptomycetes). Barakate et al. (2002) presented that 14 and 68% of the 131 streptomycetes from plant rhizospheric soils showed antimicrobial activity against *Escherichia coli* and *Staphylococcus aureus*, respectively. Several researchers had reported antimicrobial activity of actinomycetes against various pathogenic microorganisms from other unique habitats. Thirty nine actinomycetes recovered from the Antarctic soils, of which, fifteen displayed antagonistic activity against clinical Gram-positive and Gram-negative bacteria (Lee et al., 2012). Ramesh and Mathivanan (2009) obtained 208 marine actinomycetes, of which, 14.9, 8.7, and 13.5% exhibited antimicrobial activity against *E. coli*, *P. aeruginosa* and *C. albicans*, respectively. These results revealed that the unexplored unique habitats have the potential to discover actinomycetes with antimicrobial activities as well as various bioactive compounds.

To the best of our knowledge, this study offers for the first time a prelude about the unexplored culturable soil actinomycetes diversity associated with the typical alpine habitats on the Qinghai-Tibetan Plateau and their bioactive capabilities. However, more in-depth investigations on extraction, purification of the bioactive compounds produced by the actinomycetes, as well as the cold adaption mechanism of actinomycetes in alpine habitats will strengthen the development and utilization of those actinomycete isolates.

DATA AVAILABILITY STATEMENT

The datasets presented in this study can be found in online repositories. The names of the repository/repositories and accession number(s) can be found in the article/**Supplementary Material**.

AUTHOR CONTRIBUTIONS

SX, XZ, and CZ planned and designed the research. KJ, JLL, MDW, and YW provided the help in sampling. MMW and JHL analyzed the data. AM conducted the experiments and wrote the manuscript. All authors were involved in revising the manuscript critically.

FUNDING

This study was funded jointly by grants from the National Science Foundation of China (nos. 31870470 and 31570393).

ACKNOWLEDGMENTS

We are grateful to Editor and reviewers for helpful comments that improved this manuscript and to Cryosphere Research Station on the Qinghai-Tibet Plateau, Chinese Academy of Sciences for sampling the Gaize soils.

SUPPLEMENTARY MATERIAL

The Supplementary Material for this article can be found online at: https://www.frontiersin.org/articles/10.3389/fmicb.2020.555351/full#supplementary-material

REFERENCES

Adil, E., Nicholas, L., Kistler, H. C., and Kinkel, L. L. (2017). Plant community richness mediates inhibitory interactions and resource competition between *Streptomyces* and *Fusarium* Populations in the Rhizosphere. *Microbiol. Ecol.* 74, 157–167. doi: 10.1007/s00248-016-0907-5

Anand, T. P., Bhat, A. W., Shouche, Y. S., Roy, U., Siddharth, J., and Sarma, S. P. (2006). Antimicrobial activity of marine bacteria associated with sponges from the waters off the coast of south east india. *Microbiol. Res.* 161, 252–262. doi: 10.1016/j.micres.2005.09.002

Babalola, O. O., Kirby, B. M., Le Roes-Hill, M., Cook, A. E., Cary, S. C., Burton, S. G., et al. (2009). Phylogenetic analysis of actinobacterial populations associated with Antarctic Dry Valley mineral soils. *Environ. Microbiol.* 11, 566–576. doi: 10.1111/j.1462-2920.2008.01809.x

Bais, H. P., Weir, T. L., Perry, L. G., Gilroy, S., and Vivanco, J. M. (2006). The role of root exudates in rhizosphere interactions with plants and other organisms. *Ann. Rev. Plant Biol.* 57, 233–266. doi: 10.1146/annurev.arplant.57.032905.105159

Barakate, M., Ouhdouch, Y., Oufdou, K., and Beaulieu, C. (2002). Characterization of rhizospheric soil streptomycetes from Moroccan habitats and their antimicrobial activities. *World J. Microbiol. Biotechnol.* 18, 49–54. doi: 10.1023/A:1013966407890

Barka, E. A., Vatsa, P., Sanchez, L., Gaveau-Vaillant, N., Jacquard, C., Meier-Kolthoff, J. P., et al. (2016). Taxonomy, physiology, and natural products of actinobacteria. *Microbiol. Mol. Biol. Rev.* 80, 1–43. doi: 10.1128/mmbr.00019-15

Bhatnagar, I., and Kim, S. K. (2010). Immense essence of excellence: marine microbial bioactive compounds. *Mar. Drugs* 8, 2673–2701. doi: 10.3390/md8102673

Bredholt, H., Fjaervik, E., Johnsen, G., and Zotchev, S. B. (2008). Actinomycetes from sediments in the trondheim fjord, norway: diversity and biological activity. *Mar. Drugs* 6, 12–24. doi: 10.3390/md6010012

Chen, J., Chen, H. M., Zhang, Y. Q., Wei, Y. Z., Li, Q. P., Liu, H. Y., et al. (2011). *Agromyces flavus* sp. nov., an actinomycete isolated from soil. *Int. J. Syst. Evol. Microbiol.* 61, 1705–1709. doi: 10.1099/ijs.0.023242-0

Chevrette, M. G., Carlos-Shanley, C., Louie, K. B., Bowen, B. P., and Currie, C. R. (2019). Taxonomic and metabolic incongruence in the ancient genus *Streptomyces*. *Front. Microbiol.* 10:2170. doi: 10.3389/fmicb.2019.02170

Dillon, J. G., Miller, S. R., and Castenholz, R. W. (2003). UV-acclimation responses in natural populations of cyanobacteria (Calothrix sp.). *Environ. Microbiol.* 5, 473–483. doi: 10.1046/j.1462-2920.2003.00435.x

Felsenstein, J. (1985). Confidence limits on phylogenies: an approach using the bootstrap. *Evolution* 39, 783–791. doi: 10.1111/j.1558-5646.1985.tb00420.x

Fong, N. J., Burgess, M. L., Barrow, K. D., and Glenn, D. R. (2001). Carotenoid accumulation in the psychrotrophic bacterium *Arthrobacter agilis* in response to thermal and salt stress. *Appl. Microbiol. Biotechnol.* 56, 750–756. doi: 10.1007/s002530100739

Genilloud, O., Gonzalez, I., Salazar, O., Martin, J., Tormo, J. R., and Vicente, F. (2011). Current approaches to exploit actinomycetes as a source of novel natural products. *J. Ind. Microbiol. Biotechnol.* 38, 375–389. doi: 10.1007/s10295-010-0882-7

Goodfellow, M., and Williams, S. T. (1983). Ecology of actinomycetes. *Ann. Rev. Microbiol.* 37, 189–216. doi: 10.1146/annurev.mi.37.100183.001201

Guo, X., Liu, N., Li, X., Ding, Y., Fei, S., Gao, Y., et al. (2015). Red soils harbor diverse culturable actinomycetes that are promising sources of novel secondary metabolites. *Appl. Environ. Microbiol.* 81, 3086–3103. doi: 10.1128/AEM.03859-14

Hansen, A. A., Herbert, R. A., Mikkelsen, K., Jensen, L. L., Kristoffersen, T., Tiedje, J. M., et al. (2007). Viability, diversity and composition of the bacterial community in a high arctic permafrost soil from spitsbergen, northern norway. *Environ. Microbiol.* 9, 2870–2884. doi: 10.1111/j.1462-2920.2007.01403.x

Horner-Devine, M. C., Lage, M., Hughes, J. B., and Bohannan, B. J. (2004). A taxa-area relationship for bacteria. *Nature* 432, 750–753. doi: 10.1038/nature03073

Intra, B., Mungsuntisuk, I., Nihira, T., Igarashi, Y., and Panbangred, W. (2011). Identification of actinomycetes from plant rhizospheric soils with inhibitory activity against *Colletotrichum* spp., the causative agent of anthracnose disease. *BMC Res. Notes* 4:98. doi: 10.1186/1756-0500-4-98

Ivanova, V., Lyutskanova, D., Kolarova, M., Aleksieva, K., and Stoilova-Disheva, M. (2010). Structural Elucidation of a Bioactive Metabolites Produced by *Streptomyces avidinii* SB9 strain, isolated from permafrost soil in Spitsbergen, Arctic. *Biotechnol. Biotechnol. Equipment* 24, 2092–2095. doi: 10.2478/V10133-010-0080-9

Ivanova, V., Lyutskanova, D., Stoilova-Disheva, M., Kolarova, M., Aleksieva, K., Raykovska, V., et al. (2009). Isolation and identification of alpha,alpha-trehalose and glycerol from an arctic psychrotolerant *Streptomyces* sp. SB9 and their possible role in the strain's survival. *Prep. Biochem. Biotechnol.* 39, 46–56. doi: 10.1080/10826060802589585

Kamjam, M., Nopnakorn, P., Zhang, L., Peng, F., Deng, Z., and Hong, K. (2019). *Streptomyces* polaris sp. nov. and *Streptomyces* septentrionalis sp. nov., isolated from frozen soil. *Antonie Van Leeuwenhoek* 112, 375–387. doi: 10.1007/s10482-018-1166-x

Le Roes-Hill, M., Rohland, J., Meyers, P. R., Cowan, D. A., and Burton, S. G. (2009). *Streptomyces hypolithicus* sp. nov., isolated from an Antarctic hypolith community. *Int. J. Syst. Evol. Microbiol.* 59, 2032–2035. doi: 10.1099/ijs.0.007971-0

Lee, L. H., Cheah, Y. K., Mohd Sidik, S., Ab Mutalib, N. S., Tang, Y. L., Lin, H. P., et al. (2012). Molecular characterization of antarctic actinobacteria and screening for antimicrobial metabolite production. *World J. Microbiol. Biotechnol.* 28, 2125–2137. doi: 10.1007/s11274-012-1018-1

Li, J., Tian, X. P., Zhu, T. J., Yang, L. L., and Li, W. J. (2011). *Streptomyces* fildesensis sp. nov., a novel streptomycete isolated from antarctic soil. *Antonie Van Leeuwenhoek* 100, 537–543. doi: 10.1007/s10482-011-9609-7

Li, J., Zhao, G.-Z., Chen, H.-H., Wang, H.-B., Qin, S., Zhu, W.-Y., et al. (2008). Antitumour and antimicrobial activities of endophytic streptomycetes from pharmaceutical plants in rainforest. *Lett. Appl. Microbiol.* 47, 574–580. doi: 10.1111/j.1472-765X.2008.02470.x

Maldonado, L., Fragoso-Yáñez, D., Pérez-García, A., Rosellón-Druker, J., and Quintana, E. (2008). Actinobacterial diversity from marine sediments collected in Mexico. *Antonie van Leeuwenhoek* 95, 111–120. doi: 10.1007/s10482-008-9294-3

Malviya, M. K., Pandey, A., Trivedi, P., Gupta, G., and Kumar, B. (2009). Chitinolytic activity of cold tolerant antagonistic species of *Streptomyces* isolated from glacial sites of Indian himalaya. *Curr. Microbiol.* 59, 502–508. doi: 10.1007/s00284-009-9466-z

Martina, O., Jaqueline, H., Marlene, L., Florian, G., Thomas, R., Christoph, W., et al. (2019). Exploring actinobacteria associated with rhizosphere and endosphere of the native alpine medicinal plant leontopodium nivale subspecies alpinum. *Front. Microbiol.* 10:2531. doi: 10.3389/fmicb.2019.02531

Meier-Kolthoff, J. P., Göker, M., Spröer, C., and Klenk, H. P. (2013). When should a DDH experiment be mandatory in microbial taxonomy? *Arch. Microbiol.* 195, 413–418. doi: 10.1007/s00203-013-0888-4

Mikami, Y., Miyashita, K., and Arai, T. (1982). Diaminopimelic acid profiles of alkalophilic and alkaline-resistant strains of *Actinomycetes*. *J. Gen. Microbiol.* 128, 1709–1712. doi: 10.1099/00221287-128-8-1709

Mingma, R., Pathom-aree, W., Trakulnaleamsai, S., Thamchaipenet, A., and Duangmal, K. (2014). Isolation of rhizospheric and roots endophytic actinomycetes from leguminosae plant and their activities to inhibit soybean pathogen, xanthomonas campestris pv. glycine. *World J. Microbiol. Biotechnol.* 30, 271–280. doi: 10.1007/s11274-013-1451-9

Naylor, D., DeGraaf, S., Purdom, E., and Coleman-Derr, D. (2017). Drought and host selection influence bacterial community dynamics in the grass root microbiome. *Isme J.* 11, 2691–2704. doi: 10.1038/ismej.2017.118

Okoro, C. K., Brown, R., Jones, A. L., Andrews, B. A., Asenjo, J. A., Goodfellow, M., et al. (2009). Diversity of culturable actinomycetes in hyper-arid soils of the Atacama Desert. *Chile. Antonie Van Leeuwenhoek* 95, 121–133. doi: 10.1007/s10482-008-9295-2

Orsini, M., and Romano-Spica, V. (2001). A microwave-based method for nucleic acid isolation from environmental samples. *Lett. Appl. Microbiol.* 33, 17–20. doi: 10.1046/j.1472-765X.2001.00938.x

Ortiz-López, F. J., Alcalde, E., Sarmiento-Vizcaíno, A., Díaz, C., Cautain, B., García, L. A., et al. (2018). New 3-Hydroxyquinaldic acid derivatives from cultures of the marine derived actinomycete *Streptomyces cyaneofuscatus* M-157. *Mar. Drugs* 16:371. doi: 10.3390/md16100371

Ouyang, Y., Wu, H., Xie, L., Wang, G., Dai, S., Chen, M., et al. (2011). A method to type the potential angucycline producers in actinomycetes isolated from

marine sponges. *Antonie Van Leeuwenhoek* 99, 807–815. doi: 10.1007/s10482-011-9554-5

Patrycja, G., Magdalena, W., Gauravi, A., Dnyaneshwar, R., Hanna, D., and Mahendra, R. (2015). Endophytic actinobacteria of medicinal plants: diversity and bioactivity. *Antonie van Leeuwenhoek* 108, 267–289. doi: 10.1007/s10482-015-0502-7

Ponder, M. A., Gilmour, S. J., Bergholz, P. W., Mindock, C. A., Hollingsworth, R., Thomashow, M. F., et al. (2005). Characterization of potential stress responses in ancient Siberian permafrost psychroactive bacteria. *FEMS Microbiol. Ecol.* 53, 103–115. doi: 10.1016/j.femsec.2004.12.003

Prieto-Davo, A., Dias, T., Gomes, S. E., Rodrigues, S., Parera-Valadez, Y., Borralho, P. M., et al. (2016). The madeira archipelago as a significant source of marine-derived actinomycete diversity with anticancer and antimicrobial potential. *Front. Microbiol.* 7:1594. doi: 10.3389/fmicb.2016.01594

Qiao, Y., Zhao, L., Pang, Q., Chen, J., Zou, D., and Gao, Z. (2015). [Characteristics of permafrost in gerze county on the Tibetan Plateau]. *J. Glaciol. Geocryol.* 37, 1453–1460. doi: 10.7522/j.isnn.1000-0240.2015.0161

Ramesh, S., and Mathivanan, N. (2009). Screening of marine actinomycetes isolated from the Bay of Bengal, India for antimicrobial activity and industrial enzymes. *World J. Microbiol. Biotechnol.* 25, 2103–2111. doi: 10.1007/s11274-009-0113-4

Rasche, F., Knapp, D., Kaiser, C., Koranda, M., Kitzler, B., Zechmeister-Boltenstern, S., et al. (2011). Seasonality and resource availability control bacterial and archaeal communities in soils of a temperate beech forest. *Isme J.* 5, 389–402. doi: 10.1038/ismej.2010.138

Rodríguez, V., Martín, J., Sarmiento-Vizcaíno, A., de la Cruz, M., García, L. A., Blanco, G., et al. (2018). Anthracimycin B, a potent antibiotic against gram-positive bacteria isolated from cultures of the deep-sea actinomycete *Streptomyces cyaneofuscatus* M-169. *Mar. Drugs* 16:406. doi: 10.3390/md16110406

Ruan, J. (2013). [Bergey's manual of systematic bacteriology (second edition) volume 5 and the study of actinomycetes systematic in China]. *Acta Microbiol. Sinica* 53, 521–530.

Sanchez-Porro, C., Martin, S., Mellado, E., and Ventosa, A. (2003). Diversity of moderately halophilic bacteria producing extracellular hydrolytic enzymes. *J. Appl. Microbiol.* 94, 295–300. doi: 10.1046/j.1365-2672.2003.01834.x

Shirling, E. B., and Gottlieb, D. (1966). Methods for characterization of Streptomyces species. *Int. J. Bacteriol.* 16, 312–340. doi: 10.1099/00207713-16-3-313

Shivlata, L., and Satyanarayana, T. (2015). Thermophilic and alkaliphilic Actinobacteria: biology and potential applications. *Front. Microbiol.* 6:1014. doi: 10.3389/fmicb.2015.01014

Sivalingam, P., Hong, K., Pote, J., and Prabakar, K. (2019). Extreme environment streptomyces: potential sources for new antibacterial and anticancer drug leads? *Int. J. Microbiol.* 2019:5283948. doi: 10.1155/2019/5283948

Stach, J. E. M., Maldonado, L. A., Masson, D. G., Ward, A. C., Goodfellow, M., and Bull, A. T. (2003). Statistical approaches for estimating actinobacterial diversity in marine sediments. *Appl. Environ. Microbiol.* 69, 6189–6200. doi: 10.1128/AEM.69.10.6189-6200.2003

Suela Silva, M., Naves Sales, A., Teixeira Magalhaes-Guedes, K., Ribeiro Dias, D., and Schwan, R. F. (2013). Brazilian cerrado soil actinobacteria ecology. *Biomed. Res. Int.* 2013:503805. doi: 10.1155/2013/503805

Tamura, K., and Nei, M. (1993). Estimation of the number of nucleotide substitutions in the control region of mitochondrial DNA in humans and chimpanzees. *Mol. Biol. Evol.* 10, 512–526. doi: 10.1093/oxfordjournals.molbev.a040023

Tiwari, K., and Gupta, R. K. (2013). Diversity and isolation of rare actinomycetes: an overview. *Crit. Rev. Microbiol.* 39, 256–294. doi: 10.3109/1040841x.2012.709819

Verma, V. C., Gond, S. K., Kumar, A., Mishra, A., Kharwar, R. N., and Gange, A. C. (2009). Endophytic actinomycetes from Azadirachta indica A. Juss.: isolation, diversity, and anti-microbial activity. *Microb. Ecol.* 57, 749–756. doi: 10.1007/s00248-008-9450-3

Wang, Q. L., Cao, G. M., Jiang, W. B., and Zhang, Y. S. (2004). [Study on actinomycetes population of alpine meadow soil in Qinghai]. *Wei Sheng Wu Xue Bao* 44, 733–736. doi: 10.1161/01.ATV.0000116865.98067.31

Xu, L., Li, Q., and Jiang, C. (1996). Diversity of soil actinomycetes in yunnan, china. *Appl. Environ. Microbiol.* 62, 244–248. doi: 10.1021/bk-1996-0647.ch017

Zhang, B., Tang, S., Chen, X., Zhang, L., Zhang, G., Zhang, W., et al. (2016a). Streptomyces lacrimifluminis sp. nov., a novel actinobacterium that produces antibacterial compounds, isolated from soil. *Int. J. Syst. Evol. Microbiol.* 66, 4981–4986. doi: 10.1099/ijsem.0.001456

Zhang, L., Ruan, C., Peng, F., Deng, Z., and Hong, K. (2016b). Streptomyces arcticus sp. nov., isolated from frozen soil. *Int. J. Syst. Evol. Microbiol.* 66, 1482–1487. doi: 10.1099/ijsem.0.000907

Zhang, B., Tang, S., Yang, R., Chen, X., Zhang, D., Zhang, W., et al. (2019). Streptomyces dangxiongensis sp. nov., isolated from soil of Qinghai-Tibet Plateau. *Int. J. Syst. Evol. Microbiol.* 69, 2729–2734. doi: 10.1099/ijsem.0.003550

Zhang, G., Ma, X., Niu, F., Dong, M., Feng, H., An, L., et al. (2007a). Diversity and distribution of alkaliphilic psychrotolerant bacteria in the Qinghai-Tibet Plateau permafrost region. *Extremophiles* 11, 415–424. doi: 10.1007/s00792-006-0055-9

Zhang, G., Niu, F., Ma, X., Liu, W., Dong, M., Feng, H., et al. (2007b). Phylogenetic diversity of bacteria isolates from the Qinghai-Tibet Plateau permafrost region. *Can. J. Microbiol.* 53, 1000–1010. doi: 10.1139/w07-031

Zhang, X. F., Yao, T. D., Tian, L. D., Xu, S. J., and An, L. Z. (2008). Phylogenetic and physiological diversity of bacteria isolated from Puruogangri ice core. *Microb. Ecol.* 55, 476–488. doi: 10.1007/s00248-007-9293-3

Zhang, X. F., Zhao, L., Xu, S. J. Jr., Liu, Y. Z., Liu, H. Y., et al. (2013). Soil moisture effect on bacterial and fungal community in Beilu River (Tibetan Plateau) permafrost soils with different vegetation types. *J. Appl. Microbiol.* 114, 1054–1065. doi: 10.1111/jam.12106

Zhao, K., Penttinen, P., Chen, Q., Guan, T., and Lindström, K. (2012). The rhizospheres of traditional medicinal plants in Panxi, China, host a diverse selection of actinobacteria with antimicrobial properties. *Appl. Microbiol. Biotechnol.* 94, 1321–1335. doi: 10.1007/s00253-011-3862-6

Zothanpuia, Passari, A. K., Leo, V. V., Chandra, P., Kumar, B., Nayak, C., et al. (2018). Bioprospection of actinobacteria derived from freshwater sediments for their potential to produce antimicrobial compounds. *Microb. Cell Fact* 17:68. doi: 10.1186/s12934-018-0912-0

Conflict of Interest: The authors declare that the research was conducted in the absence of any commercial or financial relationships that could be construed as a potential conflict of interest.

frontiers in Microbiology

ORIGINAL RESEARCH
published: 9 October 2020
doi: 10.3389/fmicb.2020.573302

Effects of Sea Animal Activities on Tundra Soil Denitrification and nirS- and nirK-Encoding Denitrifier Community in Maritime Antarctica

Hai-Tao Dai[1], Ren-Bin Zhu[1], Bo-Wen Sun[1], Chen-Shuai Che[1] and Li-Jun Hou[2]*

[1]Anhui Province Key Laboratory of Polar Environment and Global Change, School of Earth and Space Sciences, University of Science and Technology of China, Hefei, China, [2]State Key Laboratory of Estuarine and Coastal Research, East China Normal University, Shanghai, China

OPEN ACCESS

Edited by:
Laura Zucconi, University of Tuscia, Italy

Reviewed by:
Patricia M. Valdespino-Castillo, Lawrence Berkeley National Laboratory, United States
Feth-el-Zahar Haichar, UMR5240 Microbiologie, Adaptation et Pathogenie (MAP), France
Fabiana Canini, University of Tuscia, Italy

***Correspondence:**
Ren-Bin Zhu
zhurb@ustc.edu.cn

Specialty section:
This article was submitted to Extreme Microbiology, a section of the journal Frontiers in Microbiology

Received: *16 June 2020*
Accepted: *22 September 2020*
Published: *9 October 2020*

Citation:
Dai H-T, Zhu R-B, Sun B-W, Che C-S and Hou L-J (2020) Effects of Sea Animal Activities on Tundra Soil Denitrification and nirS- and nirK-Encoding Denitrifier Community in Maritime Antarctica. Front. Microbiol. 11:573302. doi: 10.3389/fmicb.2020.573302

In maritime Antarctica, sea animals, such as penguins or seals, provide a large amount of external nitrogen input into tundra soils, which greatly impact nitrogen cycle in tundra ecosystems. Denitrification, which is closely related with the denitrifiers, is a key step in nitrogen cycle. However, effects of sea animal activities on tundra soil denitrification and denitrifier community structures still have received little attention. Here, the abundance, activity, and diversity of nirS- and nirK-encoding denitrifiers were investigated in penguin and seal colonies, and animal-lacking tundra in maritime Antarctica. Sea animal activities increased the abundances of nirS and nirK genes, and the abundances of nirS genes were significantly higher than those of nirK genes ($p < 0.05$) in all tundra soils. Soil denitrification rates were significantly higher ($p < 0.05$) in animal colonies than in animal-lacking tundra, and they were significantly positively correlated ($p < 0.05$) with nirS gene abundances instead of nirK gene abundances, indicating that nirS-encoding denitrifiers dominated the denitrification in tundra soils. The diversity of nirS-encoding denitrifiers was higher in animal colonies than in animal-lacking tundra, but the diversity of nirK-encoding denitrifiers was lower. Both the compositions of nirS- and nirK-encoding denitrifiers were similar in penguin or seal colony soils. Canonical correspondence analysis indicated that the community structures of nirS- and nirK-encoding denitrifiers were closely related to tundra soil biogeochemical processes associated with penguin or seal activities: the supply of nitrate and ammonium from penguin guano or seal excreta, and low C:N ratios. In addition, the animal activity-induced vegetation presence or absence had an important effect on tundra soil denitrifier activities and nirK-encoding denitrifier diversities. This study significantly enhanced our understanding of the compositions and dynamics of denitrifier community in tundra ecosystems of maritime Antarctica.

Keywords: denitrification, nirS and nirK genes, quantitative PCR, community structure, tundra soils, maritime Antarctica

INTRODUCTION

Nitrogen (N) is an essential element for the biosynthesis of key cellular components, such as proteins and nucleic acids, in all organisms (Kuypers et al., 2018). Nitrogen can be converted into multiple chemical forms as it circulates among atmosphere, terrestrial, and marine ecosystems, and microbial nitrogen conversion plays an important role in the nitrogen cycle (Lee and Francis, 2017). Denitrification is one of major biological nitrogen loss processes from natural ecosystems to atmosphere, contributing more than 70% of nitrogen loss (Dalsgaard et al., 2012; Hou et al., 2013; Babbin et al., 2014; Zheng et al., 2015). The denitrification processes are catalyzed by diverse types of metabolic enzymes, and closely related with the denitrifying microorganisms (Baker et al., 2015). Therefore, the abundance, activity, and diversity of denitrifying microorganisms have become research hotspots in the environments.

Nitrite reductases (Nir) is the rate-limiting enzyme among the enzymes that catalyze the denitrification processes (Baker et al., 2015; Chen et al., 2017). Nir encoded by nirS or nirK is structurally different but functionally equivalent (Shrewsbury et al., 2016). The nirS and nirK have been investigated in a variety of environments, including ocean (Braker et al., 2000; Shi et al., 2019), estuarine (Zheng et al., 2015; Gao et al., 2016), river and bay (Huang et al., 2011; Lee and Francis, 2017), wetland (Priemé et al., 2002), glacier foreland and arctic tundra (Heylen et al., 2006; Palmer et al., 2012), and in the rhizosphere (Guyonnet et al., 2018; Achouak et al., 2019). The nirK is found to be far less abundant than nirS in many environments (Mosier and Francis, 2010; Francis et al., 2013; Smith et al., 2015). The abundance, distribution, and diversity of denitrifying genes in environments are affected by multiple environmental variables, such as temperature, pH, salinity, dissolved oxygen, organic matter, and dissolved inorganic nitrogen (NO_3^-, NO_2^-, and NH_4^+) (Cornwell et al., 2014; Zheng et al., 2015; Gao et al., 2016; Li et al., 2017). At present, the abundance, diversity, and distribution of denitrifying genes have been investigated in the Antarctic environment, mainly concentrating on soils of King Sejong Station and the Cape Burk area (Jung et al., 2011; Han, 2013), Antarctic Peninsula (Yergeau et al., 2007; Vero et al., 2019), and the McMurdo Dry Valley (Ward and Priscu, 1997), and microbial mats of King George Island (Alcántara-Hernández et al., 2014; Valdespino-Castillo et al., 2018). However, the information on the distribution of nirS- and nirK-encoding denitrifiers, and their major environmental drivers is still limited in tundra soils of maritime Antarctica.

It is well known that Antarctica has extreme climate conditions with strong winds, limited liquid water availability, and low nutrient contents (Alcántara-Hernández et al., 2014). In coastal Antarctica, the ice-free tundra areas are often colonized by sea animals, such as penguins and seals, and tundra vegetation such as mosses, lichens, and algae. Penguin colonies, tundra vegetation around, and their interactions form a special ornithogenic tundra ecosystem (Tatur et al., 1997; Tatur, 2002). The global seabird database indicates that 69 million pairs of penguins are distributed on Antarctica and the sub-Antarctic islands (Riddick et al., 2012). Penguins provide a large amount of external nitrogen input to their colony soils through direct input of their guano and atmosphere deposition through ammonia volatilization (Sun et al., 2000; Zhu et al., 2011; Riddick et al., 2012). The N and P cycles in the ornithogenic tundra ecosystems are significantly affected by the deposition of a large amount of penguin guano (Riddick et al., 2012; Zhu et al., 2013, 2015b), which is abundant in organic carbon, nitrogen, and phosphorus (Zhu et al., 2011; Otero et al., 2018). The degradation of uric acid, as the main N compound in penguin guano, through mineralization and ammonification, produces NH_3 or NH_4^+, which is subsequently oxidized to nitrate through nitrification, and eventually converted to N_2 through denitrification (Kuypers et al., 2018; Otero et al., 2018). In addition, nitrous oxide (N_2O), as a strong greenhouse gas and stratospheric ozone depletion substance, can be produced during the denitrification in soils (Bothe, 2000; Zhu et al., 2013). It has been found that sea animals significantly increased tundra N_2O emissions in coastal Antarctica (Zhu et al., 2011, 2013, 2015b; Bao et al., 2018). Furthermore, penguin and seal colonies have a significant impact on tundra soil bacterial community structure (Ma et al., 2013; Zhu et al., 2015a), and the abundances, community compositions, and activities of ammonia oxidation archaea (AOA) and bacteria (AOB) are closely related to sea animal activities (Wang Q. et al., 2019). Every summer, a large number of penguin and seal breed on the ice-free land along the coasts of Antarctica and surrounding islands. Therefore, it is of great significance to examine the effects of penguin or seal activities on denitrification for understanding the nitrogen cycle process in tundra ecosystems. However, effects of penguin or seal activities on the abundances, community compositions, and activities of the denitrifiers still have received little attention in tundra soils of maritime Antarctica.

In this study, the soils were collected from a penguin colony, a seal colony, the adjacent animal-lacking tundra, and the slurry experiments were conducted to investigate the denitrification rates of tundra soils. Real-time quantitative PCR (qPCR) and high-throughput sequencing were conducted to investigate the abundance and diversity of nirS- and nirK-encoding denitrifiers in different tundra soils. Our main objectives were (1) to examine potential denitrification rates in tundra soils; (2) to investigate the abundance, diversity, and community structures of nirS- and nirK-encoding denitrifiers; and (3) to determine effects of sea animal activities and environmental variables on the abundances, community compositions, and activities of the denitrifiers in tundra soils of maritime Antarctica.

MATERIALS AND METHODS

Study Area

The study area is located on the Fildes Peninsula (61°51′–62°15′S, 57°30′–59°00′W) and Ardley Island (62°13′S, 58°56′W) in the southwest of King George Island (**Figure 1**). Fildes Peninsula is the largest ice-free area on King George Island in austral summer, covering an area of about 30 km^2. It is one of the warmest and humidest areas in Western Antarctica due to effects of sub-Antarctic maritime climate. According to the long-term

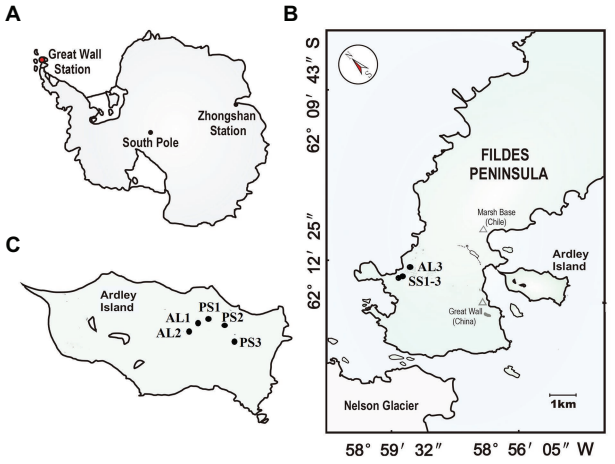

FIGURE 1 | Soil sampling sites. **(A)**: The red dot indicates the location of the study area in maritime Antarctica; **(B)**: the location of the sampling sites on the Fildes Peninsula. The tundra soils included seal colony soils SS (SS1–SS3) in the western coast of the Fildes Peninsula and adjacent seal-lacking tundra soil AL3; **(C)**: the location of the sampling sites on Ardley Island. The tundra soils included the eastern active penguin colony tundra soils PS (PS1–PS3) and the adjacent penguin-lacking tundra soils AL1 and AL2.

meteorological data collected at Great Wall Station on this peninsula, the mean annual temperature is about −2.5°C with a range of −26.6 ~ 11.7°C, and mean annual precipitation is 630 mm with the main form of snowfall.[1] The lichens and mosses dominate local vegetation. On its western coast, there are some seal aggregations including elephant seal (*Mirounga leonine*), Weddell seal (*Leptonychotes weddellii*), fur seal (*Arctocephalus gazella*), and leopard seal (*Hydrurga leptonyx*) (Sun et al., 2004). During the breeding period every summer, a large amount of seal excreta is deposited into tundra soils by snowmelt water. In seal colonies, some seal wallows have been established due to strong seal activity, and tundra patches with sporadic vegetation have formed in the marginal zones of seal wallows, whereas the adjacent seal-lacking tundra areas are predominantly covered by mosses, lichens, and algae (85–90%) due to moderate soil fertility and the absence of seal tramp (Zhu et al., 2013).

Ardley Island, with about 2.0 km in length and 1.5 km in width, is connected to the Fildes Peninsula *via* a sand dam. This island is an important ecological reserve for penguins in Western Antarctica. The local prevailing wind direction is from west or northwest, which leads to the accumulation of less snow in the east of this island (i.e., the leeward slope), and allows the establishment of active penguin colonies mainly in the eastern coast. There are approximately 5,100 breeding pairs including Gentoo (*Pygoscelis papua*), Adélie (*Pygoscelis adeliae*), and Chinstrap penguins (*Phyllophora antarctica*) in the austral summer (Sun et al., 2004). In penguin colonies, many nesting sites and some small puddles are created by penguins. These nesting sites and puddles are highly enriched with penguin guano and devoid of vegetation due to toxic overmanuring and trampling. Many tundra patches with sporadic mosses, algae, and lichens have been formed around penguin nests and puddles. Ornithogenic Cryosols, rich in nitrogen and phosphorus, are well developed due to chemical weathering favored by penguin guano deposition and mineralization (Simas et al., 2007). The adjacent penguin-lacking tundra areas are almost completely (90–95%) covered by cushions of mosses, lichens, and algae. More detailed information about the study area had been given by Zhu et al. (2013).

[1]http://chinare.mnr.gov.cn/catalog/meteorological

Tundra Soil Collection

In our study area, penguin and seal populations are spatially segregated, and penguin guano and seal excreta are transported by snowmelting water, respectively, and accumulated in local tundra soils or washed away in austral summer. During the period from December, 2018 to January, 2019, soil samples were collected from active seal colonies in the western coast of Fildes Peninsula, active penguin colonies in the east of Ardley Island and their adjacent animal-lacking tundra, to study effects of penguin and seal activities on tundra soil denitrification and nirS- and nirK-encoding denitrifier communities, although our soil sample numbers are limited due to local severe climatic conditions and the inaccessible areas. Over three soil samples PS1, PS2, and PS3 were collected from three sites of active penguin colonies, respectively, with the highest density and frequency of penguin populations during the breeding period. The two soil samples AL1 and AL2 were collected from two sites in adjacent penguin-lacking tundra, near the middle upland of Ardley Island, where penguins occasionally wander. In addition, three soil samples SS1, SS2, and SS3 were also collected at three sites of seal colonies, respectively, and one soil sample AL3 in adjacent seal-lacking tundra. All soils were collected from the top 5–10 cm using a clean stainless scoop. For each sampling site, triplicate sub-samples were collected, mixed, and homogenized to constitute a sample (about 300 g). After collection, each soil sample was divided into two parts: one part was stored at −80°C for microbial molecular analysis, and the other part was stored at −20°C for the analyses of soil physicochemical properties and denitrification activity.

Analyses of Tundra Soil Physicochemical Properties

Soil samples were dried at 105°C to a constant weight to measure moisture content expressed as the percentage of weight lost. Organic matter (OM) was determined through the loss of ignition protocol, where soils were ignited in a muffle furnace for 4 h at 550°C after initial oven drying at 105°C. Soil pH was measured by mixing soil and Milli-Q water (1:2.5 ratio). Total nitrogen (TN), total carbon (TC), and total sulfur (TS) were measured using an elemental analyzer (vario MACRO, Elementar, Germany) (Zhu et al., 2011; Hou et al., 2015). The ammonium (NH_4^+-N) and nitrate (NO_3^--N) were extracted from soils with 2 mol L^{-1} KCl, and measured using a continuous-flow nutrient analyzer (Skalar Analytical B.V., Netherlands) (Cheng et al., 2016). After digestion in Teflon tubes using

HNO_3-HCl-HF-$HClO_4$ at 190°C, total phosphorus (TP) was measured using Inductively Coupled Plasma Optical Emission Spectrometer (ICP-OES; Perkin Elmer 2100DV, Waltham, MA, United States) (Gao et al., 2018).

Determination of Denitrification Rates in Tundra Soils

The potential denitrification rates were determined using soil slurry experiments with a nitrogen isotope tracing method. Briefly, slurries were prepared with fresh soils and helium-purged ultrapure water at a soil/water volume ratio of 1:7. The slurries were transferred into a series of glass vials and pre-incubated for 48 h at 10°C, close to the highest air temperature (11.7°C) under summer collection conditions. After pre-incubated, the vials were spiked with helium-purged solutions of $^{15}NO_3^-$. The final concentration of ^{15}N in each vial was approximately 100 μmol L^{-1}. Half of the vials were immediately injected 200 μl 50% $ZnCl_2$ solution into each vial to block slurry incubation. The remaining vials were incubated for 8 h at 10°C, and then were blocked by injecting 200 μl 50% $ZnCl_2$ solution. The concentrations of $^{29}N_2$ and $^{30}N_2$ produced during the incubation were measured by membrane inlet mass spectrometry. The calculation of denitrification rates and more detailed information on slurry experiments have been described in the references (Hou et al., 2015; Cheng et al., 2016).

DNA Extraction and High-Throughput Sequencing

Total DNA was extracted from 0.20 g soil with E.Z.N.ATM Mag-Bind Soil DNA Kit (OMEGA, United States). The extracted DNA was eluted in 60 μl of elution buffer. DNA integrity was checked by agarose gel electrophoresis (DYCZ-21, Beijing). The genomic DNA was quantified using Qubit2.0 DNA Assay Kit (Life, United States). The nirS gene fragment (425 bp) was amplified using primers Cd3aF (5'-GTSAACGTSAAGGAR ACSGG-3') and R3cdR (5'-GASTTCGGRTGSGTCTTGA-3') (Hallin and Lindgren, 1999; Yi et al., 2015). The nirK gene fragment (473 bp) was amplified using primers FlaCu (5'-ATCATGGTSCTG CCGCG-3') and R3Cu (5'-GCCTCGATCAGRTTGTGGTT-3') (Throbäck et al., 2004; Zheng et al., 2015). The 50 μl PCR mixtures contained 25 μl of *Taq* PCR Master Mix, 1 μl of template DNA, 2 μl of each primer (10 μM) and 20 μl of Nuclease-free ddH_2O up to 50 μl (Sangon Biotech, Shanghai, China). The PCR condition was 2 min at 94°C, followed by 35 cycles of 94°C (30 s), 57°C (30 s), and 72°C (1 min) and a final step of 72°C (10 min) for both the nirS and nirK genes. The amplification products were sequenced using Illumina MiSeq in Sangon Company (Shanghai, China). Although primers Cd3aF:R3cdR and FlaCu:R3Cu set are not comprehensive enough to target all nirS-encoding and nirK-encoding denitrifiers, they can be used to compare the denitrifier diversity between soil samples (Throbäck et al., 2004; Blackwood et al., 2005).

Real-Time Quantitative PCR

The abundances of nirS and nirK genes were determined in triplicate by qPCR using a LightCycler480 II Real-time PCR System (Rotkreuz, Switzerland). The primers were the same as those used in high-throughput sequencing. The standard curves showed strong correlations between the threshold cycle (Ct) and the lg values of gene copy numbers (R^2 = 0.9994 for nirS; R^2 = 0.9992 for nirK). The melt curve was checked, and the amplification efficiencies for nirS and nirK were 90.3 and 107.6%, respectively. The standard curves were used to calculate the abundance of nirS and nirK in tundra soils.

Sequence Processing and Phylogenetic Analysis

The nirS and nirK genes sequences were processed using Quantitative Insights Into Microbial Ecology (QIIME) 2 Version:2019.07 (Bolyen et al., 2019). QIIME 2 plugins, including Cutadapt, DeMUX, and DADA2 were used to control sequence quality (Martin, 2011; Callahan et al., 2016). The sequences with 97% similarity were assigned to one operational taxonomic unit (OTU) by QIIME2 plugins, q2-vsearch Version:2019.07 (Rognes et al., 2016). The closest gene sequences in the NCBI database were obtained using NCBI BLASTn tools with a cutoff *E* value $<1e^{-6}$ (Xiong, 2006; Pearson, 2013). Neighbor-Joining Trees was created by MEGA X program and the reliability of the tree topologies was estimated by performing 1,000 bootstrapping replicates.

Statistical Analysis

The diversity indexes, including Chao 1, Shannon-Wiener (*H*), Simpson index (1/*D*), and Pielou's evenness, and the abundance-based coverage estimate Ace were calculated by the R Version:3.6.1 (Shi et al., 2019). Chao 1 was used to estimate total OTU number for the sequences of nirS or nirK genes, Shannon-Wiener (*H*) and Simpson index (1/*D*) indicated alpha diversity for nirS- or nirK-encoding denitrifiers, and Pielou's eveness represented the evenness of the denitrifier community in tundra soils. The abundance-based coverage was used to estimate the gene library coverage. One-way analysis of variation (ANOVA) and *T*-test were calculated for the comparisons between nirS, nirK gene abundances, diversity, and denitrification rates between tundra soils using SPSS Version:20. Correlations between nirS and nirK gene abundances, denitrification rates, and environmental factors were obtained by Pearson correlation analysis (Xiong et al., 2012). The relationships between denitrifying bacterial community structure and environmental factors were explored using canonical correspondence analysis (CCA) on the basis of the results of detrended correspondence analysis (DCA) in the software Canoco Version: 5.0 (Danovaro and Gambi, 2002).

RESULTS

Physicochemical Properties of Tundra Soils

Soil physicochemical properties showed high heterogeneity across different types of tundra sites in maritime Antarctica (**Table 1**). Penguin colony soils (PS1, PS2, and PS3) and the adjacent penguin-lacking tundra soils (AL1 and AL2) were slightly acidic with the pH range from 5.3 to 6.2, whereas

TABLE 1 | Soil properties at tundra sites on Ardley Island and Fildes Peninsula in maritime Antarctica.

Sampling No.	pH	MC	OM	TN	TC	TS	TP	C:N	NH_4^+-N	NO_3^--N
		(%)	(%)	(mg g^{-1})					(mg Kg^{-1})	
Seal colony soils										
SS1	7.0 ± 0.2	23.2	5.54	1.8 ± 0.5	11.1 ± 2.5	1.3 ± 0.2	1.3 ± 0.1	6.0	22.9 ± 5.8	0.1 ± 0.0
SS2	7.3 ± 0.1	28.8	9.09	6.6 ± 0.5	34.6 ± 2.9	2.6 ± 0.3	5.0 ± 0.2	5.3	77.7 ± 10.2	0.2 ± 0.1
SS3	7.6 ± 0.1	21.6	8.48	4.8 ± 0.3	21.1 ± 1.8	2.3 ± 0.2	3.6 ± 0.2	4.4	85.4 ± 11.1	0.1 ± 0.0
Mean	7.3 ± 0.3[a]	24.5[a]	7.70[a]	4.4 ± 2.1[a]	22.3 ± 10.4[a]	2.1 ± 0.6[ab]	3.3 ± 1.9[a]	5.2 ± 0.8[a]	62.0 ± 31.8[a]	0.1 ± 0.1[a]
Penguins colony soils										
PS1	5.4 ± 0.1	68.2	47.9	20.5 ± 0.2	194.7 ± 1.5	3.4 ± 0.2	23.7 ± 0.3	9.5	67.2 ± 14.0	1.5 ± 0.4
PS2	5.3 ± 0.2	69.8	43.7	27.5 ± 0.7	180.5 ± 2.8	6.7 ± 0.2	32.9 ± 0.3	6.6	119.5 ± 29.3	1.4 ± 0.5
PS3	5.5 ± 0.1	64.7	20.9	9.6 ± 0.5	92.0 ± 5.6	2.8 ± 0.3	12.5 ± 0.3	9.6	33.5 ± 6.0	0.2 ± 0.1
Mean	5.4 ± 0.2[b]	67.5[b]	37.5[b]	19.2 ± 7.8[b]	155.7 ± 48.3[b]	4.3 ± 1.8[a]	23.0 ± 10.2[b]	8.6 ± 1.7[ab]	73.4 ± 41.0[b]	1.0 ± 0.9[a]
Animal-lacking soils										
AL1	5.7 ± 0.2	46.01	15.2	4.3 ± 0.1	39.0 ± 1.0	0.9 ± 0	8.1 ± 0.2	9.1	9.7 ± 2.8	12.0 ± 2.2
AL2	6.2 ± 0.1	35.48	8.80	2.3 ± 0.1	22.1 ± 1.3	0.5 ± 0.3	5.7 ± 0.1	9.5	2.7 ± 0.8	0.2 ± 0.0
AL3	7.1 ± 0.1	25.02	9.05	0.2 ± 0.0	3.2 ± 0.2	0.1 ± 0.0	0.2 ± 0.0	16.0	0.1 ± 0.1	0.1 ± 0.0
Mean	6.3 ± 0.6[c]	35.50[a]	11.0[a]	2.3 ± 1.8[a]	21.4 ± 15.5[a]	0.5 ± 0.4[b]	4.7 ± 4.1[a]	11.5 ± 3.9[b]	4.2 ± 3.6[a]	4.1 ± 6.9[a]

MC, the moisture content of soil; ND indicated that the soil sample was not determined. For the measured soil properties of each tundra, tundra soil types with different letters (a, b, or c) are significantly different from one another (ANOVA, $p < 0.05$).

seal colony soils (SS1–SS3, AL3) were neutral to slightly alkaline with small pH variation (7.0–7.6). The highest levels of MC, OM, TN, TC, TS, TP, and NH_4^+-N occurred in penguin colony soils (PS1–PS3). Compared with animal-lacking tundra soils, active penguin and seal colony soils had much higher TN, TS, TP, and NH_4^+-N contents most likely due to the deposition of penguin guano or seal excreta. Especially, the NH_4^+-N and TS contents in penguin colony soils (means: 73.4 mg NH_4^+-N kg^{-1} and 4.3 mg S g^{-1}) and seal colony soils (means: 62.0 mg NH_4^+-N kg^{-1} and 2.1 mg S g^{-1}) were one to two orders of magnitude higher than those in animal-lacking tundra soils (means: 4.2 mg NH_4^+-N kg^{-1} and 0.5 mg S g^{-1}). In addition, penguin colony soils (PS1–PS3) and its adjacent tundra soils AL1 had higher NO_3^--N (1.0–12.0 mg kg^{-1}) than seal colony soils (SS1–SS3) and animal-lackingtundra soils AL2 and AL3 (0.1–0.2 mg kg^{-1}). Seal colony soils had lower C:N ratios (mean:5.2) than penguin colony soils (mean:8.6) and animal-lacking tundra soils (mean:11.5). Overall, the deposition of penguin guano or seal excreta altered local soil biogeochemical properties, leading to generally low C:N ratios and high TN, TS, TP, and NH_4^+-N contents in fauna-related tundra soils.

Gene Abundances of nirS and nirK in Tundra Soils

The abundances of nirS genes were significantly higher than those of nirK genes in all tundra soils (*t*-test, $n = 9$, $p < 0.05$). The abundances of nirS genes in penguin and seal colony soils (3.5×10^6–2.5×10^7 copies g^{-1}) were two to four orders of magnitude higher than those in the animal-lacking tundra soils (5.9×10^3–4.9×10^5 copies g^{-1}). The highest nirS gene abundance was detected in SS2, whereas the lowest occurred in AL3 (**Figure 2A**). The abundances of nirK genes showed heterogeneous distribution patterns among the tundra soils (**Figure 2B**). Overall, the abundances of nirK genes in PS (PS1–PS3) and SS (SS1–SS3) were higher than those in animal-lacking tundra soils AL (AL1–AL3). The gene abundances, especially for nirK genes, show a high variability even within the same sample types due to effects of the deposition of penguin guano or seal excreta, and levels of animal activities. The extremely high abundances of nirK genes occurred in SS1 (6.2×10^5 copies g^{-1}) and PS3 (3.2×10^5 copies g^{-1}), one to three orders of magnitude higher than those in other soils within animal colonies (4.5×10^4–9.1×10^4 copies g^{-1}) and in adjacent animal-lacking tundra soils (7.4×10^2–1.5×10^4 copies g^{-1}). The lg values of both nirS and nirK genes abundances showed significant negative correlations ($r = -0.791$, $p = 0.011$ for nirS; $r = -0.708$, $p = 0.033$ for nirK) with C:N ratios in tundra soils (**Figures 3A,B**). No significant correlation was obtained between nirS and nirK genes abundances and other environmental parameters (**Supplementary Table S1**). Therefore, tundra soil C:N ratios were predominant factors affecting nirS and nirK gene abundances in maritime Antarctica.

Denitrification Rates in Tundra Soils

The heterogeneous distribution pattern for denitrification rates was observed among different tundra soils, with the range

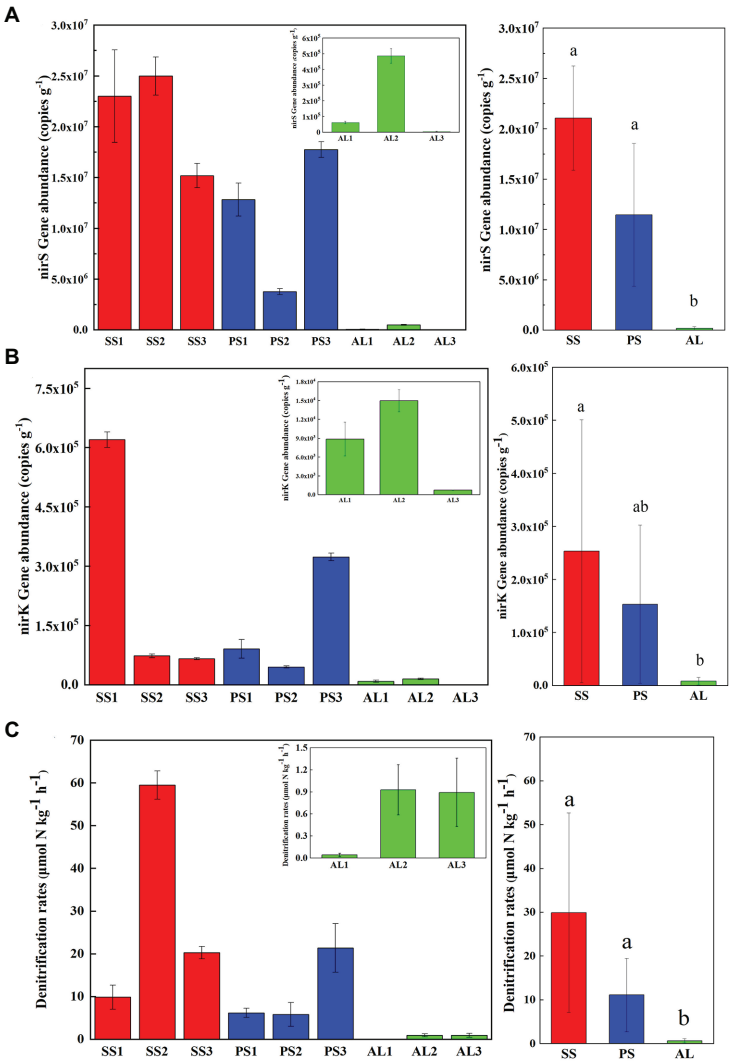

FIGURE 2 | Comparisons of the abundances of nirS **(A)** and nirK **(B)** genes, and denitrification rates **(C)** in tundra soils of maritime Antarctica. Left figures presented the mean abundances of nirS **(A)** and nirK **(B)** genes, and the mean denitrification rates **(C)** in the soils of individual tundra site; Right figures indicated the mean abundances of nirS **(A)** and nirK **(B)** genes, and the mean denitrification rates in seal colony soils (SS), penguin colony soils (PS), and animal-lacking tundra soils (AL). The different letters indicated statistically significant differences (ANOVA, $p < 0.05$). The error bars indicate standard deviations of the averages.

from 0.04 to 59.49 μmol N kg^{-1} h^{-1} (**Figure 2C**). Overall, the denitrification rates in penguin or seal colony soils were significantly higher ($p < 0.05$) than those in animal-lacking tundra soils. The mean highest rate occurred in seal colony soils (mean 29.88 ± 22.77 μmol N kg^{-1} h^{-1}), followed by penguin colony soils (mean 11.10 ± 8.34 μmol 11 N kg^{-1} h^{-1}), two orders of magnitude higher than those in animal-lacking tundra soils (mean 0.62 ± 0.50 μmol N kg^{-1} h^{-1}). Of all tundra soils, the highest rate occurred at SS2 (59.49 ± 3.3 μmol N kg^{-1} h^{-1}) with the highest nirS gene abundance. Even within penguin or seal colony, the denitrification rates also showed high variability between tundra soil samples due to effects of these animal activities and the deposition of their excreta. The denitrification rates in SS2, SS3, and PS3 (20.29–59.49 μmol N kg^{-1} h^{-1}) were one order of magnitude higher than those in SS1, PS1, and PS2 (5.79–9.85 μmol N kg^{-1} h^{-1}). The denitrification rates were significantly positively correlated with nirS gene abundances ($r = 0.733$, $p = 0.02$) in tundra soils, but no correlation was obtained between denitrification rates and nirK gene abundances (**Figures 3C,D**). In addition, no significant correlations were found between the denitrification rates and soil physicochemical properties in maritime Antarctic tundra (**Supplementary Table S1**).

Diversity for nirS- and nirK-Encoding Denitrifiers in Tundra Soils

In total, 470,556 high-quality sequences of nirS genes were obtained from all tundra soils. These sequences were clustered into 1,095 OTUs with 97% similarity. As for nirK genes, 385,042 high-quality sequences were obtained and clustered

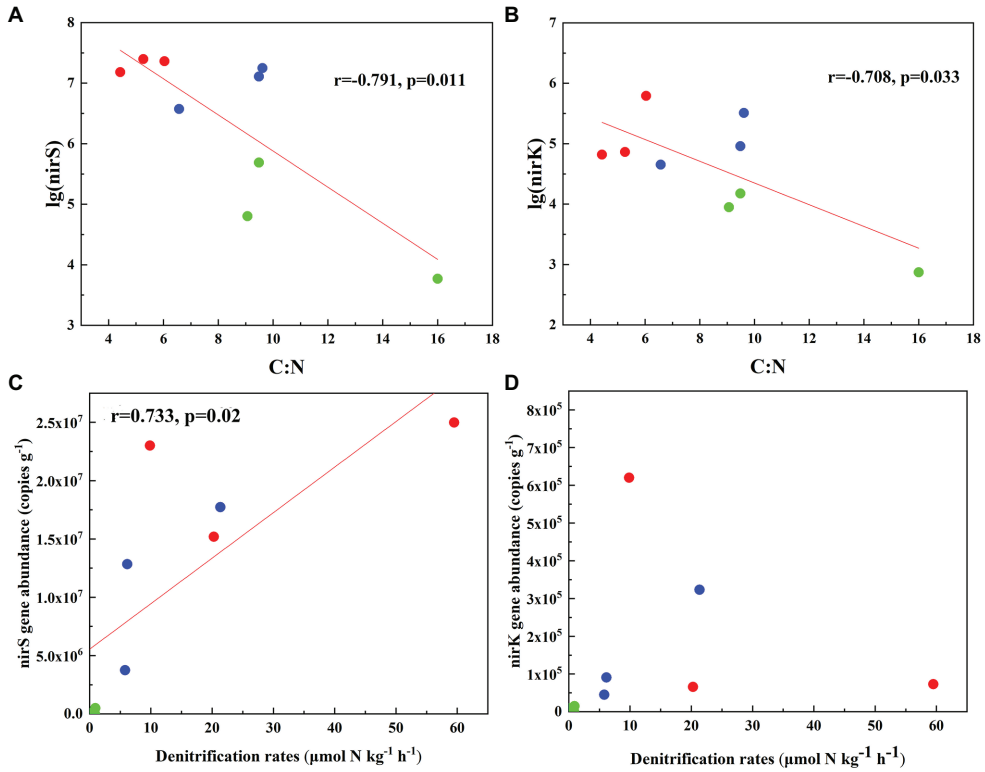

FIGURE 3 | Pearson's correlation between nirS and nirK genes abundances and tundra soil C:N **(A,B)**, and between denitrification rates and nirS, nirK gene abundances **(C,D)** in tundra soils of maritime Antarctica. The red, blue, and green dots represent the soils from SS, PS, and AL sites, respectively.

into 1,692 OTUs with 97% similarity. The Chao 1 of nirK-encoding denitrifiers (120–458) was higher than that of nirS-encoding denitrifiers (128–304) (**Supplementary Table S2**). The Pielou's evenness, Shannon-Wiener, and Simpson (1/*D*) indexes of nirK-encoding denitrifiers were higher than those of nirS-encoding denitrifiers in animal-lacking tundra soils (AL1, AL2, and AL3) but lower in sea animal colony soils. The three indexes for the nirS-encoding denitrifiers were higher in penguin or seal colony soils than in animal-lacking tundra soils (**Figure 4**). On the contrary, the three indexes of nirK-encoding denitrifiers were lower in animal colony soils than those in animal-lacking tundra soils. The Pielou's evenness indexes for nirS- and nirK-encoding denitrifiers in penguin colony soils had significant difference (ANOVA, $p < 0.05$) from those in animal-lacking tundra soils. The Simpson (1/*D*) indexes for the nirK-encoding denitrifiers were significantly lower in penguin colony soils than in animal-lacking tundra soils (ANOVA, $p < 0.05$). For the same soil sample types, the Pielou's Evenness Index and Shannon-Wiener Index (*H*) for the nirS- and nirK-encoding denitrifiers showed a low variability with the small standard deviations of the means. However, the Simpson Index (1/*D*) showed a high variability even between the same soil sample types (**Supplementary Table S2**). In addition, the Pielou's evenness index of nirS-encoding denitrifiers showed significant negative relationships with C:N ratios ($R = -0.68$, $p < 0.05$), whereas the evenness index of nirK-encoding denitrifiers showed significant negative relationships with TN, TC, and TS (**Figure 5**).

Compositions of nirS- and nirK-Encoding Denitrifiers in Tundra Soils

Phylogenetic analysis of nirS genes showed that a large proportion of unique OTUs matched to uncultured environmental nirS assemblages (**Figure 6A**). The majority of tundra soil nirS OTUs found in maritime Antarctica, closely matching to the sequences in the Genbank, were obtained from some environments but not always from obviously similar environments. The minor nirS OTUs matching to bacteria were assigned to *Proteobacteria* in tundra soils. The most abundant 50 OTUs were grouped into distinctly defined seven clusters (I–VII) on the basis of evolutionary distance. The cluster I contained eight OTUs, and 31,340 nirS gene sequences with 53.3% of the sequences from AL, 36.5% from PS, and 10.2% from SS, and they were closely related to those in sediments of Qinghai-Tibetan Plateau river (MH634647) and Tibetan Plateau wetland (KC468828). The cluster II contained eight OTUs, and 51,450 sequences with 45.8% of the sequences from AL, 35.6% from PS, and 18.6% from SS, and they closely matched to those in estuarine sediments from San Francisco Bay (GQ453804) (Mosier and Francis, 2010). The cluster III contained four OTUs and 25,099 sequences with 77.7% from SS, 11.6% from PS, and only 10.7% from AL, and their sequences

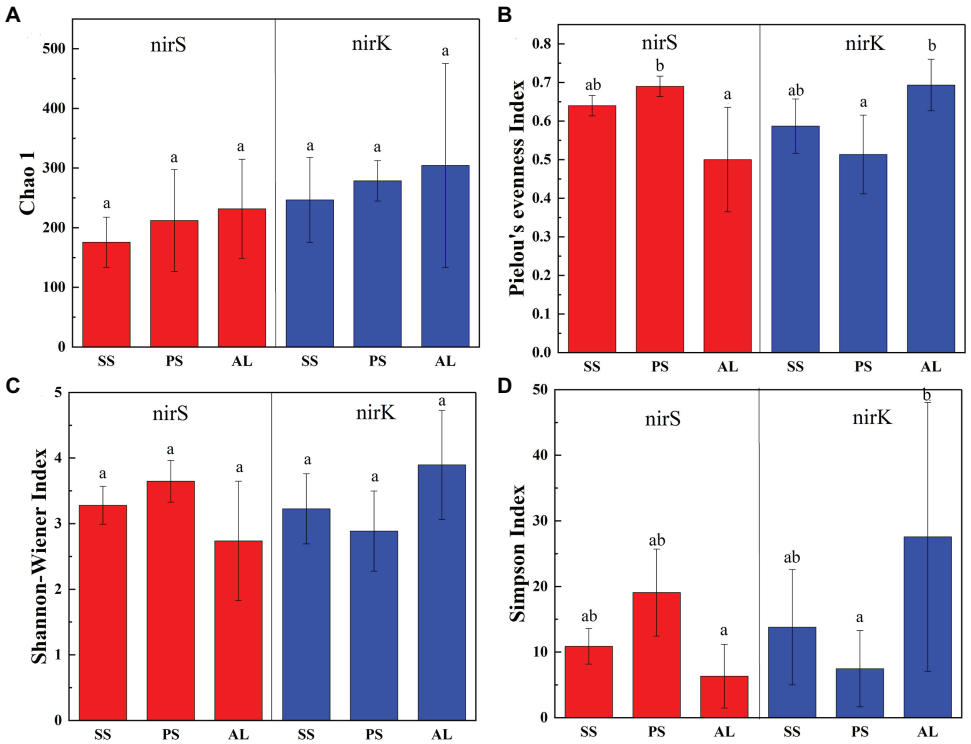

FIGURE 4 | Richness and diversity of nirS and nirK genes in seal colony soils (SS), penguin colony soils (PS), and animal-lacking tundra soils (AL) in maritime Antarctica. **(A)** Chao 1, **(B)** Pielou's evenness Index, **(C)** Shannon-Wiener Index, **(D)** Simpson Index. The error bars indicate standard deviations of the averages. The different letters indicated statistically significant differences (ANOVA, $p < 0.05$).

were closely related to those found in the microbial mats of King George Island (KC951310) (Alcántara-Hernández et al., 2014). The cluster IV contained 13 OTUs and 69,288 sequences, and 50.5% of sequences were from SS, 34.2% from PS, and only 15.3% from AL. The cluster V contained three OTUs and 8,986 sequences, only accounting for 2.5%, and phylogenetically similar to *Proteobacteria*, with 47.2% of sequences from PS, 42.2% from AL, and 10.6% from SS. The cluster VI contained five OTUs and 37,097 sequences, and 39.8% of sequences were from PS, 49.3% from SS, and only 10.9% from AL. The cluster VII had nine OTUs and the most nirS gene sequences (130,157), accounting for 36.8% of the total 50 OTU sequences, with 43.9% from AL, 29.7% PS, and 26.4% from SS, and they closely matched to those found in Baltic Sea (EF615460.1), Yangtze lakes (KU159637), and Pearl River (JN016582). Overall, tundra soils contained all the seven clusters except AL1 and AL3. The clusters III, IV, VI, and VII appeared in all tundra soils. The dominant clusters in nirS genes from penguin and seal colony soils were II, IV, VI, and VII, accounting for 58.3–92.0% of nirS gene sequences (**Figure 7A**). The dominant clusters in AL1 were clusters I and II, accounting for 79.8%. As for AL2 and AL3, the most dominant cluster was cluster VII, accounting for 59.7 and 99.0%, respectively. The nirS gene sequences of AL3 had only one OTU (OTU1) in cluster VII, which was aligned with *Pseudomonas stutzeri* SLG510A3-8 (CP011854) and had 100.0% identity from the Genbank.

Similar to nirS genes, phylogenetic analysis of nirK genes also showed that a large proportion of unique OTUs matched to uncultured environmental nirK assemblages. The most abundant 50 nirK OTUs were grouped into six distinctly defined clusters (I–VI) on the basis of evolutionary distance (**Figure 6B**). The most abundant cluster I contained 15 OTUs and 78,457 sequences, accounting for 29.0% of total 50 OTU sequences, with 44.1% from PS, 50.5% from SS, and only 5.4% from AL, and they were closely related to *Mesorhizobium* sp. (AY078254) (Song and Ward, 2006) and similar environment sequences from acidic peat soils in arctic tundra (FR865824) (Palmer et al., 2012). The cluster II contained four OTUs and 17,862 sequences with 3.7% of sequences from PS, 3.1% from SS, and 93.2% from AL. The cluster III contained 16 OTUs and 66,761 sequences with 24.0% from PS, 49.8% from SS, and 26.2% from AL, whereas the cluster IV contained 13 OTUs and 42,125 sequences with 8.7% from PS, 39.2% from SS, and 52.1% from AL. These two clusters included 24.7 and 15.6% of total sequences, respectively, and were closely related to those from some lake or estuarine sediments, such as Yangtze lakes (MF776282; KU159621) (Jiang et al., 2017), San Francisco Bay estuary (KR060158; KR060517) (Lee and Francis, 2017), Yellow River Estuary (KF144040; KX952261) (Li et al., 2014), Lake Baikal (MK460630), Chesapeake Bay estuary (EU725900) (Fortunato et al., 2009), and microbial mats on King George Island (KC951296; KC951293; KC951286) (Alcántara-Hernández et al., 2014).

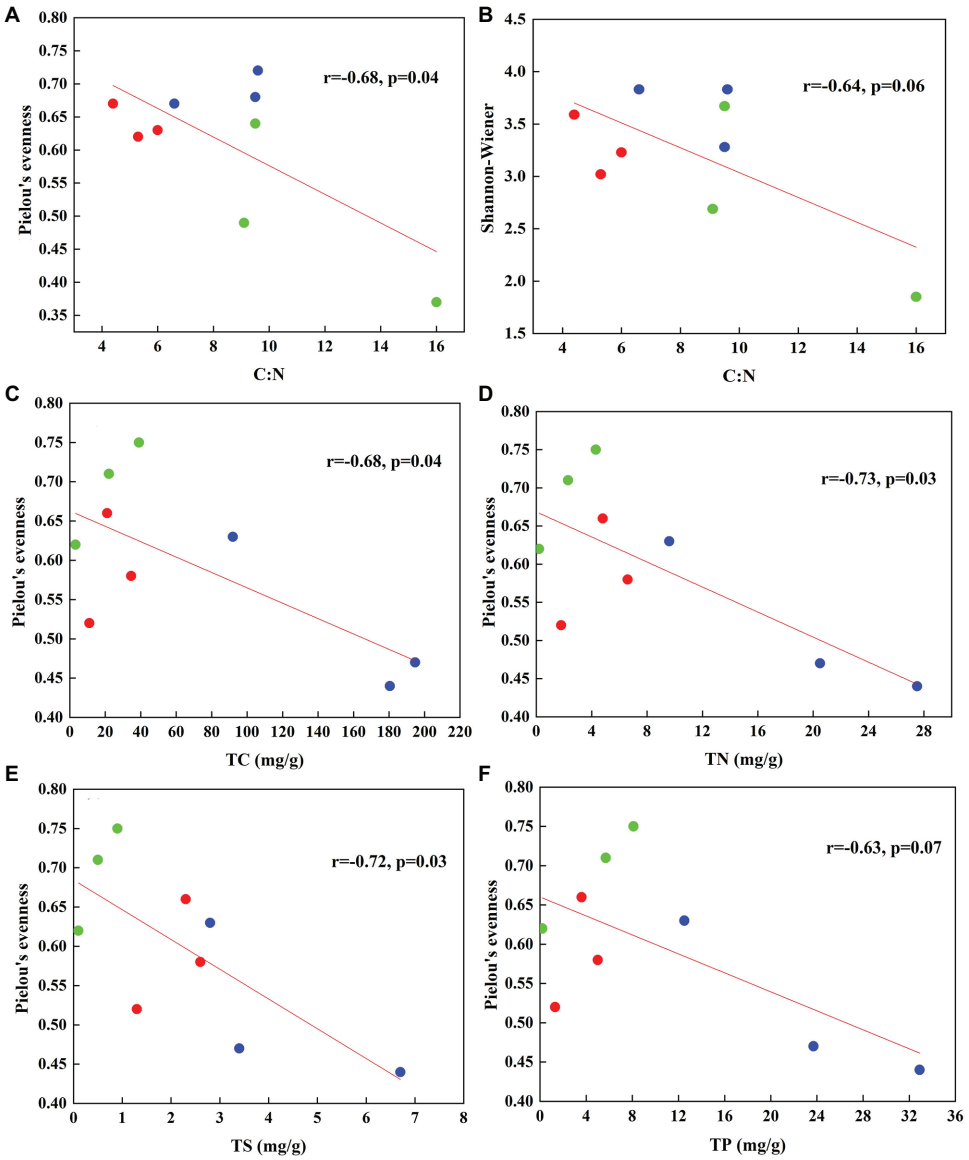

FIGURE 5 | The relationships between the diversity of nirS type **(A,B)** and nirK type **(C–F)** denitrifiers and soil biogeochemical parameters associated with sea animal activities in tundra soils of maritime Antarctica (n = 9). The red, blue, and green dots represent the soils from SS, PS, and AL sites, respectively.

The cluster V contained one OTU and 53,453 sequences with 75.2% from AL, 24.7% from SS, and 0.1% from PS, and cluster VI also contained one OTU and 1,578 sequences with 88.7% from SS, 10.9% from AL, and 0.4% from PS. These two clusters accounted for 23.5 and 0.6% of total sequences, respectively, and were related to *Nitrosospira* (CP021106) (Urakawa et al., 2015) and *Desulfosarcina* (AP021879), respectively. Overall, the clusters II, III, and IV were found in all the nine tundra soils. The dominant clusters from penguin and seal colony soils were I, III, and V, accounting for 62.0 to 99.7% of total sequences (**Figure 7B**). Clusters III and IV were the dominant clusters for tundra soils AL1 and AL2, respectively, whereas the dominant cluster was II in tundra soils AL3, accounting for 81.2%.

Relationships of Denitrifier Community Structure With Environmental Variables in Tundra Soils

The relationships of the nirS- and nirK-encoding denitrifier community structure with environmental variables were analyzed by the CCA. The environmental variables in the first two CCA dimensions (CCA1 and CCA2) provided 67.7% of cumulative variation of the nirS-encoding denitrifying community-environment relationship (**Figure 8**). The nirS community structure significantly correlated with NO_3^--N (F = 3.2, p = 0.012, 1,000 Monte Carlo permutations) and NH_4^+-N (F = 2.5, p = 0.023), which together explained 53.6% of the variation (**Table 2**). Although other environmental variables, including

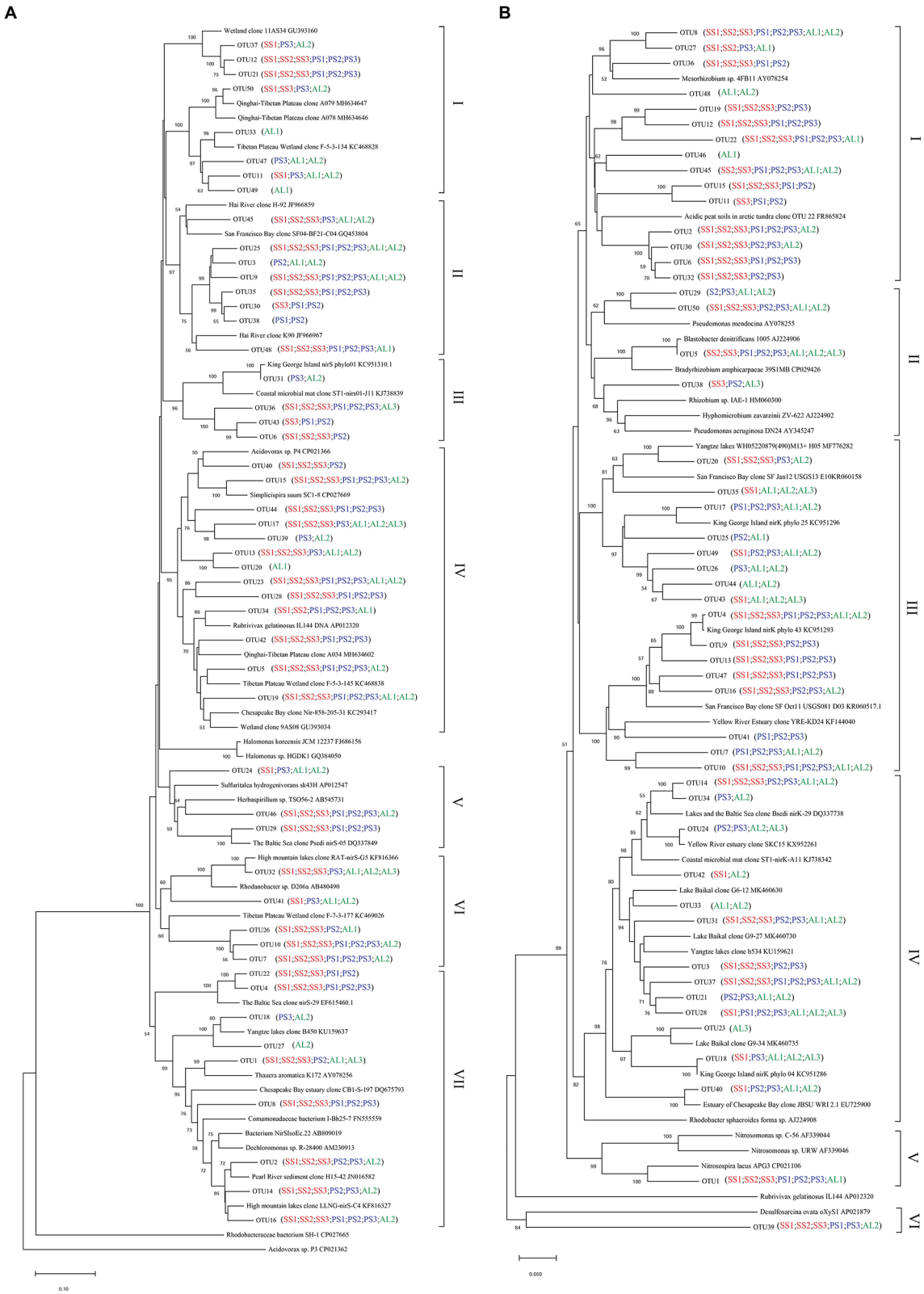

FIGURE 6 | Neighbor-joining phylogenetic tree of nirS **(A)** and nirK **(B)** sequences in tundra soils of maritime Antarctica. Bootstrap values ≥ 50% (n = 1,000) are shown near the nodes. Operational taxonomic units (OTUs) were defined at 97% similarity.

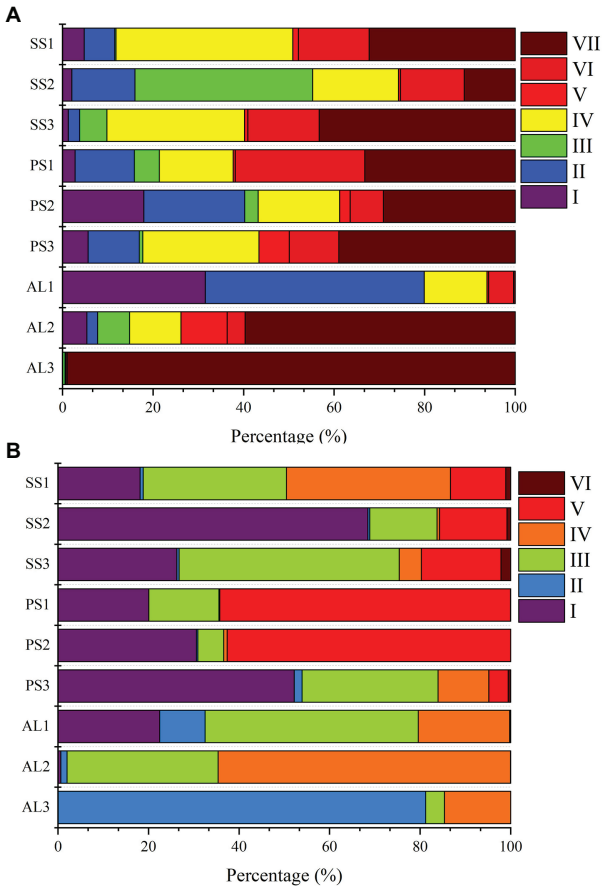

FIGURE 7 | Relative abundances of nirS-encoding **(A)** and nirK-encoding **(B)** denitrifiers sequences retrieved from penguin and seal colony soils and animal-lacking tundra soils, as related to different nirS-encoding and nirK-encoding denitrifier clusters. The analysis was based on the most abundant 50 OTUs from different tundra soils of maritime Antarctica.

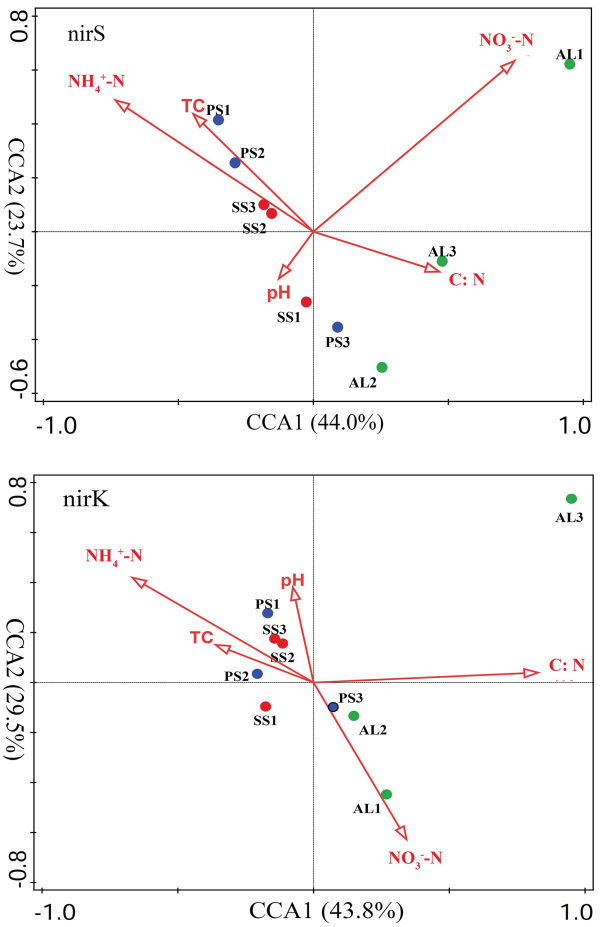

FIGURE 8 | Canonical correspondence analysis (CCA) ordination plots for the relationship between the nirS and nirK community structures with environmental variables. C:N, TC, NH_4^+-N, NO_3^--N represent C:N ratios, total carbon, ammonium, and nitrate, respectively.

pH, C:N, and TC were not statistically significant ($p > 0.05$), these variables additionally explained 40.7% of the variation. The first two dimensions explained 73.3% of the cumulative variation of the nirK-encoding denitrifying community-environment relationship. The nirK community structure significantly correlated with C:N ($F = 2.7$, $p = 0.011$) and NH_4^+-N ($F = 2.2$, $p = 0.025$), which together explained 51.3% of the variation. Other environmental variables, including NO_3^--N, pH, and TC, accounted for 43.8% of the variation.

TABLE 2 | Individual and combined contributions of soil biogeochemical properties to the nirS and nirK community structures in maritime Antarctica.

Gene	Soil properties	*F*	*p*	Individual contribution
nirS	NO_3^--N	3.2	0.012	31.2%
	NH_4^+-N	2.5	0.023	22.4%
	TC	1.5	0.147	17.2%
	C:N	1.3	0.216	15.7%
	pH	0.8	0.634	7.8%
	Combined effect			94.3%
nirK	C:N	2.7	0.011	27.5%
	NH_4^+-N	2.2	0.025	23.8%
	NO_3^--N	1.8	0.176	20.8%
	TC	1.0	0.390	12.9%
	pH	0.8	0.631	10.1%
	Combined effect			95.1%

DISCUSSION

Effects of Sea Animal Activities on the Abundances of Tundra Soil Denitrifiers

In this study, although nirS- and nirK-encoding denitrifiers were detected in all tundra soils, the abundances of nirS-encoding denitrifiers were significantly higher than those of nirK-encoding denitrifiers (**Figure 2**), which agreed with the results from other environments, such as the Yellow River Estuary (Li et al., 2017), Daya Bay (Shi et al., 2019), San Francisco Bay (Lee and Francis, 2017), and Antarctic King Sejong Station (Jung et al., 2011). The nirS gene abundances

(3.8×10^6–2.5×10^7 copies g^{-1}) in penguin and seal colony soils were close to those from the soils of King Sejong Station in Antarctica (Jung et al., 2011) (10^7–10^8 copies g^{-1} soil), higher than those in Tibet Plateau soils (2.03×10^4–1.28×10^6 copies g^{-1}) (Wang S. et al., 2019), but lower than those in Arctic seabird-affected taluses soils (6.2×10^8–1.8×10^9 copies g^{-1}) (Hayashi et al., 2018). The nirK gene abundances (7.4×10^2–6.2×10^5 copies g^{-1}) were significantly lower compared with nirS gene, consistent with those (10^3–10^6 copies g^{-1} soil) in soils from King Sejong Station in Antarcitc (Jung et al., 2011), and Svalbard (Hayashi et al., 2018). In addition, both the abundances of nirS and nirK genes were two to four orders of magnitude higher in penguin or seal colony soils than in animal-lacking tundra soils, indicating that sea animal activities greatly increased tundra soil nirS and nirK gene abundances, which were consistent with high bacterial abundances in penguin or seal colony soils and ornithogenic sediments in maritime Antarctica (Ma et al., 2013; Zhu et al., 2015a) and high denitrifier genes in seabird-affected taluses in High Arctic (Hayashi et al., 2018). The nirS gene abundances accounted for only 0.20–0.25% of the bacterial abundances (1.88×10^9–1.00×10^{10} gene copies g^{-1}) in penguin and seal colony soils, whereas the proportion of nirK gene abundances in the bacterial abundances were two to three orders of magnitude lower than that of nirS gene abundances (Ma et al., 2013).

Our previous studies showed that penguin or seal activities led to generally low C:N ratios, which had been used as an indicator for the intensity of penguin or seal activities in maritime Antarctica (Wang Q. et al., 2019). The abundances of nitrifiers and denitrifiers in soils were significantly correlated with C:N ratios in previous study (Fu et al., 2016). The negative correlations of the lg values of nirS and nirK gene abundances with C:N ratios (**Figure 3**) indicated that sea animal activities, which changed tundra soil C:N ratios, had an important effect on the denitrifier abundances in tundra soils. Many environmental variables (e.g., temperature, pH, salinity, dissolved oxygen, organic matter, and dissolved inorganic nitrogen) could affect the abundances of soil nirS and nirK genes (Zheng et al., 2015; Fu et al., 2016; Gao et al., 2016; Li et al., 2019; Shi et al., 2019). However, in this study, nirS and nirK gene abundances were not significantly related with other environmental variables (**Supplementary Table S1**), possibly due to the low number of soil sample replicates within the same type of tundra soils. Overall, the lg values of nirS and nirK gene abundances showed a significant negative correlation with soil C:N ratios across different types of tundra soils. Therefore, the change in tundra soil C:N ratios, associated with sea animal activities, was the predominant factor affecting the denitrifier abundances in tundra soils of maritime Antarctica.

Effects of Sea Animal Activities on the Activities of Tundra Soil Denitrifiers

The denitrification rates in animal colony soils (5.78–59.49 μmol N kg^{-1} h^{-1}) were significantly higher than those in adjacent animal-lacking tundra soils (0.04–0.93 μmol N kg^{-1} h^{-1}) (**Figure 2**), similar to ammonia oxidation rates measured in tundra soils (Wang Q. et al., 2019), indicating that penguin or seal activities had important effects on tundra soil denitrification rates in maritime Antarctica. In addition, the denitrification rates in animal colony soils were also higher than those measured in Tibet Plateau soils (0.39–2.57 μmol N kg^{-1} h^{-1}) (Wang S. et al., 2019), but significantly lower than those in Arctic seabird-affected taluses soils (187.1–348.6 μmol N kg^{-1} h^{-1}) (Hayashi et al., 2018), similar to those measured in northern Sweden tundra soils (7.1–114.3 μmol N kg^{-1} h^{-1}) (Björk et al., 2007), northeast Finland fen soils (36.4 μmol N kg^{-1} h^{-1}) (Palmer et al., 2012), and Russian discontinuous permafrost soils (35.7–55.7 μmol N kg^{-1} h^{-1}) (Palmer and Horn, 2015) although they were detected at higher temperature (20°C) in these other environments (**Supplementary Table S4**). The denitrification rates in animal-lacking tundra soils were similar to those in Tibet Plateau soils (Wang S. et al., 2019), but much lower than those in northern Sweden tundra soils (Björk et al., 2007), northeast Finland fen soils (Palmer et al., 2012), Russian discontinuous permafrost soils (Palmer and Horn, 2015), and Arctic seabird-affected talus soils (Hayashi et al., 2018).

Generally, the denitrification rates were affected by the abundances of nirS-encoding denitrifiers (Mosier and Francis, 2010; Gao et al., 2016). In this study, the denitrification rates were significantly positively correlated with nirS gene abundances ($r = 0.733$, $p = 0.02$). However, no significant statistical correlation was obtained between the denitrification rates and nirK gene abundances, tundra soil physicochemical properties. Therefore, compared to nirK gene abundances and soil physicochemical properties, the abundances of nirS genes better predicted the denitrifier activities in tundra soils of maritime Antarctica. In this study, the animal-lacking tundra areas were covered with the cushions of mosses and lichens due to moderate amount of nutrients and the absence of animal trampling. These tundra plants can absorb the limited soil N, highly limit the inorganic N (NH_4^+-N) availability for the denitrifiers (**Table 1**), thus might restrict the denitrification rates in tundra soils (Marushchak et al., 2011; Zhu et al., 2013). In addition, the positive relationship between denitrification rates and temperature had been reported by Hou et al. (2015) and Cheng et al. (2016), which was likely due to the increase in the denitrifier activity (Wallenstein et al., 2006). The denitrifiers are sensitive to temperature with the optimal temperature of 25–27°C for denitrification (Canion et al., 2014), implying that the denitrification rates in tundra soils will be likely to further increase in the context of global warming under the disturbance of penguin or seal activities in maritime Antarctica.

Effects of Sea Animal Activities on the Diversity of Tundra Soil Denitrifiers

Biological diversity metrics are based on species counts, which require DNA sequence data to be clustered into taxonomic units. Different OTU cutoffs of DNA sequence identity generated different OTU number and Chao 1 index (Lee and Francis, 2017). The OTU number and Chao1 of nirK-encoding denitrifiers were higher than those of nirS-encoding denitrifiers except sites PS2 and AL3. For nirS and nirK, different OTU cutoffs generated little difference in diversity, and all clustering levels led to similar conclusions about the environmental factors

influencing denitrifier community compositions (Lee and Francis, 2017). For nirS- and nirK-encoding denitrifiers, the Pielou's Evenness Index and Shannon-Wiener Index (*H*) showed a low variability within the same sample types (**Figure 4**). However, the Simpson Index (1/*D*) showed a heterogeneous distribution pattern, possibly because the inverse of Simpson Index (1/*D*) is sensitive to the level of dominance in a community (Magurran, 1988). Compared with animal-lacking tundra soils, Shannon and Simpson indexes of nirS-encoding denitrifiers were higher in penguin or seal colony soils (**Figure 4**), indicating that sea animal activities influenced the nirS-encoding denitrifier diversity in tundra soils. Generally, penguin or seal activities led to generally low C:N ratios, compared to normal tundra soils in maritime Antarctica (Wang Q. et al., 2019). The significant negative correlation ($R = -0.68$, $p = 0.04$) between Pielou's evenness of nirS-encoding denitrifiers and tundra soil C:N ratios (**Figure 5**) further indicated a relationship between nirS-encoding denitrifier diversity and sea animal activities.

For nirK-encoding denitrifiers, their diversity was lower than nirS-encoding denitrifiers in sea animal colonies, which was in accordance with other environments, such as sediments of San Francisco Bay (Lee and Francis, 2017), Yangtze Estuary (Zheng et al., 2015), and acidic peat soil in arctic tundra (Palmer et al., 2012). However, in animal-lacking tundra soils (AL1, AL2, and AL3), the diversity of nirK-encoding denitrifiers was higher than that of nirS-encoding denitrifiers (**Figure 4**). Desnues et al. (2007) found that nirS-encoding denitrifiers were mainly located in the permanent anoxic layer, whereas nirK-encoding denitrifiers were found in zones with high oxygen and pH fluctuations. Animal-lacking tundra soils were covered with cushions of mosses and lichens, which were vertically layered communities with high photosynthetic production rates (Stal, 2012), whereas animal colony soils were devoid of the coverage of tundra vegetation due to toxic overmanuring and trampling (**Supplementary Figure S1**) (Zhu et al., 2013). Compared with animal colony soils, oxygen concentration fluctuated in animal-lacking tundra soils because of the photosynthesis of mosses or lichens (Fernández-Valiente et al., 2007). Therefore, nirK-encoding denitrifiers more adapted to animal-lacking tundra soils covered with vegetation, compared with animal colony soils. Alcántara-Hernández et al. (2014) also reported that the diversity of nirK-encoding denitrifiers was greater than that of nirS-encoding denitrifiers in microbial mats on King George Island of maritime Antarctica. In addition, significant negative relationship of the Pielou's evenness of nirK genes with TN, TC, and TS levels (**Figure 5**), further indicated that animal activities probably decreased the nirK-encoding denitrifier diversity in tundra soils of maritime Antarctica. However, there was no significant relationship between Shannon-Wiener Index (*H*) and Simpson Index (1/*D*) for the denitrifiers and soil environmental variables, which could be due to the low number of soil sample replication within the same tundra types.

Effects of Sea Animal Activities on Compositions of Tundra Soil Denitrifiers

Our previous studies showed that the dominant bacterial phyla in animal colony and tundra soils in Antarctica were *Proteobacteria* (mean 48.6%), *Actinobacteria* (mean 16.3%), and *Bacteroidetes* (mean 8.6%), and *Proteobacteria* was the most dominant bacterial phylum (Ma et al., 2013). However, in this study, the minor nirS and nirK OTUs matching to bacteria were assigned to *Proteobacteria*. Phylogenetic analysis of nirS and nirK genes showed that a large proportion of OTUs matched to uncultured environmental assemblages (**Figure 6**). In addition, the nirS- and nirK-encoding denitrifier compositions were similar among the soils in penguin or seal colony, but they were different among animal-lacking tundra soils. Within all seven clusters in nirS genes, clusters II, IV, VI, and VII were the dominant phylotypes of animal colony soils, while the dominant phylotypes of AL2 and AL3 was only cluster VII. As for nirK genes, the dominant phylotypes in animal colony soils were clusters I, III, and V, whereas clusters II, III, and IV were dominant phylotypes in animal-lacking tundra soils. This result indicated that the denitrifier community structure in tundra soils was affected by sea animal activities, similar to tundra soil AOA and AOB in maritime Antarctica (Wang Q. et al., 2019). Nitrate and ammonium concentrations, and C:N ratios were closely related to sea animal activities in coastal Antarctica (Riddick et al., 2012; Zhu et al., 2013, 2015b; Otero et al., 2018). Significant correlations between the nirS-encoding denitrifier community structures and NO_3^- and NH_4^+-N concentrations, and between nirK-encoding denitrifier community structures and C:N ratios and NH_4^+-N concentrations, further confirmed that sea animal activity had an important effect on the denitrifier community structure in tundra soils of maritime Antarctica (**Figure 8** and **Table 2**).

Generally, the nutrient contents are low in normal tundra soils of maritime Antarctica. Sea animals provided considerable external N inputs for their colony soils through direct input of their excreta and ammonia volatilization (Zhu et al., 2011; Riddick et al., 2012). The uric acid from penguin guano or seal excreta produced NH_3 or NH_4^+ through mineralization and ammonification, which increased the nutrient availability in soils (Kuypers et al., 2018; Otero et al., 2018). As summarized in **Table 1**, ammonium concentrations were one to two orders of magnitude higher in penguin or seal colony soils than in animal-lacking tundra soils. Ammonium levels were one of important environmental parameters affecting the denitrifier community compositions (**Figure 8** and **Table 2**), and it could be oxidized to nitrate by nitrification, and bacteria respired nitrate as a substitute terminal electron acceptor for denitrification (Cornwell et al., 2014). Our previous studies indicated that ammonia oxidation rates were significantly higher in animal colony soils (mean 70.4 μg N kg^{-1} h^{-1}) than in non-animal tundra soils. Therefore, the NO_3^- from ammonium nitrification was likely important substrate for soil denitrification in sea animal colony (Wang Q. et al., 2019). At the same time, denitrification rates were also greatly higher in sea animal colony soils than in animal-lacking tundra soils (**Figure 2**), which might greatly consume considerable nitrate in tundra soils, and lead to low nitrate levels in animal colony soils, even closed to or lower than those in animal-lacking tundra soils (**Table 1**). The community structures of nirS-encoding denitrifiers had significant correlation with nitrate and

ammonium concentrations in tundra soils (**Figure 8**), which was consistent with previous studies (Zheng et al., 2015; Gao et al., 2016; Lee and Francis, 2017; Shi et al., 2019).

In addition, the community compositions of nirK-encoding denitrifiers were also significantly affected by ammonium. The C:N ratios were also found to be important environmental parameters influencing the community structure of nirK-encoding denitrifiers, which was consistent with the results from different environments (Saleh-Lakha et al., 2009; Mosier and Francis, 2010; Li et al., 2019). Soil pH was an important factor controlling the diversity and composition of denitrifying communities in the environments (Saleh-Lakha et al., 2009; Wise et al., 2019). However, there were no significant correlation between pH and denitrifier diversity, nirS-encoding or nirK-encoding denitrifier community structures in tundra soils (**Supplementary Table S3**), similar to the results in Tibetan wetlands reported by Jiang et al. (2020). Other environmental factors, such as organic carbon and nitrite, had no significant contribution to nirS and nirK-encoding denirifiers community structures in this study, although they had been reported to have significant impact on denitrifying community compositions (Mosier and Francis, 2010; Francis et al., 2013). Therefore, the community structures of nirS- and nirK-encoding denirifiers were closely related to the biogeochemical factors associated with sea animal activities, such as the supply of nitrate and ammonium from sea animal excreta and low C:N ratios, in tundra soils of maritime Antarctica.

CONCLUSION

This study provided a comprehensive insight into abundance, activity, diversity, and composition of nirS- and nirK-encoding denitrifier communities in tundra soils of maritime Antarctica. The abundances of nirS genes were significantly higher than those of nirK genes in all tundra soils. The denitrification rates in sea animal colony soils were significantly higher than those in adjacent animal-lacking tundra soils, and they were significantly correlated with nirS gene abundances, instead of nirK gene abundances. The lg values of nirS and nirK gene abundances were significantly negatively correlated with tundra soil C:N ratios, indicating that sea animal activities had an important effect on the abundances of tundra soil denitrifiers. The diversity for nirS-encoding denitrifier community was higher in seal or penguin colony soils than in adjacent animal-lacking tundra soils, but the diversity for nirK-encoding denitrifier was lower. The nirS- and nirK-encoding denitrifier community structures were influenced by soil biogeochemical processes related to marine animal activities, such as soil C:N alteration, the supply of NH_4^+-N and NO_3^--N from animal excreta. This study contributes to understand soil denitrifier communities in tundra environment of maritime Antarctica.

DATA AVAILABILITY STATEMENT

The datasets presented in this study can be found in online repositories. The names of the repository/repositories and accession number(s) can be found in the article/ **Supplementary Material**.

AUTHOR CONTRIBUTIONS

R-BZ, H-TD, and B-WS designed the experiments. L-JH provided experiments platform. H-TD, B-WS, and C-SC performed the experiments and analyzed the data. H-TD and R-BZ prepared original draft. R-BZ and H-TD reviewed and edited the manuscript. All authors contributed to the manuscript and gave final approval for publication.

FUNDING

This research was funded by the National Natural Science Foundation of China (grant no. 41776190; 41976220) and the Strategic Priority Research Program of Chinese Academy of Sciences (no. XDB40010200).

ACKNOWLEDGMENTS

We are thankful to the Polar Office of the National Ocean Bureau of China and the teammates of the Chinese National Antarctic Research Expedition for their support and help.

SUPPLEMENTARY MATERIAL

The Supplementary Material for this article can be found online at: https://www.frontiersin.org/articles/10.3389/fmicb.2020.573302/full#supplementary-material

REFERENCES

Achouak, W., Abrouk, D., Guyonnet, J., Barakat, M., Ortet, P., Simon, L., et al. (2019). Plant hosts control microbial denitrification activity. *FEMS Microbiol. Ecol.* 95, 1–13. doi: 10.1093/femsec/fiz021

Alcántara-Hernández, R. J., Centeno, C. M., Ponce-Mendoza, A., Batista, S., Merino-Ibarra, M., Campo, J., et al. (2014). Characterization and comparison of potential denitrifiers in microbial mats from King George Island, coastal Antarctica. *Polar Biol.* 37, 403–416. doi: 10.1007/s00300-013-1440-3

Babbin, A. R., Keil, R. G., Devol, A. H., and Ward, B. B. (2014). Organic matter stoichiometry, flux, and oxygen control nitrogen loss in the ocean. *Science* 344, 406–408. doi: 10.1126/science.1248364

Baker, B. H., Kröger, R., Brooks, J. P., Smith, R. K., and Prince Czarnecki, J. M. (2015). Investigation of denitrifying microbial communities within an agricultural drainage system fitted with low-grade weirs. *Water Res.* 87, 193–201. doi: 10.1016/j.watres.2015.09.028

Bao, T., Zhu, R., Wang, P., Ye, W., Ma, D., and Xu, H. (2018). Potential effects of ultraviolet radiation reduction on tundra nitrous oxide and methane fluxes in coastal Antarctica. *Sci. Rep.* 8:3716. doi: 10.1038/s41598-018-21881-1

Björk, R. G., Klemedtsson, L., Molau, U., Harndorf, J., Ödman, A., and Giesler, R. (2007). Linkages between N turnover and plant community structure in a tundra landscape. *Plant Soil* 294, 247–261. doi: 10.1007/s11104-007-9250-4

Blackwood, C. B., Oaks, A., and Buyer, J. S. (2005). Phylum- and class-specific PCR primers for general microbial community analysis. *Appl. Environ. Microbiol.* 71, 6193–6198. doi: 10.1128/AEM.71.10.6193-6198.2005

Bolyen, E., Rideout, J. R., Dillon, M. R., Bokulich, N. A., Abnet, C. C., Al-Ghalith, G. A., et al. (2019). Reproducible, interactive, scalable and extensible microbiome data science using QIIME 2. *Nat. Biotechnol.* 37, 852–857. doi: 10.1038/s41587-019-0209-9

Bothe, H. (2000). Molecular analysis of ammonia oxidation and denitrification in natural environments. *FEMS Microbiol. Rev.* 24, 673–690. doi: 10.1016/S0168-6445(00)00053-X

Braker, G., Zhou, J., Wu, L., Devol, A. H., and Tiedje, J. M. (2000). Nitrite reductase genes (nirK and nirS) as functional markers to investigate diversity of denitrifying bacteria in Pacific northwest marine sediment communities. *Appl. Environ. Microbiol.* 66, 2096–2104. doi: 10.1128/AEM.66.5.2096-2104.2000

Callahan, B. J., McMurdie, P. J., Rosen, M. J., Han, A. W., Johnson, A. J. A., and Holmes, S. P. (2016). DADA2: high-resolution sample inference from Illumina amplicon data. *Nat. Methods* 13, 581–583. doi: 10.1038/nmeth.3869

Canion, A., Overholt, W. A., Kostka, J. E., Huettel, M., Lavik, G., and Kuypers, M. M. M. (2014). Temperature response of denitrification and anaerobic ammonium oxidation rates and microbial community structure in Arctic fjord sediments. *Environ. Microbiol.* 16, 3331–3344. doi: 10.1111/1462-2920.12593

Chen, J., Ying, G. -G., Liu, Y. -S., Wei, X. -D., Liu, S. -S., He, L. -Y., et al. (2017). Nitrogen removal and its relationship with the nitrogen-cycle genes and microorganisms in the horizontal subsurface flow constructed wetlands with different design parameters. *J. Environ. Sci. Health A Tox. Hazard. Subst. Environ. Eng.* 52, 804–818. doi: 10.1080/10934529.2017.1305181

Cheng, L., Li, X., Lin, X., Hou, L., Liu, M., Li, Y., et al. (2016). Dissimilatory nitrate reduction processes in sediments of urban river networks: spatiotemporal variations and environmental implications. *Environ. Pollut.* 219, 545–554. doi: 10.1016/j.envpol.2016.05.093

Cornwell, J. C., Glibert, P. M., and Owens, M. S. (2014). Nutrient fluxes from sediments in the San Francisco Bay Delta. *Estuaries Coasts* 37, 1120–1133. doi: 10.1007/s12237-013-9755-4

Dalsgaard, T., Thamdrup, B., Farías, L., and Revsbech, N. P. (2012). Anammox and denitrification in the oxygen minimum zone of the eastern South Pacific. *Limnol. Oceanogr.* 57, 1331–1346. doi: 10.4319/lo.2012.57.5.1331

Danovaro, R., and Gambi, C. (2002). Biodiversity and trophic structure of nematode assemblages in seagrass systems: evidence for a coupling with changes in food availability. *Mar. Biol.* 141, 667–677. doi: 10.1007/s00227-002-0857-y

Desnues, C., Michotey, V. D., Wieland, A., Zhizang, C., Fourçans, A., Duran, R., et al. (2007). Seasonal and diel distributions of denitrifying and bacterial communities in a hypersaline microbial mat (Camargue, France). *Water Res.* 41, 3407–3419. doi: 10.1016/j.watres.2007.04.018

Fernández-Valiente, E., Camacho, A., Rochera, C., Rico, E., Vincent, W. F., and Quesada, A. (2007). Community structure and physiological characterization of microbial mats in Byers Peninsula, Livingston Island (South Shetland Islands, Antarctica). *FEMS Microbiol. Ecol.* 59, 377–385. doi: 10.1111/j.1574-6941.2006.00221.x

Fortunato, C. S., Carlini, D. B., Ewers, E., and Bushaw-Newton, K. L. (2009). Nitrifier and denitrifier molecular operational taxonomic unit compositions from sites of a freshwater estuary of Chesapeake Bay. *Can. J. Microbiol.* 55, 333–346. doi: 10.1139/W08-124

Francis, C. A., O'Mullan, G. D., Cornwell, J. C., and Ward, B. B. (2013). Transitions in nirS-type denitrifier diversity, community composition, and biogeochemical activity along the Chesapeake Bay estuary. *Front. Microbiol.* 4:237. doi: 10.3389/fmicb.2013.00237

Fu, G., Yu, T., Ning, K., Guo, Z., and Wong, M. -H. (2016). Effects of nitrogen removal microbes and partial nitrification-denitrification in the integrated vertical-flow constructed wetland. *Ecol. Eng.* 95, 83–89. doi: 10.1016/j.ecoleng.2016.06.054

Gao, J., Hou, L., Zheng, Y., Liu, M., Yin, G., Li, X., et al. (2016). nirS-encoding denitrifier community composition, distribution, and abundance along the coastal wetlands of China. *Appl. Microbiol. Biotechnol.* 100, 8573–8582. doi: 10.1007/s00253-016-7659-5

Gao, Y., Yang, L., Wang, J., Xie, Z., Wang, Y., and Sun, L. (2018). Penguin colonization following the last glacial-interglacial transition in the Vestfold Hills, East Antarctica. *Palaeogeogr. Palaeoclimatol. Palaeoecol.* 490, 629–639. doi: 10.1016/j.palaeo.2017.11.053

Guyonnet, J. P., Guillemet, M., Dubost, A., Simon, L., Ortet, P., Barakat, M., et al. (2018). Plant nutrient resource use strategies shape active rhizosphere microbiota through root exudation. *Front. Plant Sci.* 871:1662. doi: 10.3389/fpls.2018.01662

Hallin, S., and Lindgren, P. E. (1999). PCR detection of genes encoding nitrite reductase in denitrifying bacteria. *Appl. Environ. Microbiol.* 65, 1652–1657. doi: 10.1128/AEM.65.4.1652-1657.1999

Han, J. (2013). Short-term effect of elevated temperature on the abundance and diversity of bacterial and archaeal amoA genes in Antarctic soils. *J. Microbiol. Biotechnol.* 23, 1187–1196. doi: 10.4014/jmb.1305.05017

Hayashi, K., Tanabe, Y., Ono, K., Loonen, M. J. J. E., Asano, M., Hayatsu, M., et al. (2018). Seabird-affected taluses are denitrification hotspots and potential N_2O emitters in the High Arctic. *Sci. Rep.* 8, 1–11. doi: 10.1038/s41598-018-35669-w

Heylen, K., Gevers, D., Vanparys, B., Wittebolle, L., Geets, J., Boon, N., et al. (2006). The incidence of nirS and nirK and their genetic heterogeneity in cultivated denitrifiers. *Environ. Microbiol.* 8, 2012–2021. doi: 10.1111/j.1462-2920.2006.01081.x

Hou, L., Zheng, Y., Liu, M., Gong, J., Zhang, X., Yin, G., et al. (2013). Anaerobic ammonium oxidation (anammox) bacterial diversity, abundance, and activity in marsh sediments of the Yangtze estuary. *J. Geophys. Res. Biogeosci.* 118, 1237–1246. doi: 10.1002/jgrg.20108

Hou, L., Zheng, Y., Liu, M., Li, X., Lin, X., Yin, G., et al. (2015). Anaerobic ammonium oxidation and its contribution to nitrogen removal in China's coastal wetlands. *Sci. Rep.* 5:15621. doi: 10.1038/srep15621

Huang, S., Chen, C., Yang, X., Wu, Q., and Zhang, R. (2011). Distribution of typical denitrifying functional genes and diversity of the nirS-encoding bacterial community related to environmental characteristics of river sediments. *Biogeosciences* 8, 3041–3051. doi: 10.5194/bg-8-3041-2011

Jiang, X., Liu, W., Yao, L., Liu, G., and Yang, Y. (2020). The roles of environmental variation and spatial distance in explaining diversity and biogeography of soil denitrifying communities in remote Tibetan wetlands. *FEMS Microbiol. Ecol.* 96:fiaa063. doi: 10.1093/femsec/fiaa063

Jiang, X., Yao, L., Guo, L., Liu, G., and Liu, W. (2017). Multi-scale factors affecting composition, diversity, and abundance of sediment denitrifying microorganisms in Yangtze lakes. *Appl. Microbiol. Biotechnol.* 101, 8015–8027. doi: 10.1007/s00253-017-8537-5

Jung, J., Yeom, J., Kim, J., Han, J., Lim, H. S., Park, H., et al. (2011). Change in gene abundance in the nitrogen biogeochemical cycle with temperature and nitrogen addition in Antarctic soils. *Res. Microbiol.* 162, 1018–1026. doi: 10.1016/j.resmic.2011.07.007

Kuypers, M. M. M., Marchant, H. K., and Kartal, B. (2018). The microbial nitrogen-cycling network. *Nat. Rev. Microbiol.* 16, 263–276. doi: 10.1038/nrmicro.2018.9

Lee, J. A., and Francis, C. A. (2017). Spatiotemporal characterization of San Francisco Bay denitrifying communities: a comparison of nirK and nirS diversity and abundance. *Microb. Ecol.* 73, 271–284. doi: 10.1007/s00248-016-0865-y

Li, F., Li, M., Shi, W., Li, H., Sun, Z., and Gao, Z. (2017). Distinct distribution patterns of proteobacterial nirK- and nirS-type denitrifiers in the Yellow River estuary, China. *Can. J. Microbiol.* 63, 708–718. doi: 10.1139/cjm-2017-0053

Li, J., Wang, J. T., Hu, H. W., Cai, Z. J., Lei, Y. R., Cui, L. J., et al. (2019). Changes of the denitrifying communities in a multi-stage free water surface constructed wetland. *Sci. Total Environ.* 650, 1419–1425. doi: 10.1016/j.scitotenv.2018.09.123

Li, J., Wei, G., Wang, N., and Gao, Z. (2014). Diversity and distribution of nirK-harboring denitrifying bacteria in the water column in the yellow river estuary. *Microbes Environ.* 29, 107–110. doi: 10.1264/jsme2.ME13111

Ma, D., Zhu, R., Ding, W., Shen, C., Chu, H., and Lin, X. (2013). Ex-situ enzyme activity and bacterial community diversity through soil depth profiles in penguin and seal colonies on Vestfold Hills, East Antarctica. *Polar Biol.* 36, 1347–1361. doi: 10.1007/s00300-013-1355-z

Magurran, E. (1988). *Ecological diversity and its measurement*. Princeton, NJ: Princeton University Press.

Martin, M. (2011). Cutadapt removes adapter sequences from high-throughput sequencing reads. *EMBnet J.* 17:10. doi: 10.14806/ej.17.1.200

Marushchak, M. E., Pitkamaki, A., Koponen, H., Biasi, C., Seppala, M., and Martikainen, P. J. (2011). Hot spots for nitrous oxide emissions found in

different types of permafrost peatlands. *Glob. Chang. Biol.* 17, 2601–2614. doi: 10.1111/j.1365-2486.2011.02442.x

Mosier, A. C., and Francis, C. A. (2010). Denitrifier abundance and activity across the San Francisco Bay estuary. *Environ. Microbiol. Rep.* 2, 667–676. doi: 10.1111/j.1758-2229.2010.00156.x

Otero, X. L., De La Peña-Lastra, S., Pérez-Alberti, A., Ferreira, T. O., and Huerta-Diaz, M. A. (2018). Seabird colonies as important global drivers in the nitrogen and phosphorus cycles. *Nat. Commun.* 9:246. doi: 10.1038/s41467-017-02446-8

Palmer, K., Biasi, C., and Horn, M. A. (2012). Contrasting denitrifier communities relate to contrasting N_2O emission patterns from acidic peat soils in arctic tundra. *ISME J.* 6, 1058–1077. doi: 10.1038/ismej.2011.172

Palmer, K., and Horn, M. A. (2015). Denitrification activity of a remarkably diverse fen denitrifier community in Finnish Lapland is noxide limited. *PLoS One* 10:e0123123. doi: 10.1371/journal.pone.0123123

Pearson, W. R. (2013). An introduction to sequence similarity ("homology") searching. *Curr. Protoc. Bioinformatics* 42, 3.1.1–3.1.8. doi: 10.1002/0471250953.bi0301s42

Priemé, A., Braker, G., and Tiedje, J. M. (2002). Diversity of nitrite reductase (nirK and nirS) gene fragments in forested upland and wetland soils. *Appl. Environ. Microbiol.* 68, 1893–1900. doi: 10.1128/AEM.68.4.1893-1900.2002

Riddick, S. N., Dragosits, U., Blackall, T. D., Daunt, F., Wanless, S., and Sutton, M. A. (2012). The global distribution of ammonia emissions from seabird colonies. *Atmos. Environ.* 55, 319–327. doi: 10.1016/j.atmosenv.2012.02.052

Rognes, T., Flouri, T., Nichols, B., Quince, C., and Mahé, F. (2016). VSEARCH: a versatile open source tool for metagenomics. *PeerJ* 4:e2584. doi: 10.7717/peerj.2584

Saleh-Lakha, S., Shannon, K. E., Henderson, S. L., Goyer, C., Trevors, J. T., Zebarth, B. J., et al. (2009). Effect of pH and temperature on denitrification gene expression and activity in Pseudomonas mandelii. *Appl. Environ. Microbiol.* 75, 3903–3911. doi: 10.1128/AEM.00080-09

Shi, R., Xu, S., Qi, Z., Huang, H., and Liang, Q. (2019). Seasonal patterns and environmental drivers of nirS- and nirK-encoding denitrifiers in sediments of Daya Bay, China. *Oceanologia* 61, 308–320. doi: 10.1016/j.oceano.2019.01.002

Shrewsbury, L. H., Smith, J. L., Huggins, D. R., Carpenter-Boggs, L., and Reardon, C. L. (2016). Denitrifier abundance has a greater influence on denitrification rates at larger landscape scales but is a lesser driver than environmental variables. *Soil Biol. Biochem.* 103, 221–231. doi: 10.1016/j.soilbio.2016.08.016

Simas, F. N. B., Schaefer, C. E. G. R., Melo, V. F., Albuquerque-Filho, M. R., Michel, R. F. M., Pereira, V. V., et al. (2007). Ornithogenic cryosols from maritime Antarctica: phosphatization as a soil forming process. *Geoderma* 138, 191–203. doi: 10.1016/j.geoderma.2006.11.011

Smith, J. M., Mosier, A. C., and Francis, C. A. (2015). Spatiotemporal relationships between the abundance, distribution, and potential activities of ammonia-oxidizing and denitrifying microorganisms in intertidal sediments. *Microb. Ecol.* 69, 13–24. doi: 10.1007/s00248-014-0450-1

Song, B., and Ward, B. B. (2006). Nitrite reductase genes in halobenzoate degrading denitrifying bacteria. *FEMS Microbiol. Ecol.* 43, 349–357. doi: 10.1111/j.1574-6941.2003.tb01075.x

Stal, L. J. (2012). "Cyanobacterial mats and stromatolites" in *Ecology of cyanobacteria II: Their diversity in space and time*. ed. B. A. Whitton (Dordrecht: Springer Netherlands), 65–125.

Sun, L., Liu, X., Yin, X., Zhu, R., Xie, Z., and Wang, Y. (2004). A 1,500-year record of Antarctic seal populations in response to climate change. *Polar Biol.* 27, 495–501. doi: 10.1007/s00300-004-0608-2

Sun, L., Xie, Z., and Zhao, J. (2000). A 3,000-year record of penguin populations. *Nature* 407:858. doi: 10.1038/35038163

Tatur, A., (2002). "Ornithogenic ecosystems in the coastal Antarctic—formation, development and disintegration" in *Geoecology of Antarctic Ice-Free Coastal Landscapes*. ed. L. Beyer and M. Bölter (Berlin, Heidelberg: Springer), 161–184.

Tatur, A., Myrcha, A., and Niegodzisz, J. (1997). Formation of abandoned penguin rookery ecosystems in the maritime Antarctic. *Polar Biol.* 17, 405–417. doi: 10.1007/s003000050135

Throbäck, I. N., Enwall, K., Jarvis, Å., and Hallin, S. (2004). Reassessing PCR primers targeting nirS, nirK and nosZ genes for community surveys of denitrifying bacteria with DGGE. *FEMS Microbiol. Ecol.* 49, 401–417. doi: 10.1016/j.femsec.2004.04.011

Urakawa, H., Garcia, J. C., Nielsen, J. L., Le, V. Q., Kozlowski, J. A., Stein, L. Y., et al. (2015). Nitrosospira lacus sp. nov., a psychrotolerant, ammonia-oxidizing bacterium from sandy lake sediment. *Int. J. Syst. Evol. Microbiol.* 65, 242–250. doi: 10.1099/ijs.0.070789-0

Valdespino-Castillo, P. M., Cerqueda-García, D., Espinosa, A. C., Batista, S., Merino-Ibarra, M., Taş, N., et al. (2018). Microbial distribution and turnover in Antarctic microbial mats highlight the relevance of heterotrophic bacteria in low-nutrient environments. *FEMS Microbiol. Ecol.* 94:fiy129. doi: 10.1093/femsec/fiy129

Vero, S., Garmendia, G., Martínez-Silveira, A., Cavello, I., and Wisniewski, M. (2019). "Yeast activities involved in carbon and nitrogen cycles in Antarctica" in *The ecological role of micro-organisms in the Antarctic environment*. ed. S. Castro-Sowinski (Cham: Springer International Publishing), 45–64.

Wallenstein, M. D., Myrold, D. D., Firestone, M., and Voytek, M. (2006). Environmental controls on denitrifying communities and denitrification rates: insights from molecular methods. *Ecol. Appl.* 16, 2143–2152. doi: 10.1890/1051-0761(2006)016[2143,ECODCA]2.0.CO;2

Wang, S., Liu, W., Zhao, S., Wang, C., Zhuang, L., Liu, L., et al. (2019). Denitrification is the main microbial N loss pathway on the Qinghai-Tibet Plateau above an elevation of 5000 m. *Sci. Total Environ.* 696:133852. doi: 10.1016/j.scitotenv.2019.133852

Wang, Q., Zhu, R., Zheng, Y., Bao, T., and Hou, L. (2019). Effects of sea animal colonization on the coupling between dynamics and activity of soil ammonia-oxidizing bacteria and archaea in coastal Antarctica. *Biogeosciences* 16, 4113–4128. doi: 10.5194/bg-16-4113-2019

Ward, B. B., and Priscu, J. C. (1997). Detection and characterization of denitrifying bacteria from a permanently ice-covered Antarctic Lake. *Hydrobiologia* 347, 57–68. doi: 10.1023/A:1003087532137

Wise, B. R., Roane, T. M., and Mosier, A. C. (2019). Community composition of nitrite reductase gene sequences in an acid mine drainage environment. *Microb. Ecol.* 79, 562–575. doi: 10.1007/s00248-019-01420-9

Xiong, J. (2006). *Essential bioinformatics*. Cambridge: Cambridge University Press.

Xiong, J., Liu, Y., Lin, X., Zhang, H., Zeng, J., Hou, J., et al. (2012). Geographic distance and pH drive bacterial distribution in alkaline lake sediments across Tibetan Plateau. *Environ. Microbiol.* 14, 2457–2466. doi: 10.1111/j.1462-2920.2012.02799.x

Yergeau, E., Kang, S., He, Z., Zhou, J., and Kowalchuk, G. A. (2007). Functional microarray analysis of nitrogen and carbon cycling genes across an Antarctic latitudinal transect. *ISME J.* 1, 163–179. doi: 10.1038/ismej.2007.24

Yi, N., Gao, Y., Zhang, Z., Wang, Y., Liu, X., Zhang, L., et al. (2015). Response of spatial patterns of denitrifying bacteria communities to water properties in the stream inlets at Dianchi Lake, China. *Int. J. Genomics* 2015:572121. doi: 10.1155/2015/572121

Zheng, Y., Hou, L., Liu, M., Gao, J., Yin, G., Li, X., et al. (2015). Diversity, abundance, and distribution of nirS-harboring denitrifiers in intertidal sediments of the Yangtze estuary. *Microb. Ecol.* 70, 30–40. doi: 10.1007/s00248-015-0567-x

Zhu, R., Liu, Y., Xu, H., Ma, D., and Jiang, S. (2013). Marine animals significantly increase tundra N_2O and CH_4 emissions in coastal Antarctica. *J. Geophys. Res. Biogeosci.* 118, 1773–1792. doi: 10.1002/2013JG002398

Zhu, R., Shi, Y., Ma, D., Wang, C., Xu, H., and Chu, H. (2015a). Bacterial diversity is strongly associated with historical penguin activity in an Antarctic lake sediment profile. *Sci. Rep.* 5:17231. doi: 10.1038/srep17231

Zhu, R., Sun, J., Liu, Y., Gong, Z., and Sun, L. (2011). Potential ammonia emissions from penguin guano, ornithogenic soils and seal colony soils in coastal Antarctica: effects of freezing-thawing cycles and selected environmental variables. *Antarct. Sci.* 23, 78–92. doi: 10.1017/S0954102010000623

Zhu, R., Wang, Q., Ding, W., Wang, C., Hou, L., and Ma, D. (2015b). Penguins significantly increased phosphine formation and phosphorus contribution in coastal Antarctic soils. *Sci. Rep.* 4:7055. doi: 10.1038/srep07055

Conflict of Interest: The authors declare that the research was conducted in the absence of any commercial or financial relationships that could be construed as a potential conflict of interest.

frontiers in Microbiology

ORIGINAL RESEARCH
published: 23 October 2020
doi: 10.3389/fmicb.2020.575563

Fungal Symbionts Enhance N-Uptake for Antarctic Plants Even in Non-N Limited Soils

*Ian S. Acuña-Rodríguez[1], Alexander Galán[2,3,4], Cristian Torres-Díaz[5], Cristian Atala[6] and Marco A. Molina-Montenegro[1,2,7]**

[1] Laboratorio de Biología Vegetal, Instituto de Ciencias Biológicas, Universidad de Talca, Talca, Chile, [2] Centro de Investigación en Estudios Avanzados del Maule (CIEAM), Vicerrectoría de Investigación y Postgrado, Universidad Católica del Maule, Talca, Chile, [3] Departamento de Obras Civiles, Facultad de Ciencias de la Ingeniería, Universidad Católica del Maule, Talca, Chile, [4] Centro Regional de Estudios Ambientales (CREA), Universidad Católica de la Santísima Concepción, Concepción, Chile, [5] Laboratorio de Genómica y Biodiversidad (LGB), Departamento de Ciencias Naturales, Universidad del Bío-Bío, Chillán, Chile, [6] Laboratorio de Anatomía y Ecología Funcional de Plantas (AEF), Instituto de Biología, Pontificia Universidad Católica de Valparaíso, Campus Curauma, Valparaíso, Chile, [7] Centro de Estudios Avanzados en Zonas Áridas (CEAZA), Facultad de Ciencias del Mar, Universidad Católica del Norte, Coquimbo, Chile

Plant-fungi interactions have been identified as fundamental drivers of the plant host performance, particularly in cold environments where organic matter degradation rates are slow, precisely for the capacity of the fungal symbiont to enhance the availability of labile nitrogen (N) in the plant rhizosphere. Nevertheless, these positive effects appear to be modulated by the composition and amount of the N pool in the soil, being greater when plant hosts are growing where N is scarce as is the case of Antarctic soils. Nevertheless, in some coastal areas of this continent, seabirds and marine mammal colonies exert, through their accumulated feces and urine a strong influence on the edaphic N content surrounding their aggregation points. To evaluate if the fungal symbionts (root endophytes), associated to the only two Antarctic vascular plants *Colobanthus quitensis* and *Deschampsia antarctica*, act as N-uptake enhancers, even in such N-rich conditions as those found around animal influence, we assessed, under controlled conditions, the process of N mineralization in soil by the accumulation of NH_4^+ in the rizhosphere and the biomass accumulation of plants with (E+) and without (E−) fungal symbionts. Complementarily, taking advantage of the isotopic N-fractionation that root-fungal symbionts exert on organic N molecules during its acquisition process, we also determined if endophytes actively participate in the Antarctic plants N-uptake, when inorganic N is not a limiting factor, by estimating the $\delta^{15}N$ isotopic signatures in leaves. Overall, symbiotic interaction increased the availability of NH_4^+ in the rhizosphere of both species. As expected, the enhanced availability of inorganic N resulted in a higher final biomass in E + compared with E− plants of both species. In addition, we found that the positive role of fungal symbionts was also actively linked to the process of N-uptake in both species, evidenced by the contrasting $\delta^{15}N$ signatures present in E+ (−0.4 to −2.3‰) relative to E− plants (2.7–3.1‰). In conclusion, despite being grown

OPEN ACCESS

Edited by:
Pietro Buzzini,
University of Perugia, Italy

Reviewed by:
Natasja Van Gestel,
Texas Tech University, United States
Alfonso Esposito,
University of Trento, Italy

***Correspondence:**
Marco A. Molina-Montenegro
marco.molina@utalca.cl

Specialty section:
This article was submitted to Extreme Microbiology, a section of the journal Frontiers in Microbiology

Received: *23 June 2020*
Accepted: *05 October 2020*
Published: *23 October 2020*

Citation:
Acuña-Rodríguez IS, Galán A, Torres-Díaz C, Atala C and Molina-Montenegro MA (2020) Fungal Symbionts Enhance N-Uptake for Antarctic Plants Even in Non-N Limited Soils. Front. Microbiol. 11:575563. doi: 10.3389/fmicb.2020.575563

under rich N soils, the two Antarctic vascular plants showed that the presence of root-fungal endophytes, furthermore enhanced the availability of inorganic N sources in the rhizosphere, has a positive impact in their biomass, remarking the active participation of these endophytes in the N-uptake process for plants inhabiting the Antarctic continent.

Keywords: plant-fungi interactions, nitrogen, endophytes, Antarctic vascular plants, ornithogenic soils

INTRODUCTION

In cold environments as polar and alpine regions the edaphic nitrogen is mainly available as organic compound, imposing metabolic restrictions to the biological mineralization of nitrogen (Shaver and Chapin, 1980; Pietr et al., 1983; Atkin, 1996). To cope with the inorganic N scarcity, plants take advantage of symbiotic interaction with microorganisms (e.g., root mycorrhizal symbionts and root endophytes), as a strategy to enhance their nutritional status (Hobbie et al., 2000; Newsham, 2011; Acuña-Rodríguez et al., 2020). The benefit of the interactions, as described in plant-mycorrhyzae interactions from the Arctic tundra (Hobbie and Högberg, 2012), are related to the capacity of the microbial symbionts to mineralize complex organic N compounds into inorganic forms like ammonium (NH_4^+) and nitrate (NO_3^-), which are easily absorbed by the plant's roots. In consequence, the plant-microorganisms association increases N acquisition and enhances the ecophysiological performance of plants (Hobbie and Hobbie, 2008).

The microbiome associated with the Antarctic vascular flora is dominated by the ascomycetous fungi known as dark septate endophytes or DSE (Upson et al., 2009b; Newsham, 2011; Ruotsalainen, 2018). These symbiotic fungi, usually found in the roots, can enhance plant nutrient acquisition, particularly N and P (Newsham, 2011; Hill et al., 2019). However, the shift from organic to inorganic N as nutrient source seems to alter the effect of some root DSE in their host plants, either positively or negatively. This is similar to what has been found for the plant-mycorrhizae interaction of the Arctic tundra in which the role of mycorrhizae on the net plant N-uptake decrease if inorganic N become more available (Hobbie et al., 2000; Johnson et al., 2010). As shown by Upson et al. (2009a), under controlled conditions, four out of six DSE strains had positive effects on shoot and root biomasses of *Deschampsia antarctica* (Poaceae) individuals only when grown using organic N as nutrient source. When supplied with inorganic N, some detrimental effects on the plant were observed (Upson et al., 2009a), presumably because both plant and fungi compete for soil resources, shifting the plant-DSE association from beneficial to negative for the host. Thus, the positive role of DSE root-symbionts on their host plants' performance is still not conclusive and appears to be highly dependent on the environmental conditions (Newsham, 2011; Acuña-Rodríguez et al., 2020).

Among the terrestrial ice-free areas that allow the life of vascular plants in Maritime Antarctic, those that harbor ornithogenic soil, represent a particular edaphic environment due to their extremely high N concentration (Pires et al., 2017). During the summer, the animal N input produces a patchy spatial distribution of edaphic N, which concentrates around colonies (Bölter et al., 1997; Park et al., 2007). For example, it has been estimated that in Maritime Antarctica, total soil N could vary from highly enriched (N_{tot} = 14.9–8.8 g kg^{-1}) surrounding animal colonies, to highly depleted (N_{tot} = 0.5–0.17 g kg^{-1}) approximately 800 m away from the colony's influence (Bölter et al., 1997; Łachacz et al., 2018). Furthermore, the composition of the N pool can also vary drastically depending on the distance to these colonies. The rapid mineralization of animal urea not only raise local ammonium$^+$ concentrations in the presence of water, but also produces a volatile N source through the emanation of gaseous ammonia (Pietr et al., 1983), which can be exported up to 1 km away from the bird colonies, depending on the local topography and wind dynamics (Erskine et al., 1998; Bokhorst et al., 2019a). This inorganic N input, spontaneously mineralized from animal-originated N-forms, has been related to the greater performance of lowland coastal plant populations compared with those from more inland locations (Androsiuk et al., 2015). Thus, given that the composition of the N-pool (i.e., organic or inorganic) is known to alter the effect of microbial symbiotic on plants (beneficial or costly), it can be predicted that in ornithogenic N-enriched soils, N-acquisition by Antarctic vascular plants might not be exclusively attributed to the role of symbiotic microorganisms.

Several studies have tested this hypothesis using the isotopic fractionation that occurs during the biological N mineralization in some fungal symbiont-plant associations (Benavent-González et al., 2019 and references therein). Given the natural existence of two stable isotopes of nitrogen (^{14}N and ^{15}N), the proportion of the heavier isotope in both the N source (soil) and N products (i.e., plant and fungal tissues), has been proposed to be affected by the active role of fungal symbionts in the process of N uptake (Högberg, 1997). For example, during the acquisition of organic N mycorrhizal fungi is prone to retain ^{15}N-enriched N, while ^{15}N-depleted N is transferred to the plant hosts (reviewed in: Hobbie and Högberg, 2012). Hence, in this plant-fungi interaction model, the intermediate step of acquiring N through the fungal symbiont generates low $\delta^{15}N$ values in foliar tissues compared to the isotopic signature of the soil N source (Michelsen et al., 1998; Hobbie et al., 2000). Nevertheless, unlike most plant communities, the microbiota associated to the roots of the Antarctic plants is dominated by DSE instead of mycorrhizal fungi (Upson et al., 2009b). Antarctic endophytes and mycorrhizal fungi, however, seem to play a similar ecological role enhancing nutrient acquisition and N in particular (Hill et al., 2019; Acuña-Rodríguez et al., 2020).

The main goal of the present study was to explore the role of fungal endophytes on the N biological mineralization and

plant N-acquisition processes when inorganic N is not limiting. We specifically addressed two questions: (i) is the organic N-mineralization in the rhizosphere of two vascular Antarctic plants enhanced by the presence of root endophytes under N-enriched conditions? and (ii) does root endophytes participate in the N-uptake of these plant species when inorganic N is not a limiting factor? To answer these questions we specifically measured: (a) the percentage of NH_4^+ accumulated in the soil through time in plants inoculated and non-inoculated with root fungal endophytes to determine the relevance of this symbiotic association on the process of N biological mineralization, (b) the differences in biomass accumulation between those inoculated and non-inoculated plants and (c) the $\delta^{15}N$ isotopic signature in foliar tissues, we determined if fungal endophytes actively participate in the process of N-acquisition when inorganic N is not a limiting factor. By answering these questions, we are able to evaluate if the root fungal endophytes maintain their positive role as N-uptake enhancers for their hosting plants when grown in N-rich ornithogenic soils, such as those found in some Antarctic habitats.

MATERIALS AND METHODS

Sampling Site and Plant Material

Healthy individuals of *C. quitensis* and *D. antarctica* (n = 30 per species) were collected along with their rhizospheric soil from populations located in the western coast of Admiralty Bay, King George Island, Southern Shetlands, Maritime Antarctica (**Figure 1**). We focused our sampling on those individuals inhabiting microhabitats surrounding colonies of marine birds and mammals (mostly Gentoo penguin, *Pygoscelis papua*) present along the shore (Bölter, 2011; **Figure 1**). As most of these ornithogenic coastal soils, the sampled sites had primarily rocky-sandy substrates with a marked presence of coarse skeletal fractions and incipient stratification (Bölter, 2011). Collected plants were carefully put in plastic containers and transported from the field to the laboratory within 2 days, trying to avoid plant stress due to drought or extreme temperatures. Once in the laboratory, all plants were maintained at 5°C in an automatic air-cooling growth chamber (model: LTJ300LY; Tianyi Cool, China), and at a constant photosynthetic photon flux density (PPFD) of 240 μmol m^{-2} s^{-1} in daily photoperiods of 19/5 h light/dark to simulate the study site environmental conditions during the austral growing season.

Production of Axenic (E−) and Inoculated (E+) Plants

After 2 weeks of acclimation, plants from each species were vegetativelly propagated. Five tillers from 10 field-collected individual were separated, rinsed with distilled water, and treated with a 1 h submersion in 2 g l^{-1} of Benlate® (benomyl [methyl [1-butylamino carbonyl]-1H-benzimidazol-2-yl] carbamate (DuPont, Wilmington, United States) at room temperature. The resulting 50 tillers per species were transplanted to 50 cc cells pot-in-frame in a speedling tray. Cells were previously filled with autoclavated soil from the study site. The selection of the fungicide was based on its broad spectrum of action, low leaching rates (Rhodes and Long, 1974), and because it is harmless to Antarctic plants, as it has been observed

FIGURE 1 | Antarctic plant community growing near a big penguin colony in the study site (Admiralty bay, King George Island, South Shetland, Antarctica).

in previous experiments made by our research group (Ramos et al., 2018; Barrera et al., 2020; Hereme et al., 2020). After 4 weeks, endophyte infection was assessed by counting aniline blue-stained fungal hyphaes in root cross-sections in 10% of the produced plants as the percentage of infested root length (Bacon and White, 2000). Complementarily, sterilized root fragments from the selected individuals were plated on Petri dishes containing potato dextrose agar (PDA, Difco, United States) plus chloramphenicol at 100g ml^{-1} and were incubated for a 30-days at 18°C. Only those plants that showed <5% of infested-root length and no outgrowth of fungi into the PDA media were considered as "fungal endophyte-free" (E−), becoming suitable for their use in the subsequent experiment. Until the beginning of the experiment, E− tillers were sprinkled once a week during this process with the same Benlate solution (2 g l^{-1}, see above) to extend the time of the axenic state.

Half of the obtained E− individuals were re-inoculated with fungal spores from the most abundant root fungal endophyte reported for the studied populations of each plant species; these correspond to *Penicillium chrysogenum* (strain AFE001, Genebank Accession Number: KJ881371) in *C. quitensis* and *Penicillium brevicompactum* (strain AFE002, GeneBank Accession Number: KJ881370) in *D. antarctica* (Molina-Montenegro et al., 2016). In each case, the inoculum consisted of a concentrated mix of spores (5,000 spores g^{-1}) obtained from stored cultures of the referred fungal strains that are routinely maintained at the laboratories of the Instituto de Ciencias Biológicas, Universidad de Talca[1]. The liquid inoculum-mix was added three times during a week (10 ml per individual) to ensure fungal association. Two weeks after the first inoculation, occurrence of effective symbiosis was corroborated by routine staining and microscopic observation in three randomly selected individuals from each species (**Supplementary Figure 1**). The resultant endophyte free (E−, n = 20 for each species) and endophyte free, but reinoculated (E+, n = 19 for *C. quitensis*; 18 for *D. antarctica*) individuals, were then transplanted to 300 ml pots filled with sterilized Antarctic soil. We conducted a previous verification of the soil microbiological condition by cultivation of a subsample of the sterilized Antarctic soil on PDA plates where after 2 weeks no fungal growth was subsequently observed. The experiment lasted for 60 days. During that time, all plants were maintained in the same light conditions (PFD of 240 μmol m^{-2} s^{-1} in a 19/5 h light/dark day), and 40 ml of tap water were added to each plant every week.

Role of the Plant Symbiont on Soil N Mineralization

To estimate if fungal endophytes participate in the mineralization of organic N, we compared the percentage of ammonium (NH_4^+) in the rhizospheric soils from E+ and E− individuals (n = 7/fungal treatment) of each species prior to the transplant, and after 7, 15, 30, and 60 days of experiment. The substrate used for plant growing was obtained from 15 soil samples of 1 kg (1–5 cm depth) collected near Arctowski station (Antarctica) in a zone without Penguin colony influences. Those soil samples were homogenized before measuring their total N content (n = 3, N content = 7.8 ± 0.8 g of N kg^{-1}). After being autoclavated, the substrate was enriched with an organic N source (urea) to mimic the average N condition (∼16 g N kg^{-1}) described for the local coastal soils around penguin colonies, which represents an enriched N condition for Antarctic soils (Kozeretska et al., 2010). We used urea because it is an intermediate compound in the degradation pathway of uric acid, which is heavily deposited in soils close to coastal colonies of birds and mammals (Pietr et al., 1983), and because despite its spontaneous degradation at acidic conditions in the presence of water, it can be mineralized by other fungal endophyte species (Jumpponen et al., 1998).

Soil sampling from each experimental plant focused on the soil material around the roots by a careful removal of the plant from its pot. For the total N estimation, the Kjeldahl digestion method was used (Allen, 1989). Briefly, a 0.2 g soil sample was added to 0.05 g of catalyst (Li_2SO_4:$CuSO_4$ in 10:1 ratio) and 1 ml of a digestion reagent (33 g of $C_7H_6O_3$ in 1 l of H_2SO_4) in a digestion tube, and then further heated to 370°C in a digestion block until the solution was clear (∼ 6 h). The cooled digested soil sample was diluted in 10 ml of distilled water, filtered (Whatman filter paper N°44), and then diluted in 50 ml of distilled water. Flame atomic absorption spectrometry was finally used to determine the individual element concentrations. Ammonium was also determined by the colorimetric analysis of 5 g of air-dried soil samples immersed on 50 ml of 2 M KCl for 30 min and filtered through filter paper (Whatman N° 42) (Knepel, 2003), using a continuous flow injection analyzer (FIAflow2, Burkard Scientific, Uxbridge, United Kingdom). Nitrogen mineralization was then estimated to 7, 15, 30, and 60 days after the beginning of the experiment in the soil from pots containing E+ and E− individuals of both species as the relative N-NH_4^+ content (%) compared with the initial concentration observed in the soil substrate at day 0. Since thermal soil sterilization may affect nutrient availability, soil samples were tested for differences in total N in sterilized and non-sterilized soil samples (n = 5) prior to being enriched for experimentation, and no statistical differences were found between them (t-test = 0.93; p = 0.77).

Effect of DSE on Plant N Uptake

To determine the participation of fungal endophytes on the process of plant N-uptake, we estimate the foliar $\delta^{15}N$ signature of E+ and E− individuals at day 60 (n = 10 per species) and compare their patterns of ^{15}N isotopic discrimination with respect to the initial soil substrate. To calculate the latter, we estimated the $\delta^{15}N$ signature in five substrate samples ($\delta^{15}N$ = 8.8 ± 0.52‰), and five samples with the added urea ($\delta^{15}N$ = −1.46 ± 0.02‰). Then, the final value of the experimental substrate ($\delta^{15}N$ = 3.67) was calculated as:

$$\delta^{15}N_{total} = (\delta^{15}N_{soil} \times [N]_{soil} + \delta^{15}N_{urea} \times [urea])/[N]_{total}$$

The $\delta^{15}N$ isotopic ratios were assessed in the Laboratory of Biogeochemistry and Applied Stable Isotopes at the Pontificia Universidad Católica de Chile (Santiago, Chile) using an Isotope Ratio Mass Spectrometer, IRMS (Thermo Delta Advantage)

[1]http://biologia.utalca.cl

coupled to an Elemental Analyzer (Flash EA2000). Stable isotope abundances were expressed in δ-notation as the deviation from standards in parts per thousand (‰) obtained from:

$$\delta^{15}N = 1000 \times [(R_{sample}/R_{standard}) - 1]$$

where R is the corresponding $^{15}N/^{14}N$ ratio for either a given sample or the atmospheric N_2 standard for ^{15}N isotopic fractionation (Hobbie et al., 1999). The analytical precision of the isotopic measurements of multiple replicate analyses was 0.2‰. Complementarily, to estimate the overall effect of the symbiosis on the plant individual performances, the total dry biomass of 10 E+ and 10 E− plants per species was estimated at the end of the experiment. All tissues (included fallen leaves) were oven-dried at 70°C for 72 h and weighted with an electronic precision balance (Boeco BBl-54, Germany).

Data Analysis

We used General Additive Mixed Models (GAMMs) to evaluate in each species the shape of the temporal trend of the edaphic NH_4^+ concentrations, and the potential effect that the infection status (E + and E−) can exert on its direction. Using the "gamm" function from the *mgcv* R-package v.1.8.32 (Wood, 2017), we modeled the soil NH_4^+ content along time in response to the infection status of the plants by fitting a smoothed spline to the data according to the following equation:

$$y_{ij} = \alpha_0 + \alpha_{1k} infectionstatus_k + f_{ijk}(day_{ij}, infectionstatus_k) + \varepsilon_i$$

Where the response of the *i*th individual at the *j*th day (y_{ij}) is defined by the model intercept (α_0), the difference between α_0 and the mean response of the respective infection status k (α_{1k}), the smooth temporal function by infection status k, f_{ijk}, and the individual error (ε_i), which is assumed to be a random factor with a Gaussian distribution $\varepsilon_i \sim N(0, \sigma^2)$. In this sense, within each species a fitted spline an its approximated 95% confidence interval was calculated for each experimental group (E+ or E−). In addition, the final average NH_4^+ content in soils, the $\delta^{15}N$ isotopic values at day 60, and the average final dry biomasses were all analyzed using a two-way ANOVA's including endophyte treatment (E+ or E−) and the species of host plant as fixed factors. For the *post-hoc* contrast of treatments between species, the Honest Significant Difference (HSD) test of Tukey was applied on the two-way ANOVA outputs from the final biomass and $\delta^{15}N$ isotopic signature datasets. All statistical analyses were carried out in the R Language and Statistical Environment v3.6.2 (R Core Team, 2019), after testing for normality and homogeneity of variances assumptions using the Shapiro-Wilks and Bartlett tests, respectively.

RESULTS

Microscopy analyses demonstrated that E+ individuals were progressively colonized by DSE both extra and intracellularly. Considering that at the beginning of experiments there was no evidence of root colonization, the root infection process was successfully (Data not shown). By the end of the N-mineralization experiment (60 days), the percentage of infested roots in *C. quitensis* inoculated with *P. chrysogenum* reached 88.5 ± 1.6% and was 91.2 ± 0.9% in *D. antarctica* plants inoculated with *P. brevicompactum*. Relative to the temporal dynamic of the available NH_4^+ in the substrate of the experimental plants, GAMM models revealed for *C. quitensis* and *D. antarctica* a significant increase in time among the rhizospheric soil of both E− and E + plants (**Supplementary Table 1**). However, despite this general increase among all experimental groups, there was a significant influence of the infection status in both species, and particularly in *C. quitensis*, where E+ plants showed greater contents of NH4+ in their rhizospheres if compared with E− individuals (**Figure 2**). This can be easily observed in the absence of confidence interval overlapping in *C. quitensis*. By contrast, in *D. antarctica* the fitted splines for E+ and E− individuals appear close to each other, such as to do not appear statistically different in some time periods toward the end of the experiment (**Figure 2**).

For both species, the enhanced availability of inorganic N in the form of NH_4^+ in soil of E+ individuals may explain their higher average dry biomass at the end of the experiment relative to E− plants (**Figure 3**). In this sense, a significant biomass increase of 34 and 23% was found for both *C. quitensis* and *D. antarctica* in E+ individuals, relative to their respective axenic E− counterparts [endophyte treatment: $F_{(1, 24)} = 114.12$; $p \leq 0.0001$]. However, there was no significant interaction between endophyte treatment and species, meaning that the effect

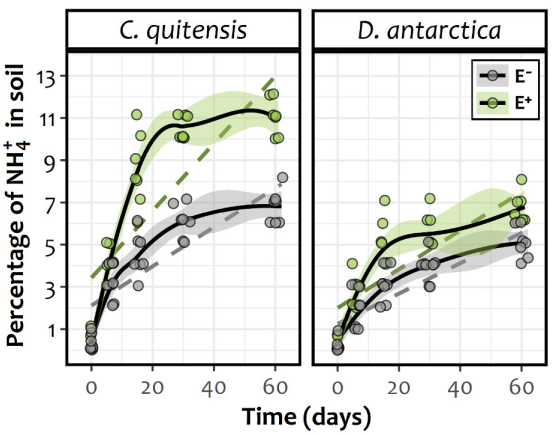

FIGURE 2 | Temporal smooth functions (solid lines) and their approximate 95% confidence intervals (shaded area) for E− (gray) and E+ (green) individuals of either Antarctic vascular plant species *Colobanthus quitensis* or *Deschampsia antarctica*, as derived from a GAMM fitted model. Confidence interval overlapping can be considered to dilute any significant difference between splines during the respective time. As a reference, dashed lines represent the simplest (i.e., linear) model fit for each experimental group. The respective coefficients were, for *C. quitensis*: slope E− = 0.093, SE E− = 0.015, df E− = 66; slope E+ = 0.161, SE E+ = 0.016, df E+ = 66 and for *D. antarctica*: slope E− = 0.071, SE E− = 0.009, df E− = 66; slope E+ = 0.091, SE E+ = 0.010, df E+ = 66. All linear regression slopes were statistically different from zero (data not shown).

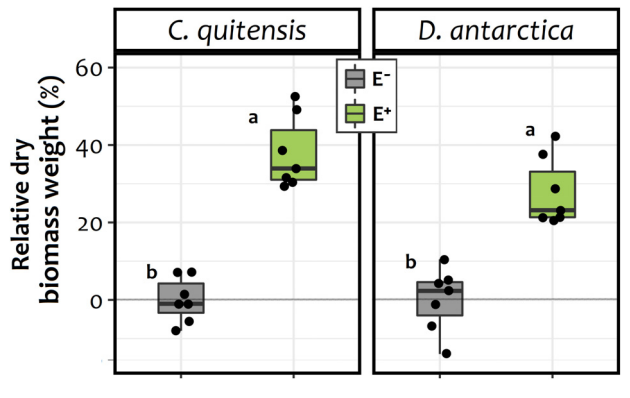

FIGURE 3 | Biomass increase percentage of endophyte free (E−, in gray) and endophyte-infected (E+, in green) individuals of *C. quitensis* and *D. antarctica*, expressed as the percentage of the average final dry biomass of the E− group of each species. Dots represent individual values (n = 7), while boxplots the data inter-quartilic distribution per group. Different letters denote significant differences ($p < 0.05$) between treatments and/or species, as determined by the Tukey a-posteriori pairwise comparison test.

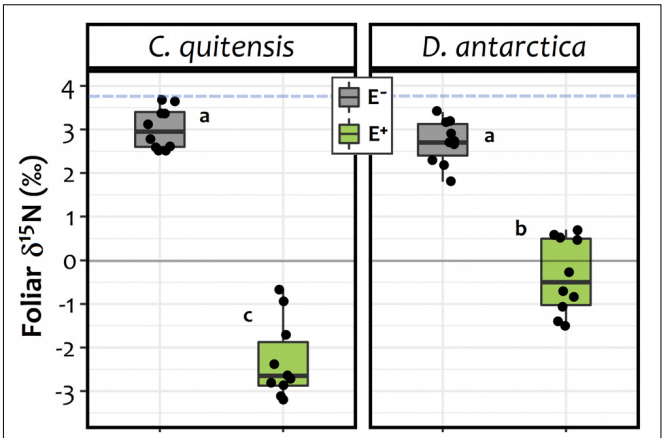

FIGURE 4 | d15N signatures observed on the foliar tissues of *C. quitensis* and *D. antarctica* growing without fungal endophytes (E−, in gray), or inoculated with their most abundant root endophyte (E+, in green). Dots represent individual values (n = 10), while boxplots the data inter-quartilic distribution per group. Different letters imply significant differences ($p < 0.05$) between treatments and/or species, as determined by the Tukey a-posteriori pairwise comparison test. The blue dashed line denotes the isotopic signature of the initial substrate (d15N = 3.7‰). The zero represent outcome among the enrichment / depletion of the 15N isotopic, relative to the standard (i.e., the atmospheric 15N/14N ratio).

of endophytes on plant biomass was similar in both *C. quitensis* and *D. antarctica* (**Figure 3**).

In relation to the ^{15}N isotopic signature of the foliar tissues, significant differences were found between experimental groups (E+ and E− plants) in both species (**Figure 4**). The average $\delta^{15}N$ values obtained showed that, relative to the isotopic fractionation in the initial substrate ($\delta^{15}N = 3.67$), the foliar tissue of *C. quitensis* and *D. antarctica* individuals from both endophyte treatments were depleted in ^{15}N. However, the fractionation among E− plants (*C. quitensis*: 3.05 ± 0.51‰; *D. antarctica*: 2.71 ± 0.49‰) was far lower than in E + plants (*C. quitensis*: −2.31 ± 0.89‰; *D. antarctica* −0.35 ± 0.86‰). This suggests that for both species, the inoculated root endophytes were significantly involved in the process of N-uptake. Furthermore, the interaction term in the two-way ANOVA was statistically significant [endophyte treatment × species: $F_{(1,\ 36)} = 25.27$; $p < 0.0001$] with N fractionation being significantly greater in *C. quitensis* than in *D. antarctica*, but only in E+ plants (Tukey test, $p < 0.05$; **Figure 4**).

DISCUSSION

Our results indicate that the presence of the studied root endophytes significantly favored organic N mineralization in the rhizospheric soil associated with Antarctic vascular plants *Colobanthus quitensis* and *Deschampsia antarctica*. Additionally, endophytes favor N-uptake independently of the availability of NH_4^+ –an inorganic and easily assimilable N-source– in both species. Previous studies on Antarctic vascular plants have shown their capacity to modify the quality and composition of the soil organic N pool (Roberts et al., 2009), and their potential to obtain free amino-acids and small peptides from the soil (Hill et al., 2011, 2019). However, it has been recently demonstrated, at least for *D. antarctica*, that much of these rhizospheric dynamics of N-transformation and uptake in this plant rely on the activity of their fungal root endophytes (Hill et al., 2019). In this sense, the present results are complementary to those of Hill et al. (2019), who demonstrated the participation of endophytes in the uptake of small peptides by *D. antarctica* under controlled conditions. The greater accumulation of NH_4^+ in the soils of E+ plants of both species found in our study suggest that, together with their capacity to metabolize amino-acids in an early stage of organic matter decomposition, the rhizospheric mineralization of organic N forms like urea is also enhanced by root fungal endophytes. Nevertheless, increase of NH_4^+ over time in soil with plants (E−) also occurred, that could be explained by direct hydrolysis of urea in the soils or even as result of the mineralization performed by plants itself. Urease activity has been reported for other root endophytes (Jumpponen et al., 1998; Narisawa, 2017), and it is likely that the species used in this study also have the same metabolic capability. On the other hand, the improvement in the mineralization of the organic N source by endophytes could be related to the higher biomass found in E+ individuals relative to E− plants at the end of the experiment. Even though it is not possible through our experimental design to define which specific N uptake pathway was favored by the fungal symbiont, its presence definitively promotes the incorporation of N into the plant hosts. However, of all the possible N forms, NH_4^+ is the most plausible compound incorporated by these Antarctic plants after endophytic mineralization from urea.

Fungal endophtytes could also explain the higher N uptake efficiency that has been observed in Antarctic vascular plant species, particularly *D. antarctica*, when the inorganic N availability increases in the soil (Rabert et al., 2017). Indeed, the preference of *D. antarctica* for NH_4^+ as its main N source

has been demonstrated, even when other inorganic N forms like NO_3^- were available in a wide range from low- to high-levels (Rabert et al., 2017). In contrast, *C. quitensis* did not show any substrate preference when exposed to similar concentrations of these inorganic N compounds (Rabert et al., 2017). This may explain the pattern of NH_4^+ accumulation in soils found in this study, which was more evident in *C. quitensis* than in *D. antarctica*. Moreover, NH_4^+ accumulation in soils was higher in *C. quitensis* toward the end of the experiment (days 30 and 60) compared to *D. antarctica*. Thus, the higher efficiency of *D. antarctica* in acquiring NH_4^+ could explain the lower accumulation of this substrate in the soil, even under the improved mineralization promoted by the fungal inoculation.

It is important to highlight that the presence of root endophytes significantly changed the ^{15}N isotopic signature in the foliar tissues of both species, demonstrating the active participation of this endophytic fungi in the process of N uptake by the host plant roots. Despite the ^{15}N signature found in leaves of E+ and E− plant tissues from both species appear to be depleted relative to the substrate, this effect was significantly larger in leaves of inoculated (E+) individuals, particularly in *C. quitensis*. The slightly depleted, and still positive, ^{15}N signal observed in the foliar tissues of E− plants is consistent with plants being grown on a ^{15}N-enriched substrate, which is typical of ornithogenic soils (Zhu et al., 2009). This is because the process of ammonia volatilization that occurs spontaneously in the presence of water after an input of uric acid in the soil, strongly discriminates against the heavier N isotopes, increasing its proportion in the soil substrate as the lighter isotope leaves the soil pool as volatile NH_3 (Erskine et al., 1998; Bokhorst et al., 2019b). For this reason, among E− plants, which acquire N without the aid of microbial symbionts, the isotopic signal in their tissues was similar to those of the substrate. Contrastingly, infected individuals (E+) of both species showed a negative isotopic ^{15}N signature, indicating a larger depletion of the heavier isotope in the assimilated N, presumably by the N-fractionation generated by the fungal symbiont. This mineralization process, which should be analogous to those exerted by mycorrhizal fungi in Arctic plant species, produces ^{15}N-enriched fungal tissues, while transferring ^{15}N-depleted nitrogen forms to the plant host (Hobbie and Colpaert, 2003; Hobbie and Högberg, 2012). This would suggest that the $\delta^{15}N$ signature in the endophyte biomass should also be enriched in ^{15}N. However, due the anatomical distribution of the fungal endophytes inside the root tissues, it was not possible for us to measure this signature in the fungal biomass.

Several studies have estimated the proportion of N isotopes among the Antarctic biota, highlighting the role of marine-derived N on the fertilization of terrestrial ecosystems in relation to their proximity to active mammal and bird colonies (Erskine et al., 1998; Park et al., 2007; Bokhorst et al., 2019a,b). Nevertheless, these values could be highly variable depending on the local conditions. For example, Park et al. (2007) reported in the surroundings of Palmer station in Biscoe Point $\delta^{15}N$ values of 11.2 and 11.0‰ for *C. quitensis* and *D. antarctica*, respectively, which showed also a small depletion in ^{15}N respective to a 13.4‰ found in the soil (Park et al., 2007). However, in a similar study, Lee et al. (2009) found that the ^{15}N isotopic signatures of *D. antarctica* from Barton peninsula (King George Island) varied between 0.4 and 4.5‰, depending on how influenced the plants were by the local bird nesting sites. In the light of this, the isotopic signatures found here appear particularly depleted in ^{15}N (negative values for both species) probably because in our experimental setup we did not reproduce the continuous input of enriched ^{15}N produced by animal colonies in the field and because the experimental soil was retrieved from a zone without marine animal influence.

It is important to acknowledge that experimental and laboratory conditions are drastically different from the field. For example, by accelerating the rate of N uptake process because growth chambers cannot mimic the exact interaction between temperatures, relative humidity, and radiation experienced by plant in natural conditions. Nonetheless, this do not override the positive effect of fungal endophytes in process uptake here. Similar to the plant-mycorrhiza model, a depleted isotopic signature in the leaves is a clear evidence of the fungal symbiont mediation in the N assimilation by the Antarctic host plants. However, our results suggest that the effect of fungal endophytes for N uptake is most pronounced for *C. quitensis* than for *D. antarctica*. This is because despite $\delta^{15}N$ of foliar tissue in both species was significantly depleted relative to their E− counterparts, the fractionation between the substrate and the foliar tissues was lower in E+ plants of *D. antarctica* ($\delta^{15}N_{fract} = 4.02$), than E+ plants of *C. quitensis* ($\delta^{15}N_{fract} = 5.98$). It has been demonstrated that *D. antarctica* has the metabolic capability to incorporate small organic N-forms like amino acids and short peptides directly from the soil (Hill et al., 2019); a process that seems to fractionate less against the heavier isotope than the endophytic fungi does, leaving a less depleted signature in the plant tissue. However, this was not assessed in this study. Further research is needed to fully understand how fungal symbionts module different pathways of N acquisition and their relative relevance for each Antarctic vascular plant species.

Among cold environments the genus *Penicillium* has been observed in soil permafrost and ice-caps (Gunde-Cimerman et al., 2003; Zucconi et al., 2012). But it is also present in different Antarctic substrates such as oligotrophic (Godinho et al., 2015), ornithogenic (McRae et al., 1999), and the active layer of soil permafrost, in which spores of the two species studied here were present (Kochkina et al., 2014). In addition, some *Penicillium* species were found in different tissues of the Antarctic flora, including rhizoids of the liverwort *Cephaloziella varians* (Newsham, 2010) and shoot of the moss *Bryum argenteum* (Bradner et al., 2000). Nevertheless, has been poorly demonstrated the role of fungal endophytes (e.g., *Penicillium* spp.) in the nitrogen uptake assessed by the isotopic modulation and/or fractionation rates.

Based on our experimental results, we build a conceptual model (see **Figure 5**) that illustrates the effects of DSE in the nutrient acquisition in the two native vascular Antarctic plants. In the absence of DSE endophytes, E− plants seem to mainly uptake enriched N-sources, either from the enriched NH_4^+ previously present in the field soil samples, or from the

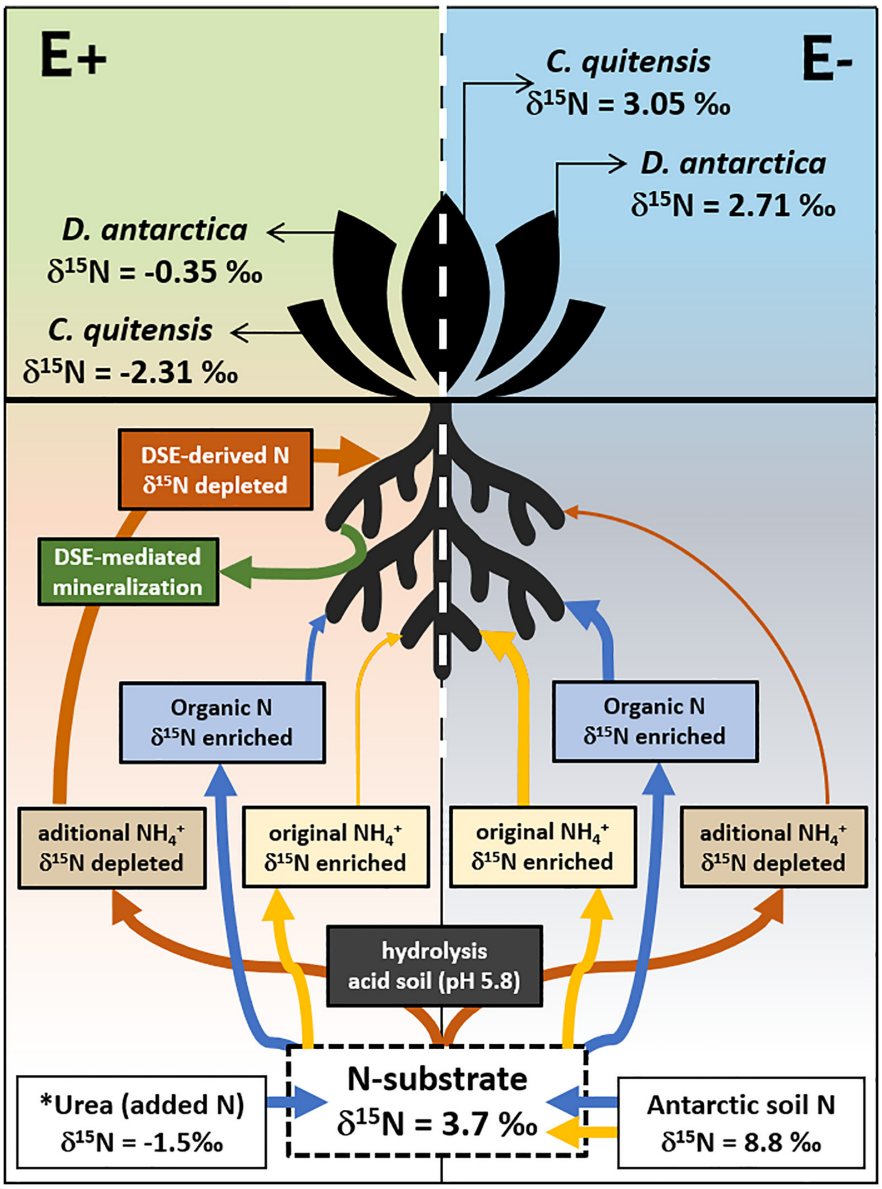

FIGURE 5 | Proposed model of the DSE-Plant interaction for N uptake in the vascular Antarctic plants *Deschampsia antarctica* and *Colobanthus quitensis*, determined by the d15N signature in soil and leaves. E denote non-infected plants while E+ their DSE-infected counterpart. Arrow's width imply preferred N-substrates uptaked/assimilated while their color represents its form in the soil (blue: organic; red/yellow: inorganic). The proportion of the urea added (8 g/kg) was equivalent to the previously estimated total N content of the experimental substrate (see methods for details). * Note that the urea added to the incubations are much more 15N depleted than the Antarctic soil used. Eliminado: Mineralization of organic N as described by the accumulation of NH4+ in the substrate of endophyte free (E−, in gray) and endophyte-infected (E+, in green) individuals of the two Antarctic vascular plant species. Boxplots represent the inter-quartilic distribution of the data (n = 7), different letters denote significant differences after a factorial pairwise comparison using Estimated-Marginal Means (EMMs) analysis with a 0.95 confidence level.

small organic compounds (e.g., amino acids and short-chain peptides) that Antarctic plant species may be capable to uptake (Hill et al., 2019). A proportion of the urea-derived NH_4^+ ($\delta^{15}N$ -1.5‰), which hydrolyzed spontaneously at the acidic conditions (pH 5.8), found in the soil, could also be uptaken due to the high affinity of plants for this N form, particularly by *D. antarctica* (Rabert et al., 2017). However, despite the presence of this ^{15}N-depleted NH_4^+ source in the substrate of all experimental plants, the ^{15}N signature in the final tissues of E− plants from both species was less fractionated ($\delta^{15}N$ 2.7–3.1‰), yet, partly depleted relative to the soil substrate ($\delta^{15}N$ 3.7‰). By contrast, the symbiotic interaction left a signature in the foliar tissues of E+ plants that was far more ^{15}N-depleted ($\delta^{15}N$ −0.4 to −2.3‰) than E− plants relative to the ^{15}N in the initial substrate, such as has been previously proposed (Hobbie and Högberg, 2012; and references therein). In this sense, this

isotopic signature strongly suggests that a large proportion of the N taken up, is preferentially managed through endophytes-mineralized N compounds, probably in the form of NH_4^+. This may be supported by the higher mineralization registered in the soils from E + individuals from both species compared with their axenic counterparts.

CONCLUSION

In conclusion, here we corroborate that despite being grown under rich N soils, DSE exert a positive effect in the N-uptake of the two Antarctic vascular plants. This effect was mediated both, by the enhanced availability of inorganic N sources in the substrate such as NH_4^+, but also by the active participation of fungal endophyte in the process of N-uptake, as suggested by the isotopic signature encountered in the foliar tissues of these plant species. Although, further research is needed to determine the specific routes by which fungal endophytes fulfill this role, here we identify some promising avenues of research to accomplish such a goal.

DATA AVAILABILITY STATEMENT

The raw data supporting the conclusions of this article will be made available by the authors, without undue reservation.

AUTHOR CONTRIBUTIONS

IA-R, CT-D, and MM-M designed and performed the experiments. IA-R, AG, and CA analyzed the data. All authors wrote and reviewed the manuscript.

FUNDING

This study was funded by the FONDECYT 1181034 and 1181873 and the ANID-PIA-Anillo INACH ACT192057.

ACKNOWLEDGMENTS

We thank the Chilean Antarctic Institute (INACH) and the "Henryk Arctowski" Polish Antarctic Station for their logistical support. Special mention to Krzysztof Herman, Bartosz Matuszczak, Cristian Fardella, and Maria Alejandra Montoya for their valuable help in the field, lab, and growth chamber experiments.

SUPPLEMENTARY MATERIAL

The Supplementary Material for this article can be found online at: https://www.frontiersin.org/articles/10.3389/fmicb.2020.575563/full#supplementary-material

REFERENCES

Acuña-Rodríguez, I. S., Newsham, K. K., Gundel, P. E., ., C., and Molina-Montenegro, M. A. (2020). Functional roles of microbial symbionts in plant cold tolerance. *Ecol. Lett.* 23, 1034–1048. doi: 10.1111/ele.13502

Allen, S. E. (1989). *Chemical Analysis of Ecological Materials*, 2nd Edn. Melbourne: Blackwell Scientific Publications.

Androsiuk, P., Chwedorzewska, K., Szandar, K., and Gielwanowska, I. (2015). Genetic variability of *Colobanthus quitensis* from King George Island (Antarctica). *Pol. Polar Res.* 36:281. doi: 10.1515/popore-2015-0017

Atkin, O. K. (1996). Reassessing the nitrogen relations of Arctic plants: a mini-review. *Plant Cell Environ.* 19, 695–704. doi: 10.1111/j.1365-3040.1996.tb00404.x

Bacon, C. W., and White, J. F. (2000). *Microbial Endophytes*. New York, NY: Marcel Dekker.

Barrera, A., Hereme, R., Ruiz-Lara, S., Larrondo, L. F., Gundel, P. E., Pollmann, S., et al. (2020). Fungal Endophytes Enhance the Photoprotective Mechanisms and Photochemical Efficiency in the Antarctic *Colobanthus quitensis* (Kunth) Bartl. Exposed to UV-B Radiation. *Front. Ecol. Evol.* 8:122. doi: 10.3389/fevo.2020.00122

Benavent-González, A., Raggio, J., Villagra, J., Blanquer, J. M., Pintado, A., Rozzi, R., et al. (2019). High nitrogen contribution by *Gunnera magellanica* and nitrogen transfer by mycorrhizas drive an extraordinarily fast primary succession in sub-Antarctic Chile. *N. Phytol.* 223, 661–674. doi: 10.1111/nph.15838

Bokhorst, S., Convey, P., and Aerts, R. (2019a). Nitrogen inputs by marine vertebrates drive abundance and richness in Antarctic terrestrial ecosystems. *Curr. Biol.* 29, 1721–1727. doi: 10.1016/j.cub.2019.04.038

Bokhorst, S., van Logtestijn, R., Convey, P., and Aerts, R. (2019b). Nitrogen isotope fractionation explains the 15 N enrichment of Antarctic cryptogams by volatilized ammonia from penguin and seal colonies. *Polar Res.* 38:3355. doi: 10.33265/polar.v38.3355

Bölter, M., Blume, H. P., Schneider, D., and Beyer, L. (1997). Soil properties and distributions of invertebrates and bacteria from King George Island (Arctowski Station), maritime Antarctic. *Polar Biol.* 18, 295–304. doi: 10.1007/s003000050191

Bölter, M. (2011). Soil development and soil biology on King George Island, maritime Antarctic. *Pol. Polar Res.* 32, 105–116. doi: 10.2478/v10183-011-0002-z

Bradner, J. R., Sidhu, R. K., Yee, B., Skotnicki, M. L., Selkirk, P. M., and Nevalainen, K. M. H. (2000). A new microfungal isolate, Embellisia sp., associated with the Antarctic moss *Bryum argenteum*. *Polar Biol.* 23, 730–732. doi: 10.1007/s003000000161

Erskine, P. D., Bergstrom, D. M., Schmidt, S., Stewart, G. R., Tweedie, C. E., and Shaw, J. D. (1998). Subantarctic Macquarie Island–a model ecosystem for studying animal-derived nitrogen sources using 15 N natural abundance. *Oecologia* 117, 187–193. doi: 10.1007/s004420050647

Godinho, V. M., Gonçalves, V. N., Santiago, I. F., Figueredo, H. M., Vitoreli, G. A., Schaefer, C. E., et al. (2015). Diversity and bioprospection of fungal community present in oligotrophic soil of continental Antarctica. *Extremophiles* 19, 585–596. doi: 10.1007/s00792-015-0741-6

Gunde-Cimerman, N., Sonjak, S., Zalar, P., Frisvad, J. C., Diderichsen, B., and Plemenitaš, A. (2003). Extremophilic fungi in arctic ice: a relationship between adaptation to low temperature and water activity. *Phys. Chem. Earth.* 28, 1273–1278. doi: 10.1016/j.pce.2003.08.056

Hereme, R., Morales-Navarro, S., Ballesteros, G., Barrera, A., Ramos, P., Gundel, P. E., et al. (2020). Fungal endophytes exert positive effects on *Colobanthus quitensis* under water stress but neutral under a projected climate change scenario in Antarctica. *Front. Microbiol.* 11:264. doi: 10.3389/fmicb.2020.00264

Hill, P. W., Farrar, J., Roberts, P., Farrell, M., Grant, H., Newsham, K. K., et al. (2011). Vascular plant success in a warming Antarctic may be due to efficient nitrogen acquisition. *Nat. Clim. Chang.*1, 50–53.

Hill, P. W., Broughton, R., Bougoure, J., Havelange, W., Newsham, K. K., Grant, H., et al. (2019). Fungal root endophytes of Antarctic angiosperms facilitate the

acquisition of organic nitrogen from ancient soil organic matter. *Ecol. Lett.* 22, 2111–2119. doi: 10.1038/nclimate1060

Hobbie, E. A., and Colpaert, J. V. (2003). Nitrogen availability and colonization by mycorrhizal fungi correlate with nitrogen isotope patterns in plants. *N. Phytol.* 157, 115–126. doi: 10.1046/j.1469-8137.2003.00657.x

Hobbie, E. A., and Hobbie, J. E. (2008). Natural abundance of 15 N in nitrogen-limited forests and tundra can estimate nitrogen cycling through mycorrhizal fungi: a review. *Ecosystems* 11:815. doi: 10.1007/s10021-008-9159-7

Hobbie, E. A., and Högberg, P. (2012). Nitrogen isotopes link mycorrhizal fungi and plants to nitrogen dynamics. *N. phytol.* 196, 367–382. doi: 10.1111/j.1469-8137.2012.04300.x

Hobbie, E. A., Macko, S. A., and Shugart, H. H. (1999). Interpretation of nitrogen isotope signatures using the NIFTE model. *Oecologia* 120, 405–415. doi: 10.1007/s004420050873

Hobbie, E. A., Macko, S. A., and Williams, M. (2000). Correlations between foliar δ 15 N and nitrogen concentrations may indicate plant-mycorrhizal interactions. *Oecologia* 122, 273–283. doi: 10.1007/PL00008856

Högberg, P. (1997). Tansley review no. 95 15 N natural abundance in soil–plant systems. *N. Phytol.* 137, 179–203. doi: 10.1046/j.1469-8137.1997.00808.x

Johnson, N. C., Wilson, G. W., Bowker, M. A., Wilson, J. A., and Miller, R. M. (2010). Resource limitation is a driver of local adaptation in mycorrhizal symbioses. *Proc. Natl. Acad. Sci. U S A* 107, 2093–2098. doi: 10.1073/pnas.0906710107

Jumpponen, A., Mattson, K. G., and Trappe, J. M. (1998). Mycorrhizal functioning of *Phialocephala fortinii* with *Pinus contorta* on glacier forefront soil: interactions with soil nitrogen and organic matter. *Mycorrhiza* 7, 261–265. doi: 10.1007/s005720050190

Knepel, K. (2003). Determination of nitrate in 2M KCl soil extracts by flow injection analysis. *Quik Chem. Method*. 12, 107–104.

Kochkina, G. A., Ozerskaya, S. M., Ivanushkina, N. E., Chigineva, N. I., Vasilenko, O. V., Spirina, E. V., et al. (2014). Fungal diversity in the Antarctic active layer. *Microbiology* 83, 94–101. doi: 10.1134/S002626171402012X

Kozeretska, I. A., Parnikoza, I. Y., Mustafa, O., Tyschenko, O. V., Korsun, S. G., and Convey, P. (2010). Development of Antarctic herb tundra vegetation near Arctowski station, King George Island. 3, 254–261. doi: 10.1016/j.polar.2009.10.001

Łachacz, A., Kalisz, B., Giełwanowska, I., Olech, M., Chwedorzewska, K. J., and Kellmann-Sopyła, W. (2018). Nutrient abundance and variability from soils in the coast of king George Island. *J. Soil Sci. Plant Nut.* 18, 294–311. doi: 10.4067/S0718-95162018005001101

Lee, Y. I., Lim, H. S., and Yoon, H. I. (2009). Carbon and nitrogen isotope composition of vegetation on King George Island, maritime Antarctic. *Polar Biol.* 32, 1607–1615. doi: 10.1007/s00300-009-0659-5

McRae, C. F., Hocking, A. D., and Seppelt, R. D. (1999). *Penicillium* species from terrestrial habitats in the Windmill Islands. East Antarctica, including a new species, Penicillium antarcticum. *Polar Biol.* 21, 97–111. doi: 10.1007/s003000050340

Michelsen, A., Quarmby, C., Sleep, D., and Jonasson, S. (1998). Vascular plant ^{15}N natural abundance in heath and forest tundra ecosystems is closely correlated with presence and type of mycorrhizal fungi in roots. *Oecologia* 115, 406–418. doi: 10.1007/s004420050535

Molina-Montenegro, M. A., Oses, R., Torres-Díaz, C., Atala, C., Zurita-Silva, A., and Ruiz-Lara, S. (2016). Root-endophytes improve the ecophysiological performance and production of an agricultural species under drought condition. *AoB Plants* 8:lw062. doi: 10.1093/aobpla/plw062

Narisawa, K. (2017). The dark septate endophytic fungus *Phialocephala fortinii* is a potential decomposer of soil organic compounds and a promoter of Asparagus officinalis growth. *Fungal Ecol.* 28, 1–10. doi: 10.1016/j.funeco.2017.04.001

Newsham, K. K. (2010). The biology and ecology of the liverwort *Cephaloziella varians* in Antarctica. *Antarct. Sci.* 22, 131–143. doi: 10.1017/S0954102009990630

Newsham, K. K. (2011). A meta-analysis of plant responses to dark septate root endophytes. *N. Phytol.* 190, 783–793. doi: 10.1111/j.1469-8137.2010.03611.x

Park, J. H., Day, T. A., Strauss, S., and Ruhland, C. T. (2007). Biogeochemical pools and fluxes of carbon and nitrogen in a maritime tundra near penguin colonies along the Antarctic Peninsula. *Polar Biol.* 30, 199–207. doi: 10.1007/s00300-006-0173-y

Pietr, S. J., Tatur, A., and Myrcha, A. (1983). Mineralization of penguin excrements in the Admiralty Bay region (King George Island, South Shetland Islands, Antarctica). *Pol. Polar Res.* 4, 97–112.

Pires, C. V., Schaefer, C. E., Hashigushi, A. K., Thomazini, A., and Mendonça, E. S. (2017). Soil organic carbon and nitrogen pools drive soil C-CO2 emissions from selected soils in Maritime Antarctica. *Sci. Total Environ.* 596, 124–135. doi: 10.1016/j.scitotenv.2017.03.144

R Core Team (2019). *R: A Language and Environment for Statistical Computing*. Vienna: R Foundation for Statistical Computing.

Rabert, C., Reyes-Díaz, M., Corcuera, L. J., Bravo, L. A., and Alberdi, M. (2017). Contrasting nitrogen use efficiency of Antarctic vascular plants may explain their population expansion in Antarctica. *Polar Biol.* 40, 1569–1580. doi: 10.1007/s00300-017-2079-2

Ramos, P., Rivas, N., Pollmann, S., Casati, P., and Molina-Montenegro, M. A. (2018). Hormonal and physiological changes driven by fungal endophytes increase Antarctic plant performance under UV-B radiation. *Fungal Ecol.* 34, 76–82. doi: 10.1016/j.funeco.2018.05.006

Rhodes, R. C., and Long, J. D. (1974). Run-off and mobility studies on benomyl in soils and turf. *B. Environ. Contam. Tox.* 12, 385–393. doi: 10.1007/BF01709137

Roberts, P., Newsham, K. K., Bardgett, R. D., Farrar, J. F., and Jones, D. L. (2009). Vegetation cover regulates the quantity, quality and temporal dynamics of dissolved organic carbon and nitrogen in Antarctic soils. *Polar Biol.* 32, 999–1008. doi: 10.1007/s00300-009-0599-0

Ruotsalainen, A. L. (2018). "Dark Septate Endophytes (DSE) in Boreal and Subarctic Forests," in *Endophytes of Forest Trees*. eds A.M. Pirttilä., and A.C. Frank (Cham: Springer), 105–117. doi: 10.1007/978-3-319-89833-9_5

Shaver, G. R., and Chapin, F. S. III (1980). Response to fertilization by various plant growth forms in an Alaskan tundra: nutrient accumulation and growth. *Ecology* 61, 662–675. doi: doi.org/10.2307/1937432

Upson, R., Newsham, K. K., Bridge, P. D., Pearce, D. A., and Read, D. J. (2009a). Taxonomic affinities of dark septate root endophytes of *Colobanthus quitensis* and *Deschampsia antarctica*, the two native Antarctic vascular plant species. *Fungal Ecol.* 2, 184–196.

Upson, R., Read, D. J., and Newsham, K. K. (2009b). Nitrogen form influences the response of *Deschampsia antarctica* to dark septate root endophytes. *Mycorrhiza* 20, 1–11. doi: 10.1007/s00572-009-0260-3

Wood, S. N. (2017). *Generalized Additive Models: An Introduction With R*, 2nd Edn. United States: Chapman and Hall/CRC.

Zhu, R., Liu, Y., Ma, E., Sun, J., Xu, H., and Sun, L. (2009). Nutrient compositions and potential greenhouse gas production in penguin guano, ornithogenic soils and seal colony soils in coastal Antarctica. *Antarct. Sci.* 21, 427–438. doi: 10.1017/S0954102009990204

Zucconi, L., Selbmann, L., Buzzini, P., Turchetti, B., Guglielmin, M., Frisvad, J. C., et al. (2012). Searching for eukaryotic life preserved in Antarctic permafrost. *Polar Biol.* 35, 749–757. doi: 10.1007/s00300-011-1119-6

Conflict of Interest: The authors declare that the research was conducted in the absence of any commercial or financial relationships that could be construed as a potential conflict of interest.

frontiers in Microbiology

ORIGINAL RESEARCH
published: 13 November 2020
doi: 10.3389/fmicb.2020.596589

The Transition From Stochastic to Deterministic Bacterial Community Assembly During Permafrost Thaw Succession

Stacey Jarvis Doherty[1,2], Robyn A. Barbato[2], A. Stuart Grandy[3], W. Kelley Thomas[1], Sylvain Monteux[4], Ellen Dorrepaal[5], Margareta Johansson[6] and Jessica G. Ernakovich[1,3]*

[1] Department of Molecular, Cellular, and Biomedical Sciences, University of New Hampshire, Durham, NH, United States, [2] Cold Regions Research and Engineering Laboratory, Engineer Research Development Center, United States Army Corps of Engineers, Hanover, NH, United States, [3] Department of Natural Resources and the Environment, University of New Hampshire, Durham, NH, United States, [4] Department of Soil and Environment, Swedish University of Agricultural Sciences, Uppsala, Sweden, [5] Climate Impacts Research Centre, Department of Ecology and Environmental Sciences, Umeå University, Abisko, Sweden, [6] Department of Physical Geography and Ecosystem Science, Lund University, Lund, Sweden

OPEN ACCESS

Edited by:
Laura Zucconi, University of Tuscia, Italy

Reviewed by:
Eric M. Bottos, Thompson Rivers University, Canada
Jackson Sorensen, University of California, Davis, United States

***Correspondence:**
Stacey Jarvis Doherty
stacey.j.doherty@erdc.dren.mil

Specialty section:
This article was submitted to Extreme Microbiology, a section of the journal Frontiers in Microbiology

Received: *19 August 2020*
Accepted: *27 October 2020*
Published: *13 November 2020*

Citation:
Doherty SJ, Barbato RA, Grandy AS, Thomas WK, Monteux S, Dorrepaal E, Johansson M and Ernakovich JG (2020) The Transition From Stochastic to Deterministic Bacterial Community Assembly During Permafrost Thaw Succession. Front. Microbiol. 11:596589. doi: 10.3389/fmicb.2020.596589

The Northern high latitudes are warming twice as fast as the global average, and permafrost has become vulnerable to thaw. Changes to the environment during thaw leads to shifts in microbial communities and their associated functions, such as greenhouse gas emissions. Understanding the ecological processes that structure the identity and abundance (i.e., assembly) of pre- and post-thaw communities may improve predictions of the functional outcomes of permafrost thaw. We characterized microbial community assembly during permafrost thaw using *in situ* observations and a laboratory incubation of soils from the Storflaket Mire in Abisko, Sweden, where permafrost thaw has occurred over the past decade. *In situ* observations indicated that bacterial community assembly was driven by randomness (i.e., stochastic processes) immediately after thaw with drift and dispersal limitation being the dominant processes. As post-thaw succession progressed, environmentally driven (i.e., deterministic) processes became increasingly important in structuring microbial communities where homogenizing selection was the only process structuring upper active layer soils. Furthermore, laboratory-induced thaw reflected assembly dynamics immediately after thaw indicated by an increase in drift, but did not capture the long-term effects of permafrost thaw on microbial community dynamics. Our results did not reflect a link between assembly dynamics and carbon emissions, likely because respiration is the product of many processes in microbial communities. Identification of dominant microbial community assembly processes has the potential to improve our understanding of the ecological impact of permafrost thaw and the permafrost–climate feedback.

Keywords: permafrost thaw, microbial community, community assembly, phylogenetic null modeling, ecological processes

INTRODUCTION

Permafrost, soil that has been frozen for two or more consecutive years, underlies approximately one fourth of the northern hemisphere (Zhang et al., 1999) and is undergoing thaw with increasing global temperature (Romanovsky et al., 2017). The Northern high latitudes are experiencing warming twice as fast as the global average (Overland et al., 2019) with an expected increase of 5°C to 6°C in the surface air temperature by the end of this century (Stocker et al., 2014). It is estimated that permafrost stores approximately 1300 Pg of carbon which is equal to that found in Earth's atmosphere and above and belowground vegetation combined (Hugelius et al., 2014). Following thaw, soil microorganisms decompose this carbon resulting in the release of greenhouse gases such as carbon dioxide (CO_2), methane (CH_4), and nitrous oxide (N_2O) to the atmosphere (Schädel et al., 2014; Treat et al., 2016; Voigt et al., 2017). As a result, these gases create a positive feedback to global warming, further threatening permafrost degradation.

Permafrost thaw induces changes to microbial community composition and functional potential (Mackelprang et al., 2011; Coolen and Orsi, 2015; Hultman et al., 2015). In microbial systems, dramatic disturbances of the local environment can lead to mass extinction and essentially "reset" a community's trajectory (Ferrenberg et al., 2013). Simulated permafrost thaw experiments conducted in a controlled laboratory environment have shown that thawing over relatively short time scales (e.g., days to months) results in different microbial community structure than before thaw (Mackelprang et al., 2011; Ernakovich et al., 2017). Field thaw experiments indicate that permafrost community compositions shift over longer time scales to resemble active layer communities along depth profiles (Deng et al., 2015; Mondav et al., 2017; Monteux et al., 2018). Functional shifts have also been observed during permafrost thaw. Frozen conditions promote genes involved in stress responses and survival strategies, and thaw results in increases in genes involved in decomposition of soil organic matter and transport of soil nutrients (Mackelprang et al., 2011, 2017; Coolen and Orsi, 2015; Hultman et al., 2015).

Since soil microorganisms regulate many important biogeochemical processes, such as carbon and nitrogen cycling, it is critical to understand how microbial communities are shaped during permafrost thaw and to what degree this will affect ecosystem level processes. Microbial community structure is important for ecosystem processes (Graham et al., 2016), but to what degree it matters depends on the physical and phylogenetic scale in question (Schimel, 1995). The structure of microbial communities is influenced by both deterministic and stochastic ecological assembly processes. Deterministic processes are driven by abiotic and biotic selection pressures that influence the fitness of a population in a given environment (Vellend, 2010; Nemergut et al., 2013). Stochastic processes, which include inherent randomness, are less predictable and include diversification (genetic variation), drift (random changes in species abundances), and dispersal (movement of species across space) (Vellend, 2010; Nemergut et al., 2013). Many microbiome studies attribute patterns of community structure only to deterministic processes (reviewed in Zhou and Ning, 2017). However, stochastic processes play an important role in structuring communities that is underappreciated in microbial ecology due to difficulty in defining stochastic processes and the variety of approaches used to assess stochasticity (Nemergut et al., 2013; Zhou and Ning, 2017). When communities are shaped by deterministic processes, variations in the local environment may directly influence functional outcomes since microbial traits are selected for by environmental conditions. Alternatively, when communities are structured by stochastic processes, function may be dependent on random shifts in trait abundances within the community, rather than a direct relationship with the environment (Knelman and Nemergut, 2014).

Assembly processes in permafrost systems provide important insights into drivers of microbial community structure in intact and thawed conditions. Bottos et al. (2018) found that bacterial communities in intact permafrost are structured by dispersal limitation. The permafrost environment is also thought to be selective for organisms that can survive subzero temperatures for extended periods of time (reviewed in Jansson and Taş, 2014), suggesting deterministic processes may also play a large role. Increases in soil temperature due to either experimental warming or long-term permafrost thaw have resulted in an increase of deterministic processes structuring active layer microbial communities (Mondav et al., 2017; Feng et al., 2020). Furthermore, Tripathi et al. (2018, 2019) found stochastic processes dominate community assembly in deeper soils compared to surface soils in permafrost systems. However, these studies lack a direct comparison of assembly processes in permafrost soils pre- and post-thaw. Upon thaw, the local environment changes dramatically and may present a physiological challenge for these microbes that have become accustomed to living in permafrost conditions. Immediately after a disturbance, assembly processes are more stochastic likely due to mass extinction events leading to ecological equivalence of individuals and immigration with little competition (Ferrenberg et al., 2013; Dini-Andreote et al., 2015). As succession progresses, selection begins to play a large role in structuring communities (Ferrenberg et al., 2013; Dini-Andreote et al., 2015). Therefore, we speculate that microbial communities in newly thawed permafrost are likely structured by stochastic processes, but as time since thaw progresses there is a shift toward deterministic assembly. In order to develop a robust framework to predict permafrost community dynamics following thaw, laboratory and field studies are needed to characterize shifts in microbial community assembly during thaw in both active layer and permafrost soils. Since outcomes of stochastic assembly may be more difficult to predict due to inherit randomness, the immediate implications of permafrost thaw may be difficult to understand if stochastic assembly plays a large role in structuring post-thaw communities.

The overall objective of this study was to determine the relative contribution of stochastic and deterministic assembly processes in active layer and permafrost soils pre- and post-thaw. Specific objectives were to characterize the effect of time since thaw on assembly processes and evaluate the effect of increased temperature on assembly dynamics and microbial

functions. We used the soil depth profile as a proxy of "time since thaw" by incorporating changes in active layer thickness over a fourteen-year period at the Storflaket Mire in Abisko, Sweden. We hypothesized that the uppermost active layer and permafrost communities would be dominated by environmental selection and transition zone communities would be dominated by stochastic assembly due to recent shifts in the abiotic environment. To test the direct effect of increased temperature on assembly dynamics we subjected soil samples from four depths along the depth profile to incubation at 4°C and 15°C. We hypothesized community assembly would be more stochastic at all depths after lab-induced thaw compared to *in situ* assembly. Specifically, the warmer incubation temperature leading to the most stochastic assembly due to the higher temperature representing a greater disturbance to the community. Comparing assembly patterns between field and lab thaw scenarios will elucidate the potential differences in community assembly at long versus short timescales after thaw.

MATERIALS AND METHODS

Site Description, Sample Collection, and Processing

Permafrost and active layer soil samples were collected from control plots used in a snow manipulation experiment (Johansson et al., 2013) at the Storflaket Mire in Abisko, Sweden (68°20′48″N, 18°58′16′E). Active layer thickness measurements were recorded across experimental plots during peak thaw in September each year resulting in a detailed record of active layer thickness over a fourteen-year period. A total of four replicate cores were collected from control plots at the site. Sampling locations were chosen to ensure similar active layer thickness and thaw histories were captured in the replicate cores (**Figure 1A**). At the time of sampling in June 2019, active layer soils had only thawed to approximately 34 cm. The permafrost began at 65 cm according to the 2018 active layer thickness data that was used to estimate the permafrost depth.

The thawed active layer was collected using a sterile serrated knife cleaned with 70% ethanol, DNA Away, and RNAse Away solutions (Thermo Fisher Scientific, Waltham, MA, United States) and set aside on a clean plastic tarp. The frozen active layer and permafrost were collected using a SIPRE corer (Jon's Machine Shop, Fairbanks, AK, United States) fitted with a gas-powered motor. The soil core was reconstructed by laying each piece on a cleaned plastic tarp. The thawed active layer was sub-sectioned into 10 cm sections up to 30 cm (0–10 cm, 10–20 cm, 20–30 cm) and placed in sterile Whirlpak bags. Frozen active layer and permafrost samples were bagged intact and sub sectioned back in the lab for the remaining depths: 30–40 cm, 40–50 cm, 50–60 cm, 60–70 cm, and 70–80 cm. All samples were stored on ice during transit.

All soil samples were subsampled for DNA analysis and soil incubation in a 2°C cold room at the Abisko Scientific Research Station. Tyvek suits and face masks were worn to reduce potential contamination of samples. All tools were sterilized with 70% ethanol, DNA Away, and RNAse Away solutions (Thermo Fisher Scientific, Waltham, MA, United States). Frozen cores were subsampled every 10 cm by cutting through the core with a sterile wire hand saw and broken apart with a mallet and sterile chisel. From each 10 cm segment, three smaller pieces were taken for DNA analysis of the *in situ* ("initial") community using a sterile hole saw bit and electric drill. All samples were stored at −20°C until shipment. Samples used to assess initial communities were hand carried on dry ice during transit and stored at −80°C upon arrival. Remaining samples to be used in the soil incubation thaw experiment were shipped frozen to the University of New Hampshire (UNH) and thawed to room temperature during the 12 days in transit. Upon arrival at UNH, these samples were stored at 4°C for 3 days prior to incubation set up.

Abiotic Analyses

Physical and chemical properties were characterized for "initial" samples using the thawed soils. Gravimetric water content (GWC), pH, total combustible carbon and nitrogen were measured. Soil GWC was determined by weighing approximately 10–20 g of soil from each biological replicate and drying at 105°C to a constant mass for 24 h. GWC was calculated on a per dry mass basis. Soil pH was determined by shaking a slurry of fresh soil and water (1:10) for 1 h and measured using an Accumet basic AB 15 pH meter (Thermo Fisher Scientific, Waltham, MA, United States). Soil was air dried and ground to a fine powder using a ball mill grinder fitted with plastic inserts. Ground soils were analyzed for total combustible carbon and nitrogen via thermal oxidation with gas chromatographic separation followed by thermal conductivity detection on a Costech C/H/N/S Elemental Analyzer (Costech Analytical Technologies, Inc., Valencia, CA, United States).

Soil Incubation

A soil incubation experiment was conducted to assess microbial community assembly after lab-induced thaw. The soil incubation was conducted at two different thaw temperatures. The 4°C temperature was chosen to reflect near-term thaw conditions and the 15°C temperature emulated a more drastic thaw state representative of the predicted temperature increase for the end of this century at northern high latitudes (Stocker et al., 2014). Four depths from each core were chosen to represent upper active layer (10–20 cm), lower active layer (30–40 cm), transition zone (50–60 cm), and intact permafrost (70–80 cm). For each depth, two subsamples of approximately 40 g of fresh soil were weighed into ethanol-cleaned specimen cups and placed inside a liter sized glass jar with deionized water at the bottom to maintain moisture content (**Supplementary Figure S1**). Lids were fitted with valves to allow for headspace gas analysis to monitor heterotrophic respiration throughout the incubation. Subsamples were preincubated in a controlled incubator in the dark at either 4°C or 15°C for 5 days. After the preincubation, the jars were flushed with CO_2-free air (Airgas, Dover, NH, United States) for 10 min. Jars were then sealed and incubated at either 4°C or 15°C in the dark. Individual cores served as replicates for this experiment (4 depths × 2 temperatures × 4 replicates (cores) = 32 samples).

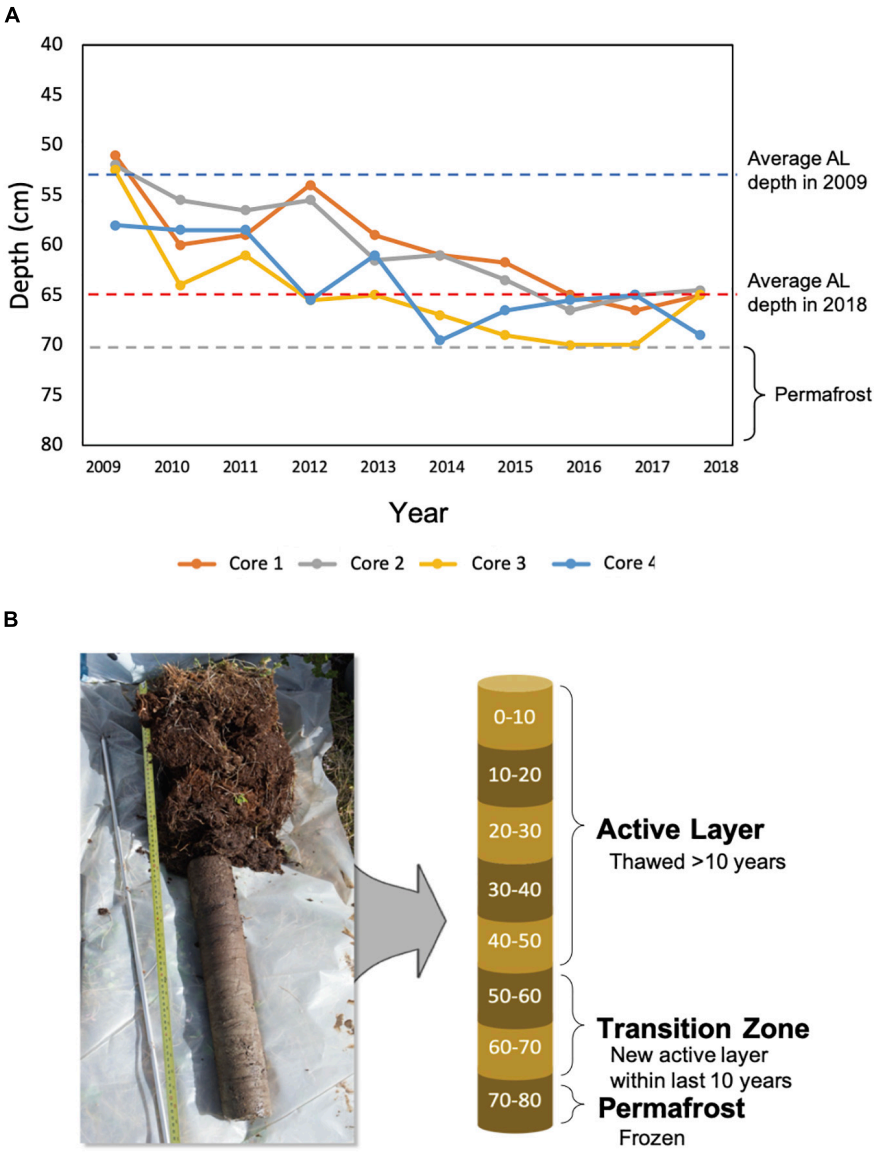

FIGURE 1 | Changes in active layer thickness and core subsampling. **(A)** The active layer thickness at sampling locations from 2009 to 2018. In 2009, the average active layer thickness across locations was 53 cm, and in 2018, it was 65 cm. Active layer thickness did not exceed 70 cm during this time period. **(B)** Each core was subsampled every 10 cm. Approximate time since thaw was used to differentiate active layer, transition zone, and permafrost soils.

Headspace gas measurements were analyzed every 2–7 days to ensure CO_2 concentrations remained below 2% and oxic. Jars were removed individually from the incubator and attached to a Picarro G2201-i cavity ring down spectrometer (Picarro, Santa Clara, CA, United States). Once readings stabilized, the CO_2 concentration was recorded, and the jar was flushed with CO_2-free air (Airgas, Dover, NH, United States) for 10 min. The spectrometer was calibrated using gas standards prepared by mixing a known volume of CO_2 calibration gas and CO_2-free air. Standards were generated to span the operational range of the instrument 100–4,000 ppm CO_2. Methane concentrations did not exceed the lower limit of the operational range of the analyzer (1.8 ppm CH_4) at any point during the incubation. Respiration rate was calculated to μg C-CO_2 g^{-1} dry soil h^{-1} (Equation 1). Dry weight was calculated using the gravimetric water content of the samples.

$$\mu g\ C\text{-}CO_2\ g^{-1} dry\ soil\ h^{-1} = \frac{CO_2\ \mu mol}{mol\ air} \times P \times V \times \frac{1}{R} \times \frac{1}{T} \times \frac{1}{g\ dry\ soil} \times \frac{12\ \mu g\ C}{1\ \mu mol\ C} \times \frac{1}{t}$$

Equation 1. Respiration rate calculation where P is atmospheric pressure in atm, V is headspace volume in L, R is ideal gas constant in L atm K^{-1} mol^{-1}, T is incubation temperature in K, and t is incubation length in hours.

Temperature sensitivity (Q_{10}) was also calculated to investigate the effect of warming on carbon processing rates, as measured by CO_2 production (Equation 2). Q_{10} values indicate the factor by which respiration increases when temperature is increased by 10°C.

$$Q_{10} = \left(\frac{k_{15}}{k_4}\right)^{\left(\frac{10}{15-4}\right)}$$

Equation 2. Temperature sensitivity (Q_{10}) calculation where k_{15} and k_4 are respiration rates at 15°C and 4°C, respectively.

Samples were harvested after 193 days of incubation ("post-thaw") to determine microbial community composition and assembly processes at the two incubation temperatures.

Microbial Community Analysis

Genomic DNA was extracted from both "initial" and "post-thaw" incubation experiment samples and sequenced to assess the microbial community composition and dominant assembly mechanisms. Frozen samples were homogenized prior to analysis using a mallet to crush large chunks. DNA was extracted using the Qiagen DNeasy PowerSoil kit (Qiagen, Hilden, Germany) with minor changes to manufacture's protocol (**Supplementary Material**). Each sample was extracted in triplicate and loaded onto the same spin filter to concentrate the DNA to increase yield in the permafrost samples which were expected to have low biomass. A MoBio PowerClean kit (MoBio, Carlsbad, CA, United States) was used to remove PCR inhibitors from the extracted DNA. DNA was then quantified using the Quant-iT dsDNA High Sensitivity Assay Kit and Qubit 3.0 fluorometer (Invitrogen, Carlsbad, CA, United States).

DNA was amplified through polymerase chain reaction (PCR) using the primers 515f-806r of the V4 region of the 16S rRNA gene to profile the bacterial and archaeal communities (Apprill et al., 2015; Parada et al., 2016) and the primers ITS1f-ITS2 of the internal transcribed spacer to profile the fungal community (White et al., 1990) (**Supplementary Table S1**). The reactions were performed separately for the two primer sets as follows. Each 16S rRNA reaction contained 6 μL DreamTaq Hot Start Green (Thermo Fisher Scientific, Waltham, MA, United States), 2.6 μL sterile water, 0.7 μL forward primer (5 μM), 0.7 μL reverse primer (5 μM), and 2 μL template DNA (10× diluted). Each ITS reaction contained 6 μL DreamTaq Hot Start Green, 3 μL sterile water, 0.5 μL forward primer (5 μM), 0.5 μL reverse primer (5 μM), and 2 μL template DNA (10× diluted). Amplifications were performed using a T100 Thermal Cycler (Bio-Rad, Hercules, CA, United States). The 16S rRNA conditions were: enzyme activation at 94°C for 3 min, followed by 35 cycles of denaturation at 94°C for 45 s, annealing at 50°C for 60 s, and extension at 72°C for 90 s, followed by final extension at 72°C for 10 min. The ITS conditions were: enzyme activation at 95°C for 3 min, followed by 35 cycles of denaturation at 95°C for 30 s, annealing at 52°C for 30 s, and extension at 72°C for 60 s, followed by final extension at 72°C for 12 min. No template controls were included to verify there was no contamination during the PCR. The presence of PCR product was confirmed through gel electrophoresis and quantified using the Qubit 3.0 fluorometer. PCR product concentration ranged from 2–27 ng/μL with deeper soil samples having lower concentrations than the near surface soil samples. PCR products were sent to the Hubbard Center for Genomic Studies (University of New Hampshire, NH, United States) for sequencing by Illumina HiSeq2500 with Rapid Run© SBS V2 chemistries (Illumina, San Diego, CA, United States) and 2 × 250 bp paired-end reads. Reads were demultiplexed using CASAVA (version 1.8; Illumina, San Diego, CA, United States).

Sequences were analyzed using QIIME 2 (version 2019.4) (Bolyen et al., 2019) on the Premise high performance computing cluster (University of New Hampshire, NH, United States). Primers were removed using Cutadapt (Martin, 2011) and then quality filtered with DADA2 (Callahan et al., 2016). For ITS analysis, ITSxpress (Rivers et al., 2018) was used to remove conserved regions to improve taxonomic classification (Nilsson et al., 2009). Taxonomy was assigned to amplicon sequence variants (ASVs) using scikit-learn naïve Bayes taxonomy classifier (Pedregosa et al., 2011) against the SILVA 99% database (Quast et al., 2012) for bacteria and UNITE database (Nilsson et al., 2019) for fungi. ASVs were filtered to remove chloroplast, mitochondria, and ASVs without phylum level classification. Bacteria and archaea were split into separate ASV tables. Due to low sequencing depth of archaea, it was not analyzed further in this study. ASVs were aligned with MAFFT (Katoh and Standley, 2013) and used to construct a phylogeny with FastTree2 (Price et al., 2010). To assess community composition along the depth profile, samples were rarefied to 2500 sequences per sample for bacteria and 950 for fungi. For the incubation study, samples were rarefied to 900 sequences per sample for bacteria and 950 for fungi. Rarefaction plots can be found in the **Supplemental Material** (**Supplementary Figures S4–S7**). Rarefication depths were chosen to ensure at least three replicates remained for each treatment. QIIME 2 artifacts were exported to R (version 3.6.3) (R Core Team, 2018) using the "qiime2R" package (Bisanz, 2018) to conduct statistical analysis using the "phyloseq" (McMurdie and Holmes, 2013) and "vegan" packages (Oksanen et al., 2019). Rarefied ASV tables and rooted trees were used for the community assembly analysis.

Statistical Analysis

All statistical analyses were conducted in R (version 3.6.3) (R Core Team, 2018). One-way analysis of variance (ANOVA) was used to assess differences in soil abiotic parameters by depth. Assumptions of normality and homogeneity were assessed using the Shapiro–Wilk and Levene tests, respectively. Two-way ANOVA was used to assess differences in soil respiration rates by incubation temperature and depth. C:N ratios and respiration rates were log transformed for statistical analysis to improve assumptions of normality. Multiple comparisons were conducted using the Tukey's HSD test to find which means were significantly different from one another.

Multivariate statistical analysis of community data was conducted using the 'vegan' package. Non-metric multidimensional scaling (NMDS) analysis using Bray–Curtis dissimilarity measure was used to evaluate differences

in microbial community composition with depth and incubation temperature. Biplot vectors were added to the "initial" community NMDS plots using the "envfit()" function. Permutational multivariate analysis of variance (PerMANOVA) was conducted using the "adonis()" function to determine significant drivers of community composition for both "initial" and "post-thaw" communities. Depth and temperature were included as fixed factors in the PerMANOVA model and permutations were constrained by the permafrost core the samples originated from to account for random factors. PerMANOVA analysis is sensitive to significant differences in dispersion across groups (Anderson, 2006). Differences between group dispersion was assessed using the "betadisper()" function to calculate the average distance of samples to the group spatial median in multivariate space. Significance was assessed using a permutation test with the "permutest()" function conducting 999 permutations.

Phylogenetic Signal and Null Modeling

The relative contribution of deterministic and stochastic assembly processes was determined for bacterial communities using phylogenetic turnover between samples and null models (Stegen et al., 2012, 2013). In order to infer ecological processes from phylogenetic information, there must be phylogenetic signal (Losos, 2008). Phylogenetic signal occurs when ecological similarity between species is related to their phylogenetic similarity. To test this assumption, phylogenetic signal was evaluated for GWC, pH, percent nitrogen, percent carbon, and the C:N ratio using the between-ASV difference in environmental optima and between-ASV phylogenetic distance. The environmental optima for each ASV was determined by calculating the abundance weighted mean for each environmental parameter tested (Stegen et al., 2012) using the "analogue" package (Simpson and Oksanen, 2020). This approximates the niche value of each abiotic variable for each ASV. A matrix of the between-ASV environmental optima differences was calculated using Manhattan distances for each abiotic variable. In addition to evaluating each abiotic variable individually, we calculated the combined ASV environmental optima using all of the abiotic variables measured. In brief, a matrix of the between-ASV combined environmental optima differences was calculated using the Euclidean distance measure of log normalized optima of all abiotic variables. The between-ASV phylogenetic distances were calculated using the "adephylo" package (Jombart and Dray, 2008). A mantel correlogram was generated using the "vegan" package by comparing each matrix of between-ASV environmental optima differences and the second matrix of between-ASV phylogenetic distances to evaluate the phylogenetic signal. Pearson's correlation coefficients were calculated for fifty phylogenetic distance classes. The Mantel test statistic was determined using 999 permutations with progressive Holm-Bonferroni correction for multiple testing. Significant positive correlations indicate ecological similarity among ASVs is higher than expected by chance within the distance class (Borcard and Legendre, 2012). Alternatively, significant negative correlations indicate ASVs are more ecologically dissimilar than expected by chance (Borcard and Legendre, 2012).

Determination of assembly processes was only conducted for bacterial communities. The ITS region is appropriate for investigations of fungal community composition, but since it is not phylogenetically conserved it is inappropriate for phylogenetic modeling. Using the framework developed by Stegen et al. (2012, 2013), phylogenetic turnover between communities was quantified as the β-mean-nearest taxon distance (βMNTD) using the "picante" package (Kembel et al., 2010). This quantifies the mean phylogenetic distance between each member of a community and its closest relative in a second community. Null modeling of each community was then performed to create a distribution ($n = 999$) of βMNTD values representing a stochastic assembled community. For each iteration of the model, the tips of phylogeny were randomized and the βMNTD was recalculated. Deviations of the observed βMNTD from the null distribution were quantified in units of standard deviation of the null to generate the β-nearest taxon index (βNTI). Sample pairwise comparisons resulting in $\beta NTI < -2$ or $\beta NTI > 2$ indicates phylogenetic turnover is less than or greater than expected by chance, respectively, suggesting niche-based processes. Pairwise comparisons resulting in $-2 > \beta NTI > 2$ indicate stochastic processes structure turnover between the two communities. A modified Raup–Crick metric calculated using the Bray–Curtis dissimilarity measure (RC_{bray}) was used to further differentiate the stochastic processes structuring the community (Chase et al., 2011). **Table 1** summarizes the βNTI and RC_{bray} output values and how assembly processes were defined. The relative contribution of assembly processes was calculated by taking the fraction of pairwise comparisons demonstrating a given process and dividing by the total pairwise comparisons.

TABLE 1 | Assembly processes and respective model conditions referenced from (Stegen et al., 2013).

Deterministic processes		**Stochastic processes**		
Homogeneous selection	**Heterogeneous selection**	**Homogenizing dispersal**	**Dispersal limitation and drift**	**Drift alone**
Environment constrains community composition through selection	Divergent environmental conditions result in each community having ecologically distinct members	High dispersal rates outweigh selective pressures	Movement of individuals is restricted	Population sizes fluctuate due to chance events
$\beta NTI < -2$	$\beta NTI > 2$	$-2 < \beta NTI < 2$		
–	–	$RC_{bray} < -0.95$	$RC_{bray} > 0.95$	$-0.95 < RC_{bray} < 0.95$

RESULTS

Community Assembly Patterns Along Depth Profile

Soil Properties

Soil abiotic properties were determined at each depth. Average gravimetric water content exceeded 100% at all depths and was highest in the upper soil layers and decreased along the soil depth profile (**Figure 2**; ANOVA; $F = 3.299$, $P = 0.0133$). Soil pH was acidic (pH < 7) at all depths, with the upper soil layers being most acidic with an average pH of 3.9 (**Figure 2**; ANOVA; $F = 6.325$, $P = 0.0003$). Total combustible carbon was approximately 46% in the first 40 cm and decreased across 40 cm to 80 cm. Total combustible nitrogen fluctuated throughout the depth profile, ranging from 0.26% to 2.47%. The soil C:N ratio was approximately four times higher in the upper active layer compared to the permafrost and consistently decreased with depth (**Figure 2**; ANOVA; $F = 7.854$, $P = 0.0000574$).

Phylogenetic Signal

Phylogenetic signal was evaluated using Mantel correlograms comparing between-ASV environmental optima and between-ASV phylogenetic distances. All Mantel correlograms showed significant positive correlations across short phylogenetic distance (**Figure 3**). This relationship is consistent with other studies and indicates closely related species are more ecologically similar (Stegen et al., 2013; Wang et al., 2013; Dini-Andreote et al., 2015). Phylogenetic signal over short distances supports the use of βMNTD in determining the degree of ecological similarity since it calculates evolutionary distance between closely related species (Stegen et al., 2012; Wang et al., 2013). Significant negative correlations over intermediate phylogenetic distance classes were also observed. This indicates that ASVs at intermediate distances were more ecologically dissimilar than expected by chance. This further supports that using βMNTD is a robust method to infer ecological assembly processes since closely related taxa are most ecologically similar according to the Mantel correlogram results.

Microbial Community Dynamics Along the Depth Profile

Microbial community composition shifted with depth as indicated by NMDS analysis of bacterial and fungal communities using Bray-Curtis dissimilarity measures (**Figure 4**). Bacterial community composition clustered by depth for samples spanning the upper active layer: 0–10, 10–20, and 20–30 cm (**Figure 4A**). Fungal community composition also shifted with depth, however more clustering was observed within the deeper soils (60–70 cm and 70–80 cm) than was for bacterial communities. Differences in dispersion across depths were non-significant for both bacteria and fungi (**Supplementary Table S1**). For both bacteria and fungi, the core that the samples originated from was a significant driver of community composition (PerMANOVA; bacteria: $F = 2.003$, $R^2 = 0.2145$, $P = 0.003$; fungi: $F = 2.342$, $R^2 = 0.2201$, $P = 0.0006$) and was used to constrain permutations when investigating significant differences in community composition by depth. Depth was a significant driver of community composition for both bacteria (PerMANOVA; $F = 1.698$, $R^2 = 0.3977$, $P = 0.0001$) and fungi (PerMANOVA; $F = 1.307$, $R^2 = 0.3034$, $P = 0.0091$). Environmental vectors were fitted onto the NMDS ordinations and significance of the fitted vectors was assessed using permutation tests of the environmental variables. The five environmental variables measured significantly correlated with bacterial and fungal community compositions, with the exception of percent nitrogen for fungal communities ($P > 0.05$). Soil pH correlated strongly with NMDS axes, reflecting that pH was a strong driver of the observed differences in community

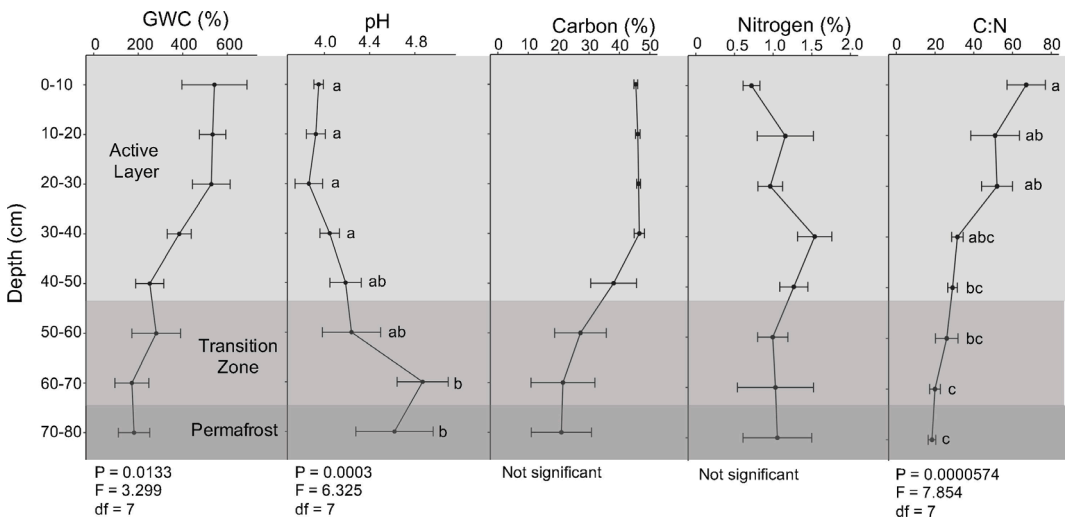

FIGURE 2 | Abiotic parameters. Gravimetric water content (GWC), pH, total combustible carbon and nitrogen, and soil carbon to nitrogen ratio (C:N) of field soils along the depth profile. Points represent mean values, and error bars indicate ± standard error of the mean ($n = 4$). Means with the same letter are not significantly different within each abiotic parameter as determined by Tukey's test ($\alpha = 0.05$). C:N ratios were log transformed for statistical analysis.

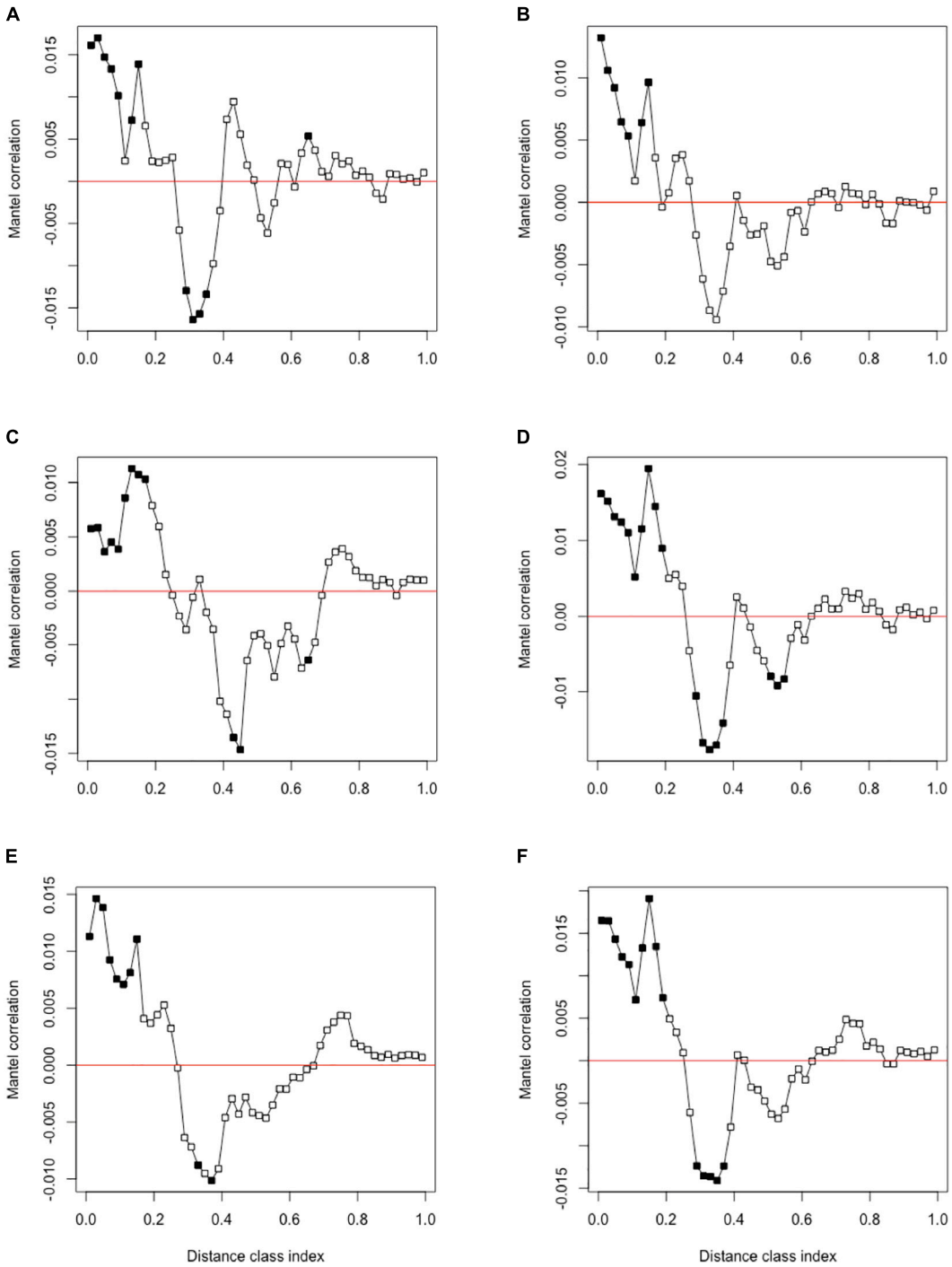

FIGURE 3 | Mantel correlogram using Pearson's correlation coefficient of between-ASV environmental optima and between-ASV phylogenetic distance for **(A)** pH, **(B)** % GWC, **(C)** % nitrogen, **(D)** % carbon, **(E)** C:N ratio, and **(F)** combined abiotic variables. Significant correlations ($P < 0.05$, solid circles) indicate phylogenetic signal in ASV ecological niche for the associated distance class. Significant positive correlations indicate that ecological similarity among ASVs is higher than expected by chance within the distance class. Alternatively, significant negative correlations indicate that ASVs are more ecologically dissimilar than expected by chance (Borcard and Legendre, 2012).

composition ($P < 0.003$). Likewise, gravimetric water content, percent carbon, and the C:N ratio were also significant abiotic drivers ($P < 0.01$).

Ecological processes structuring bacterial communities were determined using a phylogenetic null modeling approach. Assembly processes structuring bacterial communities changed

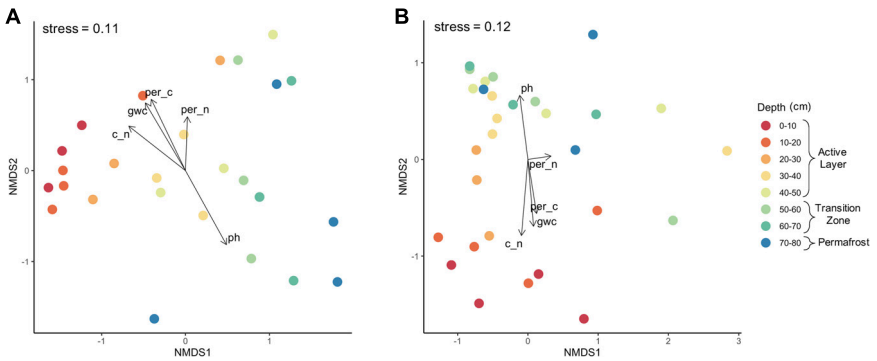

FIGURE 4 | Microbial community composition by depth. Non-metric multidimensional scaling analysis using Bray–Curtis dissimilarity of **(A)** bacterial and **(B)** fungal communities along depth profile. Depth was a significant driver of community composition for both bacteria (PerMANOVA; $F = 1.698$, $R^2 = 0.3977$, $P = 0.0001$) and fungi (PerMANOVA; $F = 1.307$, $R^2 = 0.3034$, $P = 0.0091$).

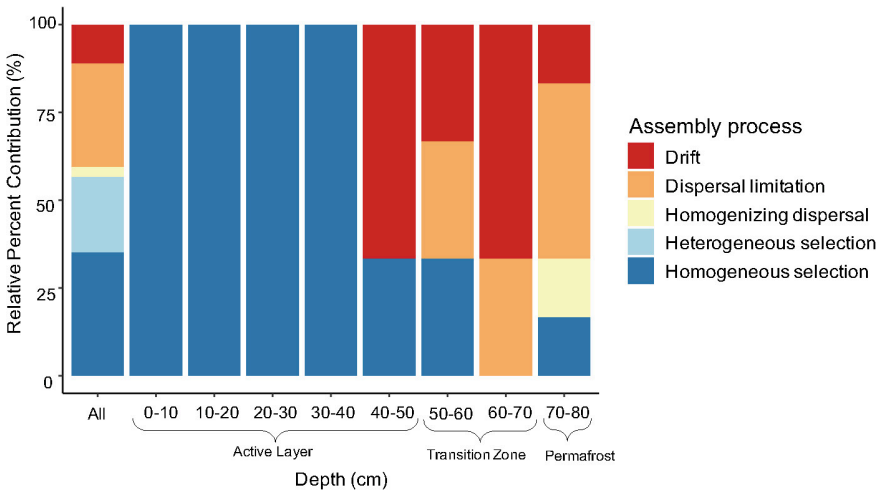

FIGURE 5 | Relative contribution of assembly process structuring bacterial communities along the depth profile. Assembly processes were determined across all pairwise comparisons ("All"; $n = 325$) and within-group pairwise comparisons ($n = 3$ to 6) calculated from three to four biological replicates. Specifically, the 10–20 cm and 70–80 cm depth comparisons had $n = 6$ and the rest were $n = 3$.

along the depth profile (**Figure 5**). When looking at all possible pairwise comparisons in the dataset, results indicate that approximately 56% of the assembly process were deterministic with homogeneous selection being the most dominant (**Figure 5**). Heterogeneous selection was also observed, likely due to varying environmental conditions between samples in the pairwise comparisons. Homogeneous selection indicates constant selection pressures (e.g., environmental conditions) resulting in low turnover between communities while heterogeneous selection suggests there are differences between selection pressures resulting in a large amount of turnover between communities (Stegen et al., 2015). We determined the assembly processes governing community composition at each depth by including only the within depth pairwise comparisons. Bacterial communities in the upper to mid active layers (0–10 cm to 30–40 cm) were structured completely by homogenous selection (**Figure 5**). There was a shift in assembly processes between the 30–40 cm and 40–50 cm depths where an increase in stochastic processes was observed, specifically drift. The 60–70 cm depth was completely dominated by the stochastic processes drift and dispersal limitation. This depth represents the most recently thawed soils which transitioned from permafrost to active layer within the last fourteen years (**Figure 1**). Permafrost (70–80 cm) bacterial communities were also structured mostly by stochastic processes, particularly dispersal limitation which represented 50% of the assembly processes (**Figure 5**). Drift, homogenizing dispersal, and homogeneous selection were also important processes structuring permafrost bacterial communities.

Community Assembly Patterns After Laboratory Thaw

Effect of Soil Depth and Incubation Temperature on Microbial Respiration

Microbial respiration was monitored throughout the incubation to assess general microbial activity and release of CO_2 with

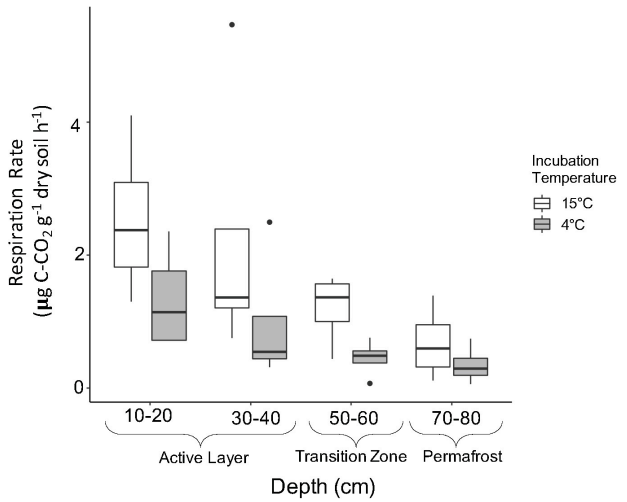

FIGURE 6 | Soil respiration rates by depth of soils incubated at 15°C (white) and 4°C (gray). Respiration rates were determined using stabilized rates from day 20 to 193 of incubation. Boxplots show median value as a solid line and upper and lower quartiles at the top and bottom of the boxes, respectively. Whiskers and points indicate the extent of the data. Respiration rates were log transformed for statistical analysis. Two-way ANOVA indicated significant effects of temperature ($F = 7.683$, $P = 0.01060$) and depth ($F = 5.134$, $P = 0.00695$) on respiration, but no combined effect.

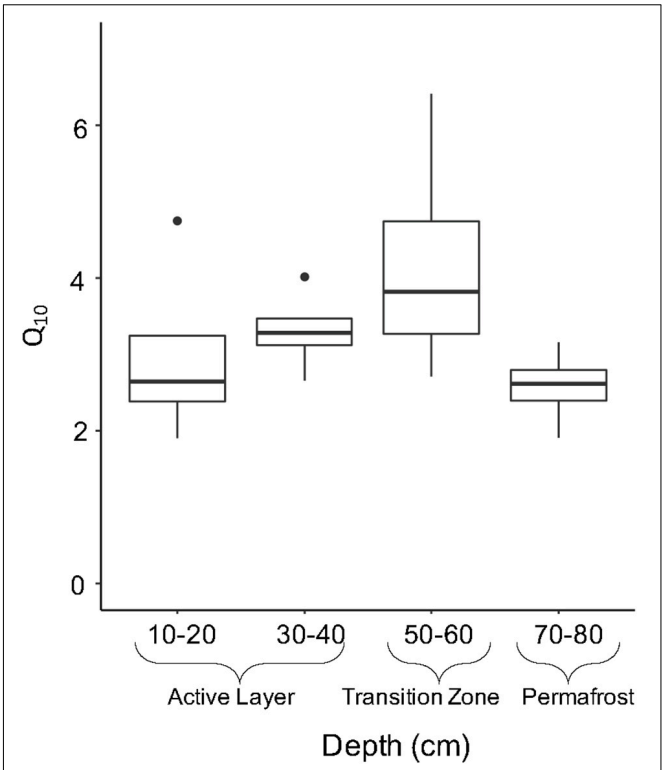

FIGURE 7 | Temperature sensitivity (Q_{10}) by soil depth. Q_{10} is an indicator of the temperature sensitivity of respiration and were calculated from CO_2 respiration rates at 15°C and 4°C. Boxplots show median value as a solid line and upper and lower quartiles at the top and bottom of the boxes, respectively. Whiskers and points indicate the extent of the data.

increased temperature. Respiration rates significantly decreased with depth (**Figure 6**; Two-way ANOVA; $F = 5.134$, $P = 0.00695$) where the 10–20 cm rate was four times greater than the 70–80 cm rate at both temperatures. Average respiration rates were significantly higher in soils incubated at 15°C compared to 4°C (**Figure 6**; Two-way ANOVA; $F = 7.683$, $P = 0.01060$). In general, average respiration was two to three times higher at 15°C compared to 4°C.

Temperature sensitivity (Q_{10}) of microbial respiration in soil samples was calculated to determine the factor by which heterotrophic respiration increases when temperature is increased by 10°C for these samples. No significant difference in Q_{10} values were observed between soil layers. The upper active layer (10–20 cm) and permafrost soils (70–80 cm) showed similar average Q_{10} values of 2.88 ± 0.59 and 2.49 ± 0.25, respectively (**Figure 7**). The transition zone soils showed the highest temperature sensitivity of all depths with an average of 4.05 ± 0.77 (**Figure 7**).

Microbial Community Dynamics With Incubation Conditions

Changes to the microbial community with thaw were assessed by comparing pre- and post-incubation communities at 4°C and 15°C. The laboratory incubation allowed us to examine the direct effect of temperature change on microbial communities found in each of the soil depth layers. Non-metric multidimensional scaling (NMDS) analysis using Bray-Curtis dissimilarity measures was used to determine if increased temperature resulted in changes to microbial community composition along the depth profile (**Figure 8**). Differences in group dispersion were non-significant for depth and temperature (**Supplementary Table S1**). For both bacteria and fungi, core was a significant driver of community composition (**Supplementary Figures S2, S3**; PerMANOVA; bacteria: $F = 2.842$, $R^2 = 0.1833$, $P = 0.0001$; fungi: $F = 2.414$, $R^2 = 0.1440$, $P = 0.0001$) and was used to constrain permutations when investigating community composition by depth and temperature. A three-dimensional NMDS solution was found (stress value < 0.2) for bacterial community structure and indicated strong clustering by depth with the deeper soils being less clustered compared to the active layer samples (**Figures 8A,B**). When looking at NMDS axes 2 and 3, the 50–60 cm and 70–80 cm depths grouped by pre- and post-incubation (**Figure 8B**). Both depth and temperature were significant drivers of bacterial community composition (PerMANOVA; depth: $F = 2.864$, $R^2 = 0.1876$, $P = 0.0001$; temperature: $F = 1.422$, $R^2 = 0.0621$, $P = 0.0027$); however, depth seemed to explain more variation in community composition compared to temperature. Depth and temperature were also significant drivers of fungal community composition (PerMANOVA; depth: $F = 2.075$, $R^2 = 0.1155$, $P = 0.0001$; temperature: $F = 3.489$, $R^2 = 0.1332$, $P = 0.0001$) with strong clustering observed by temperature (**Figure 8C**). In general, the pre- and post-incubation 10-20 cm samples clustered separately from the other three depths after incubation. The three samples

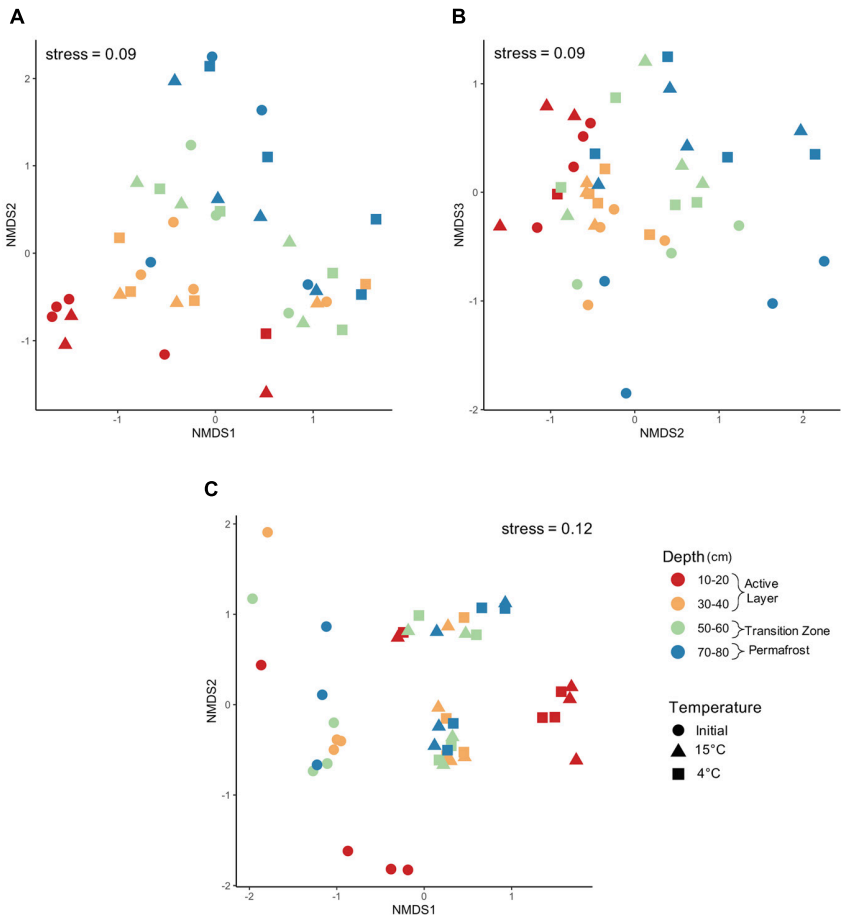

FIGURE 8 | Microbial community composition pre- and post-incubation. Non-metric multidimensional scaling analysis using Bray–Curtis dissimilarity community composition of **(A)** bacteria axes 1–2, **(B)** bacteria axes 2–3, and **(C)** fungi axes 1–2 before and after incubation at 4°C and 15°C. Bacterial communities were significantly structured by both depth and temperature (PerMANOVA; depth: $F = 2.864$, $R^2 = 0.1876$, $P = 0.0001$; temperature: $F = 1.422$, $R^2 = 0.0621$, $P = 0.0027$). Additionally, fungal communities were significantly structured by both depth and temperature (PerMANOVA; depth: $F = 2.075$, $R^2 = 0.1155$, $P = 0.0001$; temperature: $F = 3.489$, $R^2 = 0.1332$, $P = 0.0001$).

that did not follow this pattern were all from the same core which clustered somewhat on its own (**Supplementary Figure S3**).

We investigated the direct effect of increased temperature on assembly processes structuring microbial communities in along the depth profile. Dominant assembly processes were assessed to determine how assembly may differ based on near-term versus long-term thaw conditions. When looking at the effect of temperature on assembly of all depths combined, there was a slight increase in deterministic assembly between the initial and 4°C samples, but incubation at 15°C led to a 16% increase in stochastic assembly (**Figure 9A**). Laboratory incubation resulted in an increase in drift at both temperatures when all comparisons were considered. Varying shifts in assembly processes with incubation temperature were observed within each depth (**Figure 9A**). Processes structuring bacterial communities in the 10-20 cm layer remained deterministic after incubation (**Figure 9**). Only one of the 4°C samples for the 10–20 cm layer made it through quality control of the sequencing data and therefore pairwise comparisons could not be made for this treatment. An increase in stochastic processes was observed with warmer incubation temperature in the 30–40 cm depth. Within this depth, incubation at 15°C resulted in an increase from 33% to 66% stochastic assembly with drift being the dominant process (**Figure 9**). Both the 50–60 cm and 70–80 cm depths showed an increase in deterministic assembly from initial to 4°C samples and then a shift back to mostly stochastic assembly at 15°C (**Figure 9B**). The 50–60 cm depth was dominated by drift both pre- and post-incubation (**Figure 9A**). Permafrost (70–80 cm) bacterial communities were structured mainly by dispersal limitation in the frozen state, but upon thaw at 4°C and 15°C there was a shift to drift (**Figure 9A**). Heterogenous selection also emerged as an important deterministic process post-thaw for permafrost samples. Dispersal limitation and homogenizing dispersal were shown to be important processes structuring bacterial communities in the 50–60 cm and 70–80 cm samples after incubation in isolated microcosms (**Figure 9A**). However, the relative percent contribution of these two processes was less than that shown for the initial samples in both cases. The

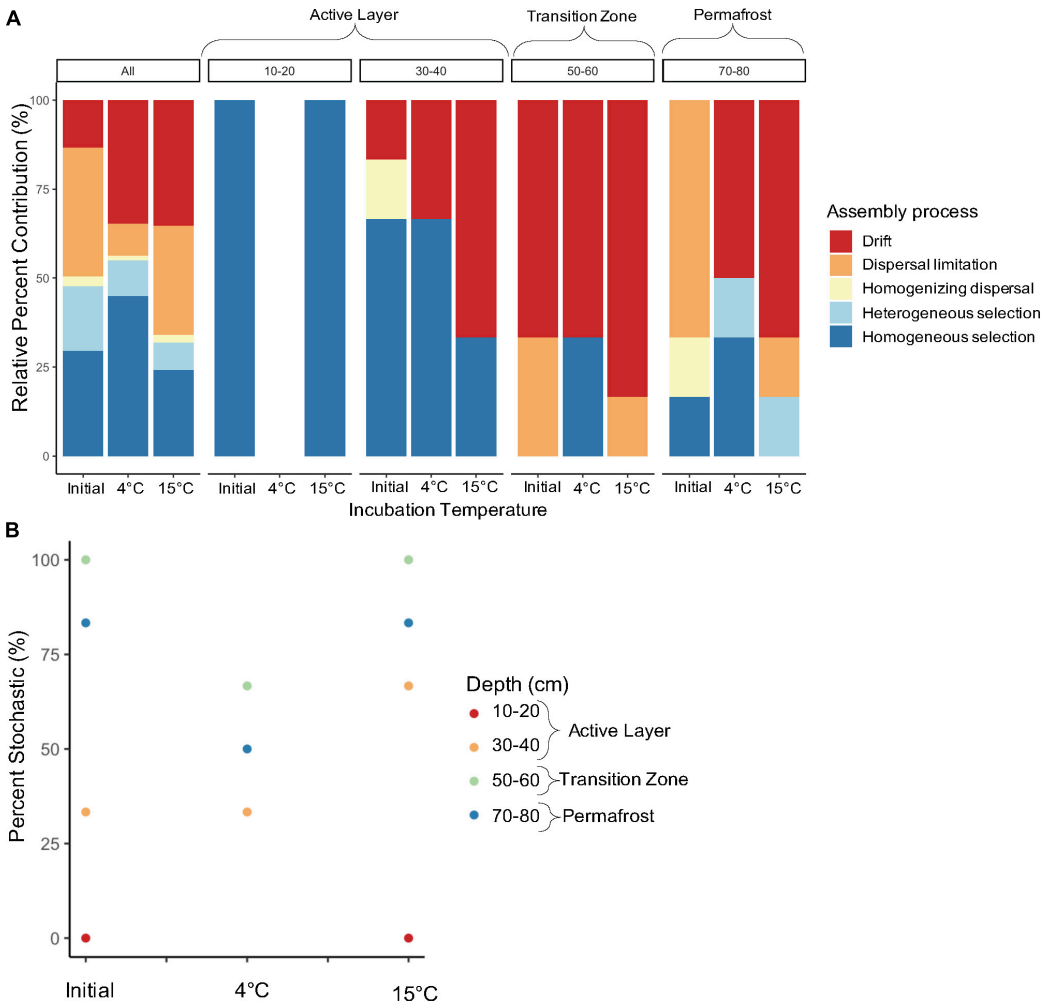

FIGURE 9 | Relative contribution of assembly process structuring bacterial communities pre- and post-incubation at 4°C and 15°C. The **(A)** relative percent contribution of each assembly process and **(B)** percent stochastic assembly are shown by depth. Assembly processes were determined across all pairwise comparisons ("All", $n = 861$) and within-group pairwise comparisons ($n = 3$ to 6) calculated from three to four biological replicates. The 10–20–4°C treatment only had one replicate and therefore pairwise comparisons for that treatment could not be made. Note that the 10–20–4°C data point on **(B)** is missing.

presence of these dispersal-based processes after incubation in isolated containers reflects their initial importance in structuring the communities in the field.

DISCUSSION

Microbial communities are structured by a combination of deterministic and stochastic processes, the outcome of which may have implications for how the community processes organic matter (Delgado-Baquerizo et al., 2016; Trivedi et al., 2016). Functional, taxonomic, and phylogenetic beta diversity are closely correlated in soil microorganisms (Fierer et al., 2012). Furthermore, Martiny et al. (2013) found that 93% of functional traits they investigated were non-randomly distributed across phylogeny with most traits being shared only among phylogenetically similar taxa. Given this relationship between phylogeny and function, the use of phylogenetic approaches to investigate drivers of community structure could be used to predict how function might change due to disturbance. Our findings suggest there is a shift toward stochastic assembly immediately after thaw, particularly the influence of drift, except in upper active layer soils. The active layer soils that have been seasonally thawed for many years exhibited mainly deterministic assembly indicating the importance of selection under long-term thaw. Understanding the processes controlling community reorganization after permafrost thaw will improve our ability to develop a robust framework to predict the ecological impact of permafrost thaw.

Permafrost Thaw Resulted in Increased Stochastic Assembly

Assembly processes structuring bacterial communities shifted along the depth profile. Transition zone soil at the active

layer-permafrost interface represents the most recently thawed soils, and the active layer soils have been seasonally thawed for a longer period of time. Permafrost and transition zone soils were dominated by stochastic community assembly, but deterministic processes also played a role in permafrost soils which is unsurprising given that stochastic and deterministic processes work in combination to influence community composition (Vellend, 2010). In intact permafrost, bacterial communities were structured mainly by dispersal limitation, but homogenizing dispersal, drift, and homogenizing selection also played a role in structuring permafrost communities. Bottos et al. (2018) also found dispersal limitation as the dominant process structuring permafrost bacterial communities across a permafrost transect in Central Alaska and found contributions of homogenizing dispersal and homogenous selection. Homogenizing dispersal describes high dispersal rates that outweigh selection pressures and is often seen in combination with dispersal limitation, but generally one is much more dominant than the other (Bottos et al., 2018; Tripathi et al., 2019). Homogenous selection occurs when a homogenous environment selects for ecologically similar taxa, which demonstrates that the permafrost environment is spatially homogenous and imposes limitations on the phylogenetic and functional diversity of the system. Our hypothesis that permafrost soils would be dominated by selection due to necessary survival strategies to tolerate adverse conditions was not supported. Instead, the physical constraints on dispersal were the dominant ecological process governing permafrost bacterial community structure. Although dispersal is often described as a stochastic process, some argue dispersal can be influenced by both stochastic and deterministic factors (reviewed in Nemergut et al., 2013; Zhou and Ning, 2017). In the case of permafrost, dispersal rates are partly dependent on the frozen environmental conditions and metabolic state of community members suggesting dispersal limitation may be partly deterministic. Frozen soil restricts the passive dispersal of microbes and cold temperature promotes a high degree of dormancy in the community therefore limiting their active dispersal abilities.

The transition zone soils, which most recently transitioned from permafrost to seasonally thawed active layer soils, were completely dominated by stochastic assembly processes which supported our hypothesis. Drift (random fluctuations in population sizes due to chance events) was the dominant process in the transition zone soils which indicates there may have been a great amount of turnover and extinction after thaw. Drift is an important process when local community size is small, selection is weak, and populations are present in low-abundances which could lead to local extinction (Chase and Myers, 2011; Nemergut et al., 2013). We did not measure population size in our study; however, in the case of permafrost thaw, it likely decreases due to drastic changes in the local environment immediately after thaw resulting in the closing of permafrost-specific niches, affecting individuals' ability to survive in the new environment. Future work should measure population size when assessing the contribution of assembly processes, particularly in the case of drift. Dispersal limitation also contributed to community assembly within transition zone soils suggesting dispersal between soil layers is still somewhat restricted immediately after thaw. The large influence of stochastic processes likely contributed to the observed variation of community composition in the permafrost and transition zone because the randomness of these processes allows for different composition trajectories (Fukami, 2015). These results are consistent with findings from Monteux et al. (2018) where the authors also observed more variation in community composition of the deeper soils at the same field site. Increases in stochastic assembly have been observed with increased depth in permafrost systems, particularly the influence of drift (Tripathi et al., 2018, 2019). Tripathi et al. (2019) also found dispersal limitation was highest in the deepest soil horizon in their study.

Active layer soils were dominated by deterministic assembly processes, suggesting that as time since thaw increases, there is a shift from stochastic to deterministic assembly. Upper active layer bacterial communities were completely dominated by homogenous selection indicating that there was less turnover between active layer communities than expected by chance. Tripathi et al. (2019) also found homogeneous selection was the dominant process structuring upper active layer bacterial communities which they attributed to minimal variation in physiochemical properties within this layer. We also observed little variation in pH and % carbon. Feng et al. (2020) observed an increase in deterministic assembly in permafrost-affected surface soils under long term warming which is consistent with our findings that the longer soils were thawed, the less stochastic assembly was observed. When investigating bacterial community assembly along a natural thaw gradient, Mondav et al. (2017) found there was a slight increase in deterministic assembly moving from intact to degraded permafrost sites. This further supports the finding that soils under long-term thaw transition from stochastic to deterministic assembly. Our hypothesis that the upper active layer would be dominated by deterministic assembly was supported. We observed assembly processes in the transition zone soils were largely stochastic and as time since thaw increased up the depth profile, the contribution of deterministic processes also increased. Our results support the framework developed by Ferrenberg et al. (2013) that community assembly immediately after a disturbance is likely to be stochastic and as succession progresses deterministic processes begin structuring communities. However, one drawback of using depth as a proxy of "time since thaw" is that it is difficult to tease apart the influence of soil physiochemical properties and the time, but these factors are intimately linked with permafrost thaw making this approach a reasonable approximation of *in situ* processes.

Laboratory Induced Thaw Increased Relative Contribution of Drift

Our hypothesis that assembly would be more stochastic at all depths after lab-induced thaw compared to *in situ* assembly, due

to the short successional time frame after the disturbance, was not supported. Instead, we observed similar percent stochasticity at pre- and post-incubation at 15°C. The permafrost and transition zone soils showed a slight decrease in stochastic assembly from pre- to post-incubation at 4°C. However, the importance of drift in structuring communities after thaw—a key finding from the field study—was confirmed in the laboratory incubations. The βNTI values from pairwise comparisons of all samples showed an increase in drift of 13% to 35% after incubation. Even larger increases in the relative contribution of drift were observed for the permafrost (70–80 cm) and lower active layer (30–40 cm) samples with the 15°C incubation temperature yielding the highest percent drift. The transition zone (50–60 cm) was initially dominated by drift, which only increased with incubation at 15°C. The observation that there is a large increase in drift upon thaw is consistent with the finding from the field study where a large increase in drift was seen in the transition zone. This suggests that laboratory incubation studies simulating permafrost thaw are good at showing the immediate effects of thaw, but that to understand the long-term effects longer incubations may be necessary. Given that the samples used in the incubation study thawed in transit, community trajectories might have been influenced by populations that emerged at room temperature. However, the large amount of turnover (i.e., drift) observed even after 193 days of incubation suggests these community members may not have had a greater fitness advantage after thaw.

When drift dominates, it may be difficult to predict the resulting community structure and function due to the random fluctuations in community member abundance. This makes inference of long-term effects of community change with thaw difficult using short-term lab studies (Elberling et al., 2013; Knoblauch et al., 2013). Lab incubations, at least those done in the short term, may not completely capture shifts in assembly at mid to late succession. Furthermore, laboratory studies usually do not incorporate the interactions between active layer and permafrost microbes, and since dispersal limitation is an important process structuring transition zone and permafrost communities, this should be considered. Experiments are needed to investigate permafrost thaw under realistic conditions where natural dispersal and seasonal changes can occur.

The Influence of Assembly Dynamics on Community Function

Disturbance events may alter ecosystem functioning when the disturbance results in a change in community composition—a common occurrence in microbial systems (Allison and Martiny, 2008). Different assembly processes can result in communities with varying compositions that harbor a distinct suite of functional traits and ultimately influence ecosystem functions (Knelman and Nemergut, 2014). Furthermore, assembly processes can influence community function due to fitness of individuals and their ability to contribute toward biogeochemical functions versus spending energy on survival and maintenance (Graham and Stegen, 2017). Some argue that information on microbial community composition is not necessary to predict how they will function (Schimel, 2001), however this is based on the assumptions that community assembly is controlled by selection (Nemergut et al., 2013) and that traits are always selected by the environment. Microbial communities structured by stochastic processes likely lack a direct link to environmental parameters and predicting functional outcomes based on environmental conditions alone may be difficult (Nemergut et al., 2013). While the synthesis by Allison and Martiny (2008) found that changes in community composition resulted in changes in function and the simulation modeling by Graham and Stegen (2017) show assembly processes can influence biogeochemical function, the assembly-function link proposed by Nemergut et al. (2013) is largely untested by experimental data.

Stochastic assembly in the months after permafrost thaw may result in decreased fitness of individuals leading to greater release of carbon from the soil. We speculate that permafrost thaw leads to a great amount of physiological stress for individuals in the community. This shift in environmental conditions may result in a stochastically assembled community dominated by drift and comprised of unfit taxa that invest most of their energy to survival and maintenance rather than biogeochemical processes (Schimel et al., 2007). Alternatively, increased CO_2 emissions could result due to fast-growing taxa proliferating after thaw. In either instance, unfit and fast-growing taxa are thought to be less efficient than their counterparts (reviewed in Molenaar et al., 2009; Roller and Schmidt, 2015) resulting in more carbon released as CO_2 in relation to carbon assimilated into biomass (Manzoni et al., 2012).

To test the link between assembly processes and carbon emission from thawing permafrost, we measured CO_2 respiration and compared it with the dominant assembly processes at each soil layer. We observed significant differences in microbial respiration along the soil depth profile and with incubation temperature. The transition zone soil showed increased temperature sensitivity (Q_{10}) indicating the respiration rate of these soils was most positively affected by an increase in temperature; however, this was not significantly higher than that of the other soil depths. Our results do not indicate there is a direct link between carbon emission from microbial respiration and assembly processes structuring communities. Respiration is conserved across many microbial taxa and shifts in assembly processes are less likely to affect broad functions that are redundant in a community. More specific traits, such as ability to use different carbon substrates, are less phylogenetically conserved and are only shared between closely related taxa (Martiny et al., 2013). In the case of these more specific functions, we would expect to see a relationship between assembly dynamics and functional outcomes. While our study suggests that differences in assembly processes do not have a direct link with CO_2 emissions, future research should investigate the assembly-function link over a broad suite of functions to better understand the role of these recently disturbed communities in the permafrost-climate feedback.

CONCLUSION

The objective of this study was to determine the ecological processes structuring microbial communities in permafrost and active layer soils. We found that depth was a strong driver of microbial community composition in both pre- and post-incubation soils. Permafrost and transition zone soils were dominated by stochastic processes with drift and dispersal limitation being the main processes controlling bacterial community structure. Deterministic processes, specifically homogeneous selection, were dominant in the active layer soils. Thawed conditions in both the field study and lab incubation increased the relative contribution of stochastic processes, particularly the importance of drift, in structuring communities. This was potentially the result of closing and opening of niches that lead to a large amount of turnover in community composition after thaw, particularly those with small population sizes. The laboratory incubation study reflected community assembly dynamics immediately after thaw, but precludes understanding the effect of assembly over long-term succession post-thaw. Our results suggest stochastic assembly immediately after thaw did not result in increased carbon emissions; however, future work should investigate the relationship between assembly dynamics and functional outcomes, particularly across the range of broad to specific functions.

DATA AVAILABILITY STATEMENT

The datasets presented in this study can be found in online repositories. The names of the repository/repositories and accession number(s) can be found below: https://www.ncbi.nlm.nih.gov/, PRJNA657840. Code used for modeling and statistical analyses is available at GitHub (https://github.com/sljarvis2).

AUTHOR CONTRIBUTIONS

SD, JE, RB, AG, and WT contributed to the experimental design. SM, ED, and MJ contributed to the field sampling design. MJ contributed to the active layer thickness data. SD and RB conducted the permafrost sampling and core processing. SD performed the experiments and analyzed the data. JE provided the experiment oversight and contributed to the data interpretation. SD wrote the first draft of the manuscript. All authors contributed to the manuscript revision, and read and approved the submitted version.

FUNDING

This work was supported by the New Hampshire Agricultural Experiment Station, the University of New Hampshire, and the Arctic Science IntegrAtion Quest Mobility Grant. Additional funding support was provided by the United States Army Engineer Research and Development Center, Basic Research Program Office, Environmental Quality and Installations.

ACKNOWLEDGMENTS

The authors would like to thank the Swedish Polar Research Secretariat, most specifically the staff of the Abisko Scientific Research Station, for their hospitality and offering logistic support. SD would like to thank Katie Bennett for assistance in the permafrost collection, Drew Ernakovich for assistance with the soil incubation setup and respiration analysis, Nate Blais for conducting soil CO_2 measurements, and David Moore for assistance in statistical analysis. SD would also like to thank Lukas Bernhardt, Sean Schaefer, and Dr. Jessica Mackay for their input on experimental design and data analysis. The content of this manuscript was previously included in a Master's thesis (Doherty, 2020).

SUPPLEMENTARY MATERIAL

The Supplementary Material for this article can be found online at: https://www.frontiersin.org/articles/10.3389/fmicb.2020.596589/full#supplementary-material

REFERENCES

Allison, S. D., and Martiny, J. B. H. (2008). Resistance, resilience, and redundancy in microbial communities. *Proc. Natl. Acad. Sci. U.S.A.* 105, 11512–11519. doi: 10.1073/pnas.0801925105

Anderson, M. J. (2006). Distance-based tests for homogeneity of multivariate dispersions. *Biometrics* 62, 245–253. doi: 10.1111/j.1541-0420.2005.00440.x

Apprill, A., McNally, S., Parsons, R., and Weber, L. (2015). Minor revision to V4 region SSU rRNA 806R gene primer greatly increases detection of SAR11 bacterioplankton. *Aquat. Microb. Ecol.* 75, 129–137. doi: 10.3354/ame01753

Bisanz, J. E. (2018). *qiime2R: Importing QIIME2 Artifacts and Associated Data into R Sessions*. Available online at: https://github.com/jbisanz/qiime2R (accessed August 7, 2020).

Bolyen, E., Rideout, J. R., Dillon, M. R., Bokulich, N. A., Abnet, C. C., Al-Ghalith, G. A., et al. (2019). Reproducible, interactive, scalable and extensible microbiome data science using QIIME 2. *Nat. Biotechnol.* 37, 852–857. doi: 10.1038/s41587-019-0209-9

Borcard, D., and Legendre, P. (2012). Is the Mantel correlogram powerful enough to be useful in ecological analysis? A simulation study. *Ecology* 93, 1473–1481. doi: 10.1890/11-1737.1

Bottos, E. M., Kennedy, D. W., Romero, E. B., Fansler, S. J., Brown, J. M., Bramer, L. M., et al. (2018). Dispersal limitation and thermodynamic constraints govern spatial structure of permafrost microbial communities. *FEMS Microbiol. Ecol.* 94:fiy110. doi: 10.1093/femsec/fiy110

Callahan, B. J., McMurdie, P. J., Rosen, M. J., Han, A. W., Johnson, A. J. A., and Holmes, S. P. (2016). DADA2: high resolution sample inference from Illumina amplicon data. *Nat. Methods* 13, 581–583. doi: 10.1038/nmeth.3869

Chase, J. M., Kraft, N. J. B., Smith, K. G., Vellend, M., and Inouye, B. D. (2011). Using null models to disentangle variation in community dissimilarity from variation in α-diversity. *Ecosphere* 2:art24. doi: 10.1890/ES10-00117.1

Chase, J. M., and Myers, J. A. (2011). Disentangling the importance of ecological niches from stochastic processes across scales. *Philos. Trans. R. Soc. London, Ser. B* 366, 2351–2363. doi: 10.1098/rstb.2011.0063

Coolen, M. J. L., and Orsi, W. D. (2015). The transcriptional response of microbial communities in thawing Alaskan permafrost soils. *Front. Microbiol.* 6:197. doi: 10.3389/fmicb.2015.00197

Delgado-Baquerizo, M., Giaramida, L., Reich, P. B., Khachane, A. N., Hamonts, K., Edwards, C., et al. (2016). Lack of functional redundancy in the relationship between microbial diversity and ecosystem functioning. *J. Ecol.* 104, 936–946. doi: 10.1111/1365-2745.12585

Deng, J., Gu, Y., Zhang, J., Xue, K., Qin, Y., Yuan, M., et al. (2015). Shifts of tundra bacterial and archaeal communities along a permafrost thaw gradient in Alaska. *Mol. Ecol.* 24, 222–234. doi: 10.1111/mec.13015

Dini-Andreote, F., Stegen, J. C., van Elsas, J. D., and Salles, J. F. (2015). Disentangling mechanisms that mediate the balance between stochastic and deterministic processes in microbial succession. *Proc. Natl. Acad. Sci. U.S.A.* 112, E1326–E1332. doi: 10.1073/pnas.1414261112

Doherty, S. J. (2020). *The Transition From Stochastic to Deterministic Bacterial Community Assembly During Permafrost Thaw Succession*. Master's thesis, University of New Hampshire, Durham, NH.

Elberling, B., Michelsen, A., Schädel, C., Schuur, E. A. G., Christiansen, H. H., Berg, L., et al. (2013). Long-term CO2 production following permafrost thaw. *Nat. Clim. Change* 3, 890–894. doi: 10.1038/nclimate1955

Ernakovich, J. G., Lynch, L. M., Brewer, P. E., Calderon, F. J., and Wallenstein, M. D. (2017). Redox and temperature-sensitive changes in microbial communities and soil chemistry dictate greenhouse gas loss from thawed permafrost. *Biogeochemistry* 134, 183–200. doi: 10.1007/s10533-017-0354-5

Feng, J., Wang, C., Lei, J., Yang, Y., Yan, Q., Zhou, X., et al. (2020). Warming-induced permafrost thaw exacerbates tundra soil carbon decomposition mediated by microbial community. *Microbiome* 8:3. doi: 10.1186/s40168-019-0778-3

Ferrenberg, S., O'Neill, S. P., Knelman, J. E., Todd, B., Duggan, S., Bradley, D., et al. (2013). Changes in assembly processes in soil bacterial communities following a wildfire disturbance. *ISME J.* 7, 1102–1111. doi: 10.1038/ismej.2013.11

Fierer, N., Leff, J. W., Adams, B. J., Nielsen, U. N., Bates, S. T., Lauber, C. L., et al. (2012). Cross-biome metagenomic analyses of soil microbial communities and their functional attributes. *Proc. Natl. Acad. Sci. U.S.A.* 109, 21390–21395. doi: 10.1073/pnas.1215210110

Fukami, T. (2015). Historical contingency in community assembly: integrating niches, species pools, and priority effects. *Annu. Rev. Ecol. Evol. Syst.* 46, 1–23. doi: 10.1146/annurev-ecolsys-110411-160340

Graham, E., and Stegen, J. (2017). Dispersal-based microbial community assembly decreases biogeochemical function. *Processes* 5:65. doi: 10.3390/pr5040065

Graham, E. B., Knelman, J. E., Schindlbacher, A., Siciliano, S., Breulmann, M., Yannarell, A., et al. (2016). Microbes as engines of ecosystem function: when does community structure enhance predictions of ecosystem processes? *Front. Microbiol.* 7:214. doi: 10.3389/fmicb.2016.00214

Hugelius, G., Strauss, J., Zubrzycki, S., Harden, J. W., Schuur, E. A. G., Ping, C.-L., et al. (2014). Estimated stocks of circumpolar permafrost carbon with quantified uncertainty ranges and identified data gaps. *Biogeosciences* 11, 6573–6593. doi: 10.5194/bg-11-6573-2014

Hultman, J., Waldrop, M. P., Mackelprang, R., David, M. M., McFarland, J., Blazewicz, S. J., et al. (2015). Multi-omics of permafrost, active layer and thermokarst bog soil microbiomes. *Nature* 521, 208–212. doi: 10.1038/nature14238

Jansson, J. K., and Taş, N. (2014). The microbial ecology of permafrost. *Nat. Rev. Microbiol.* 12, 414–425. doi: 10.1038/nrmicro3262

Johansson, M., Callaghan, T. V., Bosiö, J., Åkerman, H. J., Jackowicz-Korczynski, M., and Christensen, T. R. (2013). Rapid responses of permafrost and vegetation to experimentally increased snow cover in sub-arctic Sweden. *Environ. Res. Lett.* 8:035025. doi: 10.1088/1748-9326/8/3/035025

Jombart, T., and Dray, S. (2008). *adephylo: Exploratory Analyses for the Phylogenetic Comparative Method*. Available online at: https://cran.r-project.org/web/packages/adephylo/index.html (accessed December 18, 2017).

Katoh, K., and Standley, D. M. (2013). MAFFT multiple sequence alignment software version 7: improvements in performance and usability. *Mol. Biol. Evol.* 30, 772–780. doi: 10.1093/molbev/mst010

Kembel, S. W., Cowan, P. D., Helmus, M. R., Cornwell, W. K., Morlon, H., Ackerly, D. D., et al. (2010). Picante: R tools for integrating phylogenies and ecology. *Bioinformatics* 26, 1463–1464. doi: 10.1093/bioinformatics/btq166

Knelman, J. E., and Nemergut, D. R. (2014). Changes in community assembly may shift the relationship between biodiversity and ecosystem function. *Front. Microbiol.* 5:424. doi: 10.3389/fmicb.2014.00424

Knoblauch, C., Beer, C., Sosnin, A., Wagner, D., and Pfeiffer, E.-M. (2013). Predicting long-term carbon mineralization and trace gas production from thawing permafrost of Northeast Siberia. *Glob. Change Biol.* 19, 1160–1172. doi: 10.1111/gcb.12116

Losos, J. B. (2008). Phylogenetic niche conservatism, phylogenetic signal and the relationship between phylogenetic relatedness and ecological similarity among species. *Ecol. Lett.* 11, 995–1003. doi: 10.1111/j.1461-0248.2008.01229.x

Mackelprang, R., Burkert, A., Haw, M., Mahendrarajah, T., Conaway, C. H., Douglas, T. A., et al. (2017). Microbial survival strategies in ancient permafrost: insights from metagenomics. *ISME J.* 11, 2305–2318. doi: 10.1038/ismej.2017.93

Mackelprang, R., Waldrop, M. P., DeAngelis, K. M., David, M. M., Chavarria, K. L., Blazewicz, S. J., et al. (2011). Metagenomic analysis of a permafrost microbial community reveals a rapid response to thaw. *Nature* 480, 368–371. doi: 10.1038/nature10576

Manzoni, S., Taylor, P., Richter, A., Porporato, A., and Ågren, G. I. (2012). Environmental and stoichiometric controls on microbial carbon-use efficiency in soils: research review. *New Phytol.* 196, 79–91. doi: 10.1111/j.1469-8137.2012.04225.x

Martin, M. (2011). Cutadapt removes adapter sequences from high-throughput sequencing reads. *EMBnet J.* 17:10. doi: 10.14806/ej.17.1.200

Martiny, A. C., Treseder, K., and Pusch, G. (2013). Phylogenetic conservatism of functional traits in microorganisms. *ISME J.* 7, 830–838. doi: 10.1038/ismej.2012.160

McMurdie, P. J., and Holmes, S. (2013). phyloseq: an R package for reproducible interactive analysis and graphics of microbiome census data. *PLoS One* 8:e61217. doi: 10.1371/journal.pone.0061217

Molenaar, D., van Berlo, R., de Ridder, D., and Teusink, B. (2009). Shifts in growth strategies reflect tradeoffs in cellular economics. *Mol. Syst. Biol.* 5:323. doi: 10.1038/msb.2009.82

Mondav, R., McCalley, C. K., Hodgkins, S. B., Frolking, S., Saleska, S. R., Rich, V. I., et al. (2017). Microbial network, phylogenetic diversity and community membership in the active layer across a permafrost thaw gradient: microbial community across a permafrost thaw gradient. *Environ. Microbiol.* 19, 3201–3218. doi: 10.1111/1462-2920.13809

Monteux, S., Weedon, J. T., Blume-Werry, G., Gavazov, K., Jassey, V. E. J., Johansson, M., et al. (2018). Long-term in situ permafrost thaw effects on bacterial communities and potential aerobic respiration. *ISME J.* 12, 2129–2141. doi: 10.1038/s41396-018-0176-z

Nemergut, D. R., Schmidt, S. K., Fukami, T., O'Neill, S. P., Bilinski, T. M., Stanish, L. F., et al. (2013). Patterns and processes of microbial community assembly. *Microbiol. Mol. Biol. Rev.* 77, 342–356. doi: 10.1128/MMBR.00051-12

Nilsson, R. H., Larsson, K. H., Taylor, A. F. S., Bengtsson-Palme, J., Jeppesen, T. S., Schigel, D., et al. (2019). The UNITE database for molecular identification of fungi: handling dark taxa and parallel taxonomic classifications. *Nucleic Acids Res.* 47, D259–D264. doi: 10.1093/nar/gky1022

Nilsson, R. H., Ryberg, M., Abarenkov, K., Sjokvist, E., and Kristiansson, E. (2009). The ITS region as a target for characterization of fungal communities using emerging sequencing technologies. *FEMS Microbiol. Lett.* 296, 97–101. doi: 10.1111/j.1574-6968.2009.01618.x

Oksanen, J., Blanchet, G., Friendly, M., Kindt, R., Legendre, P., McGlinn, D., et al. (2019). *vegan: Community Ecology Package*. Available online at: https://CRAN.R-project.org/package=vegan (accessed September 01, 2019).

Overland, J. E., Hanna, E., Hassen-Bauer, I., Kim, S.-J., Walsh, J. E., Wang, M., et al. (2019). *Surface Air Temperature*. Available online at: http://www.arctic.noaa.gov/Report-Card/Report-Card-2019 (accessed February 26, 2020).

Parada, A. E., Needham, D. M., and Fuhrman, J. A. (2016). Every base matters: assessing small subunit rRNA primers for marine microbiomes with mock communities, time series and global field samples. *Environ. Microbiol.* 18, 1403–1414. doi: 10.1111/1462-2920.13023

Pedregosa, F., Varoquaux, G., Gramfort, A., Michel, V., Thirion, B., Grisel, O., et al. (2011). Scikit-learn: machine learning in python. *J. Mach. Learn Res.* 12, 2825–2830.

Price, M. N., Dehal, P. S., and Arkin, A. P. (2010). FastTree 2 – approximately maximum-likelihood trees for large alignments. *PLoS One* 5:e9490. doi: 10.1371/journal.pone.0009490

Quast, C., Pruesse, E., Yilmaz, P., Gerken, J., Schweer, T., Yarza, P., et al. (2012). The SILVA ribosomal RNA gene database project: improved data processing and web-based tools. *Nucleic Acids Res.* 41, D590–D596. doi: 10.1093/nar/gks1219

R Core Team (2018). *R: A Language and Environment for Statistical Computing*. Vienna: R Foundation for Statistical Computing.

Rivers, A. R., Weber, K. C., Gardner, T. G., Liu, S., and Armstrong, S. D. (2018). ITSxpress: software to rapidly trim internally transcribed spacer sequences with quality scores for marker gene analysis. *F1000Res.* 7:1418. doi: 10.12688/f1000research.15704.1

Roller, B. R., and Schmidt, T. M. (2015). The physiology and ecological implications of efficient growth. *ISME J.* 9, 1481–1487. doi: 10.1038/ismej.2014.235

Romanovsky, V., Isaksen, K., Drozdov, D., Anisimov, O., Instanes, A., Leibman, M., et al. (2017). "Changing permafrost and its impacts," in *Snow, Water, Ice and Permafrost in the Arctic (SWIPA) 2017*, (Oslo: Arctic Monitoring and Assessment Programme (AMAP)), 65–102.

Schädel, C., Schuur, E. A. G., Bracho, R., Elberling, B., Knoblauch, C., Lee, H., et al. (2014). Circumpolar assessment of permafrost C quality and its vulnerability over time using long-term incubation data. *Glob. Change Biol.* 20, 641–652. doi: 10.1111/gcb.12417

Schimel, D. S. (1995). Terrestrial ecosystems and the carbon cycle. *Glob. Change Biol.* 1, 77–91. doi: 10.1111/j.1365-2486.1995.tb00008.x

Schimel, J. (2001). "Biogeochemical models: implicit versus explicit microbiology," in *Global Biogeochemical Cycles in the Climate System*, (Cambridge, MA: Academic Press), 177–183.

Schimel, J., Balser, T. C., and Wallenstein, M. (2007). Microbial Stress-Response Physiology and Its Implications for Ecosystem Function. *Ecology* 88, 1386–1394. doi: 10.1890/06-0219

Simpson, G. L., and Oksanen, J. (2020). *analogue: Analogue Matching and Modern Analogue Technique Transfer Function Models*. Available online at: https://cran.r-project.org/package=analogue (accessed July 28, 2020).

Stegen, J. C., Lin, X., Fredrickson, J. K., Chen, X., Kennedy, D. W., Murray, C. J., et al. (2013). Quantifying community assembly processes and identifying features that impose them. *ISME J.* 7, 2069–2079. doi: 10.1038/ismej.2013.93

Stegen, J. C., Lin, X., Fredrickson, J. K., and Konopka, A. E. (2015). Estimating and mapping ecological processes influencing microbial community assembly. *Front. Microbiol.* 6:370. doi: 10.3389/fmicb.2015.00370

Stegen, J. C., Lin, X., Konopka, A. E., and Fredrickson, J. K. (2012). Stochastic and deterministic assembly processes in subsurface microbial communities. *ISME J.* 6, 1653–1664. doi: 10.1038/ismej.2012.22

Stocker, T. F., Qin, D., Plattner, G.-K., Tignor, M. M. B., Allen, S. K., Boschung, J., et al. (eds) (2014). *Climate Change 2013: The Physical Science Basis. Contribution of Working Group I to the Fifth Assessment Report of IPCC the Intergovernmental Panel on Climate Change*. Cambridge: Cambridge University Press, doi: 10.1017/CBO9781107415324

Treat, C. C., Jones, M. C., Camill, P., Gallego-Sala, A., Garneau, M., Harden, J. W., et al. (2016). Effects of permafrost aggradation on peat properties as determined from a pan-Arctic synthesis of plant macrofossils. *J. Geophys. Res.* 121, 78–94. doi: 10.1002/2015JG003061

Tripathi, B. M., Kim, H. M., Jung, J. Y., Nam, S., Ju, H. T., Kim, M., et al. (2019). Distinct taxonomic and functional profiles of the microbiome associated with different soil horizons of a moist tussock tundra in Alaska. *Front. Microbiol.* 10:1442. doi: 10.3389/fmicb.2019.01442

Tripathi, B. M., Kim, M., Kim, Y., Byun, E., Yang, J.-W., Ahn, J., et al. (2018). Variations in bacterial and archaeal communities along depth profiles of Alaskan soil cores. *Sci. Rep.* 8:504. doi: 10.1038/s41598-017-18777-x

Trivedi, P., Delgado-Baquerizo, M., Trivedi, C., Hu, H., Anderson, I. C., Jeffries, T. C., et al. (2016). Microbial regulation of the soil carbon cycle: evidence from gene–enzyme relationships. *ISME J.* 10, 2593–2604. doi: 10.1038/ismej.2016.65

Vellend, M. (2010). Conceptual synthesis in community ecology. *Q. Rev. Biol.* 85, 183–206. doi: 10.1086/652373

Voigt, C., Lamprecht, R. E., Marushchak, M. E., Lind, S. E., Novakovskiy, A., Aurela, M., et al. (2017). Warming of subarctic tundra increases emissions of all three important greenhouse gases – carbon dioxide, methane, and nitrous oxide. *Glob. Change Biol.* 23, 3121–3138. doi: 10.1111/gcb.13563

Wang, J., Shen, J., Wu, Y., Tu, C., Soininen, J., Stegen, J. C., et al. (2013). Phylogenetic beta diversity in bacterial assemblages across ecosystems: deterministic versus stochastic processes. *ISME J.* 7, 1310–1321. doi: 10.1038/ismej.2013.30

White, T. J., Bruns, T., Lee, S. J. W. T., and Taylor, J. (1990). "Amplification and direct sequencing of fungal ribosomal RNA genes for phylogenetics," in *PCR Protocols: A Guide to Methods and Applications*, Vol. 18, eds M. A. Innis, D. H. Gelfand, J. J. Sninsky, and T. J. White (Amsterdam: Elsevier Science), 315–322. doi: 10.1016/b978-0-12-372180-8.50042-1

Zhang, T., Barry, R. G., Knowles, K., Heginbottom, J. A., and Brown, J. (1999). Statistics and characteristics of permafrost and ground-ice distribution in the Northern Hemisphere. *Polar Geogr.* 23, 132–154. doi: 10.1080/10889379909377670

Zhou, J., and Ning, D. (2017). Stochastic community assembly: does it matter in microbial ecology? *Microbiol. Mol. Biol. Rev.* 81:576. doi: 10.1128/MMBR.00002-17

Conflict of Interest: The authors declare that the research was conducted in the absence of any commercial or financial relationships that could be construed as a potential conflict of interest.

frontiers in Microbiology

ORIGINAL RESEARCH
published: 18 December 2020
doi: 10.3389/fmicb.2020.615608

A Previously Undescribed Helotialean Fungus That Is Superabundant in Soil Under Maritime Antarctic Higher Plants

Kevin K. Newsham[1]†, Filipa Cox[1,2†], Chester J. Sands[1], Mark H. Garnett[3], Naresh Magan[4], Claire A. Horrocks[5], Jennifer A. J. Dungait[5‡] and Clare H. Robinson[2]*

[1] British Antarctic Survey, Natural Environment Research Council, Cambridge, United Kingdom, [2] Department of Earth and Environmental Sciences, The University of Manchester, Manchester, United Kingdom, [3] National Environmental Isotope Facility Radiocarbon Laboratory, Glasgow, United Kingdom, [4] Applied Mycology Group, Environment and AgriFood Theme, Cranfield University, Cranfield, United Kingdom, [5] Sustainable Agriculture Sciences, Rothamsted Research, Okehampton, United Kingdom

OPEN ACCESS

Edited by:
Laura Zucconi,
University of Tuscia, Italy

Reviewed by:
Luiz H. Rosa,
Federal University of Minas Gerais, Brazil
Hyoungseok Lee,
Korea Polar Research Institute, South Korea

***Correspondence:**
Kevin K. Newsham
kne@bas.ac.uk

†These authors have contributed equally to this work

‡**Present address:**
Jennifer A. J. Dungait,
Carbon Management Center, SRUC–Scotland's Rural College, Edinburgh, United Kingdom; Department of Geography, University of Exeter, Exeter, United Kingdom

Specialty section:
This article was submitted to Extreme Microbiology, a section of the journal Frontiers in Microbiology

Received: 09 October 2020
Accepted: 24 November 2020
Published: 18 December 2020

Citation:
Newsham KK, Cox F, Sands CJ, Garnett MH, Magan N, Horrocks CA, Dungait JAJ and Robinson CH (2020) A Previously Undescribed Helotialean Fungus That Is Superabundant in Soil Under Maritime Antarctic Higher Plants. Front. Microbiol. 11:615608. doi: 10.3389/fmicb.2020.615608

We report a previously undescribed member of the Helotiales that is superabundant in soils at two maritime Antarctic islands under Antarctic Hairgrass (*Deschampsia antarctica* Desv.). High throughput sequencing showed that up to 92% of DNA reads, and 68% of RNA reads, in soils from the islands were accounted for by the fungus. Sequencing of the large subunit region of ribosomal (*r*)DNA places the fungus close to the Pezizellaceae, Porodiplodiaceae, and Sclerotiniaceae, with analyses of internal transcribed spacer regions of *r*DNA indicating that it has affinities to previously unnamed soil and root fungi from alpine, cool temperate and Low Arctic regions. The fungus was found to be most frequent in soils containing C aged to 1,000–1,200 years before present. The relative abundances of its DNA and RNA reads were positively associated with soil carbon and nitrogen concentrations and $\delta^{13}C$ values, with the relative abundance of its DNA being negatively associated with soil pH value. An isolate of the fungus produces flask-shaped phialides with a pronounced venter bearing masses of conidia measuring 4.5–6(7) × 1.8–2.5 μm, suggestive of anamorphic *Chalara*. Enzymatic studies indicate that the isolate strongly synthesizes the extracellular enzyme acid phosphatase, and also exhibits alkaline phosphatase and naphthol-AS-BI-phosphohydrolase activities. Ecophysiological measurements indicate optimal hyphal growth of the isolate at a pH of 4.2–4.5 and a water potential of −0.66 MPa. The isolate is a psychrotroph, exhibiting measureable hyphal growth at −2°C, optimal hyphal extension rate at 15°C and negligible growth at 25°C. It is proposed that the rising temperatures that are predicted to occur in maritime Antarctica later this century will increase the growth rate of the fungus, with the potential loss of ancient C from soils. Analyses using the GlobalFungi Database indicate that the fungus is present in cold, acidic soils on all continents. We advocate further studies to identify whether it is superabundant in soils under *D. antarctica* elsewhere in maritime Antarctica, and for further isolates to be obtained so that the species can be formally described.

Keywords: Antarctica, ^{14}C (or carbon-14), carbon, ^{13}C, *Chalara*, Helotiales

INTRODUCTION

Although Antarctica has been neglected in global mass sequencing studies of soil fungi (Tedersoo et al., 2014; Bahram et al., 2018; Egidi et al., 2019; Větrovský et al., 2019), several features are starting to emerge of the fungal communities found in the soils that form on the continent (Bockheim, 2015). One characteristic of Antarctic soil fungal communities is their relatively low alpha diversity (Canini et al., 2020), with reductions in the number of species present in soils at higher southern latitudes (*c.f.* Větrovský et al., 2019), which are associated with decreasing air temperature and, most probably, liquid water availability (Newsham et al., 2016). Perhaps surprisingly for such an isolated continent, another feature of the fungal communities in Antarctic soils is that they exhibit low endemism, with many taxa either having cosmopolitan or bipolar distributions (Cox et al., 2016). Specific fungal taxa are also characteristic of maritime Antarctic soils, with perhaps the foremost example being *Pseudogymnoascus roseus*, which is widespread in the barren fellfield soils of the region (see Supplementary Figure S3 in Newsham et al., 2016). In contrast, fungi in the class Leotiomycetes and the order Helotiales are frequent in the roots of Antarctic Hairgrass (*Deschampsia antarctica*), one of the only two native Antarctic higher plant species, and in the soils that form under the grass (Upson et al., 2009; Cox et al., 2016, 2019).

In the course of studies on maritime Antarctic soils sampled from under *D. antarctica*, a member of the Helotiales was identified that was frequent at Signy Island in the South Orkney Islands and Léonie Island in southern maritime Antarctica (Cox et al., 2016, 2019; Newsham et al., 2018). This fungus, referred to previously as Helotiales sp. 1, respires significant volumes of CO_2 from ancient (> 1,000 years before present, BP) soil carbon (C) sources (Newsham et al., 2018). Here, we conduct preliminary taxonomic analyses on this fungus by sequencing the large subunit (LSU) and internal transcribed spacer (ITS) regions of its ribosomal (*r*)DNA, describe its anamorph, report its associations with edaphic factors and its enzymatic capabilities, determine its growth responses under controlled conditions to different pH values, soil water potentials and temperatures, and compare these responses with information in the GlobalFungi database (globalfungi.com; Větrovský et al., 2020). In doing so, we build up a picture of how this apparently frequent soil fungus might respond to climatic change in maritime Antarctica (Bracegirdle et al., 2008; Bracegirdle and Stephenson, 2012; Turner et al., 2016), and what the consequences of these responses might be for the soils of the region during the twenty first century.

MATERIALS AND METHODS

Sampling

Soils used in the analyses were sampled in October and November 2011 from active layers overlaying permafrost in six pits (0.40 m × 0.40 m) dug under turves of *D. antarctica*. Three pits were dug at Polynesia Point on Signy Island (60.7107°S, 45.5849°W; altitude 35–45 m a.s.l.) and three were dug on Walton Terraces on the north-western side of Léonie Island (67.5984°S, 68.3561°W; altitude 50–60 m a.s.l.). The three pits dug at each island were separated by a mean distance of 311 m. Soils were sampled by hammering five sterile tubes (50 ml capacity) horizontally into the vertical faces of each pit at depths of 2, 4, and 8 cm, generating 15 soil samples from each pit. Further details of sampling are provided by Cox et al. (2016, 2019) and Newsham et al. (2018). Soil was frozen at −20 or −80°C within a few hours of sampling and was transported back to the United Kingdom at these temperatures, where it was thawed prior to the analyses described below.

Edaphic Factors

Soil pH, moisture and C and N concentrations were measured in bulked soils from each of the three depths in the three pits dug at each island, generating 18 soil samples in total. Soil pH was measured by adding approximately the same volume of deionized water to each soil sample to generate slurries and recording pH with a glass electrode (pH 21, Hanna Instruments, Leighton Buzzard, United Kingdom). Soil moisture was measured gravimetrically after drying *c.* 1 g of fresh soil at 105°C for 17 h. Sub-samples (*c.* 2.5 mg) of air-dried soil were weighed into foil capsules and were analyzed for total C and N (Carlo Erba NA1500 elemental analyser, CE Instruments, Wigan, United Kingdom). Details of samples are provided by Robinson et al. (2020).

^{14}C and ^{13}C Determinations

Owing to the expense of these determinations, analyses were made on the five replicate soils sampled from depths of 2, 4, and 8 cm in one of the three pits dug at each island, generating 30 samples in total. The soils were submitted to the NERC (now NEIF) Radiocarbon Laboratory, where soil C was converted to carbon dioxide (CO_2) using either bomb combustion in a high-pressure oxygen atmosphere, or an elemental combustion system (Costech ECS 4010, Italy). Sample CO_2 was cryogenically purified under vacuum and split into aliquots. The $\delta^{13}C$ (relative to the Vienna PDB standard) was determined on one aliquot of sample CO_2 by isotope ratio mass spectrometry (Delta V, Thermo-Fisher, Germany). A second aliquot was converted to graphite using Fe:Zn reduction (Slota et al., 1987) and analyzed for ^{14}C content using accelerator mass spectrometry at the Scottish Universities Environmental Research Centre (East Kilbride, United Kingdom). Following convention (Stuiver and Polach, 1977), ^{14}C results were normalized to $\delta^{13}C = -25‰$ and expressed as % modern and conventional radiocarbon ages (in years BP, where 0 BP = AD1950). Mean residence time (MRT) of C in soil was determined from ^{14}C concentration using a bomb-^{14}C soil carbon turnover model (the Meathop Model; Harkness et al., 1986), as described by Horrocks et al. (2020). For samples that showed no clear evidence of bomb-^{14}C incorporation (i.e., < 97%Modern), the conventional radiocarbon age was used as the MRT (Bol et al., 1999). Sample details, including unique publication codes for each sample, are provided by Robinson et al. (2020).

DNA and RNA Library Construction

As described by Cox et al. (2016, 2019), both nucleotides were extracted simultaneously from soil samples (5 mg) using RNA PowerSoil Total RNA Isolation and DNA Elution Accessory kits (MoBio Laboratories, Carlsbad, CA, United States). Extracted RNA was treated with a Turbo DNA-free kit (Life Technologies, Carlsbad, CA, United States), checked for contaminant DNA using PCR, and reverse transcribed using AccuScript High-Fidelity Reverse Transcriptase (Agilent, Santa Clara, CA, United States) and random non-amers. Internal transcribed spacer (ITS) regions in the extracted DNA and cDNA were amplified in triplicate PCR reactions using ITS1F (Gardes and Bruns, 1993) and ITS4 (White et al., 1990) primers. The ITS4 primer was modified with the Roche 454 A adapter and a 10 bp barcode specific to each sample, and the ITS1F primer was modified with the 454 B adaptor. The triplicate PCR products were pooled and purified using AMPure XP bead purification (Beckman Coulter, Inc., Brea, CA, United States) and quantified using a Qubit dsDNA HS Assay (Life Technologies, Carlsbad, CA, United States) before normalization to consistent concentration. The purified and normalized PCR products were run on the 454 Roche Titanium FLX platform at the Liverpool Centre for Genomic Research.

The DNA and RNA sequences were processed using the QIIME pipeline (Caporaso et al., 2010). Sequences were filtered to remove reads that were of low quality, < 300 bp or $> 1{,}200$ bp, and were split according to barcodes. The remaining sequences were denoised (Reeder and Knight, 2010), and checked for potential chimeras (Edgar et al., 2011). After deleting potential chimeras, the resulting libraries from Signy Island and Léonie Island consisted of 2,313–11,401 and 1,994–15,482 DNA reads and 2,478–11,840 and 5,250–10,943 RNA reads, respectively (**Supplementary Figure S1**). The ITS2 regions of the remaining sequences were extracted using ITSx (Bengtsson-Palme et al., 2013) and grouped into operational taxonomic units (OTUs) at 97% sequence similarity using USEARCH 6.1 (Edgar, 2010). The ITS sequence of the isolate (see below) showed 100% similarity to a representative OTU in the DNA and RNA libraries, enabling its abundance in field soil to be determined (see Robinson et al., 2020). DNA and RNA sequences have been deposited in the NCBI Sequence Read Archive (accession codes SRP068654 and PRJNA518063, respectively).

Isolation, Agar Media, and Microscopy

The fungus was isolated in 2012 from surface sterilized organic matter (OM). Briefly, decomposing OM picked from Léonie Island soil was washed 30 times in sterile water, blotted dry on sterile filter paper and pressed into soil extract medium (SEM) before incubation at 7°C for up to 16 weeks (Newsham et al., 2018). An isolate of the fungus was subsequently maintained at *c.* 15°C on half strength potato dextrose agar (PDA) medium. The isolate was also inoculated onto oat agar (OA) and Azure B agar media (Newsham et al., 2018). Phialides and conidia formed on the latter medium at the inoculation point after 6 weeks of growth at *c.* 15°C. Squash mounts in water were examined at $\times 400$ and $\times 1{,}000$ magnifications using light microscopy (Olympus BX51, Olympus Life Sciences, Tokyo, Japan), with images of structures being captured using Cell P software (Olympus Life Sciences).

Taxonomic Placement

DNA was extracted from hyphae of the isolate growing on sterile cellophane overlaying half strength PDA medium using a commercially available kit (Extract-n-Amp Plant PCR, Sigma-Aldrich, St Louis, United States). Following standard protocols, the ITS region of *r*DNA was amplified with the ITS1F (5′-CTTGGTCATTTAGAGGAAGTAA-3′)/ITS4 (5′-TCCTCCGCTTATTGATATGC-3′) primer pair, and a portion of the large subunit (LSU) gene was amplified with the JS-1 (5′-CGCTGAACTTAAGCATAT-3′)/LR5 (5′-TCCTGAGGGAAACTTCG-3′) primer pair. The amplicons were bidirectionally sequenced at a commercial facility, using the same primers. The sequences were manually trimmed and consensus sequences were generated prior to deposition in GenBank (accession codes MW033386 and MW033387). The ITS sequences were subjected to blastn searches in UNITE v. 8.2[1] to determine if the fungus had been sampled and sequenced previously, and to provide a starting point for a taxonomic placement. In order to better place the fungus taxonomically, an exemplar sequence of a voucher LSU sequence was downloaded from NCBI GenBank from each of the classes Orbiliomycetes and Pezizomycetes (as outgroups), and sequences for exemplars from each order within the class Leotiomycetes. Where possible, sequences from type material were chosen to add rigor to the taxonomic placement, with other sequences being derived from material deposited in the Centraalbureau voor Schimmelcultures (CBS) culture collection, the majority of which are reported by Vu et al. (2019), or from vouchered specimens. Sequences were aligned using MAFFT 7.450 (Katoh and Standley, 2013) in the GENEIOUS R11 package (Biomatters, Ltd., Auckland, New Zealand). Ambiguous columns were excised where alignment ambiguities existed around regions containing gaps. A phylogenetic analysis was undertaken to place the test LSU sequence against the voucher sequences, and to identify the likely order to which it belonged. An exemplar sequence from each family in the order was downloaded and a new round of phylogenetic analyses was conducted to place the test LSU sequence to family. An exemplar from each genus of the likely family and closely related families was downloaded to further refine the taxonomic placement. A similar strategy was used to provide context to closely matching ITS sequences in order to produce an ITS phylogeny. Phylogenetic analyses were conducted using approximate maximum likelihood in the package FastTrees 2.1.11 (Price et al., 2010) in the GENEIOUS package using a General Time Reversible (GTR) model, four rate categories per site and the Gamma20 likelihood optimized. The final phylogeny was produced in MrBayes 3.2.3 (Ronquist et al., 2012) using a GTR model with a gamma distribution. The analysis used four heated chains and four replicates. Twenty million generations were run, with sampling every

[1] https://unite.ut.ee/

thousandth generation. Convergence, stability and stationarity were determined using Tracer 1.7.1 (Rambaut et al., 2018).

Responses to pH

The isolate was grown on half strength PDA medium amended to pH values of 3.9, 4.2, 4.5, 5.1, 5.6, and 6.1 with citric acid/phosphate buffer (Stoll and Blanchard, 1990). The pH values of the media were measured with a Jencons pH meter (Jencons Scientific Ltd., Leighton Buzzard, United Kingdom) prior to autoclaving. Media at pH 3.9 and pH 4.2–6.1 were solidified with 2 and 1.5% technical agar (Oxoid no. 1, Thermo Fisher Scientific Ltd., Basingstoke, United Kingdom), respectively. The medium at each pH was poured into six replicate 90 mm diameter non-vented Petri dishes and was inoculated with plugs (7 mm diameter) of the fungus bored from the margins of actively growing colonies on half strength PDA medium. The dishes were incubated at 15°C in the dark for 5 weeks. Two measurements of each colony's diameter were recorded weekly at *c*. 90° to each other and radial extension rates (mm d^{-1}) were subsequently calculated.

Responses to Temperature

Plugs (7 mm diameter) bored from the margins of the isolate growing on half strength PDA medium were inoculated onto SEM in 0.2 μm-vented sterile cell culture flasks (Thermo Fisher Scientific BioLite, 130189, Loughborough, United Kingdom) that were incubated at −2, 2, 4, 9, 15, 20, and 25°C for up to 5 weeks. Four flasks were prepared for incubation at each temperature. Those at 4 and 15–25°C were incubated in refrigerators or cabinets, the temperatures of which were monitored hourly using TinyTag Plus 2 TGP-4017 loggers (Gemini Data Loggers Ltd., Chichester, United Kingdom). Those at −2, 2, and 9°C were submerged vertically into coolant in recirculating water baths (Newsham and Garstecki, 2007), with all of the flask except the neck being submerged in the coolant. Temperatures were monitored regularly using a thermometer set into SEM in a dummy flask. Measurements of the diameter of each colony recorded at 7 d intervals were subsequently used to calculate radial extension rates (mm d^{-1}).

Responses to Water Potential

Sterile capillary matting (Gardman, Huntingdon, United Kingdom) was placed into 90 mm Petri dishes and was soaked with liquid SEM modified with PEG 8000 to water potentials of −0.66, −0.96, −2.22, −3.15, −4.90, −6.17, and −8.24 MPa, measured using a dew point potentiameter. Sterile black cotton cloth was placed on top of the matting, followed by sterile cellophane film (55 mm × 55 mm; Natureflex 28 NP, Innovia Films, Wigton, United Kingdom). Air bubbles were removed from under the cellophane with a sterile L-shaped spreader. Plugs (7 mm diameter), bored from the margins of colonies grown on SEM for 3 weeks at 15°C, were placed in the centre of the cellophane. The dishes, three of which were prepared for each water potential, were sealed with Parafilm and incubated in the dark at 15°C. Each colony was photographed at weekly intervals for up to 6 weeks. Using ImageJ (National Institute of Health, Bethesda, MD, United States), two measurements of each colony's diameter were recorded at *c*. 90° to each other. Radial extension rates (mm d^{-1}) were subsequently calculated.

Extracellular Enzyme Analyses

Measurements of extracellular phosphatase activities using *p*-nitrophenol assays were made using the methods described by Newsham et al. (2018), except that the substrate for the assays was 4-nitrophenyl phosphate disodium salt hexahydrate (Sigma-Aldrich, St Louis, United States), with the pH values of the acetate buffer being adjusted to 6.0 and 8.0 for acid and alkaline phosphatase assays, respectively. Semi-quantitative measurements of the activities of these two enzymes were also made at pH 5.4 and pH 8.5 with 2-naphthyl phosphate as the substrate using the methods described by Newsham et al. (2018) and API ZYM kits (bioMérieux Ltd., Basingstoke, United Kingdom). The same methods were also used to semi-quantitatively test for the activities of lipase, trypsin, α-chymotrypsin and α-galactosidase with the substrates 2-naphthyl myristate (pH 7.5), N-benzoyl-DL-arginine-2-naphthylamide (pH 8.5), N-glutaryl-phenylalanine-2-naphthylamide (pH 7.5), and 6-Br-2-naphthyl-αD-galactopyranoside (pH 5.4), respectively.

Geographical Distribution

The ITS2 region of the fungus was entered into the GlobalFungi database (Větrovský et al., 2020) and the geolocations of exact hits were recorded. After excluding the data reported for Signy Island and Léonie Island reported by Cox et al. (2016), the details of substrates, soil pH, and mean annual temperature and precipitation were noted for the 285 exact hits in the database.

Statistical Analyses

The effects of soil depth on the relative abundance of the fungus in DNA and RNA communities, and the influence of pH, temperature and water potential on the radial extension rate of the isolate, were tested with ANOVA and Tukey's multiple range tests. Associations between the relative abundance of the fungus and edaphic factors were tested with linear and three part Gaussian regressions. Analyses were made in Sigmaplot 14 (Systat Software Inc., San Jose, CA, United States) and MINITAB 18 (State College, PA, United States).

RESULTS

Relative Abundance in DNA and RNA Libraries

The fungus was present in all 45 soil samples from Signy Island from which DNA libraries were made. Its mean relative abundance in DNA libraries from the island was 39% (range 19–66%; **Supplementary Figure S1C**). At Léonie Island, it was present in 42 of the 45 soil samples from which DNA libraries were made, with a mean relative abundance of 46% (range 0–92%; **Supplementary Figure S1C**). RNA of the fungus was detected in 43 out of 45 libraries constructed from Signy Island soil, but at

a much lower relative abundance than in DNA libraries (mean relative abundance 2%, range 0–8%; **Supplementary Figure S1F**), and its RNA was detected in 36 of the 45 RNA libraries from Léonie Island, with a mean relative abundance of 17% (range 0–68%; **Supplementary Figure S1F**).

Changes in Relative Abundance With Soil Depth and Soil Fraction

The relative abundance of the DNA of the fungus changed with depth at Signy island, with a doubling in its abundance from 25 to 50% of the DNA community as depth increased from 2 to 8 cm [$F_{(2,\ 42)} = 37.35$, $P < 0.001$; **Figure 1A**]. There were no apparent effects of soil depth on the relative abundance of the fungus in DNA and RNA communities at Léonie Island and Signy Island, respectively (**Figures 1B,C**), but its mean abundance in the RNA community at Léonie Island increased from 6 to 24% as depth increased from 2 to 8 cm [$F_{(2,\ 42)} = 3.87$, $P = 0.029$; **Figure 1D**].

Associations With Edaphic Factors

Correlative analyses between the relative abundance of the fungus in the DNA and RNA communities at Signy Island and Léonie Island indicated that it was more frequent and active in soils with lower radiocarbon (^{14}C) enrichment (**Figures 2A,G**), with significant negative linear associations between its abundance in the two communities and ^{14}C enrichment ($r = -0.670$ and -0.743, both $P < 0.001$). There were also significant associations between the MRT of soil C and the relative abundance of the DNA and RNA of the fungus, with peak abundance of each nucleotide in soils aged approximately 1,000 and 1,200 years BP, respectively ($r = 0.835$ and 0.965, both $P < 0.001$; **Figures 2B,H**). The relative abundances of the DNA and RNA of the fungus were positively and linearly associated with soil δ^{13}C value and C and N concentrations ($r = 0.525$–0.699, all $P < 0.025$; **Figures 2C–E,I–K**), whereas the abundance of its DNA was negatively associated with soil pH value ($r = -0.646$, $P = 0.004$; **Figure 2F**). Soil moisture concentration, which ranged from 58.4 to 76.2%, was not associated with the relative abundance of the fungus in the DNA or RNA communities (data not shown).

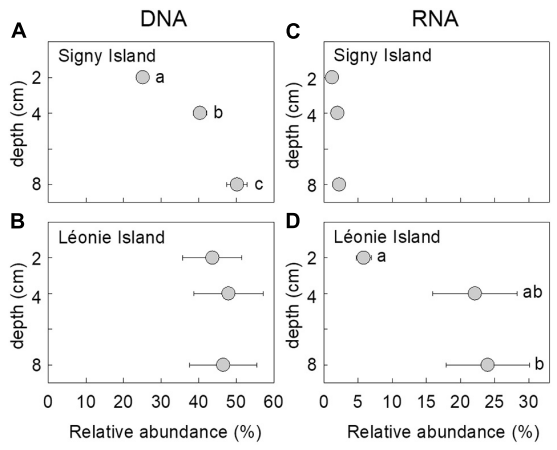

FIGURE 1 | Relative abundances of the fungus in **(A,B)** DNA and **(C,D)** RNA communities as a function of soil depth at Signy Island **(A,C)** and Léonie Island **(B,D)**. Values shown are means ± standard error of the mean. Values marked with different letters differed following Tukey's tests.

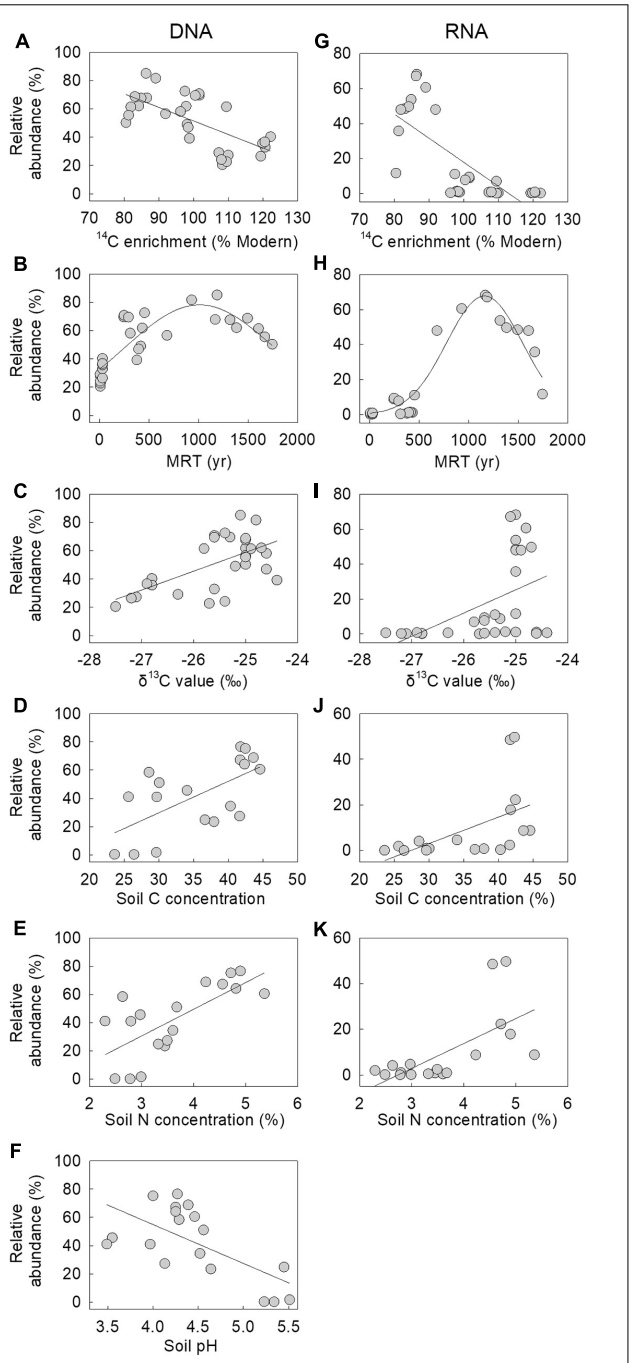

FIGURE 2 | Relative abundances of the fungus in **(A–F)** DNA and **(G–K)** RNA communities as a function of soil ^{14}C enrichment, mean residence time (MRT), δ^{13}C content, C and N concentrations and pH value. Lines are best fits, derived from linear and **(B,H)** three-parameter Gaussian functions. Note that one sample, assigned a MRT of 9 or 77 years, was excluded from **(B)** and **(H)**, and that the association between the relative abundance of the fungus in the RNA community and soil pH value was not significant.

Taxonomic Placement

The LSU phylogeny placed the fungus in the order Helotiales. Type, CBS and voucher LSU sequences were able to refine the test sequence to matching to members of the families Pezizellaceae, Porodiplodiaceae, and Sclerotiniaceae, such as *Chalara clidemiae* and species of *Calycina*, *Porodiplodia*, *Monilinia*, *Botryotinia,* and *Streptotinia* (**Figure 3**), but with low support (posterior probability of 0.94) and without sufficient taxonomic coverage of genera available to gain any more precision. The ITS phylogeny similarly placed the fungus in the Helotiales, and indicated close matches to sequences assigned to the families Pezizellaceae, Hyaloscyphaceae, and Dermateaceae (**Supplementary Figure S2**). Comparisons of the ITS region sequence of the fungus with those in the UNITE database indicated that it bore close (> 99%) similarities to soil and root fungi from cold regions (**Table 1**). The best match was to the sequence of a fungus cloned from acidic (pH 4.4) soil under *Eriophorum*, *Betula*, *Ledum,* and *Vaccinium* spp. at Toolik Lake in the Low Arctic (**Table 1**). Other close matches were recorded with a *Phialea* species inhabiting the hair roots of the ericaceous plant species *Phyllodoce aleutica* growing in an alpine region of Japan, and members of the Helotiales in soil under the shrub *Salix*

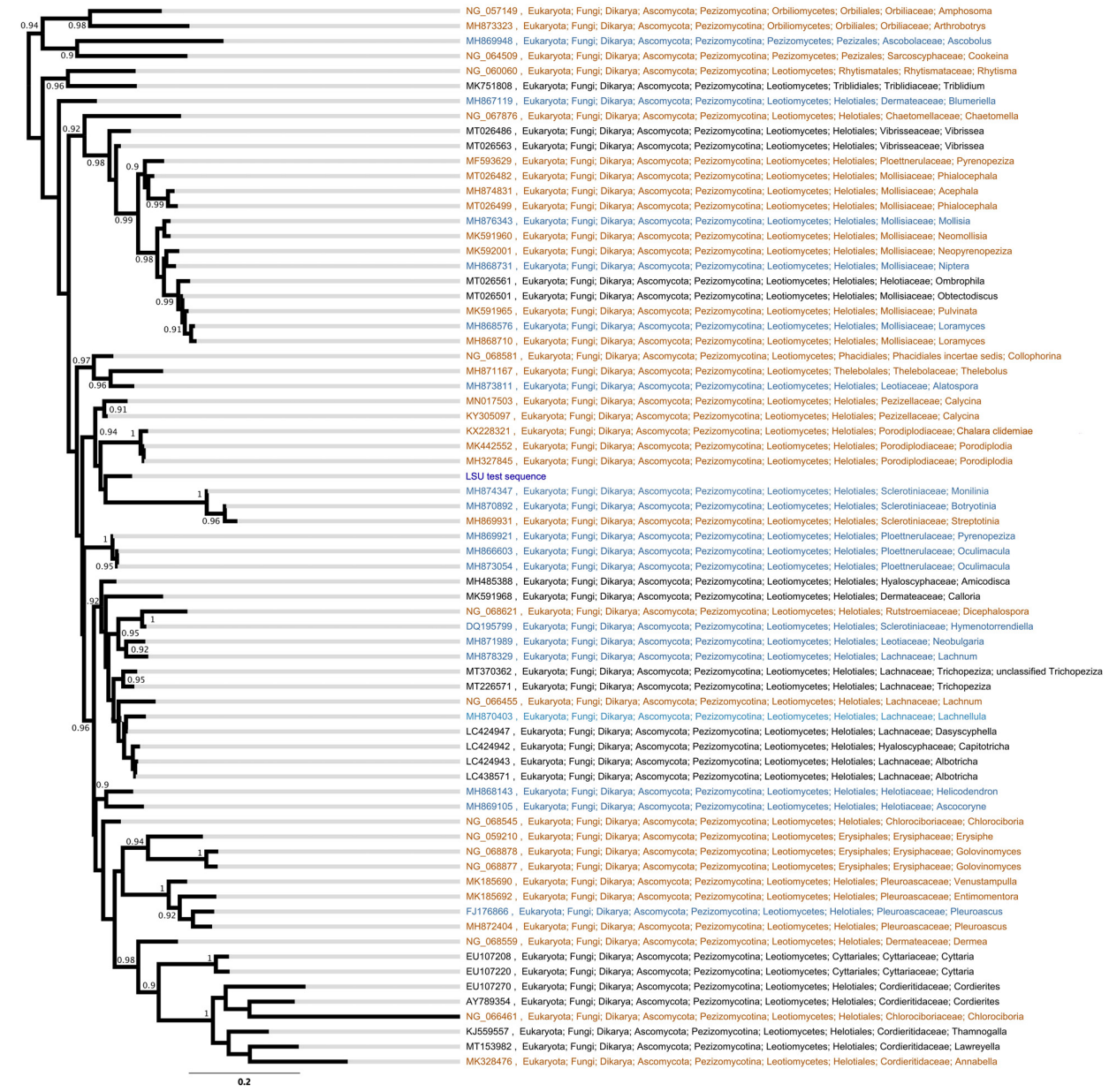

FIGURE 3 | Bayesian phylogeny of large ribosomal subunit (LSU) sequences from type material (orange), CBS cultures (blue), and vouchered specimens (black). Node support numbers are posterior probabilities. Tip labels are GenBank accession codes and the taxonomic cascade is derived from NCBI GenBank.

TABLE 1 | The 10 closest matches to the ITS sequence of the fungus derived from UNITE v. 8.2 (accessed August 2020), showing accession codes, UNITE taxon names, similarity scores and percentage similarities and regions and substrates of origin.

Accession code*	UNITE taxon name	Score	Coverage (%)	Similarity (%)	Region of origin	Substrate	References
HQ211994	Helotiales	983	89	99.813	Low Arctic (Alaska)	Soil	Deslippe et al., 2012
HQ211950	Helotiales	983	89	99.813	Low Arctic (Alaska)	Soil	Deslippe et al., 2012
UDB0756281	Envir: Fungi	983	51	99.813	United States	Soil	Tedersoo et al., 2014
LC131017	*Phialea*	981	99	99.813	Tateyama Kurobe Alpine Route (Japan)	*Phyllodoce aleutica* hair roots	Unpublished
EU529971	Helotiales	981	100	99.813	Sub-Arctic (Abisko, Sweden)	Soil under *Salix polaris*	Hrynkiewicz et al., 2009
HQ212087	Helotiales	977	89	99.626	Low Arctic (Alaska)	Soil	Deslippe et al., 2012
MN328304	Helotiales	974	99	99.811	Cool southern temperate (Falkland Islands)	*Poa flabellata* root	Unpublished
MN328301	Helotiales	974	99	99.811	Cool southern temperate (Falkland Islands)	*P. flabellata* root	Unpublished
MN328296	Helotiales	974	99	99.811	Cool southern temperate (Falkland Islands)	*P. flabellata* root	Unpublished
KF359562	Helotiaceae	972	100	99.440	Great Smoky Mountains (United States)	*Tsuga canadensis* root	Baird et al., 2014

Note that UDB0756281 is deposited in UNITE. All other sequences are deposited in GenBank.

polaris growing at Abisko in sub-Arctic Sweden, in *Poa flabellata* roots from the Falkland Islands, and a member of the Helotiaceae from the roots of *Tsuga canadensis* growing in an alpine region of North America (**Table 1**).

Descriptions of Colonies and Anamorph

On half strength PDA and OA medium, colonies of the fungus are thin and white with well-defined margins. Sclerotia and stroma are absent. Conidia are produced in masses at the apices of pigmented, flask-shaped phialides of length 25–37 μm and widths 5–7 μm (venter) and 2.0–2.5 μm (collarette; **Figures 4A,B**). The apices of phialides are not flared (**Figure 4C**). Conidia, which were not observed to form in basipetal chains, are hyaline, cylindrical with rounded ends, 0(–1) septate and measure 4.5–6(7) × 1.8–2.5 μm (**Figure 4D**).

Responses to pH, Temperature, and Water Potential

The isolate is an acidophile, exhibiting maximum hyphal growth at pH 4.2–4.5, and slower growth at pH 6.1 compared with pH 3.9–5.6 (**Figure 5A**). It was also found to be a psychrotroph, with measurable hyphal growth at −2°C (0.04 mm d^{-1}) and optimum hyphal extension rate at 15°C (0.93 mm d^{-1}). Radial extension rate at 25°C was negligible (0.02 mm d^{-1}; **Figure 5B**). Measurements of hyphal growth on SEM modified with PEG 8000 to a range of water potentials indicated that radial extension rate was fastest at −0.66 MPa, with rapidly declining extension rates between −0.66 and −3.15 MPa, and no growth at below −4.9 MPa (**Figure 5C**).

Enzyme Analyses

Analyses using *p*-nitrophenyl assays indicated mean acid phosphatase activity of the isolate of 12 μM h^{-1} *p*-nitrophenol liberated, with no apparent alkaline phosphatase activity (data not shown). API ZYM assays indicated strong acid phosphatase activity, and weak alkaline phosphatase activity. These assays also showed weak naphthol-AS-BI-phosphohydrolase activity, and no activities for lipase, trypsin, α-chymotrypsin and α-galactosidase (data not shown).

Geographical Distribution

Analyses using the GlobalFungi Database indicated that fungi with ITS2 regions bearing 100% similarities to that of the fungus reported here are present on all continents (**Figure 6**). These analyses also indicated increased relative abundances (> 1%) of the fungus at high latitudes in the southern hemisphere and alpine regions in the northern hemisphere (**Figure 6**). DNA of the fungus has mainly been amplified from soils in forest, desert, tundra and grassland biomes (91.6% of records), with occasional records from litter, bryophyte tissues and roots. The locations in which the fungus has been recorded have a mean annual temperature of 5.0°C (range −10.4–17.7°C) and a mean annual precipitation of 1,077 mm per annum (range 206–4,251 mm). The mean pH value of the soils from which the DNA of the fungus has been amplified is 4.8 (range 2.6–6.1).

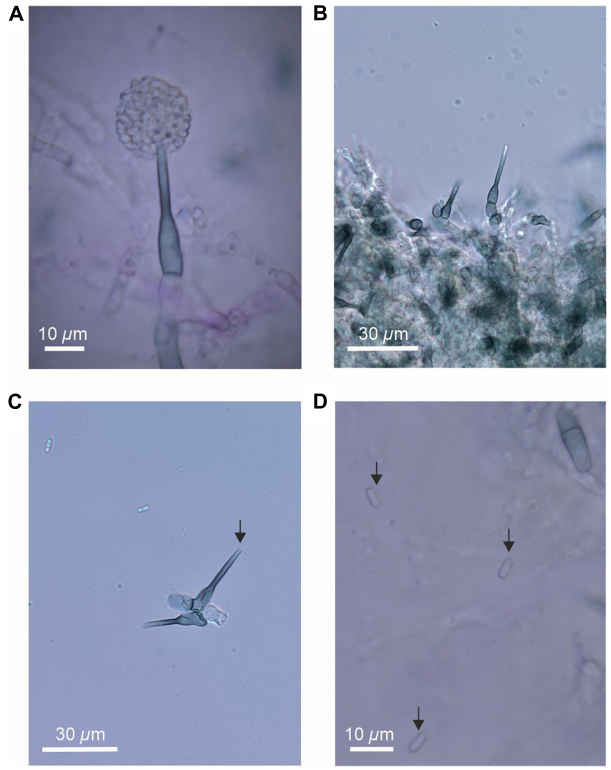

FIGURE 4 | The anamorph of the fungus, showing **(A)** flask-shaped phialide with a pronounced venter bearing masses of conidia, **(B)** phialides and swollen cells, **(C)** phialide without flared apex (arrowed), and **(D)** conidia (arrowed).

DISCUSSION

The observations reported here indicate the superabundance of a fungus in two maritime Antarctic soils under *Deschampsia antarctica*. The fungus was recorded in all DNA libraries constructed from soil sampled from Signy Island and all but three of the 45 DNA libraries made from Léonie Island soil, with maximum abundances in the soils from each island of 66 and 92%, respectively. It also occurred in 36–43 of the RNA libraries constructed from each island, but, as noted previously by Cox et al. (2019), its relative abundance in the RNA community (0–68%) was lower than in the DNA community. Although the abundance of the fungus in DNA and RNA libraries may be owing to its nucleic acids being more resistant to damage than those of other fungal taxa (Willerslev et al., 2004), it exhibits similar features to those of other abundant soil fungi. In a recent analysis, it was shown that just 83 fungal taxa, all but three of which are ascomycetes, account for about one fifth of DNA reads from soils sampled from six other continents (Egidi et al., 2019). These fungal taxa, five of which belong to the Helotiales, are characterized by the expression of genes for stress tolerance, CAZymes (carbohydrate active enzymes) and competitive ability (Egidi et al., 2019). Although the competitive abilities of the fungus reported here have yet to be tested, it strongly synthesizes extracellular enzymes for carbohydrate breakdown (Newsham et al., 2018), and it is abundant and active in soils that are frozen for *c.* 8 months per annum (Convey et al., 2018) and which are exposed to annual temperature ranges of 48°C and midwinter temperatures below −20°C (Bokhorst et al., 2011), suggesting that it expresses stress tolerance genes. We hence propose that a combination of these characteristics enable the survival of the fungus in the harsh environments of maritime Antarctica, leading to its superabundance in the soils of Signy and Léonie islands.

In agreement with previous studies showing significant effects of depth on the frequencies of distinct fungal guilds and taxa in soil (Dickie et al., 2002; Lindahl et al., 2006), the fungus reported here was more abundant and active in deeper soils, with, as depth increased from 2 to 8 cm, a doubling in its relative abundance in the DNA community at Signy Island, and a threefold increase in its abundance in the RNA community at Léonie Island. The preference of the fungus for deeper, and hence older (Horrocks et al., 2020), soils resulted in its relative abundance in both nucleic acid communities being negatively associated with soil ^{14}C enrichment, with peak abundances of DNA and RNA reads in soils with MRT of C of 1,000–1,200 years BP. The increased relative abundance of the fungus in soils with enriched ^{13}C values, derived from plants growing under wetter conditions (Wasley et al., 2006), also agrees with its preference for growth at increased water availability,

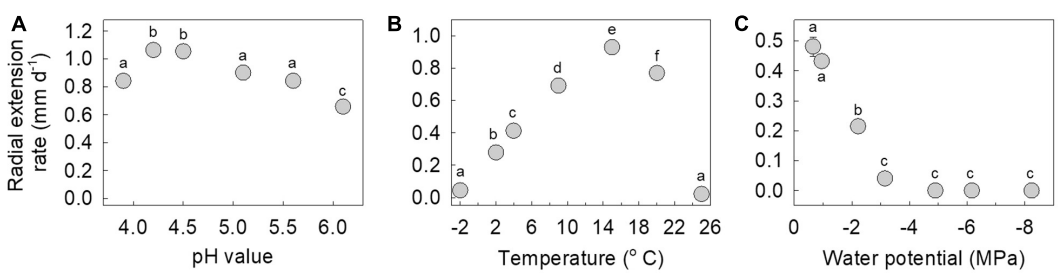

FIGURE 5 | Radial extension rate of the fungus in response to **(A)** pH values between 3.9 and 6.1, **(B)** temperatures between –2 and 25°C, and **(C)** water potentials between –0.66 and –8.24 MPa. Note that values are means of 3–6 replicates ± standard error of the mean, with all but one of the error bars being obscured by the data points. Distinct letters within each panel denote values that differed significantly following Tukey's tests.

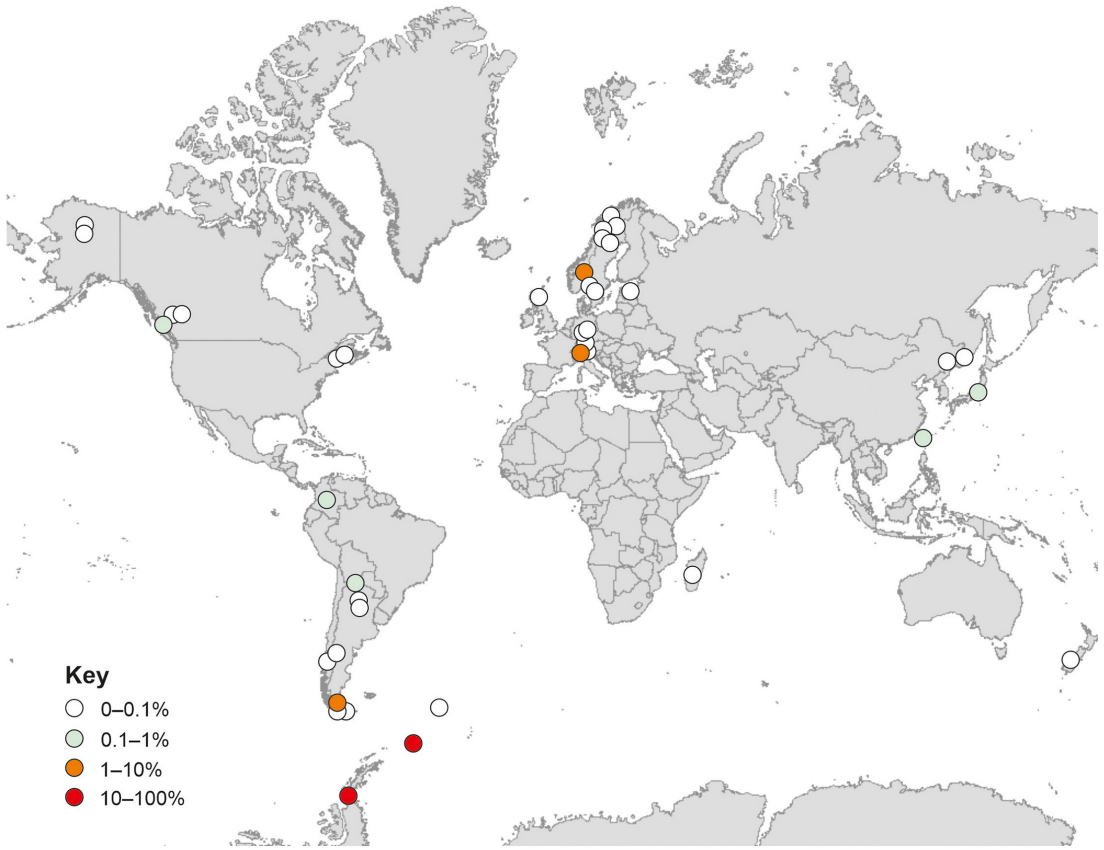

FIGURE 6 | Global distribution of the fungus. Data are from GlobalFungi.com (Větrovský et al., 2020), accessed in September 2020. Colours denote different relative abundances in high throughput sequencing libraries (see key).

with maximum hyphal extension rate being recorded here at a water potential of −0.66 MPa. However, we cannot discount the possibility that the positive association between the relative abundances of the fungus in DNA and RNA communities and soil ^{13}C value may have arisen from ^{13}C enrichment at increased soil depth (Horrocks et al., 2020), possibly arising from isotopic fractionation or the addition of ^{13}C-enriched microbially-derived C during decomposition (Schweizer et al., 1999; Boström et al., 2007), or from the depletion of the ^{13}C content of plant material entering soil over the previous 150 years (Leavitt and Lara, 1994; Royles et al., 2013).

A previous biogeographical study concluded that the fungal taxa encountered in maritime Antarctic soils tend not be endemic to the region, but instead usually have bipolar or cosmopolitan distributions (Cox et al., 2016). In support of this, analyses using the GlobalFungi Database (Větrovský et al., 2020) confirmed that the fungus studied here is apparently globally distributed, with exact matches of its ITS2 region to DNA sequences amplified from soils on all continents. Excluding the data reported here, further analyses using the GlobalFungi Database indicated that the fungus is most frequent in soils with a mean pH value of 4.8, and is apparently not present in soils with pH values of > 6.2. These findings closely corroborate the analyses here, with the relative abundance of the DNA of the fungus being negatively associated with soil pH, and with the isolate of the fungus exhibiting optimum hyphal extension rate at pH 4.2–4.5 and a marked reduction in extension rate at pH 6.1. As well as being an acidophile, the isolate is a psychrotroph, exhibiting measurable growth at −2°C, optimum hyphal extension rate at 15°C, and negligible growth at 25°C. These findings corroborate analyses using both the GlobalFungi and UNITE databases, which indicate that the fungus tends to occur in cold habitats with a MAT of 5°C, and that its closest matches are found in cold regions, with 99.4–99.8% similarity of its ITS region to members of the Helotiales in soils and roots in the Low Arctic, alpine regions and the cool temperate Falkland Islands (Hrynkiewicz et al., 2009; Deslippe et al., 2012; Baird et al., 2014). These analyses were also in agreement with the wider ITS phylogeny, which showed a distinctive clade formed by the test sequence and its closest matches with no clear generic or familial alignment, suggestive of an as yet undescribed taxon group encompassing cold tolerant fungi.

Phylogenetic analyses of the LSU region of *r*DNA of the isolate provided better resolution at the family level, with the test sequence grouping, albeit at low support, with members

of the Sclerotiniaceae, Pezizellaceae and the recently recognized family Porodiplodiaceae (Crous et al., 2018). Morphological characters suggest that membership of the Sclerotiniaceae is unlikely, with an absence of sclerotia and stroma in culture (Carbone and Kohn, 1993). However, the morphology of the phialides is suggestive of *Chalara*, members of which produce flask-shaped, obclavate phialides with pronounced venters (Nag Raj and Kendrick, 1975) and are frequent in the Pezizellaceae. We note that the isolate is dissimilar to *Chalara antarctica*, a member of the family isolated from soils under *D. antarctica* and *Colobanthus quitensis* on the Danco Coast, which has floccose or tufted brown colonies with slender phialides of length 25–30 μm and width 3 μm that lack a pronounced venter, and has a flared collar bearing 2–3 conidia borne in chains (Cabello, 1989). It does, however, bear similarities to the *Chalara* anamorph of *Cyathicula strobilina*, recorded on decomposing cones of *Picea abies* from northern Europe, the colonies of which, as here, display optimal hyphal extension at 10–20°C, but minimal growth at 24°C (Gams and Philippi, 1992). Although dissimilar to *Porodiplodia*, the type genus in the Porodiplodiaceae, colonies of which are darkly pigmented on PDA and OA and produce broad, pigmented, 1-septate conidia in short chains (Crous et al., 2018, 2019), the isolate bears morphological similarities to *C. clidemiae*, another member of this family (Crous et al., 2016). In addition, it has an LSU region sequence with 94% pairwise identity (sequence length 807, identical bases 756) to that of the holotype of *C. clidemiae* (GenBank accession code KX228321; Crous et al., 2016). However, despite these similarities to *Chalara*, given the low levels of support for placement of the isolate at the family level, it is apparent that further research is needed to accurately determine its taxonomic position.

In the latter half of the twentieth century, surface air temperatures in maritime Antarctica rose by *c.* 0.7–2.8°C (Adams et al., 2009), with widespread effects in the environment, such as glacial recession (Cook et al., 2005), ice shelf disintegration (Cook and Vaughan, 2010) and the expansion of populations of vascular plant species, notably *D. antarctica* (Fowbert and Smith, 1994; Gerighausen et al., 2003). Although this warming trend has slowed in the last two decades (Turner et al., 2016), further increases in atmospheric greenhouse gas concentrations are predicted to lead to 2–4°C rises in air temperature by the end of the twenty first century (Bracegirdle et al., 2008; Bracegirdle and Stephenson, 2012), with consequent rises in surface soil temperatures (Qian et al., 2011). Given the superabundance of the fungus reported here in soils at two maritime Antarctic islands, the question arises of what the effects will be of these changes in soil temperature on its growth and activity. It seems likely, given the positive growth response of the fungus to increasing temperatures between −2 and 15°C, and with mean summertime soil surface temperatures on Signy Island and Anchorage Island, a member of the Léonie Islands group, of 2.2–4.4°C (Bokhorst et al., 2008), that warming will lead to increased hyphal growth of the fungus in soil during summer. With soil surface temperatures at Signy Island and Léonie Island reaching 21.2–27.4°C under cloudless skies during austral summer (Bokhorst et al., 2011), it is also possible that the hyphal growth of the fungus, which exhibits marked reductions at > 20°C, may be inhibited. However, we do not anticipate substantial inhibitory effects on its growth rate, since the fungus is most frequent in maritime Antarctic soils at depths of at least 8 cm, which do not heat to the same extent as surface soils (Bokhorst et al., 2013).

What are the likely effects of increased growth and activity of the fungus on the cycling of elements in maritime Antarctic soils? Assuming that the water potential of these soils does not fall below −4.9 MPa—at which point hyphal growth halts—it is likely that C cycling will be accelerated, since the fungus strongly synthesizes extracellular cellulase enzymes (Newsham et al., 2018). With the analyses here showing that the fungus is most frequent in soils containing C with a MRT of 1,000–1,200 years BP, along with data from *in vitro* experiments showing that it respires CO_2 from Léonie Island soil aged up to *c.* 1,171 years BP (Newsham et al., 2018), it is reasonable to conclude that as soils warm, increased hyphal growth will lead to the loss of ancient C, potentially aged up to 5,500 years BP (Björck et al., 1991). In agreement with previous studies on other Ascomycetes (e.g., Oses-Pedraza et al., 2020), effects of the fungus on the sparse lignin moieties present in maritime Antarctic soils are unlikely, as it displays no apparent activity of peroxidase-type lignin modifying enzymes (Newsham et al., 2018). Data from the present study and that of Newsham et al. (2018) also indicate few effects of the fungus on the breakdown of glycoproteins, glycolipids, esters, proteins, polypeptides or amino acids, with the fungus exhibiting minimal or no activity of esterase, esterase lipase, α-galactosidase, trypsin, α-chymotrypsin or cysteine or valine arylamidases. Nevertheless, as reported here, the fungus strongly synthesizes acid phosphatase and weakly synthesizes alkaline phosphatase and naphthol-AS-BI-phosphohydrolase, with potential effects on the cycling of phosphorus (P) in soils under *D. antarctica* as they warm in future decades. However, with comparatively high extractable concentrations of P in soil under the grass on Signy Island (50–130 mg P kg^{-1} soil; Allen et al., 1967), it is possible that these effects will not influence P cycling to the extent that primary productivity is affected.

CONCLUSION

We report a previously undescribed member of the Helotiales that is superabundant in soils under *Deschampsia antarctica* at two maritime Antarctic islands. The relative abundances of its DNA and RNA reads were closely associated with ^{14}C enrichment and MRT of soil C, which, together with strong cellulase activity (Newsham et al., 2018), imply significant loss of ancient C from soils as the maritime Antarctic warms over future decades. Phylogenetic analyses based on the LSU region of *r*DNA indicate its placement in, or close to, the families Porodiplodiaceae, Sclerotiniaceae, and Pezizellaceae, with similarities to anamorphic *Chalara*. We advocate that further isolates of the fungus should be obtained prior to the formal description of what appears to be a previously undescribed, globally distributed soil fungus.

DATA AVAILABILITY STATEMENT

The data are reported by Robinson et al. (2020) at this link: https://doi.org/10.5285/65359151-158C-47D1-8C04-A59BC3A28F53.

AUTHOR CONTRIBUTIONS

CR, KN, and JD secured the funding. KN, CR, and FC conducted the fieldwork. FC created DNA and RNA libraries and, with KN, isolated the fungus. CS performed the phylogenetic analyses. MG made ^{14}C and ^{13}C determinations. CH measured soil C and N concentrations. KN and NM conducted the ecophysiological studies. KN wrote the manuscript, which was commented on and improved by the other authors. All authors contributed to the article and approved the submitted version.

FUNDING

This research was funded by an Antarctic Funding Initiative grant and associated awards from the United Kingdom Natural Environment Research Council (grant nos. NE/H014098/1, NE/H014772/1, and NE/H01408X/1).

ACKNOWLEDGMENTS

The British Antarctic Survey's Logistics Group and the officers and ship's company of the RRS James Clark Ross provided transport to and from the sampling sites. Andy Wood, Mike Dunn, Ash Cordingley, and Ian Rudkin assisted with fieldwork and Marta Misiak helped with enzyme analyses. Laura Gerrish drew the map shown in **Figure 6** and Paul Kirk (Royal Botanic Gardens, Kew) supplied literature. Two reviewers provided helpful comments. All are gratefully acknowledged.

SUPPLEMENTARY MATERIAL

The Supplementary Material for this article can be found online at: https://www.frontiersin.org/articles/10.3389/fmicb.2020.615608/full#supplementary-material

REFERENCES

Adams, B., Athern, R., Atkinson, A., Barbante, C., Bargagli, R., Bergstrom, D., et al. (2009). "The instrumental period," in *Antarctic Climate Change and the Environment*, eds J. Turner, R. A. Bindschadler, P. Convey, G. Di Prisco, E. Fahrbach, J. Gutt, et al. (Cambridge: Scientific Committee on Antarctic Research), 183–298.

Allen, S. E., Grimshaw, H. M., and Holdgate, M. W. (1967). Factors affecting the availability of plant nutrients on an Antarctic island. *J. Ecol.* 55, 381–396. doi: 10.2307/2257883

Bahram, M., Hildebrand, F., Forslund, S. K., Anderson, J. L., Soudzilovskaia, N. A., Bodegom, P. M., et al. (2018). Structure and function of the global topsoil microbiome. *Nature* 560, 233–237. doi: 10.1038/s41586-018-0386-6

Baird, R., Stokes, C. E., Wood-Jones, A., Watson, C., Alexander, M., Johnson, G. T. K., et al. (2014). Molecular clone and culture inventory of the root fungal community associated with eastern hemlock in Great Smoky Mountains National Park. *Southeast. Nat.* 13, 219–237. doi: 10.1656/058.013.s601

Bengtsson-Palme, J., Ryberg, M., Hartmann, M., Branco, S., Wang, Z., Godhe, A., et al. (2013). Improved software detection and extraction of ITS1 and ITS2 from ribosomal ITS sequences of fungi and other eukaryotes for analysis of environmental sequencing data. *Methods Ecol. Evol.* 4, 914–919. doi: 10.1111/2041-210X.12073

Björck, S., Malmer, N., Hjort, C., Sandgren, P., Ingólfsson, Ó, Wallén, B., et al. (1991). Stratigraphic and paleoclimatic studies of a 5500-year-old moss bank on Elephant Island, Antarctica. *Arct. Alp. Res.* 23, 361–374. doi: 10.1080/00040851.1991.12002857

Bockheim, J. G. (2015). *The Soils of Antarctica*. Berlin: Springer.

Bokhorst, S., Huiskes, A., Aerts, R., Convey, P., Cooper, E. J., Dalen, L., et al. (2013). Variable temperature effects of open top chambers at polar and alpine sites explained by irradiance and snow depth. *Glob. Chang. Biol.* 19, 64–74. doi: 10.1111/gcb.12028

Bokhorst, S., Huiskes, A., Convey, P., Sinclair, B. J., Lebouvier, M., and Van de Vijver, B. (2011). Microclimate impacts of passive warming methods in Antarctica: implications for climate change studies. *Polar Biol.* 34, 1421–1435. doi: 10.1007/s00300-011-0997-y

Bokhorst, S., Huiskes, A., Convey, P., van Bodegom, P. M., and Aerts, R. (2008). Climate change effects on soil arthropod communities from the Falkland Islands and the Maritime Antarctic. *Soil Biol. Biochem.* 40, 1547–1556. doi: 10.1016/j.soilbio.2008.01.017

Bol, R. A., Harkness, D. D., Huang, Y., and Howard, D. M. (1999). The influence of soil processes on carbon isotope distribution and turnover in the British uplands. *Eur. J. Soil Sci.* 50, 41–51. doi: 10.1046/j.1365-2389.1999.00222.x

Boström, B., Comstedt, D., and Ekblad, A. (2007). Isotope fractionation and ^{13}C enrichment in soil profiles during the decomposition of soil organic matter. *Oecologia* 153, 89–98. doi: 10.1007/s00442-007-0700-8

Bracegirdle, T. J., Connolley, W. M., and Turner, J. (2008). Antarctic climate change over the Twenty First century. *J. Geophys. Res.* 113:D03103. doi: 10.1029/2007JD008933

Bracegirdle, T. J., and Stephenson, D. (2012). Higher precision estimates of regional polar warming by ensemble regression of climate model projections. *Clim. Dyn.* 39, 2805–2821. doi: 10.1007/s00382-012-1330-3

Cabello, M. (1989). Deuteromycotina from Antarctica. New species of hyphomycetes from Danco Coast, Antarctic Peninsula. *Mycotaxon* 36, 91–94.

Canini, F., Geml, J., D'Acqui, L. P., Selbmann, L., Onofri, S., Ventura, S., et al. (2020). Exchangeable cations and pH drive diversity and functionality of fungal communities in biological soil crusts from coastal sites of Victoria Land, Antarctica. *Fung. Ecol.* 45:100923. doi: 10.1016/j.funeco.2020.100923

Caporaso, J. G., Kuczynski, J., Stombaugh, J., Bittinger, K., Bushman, F. D., Costello, E. K., et al. (2010). QIIME allows analysis of high-throughput community sequencing data. *Nat. Methods* 7, 335–336. doi: 10.1038/nmeth.f.303

Carbone, I., and Kohn, L. M. (1993). Ribosomal DNA sequence divergence within internal transcribed spacer I of the *Sclerotiniaceae*. *Mycologia* 85, 415–427. doi: 10.1080/00275514.1993.12026293

Convey, C., Coulson, S. J., Worland, M. R., and Sjöblom, A. (2018). The importance of understanding annual and shorter-term temperature patterns and variation in the surface levels of polar soils for terrestrial biota. *Polar Biol.* 41, 1587–1605. doi: 10.1007/s00300-018-2299-0

Cook, A. J., Fox, A. J., Vaughan, D. G., and Ferrigno, J. G. (2005). Retreating glacier fronts on the Antarctic Peninsula over the past half-century. *Science* 308, 541–544. doi: 10.1126/science.1104235

Cook, A. J., and Vaughan, D. G. (2010). Overview of areal changes of the ice shelves on the Antarctic Peninsula over the past 50 years. *Cryosphere* 4, 77–98. doi: 10.5194/tc-4-77-2010

Cox, F., Newsham, K. K., Bol, R., Dungait, J. A. J., and Robinson, C. H. (2016). Not poles apart: Antarctic soil fungal communities show similarities to those of the distant Arctic. *Ecol. Lett.* 19, 528–536. doi: 10.1111/ele.12587

Cox, F., Newsham, K. K., and Robinson, C. H. (2019). Endemic and cosmopolitan fungal taxa exhibit differential abundances in total and active communities of Antarctic soils. *Environ. Microbiol.* 21, 1586–1596. doi: 10.1111/1462-2920.14533

Crous, P. W., Schumacher, R. K., Akulov, A., Thangavel, R., Hernández-Restrepo, M., Carnegie, A. J., et al. (2019). New and interesting fungi. 2. *Fung. Syst. Evol.* 3, 57–134. doi: 10.3114/fuse.2019.03.06

Crous, P. W., Wingfield, M. J., Burgess, T. I., St. Hardy, G. E. J., Gené, J., Guarro, J., et al. (2018). Fungal planet description sheets: 716-784. *Persoonia* 40, 240–393. doi: 10.3767/persoonia.2018.40.10

Crous, P. W., Wingfield, M. J., Richardson, D. M., Le Roux, J. J., Strasberg, D., Edwards, J., et al. (2016). Fungal planet description sheets: 400-468. *Persoonia* 36, 316–458. doi: 10.3767/003158516X692185

Deslippe, J. R., Hartmann, M., Simard, S. W., and Mohn, W. W. (2012). Long-term warming alters the composition of Arctic soil microbial communities. *FEMS Microbiol. Ecol.* 82, 303–315. doi: 10.1111/j.1574-6941.2012.01350.x

Dickie, I. A., Xu, B., and Koide, R. T. (2002). Vertical niche differentiation of ectomycorrhizal hyphae in soil as shown by T-RFLP analysis. *New Phytol.* 156, 527–535. doi: 10.1046/j.1469-8137.2002.00535.x

Edgar, R. C. (2010). Search and clustering orders of magnitude faster than BLAST. *Bioinformatics* 26, 2460–2461. doi: 10.1093/bioinformatics/btq461

Edgar, R. C., Haas, B. J., Clemente, J. C., Quince, C., and Knight, R. (2011). UCHIME improves sensitivity and speed of chimera detection. *Bioinform.* 27, 2194–2200. doi: 10.1093/bioinformatics/btr381

Egidi, E., Delgado-Baquerizo, M., Plett, J. M., Wang, J., Eldridge, D. J., Bardgett, R. D., et al. (2019). A few ascomycete taxa dominate soil fungal communities worldwide. *Nat. Comms.* 10:2369. doi: 10.1038/s41467-019-10373-z

Fowbert, J. A., and Smith, R. I. L. (1994). Rapid population increases in native vascular plants in the Argentine Islands, Antarctic Peninsula. *Arct. Alp. Res.* 26, 290–296. doi: 10.1080/00040851.1994.12003068

Gams, W., and Philippi, S. (1992). A study of *Cyathicula strobilina* and its *Chalara* anamorph *in vitro*. *Persoonia* 14, 547–552.

Gardes, M., and Bruns, T. D. (1993). ITS primers with enhanced specificity for basidiomycetes-application to the identification of mycorrhizae and rusts. *Mol. Ecol.* 2, 113–118. doi: 10.1111/j.1365-294X.1993.tb00005.x

Gerighausen, U., Bräutigam, K., Mustafa, O., and Peter, H.-U. (2003). "Expansion of vascular plants on an Antarctic island - a consequence of climate change?," in *Antarctic Biology in a Global Context*, eds A. H. L. Huiskes, W. W. C. Gieskes, J. Rozema, R. M. L. Schorno, S. M. van der Vies, and W. J. Wolff (Leiden: Backhuys Publishers), 79–83.

Harkness, D. D., Harrison, A. F., and Bacon, P. J. (1986). The temporal distribution of 'bomb' ^{14}C in a forest soil. *Radiocarb. Lab.* 28, 328–337. doi: 10.1017/S0033822200007426

Horrocks, C. A., Newsham, K. K., Cox, F., Garnett, M. H., Robinson, C. H., and Dungait, J. A. J. (2020). Predicting the impacts of climate warming on maritime Antarctic soils: a space-for-time substitution study. *Soil Biol. Biochem.* 141:107682. doi: 10.1016/j.soilbio.2019.107682

Hrynkiewicz, K., Baum, C., and Leinweber, P. (2009). Mycorrhizal community structure, microbial biomass P and phosphatase activities under *Salix polaris* as influenced by nutrient availability. *Eur. J. Soil Biol.* 45, 168–175. doi: 10.1016/j.ejsobi.2008.09.008

Katoh, K., and Standley, D. M. (2013). MAFFT multiple sequence alignment software version 7: improvements in performance and usability. *Mol. Biol. Evol.* 30, 772–780. doi: 10.1093/molbev/mst010

Leavitt, S. W., and Lara, A. (1994). South American tree rings show declining δ^{13}C trend. *Tellus* 46, 152–157. doi: 10.1034/j.1600-0889.1994.t01-1-00007.x

Lindahl, B. D., Ihrmark, K., Boberg, J., Trumbore, S. E., Högberg, P., Stenlid, J., et al. (2006). Spatial separation of litter decomposition and mycorrhizal nitrogen uptake in a boreal forest. *New Phytol.* 173, 611–620. doi: 10.1111/j.1469-8137.2006.01936.x

Nag Raj, T. R., and Kendrick, B. (1975). *A Monograph of Chalara and Allied Genera*. Waterloo, ON: Wilfred Laurier University Press.

Newsham, K. K., Garnett, M. H., Robinson, C. H., and Cox, F. (2018). Discrete taxa of saprotrophic fungi respire different ages of carbon from Antarctic soils. *Sci. Rep.* 8:7866. doi: 10.1038/s41598-018-25877-9

Newsham, K. K., and Garstecki, T. (2007). Interactive effects of warming and species loss on model Antarctic microbial food webs. *Funct. Ecol.* 21, 577–584. doi: 10.1111/j.1365-2435.2007.01250.x

Newsham, K. K., Hopkins, D. W., Carvalhais, L. C., Fretwell, P. T., Rushton, S. P., O'Donnell, A. G., et al. (2016). Relationship between soil fungal diversity and temperature in the maritime Antarctic. *Nat. Clim. Chang.* 6, 182–186. doi: 10.1038/nclimate2806

Oses-Pedraza, R., Torres-Díaz, C., Lavín, P., Retamales-Molina, P., Atala, C., Gallardo-Cerda, J., et al. (2020). Root endophytic *Penicillium* promotes growth of Antarctic vascular plants by enhancing nitrogen mineralization. *Extremophiles* 24, 721–732. doi: 10.1007/s00792-020-01189-7

Price, M. N., Dehal, P. S., and Arkin, A. P. (2010). FastTree 2 - approximately maximum-likelihood trees for large alignments. *PLoS One* 5:e9490. doi: 10.1371/journal.pone.0009490

Qian, B., Gregorich, E. G., Gameda, S., Hopkins, D. W., and Wang, X. L. (2011). Observed soil temperature trends associated with climate change in Canada. *J. Geophys. Res.* 116:D02106. doi: 10.1029/2010JD015012

Rambaut, A., Drummond, A. J., Xie, D., Baele, G., and Suchard, M. A. (2018). Posterior summarisation in Bayesian phylogenetics using Tracer 1.7. *Syst. Biol.* 67, 901–904. doi: 10.1093/sysbio/syy032

Reeder, J., and Knight, R. (2010). Rapidly denoising pyrosequencing amplicon reads by exploiting rank-abundance distributions. *Nat. Methods* 7, 668–669. doi: 10.1038/nmeth0910-668b

Robinson, C. H., Cox, F., Garnett, M. H., Horrocks, C. A., Dungait, J. A. J., and Newsham, K. K. (2020). *Relative Abundances of DNA and RNA of a Previously Undescribed Helotiales species in Soils from Signy Island and Léonie Island, Along with Edaphic Factors*. Cambridge: UK Polar Data Centre, British Antarctic Survey.

Ronquist, F., Teslenko, M., van der Mark, P., Ayres, D. L., Darling, A., Höhna, S., et al. (2012). MrBayes 3.2: efficient bayesian phylogenetic inference and model choice across a large model space. *Syst. Biol.* 61, 539–542. doi: 10.1093/sysbio/sys029

Royles, J., Amesbury, M. J., Convey, P., Griffiths, H., Hodgson, D. A., Leng, M. J., et al. (2013). Plants and soil microbes respond to recent warming on the Antarctic Peninsula. *Curr. Biol.* 23, 1702–1706. doi: 10.1016/j.cub.2013.07.011

Schweizer, M., Fear, J., and Cadisch, G. (1999). Isotopic (^{13}C) fractionation during plant residue decomposition and its implications for soil organic matter studies. *Rapid Commun. Mass Spectrom.* 13, 1284–1290. doi: 10.1002/(sici)1097-0231(19990715)13:13<1284::aid-rcm578>3.0.co;2-0

Slota, P., Jull, A. J. T., Linick, T., and Toolin, L. J. (1987). Preparation of small samples for ^{14}C accelerator targets by catalytic reduction of CO. *Radiocarbon* 29, 303–306. doi: 10.1017/S0033822200056988

Stoll, V. S., and Blanchard, J. S. (1990). Buffers: principles and practice. *Meth. Enzymol.* 182, 24–38. doi: 10.1016/0076-6879(90)82006-n

Stuiver, M., and Polach, H. A. (1977). Reporting of ^{14}C data. *Radiocarbon* 19, 355–363. doi: 10.1017/S0033822200003672

Tedersoo, L., Bahram, M., Põlme, S., Kõljalg, U., Yorou, N. S., Wijesundera, R., et al. (2014). Global diversity and geography of soil fungi. *Science* 346:1256688. doi: 10.1126/science.1256688

Turner, J., Lu, H., White, I., King, J. C., Phillips, T., Hosking, J. S., et al. (2016). Absence of 21st century warming on Antarctic Peninsula consistent with natural variability. *Nature* 535, 411–415. doi: 10.1038/nature18645

Upson, R., Newsham, K. K., Bridge, P. D., Pearce, D. A., and Read, D. J. (2009). Taxonomic affinities of dark septate root endophytes in the roots of *Colobanthus quitensis* and *Deschampsia antarctica*, the two native Antarctic vascular plant species. *Fung. Ecol.* 2, 184–196. doi: 10.1016/j.funeco.2009.02.004

Větrovský, T., Kohout, P., Kopecký, M., Machac, A., Man, M., and Bahnmann, B. D. (2019). A meta-analysis of global fungal distribution reveals climate-driven patterns. *Nat. Comms.* 10:5142. doi: 10.1038/s41467-019-13164-8

Větrovský, T., Morais, D., Kohout, P., Lepinay, C., Algora, C., Hollá, S. A., et al. (2020). GlobalFungi, a global database of fungal occurrences from high-throughput-sequencing metabarcoding studies. *Sci. Data* 7:228. doi: 10.1038/s41597-020-0567-7

Vu, D., Groenewald, M., de Vries, M., Gehrmann, T., Stielow, B., Eberhardt, U., et al. (2019). Large-scale generation and analysis of filamentous fungal DNA barcodes boosts coverage for kingdom fungi and reveals thresholds for fungal species and higher taxon delimitation. *Stud. Mycol.* 92, 135–154. doi: 10.1016/j.simyco.2018.05.001

Wasley, J., Robinson, S. A., Lovelock, C. E., and Popp, M. (2006). Some like it wet - biological characteristics underpinning tolerance of extreme water stress events in Antarctic bryophytes. *Funct. Plant Biol.* 33, 443–455. doi: 10.1071/FP05306

White, T. J., Bruns, T., Lee, S., and Taylor, J. (1990). "Amplification and direct sequencing of fungal ribosomal RNA genes for phylogenetics," in *PCR Protocols: A Guide to Methods and Applications*, eds T. White, T. Bruns, S. Lee, J. Taylor, M. Innis, D. Gelfand, et al. (New York, NY: Academic Press), 315–322. doi: 10.1016/b978-0-12-372180-8.50042-1

Willerslev, E., Hansen, A. J., and Poinar, H. N. (2004). Isolation of nucleic acids and cultures from fossil ice and permafrost. *Trends Ecol. Evol.* 19, 141–147. doi: 10.1016/j.tree.2003.11.010

Conflict of Interest: The authors declare that the research was conducted in the absence of any commercial or financial relationships that could be construed as a potential conflict of interest.

frontiers in Microbiology

ORIGINAL RESEARCH
published: 08 January 2021
doi: 10.3389/fmicb.2020.607396

Distinct Microbial Communities in Adjacent Rock and Soil Substrates on a High Arctic Polar Desert

*Yong-Hoe Choe, Mincheol Kim and Yoo Kyung Lee**

Korea Polar Research Institute, Incheon, South Korea

Understanding microbial niche variability in polar regions can provide insights into the adaptive diversification of microbial lineages in extreme environments. Compositions of microbial communities in Arctic soils are well documented but a comprehensive multidomain diversity assessment of rocks remains insufficiently studied. In this study, we obtained two types of rocks (sandstone and limestone) and soils around the rocks in a high Arctic polar desert (Svalbard), and examined the compositions of archaeal, bacterial, fungal, and protistan communities in the rocks and soils. The microbial community structure differed significantly between rocks and soils across all microbial groups at higher taxonomic levels, indicating that Acidobacteria, Gemmatimonadetes, Latescibacteria, Rokubacteria, Leotiomycetes, Pezizomycetes, Mortierellomycetes, Sarcomonadea, and Spirotrichea were more abundant in soils, whereas Cyanobacteria, Deinococcus-Thermus, FBP, Lecanoromycetes, Eurotiomycetes, Trebouxiophyceae, and Ulvophyceae were more abundant in rocks. Interestingly, fungal communities differed markedly between two different rock types, which is likely to be ascribed to the predominance of distinct lichen-forming fungal taxa (Verrucariales in limestone, and Lecanorales in sandstone). This suggests that the physical or chemical properties of rocks could be a major determinant in the successful establishment of lichens in lithic environments. Furthermore, the biotic interactions among microorganisms based on co-occurrence network analysis revealed that *Polyblastia* and *Verrucaria* in limestone, and *Atla*, *Porpidia*, and *Candelariella* in sandstone play an important role as keystone taxa in the lithic communities. Our study shows that even in niches with the same climate regime and proximity to each other, heterogeneity of edaphic and lithic niches can affect microbial community assembly, which could be helpful in comprehensively understanding the effects of niche on microbial assembly in Arctic terrestrial ecosystems.

Keywords: polar desert, lithic niche, edaphic niche, rock microbes, Arctic

OPEN ACCESS

Edited by:
Laura Zucconi,
University of Tuscia, Italy

Reviewed by:
Asuncion de los Ríos,
Consejo Superior de Investigaciones Científicas (CSIC), Spain
Eduardo Castro-Nallar,
Andrés Bello University, Chile

***Correspondence:**
Yoo Kyung Lee
yklee@kopri.re.kr

Specialty section:
This article was submitted to Extreme Microbiology, a section of the journal Frontiers in Microbiology

Received: *17 September 2020*
Accepted: *08 December 2020*
Published: *08 January 2021*

Citation:
Choe Y-H, Kim M and Lee YK (2021) Distinct Microbial Communities in Adjacent Rock and Soil Substrates on a High Arctic Polar Desert. Front. Microbiol. 11:607396. doi: 10.3389/fmicb.2020.607396

INTRODUCTION

Understanding the microbial community structure and diversity in polar regions is fundamentally important in both microbial ecology and evolution (Allen and Banfield, 2005). The microbial colonization found in these habitats not only provides insights into microbial succession on uncolonized niches such as glacial forelands, but also helps understand the adaptive mechanisms to

the extreme environment for their stressful factors. Studies to identify the diversity and dynamics of the microbial community have been conducted in a variety of extreme terrestrial ecosystems, including the tundra region (McCann et al., 2016), high-altitude areas (Wong et al., 2010; Tolotti et al., 2020), hyper-arid deserts (Wierzchos et al., 2006, 2013), and Antarctic deserts (de los Rios et al., 2005; Lee et al., 2019). In the case of high Arctic regions, although the distribution pattern and function of edaphic microbial communities have been extensively documented (Kastovska et al., 2005; Schutte et al., 2009; Wilhelm et al., 2011; Tveit et al., 2013; Blaud et al., 2015; McCann et al., 2016), few studies have investigated lithic microbial communities, and these have mainly focused on bacteria and/or fungi (Omelon et al., 2006, 2007; Omelon, 2008; Ziolkowski et al., 2013; Choe et al., 2018). These studies suggest that rocks can be a hotspot for microbial diversity and that the physical and chemical properties of lithic substrates affect microbial colonization. However, there have been few comprehensive multidomain biodiversity assessments on polar regions (Pointing et al., 2009; Garrido-Benavent et al., 2020), and variations in the microbial diversity between different niches (rocks and soils) are still poorly understood.

The climate regime plays a major role in determining the diversity and dynamics of microbial communities, and niche characteristics can also be one of the crucial factors affecting phylogenetic diversity as well as their survival strategies, especially in polar regions (Pointing and Belnap, 2012). Several studies have attempted to demonstrate the microstructure, physicochemical properties, and nutrient availability of the habitat, which are thought to be determinants of microbial diversity and survival strategies (Rogers and Bennett, 2004; Carson et al., 2009). In the case of lithic habitat, the microhabitat architecture of the rock, such as translucence, thermal conductivity, the pore network, and chemical composition is one of main drivers of lithic microbial colonization (Wierzchos et al., 2015). Furthermore, rock weathering in the early stages of soil development in the polar regions, such as the glacial foreland, can promote certain microbial communities in the surrounding soil by leaching of rock minerals (Borin et al., 2010). Similarly, soils are also heterogeneous habitats, containing a variety of spatial scales and environmental gradients (Lehmann et al., 2008). These characteristics provide a large potential for niche differentiation and may be an important factor in developing the diversity of microbial communities in soil (Young et al., 2008). These studies have shown distinct microbial communities that are specialized in soil and rock, respectively. However, it remains unexplored whether the differences in microbial composition are also observed in an adjacent edaphic and lithic niche.

In this s tudy, we examined the diversity and structure of four microbial groups (archaea, bacteria, fungi, and protists) of two selected rocks (sandstone and limestone) and two types of soils around the limestone and sandstone each, and then confirmed whether these groups were specialized in niches. We conducted the test in the same climate regime to minimize the impact of climate variability. Soil and rock chemical characteristics were analyzed to account for the differences in niches. Furthermore, microstructural analyses of rock were used to identify the differences in physical properties between the two types of rock and the potential contributions of structural differences to lithic microbial colonization. This study offers a holistic view of edaphic and lithic microbial communities and helps understand the relationship between niche characteristics and microbial community structure in a polar desert.

MATERIALS AND METHODS

Field Sampling

The sampling site was located in an exposed knoll about 4 km NW of Ny-Ålesund in Svalbard. The site was composed mainly of dolomitic limestone and sandstone of the Carboniferous age (**Figures 1A,B**). A total of 76 samples consisting of limestone (Lime), sandstone (Sand), soil around limestone (Lime-Soil), and soil around sandstone (Sand-Soil) were collected from the site in August 2016 (**Supplementary Table 1**). For rock samples, three different parts of each rock were randomly sampled and pooled into a sterile plastic bag without discriminating the surface and inner parts. In the case of soil samples, soils at three points around each rock sample were pooled into a sterile plastic bag. The samples were placed in a cooler with ice packs during transport to the laboratory at Dasan Research Station, and then stored at −20°C until analysis. Soil samples were not sieved, but gravels larger than 3–4 cm size were removed. Rock samples were crushed using a Mixer Mill (Retsch, Germany) for genomic DNA extraction.

Microclimate Data

The climate data of the study area were recorded during every 10 min intervals using an Onset HOBO® Micro weather Station Data Logger (H21-002), from August 10th, 2015 to July 25th, 2016. Relative humidity (RH) and air temperature (T) were recorded using RH/T sensors (HOBO® S-THB-M002) shaded from the sun 100 cm above the rock surface. Solar flux was measured using a quantum sensor (S-LIA-M003 and S-LIB-M003) for photosynthetic active radiation (PAR) and total solar radiation.

Major and Trace Element Analysis

The major element compositions of the rock and soil samples were determined using a wavelength-dispersive XRF spectrometer (Panalytical, Netherlands) at the Korea Polar Research Institute. Three glass disks per sample prepared by fusing a powdered sample with LT 100 flux (100% Li tetraborate; XRF Scientific, Australia) were used for XRF analysis. Each disk was measured three times, and the average value was taken. To determine trace element concentrations of rocks and soils, finely ground samples were dissolved by acid digestion. The concentration of the final solutions was determined using an inductively coupled plasma mass spectrometry (ICP-MS) using a Thermo ICAP-Q mass spectrometer at the Korea Polar Research Institute.

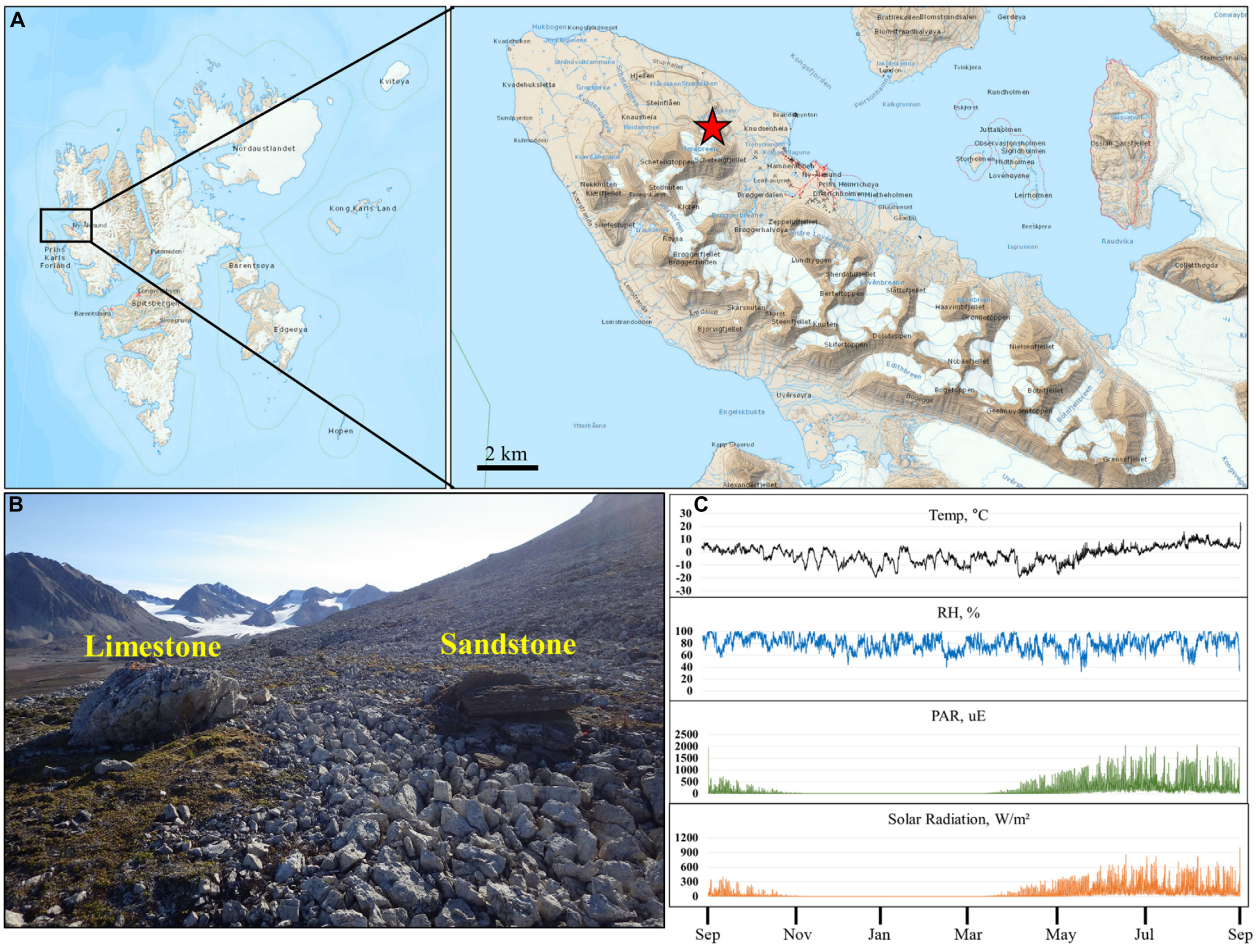

FIGURE 1 | Location and microclimate data of the study site. **(A,B)** Present location and landscape of the sampling sites. **(C)** Present annual temperature, relative humidity, photosynthetically active radiation, and total solar radiation of the study site. The map was prepared based on the map of TopoSvalbard made by the Norwegian Polar Institute.

Pore Structure of Lithic Substrates

The pore size distribution and porosity of limestone and sandstone were characterized by mercury intrusion porosimetry (MIP) at the Korea Basic Science Institute using an AutoPore IV 9500 (Micromeritics Instrument, Norcross, United States) instrument. Three subsamples were prepared for each rock sample, and each subsample was measured three times.

X-ray CT was used to characterize three-dimensional images of the pore structure and distribution in the subsurface of the rock samples. Three cylindrical samples (average height of 20 mm) were cut from limestone (n = 3) and sandstone (n = 3). X-ray CT analysis was carried out using an X-EYE system at the Korea Institute of Civil Engineering and Building Technology. Pore images were acquired using an adaptive thresholding technique based on X-ray CT images.

Total Water Retention Capacity

Rock samples of approximately 5 cm^3 were weighed prior to immersion in H_2O, and then the rock samples were immersed in H_2O. After 24 h, the rock samples were weighed again by removing the excess gravitational water. The total water retention capacity (TWRC) is shown as (%) w/w of retained water per g of rock. Triplicates were performed for limestone and sandstone.

Processing of Illumina Amplicon Sequence Data

Total DNA was extracted from 3 g of powdered rock and 3 g of soil using the FastDNA SPIN kit (MP Biomedicals, Illkirch, France), following the manufacturer's protocol. DNA samples were submitted for PCR amplification, library preparation, and paired-end Illumina MiSeq sequencing (2 × 300 bp) to the Integrated Microbiome Resource (IMR) facility at the Centre for Genomics and Evolutionary Bioinformatics at Dalhousie University (Halifax, Canada). The extracted DNA was amplified using primers 956F and 1401R targeting the V6-V8 region of the archaeal 16S rRNA gene (Comeau et al., 2011), the primer pair 515F-926R targeting the V4-V5 region of the bacterial 16S rRNA gene (Parada et al., 2016; Walters et al., 2016), the

primer pair 572F-1009R targeting the V4 region of the eukaryotic 18S rRNA gene (Comeau et al., 2011), and the pair ITS86F-TS4R targeting the ITS2 region of the fungal nuclear ribosomal internal transcribed spacer (De Beeck et al., 2014). Samples that were not amplified were excluded from further analysis (see **Supplementary Table 1**).

Quality control analysis of the paired-end reads was conducted to determine the length of the reads that can be trimmed in downstream steps, using FastQC[1]. Cutadapt v2.10 was run to remove the remaining adapter and primer sequences from both ends (Martin, 2011). The sequence reads were processed following the QIIME2 pipeline (version 2018.2 platform)[2] (Bolyen et al., 2018). Briefly, the sequence reads of archaeal 16S rRNA genes (at base position 240 and 200 bp for forward and reverse reads, respectively), bacterial 16S rRNA genes (270 and 230 bp), fungal ITS2 regions (250 and 220 bp), and eukaryotic 18S rRNA genes (260 and 220 bp) were trimmed to discard base pairs with average Phred quality score less than 30 and dereplicated using DADA2 (Callahan et al., 2016) as implemented in QIIME2 with paired-end setting (including quality control, trimming, pair-joining, and chimera removals). The QIIME2 q2-feature-classifier[3], a naive Bayes classifier, was used to assign taxonomy. All ASVs were assigned a taxonomic classification using the Silva database (release 128, Quast et al., 2013) for archaeal and bacterial 16S rRNA gene, the UNITE database (v8.0, Abarenkov et al., 2010) as a reference database for fungal ITS2 region, and the PR^2 database (v.4.10.0, Guillou et al., 2013) as a reference database for the 18S rRNA gene. To selectively analyze protistan communities in the 18S rRNA sequence data, the sequences assigned to the fungal 18S rRNA gene were filtered out prior to further analyses.

Statistical Analyses

Alpha diversity, including richness, Shannon and Simpson indices, and evenness of rock and soil samples were calculated using QIIME2 (version 2018.2 platform; see text footnote 2) with subsampling depth based on the lowest sequences of sample for each domain. A one-way between subjects ANOVA and *post hoc* comparison using the Duncan's LSR test were conducted to compare relative abundance among the niches for all domains at the phylum (or class) level. Where assumptions for parametric tests were not met, a Kruskal-Wallis test for independent samples and a Dunn's *post hoc* test were performed (R's agricolae and FSA package). Non-metric multidimensional scaling (NMDS) ordinations were constructed on the basis of Bray-Curtis dissimilarities to demonstrate differences in the composition of microbial communities across sample groups. The differences in microbial community structure between two substrates (rock and soil) were identified by analysis of similarities (ANOSIM) (Clarke, 1993). The effects of substrates and rock types (limestone and sandstone) and their interaction on the microbial dissimilarity were tested by a two-way permutational multivariate analysis of variance using the Adonis function in the Vegan package[4]. We also tested for differences in the dispersion of substrates by performing an analysis of multivariate homogeneity [PERMDISP, (Anderson, 2006)] with the function "betadisper" implemented in the R package "vegan" (Oksanen et al., 2016) using default parameters. ASVs that predominantly contributed to these differences were identified using similarity percentage (SIMPER) analysis using PRIMER-E (Clarke and Gorley, 2006). Furthermore, we identified the "niche breadth" using the formula

$$B_j = \frac{1}{\sum_i^N P_{ij}^2}$$

where B_j is the niche breadth and P_{ij} indicates the proportion of individuals of species j found in a given niche i. ASVs that were more evenly distributed along a wider range of niches were considered as generalists, whereas ASVs with a lower B-value were regarded as specialists. Niche breadth was calculated for the 500 ASVs with the highest mean relative abundance. The values for niche breadth ranged from 1 to 25. ASVs with B $>$3.5 were regarded as generalists, and ASVs with B $<$ 1.5 were considered specialists, which were identified according to the approach by Logares et al. (2013) and Maier et al. (2018).

Co-occurrence networks for lithic niches were constructed using the SParse InversE Covariance Estimation for Ecological Association Inference (SPIEC-EASI) for combined bacterial and fungal datasets (Kurtz et al., 2015; Tipton et al., 2018). To reduce the complexity of network visualization, rare ASVs were filtered out by defining thresholds of a relative abundance $>$0.001% and a minimum of six occurrences in a dataset consisting of samples that recovered both bacteria and fungi (18 limestone samples and 18 sandstone samples). We used the MB (Meinshausen and Bühlmann) method as an inference scheme, and the StARS variability threshold was set to 0.05 for all networks. The topological properties of networks were analyzed using the package "igraph" (Csardi and Nepusz, 2006). We considered ASVs with highest betweenness centrality in the network as keystone taxa (Martin González et al., 2010; Vick-Majors et al., 2014; Banerjee et al., 2016).

RESULTS

Microclimate Data

Microclimatic parameters such as relative humidity, photosynthetically active radiation (PAR), and air temperature were recorded for 12 months, from August 2015, at close proximity to the sampling site (**Figure 1C**). Solar radiation and PAR values showed a similar pattern throughout the year. During the summer period, the spikes of solar radiation and PAR values were up to 1004 W/m^2 and 2066 μE, respectively. The fluctuation in annual air temperatures was in accordance with seasonal changes in solar irradiance. The annual mean temperature for the 12 month period was −1.8°C. The mean daily maximum temperature in summer (June-August) was

[1] https://www.bioinfor-matics.babraham.ac.uk/projects/fastqc/

[2] https://qiime2.org/

[3] https://github.com/qiime2/q2-feature-classifier

[4] https://cran.r-project.org/web/packages/vegan/index.html

10.2°C with a maximum of 23.3°C. The minimum recorded air temperature was −19.7°C in January. Relative humidity rarely fell below 40%, rose above 60% during a year, and occasionally reached 100%.

Chemical and Physical Characterization of Niches

The major and trace element compositions of selected rock (Limestone and Sandstone) and soil (Lime-Soil and Sand-Soil) samples are shown in **Supplementary Table 3**. In limestone, Ca and Mg were relatively high, and the content of Sr was the highest among the trace elements. In contrast, the content of Si was significantly higher in sandstone, and V, Cr, Zn, Rb, Sr, and Ba were also abundant in sandstone. In soil, Lime-Soil and Sand-Soil showed similar elemental distributions with relatively high contents of Si, Ca, V, Cr, Zn, Rb, Sr, and Ba, which were significantly different from limestone but similar to that of sandstone.

X-ray computerized tomography (CT) was used to better characterize the subsurface microstructure of limestone and sandstone (**Supplementary Figure 1**). The resulting X-ray CT scans showed a different pore distribution in the subsurface between limestone and sandstone. In terms of the spatial distribution of pores, the pores of the sandstone were distributed mainly from the surface to a depth of 5 mm (**Supplementary Figure 1A**). Conversely, in the limestone, the pores were evenly distributed throughout (**Supplementary Figure 1D**). These distributions correspond to longitudinal section images with pores marked in black spots (**Supplementary Figures 1B,E**). These results were also observed in the graph of porosity change with height (**Supplementary Figures 1C,F**).

Mercury intrusion porosimetry (MIP) analysis was conducted to analyze the distribution of smaller pores (**Supplementary Table 4**). The results showed that the limestone has a greater mean pore diameter (294.333 ± 49.460 nm) and median pore diameter (2100.867 ± 123.727 nm) than sandstone. However, the porosities of limestone and sandstone were not significantly different. In addition, the total water retention capacity (TWRC) was measured as a feature related to the difference in the physical structure of the rock. Although the difference in TWRC between limestone and sandstone was statistically significant, it was very small.

Microbial Community Composition

Rock and soil samples showed distinct differences in relative abundance and microbial diversity under the same climatic regime. After the quality filtering processes on positive amplifications were completed, we obtained a total of 456432, 924726, 980868, and 239390 high-quality sequences for archaea, bacteria, fungi, and protists, respectively (**Supplementary Tables 1**, **2**). Rarefaction curves approached plateau at their respective maximum sampling depths, indicating that sequencing depth was sufficient to identify the majority of ASVs within microbial communities at each niche (**Supplementary Figure 2**).

The most abundant archaeal phyla were Thaumarchaeota (average: 99 ± 1.35% across all samples) with small contributions from Euryarchaeota (average: 1 ± 1.35% soil samples only) (**Figure 2A** and **Supplementary Table 5**). At the class level, Nitrososphaera (100 ± 1.03%) mainly contributed across all niches and Nitrososphaera were primarily represented by the order Nitrososphaerales (100 ± 1.03%). Although there was a significant difference in community composition between edaphic and lithic niches, we could not find any taxonomic differences at a fine level due to the limitation of taxonomic assignment at a lower level.

A total of 28 bacterial phyla were identified in the edaphic and lithic communities. Proteobacteria was the most abundant phylum across the entire sample set (average: 24.7 ± 5.4% across all samples), followed by Actinobacteria (18.3 ± 6.6%), Bacteroidetes (13.8 ± 4.1%), Acidobacteria (12.5 ± 3.4%), Cyanobacteria (8.8 ± 4.8%), Planctomycetes (7.0 ± 2.6%), Chloroflexi (4.8 ± 2.1%), and FBP (2.2 ± 2.1%) (**Figure 2A** and **Supplementary Table 5**). At the class level, Alphaproteobacteria (16.4 ± 6.3%), Bacteroidia (12.5 ± 4.2%), Thermoleophilia (11.9 ± 5.4%), Oxyphotobacteria (8.8 ± 4.8%), Gammaproteobacteria (7.9 ± 5.3%), Blastocatellia (5.6 ± 2.7%), Planctomycetacia (4.1 ± 1.9%), and Actinobacteria (3.6 ± 1.9%) were highly abundant. We also observed statistically significant differences in the relative abundance between the lithic and soil niches (mean relative abundance >1%; **Figure 2A** and **Supplementary Table 5**). The relative abundances of Acidobacteria, Gemmatimonadetes, Latescibacteria, and Rokubacteria were significantly higher in soil samples than in rock samples, whereas the relative abundance of Cyanobacteria, Deinococcus-Thermus, and FBP were significantly higher in rock samples than in soil samples.

Across all samples, the most abundant fungal classes were Lecanoromycetes (average: 34.5 ± 25.9%), unclassified fungi (26.7 ± 15.6%), Leotiomycetes (13.9 ± 18.1%), and Eurotiomycetes (12.0 ± 10.8%), with smaller contributions from Pezizomycetes (3.5 ± 13.9%), Agaricomycetes (3.4 ± 6.7%), Mortierellomycetes (2.3 ± 3.3%), and Dothideomycetes (1.9 ± 1.8%). At the order level, Lecanorales (26.5 ± 23.2%), unclassified Ascomycota (18.2 ± 12.2%), Verrucariales (11.5 ± 10.9%), unclassified fungi (8.2 ± 7.3%), Thelebolales (6.9 ± 11.7%), Helotiales (6.7 ± 11.2%), and Pezizales (3.5 ± 13.9%) mainly contributed to the fungal community. The relative abundances of Leotiomecetes, Pezizomycetes, and Mortierellomycetes were significantly higher in edaphic niches than in lithic niches, whereas the relative abundance of Lecanoromycetes and Eurotiomycetes were significantly higher in lithic niches than in edaphic niches (**Figure 2B** and **Supplementary Table 5**). In lithic fungal communities, Eurotiomycetes and Lecanoromycetes were most abundant in both limestone and sandstone, but the relative abundance at the order level was different. Eurotiales, Hymeneliales, and Verrucariales were more abundant in limestone communities than in sandstone communities, but the relative abundance of Acarosporales, Candelariales, Lecanorales, Lecideales, Ostropales, Peltigerales, Rhizocarpales, and Umbilicariales were higher in the latter (**Supplementary Figure 3**).

The inferred protistan ASVs were mainly assigned to the phyla Chlorophyta (average: 76.0 ± 31.5% across all samples), followed by Cercozoa (11.5 ± 16.2%), Ciliophora (5.2 ± 7.4%),

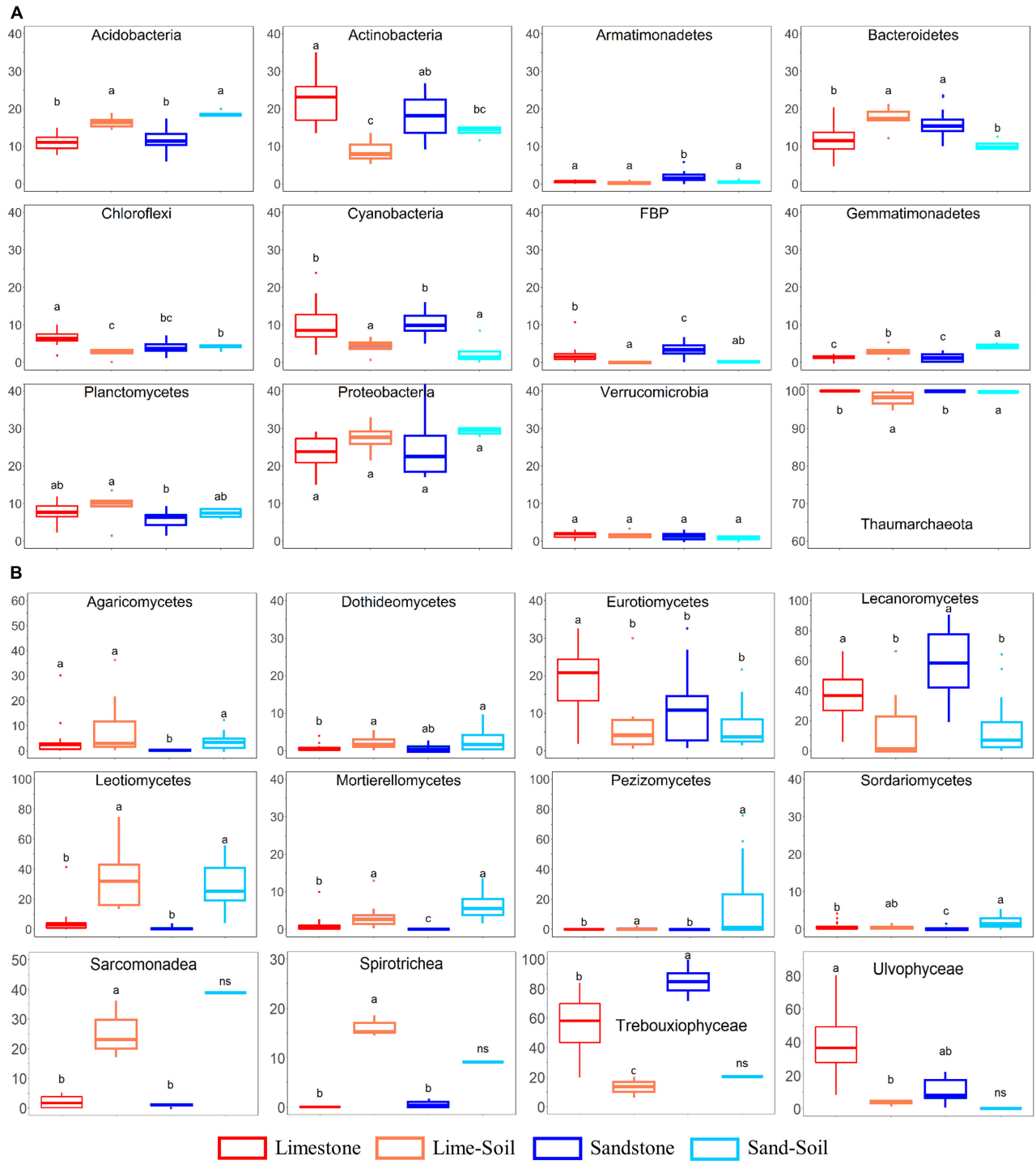

FIGURE 2 | The relative abundance of bacterial, archaeal, fungal, and protistan taxa in four different niches. **(A)** Bacterial and archaeal taxa; **(B)** fungal and protistan taxa. Boxes limit the 25th- and 75th percentile with the median presented as the line. Error bars present the 1st and 99th percentile and outliers are shown as dots below and above. Significant differences ($P < 0.05$) are marked by different letters (see also **Supplementary Table 5**).

and Ochrophyta (1.9 ± 4.2%). At the class level, we also observed statistically significant differences in the relative abundance between the lithic and edaphic niches (mean relative abundance >5%; **Figure 2B** and **Supplementary Table 5**). The relative abundances of Sarcomonadea and Spirotrichea were significantly higher in lithic niches than in edaphic niches, whereas the relative abundances of Trebouxiophyceae and Ulvophyceae were significantly higher in edaphic niches.

Alpha diversity indices, such as richness, and Shannon and Simpson indices tended to be higher in edaphic than in lithic archaeal, bacterial, and protistan communities (**Supplementary Figure 4**). For fungi, these indices were comparable for both niches, except for ASV richness which was higher in lithic than in edaphic communities. The evenness of edaphic communities of bacteria and protists was higher than that of lithic communities, whereas archaeal and fungal communities were similar in both niches (**Supplementary Figure 4**).

Niche Differentiation of Microbial Communities in Rock and Soil

The community structure of all four microbial groups (bacteria, archaea, fungi, and protists) differed mainly by substrate type (rock vs. soil), followed by rock type (limestone vs. sandstone) (**Figure 3** and **Supplementary Table 6**). The similarity percentage analysis (SIMPER) was used to determine the relative contribution of an individual ASV to the community dissimilarity among the niches (**Supplementary Table 7**). To achieve the higher taxonomic resolution of those ASVs, the ASVs were further BLAST-searched against the NCBI nucleotide collection database (nr/nt). For archaea, the average dissimilarity between lithic and edaphic niches was 71.98% and was driven by ASV062 (contribution to dissimilarity: 10.4%), ASV050 (7.0%), and ASV031 (6.8%). The average dissimilarity between limestone and sandstone was 52.16% and was driven by ASV036 (11.4%), ASV075 (8.4%), and ASV062 (7.3%). For bacteria, the members of the Gemmatimonadetes contributed to 1.24–1.56% of the dissimilarity of bacterial communities between the lithic niches and soil niches. Although many bacterial phyla consistently contributed to community dissimilarity between limestone and sandstone, the top 3 ASVs that contributed the most to community dissimilarity were the members of Actinobacteria and Chloroflexi (0.40–0.46%). Among the ASVs largely responsible for the dissimilarity of fungal communities between rock and soil, the top 3 genera were *Geomyces* (3.36%), *Pulvinula* (1.07%), and *Mortierella* (1.03%) (**Supplementary Table 7**). In lithic niches, the ASVs belonging to Lecanoromycetes contributed the most to the dissimilarity between limestone and sandstone. In protistan communities, although there was the limitation of taxonomic assignment at a lower level, the ASVs, which contributed to the dissimilarity of protistan communities, were members of Cercozoa and Chlorophyta (**Supplementary Table 7**). Furthermore, the results of the PERMDISP analysis revealed differentiation among edaphic and lithic bacterial and fungal communities, indicating that lithic bacterial and fungal communities were significantly more variable in their intra-ASV composition than the edaphic ones (**Supplementary Figures 5**, **6**).

For bacteria and fungi, in which the number of recovered samples was sufficient and well assigned to the lower taxonomic level, we performed further analysis to identify generalists and specialists between rocks and soils. The analyses used the 500 ASVs with the highest mean relative abundance in rock and soil samples. For bacteria, we identified 304 ASVs (out of 500 ASVs, 60.8%) as generalists and 84 ASVs as specialists (16.8%) (**Figures 4A,C**). Among bacterial generalists, ASVs belonging to Proteobacteria (85 ASVs) and Actinobacteria (85 ASVs) were the most abundant phyla, followed by Cyanobacteria (43 ASVs), Bacteroidetes (31 ASVs), and Acidobactera (20 ASVs). Among all specialists, ASVs belonging to Bacteroidetes (24 ASVs), Acidobacteria (16 ASVs), and Proteobacteria (15 ASVs) were dominant. A much higher proportion of Proteobacteria, Actinobacteria, Cyanobacteria, FBP, and Chloroflexi was present within generalists than specialists, whereas the proportion of specialists in Acidobacteria, Bacteroidetes, and Planctomycetes was higher or similar to that of generalists. The specialists belonging to Bacteroidetes were most abundant in lithic niches, whereas Proteobacteria were more abundant in the edaphic niches (**Supplementary Table 9**). For fungi, among 500 ASVs, 198 generalist (39.6%) and 98 specialist ASVs (19.6%) were detected (**Figures 4B,D**). In all taxa, Lecanoromycetes were detected as the most abundant classes (except unclassified 185 ASVs), followed by Eurotiomycetes (79 ASVs), Leotiomycetes (43 ASVs), Agaricomycetes (25 ASVs), Dothideomycetes (14 ASVs), Mortierellomycetes (14 ASVs), Sordariomycetes (12 ASVs), and Pezizomycetes (4 ASVs). Among generalist ASVs, members of Eurotiomycetes, Lecanoromycetes, and Leotiomycetes were the most abundant. The proportion of generalists was higher than that of specialists in most taxa, except for Dothideomycetes. The ASVs belonging to Eurotiomycetes and Lecanoromycetes were the most abundant as a specialist in lithic niches, whereas most abundant specialists in edaphic niches were Leotiomycetes (**Supplementary Table 8**).

Co-occurrence Patterns of Bacterial and Fungal Communities in Lithic Niches

Limestone and sandstone showed clear differences in terms of their physical and chemical properties (**Supplementary Figure 1** and **Supplementary Table 3**). Moreover, the microbial community composition between limestone and sandstone also differed significantly. We further conducted a network analysis to identify the difference in the biotic interactions among microorganisms between two types of rocks. Two networks were generated by rock type (**Figure 5**), and both limestone and sandstone networks were very sparse, with an average node degree of 2.699 and 3.248, respectively. The modularity, clustering coefficient, average path length, positive/negative edge ratio, and network diameter of the limestone network were greater than those of the sandstone network (**Supplementary Table 9**). In terms of interactions between taxa in the network, the number of intra-kingdom links in bacterial taxa or fungal taxa was higher than the number of inter-kingdom links between bacterial and fungal taxa (**Supplementary Table 10**).

Among ASVs identified as keystone taxa (i.e., the largest number of degrees and greatest betweenness) for each network, most of them were affiliated with lichen-forming fungal taxa in both limestone and sandstone, but the taxonomic affiliations at the genus level of those ASVs differed depending on the rock type. The keystone fungal ASVs within the limestone included genera *Polyblastia* and *Verrucaria*, whereas the keystone ASVs within sandstone were assigned to genera such as *Atla*, *Porpidia*,

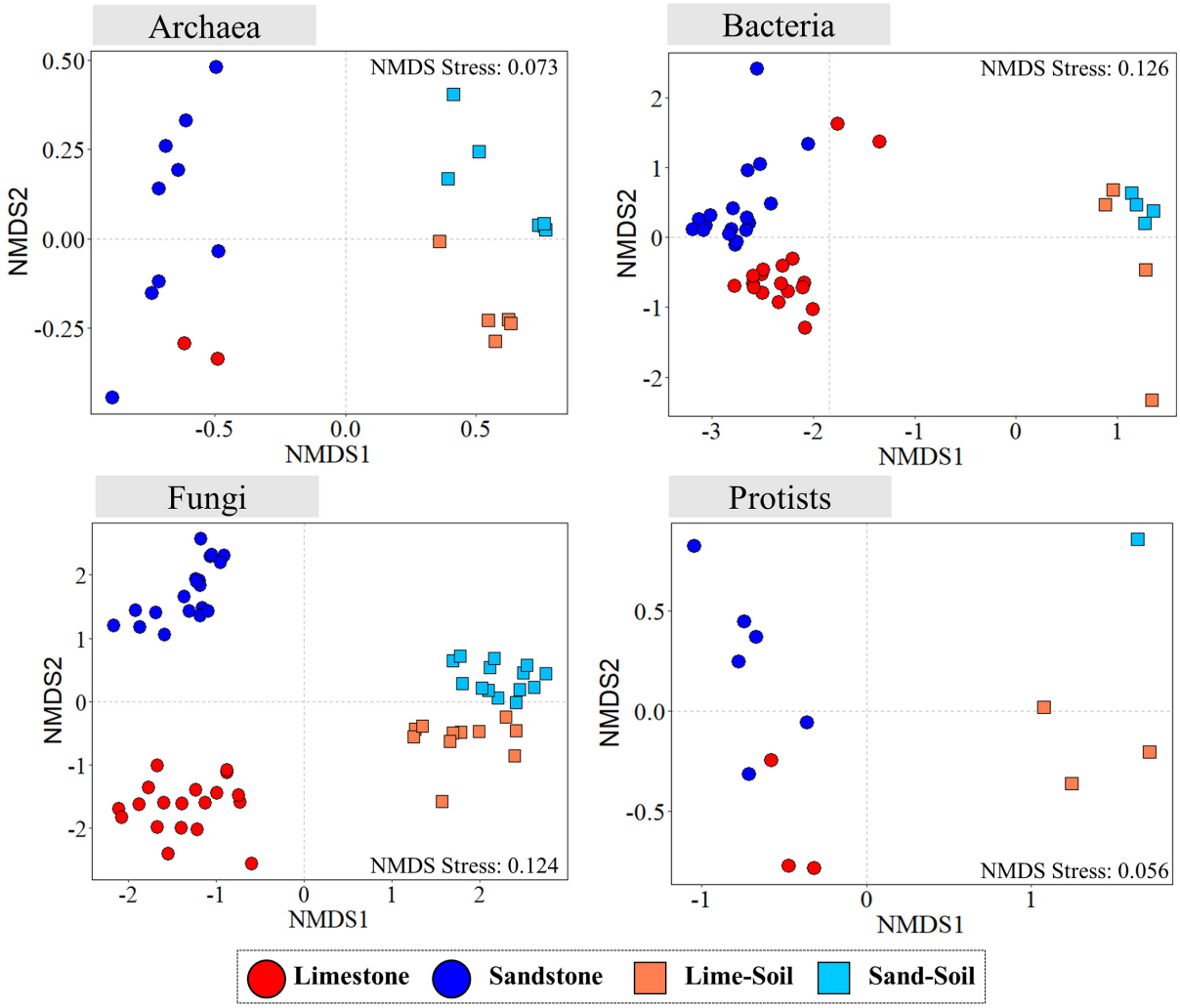

FIGURE 3 | Non-metric multidimensional scaling (NMDS) ordination plots of Bray–Curtis dissimilarities for archaeal, bacterial, fungal, and protistan communities across sample categories.

and *Candelariella* (**Supplementary Table 11**). The bacterial taxa that appeared to be positively correlated with fungal keystone ASVs were also different between limestone and sandstone. For example, *Polyblastia* and *Verrucaria* in limestone correlated with ASVs belonging to the order Burkholderiales (R = 0.546, P = 0.018) and Rhizobiales (R = 0.545, P = 0.019), whereas *Porpidia* in sandstone correlated with genera *Singulisphaera* (R = 0.679, P = 0.001) and *Polymorphobacter* (R = 0.537, P = 0.021).

DISCUSSION

In this study, we showed that the community structure of four taxonomic groups (archaea, bacteria, fungi and protists) differed significantly between rocks and soils. Previous studies have demonstrated that the habitat heterogeneity has strong influences on lithic and edaphic microbial communities (Pointing et al., 2009; Lee et al., 2016; Meslier et al., 2018). For example, the diversity of microbial communities in four different lithic substrates from the Atacama Desert was found to be strongly correlated with those substrates (Meslier et al., 2018). Similarly, differences in diversity and structure of the microbial community have been reported for lithic and soil niches in Plateau Desert and McMurdo Dry Valleys (Pointing et al., 2009; Lee et al., 2016). To our knowledge, no study has compared community assembly across lithic and edaphic niches and without the confounding effect of different climate regimes in the high Arctic cold desert. We also presented for the first time a comprehensive multidomain diversity of lithic and edaphic microbial communities from Svalbard. Although lithic colonizations in Svalbard were previously reported, target taxa were mostly confined to bacteria and fungi.

A comprehensive assessment of the microbiome of rock and soil showed that Thaumarchaeota, Proteobacteria, Ascomycota, and Chlorophyta were the most abundant archaeal, bacterial,

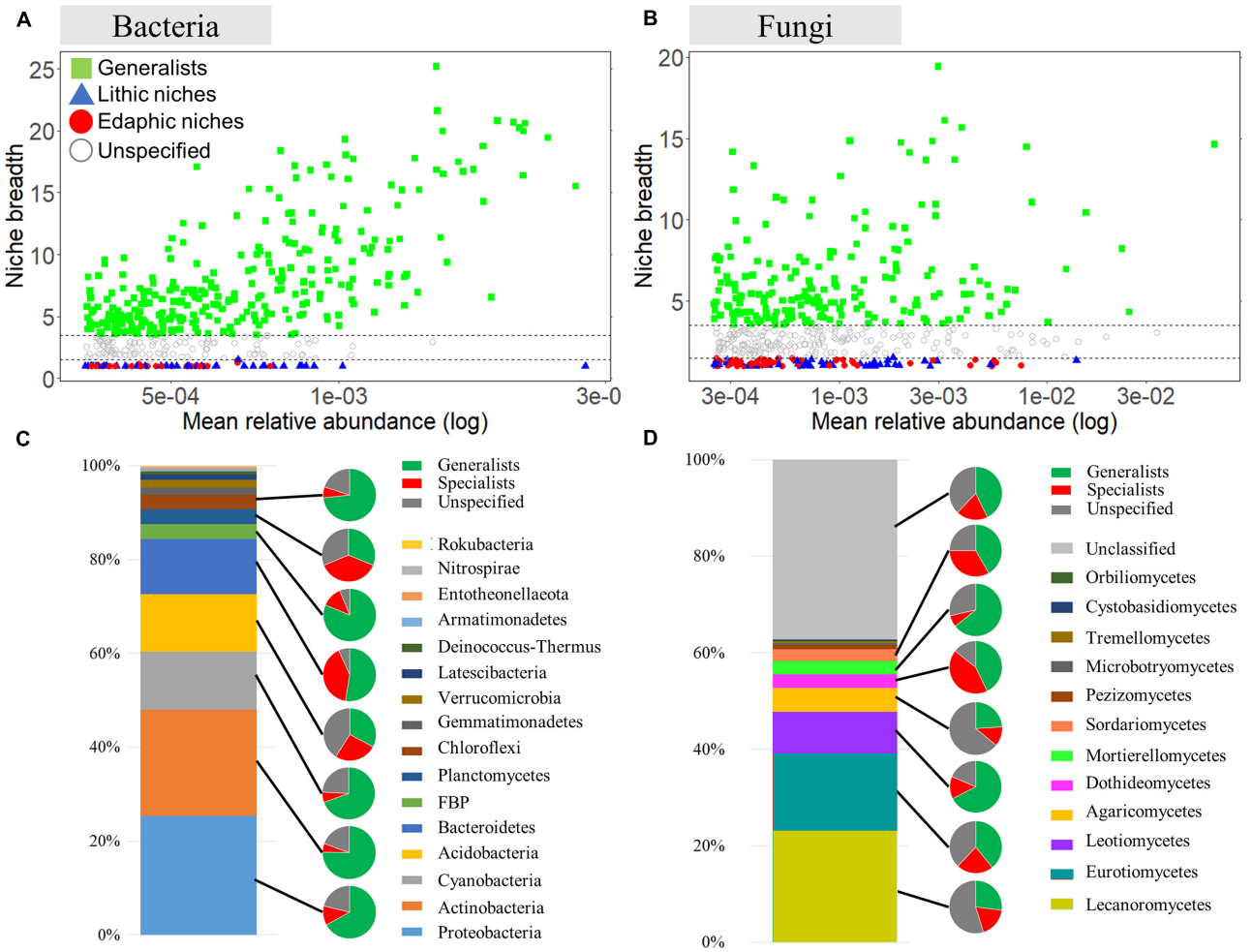

FIGURE 4 | Analysis of niche specialists and generalists. Niche breadth of bacterial ASVs **(A)** and fungal ASVs **(B)** identified in lithic and edaphic niches. Each symbol represents an ASV. ASVs with a *B* value >3.5 are considered niche generalists, while ASVs with a *B* value < 1.5 are considered niche specialists. Phylum compositions of all taxa, specialists, generalists are shown. The bar graph shows the phylum compositions of total bacteria **(C)** and fungi **(D)**. The smaller pies show the proportions of specialists, generalists and unspecified ASVs.

fungal, and protistan taxa, respectively. Thaumarchaeota, which is mostly composed of class Nitrososphaeria including a number of ammonia-oxidizing archaea (AOA), is globally distributed in aquatic and terrestrial ecosystems (Alves et al., 2018). AOA is especially known as a pioneer that can thrive in extreme and oligotrophic environments (Stahl and de la Torre, 2012; Alves et al., 2018). Their genetic flexibility and niche adaptability not only allow them to adapt to harsh environments but also potentially play a role as primary producers in the ecosystems, contributing to nitrogen cycling in nitrogen-limited ecosystems (Stahl and de la Torre, 2012; Beam et al., 2014). Proteobacteria are also known to contain a number of phototrophic, photoheterotrophic, and chemolithotrophic taxa that are able to survive in oligotrophic niches such as polar regions (Wei et al., 2016; Choe et al., 2018). For example, N-fixing Rhizobiales, Burkholderiales, Xanthomonadales, and Myxococcales belonging to the Proteobacteria have been reported to dominate in Arctic soils as well as in Antarctica (Cary et al., 2010; Kim et al., 2015; Malard and Pearce, 2018). Among the microbial eukaryotic groups, despite varying in relative abundance at lower taxonomic levels, the fungal phyla Ascomycota and the phyla Chlorophyta belonging to green algae dominated the study area. The Ascomycota contain a variety of taxonomic groups that can resist environmental stresses (Selbmann et al., 2005). For example, certain species of the class Lecanoromycetes and Leotiomycetes belonging to Ascomycota are able to produce fungal secondary metabolites such as atranorin, calycin, pinastric acid, and pulvinic acid that absorb strong UV and filter out excessive UV irradiation (Molnár and Farkas, 2010). Moreover, the ecological characteristics of various lichen-forming fungi, which comprise a large part of Ascomycota (about 40% of all Ascomycota), could be a possible reason for the predominance of these fungal phyla in the study area (Lawrey and Diederich, 2003). In this context, the high relative abundance of Trebouxiophyceae and Ulvophyceae belonging to Chlorophyta, which include symbiotic photobionts, parallels that of Ascomycota, and this correlation makes sense

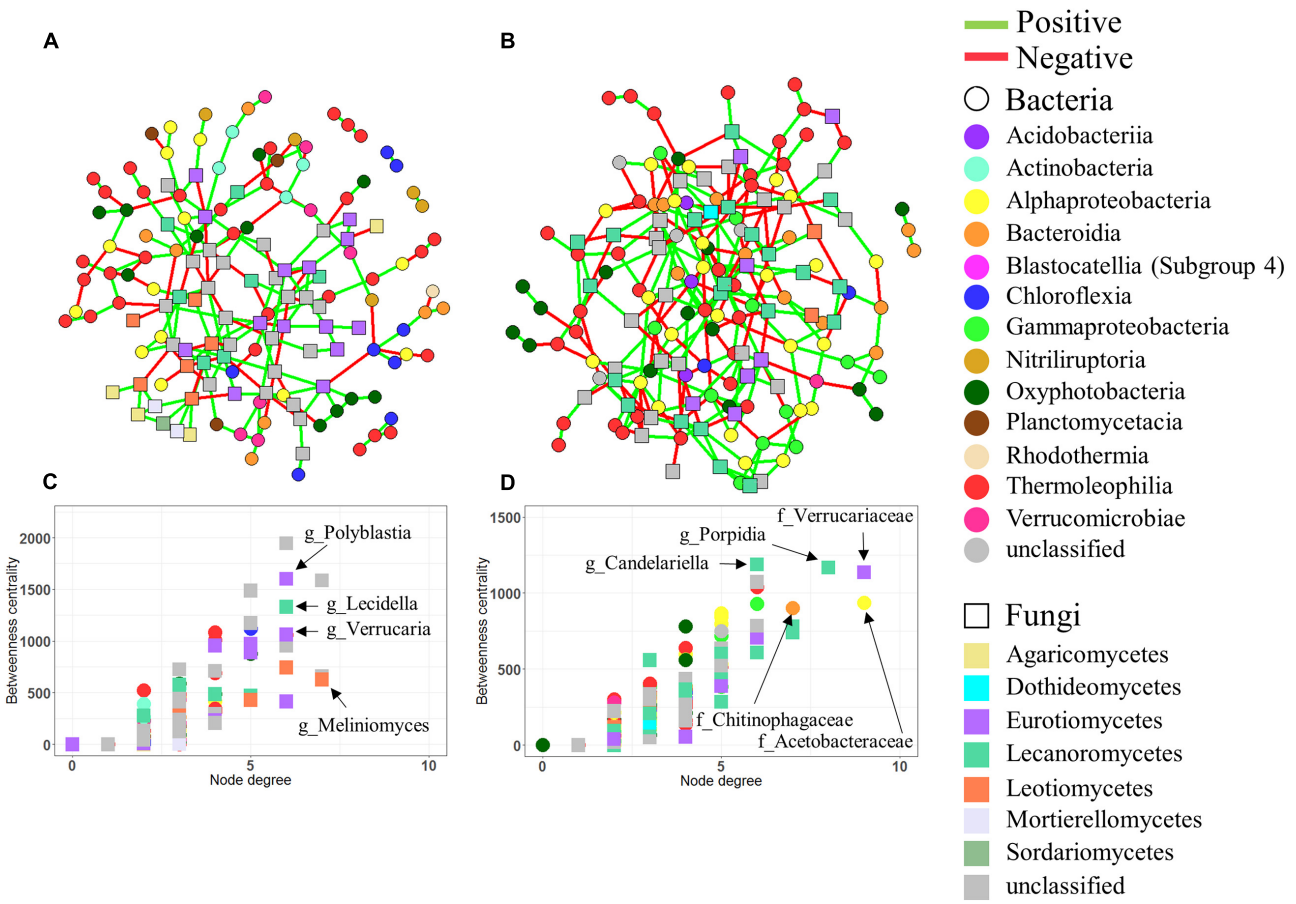

FIGURE 5 | Co-occurrence networks. Networks based on bacterial and fungal ASVs combined in limestone **(A)** and sandstone **(B)**. In all networks, circles and squares correspond to bacterial and fungal ASVs, respectively, with colors representing each taxonomic rank, class. Edges represent positive (green) or negative (red) interactions. Betweenness centrality and degree of each ASV in the limestone network **(C)** and sandstone network **(D)**. Nodes with high betweenness centrality and high degree values are considered to be keystone taxa in the networks. The genera of the bacterial and fungal ASVs with the highest degree and centrality are shown.

since the former includes symbiotic photobionts within lichens (Faluaburu et al., 2019).

Distinct differences were observed in the composition of microbial communities between lithic and edaphic niches. Similar results were also observed in previous studies by Pointing et al. (2009); Yung et al. (2014), Van Goethem et al. (2016), and Garrido-Benavent et al. (2020) which compared rock and soil microbial communities in Antarctic regions. In line with our findings, Garrido-Benavent et al. (2020) revealed differentially abundant bacterial and fungal taxa in rock and soil, showing that Deinococcus-Thermus and Lecanoromycetes were more abundant in lithic than edaphic communities, and the opposite was true for Agaricomycetes and Leotiomycetes. In contrast with our findings, Chloroflexi and Cyanobacteria showed low abundance in examined rock (igneous rock) in the study. These contrasting results are likely due to different rock types, supported by previous findings by Choe et al. (2018), which showed that Chloroflexi and Cyanobacteria were more abundant in sedimentary rocks than igneous rocks. This differential selection for taxa in the two niches is likely related to the capacity of the microorganisms to adapt to the niche and the biotic interactions between them. For example, bacterial phyla, Acidobacteria and Gemmatimonadetes were significantly higher in the edaphic niche than in the lithic niche. Additionally, Proteobacteria were identified as the most abundant edaphic specialist. These phyla are known to include aerobic anoxygenic phototrophic bacteria, which may play an important role in contributing to organic carbon cycling in nutrient-poor arid soils (Csotonyi et al., 2010). Furthermore, a previous study showed high proportions of Gemmatimonadetes in arid soils, suggesting an adaption to low-moisture environments (DeBruyn et al., 2011). As such, the functional similarity required to adapt to the extreme environment of the dominant taxa despite the different characteristics of the niche may be an example of functional redundancy (Louca et al., 2018). Functional redundancy has been observed in extreme environments such as deep subseafloor aquifer (Tully et al., 2018) and Antarctic terrestrial ecosystems (Yergeau et al., 2007, 2012; Pointing et al., 2009). For example, Pointing et al. (2009) showed little functional variation between the bare soil samples, despite the

samples having heterogeneous phylogenetic diversity. Similarly, Yergeau et al. (2012) revealed that the major members of the soil community were functionally similar despite differences in microbial diversity between distinct habitats.

Lithic microbial communities are frequently dominated by Cyanobacteria, which are the major drivers of photosynthetic carbon fixation and nitrogen cycling in desert ecosystems (Warren-Rhodes et al., 2006; Chan et al., 2012). Consistent with these studies, our data showed that Cyanobacteria was significantly higher in the lithic niches than in edaphic niches. Particularly, ASVs belonging to the family Chroococcidiopsidaceae were significantly higher in both limestone and sandstone than in soils. Among the species belonging to Chroococcidiopsidaceae, Chroococcidiopsis, which are most commonly observed in the lithic niche, have relatively small coccoid cells. It is well adapted to entering pore spaces in the rock matrix as well as secreting extracellular polymeric substances that are implicated in various stress resistances in rocks (Chan et al., 2012; Pointing, 2016). These characteristics could be a possible reason for the predominance of the cyanobacterial family in the lithic niches. The relative abundances of Actinobacteria, FBP, and Deinococcus-Thermus were also higher in the lithic communities. The order Solirubrobacterales in Actinobacteria were the most abundant group observed in lithic niches, consistent with previous studies that have been observed in rocks (Esposito et al., 2015; Khilyas et al., 2019). The 16S rRNA sequence of candidate division FBP was first reported from a lichen-dominated lithic habitat in Antarctica (de la Torre et al., 2003), and Deinococcus-Thermus was also dominant in cryptoendolithic environments (Cary et al., 2010). The prominent features of these phyla are that they can be adapted to various environmental stresses, such as fluctuating temperature and strong UV radiation (Suzuki and Whitman, 2012). Such stress tolerance traits can help them survive in lithic habitats in polar regions.

Fungal ASVs belonging to Lecanoromycetes and Eurotiomycetes were notably higher in both limestone and sandstone than in soils and were also the most abundant specialists in the lithic niche. The majority of the Lecanoromycetes and Eurotiomycetes were identified as members of the lichen-forming order Lecanorales and Verrucariales. Lichens are considered especially well adapted to the lithic niche under cold environments, owing to their freezing tolerance, low mineral nutrient demand, and ability to be photosynthetically active at low temperatures (Kappen, 2000). Consistent with our findings, a recent study on lithic colonization patterns in Axel Heiberg Island, Inglefield Land, and Svalbard has reported a lichen mycobiont prevalence in lithic niches (Hansen et al., 2006; Ziolkowski et al., 2013; Choe et al., 2018). Unlike lithic niches, the relative abundance of ASVs belonging to class Leotiomycetes was not only higher in the edaphic niche than in the lithic niche, but was also identified as a specialist in the soils. The dominant fungal orders detected in this study belonged to Helotiales (Leotiomycetes) in Ascomycota. In previous studies, Helotiales was found in the rhizosphere in Arctic regions (Bjorbaekmo et al., 2010; Walker et al., 2011). Deslippe et al. (2012) observed that Ascomycota was dominated by Helotiales in Alaska (low Arctic). In the Siberian tundra (High Arctic), Ascomycota was also dominated by Leotimycetes (Gittel et al., 2014). In this respect, Leotimycetes seem to be more optimized or preferred for the edaphic niche.

The classes Trebouxiophyceae and Ulvophyceae in Chlorophyta were notably higher in both limestone and sandstone than in soils. According to previous studies, Cyanobacteria and Chlorophyta (green algae) are regarded as the pioneering inhabitants in the colonization of the lithic niche (Tiano et al., 1995). Their biofilm-forming and photosynthetic ability allow them to colonize on a rock by developing a symbiotic relationship with lichen-forming fungal taxa (de los Rios et al., 2007). The higher relative abundances of Sarcomonadea and Spirotrichea in soils were in line with previous soil eukaryotic DNA studies as well as microscopic studies (Adl and Gupta, 2006; Bates et al., 2013; Harder et al., 2016; Seppey et al., 2017). Cercozoa, to which Sarcomonadea belongs, tended to be more abundant in arid soils, and ciliate taxa such as Spirotrichea are known to survive in arid conditions such as polar deserts (Adl and Gupta, 2006; Bates et al., 2013). The distinct communities between rocks and soils demonstrate that distinct microbial communities can be induced by different niche characteristics, even though they are close to each other.

Interestingly, our results provide evidence for ecological coherence at higher taxonomic ranks in lithic bacterial and fungal communities. The lithic niches were dominated by similar phyla that were clearly distinguished from those of the edaphic niches, but the composition of lithic communities at lower taxonomic levels differed by rock type. This ecological coherence depending on niche implies that its members share life strategies or specific traits that distinguish them from other taxa, but the functional traits of those communities need further investigation (Philippot et al., 2010). In other words, the spatial heterogeneity of the lithic microhabitats likely exerts a stronger filter on the ability of airborne microorganisms to colonize the lithic substrate compared to the edaphic substrate in the stochastic process of dispersal, which is consistent with the results in previous studies (de los Rios et al., 2007; Meslier et al., 2018).

Rocks provide habitats for microorganisms, and they also affect the microbial community structure (Meslier et al., 2018). Although Meslier et al. (2018) suggested that the chemical properties of the rock may not be an essential driver of community composition and diversity, the ability of microorganisms to use nutrients leached from rocks can affect the community composition in their niche. In addition, Cámara et al. (2008) suggested that the microstructure of the rock, such as the space available for colonization and its physical structure, linked to water retention capabilities, can be a determinant of the potential bioreceptivity of lithic habitat. In our study, despite the clearly different chemical composition and microhabitat architecture of limestone and sandstone, the structures of archaeal, bacterial, and protistan communities were similar in both limestone and sandstone, which is consistent with the previous studies on lithic communities from polar deserts (de la Torre et al., 2003; Pointing et al., 2007; Archer et al., 2017). This suggests that the dominant microbial taxa

of these communities consist of common microorganisms that can colonize lithic microhabitats, supporting the microbial metacommunity concept (Walker and Pace, 2007) and also imply that the climatic characteristics of the habitat could be major drivers determining the dominant taxa in lithic niches (Pointing et al., 2009; Cowan et al., 2010).

Nevertheless, our results revealed obvious differences that were mainly caused by lichen-forming fungal taxa in the fungal community structure between limestone and sandstone. Such differences were not only observed in relative abundance at the low taxonomic level between limestone and sandstone but the network analysis also showed that different fungal genera are keystone taxa in limestone and sandstone. The fungal ASVs identified as keystone taxa in limestone were mostly assigned to *Polyblastia* and *Verrucaria* belonging to Verrucariales. Members of these genera are well known to form calcicolous endolithic lichens (Halda, 2003; Hoppert et al., 2004). In contrast to limestone, fungal ASVs belonging to *Porpidia* and *Candelariella* were identified as keystone taxa in sandstone. They are frequently observed in siliceous rocks such as sandstone (Dobson, 1979). Although biophysical and biochemical mechanisms of rock weathering by lichens have been extensively studied (Mccarroll and Viles, 1995; Matthews and Owen, 2008; de los Rios et al., 2009; Favero-Longo et al., 2011), evolutionary links between habitat preference and lichen-forming fungal taxa have been rarely investigated (Hoppert et al., 2004). One possible reason for this could be that bioreceptivity of rocks is determined by chemical, mineralogical, and physical properties such as porosity, pore size, pore distribution, pore connectivity, water retention capacity, and light transmittance (Wierzchos et al., 2015). Previous studies showed that the differential rock colonization by lichen-associated fungi is largely determined by differences in the physicochemical characteristics of the lithic substrate (Kurtz and Netoff, 2001; Hoppert et al., 2004; Favero-Longo et al., 2011). Furthermore, lichenized fungi play a pivotal role in the production of extracellular compounds as well as in the formation of lichen thallus structures (Lawrey and Diederich, 2003). In this context, it is not surprising that lichen-associated fungi might act as hubs in the community network, and could be habitat specialized taxa depending on rock type.

CONCLUSION

Niche differentiation of the microbiomes in lithic and edaphic substrates in this study was demonstrated using the multidomain diversity assessment by sampling strategy that minimized the effect of biogeography. The different physical and chemical properties of lithic and edaphic niches supported the distinct microbial communities, even in close spatial proximity. In particular, for lithic niches, we found that lichen-forming fungi played key roles as a hub in the communities in the cold desert. Taken together, this study provides insights into the microbial ecology of lithic and edaphic niches that influence microbial community composition in a high arctic polar desert. To comprehensively understand the mechanisms of microbial community assembly, ongoing work examining their functional diversity and environmental factors at the micro-scale will help understand how the microbial assemblages adapt to their niches in the cold desert.

DATA AVAILABILITY STATEMENT

The datasets generated for this study can be found in the Raw sequencing data were deposited in the Sequence Read Archive (SRA) of NCBI under the BioProject ID PRJNA380676.

AUTHOR CONTRIBUTIONS

Y-HC conceived the setup, did rock and soil sample fieldwork, conducted the microbial lab work, analyzed the data, and wrote the manuscript. MK provided a range of feedback on the analyses and the manuscript. YL supervised the setup and provided funding. All authors reviewed and contributed to the final version of the manuscript.

FUNDING

This work was supported by a grant from Korea Polar Research Institute (KOPRI-PE16030) and from a National Research Foundation of Korea Grant from the Korean Government (MSIT; the Ministry of Science and ICT) (NRF-2016M1A5A1901769) (KOPRI-PN20081).

ACKNOWLEDGMENTS

We would like to thank Yunseok Yang and Seunghee Han of the Korea Polar Research Institute for the XRF and ICP-MS measurements, respectively. Y-HC wishes to acknowledge Jaeryong Oh for his help during sampling in Svalbard.

SUPPLEMENTARY MATERIAL

The Supplementary Material for this article can be found online at: https://www.frontiersin.org/articles/10.3389/fmicb.2020.607396/full#supplementary-material

REFERENCES

Abarenkov, K., Nilsson, R. H., Larsson, K. H., Alexander, I. J., Eberhardt, U., Erland, S., et al. (2010). The UNITE database for molecular identification of fungi - recent updates and future perspectives. *New Phytol.* 186, 281–285. doi: 10.1111/j.1469-8137.2009.03160.x

Adl, M. S., and Gupta, V. V. S. R. (2006). Protists in soil ecology and forest nutrient cycling. *Can. J. Forest. Res.* 36, 1805–1817. doi: 10.1139/X06-056

Allen, E. E., and Banfield, J. F. (2005). Community genomics in microbial ecology and evolution. *Nat. Rev. Microbiol.* 3, 489–498. doi: 10.1038/nrmicro1157

Alves, R. J. E., Minh, B. Q., Urich, T., von Haeseler, A., and Schleper, C. (2018). Unifying the global phylogeny and environmental distribution of ammonia-oxidising archaea based on amoA genes. *Nat. Commun.* 9, 1517. doi: 10.1038/s41467-018-03861-1

Anderson, M. J. (2006). Distance-based tests for homogeneity of multivariate dispersions. *Biometrics* 62, 245–253. doi: 10.1111/j.1541-0420.2005.00440.x

Archer, S. D. J., de los Rios, A., Lee, K. C., Niederberger, T. S., Cary, S. C., Coyne, K. J., et al. (2017). Endolithic microbial diversity in sandstone and granite from the McMurdo Dry Valleys, Antarctica. *Polar Biol.* 40, 997–1006. doi: 10.1007/s00300-016-2024-9

Banerjee, S., Baah-Acheamfour, M., Carlyle, C. N., Bissett, A., Richardson, A. E., Siddique, T., et al. (2016). Determinants of bacterial communities in C anadian agroforestry systems. *Environ. Microbiol.* 18, 1805–1816. doi: 10.1111/1462-2920.12986

Bates, S. T., Clemente, J. C., Flores, G. E., Walters, W. A., Parfrey, L. W., Knight, R., et al. (2013). Global biogeography of highly diverse protistan communities in soil. *ISME J.* 7, 652–659. doi: 10.1038/ismej.2012.147

Beam, J. P., Jay, Z. J., Kozubal, M. A., and Inskeep, W. P. (2014). Niche specialization of novel Thaumarchaeota to oxic and hypoxic acidic geothermal springs of Yellowstone National Park. *ISME J.* 8, 938–951. doi: 10.1038/ismej.2013.193

Bjorbaekmo, M. F. M., Carlsen, T., Brysting, A., Vralstad, T., Hoiland, K., Ugland, K. I., et al. (2010). High diversity of root associated fungi in both alpine and arctic *Dryas octopetala*. *BMC Plant Biol.* 10:244. doi: 10.1186/1471-2229-10-244

Blaud, A., Phoenix, G. K., and Osborn, A. M. (2015). Variation in bacterial, archaeal and fungal community structure and abundance in High Arctic tundra soil. *Polar Biol.* 38, 1009–1024. doi: 10.1007/s00300-015-1661-8

Bolyen, E., Rideout, J. R., Dillon, M. R., Bokulich, N. A., Abnet, C., Al-Ghalith, G. A., et al. (2018). QIIME 2: reproducible, interactive, scalable, and extensible microbiome data science. *Nat. Biotechnol.* 37, 852–857.

Borin, S., Ventura, S., Tambone, F., Mapelli, F., Schubotz, F., Brusetti, L., et al. (2010). Rock weathering creates oases of life in a High Arctic desert. *Environ. Microbiol.* 12, 293–303. doi: 10.1111/j.1462-2920.2009.02059.x

Callahan, B. J., McMurdie, P. J., Rosen, M. J., Han, A. W., Johnson, A. J. A., and Holmes, S. P. (2016). DADA2: high-resolution sample inference from Illumina amplicon data. *Nat. Methods* 13, 581–583. doi: 10.1038/Nmeth.3869

Cámara, B., de los Ríos, A., del Cura, M. G., Galván, V., and Ascaso, C. (2008). Dolostone bioreceptivity to fungal colonization. *Mater. Construcción* 58, 113–124. doi: 10.3989/mc.2008.v58.i289-290.71

Carson, J. K., Campbell, L., Rooney, D., Clipson, N., and Gleeson, D. B. (2009). Minerals in soil select distinct bacterial communities in their microhabitats. *FEMS Microbiol. Ecol.* 67, 381–388. doi: 10.1111/j.1574-6941.2008.00645.x

Cary, S. C., McDonald, I. R., Barrett, J. E., and Cowan, D. A. (2010). On the rocks: the microbiology of Antarctic Dry Valley soils. *Nat. Rev. Microbiol.* 8, 129–138. doi: 10.1038/nrmicro2281

Chan, Y. K., Lacap, D. C., Lau, M. C. Y., Ha, K. Y., Warren-Rhodes, K. A., Cockell, C. S., et al. (2012). Hypolithic microbial communities: between a rock and a hard place. *Environ. Microbiol.* 14, 2272–2282. doi: 10.1111/j.1462-2920.2012.02821.x

Choe, Y. H., Kim, M., Woo, J., Lee, M. J., Lee, J. I., Lee, E. J., et al. (2018). Comparing rock-inhabiting microbial communities in different rock types from a high arctic polar desert. *FEMS Microbiol. Ecol.* 94, fiy070. doi: 10.1093/femsec/fiy070

Clarke, K. (1993). Non-parametric multivariate analyses of changes in community structure. *Aust. J. Ecol.* 18, 117–143. doi: 10.1111/j.1442-9993.1993.tb00438.x

Clarke, K. R., and Gorley, R. N. (2006). *PRIMER v6: User Manual/tutorial*. Plymouth: PRIMER-E Ltd.

Comeau, A. M., Li, W. K., Tremblay, J. É, Carmack, E. C., and Lovejoy, C. (2011). Arctic Ocean microbial community structure before and after the 2007 record sea ice minimum. *PLoS One* 6:e27492. doi: 10.1371/journal.pone.0027492

Cowan, D. A., Khan, N., Pointing, S. B., and Cary, S. C. (2010). Diverse hypolithic refuge communities in the McMurdo Dry Valleys. *Antarct. Sci.* 22, 714–720. doi: 10.1017/S0954102010000507

Csardi, G., and Nepusz, T. (2006). The igraph software package for complex network research. *InterJ. Complex Syst.* 1695, 1–9.

Csotonyi, J. T., Swiderski, J., Stackebrandt, E., and Yurkov, V. (2010). A new environment for aerobic anoxygenic phototrophic bacteria: biological soil crusts. *Environ. Microbiol. Rep.* 2, 651–656. doi: 10.1111/j.1758-2229.2010.00151.x

De Beeck, M. O., Lievens, B., Busschaert, P., Declerck, S., Vangronsveld, J., and Colpaert, J. V. (2014). Comparison and validation of some ITS primer pairs useful for fungal metabarcoding studies. *PLoS One* 9:e97629. doi: 10.1371/journal.pone.0097629

de la Torre, J. R., Goebel, B. M., Friedmann, E. I, and Pace, N. R. (2003). Microbial diversity of cryptoendolithic communities from the McMurdo Dry Valleys, Antarctica. *Appl. Environ. Microb.* 69, 3858–3867. doi: 10.1128/Aem.69.7.3858-3867.2003

de los Rios, A., Cámara, B., del Cura, M. ÁG., Rico, V. J., Galván, V., and Ascaso, C. (2009). Deteriorating effects of lichen and microbial colonization of carbonate building rocks in the Romanesque churches of Segovia (Spain). *Sci. Total Environ.* 407, 1123–1134. doi: 10.1016/j.scitotenv.2008.09.042

de los Rios, A., Grube, M., Sancho, L. G., and Ascaso, C. (2007). Ultrastructural and genetic characteristics of endolithic cyanobacterial biofilms colonizing Antarctic granite rocks. *FEMS Microbiol. Ecol.* 59, 386–395. doi: 10.1111/j.1574-6941.2006.00256.x

de los Rios, A., Sancho, L. G., Grube, M., Wierzchos, J., and Ascaso, C. (2005). Endolithic growth of two Lecidea lichens in granite from continental Antarctica detected by molecular and microscopy techniques. *New Phytol.* 165, 181–189. doi: 10.1111/j.1469-8137.2004.01199.x

DeBruyn, J. M., Nixon, L. T., Fawaz, M. N., Johnson, A. M., and Radosevich, M. (2011). Global biogeography and quantitative seasonal dynamics of gemmatimonadetes in soil. *Appl. Environ. Microb.* 77, 6295–6300. doi: 10.1128/Aem.05005-11

Deslippe, J. R., Hartmann, M., Simard, S. W., and Mohn, W. W. (2012). Long-term warming alters the composition of Arctic soil microbial communities. *FEMS Microbiol. Ecol.* 82, 303–315. doi: 10.1111/j.1574-6941.2012.01350.x

Dobson, F. (1979). *Lichens, A Field Guide*. Richmond: Kingprint Ltd.

Esposito, A., Ahmed, E., Ciccazzo, S., Sikorski, J., Overmann, J., Holmstrom, S. J. M., et al. (2015). Comparison of rock varnish bacterial communities with surrounding non-varnished rock surfaces: taxon-specific analysis and morphological description. *Microb. Ecol.* 70, 741–750. doi: 10.1007/s00248-015-0617-4

Faluaburu, M. S., Nakai, R., Imura, S., and Naganuma, T. (2019). Phylotypic characterization of mycobionts and photobionts of rock tripe lichen in East Antarctica. *Microorganisms* 7, 203. doi: 10.3390/microorganisms7070203

Favero-Longo, S. E., Gazzano, C., Girlanda, M., Castelli, D., Tretiach, M., Baiocchi, C., et al. (2011). Physical and chemical deterioration of silicate and carbonate rocks by Meristematic Microcolonial fungi and Endolithic lichens (Chaetothyriomycetidae). *Geomicrobiol. J.* 28, 732–744. doi: 10.1080/01490451.2010.517696

Garrido-Benavent, I., Pérez-Ortega, S., Durán, J., Ascaso, C., Pointing, S. B., Rodríguez-Cielos, R., et al. (2020). Differential colonization and succession of microbial communities in rock and soil substrates on a maritime Antarctic Glacier Forefield. *Front. Microbiol.* 11:126. doi: 10.3389/fmicb.2020.00126

Gittel, A., Barta, J., Kohoutova, I., Mikutta, R., Owens, S., Gilbert, J., et al. (2014). Distinct microbial communities associated with buried soils in the Siberian tundra. *ISME J.* 8, 841–853. doi: 10.1038/ismej.2013.219

Guillou, L., Bachar, D., Audic, S., Bass, D., Berney, C., Bittner, L., et al. (2013). The Protist Ribosomal Reference database (PR2): a catalog of unicellular eukaryote Small Sub-Unit rRNA sequences with curated taxonomy. *Nucleic Acids Res.* 41, D597–D604. doi: 10.1093/nar/gks1160

Halda, J. J. (2003). *A taxonomic Study of the Calcicolous Endolitic Species of the Genus Verrucaria (Ascomycotina, Verrucariales) with the Lid-like and Radiately Opening Involucrellum*. Rychnov nad Kněžnou: Muzeum a galerie Orlických hor.

Hansen, E. S., Dawes, P. R., and Thomassen, B. (2006). Epilithic lichen communities in High Arctic Greenland: physical, environmental, and geological aspects of their ecology in Inglefield Land (78 degrees-79 degrees N). *Arct. Antarct. Alp. Res.* 38, 72–81. doi: 10.1657/1523-0430(2006)038[0072:elciha]2.0.co;2

Harder, C. B., Ronn, R., Brejnrod, A., Bass, D., Abu Al-Soud, W., and Ekelund, F. (2016). Local diversity of heathland Cercozoa explored by in-depth sequencing. *ISME J.* 10, 2488–2497. doi: 10.1038/ismej.2016.31

Hoppert, M., Flies, C., Pohl, W., Gunzl, B., and Schneider, J. (2004). Colonization strategies of lithobiontic microorganisms on carbonate rocks. *Environ. Geol.* 46, 421–428. doi: 10.1007/s00254-004-1043-y

Kappen, L. (2000). Some aspects of the great success of lichens in Antarctica. *Antarct. Sci.* 12, 314–324. doi: 10.1017/S0954102000000377

Kastovska, K., Elster, J., Stibal, M., and Santruckova, H. (2005). Microbial assemblages in soil microbial succession after glacial retreat in Svalbard (high Arctic). *Microb. Ecol.* 50, 396–407. doi: 10.1007/s00248-005-0246-4

Khilyas, I. V., Sorokina, A. V., Elistratova, A. A., Markelova, M. I., Siniagina, M. N., Sharipova, M. R., et al. (2019). Microbial diversity and mineral composition of weathered serpentine rock of the Khalilovsky massif. *PLoS One* 14:e0225929. doi: 10.1371/journal.pone.0225929

Kim, M., Cho, A., Lim, H. S., Hong, S. G., Kim, J. H., Lee, J., et al. (2015). Highly heterogeneous soil bacterial communities around Terra Nova Bay of Northern Victoria Land, Antarctica. *PLoS One* 10:e0119966. doi: 10.1371/journal.pone.0119966

Kurtz, H. D., and Netoff, D. I. (2001). Stabilization of friable sandstone surfaces in a desiccating, wind-abraded environment of south-central Utah by rock surface microorganisms. *J. Arid Environ.* 48, 89–100. doi: 10.1006/jare.2000.0743

Kurtz, Z. D., Muller, C. L., Miraldi, E. R., Littman, D. R., Blaser, M. J., and Bonneau, R. A. (2015). Sparse and compositionally robust inference of microbial ecological networks. *PLoS Comput. Biol.* 11:e1004226. doi: 10.1371/journal.pcbi.1004226

Lawrey, J. D., and Diederich, P. (2003). Lichenicolous fungi: Interactions, evolution, and biodiversity. *Bryologist* 106, 80–120. doi: 10.1639/0007-2745(2003)106[0080:lfieab]2.0.co;2

Lee, J., Cho, J., Cho, Y. J., Cho, A., Woo, J., Lee, J., et al. (2019). The latitudinal gradient in rock-inhabiting bacterial community compositions in Victoria Land, Antarctica. *Sci. Total Environ.* 657, 731–738. doi: 10.1016/j.scitotenv.2018.12.073

Lee, K. C., Archer, S. D. J., Boyle, R. H., Lacap-Bugler, D. C., Belnap, J., and Pointing, S. B. (2016). Niche filtering of bacteria in soil and rock habitats of the Colorado Plateau Desert, Utah, USA. *Front. Microbiol.* 7:1489. doi: 10.3389/fmicb.2016.01489

Lehmann, J., Solomon, D., Kinyangi, J., Dathe, L., Wirick, S., and Jacobsen, C. (2008). Spatial complexity of soil organic matter forms at nanometre scales. *Nat. Geosci.* 1, 238–242. doi: 10.1038/ngeo155

Logares, R., Lindstrom, E. S., Langenheder, S., Logue, J. B., Paterson, H., Laybourn-Parry, J., et al. (2013). Biogeography of bacterial communities exposed to progressive long-term environmental change. *ISME J.* 7, 937–948. doi: 10.1038/ismej.2012.168

Louca, S., Polz, M. F., Mazel, F., Albright, M. B., Huber, J. A., O'Connor, M. I., et al. (2018). Function and functional redundancy in microbial systems. *Nat. Ecol. Evol.* 2, 936–943. doi: 10.1038/s41559-018-0519-1

Maier, S., Tamm, A., Wu, D., Caesar, J., Grube, M., and Weber, B. (2018). Photoautotrophic organisms control microbial abundance, diversity, and physiology in different types of biological soil crusts. *ISME J* 12, 1032–1046. doi: 10.1038/s41396-018-0062-8

Malard, L. A., and Pearce, D. A. (2018). Microbial diversity and biogeography in Arctic soils. *Env. Microbiol. Rep.* 10, 611–625. doi: 10.1111/1758-2229.12680

Martin, M. (2011). Cutadapt removes adapter sequences from high-throughput sequencing reads. *EMBnet. J.* 17, 10–12. doi: 10.14806/ej.17.1.200

Martin González, A. M. M., Dalsgaard, B., and Olesen, J. M. (2010). Centrality measures and the importance of generalist species in pollination networks. *Ecol. Complex* 7, 36–43. doi: 10.1016/j.ecocom.2009.03.008

Matthews, J. A., and Owen, G. (2008). Endolithic lichens, rapid biological weathering and schmidt hammer R-values on recently exposed rock surfaces: storbreen glacier Foreland, Jotunheimen, Norway. *Geogr. Ann. A.* 90a, 287–297. doi: 10.1111/j.1468-0459.2008.00346.x

McCann, C. M., Wade, M. J., Gray, N. D., Roberts, J. A., Hubert, C. R. J., and Graham, D. W. (2016). Microbial communities in a high Arctic polar desert landscape. *Front. Microbiol.* 7:419. doi: 10.3389/fmicb.2016.00419

Mccarroll, D., and Viles, H. (1995). Rock-weathering by the lichen Lecidea-Auriculata in an arctic alpine environment. *Earth Surf. Process.* 20, 199–206. doi: 10.1002/esp.3290200302

Meslier, V., Casero, M. C., Dailey, M., Wierzchos, J., Ascaso, C., Artieda, O., et al. (2018). Fundamental drivers for endolithic microbial community assemblies in the hyperarid Atacama Desert. *Environ. Microbiol.* 20, 1765–1781. doi: 10.1111/1462-2920.14106

Molnár, K., and Farkas, E. (2010). Current results on biological activities of lichen secondary metabolites: a review. *Z. Naturforsch. C* 65, 157–173. doi: 10.1515/znc-2010-3-401

Oksanen, J., Blanchet, F., Kindt, R., Legendre, P., Minchin, P., O'hara, R., et al. (2016). *Package Vegan: Community Ecology Package in R*. Available online at: http://cran. ism. ac.jp/web/packages/vegan/ vegan. Pdf/ (accessed October, 2016)

Omelon, C. R. (2008). Endolithic microbial communities in polar desert habitats. *Geomicrobiol. J.* 25, 404–414. doi: 10.1080/01490450802403057

Omelon, C. R., Pollard, W. H., and Ferris, F. G. (2006). Environmental controls on microbial colonization of high Arctic cryptoendolithic habitats. *Polar Biol.* 30, 19–29. doi: 10.1007/s00300-006-0155-0

Omelon, C. R., Pollard, W. H., and Ferris, F. G. (2007). Inorganic species distribution and microbial diversity within high arctic cryptoendolithic habitats. *Microb. Ecol.* 54, 740–752. doi: 10.1007/s00248-007-9235-0

Parada, A. E., Needham, D. M., and Fuhrman, J. A. (2016). Every base matters: assessing small subunit rRNA primers for marine microbiomes with mock communities, time series and global field samples. *Environ. Microbiol.* 18, 1403–1414. doi: 10.1111/1462-2920.13023

Philippot, L., Andersson, S. G. E., Battin, T. J., Prosser, J. I., Schimel, J. P., Whitman, W. B., et al. (2010). The ecological coherence of high bacterial taxonomic ranks. *Nat. Rev. Microbiol.* 8, 523–529. doi: 10.1038/nrmicro2367

Pointing, S. B. (2016). "Hypolithic communities," in *Biological Soil Crusts: An Organizing Principle in Drylands*, eds B. Weber, B. Büdel, and J. Belnap (Berlin: Springer), 199–213. doi: 10.1007/978-3-319-30214-0_11

Pointing, S. B., and Belnap, J. (2012). Microbial colonization and controls in dryland systems. *Nat. Rev. Microbiol.* 10, 551–562. doi: 10.1038/nrmicro2831

Pointing, S. B., Chan, Y. K., Lacap, D. C., Lau, M. C. Y., Jurgens, J. A., and Farrell, R. L. (2009). Highly specialized microbial diversity in hyper-arid polar desert. *Proc. Natl. Acad. Sci. U.S.A.* 106, 19964–19969. doi: 10.1073/pnas.0908274106

Pointing, S. B., Warren-Rhodes, K. A., Lacap, D. C., Rhodes, K. L., and Mckay, C. P. (2007). Hypolithic community shifts occur as a result of liquid water availability along environmental gradients in China's hot and cold hyperarid deserts. *Environ. Microbiol.* 9, 414–424. doi: 10.1111/j.1462-2920.2006.01153.x

Quast, C., Pruesse, E., Yilmaz, P., Gerken, J., Schweer, T., Yarza, P., et al. (2013). The SILVA ribosomal RNA gene database project: improved data processing and web-based tools. *Nucleic Acids Res.* 41, D590–D596. doi: 10.1093/nar/gks1219

Rogers, J. R., and Bennett, P. C. (2004). Mineral stimulation of subsurface microorganisms: release of limiting nutrients from silicates. *Chem. Geol.* 203, 91–108. doi: 10.1016/j.chemgeo.2003.09.001

Schutte, U. M. E., Abdo, Z., Bent, S. J., Williams, C. J., Schneider, G. M., Solheim, B., et al. (2009). Bacterial succession in a glacier foreland of the High Arctic. *ISME J.* 3, 1258–1268. doi: 10.1038/ismej.2009.71

Selbmann, L., de Hoog, G. S., Mazzaglia, A., Friedmann, E. I., and Onofri, S. (2005). Fungi at the edge of life: cryptoendolithic black fungi from Antarctic desert. *Stud. Mycol.* 51, 1–32. doi: 10.1007/978-1-4020-6112-7_40

Seppey, C. V. W., Singer, D., Dumack, K., Fournier, B., Belbahri, L., Mitchell, E. A. D., et al. (2017). Distribution patterns of soil microbial eukaryotes suggests widespread algivory by phagotrophic protists as an alternative pathway for nutrient cycling. *Soil Biol. Biochem.* 112, 68–76. doi: 10.1016/j.soilbio.2017.05.002

Stahl, D. A., and de la Torre, J. R. (2012). Physiology and diversity of ammonia-oxidizing Archaea. *Annu. Rev. Microbiol.* 66, 83–101. doi: 10.1146/annurev-micro-092611-150128

Suzuki, K. I, and Whitman, W. B. (2012). "Class VI. Thermoleophilia class. nov," in *Bergey's Manual of Systematic Bacteriology 5, 2010-2028*, eds M. Goodfellow, P. H.-J. B. Kämpfer, M. E. K.-I. S. Trujillo, W. Ludwig, and W. B. Whitman (New York, NY: Springer).

Tiano, P., Accolla, P., and Tomaselli, L. (1995). Phototrophic Biodeteriogens on Lithoid surfaces – an ecological study. *Microb. Ecol.* 29, 299–309. doi: 10.1007/Bf00164892

Tipton, L., Muller, C. L., Kurtz, Z. D., Huang, L., Kleerup, E., Morris, A., et al. (2018). Fungi stabilize connectivity in the lung and skin microbial ecosystems. *Microbiome* 6, 12. doi: 10.1186/s40168-017-0393-0

Tolotti, M., Cerasino, L., Donati, C., Pindo, M., Rogora, M., Seppi, R., et al. (2020). Alpine headwaters emerging from glaciers and rock glaciers host

different bacterial communities: Ecological implications for the future. *Sci. Total. Environ.* 717, 137101. doi: 10.1016/j.scitotenv.2020.137101

Tully, B. J., Wheat, C. G., Glazer, B. T., and Huber, J. A. (2018). A dynamic microbial community with high functional redundancy inhabits the cold, oxic subseafloor aquifer. *ISME J.* 12, 1–16. doi: 10.1038/ismej.2017.187

Tveit, A., Schwacke, R., Svenning, M. M., and Urich, T. (2013). Organic carbon transformations in high-Arctic peat soils: key functions and microorganisms. *ISME J.* 7, 299–311. doi: 10.1038/ismej.2012.99

Van Goethem, M. W., Makhalanyane, T. P., Valverde, A., Cary, S. C., and Cowan, D. A. (2016). Characterization of bacterial communities in lithobionts and soil niches from Victoria Valley, Antarctica. *FEMS Microbiol. Ecol.* 92, fiw051. doi: 10.1093/femsec/fiw051

Vick-Majors, T. J., Priscu, J. C., and Amaral-Zettler, L. A. (2014). Modular community structure suggests metabolic plasticity during the transition to polar night in ice-covered Antarctic lakes. *ISME J.* 8, 778–789. doi: 10.1038/ismej.2013.190

Walker, J. F., Aldrich-Wolfe, L., Riffel, A., Barbare, H., Simpson, N. B., Trowbridge, J., et al. (2011). Diverse Helotiales associated with the roots of three species of Arctic Ericaceae provide no evidence for host specificity. *New Phytol.* 191, 515–527. doi: 10.1111/j.1469-8137.2011.03703.x

Walker, J. J., and Pace, N. R. (2007). Endolithic microbial ecosystems. *Ann. Rev. Microbiol.* 61, 331–347. doi: 10.1146/annurev.micro.61.080706.093302

Walters, W., Hyde, E. R., Berg-Lyons, D., Ackermann, G., Humphrey, G., Parada, A., et al. (2016). Improved bacterial 16S rRNA gene (V4 and V4-5) and fungal internal transcribed spacer marker gene primers for microbial community surveys. *Msystems* 1, e00009-15. doi: 10.1128/mSystems.00009-15

Warren-Rhodes, K. A., Rhodes, K. L., Pointing, S. B., Ewing, S. A., Lacap, D. C., Gomez-Silva, B., et al. (2006). Hypolithic cyanobacteria, dry limit of photosynthesis, and microbial ecology in the hyperarid Atacama Desert. *Microb. Ecol.* 52, 389–398. doi: 10.1007/s00248-006-9055-7

Wei, S. T. S., Lacap-Bugler, D. C., Lau, M. C. Y., Caruso, T., Rao, S., Rios, A. D. L., et al. (2016). Taxonomic and functional diversity of soil and hypolithic microbial communities in Miers Valley, McMurdo Dry Valleys, Antarctica. *Front. Microbiol.* 7:1642. doi: 10.3389/fmicb.2016.01642

Wierzchos, J., Ascaso, C., and McKay, C. P. (2006). Endolithic cyanobacteria in halite rocks from the hyperarid core of the Atacama Desert. *Astrobiology* 6, 415–422. doi: 10.1089/ast.2006.6.415

Wierzchos, J., Davila, A. F., Artieda, O., Camara-Gallego, B., Rios, A. D., Nealson, K. H., et al. (2013). Ignimbrite as a substrate for endolithic life in the hyperarid Atacama Desert: implications for the search for life on Mars. *Icarus* 224, 334–346. doi: 10.1016/j.icarus.2012.06.009

Wierzchos, J., DiRuggiero, J., Vitek, P., Artieda, O., Souza-Egipsy, V., Skaloud, P., et al. (2015). Adaptation strategies of endolithic chlorophototrophs to survive the hyperarid and extreme solar radiation environment of the Atacama Desert. *Front. Microbiol.* 6:934. doi: 10.3389/fmicb.2015.00934

Wilhelm, R. C., Niederberger, T. D., Greer, C., and Whyte, L. G. (2011). Microbial diversity of active layer and permafrost in an acidic wetland from the Canadian High Arctic. *Can. J. Microbiol.* 57, 303–315. doi: 10.1139/W11-004

Wong, F. K. Y., Lau, M. C. Y., Lacap, D. C., Aitchison, J. C., Cowan, D. A., and Pointing, S. B. (2010). Endolithic microbial colonization of limestone in a high-altitude arid environment. *Microb. Ecol.* 59, 689–699. doi: 10.1007/s00248-009-9607-8

Yergeau, E., Bokhorst, S., Kang, S., Zhou, J., Greer, C. W., Aerts, R., et al. (2012). Shifts in soil microorganisms in response to warming are consistent across a range of Antarctic environments. *ISME J.* 6, 692–702. doi: 10.1038/ismej.2011.124

Yergeau, E., Newsham, K. K., Pearce, D. A., and Kowalchuk, G. A. (2007). Patterns of bacterial diversity across a range of Antarctic terrestrial habitats. *Environ. Microbiol.* 9, 2670–2682. doi: 10.1111/j.1462-2920.2007.01379.x

Young, I. M., Crawford, J. W., Nunan, N., Otten, W., and Spiers, A. (2008). Microbial distribution in soils: physics and scaling. *Adv. Agron.* 100, 81–121. doi: 10.1016/S0065-2113(08)00604-4

Yung, C. C., Chan, Y., Lacap, D. C., Pérez-Ortega, S., de los Ríos-Murillo, A., Lee, C. K., et al. (2014). Characterization of chasmoendolithic community in Miers Valley, McMurdo Dry Valleys, Antarctica. *Microb. Ecol.* 68, 351–359. doi: 10.1007/s00248-014-0412-7

Ziolkowski, L. A., Mykytczuk, N. C. S., Omelon, C. R., Johnson, H., Whyte, L. G., and Slater, G. F. (2013). Arctic gypsum endoliths: a biogeochemical characterization of a viable and active microbial community. *Biogeosciences* 10, 7661–7675. doi: 10.5194/bg-10-7661-2013

Conflict of Interest: The authors declare that the research was conducted in the absence of any commercial or financial relationships that could be construed as a potential conflict of interest.

frontiers in Microbiology

ORIGINAL RESEARCH
published: 11 January 2021
doi: 10.3389/fmicb.2020.616518

Temporal, Spatial, and Temperature Controls on Organic Carbon Mineralization and Methanogenesis in Arctic High-Centered Polygon Soils

Taniya Roy Chowdhury[1†], Erin C. Berns[1], Ji-Won Moon[1†], Baohua Gu[2], Liyuan Liang[2†], Stan D. Wullschleger[2,3] and David E. Graham[1]*

[1] Oak Ridge National Laboratory, Biosciences Division, Oak Ridge, TN, United States, [2] Oak Ridge National Laboratory, Environmental Sciences Division, Oak Ridge, TN, United States, [3] Oak Ridge National Laboratory, Climate Change Science Institute, Oak Ridge, TN, United States

OPEN ACCESS

Edited by:
Laura Zucconi,
University of Tuscia, Italy

Reviewed by:
Jesper Christiansen,
University of Copenhagen, Denmark
Maria Papale,
National Research Council (CNR), Italy

***Correspondence:**
David E. Graham
grahamde@ornl.gov

†Present address:
Taniya Roy Chowdhury,
USDA-Agricultural Research Service, Crops Pathology and Genetics Research Unit, Davis, CA, United States
Ji-Won Moon,
U.S. Geological Survey, National Minerals Information Center, Reston, VA, United States
Liyuan Liang,
Department of Earth and Planetary Science, University of Tennessee Knoxville, Knoxville, TN, United States

Specialty section:
This article was submitted to Extreme Microbiology, a section of the journal Frontiers in Microbiology

Received: 12 October 2020
Accepted: 10 December 2020
Published: 11 January 2021

Citation:
Roy Chowdhury T, Berns EC, Moon J-W, Gu B, Liang L, Wullschleger SD and Graham DE (2021) Temporal, Spatial, and Temperature Controls on Organic Carbon Mineralization and Methanogenesis in Arctic High-Centered Polygon Soils. Front. Microbiol. 11:616518. doi: 10.3389/fmicb.2020.616518

Warming temperatures in continuous permafrost zones of the Arctic will alter both hydrological and geochemical soil conditions, which are strongly linked with heterotrophic microbial carbon (C) cycling. Heterogeneous permafrost landscapes are often dominated by polygonal features formed by expanding ice wedges: water accumulates in low centered polygons (LCPs), and water drains outward to surrounding troughs in high centered polygons (HCPs). These geospatial differences in hydrology cause gradients in biogeochemistry, soil C storage potential, and thermal properties. Presently, data quantifying carbon dioxide (CO_2) and methane (CH_4) release from HCP soils are needed to support modeling and evaluation of warming-induced CO_2 and CH_4 fluxes from tundra soils. This study quantifies the distribution of microbial CO_2 and CH_4 release in HCPs over a range of temperatures and draws comparisons to previous LCP studies. Arctic tundra soils were initially characterized for geochemical and hydraulic properties. Laboratory incubations at −2, +4, and +8°C were used to quantify temporal trends in CO_2 and CH_4 production from homogenized active layer organic and mineral soils in HCP centers and troughs, and methanogen abundance was estimated from *mcrA* gene measurements. Results showed that soil water availability, organic C, and redox conditions influence temporal dynamics and magnitude of gas production from HCP active layer soils during warming. At early incubation times (2–9 days), higher CO_2 emissions were observed from HCP trough soils than from HCP center soils, but increased CO_2 production occurred in center soils at later times (>20 days). HCP center soils did not support methanogenesis, but CH_4-producing trough soils did indicate methanogen presence. Consistent with previous LCP studies, HCP organic soils showed increased CO_2 and CH_4 production with elevated water content, but HCP trough mineral soils produced more CH_4 than LCP mineral soils. HCP mineral soils also

released substantial CO_2 but did not show a strong trend in CO_2 and CH_4 release with water content. Knowledge of temporal and spatial variability in microbial C mineralization rates of Arctic soils in response to warming are key to constraining uncertainties in predictive climate models.

Keywords: anaerobic carbon mineralization, methanogenesis, mcrA, permafrost, Arctic tundra

INTRODUCTION

Arctic warming will transform tundra ecosystems by increasing soil temperatures and active layer depth, lengthening the annual active layer thaw period, and releasing large quantities of soil organic carbon (SOC) (Shaver et al., 1992; Schuur et al., 2009; Waldrop et al., 2010; Yergeau et al., 2010; Mackelprang et al., 2011; Lipson et al., 2013; Olefeldt et al., 2013). These changes could promote microbial degradation of SOC, increasing the flux of carbon dioxide (CO_2) and methane (CH_4) from Arctic soils and accelerating climate warming trends (Tveit et al., 2013; Crowther et al., 2015; Tang et al., 2016; Pries et al., 2017; Jansson and Hofmockel, 2019). Polygonal – or patterned – landscapes, formed by expanding ice wedges, are common in many regions of Arctic tundra and contribute to carbon (C) release during warming. Massive ice wedges form in cracks present in drained, interstitial tundra and give rise to low centered polygons (LCPs), which are typically characterized by water-saturated centers surrounded by elevated rims and outlying troughs. As ice wedges degrade, drier high centered polygons (HCPs) are formed, which drain water outward to surrounding troughs (**Figure 1**). Utqiagvik (formerly Barrow), Alaska is located in a region dominated by thaw lakes and polygonal tundra. LCP centers, rims, and troughs make up approximately 24% of the tundra (Billings and Peterson, 1980; Hinkel and Nelson, 2003; Walker et al., 2008), whereas HCP centers and troughs comprise 11% (Lara et al., 2015; Liljedahl et al., 2016). To effectively model and evaluate warming-induced CO_2 and CH_4 fluxes from tundra soils in regions like Utqiagvik, data quantifying CO_2 and CH_4 release from both LCP and HCP soils are needed. Controlled laboratory incubation studies are routinely used to identify the key drivers of gas emission patterns and the role of microbial properties like gene abundance, that in turn can inform model parameterization (Evans and Wallenstein, 2014; Faucherre et al., 2018; Philben et al., 2020a).

The microtopographic variability of polygonal landscapes controls hydrological heterogeneities, which have been shown to correlate with differences in pH, dissolved oxygen (DO), ferrous iron [Fe(II)], nutrients, and microbial activity (Fiedler et al., 2004; Preuss et al., 2013; Herndon et al., 2015, 2020; Lipson et al., 2015; Newman et al., 2015; Taş et al., 2018; Wu et al., 2018). These biogeochemical gradients across LCPs and HCPs may control the nature and magnitude of C flux from Arctic soils. Previous research has shown variability in CO_2 and CH_4 release across HCPs and LCPs and their associated microtopographies (trough, rim, and center) (Lipson et al., 2012; Roy Chowdhury et al., 2015; Wainwright et al., 2015; Grant et al., 2017; Taş et al., 2018), and some studies have begun to develop relationships between hydrological and biogeochemical controls on CO_2 and CH_4 release from these different environments (Yang et al., 2016; Lara et al., 2019; Philben et al., 2020b). Flux measurements from Arctic tundra have shown that both LCPs and HCPs release CO_2, and that LCPs tend to release more CH_4 (often with more measurement variability) than HCPs (Wainwright et al., 2015; Vaughn et al., 2016; Arora et al., 2019). Due to their higher water content and more effective thermal insulation during cold season transitions, LCPs have been extensively studied to evaluate trends in CO_2 and CH_4 release (Zona et al., 2011; Roy Chowdhury et al., 2015; Tang et al., 2016). Though HCPs cover less area and may release less CO_2 and CH_4 than LCPs during warming (Morrissey and Livingston, 1992; Sachs et al., 2010; Wainwright et al., 2015; Vaughn et al., 2016), quantitative data for CO_2 and CH_4 release from HCPs is necessary to inform microbial SOC mineralization rates across tundra microtopographies in predictive climate models (Wang et al., 2019; Zheng et al., 2019). The purpose of the present study is to fill a data gap concerning the magnitude, rate, and temporal and spatial variability of warming-induced microbial SOC mineralization across HCP microtopographies and associated gradients in hydrology, and make comparisons to trends observed with LCPs.

The present study considers the biogeochemical and hydrological gradients across HCP microtopographies (troughs and centers) along a soil profile (from organic to mineral soils in the active layer), and quantifies temporal trends in C release. Our research questions include: (1) will all HCP soils – trough, center, organic, and mineral – release more CO_2 and CH_4 at elevated temperatures? (2) will the rates, magnitude, and composition of CO_2 and CH_4 release from HCP soils depend on hydraulic or geochemical factors, or both? and (3) will differences in HCP soil hydrological and thermal regimes, associated with HCP microtopographies, regulate methanogen abundance and thus CH_4 release?

These questions were evaluated using soil incubations from cores obtained from the Barrow Environmental Observatory (BEO). First, the geochemical and hydraulic properties of HCP soils were characterized to assign soil types as either organic or mineral. Then soils were incubated at three temperatures to evaluate changes in the rate and magnitudes of CO_2 and CH_4 release. DNA extracted from the soils was evaluated for presence of *mcrA* genes and used to interpret CH_4 release trends. Relationships between CO_2 and CH_4 release, hydraulic, and geochemical properties, and methanogen population across microtopographies and soil types were then assessed. Finally, CO_2 and CH_4 release, methanogen abundance, and water retention from HCPs were compared to LCP soil incubation results from Roy Chowdhury et al. (2015). The results from this

study provide process understanding to field-scale observations of CO_2 and CH_4 fluxes in the Arctic (Sturtevant et al., 2012; Vaughn et al., 2016; Zona et al., 2016; Raz-Yaseef et al., 2017). Relative rates of gas production from these incubations complement separate field measurements to inform parameterization of Earth systems models for Arctic ecosystems (Riley et al., 2011; Burrows et al., 2020).

MATERIALS AND METHODS

Site Description, Soil Processing, and Soil Analysis

The study site is located in the BEO in Utqiagvik, Alaska at the intensive study site B of the Next-Generation Ecosystem Experiments (NGEE) in the Arctic project (formerly Zone 1, as presented by Hubbard et al. (2013)). Located in the Arctic coastal tundra ecoregion, the site is dominated by thaw lakes and ice wedge polygons overlying continuous permafrost (Lara et al., 2015; Wainwright et al., 2015). At this site, the HCP included two microtopographic features as depicted in **Figure 1**: a drained, elevated center and a trough that is frequently water saturated (HCP photo, **Supplementary Figure S1A**). Subsurface temperatures from 2013 to 2014 at the NGEE Barrow site B varied seasonally from −18 to −1°C at 1 m below the surface[1]. Temperatures at the HCP center (0 – 25 cm) closely followed changes in air temperatures, while HCP trough temperatures varied less than the air temperature.

The core collection, soil processing, and microcosm construction methods were described previously (Roy Chowdhury et al., 2015; Yang et al., 2016). In brief, intact frozen soil cores (8.3 cm diameter) were collected in April of 2012 and 2013 using a hydraulic drill to a depth of ∼80 cm. Sample locations included the HCP center (cores NGADG0043 and NGADG0020) at N 71° 16.7583′, W 156° 36.2729′ and N 71° 16.7586′, W 156° 36.2772′, as well as the HCP trough (core NGADG0048) at N 71° 16.7576′, W 156° 36.2846′. After frozen cores were transported to Oak Ridge, TN, United States they were stored at −20°C prior to processing.

Soil cores were removed from their sterile liners and processed inside a vinyl anaerobic chamber with a N_2 atmosphere containing at least 1.0% H_2 and less than 1 ppm O_2. A multi-purpose oscillating power tool with sterilized cutting blades was used for all sediment processing and homogenization in autoclaved containers kept on ice packs. Soil cores from each site were divided into 10 cm vertical increments, which were characterized for gravimetric water content (θ_g), pH, and Fe(II). Fe(II) was used as an indication of redox conditions in the soil. The Fe(II) measurements are exchangeable Fe(II), extracted with 2 M KCl (1:5, w:v) by shaking for 1 h under anoxic conditions, and then filtering through 0.2 μm nylon syringe filters. Water content was determined by oven drying at 105°C for 24 h, pH using a 1:5 or 1:10 (soil weight: 2 M KCl volume) ratio, and Fe(II) with a 1,10-phenanothroline assay. Detailed methods were presented in Roy Chowdhury et al. (2015). Munsell color was documented, and soil horizons were determined per United States Department of Agriculture taxonomy.

Replicate incubations were made possible by homogenizing core depth increments with similar geochemistry in a vinyl anaerobic chamber. The depth increments were designated by soil type: organic (Oi, Oe, and Oa horizons), mineral (E and B horizons), or permafrost/ground ice (**Table 1**). The homogenized depth increments for microcosm incubations are as follows: HCP center organic (10–20 cm), HCP center mineral (20–50 cm), HCP trough organic (10–30 cm), and HCP trough mineral (30–50 cm). Frozen soils were homogenized using an oscillating power tool, and gravels and coarse roots were removed. This method does not affect the soil microaggregate structure or expose the samples to oxidation, drying or significant warming that could disrupt anaerobic microbial processes. Minimal oxidation occurred during this process due to handling in the anaerobic chamber. These methods are complementary to other studies that utilized less disturbed soil cubes which have more heterogeneity such as the approach of Biasi et al. (2005). Core sections from 0 to 10 cm were excluded to focus on soil processes that are not dominated by plant litter decomposition, which has been studied in many ecosystems (Hobbie and Gough, 2004; Voigt et al., 2019). Total C (TC) and nitrogen (TN) were then determined with a TruSpec CN elemental analyzer (LECO Corporation, St. Joseph, MI, United States). All measurements were conducted in triplicates and data are presented as mean ± standard deviation (**Table 1**). Soil preparation and experimental design are summarized in **Supplementary Figure S2**. Separate cores used for water potential measurements were also characterized in 10–cm increments (**Supplementary Table S2**) and additionally evaluated for soil texture (by hydrometer with 0.5% sodium hexametaphosphate solution) and mineralogy with X-ray diffraction (XRD) using an X'pert PRO (PANalytical, Natick, MA, United States) with Mo-Kα radiation at 55kV/40 mA, 5 – 35^o 2θ with 1.5^o 2θ min^{-1} scanning rate.

Soil Water Potential Analysis

Soil Water Potential Measurements

Soil water potential measurements were conducted to evaluate the water retention properties of the HCP center soils collected from BEO. These measurements and parameterized models give insight into how soil water content responds to changing hydrological conditions and future trends in water availability. HCP center soils were measured for soil water potential because it was assumed that the center soils would be more sensitive to water availability dynamics than the saturated trough soils. Two complementary systems (METER Group, Pullman, WA, United States) were employed to measure soil water potential for HCP center soils (NGADG0020) during drying: the tensiometer based HYPROP system measured matric potential (Ψ_m) for wet-end water potential, and the vapor pressure-based WP4C system measured a combination of Ψ_m and osmotic potential (Ψ_o) for dry-end water potentials. Electrical conductivity (EC)

[1]http://lapland.gi.alaska.edu/vdv/vdv_historical.php

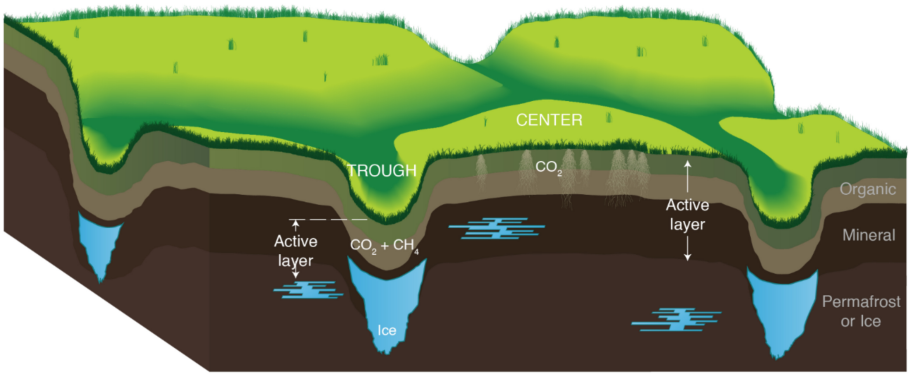

FIGURE 1 | Conceptual illustration of the soil profile in high-center polygon (HCP) troughs and centers. Melting ice wedges (blue) cause the trough areas to subside, promoting drainage from the centers that saturates the troughs. The organic and mineral soil layers comprise the active layer, which thaws annually to the top of the permafrost (horizons noted on the right side of figure). Locations of CO_2 and CH_4 production are also indicated. The lateral scale of the polygons is much larger than the exaggerated vertical scale.

TABLE 1 | Soil characteristics of high-center polygon (HCP) center and trough cores.

Micro-topography	Description		Depth (cm)	Soil horizon	Munsell color	Water * content (θg) g g^{-1} dwt.	pH_{KCl}* 1:5, w:v	Total C (%)	C/N
HCP Center	High root density		0–10	O	10YR 4/4	0.72	4.11	n/a*	n/a*
			10–20	O	10YR 4/4	0.44	3.84	20.49	20
	Dry crumbly, no structure		20–30	B	10YR 3/4	0.42	3.76	17.1	21
			30–40	B	10YR 3/4	0.99	4.89	17.1	21
		--	40–50	B	10YR 3/4	1.38	4.98	17.1	21
			50–60	ice		n/a*			
			60–70	ice		n/a*			
HCP trough	Roots, mottled, red/ox micro-regions		0–10	O	10YR 2/2, 10YR 5/4	6.47	5.57	n/a*	n/a*
			10–20	O	10YR 2/2, 10YR 5/4	3.31	5.03	31.01	20
			20–30	O	10YR 2/2, 10YR 5/4	1.09	5.08	31.01	20
	Increased OM		30–40	E	2.5Y 2/2	0.79	5.12	17.26	21
	Reduced	--	40–50	E/Bh	2.5Y 2/2	1.96	5.49	17.26	21
			50–60	ice		n/a*			

Depths determined to be plant material or litter, organic layer, mineral layer, and ice are indicated by the blue, red, green, and gray sections of the color bar, respectively. Black dashed lines within the color bar indicate the approximate depth of the active layer – permafrost boundary as determined by maximum thaw depths measured in September 2012.

**Values are an average of duplicate measurements.*

measurements (Orion 011010 cell, and Orion 115A+ meter) were used to adjust WP4C measurements to Ψ_m, allowing evaluation of Ψ_m over the full range of water contents (EC measurements at different soil: DI water ratios are presented in **Supplementary Table S2**). The HCP center core used for water potential measurements had slightly different depth increments associated with the soil horizons than the homogenized depths for the microcosm incubations. Depth increments for the water potential core were as follows: organic (0–10 cm and 10–20 cm), mineral (20–35 cm) with an organic rich zone at 35 cm, organic/mineral transition (35–50 cm) with indication of thaw depth at 45 cm, mineral/organic (50–65 cm), and ice (65–80 cm).

Soil core sections (at least 250 mL soil volume) were thawed and introduced to the sample rings (5 cm height by 8 cm I.D.) for HYPROP measurements (**Supplementary Figure S3**). Sample preparation and generation of the soil drying curve was conducted according to the manufacturer's instructions. To account for insufficient sample volume, some HCP core sections (thawed soils from organic horizons, 0–10 cm and 10–20 cm) had to be analyzed using a reduced sample volume by adding several layers of silicon gaskets. Upper and lower tensiometers measured changes in soil water tension during drying, and the Ψ_m and hydraulic gradient were calculated. During the HYPROP measurement, changes in mass were also recorded, allowing calculation of volumetric water content (θ_v). After the air entry pressure was reached, subsamples from the HYPROP sample ring were taken from the top, middle, and bottom of the device for WP4C measurements. Additional WP4C measurements utilized air-dried samples from frozen cores.

Samples lacking enough mass for WP4C measurements – namely the HCP core section from 10 to 20 cm – utilized oven-dried samples that were re-wetted. Wet end water potentials at higher θ_v were determined using the HYPROP instrument, and the dry end measurements were measured with the WP4C to produce the soil water retention curves (SWRCs), or soil water characteristic curves, which relate soil water content to soil water potential.

Soil Water Potential Hydraulic Modeling

Integrated water potential data from both systems were fit with five different models that are supported by the HYPROP-FIT software (version 3.0, Decagon), as described in the **Supplementary Material**. Model fit parameters were checked by statistical analysis of the root-mean-square error (RMSE) values of both water content data and log of conductivities and corrected Akaike Information Criterion (AICc). While five different models were evaluated, comparison of water potentials across different depth increments were made with the van Genuchten-Maulem model (Van Genuchten, 1980) (Eq. 1) because it provided the best fit for the majority of the soil depths.

$$\theta_v(\psi) = \theta_r + \frac{\theta_s - \theta_r}{\left(1 + (\alpha|\psi_m|)^n\right)^{1-1/n}} \quad (1)$$

The volumetric water content (θ_v) is presented as a function of water matric potential (Ψ_m). Fitting parameters for this study include the residual water content (θ_r), saturated water content (θ_s), and two shape parameters α and n, which represent the inverse of the air entry pressure and the soil pore size distribution, respectively.

Incubation Experiments and Gas Analyses

Microcosm experiments were conducted in triplicate to evaluate temporal trends in the rate and magnitude of potential CO_2 and CH_4 production across soil horizons and microtopographies of HCPs at representative elevated temperatures (**Supplementary Figure S2**). Wheaton serum vials (60 mL) were filled with 15 ± 0.05 g of wet soils from organic or mineral horizons of the HCP center (NGADG0043) and trough (NGADG0048), and crimp sealed with blue butyl rubber stoppers. Replicates were from the same homogenized section of soil in the same core. Based on the soil redox condition as informed by the Fe(II) concentrations, microcosms constructed from HCP trough organic and mineral horizon soils were incubated under anoxic conditions through purging the headspace with N_2. Mineral horizon soils from the HCP center were also incubated under anoxic conditions. The low concentrations of Fe(II) in the organic horizon of the HCP center (0 – 25 cm) indicated oxic conditions [Fe(II) data presented in Results section], and these microcosms were consequently incubated under an initial headspace of atmospheric oxygen to simulate *in situ* conditions. Headspace oxygen concentrations were monitored over time in a subset of these oxic samples (data not shown). Temperatures chosen for the incubations (−2, +4, and +8°C) were informed by the approximate thaw temperature of permafrost soils (−2°C) and the approximate maximum temperatures measured at 10 cm (+8°C) and 20 cm (+4°C) depths in HCP trough and center soils in Barrow during the summer of 2013[2]. Due to thermal gradients in the active layer, mineral soils below 20 cm depth are unlikely to experience temperatures as high as +8°C; mineral soil incubations at this temperature were conducted for comparison to organic soils, and implications of this comparison are noted in the discussion. Microcosms were destructively sampled after 0, 30, and either 60 or 75 days of incubation for analyses of pH and Fe(II) and for DNA extraction. The final sampling point (60 or 75 days) depended on the rates of CO_2 or CH_4 production. The total number of microcosms constructed from HCP samples was 108: 2 microtopographic features (center and trough) × 2 soil horizons (organic and mineral) × 3 temperatures (−2, +4, and +8°C) × 3 time points (0, 30, and either 60 or 75 days) × 3 replicates.

Headspace CO_2 and CH_4 concentrations during incubations were analyzed every other day for 10 days and, thereafter, every 5 days for up to 60 days. Gases were measured using a gas chromatograph equipped with a methanizer and flame ionization detector by injecting 0.5 mL of headspace into the GC inlet. Headspace pressure remained approximately 1 atm during incubation experiments, and adjustments for pressure changes were not made due to sampling of a small headspace volume. Total gas concentrations were reported as μmol g^{-1} dry weight (dwt.) soil and include dissolved gas concentrations, calculated as reported previously (Roy Chowdhury et al., 2015). Headspace O_2 concentrations were monitored for microcosms from the HCP center using a SRI 8610C gas chromatograph with a 10-port gas sampling valve, argon carrier gas, 30-foot HayeSep DB 100–120 mesh column, and a thermal conductivity detector.

Concentrations (μmol g-dwt^{-1} soil) of CO_2 and CH_4 produced over time were fit with either hyperbolic, sigmoidal, or exponential response curves. Equations utilized for the fitting are presented in the captions of **Supplementary Tables S4, S5**, and are explained in detail in Roy Chowdhury et al. (2015). Rates of gas production were calculated using first derivatives of the best response curve-fitting equation at all time points to represent the changing rates of CO_2 and CH_4 production over time. While measurements of CO_2 and CH_4 release in incubations are valuable to improve understanding of relevant biogeochemical processes that occur in Arctic soils, it is important to integrate understanding developed from incubations with other experimental approaches and field scale flux measurements to effectively parameterize soil biogeochemical models. Rates presented from homogenized incubations in this study give insight into the relative importance of processes across microtopographies and soil types but are not a direct indication of net fluxes at the soil surface in the field.

DNA Extraction and Quantitative PCR (*q*PCR) Amplification of *mcrA* Gene

Gene copies of methyl coenzyme reductase M α subunit, *mcrA*, were used to determine the presence of methanogens and further interpret CH_4 production observed in the microcosms.

[2]http://lapland.gi.alaska.edu/vdv/vdv.php/historical/59

DNA was extracted from subsamples of homogenized frozen bulk soil (pre-incubation) and microcosms incubated at −2, 4, and 8°C (after 30 and either 60 or 75 days of incubation). The total DNA was extracted from 0.25 g of wet soil using the PowerLyzer PowerSoil DNA Isolation Kit (MoBio Laboratories) according to the manufacturer's protocol. DNA quality were assessed (Nanodrop2000, Thermo Scientific) and concentrations determined by Qubit 3.0 Fluorometer (Life Technologies) using the Qubit dsDNA High Sensitivity Assay Kit (Invitrogen). Soil samples containing high concentrations of organic matter and humic acids generally resulted in low purity DNA ($A_{260}/A_{280} < 1.5$). These samples were further purified using the Wizard DNA Clean-Up System (Promega) following the manufacturer's protocol with sample recovery ranging from 70 to 98% yield. Only samples with high-purity DNA ($A_{260}/A_{280} > 1.7$) were used for downstream applications. Triplicate DNA extractions were performed, and samples were frozen at −20°C until quantitative PCR (*q*PCR) analysis.

The *q*PCR was performed with primers *mlas* (5′ GGT GGT GTM GGD TTC ACM CAR TA) and *mcrA-rev* (5′ CGT TCA TBG CGT AGT TVG GRT AGT) using the non-specific fluorophore iQ SYBR Green SuperMix (BioRad Laboratories Inc.) (Luton et al., 2002). All *q*PCR assays were performed using a Bio-Rad iCycler per the method described in **Supplementary Table S1**. Reaction mixtures contained 19 μL of the master mix and 1 μL of template DNA per reaction. Triplicates of no-template controls, containing diethylpyrocarbonate (DEPC)-treated water were included in each run. In preliminary experiments the annealing temperatures of all reactions were optimized for high-specificity and high yield when amplifying the samples. After each *q*PCR run, melt curve analysis to verify the presence of the desired amplicon was performed by increasing the temperature from 60°C to 95°C in 0.5°C increments every 5 s.

The concentration of *mcrA* gene (C_{target} [copies μL^{-1}]) in the DNA standard, *Methanococcus maripaludis* C5 genomic DNA, was calculated from the DNA concentration (C_{DNA}[ng μL^{-1}] = 6.1 of the standard), the length of the DNA standard (l_{DNA}[bp] = 1,661,137), the number of targets per DNA fragment (n_{target}[copies] = 1 *mcrA* copy per genome), Avogadro's number (N_A) (6.022×10^{23} bp mol^{-1}), and the average molar mass of a double-stranded base pair (M_{bp} = 660 g mol^{-1}) using Eq. 2 (Brankatschk et al., 2012). The C_{target} value for *M. maripaludis* C5 was 3.3×10^6 *mcrA* copies μL^{-1}.

$$C_{target} = n_{target} \times \frac{C_{DNA} \times N_A}{l_{DNA} \times M_{bp}} \quad (2)$$

Two separate strategies were employed to estimate the efficiency (E) of *q*PCR amplification of soil DNA samples based on the number of cycles necessary to reach the threshold fluorescence values (C_T). These methods estimated either the efficiency from a standard dilution series (E_{ds}) or the efficiency based on fluorescence increase (E_{fi}) for each sample, as described below.

The first approach was the frequently used standard curve (SC) method of absolute quantification wherein the linear regression of $\log(N_{0standard})$ versus C_T gives the intercept a and slope b of the standard curve (Eq. 3). The number of copies in the sample, $N_{0sample}$, can be calculated based on the linear regression of a 10-fold dilution series (*ds*) of the standard. Using this method, the limit of quantitation of *mcrA* gene concentration was estimated to be 10^2 copies μL^{-1} (C_T = 29, C.V. = 0.011). The slope b of the linear regression ($r^2 > 0.999$) was used to estimate the efficiency from dilution series, E_{ds} (Eq. 4).

$$C_{T\ sample} = a + b \times log(N_{0\ standard}) \quad (3)$$

$$E_{ds} = 10^{\left(\frac{1}{b}\right)} \quad (4)$$

Using this method, the PCR amplification efficiency for all runs was determined at 98 – 101% (E_{ds} = 1.98 to 2.01). This method assumes E_{ds} of the sample is the same as that of the standard, thus introducing the possibility of increased quantification errors.

Raw fluorescence data were exported from the Bio-Rad iCycler system and imported into the LinRegPCR program (version 2014.1) (Ruijter et al., 2009). In the program settings, all samples in one *q*PCR run were treated as one amplicon to set a common window of linearity ($r^2 > 0.999$). Subsequently, the program automatically determined the fluorescence threshold for all samples and calculated the individual C_T and efficiencies based on the fluorescence increase, E_{fi} (Ruijter et al., 2009). The results were exported, and the mean E_{fi} of each sample was calculated as the arithmetic mean of all replicates. The range of PCR amplification efficiency for individual *q*PCR reactions using this method ranged from 70 to 104% (E_{fi} = 1.73 to 2.04). This broad range demonstrates the variability of *q*PCR efficiency, in other words in amplification quality, with template source (e.g., organic vs. mineral soils). The sub-optimum efficiency reported here may be due to the degenerate primers used to account for the *mcrA* sequence variability within the methanogen lineage, or the presence of inhibitors that can affect annealing kinetics and the accuracy of the *q*PCR assay. We used this method to obtain the C_T values for samples based on the linear increase of fluorescence to account for template-related variability of E by correcting for differences in E between the samples and standard (Brankatschk et al., 2012).

Statistical Analyses

Descriptive statistics utilized for data analysis were computed in Origin Pro (version 8.6, Origin Lab). Mean comparisons were performed using Tukey's honest significant difference *post hoc* test or the non-parametric Kolmogorov-Smirnov Test. Data are presented as mean ± standard error unless otherwise noted. Analysis of variance used Welch's *t*-test and most statistical tests were done using the R statistical programming language (R Core Team, version 3.0.3). Non-linear regressions were performed using curve-fitting routines in Prism (version 8.4.3, GraphPad Software) as described previously (Roy Chowdhury et al., 2015).

RESULTS

Geochemical Characteristics of Intact HCP Cores

Key soil characteristics of the HCP cores obtained from the center and trough were measured in 10 -cm increments along the vertical profiles. The results for the cores used in the incubation experiments are summarized in **Table 1**. Both center and trough cores had high contents of undegraded roots to depths of ∼10 cm, underlain by a composite of intermediately to completely degraded organic matter. The organic horizon ranged from ∼10–20 cm in the center core and from ∼10–30 cm in the trough core, indicating a deeper organic horizon in the HCP trough. Organic horizons for both center and trough cores were underlain by the mineral horizon (E and B). The HCP center core showed an extended gradient from organic to mineral horizon across depth increments of 20–40 cm. Tile probe measurements from the same HCP, obtained in a September 2012 field campaign (when the active layer was completely thawed), determined thaw depths of 40 cm in the trough and 45 cm in the center, indicating the approximate extent of the active layer, which was comparable to other reports (Wainwright et al., 2015). Permafrost in both cores was mainly ground ice. XRD data from the HCP center showed that all depths were dominated by quartz minerals with additional peaks representing albite, illite, and kaolinite (**Supplementary Figure S4**), expanding upon previous descriptions (Black, 1964). No inorganic carbonate minerals were observed in the XRD patterns, indicating that carbonate mineral precipitation was absent in the HCP center soil. The lack of inorganic carbonate minerals was expected based on the relatively low pH measured in these soils (**Table 1**). Soil textures in the HCP center were predominantly clay loam and silt loam with sandy clay in some sections (**Supplementary Table S2**).

The gravimetric water contents (θ_g) of HCP soils increased with depth from the organic to mineral soils and were highest near the active layer-permafrost boundary. Based on volumetric water contents and soil water release measurements presented below, the HCP center active layer soils were saturated in the frozen cores. In the HCP trough, θ_g decreased with depth from the organic to mineral soils, and then increased at the active layer–permafrost transition. Profiles of θ_g variation with depth are presented in **Supplementary Figure S1**. The HCP trough showed greater variation in water content across the core profile (0.79 g g-dwt.$^{-1}$ to 6.47 g g-dwt.$^{-1}$ than the HCP center (0.42 g g-dwt.$^{-1}$ to 1.38 g g-dwt^{-1}). The organic horizon in the HCP trough had high θ_g, with evidence of gleying, and high organic content (31% total C). The mineral layer of the HCP trough (17% total C) was very dark brown (Munsell 2.5Y 2/2) at depths of approximately 30 cm with visual characteristics of hydric soil. Both the center and trough of the HCP were underlain by ground ice with low mineral content. Although the C:N ratios in the active layers did not differ significantly between the center and trough, the trough had a higher % C in the organic soils indicating that there was also a higher nitrogen concentration in the trough organic soil as compared to the center organic soil. While all soil horizons had very high organic C, the trend in organic C concentration from high to low was trough organic > center organic > trough mineral ≈ center mineral.

The extractable Fe(II) concentrations indicated a transition in redox conditions over the HCP polygon that corresponded with increasing water content. Fe(II) concentrations are plotted with depth for center and trough cores in **Figure 2**. The HCP center organic soil had minimal extractable Fe(II), indicating oxic conditions, and the mineral soils from 40 to 50 cm had Fe(II) at 42 ± 4 μmol g-dwt.$^{-1}$ Fe(II) (**Figure 2A**). Trough organic soils had even higher Fe(II) at 70 ± 15 μmol g-dwt.$^{-1}$, a very significant increase from the undetectable Fe(II) in the HCP center organic soils. Decreases in Fe(II) were observed with increasing depth from the HCP trough organic to mineral soils (**Figure 2B**). The high Fe(II) concentration observed in the HCP trough organic samples aligned with elevated θ_g,

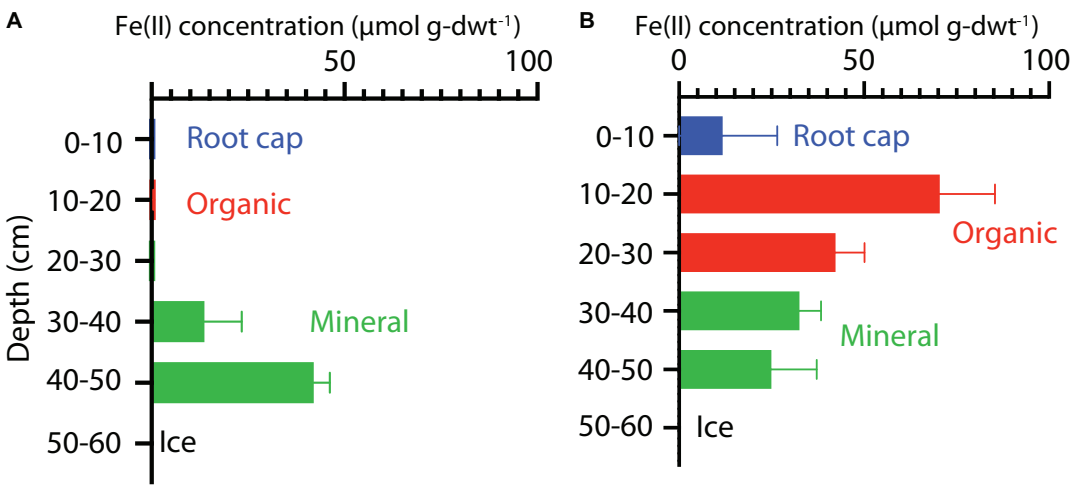

FIGURE 2 | Vertical profiles of extractable Fe(II) concentrations in soil cores from HCP center **(A)** and trough **(B)**. Bars represent data from triplicate measurements with error bars showing the standard deviations. Colors indicate the different soil layers.

indicating that the saturated organic horizon of the trough was more anoxic than the drier organic horizon in the HCP center. Trends in Fe(II) concentrations mirrored the general trends in θ_g across microtopographies and horizons, highlighting the positive relationship between Fe(II) and θ_g. However, the high volumetric water content of the HCP center organic soils with low concentrations of extractable Fe(II) demonstrates that the water content does not always indicate anoxic conditions. Overall, the Fe(II) data demonstrates a gradient from more oxidized to more reduced conditions across the relatively oxic/sub-oxic surface layers in the HCP center to the anoxic HCP trough.

Higher Fe(II) concentrations were also generally associated with higher pH. HCP trough samples had significantly higher pH than the HCP center samples ($p < 0.05$, two-tailed paired *t*-test), with the pH of the trough and center samples across all depths averaging 5.26 and 4.32, respectively. Lower pH in shallower HCP center soils (**Table 1**) may represent acidity produced during oxidation of Fe(II) and precipitation of Fe(III) oxide/hydroxides or anaerobic SOC decomposition. The lower pH in HCP center soils could also be related to decreased buffering capacity associated with lower cation concentrations in HCP center soils (Newman et al., 2015).

Soil Water Potential and Hydraulic Modeling

Soil water potential indicates how tightly water is held in a soil matrix. Measurements of soil water potential were conducted using an additional HCP center core and were used to interpret the water retention capacity of the soil (Moon and Graham, 2017). The water retention of tundra soils may have important implications for future trends in SOC mineralization, which are discussed in Section "Carbon Release From HCPs May be Associated With Higher Water Content and Total C." Soils from the HCP center were evaluated because they are expected to have more dynamic wetting and drying cycles than the mostly saturated HCP trough. Soil properties for the additional core were determined using the same techniques as the microcosm incubation cores and are presented in **Supplementary Table S2**. Electrical conductivity (EC) was also determined at different dilutions before collecting water potential data (**Supplementary Table S2**).

Properties Used for the HYPROP and WP4C Soil Water Measurement

The HCP center core used for water potential measurements (NGADG0020) had pH ranges (3.88 – 4.46) comparable to the core used for microcosm incubations (3.76 – 4.89). Total C between cores was also similar: the water potential core had 11–19% (**Supplementary Table S2**) total C and the microcosm core had ∼17–20% total C (**Table 1**). Well-decomposed organic layers in the 35–50 and 65–80 cm sections were also observed. The EC values for the HCP core exhibited a proportional dilution effect with increased water to soil ratio for most depth increments, however, the 30–50 cm and 65–80 cm sections from HCP showed similar or higher EC values with increased water volume (**Supplementary Table S2**). HCP center core depths that did not have proportional dilution for EC also had higher gravimetric water contents.

Model Fitting to Determine Retention and Conductivity Function Parameters

Water potential measurements across different soil depths were used to develop SWRCs and the data was fit with the van Genuchten model (**Figure 3**). Solid lines associated with data points in **Figure 3** are the best fit SWRCs for three selected soil depths. Fitting parameters are presented in **Supplementary Table S3**, and additional representations in terms of hydraulic conductivity are included in **Supplementary Figure S7**. All soil depths from the HCP center core had higher saturated water contents (θ_{sat}) than a common silt loam (tan line in **Figure 3**), but lower θ_{sat} than typical sphagnum peat soil. Saturated water contents determined from HCP soil model fitting (θ_s in **Supplementary Table S3**) were similar in the different soil sections (∼60–65%), except for the 50–65 cm and 65–80 cm depths which were greater (81 and 74%, respectively). These higher saturated water contents are likely due to particularly

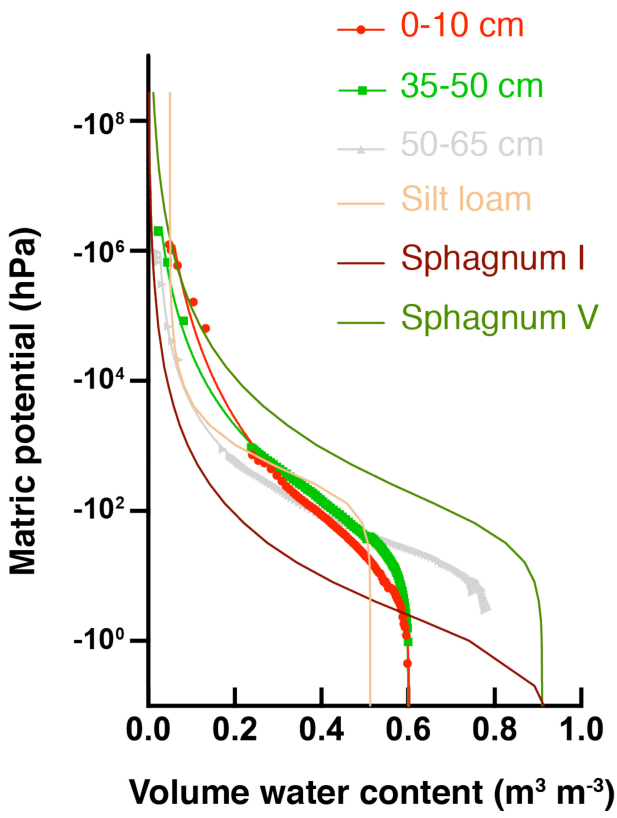

FIGURE 3 | Soil water retention curves (SWRCs) for HCP center at different soil depths (red circles = organic, green squares = mineral, and gray triangles = permafrost). Parameters for reference curves for peat soils are from Liu and Lennartz (2019): group I sphagnum had a low bulk density (BD), while group V had a relatively high bulk density. Parameters for silt loam are from Or et al. (2012). Saturated water contents (θ_{sat}) are the volumetric water content (θ_v) at the highest Ψ_m.

high porosity resulting from ice formation near the active layer – permafrost boundary.

Macroporosity of soils can be estimated from the percent pore volume extracted (beginning with saturation) under a fixed value of Ψ_m (Beven and Germann, 1982). For the present analysis, –10 hPa Ψ_m was used to evaluate macroporosity (**Supplementary Figure S8**). The macroporosity for the deepest soil layer, 65–80 cm, was quite high (35%), consistent with the interpretation that ice formed large pores at this depth. The macroporosity of the 0–10 cm depth was 13%, which is still high relative to high bulk density (BD) sphagnum soils (2.6%). Water drains quickly through larger pores in HCP center soils, but active layer organic soils (depths of 0–10 cm and 10–20 cm) show that they will retain more water under continued drying than thawed permafrost soils (depths of 50–65 cm and 65–80 cm), as indicated by the higher θ_v at lower Ψ_m for organic soils.

Other fitting parameters from the van Genuchten-Mualem model (**Supplementary Table S3**) give further insight into the hydraulic behavior of the HCP center soils. Soils from depths 50–65 cm and 65–80 cm had high porosity (>0.8) and high saturated hydraulic conductivity (K_s), and an increase in K_s (from $\sim 10^1$ to $\sim 10^4$ cm day^{-1}) was observed from top to bottom of the soil core. The shape parameter, α, shows an increase with depth for the HCP center. Elevated α values are often associated with less water retention. The data indicate that the soils near the active layer – permafrost boundary would poorly retain water. These measurements describe soil properties from a newly thawed soil core, and do not account for future compaction or subsidence that could reduce porosity and conductivity in the field.

CO_2 and CH_4 Production From HCP Incubations

HCP soils were incubated at −2, +4, and +8°C. All incubations were initially anoxic (headspace purged with N_2), except for the HCP center organic horizon incubations (initially with atmospheric oxygen). CO_2 and CH_4 were measured for at least 50 days, sampling every other day for 10 days and thereafter every 5 days, and high frequency temporal measurements of CO_2 and CH_4 allowed for response curve fitting.

Magnitude and Character of CO_2 Release Varies With Soil Type and Microtopography

Organic and mineral soils of the HCP showed differences in the magnitude and character of CO_2 production. Cumulative CO_2 production over time is plotted in **Figure 4** for organic and mineral horizons of the HCP center and trough, and higher temperatures generally resulted in elevated CO_2 production under all conditions. Parameters used to fit the response curves are presented in **Supplementary Table S4**. In the HCP center soils (**Figure 4A**), oxygen was consumed within the first 13–15 days of incubation for microcosms at +4 and +8°C (data not shown); those incubated at −2°C were not analyzed. As expected, CO_2 production in the HCP center and trough organic soils increased at elevated temperatures (**Figures 4A,B**). The rates of CO_2 production (**Supplementary Figure S5**) increased at later times (>20 days) for all temperatures in the HCP center organic soils, which contrasts with the initial increased rates of CO_2 release which peaked and then decreased at later times in HCP trough soils (except for the trough mineral soil at 4°C which showed exponential response, **Figure 4D**). Decreasing rates of CO_2 production at later incubation times has been previously observed for active layer soils over similar incubation times (Waldrop et al., 2010). The initial lag in CO_2 release in the HCP center organic soils could be related to its relatively low water content which could impact initial microbial activity, though the lower pH may also be a factor. The HCP organic trough samples showed a peak in CO_2 production rates at 2 days (∼4.9 μmol CO_2 g-dwt^{-1}d^{-1}) and 9 days (5.8 μmol CO_2 g-dwt^{-1}d^{-1}) of incubation at +8°C and +4°C, respectively (**Supplementary Figure S5**), which could indicate more efficient utilization of more bioavailable C with increasing temperature in the saturated trough organic soils (Yang et al., 2016).

In general, the mineral horizons of the HCP center and trough demonstrated lower cumulative CO_2 production than the organic horizons over the experimental time. At +8°C, mineral soils of the HCP center (**Figure 4C**) showed exponential response, with accelerating CO_2 production. This is especially clear in **Supplementary Figure S5**, which presents the rate of CO_2 production as a function of time. While HCP organic soils generally showed higher cumulative CO_2 production, mineral soils from HCPs could still be contributing to CO_2 release in Arctic permafrost regions, albeit at lower rates.

HCP Trough Soils May Be a Significant Source of CH_4

HCP trough soils demonstrated elevated cumulative CH_4 production at higher temperatures, while the HCP center soils of both the organic and mineral horizons did not show measurable CH_4 production over 50 days. **Figure 5** presents cumulative CH_4 production over time for HCP trough soils, with the mineral horizon releasing approximately twice as much CH_4 (5 μmol g-dwt.$^{-1}$) as the organic horizon (2.5 μmol g-dwt.$^{-1}$) at 8°C over 50 days. CH_4 production plateaued in the trough organic soil after 30 days (**Figure 5A**) but did not reach a plateau in the trough mineral soil even after 50 days (**Figure 5B**). Rates of CH_4 production, which are plotted against time in **Supplementary Figure S6**, peak between 5 and 20 days for all conditions, indicating that delayed methanogen activity may have been followed by a phase of substrate limitation. Previous incubations by Zona et al. (2012) with similar soil types also indicated a peak in methane production rates, though this was observed slightly later at 30 days of incubation. Overall, most of the C lost from the HCP soils was released as CO_2 rather than CH_4. However, the global warming potential of CH_4 is substantially higher than CO_2, and greenhouse gas emissions from HCP troughs may be underappreciated at present. Production of CH_4 in the mineral horizon of the HCP trough accounted for 67% of total C loss at +8°C, while CH_4 released from the organic horizon approximated ∼ 5% at +8°C. Methanogenesis at −2°C was negligible throughout.

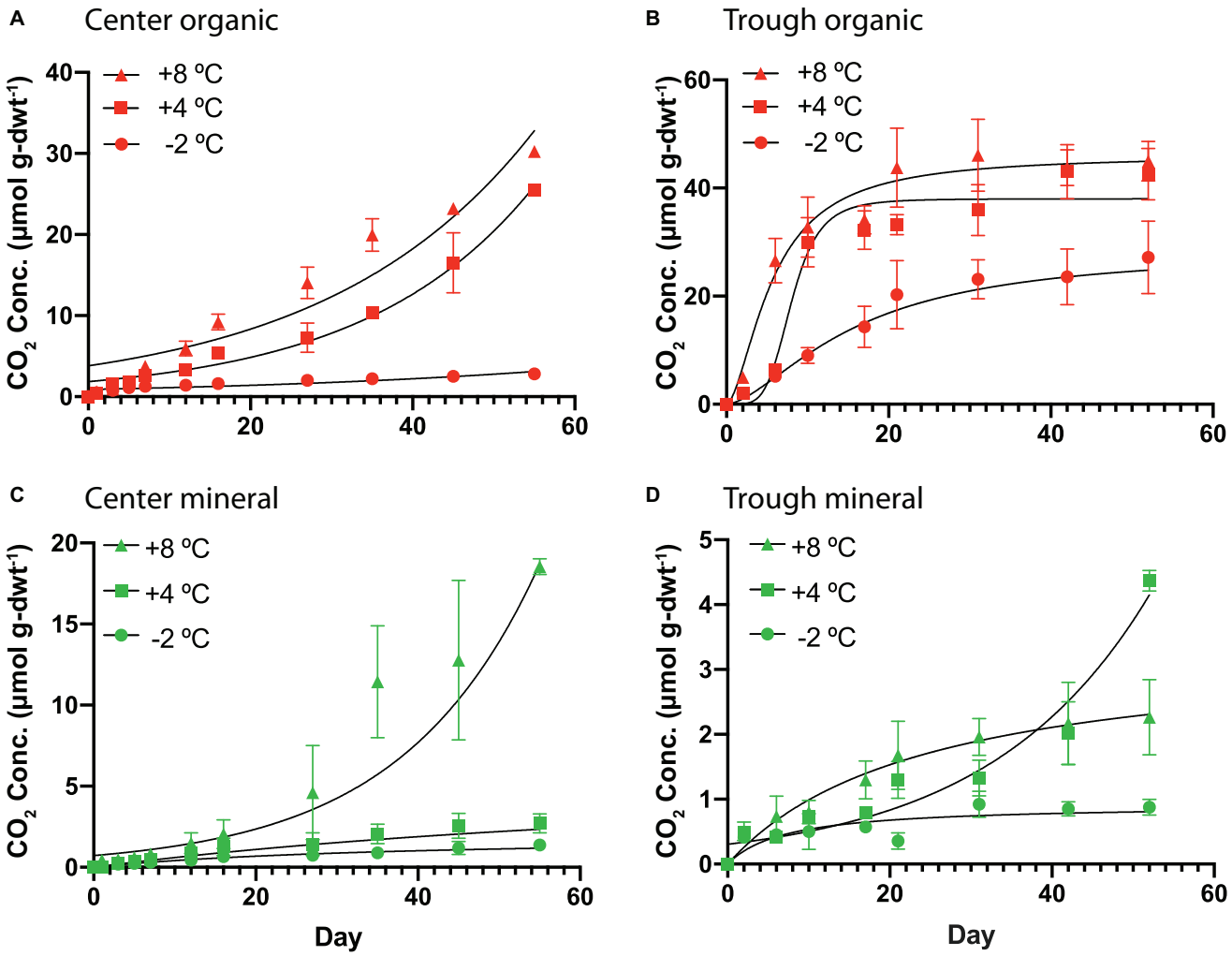

FIGURE 4 | Cumulative CO_2 production per mass of soil as dry weight (dwt.) added to the incubations over time from HCP center organic **(A)**, trough organic **(B)**, center mineral **(C)**, and trough mineral **(D)** soil samples (n = 3) incubated at –2, 4, and 8°C. The error bars represent standard deviation. Curve-fitting equations for each condition were determined following procedures described previously (Roy Chowdhury et al., 2015), and parameters are listed in **Supplementary Table S4**. Vertical scales are different for the four different plots.

mcrA Detected in Methane Producing Soils

It was expected that microcosms with elevated CH_4 production would also have larger methanogen populations. The *mcrA* abundance was quantified in microcosms after 30, 60, and/or 75 days of incubation at −2, +4 and +8°C. **Figure 6** presents the *mcrA* copy numbers for HCP trough soils. No amplifiable signature for *mcrA* could be detected in the HCP center soils ($<10^2$ copies g-dwt.$^{-1}$ soil), which was consistent with the lack of CH_4 produced. This gene also was undetected in frozen HCP trough samples before incubation, which could indicate a low methanogen population or inhibitory substances in the soil. Overall, *mcrA* copy numbers for HCP trough soils were high (10^7 to 10^9 copies g-dwt^{-1} soil) after incubation, but trends in CH_4 release between layers or across incubation temperatures were not observed (**Figure 6**).

DISCUSSION

Variation in C Release Across HCP and LCP Microtopographies and Soil Types

The present study focused on HCPs and demonstrated variations in magnitude and rate of CO_2 and CH_4 release across HCP microtopographies and soil types at different temperatures. Several previous studies have similarly quantified the magnitudes and rates of C release for LCPs during soil warming (Herndon et al., 2015; Roy Chowdhury et al., 2015; Wagner et al., 2017). **Figure 7** compares trends across all three temperatures for HCP centers and troughs with previously published data (Roy Chowdhury et al., 2015) for LCP microtopographies (center, rim, and trough). The additional rim microtopography in LCPs is defined as the raised edges between the center and the trough (not present in HCPs). As expected and consistent with previous

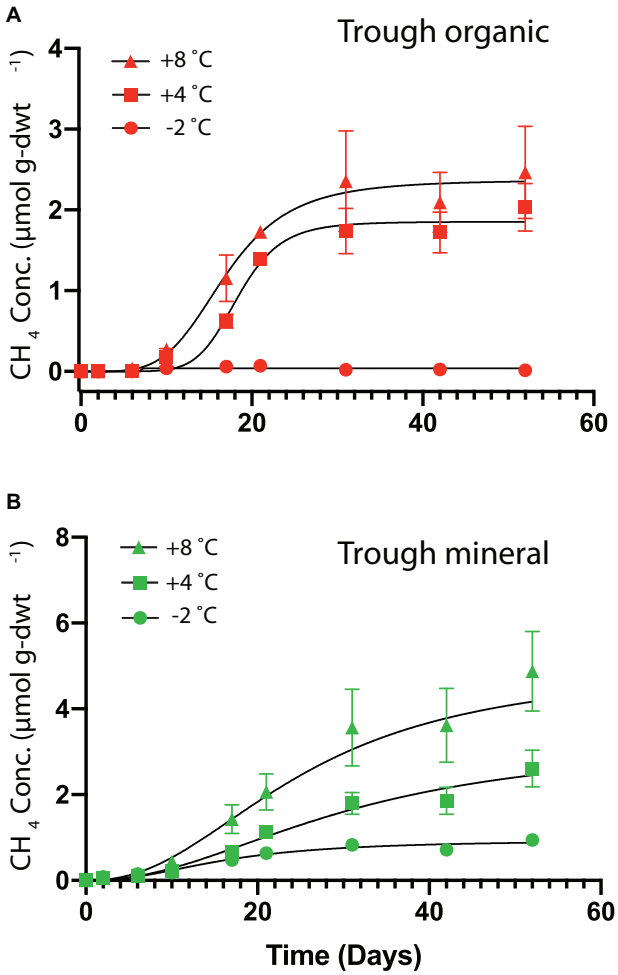

FIGURE 5 | Cumulative CH_4 production per mass of soil as dry weight (dwt.) added to the incubations over time from HCP trough organic **(A)** and trough mineral **(B)** soil samples (n = 3) incubated at –2, +4, and +8°C. No CH_4 production was observed from the HCP center soil incubations. The error bars represent standard deviations. Curve-fitting equations for each condition were determined following procedures described previously (Roy Chowdhury et al., 2015), and parameters are listed in **Supplementary Table S5**. Note: Vertical axes are different scales for the two different plots.

LCP incubations, elevated temperatures in HCP soil incubations resulted in greater cumulative CO_2 release after 60 days – increasing from −2, to 4, to 8°C – for all microtopographies and soil types (**Figures 7A,C**), with the exception of the HCP trough mineral soils (**Figure 7C**). Similarly, higher cumulative CH_4 was observed as temperatures increased for all microtopographies and soil types (**Figures 7B,D**).

Overall, the incubations indicated that soils from almost all microtopographic features of both LCPs and HCPs released more CO_2 and CH_4 with increasing temperature, which is consistent with trends in mean CO_2 production at elevated temperatures observed across as range of anoxic incubation experiments [see synthesis in Treat et al. (2015)]. While previous anoxic incubations have used elevated temperatures (in excess of 20°C) to represent the maximum possible carbon that could be released from the soils, the temperatures of −2, 4, and 8°C were used in this study to represent soil temperatures that are more likely to occur at the tested soil depths during near future warming conditions. Relative rates of gas production from these experiments help to parameterize temperature response functions that modulate gas production functions in biogeochemical models (Riley et al., 2011). For example, **Figure 4** shows that CO_2 produced from center organic soils at 8°C is approximately 15 times greater than CO_2 released from center mineral soils at 4°C after 60 days of incubation. Simulations using these response functions should be compared with future research that evaluates the magnitudes of CO_2 and CH_4 production along a soil profile with a thermal gradient representative of temperature maximums under field conditions.

Water availability appeared to impact both CH_4 and CO_2 production, consistent with previous observations (Gulledge and Schimel, 1998; Lipson et al., 2012; Kane et al., 2013; Moyano et al., 2013). In **Figure 7**, the microtopographies on the horizontal axis are arranged from highest to lowest θ_g (left to right) for organic (**Figures 7A,B**) and mineral (**Figures 7C,D**) soils. A trend showing increased CO_2 and CH_4 release with elevated θ_g is apparent for organic soils, but the same trend is not observed for the mineral soils, which have a narrower range of θ_g (0.74 – 1.38 g g^{-1}) than the organic soils (0.44 – 9.62 g g^{-1}). The relatively dry, aerobic HCP center soils had lower CO_2 and CH_4 flux than the more saturated LCP center soils, which is consistent with a synthesis of anoxic incubations by Treat et al. (2015) that showed lower CO_2 and CH_4 production from dry soils than soils that were saturated or experienced a fluctuating water table. Elevated water contents are known to limit oxygen transport in soils, restricting aerobic respiration. Ecological models commonly enforce schemes in which water saturation prohibits C mineralization and stimulates methanogenesis (Riley et al., 2011; Burrows et al., 2020), but they do not adequately account for anaerobic CO_2 production. CO_2 concentrations observed in this study (**Figure 4**) suggest that anaerobic processes are contributing CO_2 release. It has been shown that anaerobic processes such as microbial Fe(III) reduction coupled with oxidation of small organic acids can release CO_2 (Lovley and Phillips, 1988), and that this process can impact CO_2 release under some soil conditions (Chen et al., 2020).

Change in the rates of CO_2 and CH_4 release were observed for both HCP and LCP incubations. C mineralization rates in the LCP center soils generally decreased over time, while the HCP center soils under some conditions showed increasing rates of C release at later times (**Figure 4**). While some incubations plateaued in C production rate after 50 days, other incubations were just beginning to increase in C production rate (**Supplementary Figures S4, S5**); this could indicate delays in C release due to slow growth of the heterotrophic microbial community or substrate competition. Previous soil incubations from soils of drained tundra lakes also showed an earlier time peak in CO_2 production, and a delay in CH_4 production (Zona et al., 2012).

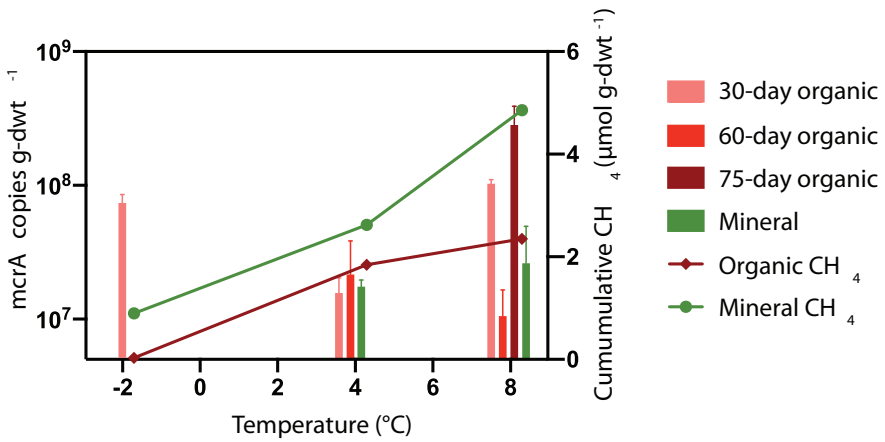

FIGURE 6 | Mean temperature responses of *mcrA* copy numbers (n = 3) for HCP trough soils. DNA was extracted for qPCR analysis after incubating organic soils for 30 and 60 or 75 days. Mineral soils were incubated for 30 and 60 days (8°C) or 75 days (4°C). The *mcrA* gene was not detected ($<10^2$ copies μL^{-1}) in HCP center soils. Mineral soils and organic soils incubated 60 days at –2°C were not analyzed.

Overall, the LCPs showed higher cumulative CO_2 and CH_4 release and more variability in the magnitude of C release than HCPs. Despite releasing less C and covering approximately half the land area as LCPs near Utqiaġvik, HCP soils can release large quantities of CH_4 and CO_2 when integrated across the large spatial domains of polygonal Artic tundra, and they need to be incorporated in models that estimate total C flux from Arctic soils. For example, data from Lara et al. (2015) indicate that HCPs cover ∼200 km^2 on the Utqiagvik Peninsula alone. Flux measurements from chamber experiments indicate that both CO_2 and CH_4 are released from HCPs and that the amount of C release varies across seasons (Wainwright et al., 2015; Arora et al., 2019). Incubation studies such as the present study allow for precise temperature control and dense temporal measurements that aid in understanding the dynamic nature of CO_2 and CH_4 release from Arctic soils. Knowing the variability in relative amounts of CO_2 and CH_4 released from incubations and the timing of peak release rates for different soil types and microtopographies may help constrain parameters needed for models that estimate carbon flux from Arctic soils. Greater understanding of processes developed from controlled, homogenized incubations can be used to inform intact soil core incubation studies, field measurements, and development of reactive transport models, which ultimately allow for better estimates of C release from Arctic tundra soils.

Carbon Release From HCPs May Be Associated With Higher Water Content and Total C

In addition to elevated incubation temperature, higher water content and total C across different soil types and microtopographies appeared to be related to greater cumulative CO_2 and CH_4 release from the HCP soils. The HCP trough organic soil, with the highest water content (1.09–3.31 g g-dwt.$^{-1}$) and organic C (31%), showed the highest cumulative CO_2 production over 50 days (**Figure 4B**) and the highest rates of CO_2 production (**Supplementary Figure S5**), indicating the potential importance of anaerobic processes such as fermentation, syntrophic oxidation, acetoclastic methanogensis, and iron reduction which produce CO_2 release under anoxic conditions. Mineral soils from both trough and center microtopographies had lower organic C, which may explain the lag and lower magnitude in CO_2 production than the organic soil – though this observation may also be due to limitations on microbial metabolism. HCP center soils with relatively low θ_g produced no CH_4 over 50 days, although O_2 was effectively consumed within the first 13–15 days of incubation. On the other hand, CH_4 was measured in both organic and mineral horizons of the HCP trough, which had higher θ_g and no initial oxygen present in the headspace (**Figure 5** and **Table 1**). Alternatively, CH_4 production may be controlled by the biomass of methanogens present in the soils.

Water Potential Influence on Carbon Release From HCP and LCP Soils

Positive correlations between C release and soil water content are discussed above, but this does not necessarily indicate the longer-term potential for CO_2 and CH_4 flux from Arctic soils. It is becoming more widely understood that climate change trends in the Artic could result in a drier landscape, exemplified by transitions from LCPs to HCPs (Raynolds et al., 2014). It will likely be comparably important to understand the ability of soil to retain water under a drying climate as it is to know the present water content at discrete time points.

In this study, soil water retention curves constructed for HCP center soils (**Figure 3**), showed water retention with relatively low potentials. This indicates that HCP soils can retain substantial amounts of water during drying. For example, at a permanent wilting point of –1.5 MPa, the HCP organic and mineral layers retain more water than a typical silt loam soil, similar to decomposed sphagnum soil. These results were different from those observed in LCP soils. Soil water retention curves for

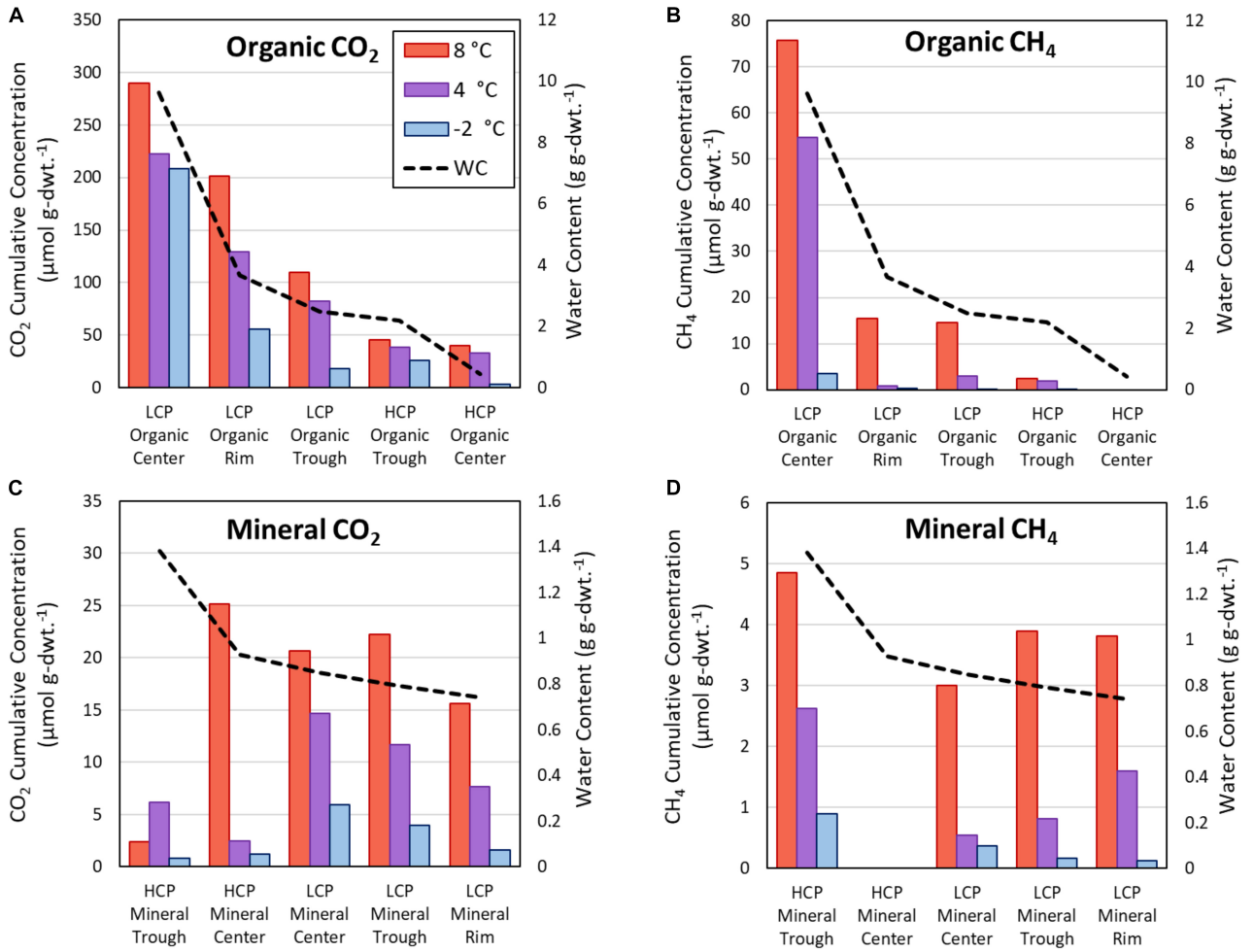

FIGURE 7 | Cumulative CO_2 and CH_4 release from active layer samples after incubations as determined from response curves at 60 days. Carbon release from organic soils for CO_2 **(A)** and CH_4 **(B)**, as well as mineral soils for CO_2 **(C)**, and CH_4 **(D)**. The vertical axes scales differ for each panel. Horizontal arrangement of LCP and HCP microtopographies progresses from highest water content (left) to lowest water content (right), and the water content relationships are different for organic and mineral soils. WC, water content.

the LCP center organic soil showed lower water retention at higher water potentials than the LCP center mineral soils and all depths of HCP center soils (**Supplementary Figure S7**). Parameter fitting indicated very high θ_s (1.0) and high hydraulic conductivity for LCP center organic soils (**Supplementary Table S3**). Estimates of macroporosity in LCP organic soils were significantly higher (23.9%) than underlying mineral soils (2.1%) and HCP active layer soils (**Supplementary Figure S8**), indicating that LCP organic soils may lose water from large pores relatively fast during dry seasons. These seasonal trends could potentially influence future ecological succession and SOC mineralization by microbial communities, which was previously proposed for soil moisture impacts on methanotrophs (Gulledge and Schimel, 1998). The large pores in these organic soils store substantial amounts of water but drain quickly from active layer soils and more slowly from thawed HCP permafrost. Previous work by Gulledge and Schimel (1998) showed faster rates of CH_4 oxidation at water holding capacities between 30 and 50%, and indicated that CH_4 oxidizers in wetter environments were less sensitive to changes in water potential than those in sampled in drier environments. Future studies should further explore the role of macroporosity and soil water retention in maintaining active microbial communities in Arctic tundra soils and the impact on CO_2 and CH_4 release.

Controls on Methanogen Presence and CH_4 Production

Counter to the original hypothesis, methanogen biomass estimated with *mcrA* marker gene copy numbers did not show a strong correlation with CH_4 release magnitude or rate. *mcrA* copy numbers in HCP trough soils did not correlate with the cumulative CH_4 production (**Figure 6**), and similar observations were made for LCP soils (**Supplementary Figure S9**). One possible explanation for this discrepancy is that the presence of *mcrA* genes does not necessarily indicate active methanogens are

present; inactive or dead organisms can still carry quantifiable amounts of *mcrA* (Freitag and Prosser, 2009). Although detectable levels of *mcrA* were present in LCP trough (2.5×10^5 copies g dwt.$^{-1}$) and center (1.3×10^7 copies g-dwt.$^{-1}$) soils measured before any incubation, significant incubation time was required before methanogenesis rates peaked in most samples (**Supplementary Figure S6**). Future studies would benefit from measuring gene expression to determine which microorganisms and enzymes are active.

While strong correlations between copy number and CH_4 release were not observed, the lack of detectable *mcrA* was consistent with HCP center soils that did not produce CH_4. Though we cannot rule out soil inhibitors preventing the amplification of *mcrA*, the replicate measurements made for all HCP center soils indicate that methanogens were not present. Low methanogen abundances or methanogenesis rates have been previously reported in permafrost environments (Wagner et al., 2007; Steven et al., 2008; Waldrop et al., 2010), and HCPs had lower relative methanogen 16S rRNA gene abundance than LCPs (Taş et al., 2018). Potential reasons for the lack of methanogens in the HCP center soils include (1) competition for substrate from other microbial communities, namely iron reducers (Roden and Wetzel, 1996), (2) limited water availability, (3) intermittent oxic conditions in the field limiting anaerobic activity and measurable methanogen growth before incubations, or (4) low pH. Previous studies have documented competition for substrate between iron reducers and methanogens (Philben et al., 2020b), but the incubations in the present study did not show a significant change in Fe(II) concentrations over the incubation time (data not shown). Water contents measured in the HCP center mineral soils were only slightly lower than the water contents in the HCP trough soils, and it is assumed that this small difference was not the main control. Fe(II) concentrations indicated that HCP center soils supported iron reduction (**Figure 2**), but it is possible that intermittent oxic conditions prevented soil redox conditions from becoming reducing enough to support methanogenesis in HCP center soils. Other geochemical controls such as pH may also influence the spatial variability in methanogenesis. While methanogens are known to grow at pH below 5, their growth is optimal between pH 6 and pH 8 (Garcia et al., 2000). The low levels of methanogenesis and *mcrA* measured in HCP soils indicate that low CH_4 production rather than robust CH_4 oxidation explains low CH_4 emissions from these elevated soil surfaces. Geochemical controls in addition to methanogen presence are likely to determine the rate and magnitude of CH_4 release from Artic tundra soils.

Implications for CO_2 and CH_4 Emissions From Warming Arctic Tundra

Knowledge of the temporal and spatial variability in microbial C mineralization rates of Arctic soils in response to warming are key to constraining uncertainties in predictive climate models. The present study focuses on CO_2 and CH_4 release from HCPs during soil incubations and quantifies nature and magnitude of C release using response functions. The magnitudes and rates of CO_2 and CH_4 production from HCPs were compared with C production from LCPs, and it was determined that the total C released from organic soils of both LCPs and HCPs is greater and more variable than the C released from mineral soils (**Figure 7**). Under our experimental conditions, it was also concluded that relatively more C is released from LCPs than HCPs, but the contributions from HCPs – especially the initial CH_4 release from the more saturated, anoxic HCP troughs – are significant and should not be neglected when evaluating soil C flux (**Figure 5** and **Supplementary Figure S6**). Anoxic soils that retain water are more likely to release CH_4, and methanogen marker gene abundance does not always correlate with increased CH_4 release magnitudes or rates when other geochemical controls are limiting.

Increased warming and thermokarst formation is predicted to increase the HCP coverage and decrease that of LCP in polygonal tundra landscapes (Lara et al., 2015). Our results suggest that this transition to drier HCPs may result in less C release as CH_4 and CO_2 from organic soils, and that releases from mineral soils should remain relatively uniform across geomorphic features. Soil warming in the present saturated landscapes and a longer thaw season can also cause an increasing positive C feedback due to accelerated loss of CO_2 and CH_4 (Hinzman et al., 1991), particularly due to high rates of methanogenesis at the end of thaw season (Windsor et al., 1992; Mastepanov et al., 2008; Sturtevant et al., 2012). The results from the present incubation study can be used to inform targeted field measurements of CO_2 and CH_4 release across soil types and microtopographies and validate relevant processes and relative rates before model implementation. Although polygon troughs make up a small proportion of the land surface, these saturated areas may contribute disproportionately to both CH_4 and CO_2 emissions. The maximum rate of CO_2 production in the saturated HCP trough organic soil was more than 3× higher than in the unsaturated HCP center (**Supplementary Figure S5**), and CH_4 in HCP trough soils was released at rates up to 0.19 μmol g-dwt.$^{-1}$ day^{-1}. Mechanisms promoting more CO_2 release from the HCP trough than the HCP center, may be due to the fitness of the microbial communities, limitations on nutrient transport in drier environments, or environmental stressors such as low pH in the HCP center. Future work should target these potential mechanisms directly. While CH_4 emissions are minor components of C loss compared to anaerobic CO_2 emissions in Utqiaġvik (Lipson et al., 2012), this proportion of CH_4 could vary significantly across the Arctic due to differences in soil freezing and the availability of alternative electron acceptors. Future studies evaluating CO_2 and CH_4 release from permafrost soils should directly evaluate the influence of soil water retention on CO_2 and CH_4 flux during soil drying, and fully explore temporal changes in microbial communities and metabolites with and without soil drying.

CONCLUSION

High centered polygons soil incubations complemented previous LCP soil incubations to provide relative rate data for CO_2 and CH_4 production across the microtopographic extremes of

polygonal tundra. Organic soils from LCPs produced the most greenhouse gases, while mineral soils had similar production rates regardless of microtopography or water content. Dynamic changes in these soils due to precipitation, freeze-thaw and drainage processes were magnified in organic layers, where temporary water saturation may not predict rates of anaerobic processes, including methanogenesis and iron reduction.

DATA AVAILABILITY STATEMENT

The original contributions presented in the study are included in the article/**Supplementary Material**, further inquiries can be directed to the corresponding author/s.

AUTHOR CONTRIBUTIONS

TRC, J-WM, BG, LL, SW, and DG designed the experiments. TRC performed the incubation experiments, chemical, and molecular analyses. J-WM performed XRD and water release experiments. TRC, EB, J-WM, and DG analyzed the data and wrote the manuscript. All authors edited and reviewed the manuscript.

FUNDING

The Next-Generation Ecosystem Experiments in the Arctic (NGEE Arctic) project was supported by the Biological and Environmental Research program in the U.S. Department of Energy (DOE) Office of Science. Support for the SULI program was also provided by the DOE Office of Science. Oak Ridge National Laboratory was managed by UT-Battelle, LLC, for the DOE under Contract No. DE-AC05-00OR22725.

ACKNOWLEDGMENTS

We gratefully acknowledge the assistance of Bob Busey, Larry Hinzman, Kenneth Lowe, Deanne Brice, Ziming Yang, Craig Ulrich, and Tommy Phelps in obtaining and analyzing frozen core samples and field measurements as well as logistical support provided by UIC Science. We thank Hannah Long for developing the soil moisture sensor calibration curve and gravimetric water content profile during a Science Undergraduate Laboratory Internship (SULI) project. Authors deeply appreciate the technical support of Mr. Leo Rivera from Decagon Devices. Finally, we thank Vladimir Romanovsky for sharing continuous subsurface temperature measurements from the Utqiaġvik site and Dami Rich for assistance preparing the illustration in **Figure 1**.

SUPPLEMENTARY MATERIAL

The Supplementary Material for this article can be found online at: https://www.frontiersin.org/articles/10.3389/fmicb.2020.616518/full#supplementary-material

REFERENCES

Arora, B., Wainwright, H. M., Dwivedi, D., Vaughn, L. J., Curtis, J. B., Torn, M. S., et al. (2019). Evaluating temporal controls on greenhouse gas (Ghg) fluxes in an Arctic tundra environment: An entropy-based approach. *Sci*. Tot. Environ. 649, 284–299.

Beven, K., and Germann, P. (1982). Macropores and water flow in soils. *Water Resour. Res.* 18, 1311–1325.

Biasi, C., Rusalimova, O., Meyer, H., Kaiser, C., Wanek, W., Barsukov, P., et al. (2005). Temperature-dependent shift from labile to recalcitrant carbon sources of arctic heterotrophs. *Rapid Commun. Mass Spectr.* 19, 1401–1408.

Billings, W., and Peterson, K. (1980). Vegetational change and ice-wedge polygons through the thaw-lake cycle in Arctic Alaska. *Arctic Alpine Res.* 12, 413–432.

Black, R. F. (1964). *Gubik formation of Quaternary age in northern*. Alaska: US Government Printing Office.

Brankatschk, R., Bodenhausen, N., Zeyer, J., and Bürgmann, H. (2012). Simple Absolute Quantification Method Correcting for Quantitative PCR Efficiency Variations for Microbial Community Samples. *Appl. Environ. Microbiol.* 78, 4481–4489.

Burrows, S., Maltrud, M., Yang, X., Zhu, Q., Jeffery, N., Shi, X., et al. (2020). The DOE E3SM v1. 1 biogeochemistry configuration: Description and simulated ecosystem-climate responses to historical changes in forcing. *J. Adv. Model. Earth Syst.* 12:e2019MS001766.

Chen, C., Hall, S. J., Coward, E., and Thompson, A. (2020). Iron-mediated organic matter decomposition in humid soils can counteract protection. *Nat. Commun.* 11, 1–13.

Crowther, T. W., Thomas, S. M., Maynard, D. S., Baldrian, P., Covey, K., Frey, S. D., et al. (2015). Biotic interactions mediate soil microbial feedbacks to climate change. *Proc. Natl. Acad. Sci.* 112, 7033–7038.

Evans, S. E., and Wallenstein, M. D. (2014). Climate change alters ecological strategies of soil bacteria. *Ecol. Lett.* 17, 155–164.

Faucherre, S., Jørgensen, C. J., Blok, D., Weiss, N., Siewert, M. B., Bang-Andreasen, T., et al. (2018). Short and Long-Term Controls on Active Layer and Permafrost Carbon Turnover Across the Arctic. *J. Geophys. Res. Biogeosci.* 123, 372–390.

Fiedler, S., Wagner, D., Kutzbach, L., and Pfeiffer, E.-M. (2004). Element redistribution along hydraulic and redox gradients of low-centered polygons, Lena Delta, Northern Siberia. *Soil Sci. Soc. Am. J.* 68, 1002–1011.

Freitag, T. E., and Prosser, J. I. (2009). Correlation of methane production and functional gene transcriptional activity in a peat soil. *Appl. Environ. Microbiol.* 75, 6679–6687.

Garcia, J.-L., Patel, B. K., and Ollivier, B. (2000). Taxonomic, phylogenetic, and ecological diversity of methanogenic Archaea. *Anaerobe* 6, 205–226.

Grant, R., Mekonnen, Z., Riley, W., Wainwright, H., Graham, D., and Torn, M. (2017). Mathematical modelling of arctic polygonal tundra with ecosys: 1. Microtopography determines how active layer depths respond to changes in temperature and precipitation. *J. Geophys. Res. Biogeosci.* 122, 3161–3173.

Gulledge, J., and Schimel, J. P. (1998). Moisture control over atmospheric CH4 consumption and CO2 production in diverse Alaskan soils. *Soil Biol. Biochem.* 30, 1127–1132.

Herndon, E. M., Yang, Z., Bargar, J., Janot, N., Regier, T. Z., Graham, D. E., et al. (2015). Geochemical drivers of organic matter decomposition in arctic tundra soils. *Biogeochemistry* 126, 397–414.

Herndon, E., Kinsman-Costello, L., and Godsey, S. (2020). Biogeochemical Cycling of Redox-Sensitive Elements in Permafrost-Affected Ecosystems. *Biogeochem. Cycles Ecol. Driv. Environ. Impact* 2020, 245–265.

Hinkel, K., and Nelson, F. (2003). Spatial and temporal patterns of active layer thickness at Circumpolar Active Layer Monitoring (CALM) sites in northern Alaska, 1995–2000. *J. Geophys. Res. Atmosph.* 108, 8168.

Hinzman, L., Kane, D., Gieck, R., and Everett, K. (1991). Hydrologic and thermal properties of the active layer in the Alaskan Arctic. *Cold Reg. Sci. Technol.* 19, 95–110.

Hobbie, S. E., and Gough, L. (2004). Litter decomposition in moist acidic and non-acidic tundra with different glacial histories. *Oecologia* 140, 113–124.

Hubbard, S. S., Gangodagamage, C., Dafflon, B., Wainwright, H., Peterson, J., Gusmeroli, A., et al. (2013). Quantifying and relating land-surface and subsurface variability in permafrost environments using LiDAR and surface geophysical datasets. *Hydrogeol. J.* 21, 149–169.

Jansson, J. K., and Hofmockel, K. S. (2019). Soil microbiomes and climate change. *Nat. Rev. Microbiol.* 18, 35–46.

Kane, E., Chivers, M., Turetsky, M., Treat, C. C., Petersen, D. G., Waldrop, M., et al. (2013). Response of anaerobic carbon cycling to water table manipulation in an Alaskan rich fen. *Soil Biol. Biochem.* 58, 50–60.

Lara, M. J., Lin, D. H., Andresen, C., Lougheed, V. L., and Tweedie, C. E. (2019). Nutrient Release From Permafrost Thaw Enhances CH4 Emissions From Arctic Tundra Wetlands. *J. Geophys. Res. Biogeosci.* 124, 1560–1573.

Lara, M. J., Mcguire, A. D., Euskirchen, E. S., Tweedie, C. E., Hinkel, K. M., Skurikhin, A. N., et al. (2015). Polygonal tundra geomorphological change in response to warming alters future CO 2 and CH 4 flux on the Barrow Peninsula. *Glob. Change Biol.* 21, 1634–1651.

Liljedahl, A. K., Boike, J., Daanen, R. P., Fedorov, A. N., Frost, G. V., Grosse, G., et al. (2016). Pan-Arctic ice-wedge degradation in warming permafrost and its influence on tundra hydrology. *Nat. Geosci.* 9, 312–318.

Lipson, D. A., Haggerty, J. M., Srinivas, A., Raab, T. K., Sathe, S., and Dinsdale, E. A. (2013). Metagenomic insights into anaerobic metabolism along an Arctic peat soil profile. *PLoS One* 8:e64659.

Lipson, D. A., Raab, T. K., Parker, M., Kelley, S. T., Brislawn, C. J., and Jansson, J. (2015). Changes in microbial communities along redox gradients in polygonized A rctic wet tundra soils. *Environ. Microbiol. Rep.* 7, 649–657.

Lipson, D. A., Zona, D., Raab, T. K., Bozzolo, F., Mauritz, M., and Oechel, W. (2012). Water-table height and microtopography control biogeochemical cycling in an Arctic coastal tundra ecosystem. *Biogeosciences* 9, 577–591.

Liu, H., and Lennartz, B. (2019). Hydraulic properties of peat soils along a bulk density gradient—A meta study. *Hydrol. Proces.* 33, 101–114.

Lovley, D. R., and Phillips, E. J. (1988). Novel mode of microbial energy metabolism: organic carbon oxidation coupled to dissimilatory reduction of iron or manganese. *Appl. Environ. Microbiol.* 54, 1472–1480.

Luton, P. E., Wayne, J. M., Sharp, R. J., and Riley, P. W. (2002). The mcrA gene as an alternative to 16S rRNA in the phylogenetic analysis of methanogen populations in landfill. *Microbiology* 148, 3521–3530.

Mackelprang, R., Waldrop, M. P., Deangelis, K. M., David, M. M., Chavarria, K. L., Blazewicz, S. J., et al. (2011). Metagenomic analysis of a permafrost microbial community reveals a rapid response to thaw. *Nature* 480, 368–371.

Mastepanov, M., Sigsgaard, C., Dlugokencky, E. J., Houweling, S., Ström, L., Tamstorf, M. P., et al. (2008). Large tundra methane burst during onset of freezing. *Nature* 456, 628–630.

Moon, J.-W., and Graham, D. (2017). *Soil water characteristics of cores from low- and high-centered polygons, Barrow, Alaska, 2012 in Next Generation Ecosystem Experiments Arctic Data Collection*, Oak Ridge: Oak Ridge National Laboratory.

Morrissey, L., and Livingston, G. (1992). Methane emissions from Alaska arctic tundra: An assessment of local spatial variability. *J. Geophys. Res. Atmosph.* 97, 16661–16670.

Moyano, F. E., Manzoni, S., and Chenu, C. (2013). Responses of soil heterotrophic respiration to moisture availability: An exploration of processes and models. *Soil Biol. Biochem.* 59, 72–85.

Newman, B. D., Throckmorton, H. M., Graham, D. E., Gu, B., Hubbard, S. S., Liang, L., et al. (2015). Microtopographic and depth controls on active layer chemistry in Arctic polygonal ground. *Geophys. Res. Lett.* 42, 1808–1817.

Olefeldt, D., Turetsky, M. R., Crill, P. M., and Mcguire, A. D. (2013). Environmental and physical controls on northern terrestrial methane emissions across permafrost zones. *Glob. Change Biol.* 19, 589–603.

Or, D., Wraith, J., Robinson, D. A., and Jones, S. B. (2012). *Soil Water Content and Water Potential Relationships in Handbook of soil sciences: properties and processes*, Florida: CRC Press.

Philben, M., Taş, N., Chen, H., Wullschleger, S. D., Kholodov, A., Graham, D. E., et al. (2020a). Influences of hillslope biogeochemistry on anaerobic soil organic matter decomposition in a tundra watershed. *J. Geophys. Res. Biogeosci.* 125:e2019JG005512.

Philben, M., Zhang, L., Yang, Z., Tas, N., Graham, D. E., and Gu, B. (2020b). Anaerobic respiration pathways and response to increased substrate availability of Arctic wetland soils. *Environ. Sci. Proces. Impacts*. 22, 2070–2083.

Preuss, I., Knoblauch, C., Gebert, J., and Pfeiffer, E.-M. (2013). Improved quantification of microbial CH 4 oxidation efficiency in arctic wetland soils using carbon isotope fractionation. *Biogeosciences* 10, 2539–2522.

Pries, C. E. H., Castanha, C., Porras, R., and Torn, M. (2017). The whole-soil carbon flux in response to warming. *Science* 355, 1420–1423.

Raynolds, M. K., Walker, D. A., Ambrosius, K. J., Brown, J., Everett, K. R., Kanevskiy, M., et al. (2014). Cumulative geoecological effects of 62 years of infrastructure and climate change in ice-rich permafrost landscapes. *Prudhoe Bay Oilfield*, *Alaska*. *Glob. Change Biol.* 20, 1211–1224.

Raz-Yaseef, N., Torn, M. S., Wu, Y., Billesbach, D. P., Liljedahl, A. K., Kneafsey, T. J., et al. (2017). Large CO2 and CH4 emissions from polygonal tundra during spring thaw in northern Alaska. *Geophys. Res. Lett.* 44, 504–513.

Riley, W., Subin, Z., Lawrence, D., Swenson, S., Torn, M., Meng, L., et al. (2011). Barriers to predicting changes in global terrestrial methane fluxes: analyses using CLM4Me, a methane biogeochemistry model integrated in CESM. *Biogeosciences* 8, 1925–1953.

Roden, E. E., and Wetzel, R. G. (1996). Organic carbon oxidation and suppression of methane production by microbial Fe (III) oxide reduction in vegetated and unvegetated freshwater wetland sediments. *Limnol. Oceanogr.* 41, 1733–1748.

Roy Chowdhury, T., Herndon, E. M., Phelps, T. J., Elias, D. A., Gu, B., Liang, L., et al. (2015). Stoichiometry and temperature sensitivity of methanogenesis and CO2 production from saturated polygonal tundra in Barrow, Alaska. *Glob. Change Biol.* 21, 722–737.

Ruijter, J., Ramakers, C., Hoogaars, W., Karlen, Y., Bakker, O., Van Den Hoff, M., et al. (2009). Amplification efficiency: linking baseline and bias in the analysis of quantitative PCR data. *Nucleic Acids Res.* 37, e45–e45.

Sachs, T., Giebels, M., Boike, J., and Kutzbach, L. (2010). Environmental controls on CH4 emission from polygonal tundra on the microsite scale in the Lena river delta. *Siberia. Glob. Change Biol.* 16, 3096–3110.

Schuur, E. A., Vogel, J. G., Crummer, K. G., Lee, H., Sickman, J. O., and Osterkamp, T. (2009). The effect of permafrost thaw on old carbon release and net carbon exchange from tundra. *Nature* 459, 556–559.

Shaver, G. R., Billings, W. D., Chapin, F. S. III, Giblin, A. E., Nadelhoffer, K. J., Oechel, W. C., et al. (1992). Global change and the carbon balance of arctic ecosystems: Carbon/nutrient interactions should act as major constraints on changes in global terrestrial carbon cycling. *Bioscience* 42, 433–441.

Steven, B., Pollard, W. H., Greer, C. W., and Whyte, L. G. (2008). Microbial diversity and activity through a permafrost/ground ice core profile from the Canadian high Arctic. *Environ. Microbiol.* 10, 3388–3403.

Sturtevant, C., Oechel, W., Zona, D., Kim, Y., and Emerson, C. (2012). Soil moisture control over autumn season methane flux, Arctic Coastal Plain of Alaska. *Biogeosciences* 9, 1423–1440.

Tang, G., Zheng, J., Xu, X., Yang, Z., Graham, D. E., Gu, B., et al. (2016). Biogeochemical modeling of CO2 and CH4 production in anoxic Arctic soil microcosms. *Biogeosciences* 13, 5021–5041.

Taş, N., Prestat, E., Wang, S., Wu, Y., Ulrich, C., Kneafsey, T., et al. (2018). Landscape topography structures the soil microbiome in arctic polygonal tundra. *Nat. Commun.* 9:777.

Treat, C. C., Natali, S. M., Ernakovich, J., Iversen, C. M., Lupascu, M., Mcguire, A. D., et al. (2015). A pan-Arctic synthesis of CH4 and CO2 production from anoxic soil incubations. *Glob. Change Biol.* 21, 2787–2803.

Tveit, A., Schwacke, R., Svenning, M. M., and Urich, T. (2013). Organic carbon transformations in high-Arctic peat soils: key functions and microorganisms. *ISME J.* 7, 299–311.

Van Genuchten, M. T. (1980). A closed-form equation for predicting the hydraulic conductivity of unsaturated soils. *Soil Sci. Soc. Am. J.* 44, 892–898.

Vaughn, L. J., Conrad, M. E., Bill, M., and Torn, M. S. (2016). Isotopic insights into methane production, oxidation, and emissions in Arctic polygon tundra. *Glob. Change Biol.* 22, 3487–3502.

Voigt, C., Marushchak, M. E., Mastepanov, M., Lamprecht, R. E., Christensen, T. R., Dorodnikov, M., et al. (2019). Ecosystem carbon response of an Arctic peatland to simulated permafrost thaw. *Glob. Change Biol.* 25, 1746–1764.

Wagner, D., Gattinger, A., Embacher, A., Pfeiffer, E. M., Schloter, M., and Lipski, A. (2007). Methanogenic activity and biomass in Holocene permafrost deposits

of the Lena Delta, Siberian Arctic and its implication for the global methane budget. *Glob. Change Biol.* 13, 1089–1099.

Wagner, R., Zona, D., Oechel, W., and Lipson, D. (2017). Microbial community structure and soil p H correspond to methane production in A rctic A laska soils. *Environ. Microbiol.* 19, 3398–3410.

Wainwright, H. M., Dafflon, B., Smith, L. J., Hahn, M. S., Curtis, J. B., Wu, Y., et al. (2015). Identifying multiscale zonation and assessing the relative importance of polygon geomorphology on carbon fluxes in an Arctic tundra ecosystem. *J. Geophys. Res. Biogeosci.* 120, 788–808.

Waldrop, M. P., Wickland, K. P., White, R. III, Berhe, A. A., Harden, J. W., and Romanovsky, V. E. (2010). Molecular investigations into a globally important carbon pool: Permafrost-protected carbon in Alaskan soils. *Glob. Change Biol.* 16, 2543–2554.

Walker, D., Epstein, H., Romanovsky, V., Ping, C., Michaelson, G., Daanen, R., et al. (2008). Arctic patterned-ground ecosystems: A synthesis of field studies and models along a North American Arctic Transect. *J. Geophys. Res. Biogeosci.* 113:G03S01.

Wang, Y., Yuan, F., Yuan, F., Gu, B., Hahn, M. S., Torn, M. S., et al. (2019). Mechanistic Modeling of Microtopographic Impacts on CO2 and CH4 Fluxes in an Alaskan Tundra Ecosystem Using the CLM-Microbe Model. *J. Adv. Model. Earth Syst.* 11, 4288–4304.

Windsor, J., Moore, T., and Roulet, N. (1992). Episodic fluxes of methane from subarctic fens. *Can. J. Soil Sci.* 72, 441–452.

Wu, Y., Ulrich, C., Kneafsey, T., Lopez, R., Chou, C., Geller, J., et al. (2018). Depth-resolved physicochemical characteristics of active layer and permafrost soils in an Arctic polygonal tundra region. *J. Geophys. Res. Biogeosci.* 123, 1366–1386.

Yang, Z., Wullschleger, S. D., Liang, L., Graham, D. E., and Gu, B. (2016). Effects of warming on the degradation and production of low-molecular-weight labile organic carbon in an Arctic tundra soil. *Soil Biol. Biochem.* 95, 202–211.

Yergeau, E., Hogues, H., Whyte, L. G., and Greer, C. W. (2010). The functional potential of high Arctic permafrost revealed by metagenomic sequencing, qPCR and microarray analyses. *ISME J.* 4, 1206–1214.

Zheng, J., Thornton, P. E., Painter, S. L., Gu, B., Wullschleger, S. D., and Graham, D. E. (2019). Modeling anaerobic soil organic carbon decomposition in Arctic polygon tundra: insights into soil geochemical influences on carbon mineralization. *Biogeosciences* 16, 663–680.

Zona, D., Gioli, B., Commane, R., Lindaas, J., Wofsy, S. C., Miller, C. E., et al. (2016). Cold season emissions dominate the Arctic tundra methane budget. *Proc. Natl. Acad. Sci.* 113, 40–45.

Zona, D., Lipson, D. A., Paw, U. K. T., Oberbauer, S. F., Olivas, P., Gioli, B., et al. (2012). Increased CO2 loss from vegetated drained lake tundra ecosystems due to flooding. *Glob. Biogeochem. Cycles* 26:GB2004.

Zona, D., Lipson, D., Zulueta, R., Oberbauer, S., and Oechel, W. (2011). Microtopographic controls on ecosystem functioning in the Arctic Coastal Plain. *J. Geophys. Res. Biogeosci.* 2011:116.

Conflict of Interest: The authors declare that the research was conducted in the absence of any commercial or financial relationships that could be construed as a potential conflict of interest.

frontiers in Microbiology

ORIGINAL RESEARCH
published: 26 January 2021
doi: 10.3389/fmicb.2020.615659

Regional Diversity of Maritime Antarctic Soil Fungi and Predicted Responses of Guilds and Growth Forms to Climate Change

Kevin K. Newsham[1], Marie L. Davey[2], David W. Hopkins[3] and Paul G. Dennis[4]*

[1]British Antarctic Survey, Natural Environment Research Council, Cambridge, United Kingdom, [2]Norwegian Institute for Nature Research, Trondheim, Norway, [3]Scotland's Rural College, Edinburgh, United Kingdom, [4]School of Earth and Environmental Sciences, The University of Queensland, Brisbane, QLD, Australia

We report a metabarcoding study documenting the fungal taxa in 29 barren fellfield soils sampled from along a 1,650 km transect encompassing almost the entire maritime Antarctic (60–72°S) and the environmental factors structuring the richness, relative abundance, and taxonomic composition of three guilds and growth forms. The richness of the lichenised fungal guild, which accounted for 19% of the total fungal community, was positively associated with mean annual surface air temperature (MASAT), with an increase of 1.7 operational taxonomic units (OTUs) of lichenised fungi per degree Celsius rise in air temperature. Soil Mn concentration, MASAT, C:N ratio, and pH value determined the taxonomic composition of the lichenised guild, and the relative abundance of the guild was best predicted by soil Mn concentration. There was a 3% decrease in the relative abundance of the saprotrophic fungal guild in the total community for each degree Celsius rise in air temperature, and the OTU richness of the guild, which accounted for 39% of the community, was negatively associated with Mn concentration. The taxonomic composition of the saprotrophic guild varied with MASAT, pH value, and Mn, NH_4^+-N, and SO_4^{2-} concentrations. The richness of the yeast community, which comprised 3% of the total fungal community, was positively associated with soil K concentration, with its composition being determined by C:N ratio. In contrast with a similar study in the Arctic, the relative abundance and richness of lichenised fungi declined between 60°S and 69°S, with those of saprotrophic Agaricales also declining sharply in soils beyond 63°S. Basidiomycota, which accounted for 4% of reads, were much less frequent than in vegetated soils at lower latitudes, with the Ascomycota (70% of reads) being the dominant phylum. We conclude that the richness, relative abundance, and taxonomic composition of guilds and growth forms of maritime Antarctic soil fungi are influenced by air temperature and edaphic factors, with implications for the soils of the region as its climate changes during the 21st century.

Keywords: Agaricales, ascomycetes, climate warming, phylogenetic marker (ITS2) sequencing, lichenised fungi, maritime Antarctica, saprotrophic fungi, yeasts

OPEN ACCESS

Edited by:
Laura Zucconi, University of Tuscia, Italy

Reviewed by:
Lucia Muggia, University of Trieste, Italy
Andrea Karime Barrera, University of Talca, Chile

****Correspondence:***
Kevin K. Newsham
kne@bas.ac.uk

Specialty section:
This article was submitted to Extreme Microbiology, a section of the journal Frontiers in Microbiology

Received: *09 October 2020*
Accepted: *22 December 2020*
Published: *26 January 2021*

Citation:
Newsham KK, Davey ML, Hopkins DW and Dennis PG (2021) Regional Diversity of Maritime Antarctic Soil Fungi and Predicted Responses of Guilds and Growth Forms to Climate Change. Front. Microbiol. 11:615659. doi: 10.3389/fmicb.2020.615659

INTRODUCTION

Although recent studies have described the fungi present in continental Antarctic soils and identified the factors controlling their activities and frequencies (Chan et al., 2013; Dreesens et al., 2014; Archer et al., 2019; Canini et al., 2020; Sannino et al., 2020), our understanding of the fungi inhabiting maritime Antarctic soils is still in its infancy. This knowledge gap is significant, since fungi have pivotal roles in all terrestrial ecosystems as decomposers of organic matter and as partners in symbioses, and notably the lichen symbiosis, which is widespread in maritime Antarctica (Øvstedal and Smith, 2001). A further imperative to study soil fungi in maritime Antarctica is that the region underwent significant change in the latter half of the 20th century, with near surface air temperatures rising by up to 3°C between the 1950s and late 1990s (Adams et al., 2009). Although this warming trend has recently slowed (Turner et al., 2016), surface air temperatures in the region are predicted to increase during the 21st century as greenhouse gases accumulate in the atmosphere (Bracegirdle et al., 2008; Bracegirdle and Stephenson, 2012). Given the roles of fungi in the decomposition process and as lichen symbionts, it follows that changes to their diversity caused by rising temperatures could influence the responses of maritime Antarctic terrestrial ecosystems to climate change.

The responses of soil fungal communities to the steep changes in environmental conditions across the maritime Antarctic – notably the significant reductions in surface air temperatures at higher latitudes in the region – have been foci for several studies (Lawley et al., 2004; Yergeau et al., 2007a; Dennis et al., 2012; Newsham et al., 2016). Although edaphic factors such as soil pH, Mn concentration, and C:N ratio account for variation in community composition (Yergeau et al., 2007a; Dennis et al., 2012; Newsham et al., 2016), the species richness of all soil fungi in the region is primarily determined by mean annual surface air temperature (MASAT), with reductions in the total number of fungal species in colder soils at higher latitudes (Newsham et al., 2016). However, the environmental factors controlling the relative abundances and taxonomic compositions of the predominant guilds and growth forms of fungi present in maritime Antarctic soils have yet to be identified. In the Arctic, research along a transect from Alaska (69°N) through to Ellef Ringnes Island in the High Arctic (79°N) indicates significant responses of three soil fungal guilds and growth forms to changes in environmental conditions at higher latitudes, with significant increases in the relative abundances of lichenised fungi and yeasts, and reductions in those of the ectomycorrhiza-forming fungi, in more northerly soils (Timling et al., 2014). It is possible that the abundances of lichen-forming fungi and yeasts might similarly alter across the maritime Antarctic, but studies have hitherto not addressed this possibility. In particular, increases in the abundances of yeasts might be anticipated in soils at higher latitudes in the region, since these are apparently the only fungi that can be isolated from soils in the McMurdo Dry Valleys in the continental Antarctic (Atlas et al., 1978), considered to be among some of the most hostile environments for life on Earth. Ectomycorrhizal symbioses, which are formed predominantly by basidiomycete fungi (Smith and Read, 2008), appear to be entirely absent from Antarctica owing to a lack of woody host plant species (Newsham et al., 2009). However, field observations suggest that another group of basidiomycetes, the sporocarp-forming Agarics, might decline in abundance at higher latitudes, with fruiting bodies of these fungi typically being restricted to habitats at the lowest latitudes in maritime Antarctica (Pegler et al., 1980).

Next generation sequencing, which offers greater sampling depth than cloning methods (Lawley et al., 2004; Yergeau et al., 2007a; Bridge and Newsham, 2009), has previously been used to determine the taxonomic compositions of soil fungal communities in the Americas, Asia, Africa, Europe, and Australasia (Tedersoo et al., 2014; Bahram et al., 2018; Egidi et al., 2019). However, Antarctica has been neglected in these studies, and, although this technique has been used several times previously to characterise the fungal communities of maritime Antarctic soils, detailed taxonomic information for the fungi present in a wide range of soils has yet to be presented. For example, two such studies have reported fungal taxa in two vegetated soils sampled from the region (Cox et al., 2016, 2019). Another study, despite basing its analyses on all fungal taxa in 29 soils sampled from across almost the entire maritime Antarctic, reported only the 50 most frequent taxa (Newsham et al., 2016). Here, we use the data reported by this study to characterise in much greater detail the regional diversity of maritime Antarctic soil fungi and to investigate the environmental factors structuring the compositions of lichenised and saprotrophic fungal guilds and yeast communities in the region, which were not addressed by Newsham et al. (2016). We sought to identify how environmental factors that can be expected to change over future decades in maritime Antarctica, such as MASAT, soil C:N ratio, and N concentrations (Newsham et al., 2016; Hill et al., 2019), are associated with the species richness, abundance, and composition of each of these guilds and growth forms, in order to predict how they will respond to further climate change in the region.

MATERIALS AND METHODS

Soils were sampled as described by Newsham et al. (2016) in November 2007 to February 2008 from 29 sites along a 1,650 km latitudinal transect between Signy Island in the South Orkney Islands (60°S) and south-eastern Alexander Island (72°S; **Figure 1A**). The soils that were collected were devoid of vegetation (**Figures 1B–E**) and were hence representative of the barren soils that typically form in maritime Antarctica. The sampling sites were either accessed by small boat or helicopter deployed from a ship, by fixed wing aircraft fitted with skis, or by foot from research stations. At each site, five samples of soil (0–50 mm depth, *c.* 50 cm^3) were placed into DNA/RNAase-treated tubes and bulked. Biological soil crusts, stones, and visible lichen thalli were avoided. The soils were frozen immediately at *c.* −80°C in a mixture of dry ice and ethanol and were kept at this temperature until processing.

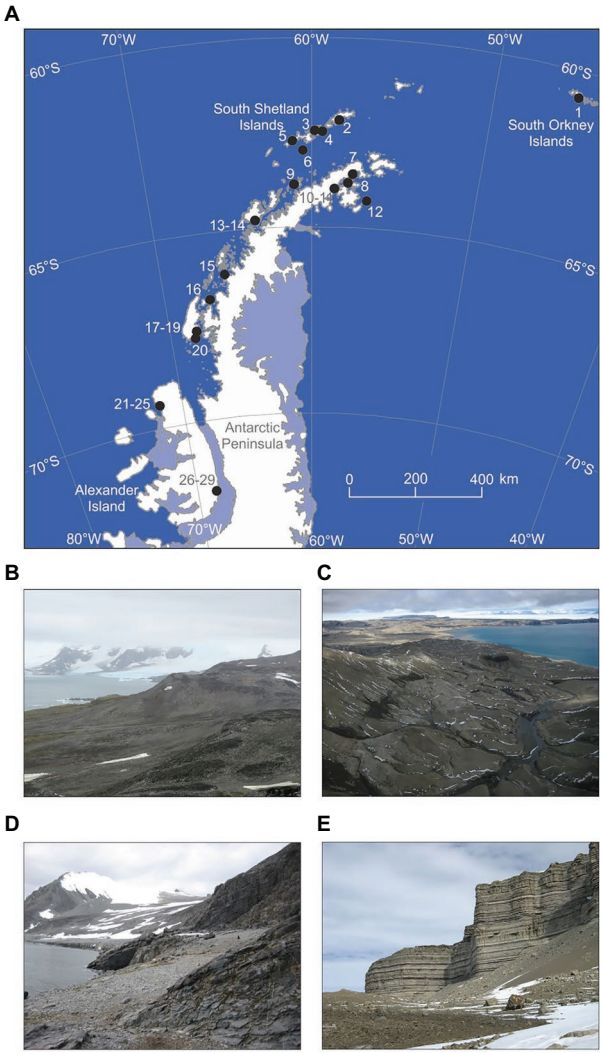

FIGURE 1 | (A) Locations of sampling sites. 1: Wynn Knolls, Signy Island (60.701°S, 45.661°W), 2: Keller Peninsula, King George Island (62.086°S, 58.399°W), 3: Orión Point, Greenwich Island (62.447°S, 59.736°W), 4: Edwards Point, Robert Island (62.460°S, 59.509°W), 5: South Beaches, Byers Peninsula, Livingston Island (62.655°S, 61.090°W), 6: Whalers Bay, Deception Island (62.977°S, 60.552°W), 7: Newsham Nunatak (63.559°S, 57.823°W), 8: Cape Lachman, James Ross Island (63.782°S, 57.783°W), 9: Spert Island (63.844°S, 60.945°W), 10–11: Alectoria Island (63.977°S, 58.640°W), 12: Marambio Station (ARG), Seymour Island (64.236°S, 56.626°W), 13: Port Lockroy, Goudier Island (64.817°S, 63.483°W), 14: Yelcho Station (CHL), Wiencke Island (64.894°S, 63.553°W), 15: Cape Evenson, Antarctic Peninsula (66.145°S, 65.717°W), 16: Detaille Island (66.790°S, 66.869°W), 17–19: Blaiklock Island, Rothera Point and Lagoon Island (67.543°S, 67.198°W, 67.568°S, 68.114°W and 67.594°S, 68.247°W, respectively), 20: Jenny Island (67.731°S, 68.365°W), 21–25: Hopkins Ridge and Mount Holt, Alexander Island (69.366°S, 71.842°W; 69.366°S, 71.844°W; 69.367°S, 71.844°W; 69.368°S, 71.844°W and 69.408°S, 71.665°W), and 26–29: Mars Oasis, Alexander Island (71.878°S, 68.248°W). **(B–E)** Show images of sites 1, 12, 20, and 26–29, respectively.

Following the methods described by Newsham et al. (2016), 20 edaphic factors were measured in each 4-mm sieved soil, *viz.*, moisture concentration, pH (H_2O), electrical conductivity, the concentrations of total organic C and N, Ca, Cu, Fe, K, Mg, Mn, Ni, P, and Zn, and those of water-extractable PO_4^{3-}, SO_4^{2-}, Cl^-, NH_4^+-N, NO_3^--N/NO_2^-N, and dissolved organic carbon (DOC). Soil C:N ratio was also calculated. Data for each of the 29 soils are shown by Dennis et al. (2020). The soils that were sampled were on average slightly acidic, had low total organic C and N concentrations, and, in comparison with mineral soils at lower latitudes, had low NH_4^+-N, NO_3^--N/NO_2^-N, and K concentrations, low to moderate concentrations of PO_4^{3-}, and high concentrations of K, Ca, Mg, and Mn (cf. Allen, 1989; **Table 1**). The remote locations of most of the studied sites precluded the direct measurement of soil temperatures, and so MASAT at each location for 2007 was derived from the Regional Atmospheric Climate Model over Antarctica (Van Lipzig et al., 1999), gridded at a horizontal resolution of 55 × 55 km. Regression analyses indicated a significant decline in MASAT from −4 to −11°C, and an increase in total C:N ratio from 3 to 10, between 60°S and 72°S (both r^2 = 31–33%, p<0.002), but no significant changes in other edaphic factors or altitude (Newsham et al., 2016).

The methods used to extract DNA from soil and amplify internal transcribed spacer 2 (ITS2) encoding genes, and the downstream processing of sequence data (which have been deposited in the NCBI short read archive), are described in detail by Newsham et al. (2016). Briefly, total DNA was extracted under aseptic conditions from soil using a commercial soil DNA isolation kit. The ITS2 region of fungal ribosomal RNA encoding genes was amplified by PCR using the primers gITS7 (5' GTGARTCATCGARTCTTTG; Ihrmark et al., 2012) and ITS4 (5' TCCTCCGCTTATTGATATGC; White et al., 1990). The use of these primers avoided the distortion of community composition associated with the ITS1F/ITS4 primer pair in next generation sequencing studies (Ihrmark et al., 2012). The forward primer was 5'-labelled with the 454 FLX sequencing primer adapter B sequence and the reverse primer with a 5'-labelled sample specific barcode sequence and the 454 FLX sequencing primer adapter A sequence. Amplicons from PCRs were purified and quantified before each sample was pooled, purified again, and then 454 pyrosequenced (Margulies et al., 2005) at a commercial facility. The sequences were quality filtered and dereplicated using the QIIME script split_libraries.py procedure, with the homopolymer filter deactivated (Caporaso et al., 2010). Acacia v. 1.48 (Bragg et al., 2012) was used to correct homopolymer errors and fungal ITS2 sequences were extracted with ITSx v. 1.0.9 (Bengtsson-Palme et al., 2013). Sequences were checked for chimeras against ITS2 sequences in UNITE v. 8.2 (Nilsson et al., 2015) using UCHIME v. 3.0.617 (Edgar, 2010). operational taxonomic units (OTUs) that could not be assigned to the kingdom Fungi were deleted from the dataset. At least 1,435 non-chimeric quality-filtered ITS2 sequences were derived from each soil sample. The sequences were clustered using UCLUST v. 1.2.22, at 97% similarity. UNITE v. 8.2 taxonomy (Kõljalg et al., 2013) was assigned to representative OTU sequences using BLAST v. 2.2.30, with the exception that members of *Mortierella* were assigned to the Mucoromycotina (Hibbett et al., 2007). Tables containing the abundances of different OTUs and their taxonomic

TABLE 1 | Summary edaphic factors of the sampled soils.

Parameter	Mean	Range
Moisture concentration	19.31	3.88–71.03
pH (H_2O)	6.64	5.26–7.76
Electrical conductivity	55.54	14.45–415.80
Organic C concentration	1.38	0.01–16.76
N concentration	0.21	0.01–2.57
Organic C:N ratio	6.64	1.59–13.87
Ca concentration	28.67	2.37–244.18
Cu concentration	66.10	0.00–290.40
Fe concentration	44.50	3.99–105.43
K concentration	2.43	0.11–10.00
Mg concentration	11.26	2.29–60.66
Mn concentration	1.06	0.15–3.67
Ni concentration	22.49	4.00–153.33
P concentration	5.41	0.16–58.84
Zn concentration	95.46	13.00–460.67
Dissolved organic C concentration	1.65	<0.01–11.45
Dissolved NO_3^--N/NO_2^--N concentration	0.08	<0.01–0.96
Dissolved NH_4^+-N concentration	0.55	<0.01–1.61
Dissolved SO_4^{2-} concentration	11.52	<0.01–180.49
Dissolved PO_4^{3-}-P concentration	4.48	<0.01–63.39
Dissolved Cl^- concentration	33.03	3.40–278.15

Units are mg kg^{-1} dry soil for all parameters except concentrations of moisture (%), Mg, P, K, Ca, Mn, and Fe (g kg^{-1}), electrical conductivity ($\mu S\ cm^{-1}$), pH, and C:N ratio (dimensionless). For methods, see Newsham et al. (2016).

assignments in each sample were generated and the number of reads was rarefied to 1,400 per sample. Richness was defined as the total number of observed OTUs per sample. In addition, guilds and growth forms were assigned to each OTU using FUNguild v. 1.0 (Nguyen et al., 2016), including taxa for which the trophic mode assignments were "highly probable" or "probable," and with minor manual adjustments (**Supplementary Table S1**). This procedure assigned a guild or growth form to 198, 238, and 66 OTUs of lichen-forming fungi, saprotrophic fungi and yeasts, respectively (**Supplementary Table S1**). Saprotrophic fungi included both filamentous fungal and obligate and facultative yeast genera (**Supplementary Table S1**). Only 10% of OTUs could be assigned to mycorrhizal, mycoparasitic, plant parasitic, or animal pathogenic fungal guilds, and so were not included in further guild level analyses.

Data analyses were implemented using R v. 3.6.3. Graphic summaries of the relative abundances of members of the soil fungal community were generated using the metacoder package (Foster et al., 2017). Regression analyses were used to determine associations between latitude and the number of OTUs and relative abundances in the total fungal community of each guild or growth form. Owing to there being *a priori* evidence of reduced frequencies of basidiocarp-forming Agarics at higher latitudes in maritime Antarctica (Pegler et al., 1980), regression analyses were also used to determine the association between the relative abundances of the saprotrophic Agaricales and latitude. Relationships between MASAT and edaphic factors and the richness and relative abundances of OTUs assigned to lichenised and saprotrophic fungal guilds, or to yeasts, were assessed using multiple linear regression with forward selection of significant predictors. The associations between MASAT and edaphic factors and the compositions of lichenised and saprotrophic fungal guilds, or yeast communities, were assessed using permutational multivariate analysis of variance (PERMANOVA), as implemented in the vegan package (Oksanen et al., 2017). The relative abundances of OTUs were Hellinger transformed prior to analysis and parsimonious PERMANOVA models were built by forward selection of significant predictors.

RESULTS

Taxonomic Composition of Maritime Antarctic Soil Fungal Communities

After rarefying the sequencing data to 1,400 reads per sample, a total of 1,220 fungal OTUs were recorded in the 29 soils, with 770 OTUs being assigned to taxa (**Supplementary Table S1**). Ascomycota dominated the soil fungal community, with 69.89% of reads being assigned to this phylum, whereas the phylum Basidiomycota accounted for only 4.36% of reads (**Supplementary Table S1**). Of the basal fungi, reads assigned to the Chytridiomycota, Glomeromycota and Mucoromycotina were present at relative abundances of 0.002, 0.007, and 8.863%, respectively (**Supplementary Table S1**). Other basal phyla or sub-phyla were not recorded in the soils.

There was a significant positive association between the occupancy of an individual OTU (the percentage of the 29 soils in which it was recorded) and its relative abundance (r^2 adj. = 52.2%, $F_{1,1,218}$ = 1332.7, p<0.001; **Figure 2**). Fungi with high occupancy or frequency, defined here as occurring in >50% of the soils and at >1% relative abundances, were almost exclusively members of the Ascomycota. The only OTU recorded in all 29 soils was *Pseudogymnoascus roseus* (**Figure 2**). The next most widespread OTUs, recorded in 24 (83%) of the soils, were a *Mortierella* species and *Cladosporium halotolerans*. Representatives of *Antarctomyces*, *Fusarium*, *Pseudeurotium*, and unclassified ascomycetes occurred in 18–20 (62–69%) of the soils. Members of the genera *Atla*, *Lobaria*, and *Catenulifera*, the family Verrucariaceae, along with two unclassified ascomycetes, occurred in 15–17 (52–59%) of the soils along the transect, but all of these taxa, except for the unidentified ascomycetes, occurred at relative abundances of <1% (**Figure 2**). Other taxa that occurred in <50% of the soils, but were present at relative abundances of >1%, were *Lecidea cancriformis*, *Mortierella polygonia*, *Penicillium polonicum*, *Verrucaria* spp., and unclassified ascomycetes (**Figure 2**).

Taxonomic Composition of Guilds and Growth Forms

Lichenised fungi accounted for 18.8% of all reads, and primarily belonged to the Verrucariaceae (Verrucariales, Eurotiomycetes; **Figure 3**; **Supplementary Table S1**). Representatives of this family consisted primarily of *Verrucaria* OTUs (8.5% of reads), but also *Polyblastia* (1.6%), *Atla* (0.7%), *Staurothele* (0.1%), and six other genera (each <0.1%; **Figure 3**; **Supplementary Table S1**). Lichenised Lecanoromycetes were also frequent, including the genera *Lecidea* (2.0%), *Acarospora*

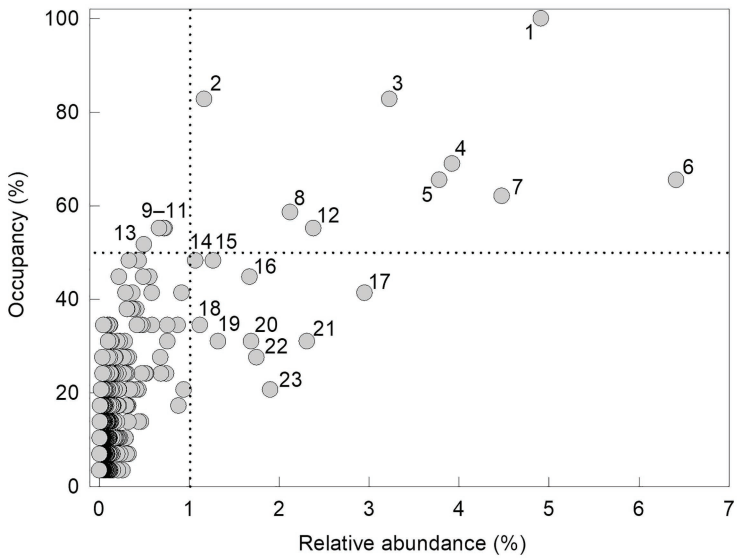

FIGURE 2 | Occupancy of operational taxonomic units (OTUs) as a function of their relative abundance. OTUs recorded in >50% of soils and at relative abundances of >1% (denoted by the dotted lines) are labelled (1: *Pseudogymnoascus roseus*, 2: *Cladosporium halotolerans*, 3: *Mortierella* sp., 4: unclassified ascomycete, 5: *Antarctomyces* sp., 6: *Fusarium* sp., 7: *Pseudeurotium hygrophilum*, 8: unclassified ascomycete, 9: *Atla* sp., 10: Verrucariaceae sp., 11: *Lobaria pseudopulmonaria*, 12: unclassified ascomycete, 13: *Catenulifera* sp., 14–15: unclassified ascomycetes, 16: *Lecidea cancriformis*, 17: *Mortierella polygonia*, 18–19: unclassified ascomycetes, 20: *Penicillium polonicum*, 21–22: *Verrucaria* spp., and 23: unclassified ascomycete).

(1.5%), *Lobaria* (0.7%), *Aspicilia* (0.6%), *Placopsis* (0.5%), *Xanthoparmelia* (0.4%), *Cetrelia* (0.4%), *Caloplaca* (0.3%), *Montanelia* (0.2%), *Psoroma* (0.2%), *Umbilicaria*, *Lecanora*, *Psilolechia*, and *Cladonia* (each 0.1%), and 20 others (each <0.1%; **Figure 3**; **Supplementary Table S1**).

Saprotrophic fungi accounted for 38.7% of all reads. Among the saprotrophs, members of the ascomycete classes Eurotiomycetes, Leotiomycetes, Dothideomycetes, and Sordariomycetes were frequent, with *Fusarium* (6.4%), *Pseudogymnoascus* (5.1%), *Pseudeurotium* (4.7%), *Antarctomyces* (3.9%), *Penicillium* (1.8%), *Cladosporium* (1.6%), *Alatospora* (1.1%), *Tetracladium* (1.1%), *Catenulifera* (0.5%), *Cladophialophora* (0.4%), *Rhinocladiella* (0.4%), *Hyaloscypha* (0.2%), *Aspergillus* (0.2%), *Acremonium* (0.2%), *Glarea* (0.2%), and *Phoma* (0.1%) being the most abundant genera detected, along with 22 other saprotrophic ascomycete genera (each <0.1%; **Figure 3**; **Supplementary Table S1**). The most abundant saprotrophic genus was *Mortierella* (8.8%), the only genus recorded in the Mucoromycotina (**Figure 3**; **Supplementary Table S1**).

The yeasts, the majority of which were basidiomycetes, accounted for 3.1% of all reads. Tremellomycetes and Microbotryomycetes were the most frequent classes, and consisted primarily of the obligate yeasts *Rhodotorula* (0.6%), *Cryptococcus* (0.3%), *Mrakia* (0.2%), and *Leucosporidiella* (0.2%), along with seven other yeast genera (**Figure 3**; **Supplementary Table S1**). Facultative ascomycete yeasts in the Chaetothyriales (Eurotiomycetes) were also recorded, with *Capronia* (0.6%), *Cladophialophora* (0.4%), and *Rhinocladiella* (0.4%) being the most frequent genera recorded in this order (**Figure 3**; **Supplementary Table S1**).

Changes in Soil Fungal Community Composition With Latitude

Lichenised Fungi

The proportion of lichenised fungi in the total soil fungal community changed significantly with latitude, with a sharp decline from 22 – 69% of the community in the South Orkney and South Shetland islands (60–63°S) to ≤8% on north-west Alexander Island at 69°S (**Figure 4A**). However, there was a subsequent increase in the relative abundance of lichenised fungi to 15–37% of the community on southern Alexander Island (72°S), resulting in a first order polynomial relationship between frequency and latitude (r^2 adj. = 57.3%, $F_{1,28}$ = 19.80, p<0.001). This increase was partly driven by increased abundance of *Acarospora*, *Polyblastia*, and *Cetrelia*, an observation supported by PERMANOVA analyses showing highly significant effects of latitude on the taxonomic composition of the lichenised fungal guild ($F_{1,27}$ = 3.35, p = 0.001). The association between the OTU richness of lichenised fungi and latitude also followed a similar pattern, and was best described by a first order polynomial (r^2 adj. = 34.8%, $F_{2,26}$ = 8.48, p=0.001; **Figure 4B**).

Saprotrophic Fungi

Regression analyses indicated that neither the proportion of saprotrophs in the total fungal community (r^2 adj. = 6.2%, $F_{1,27}$ = 2.86, p>0.1) nor saprotrophic OTU richness (r^2 adj. = 0.0%, $F_{1,27}$ = 0.47, p>0.5) varied significantly with latitude (**Supplementary Figure S1**). However, regression analyses identified declining abundance of saprotrophic Agaricales in soils beyond 63°S, with a significant hyperbolic relationship

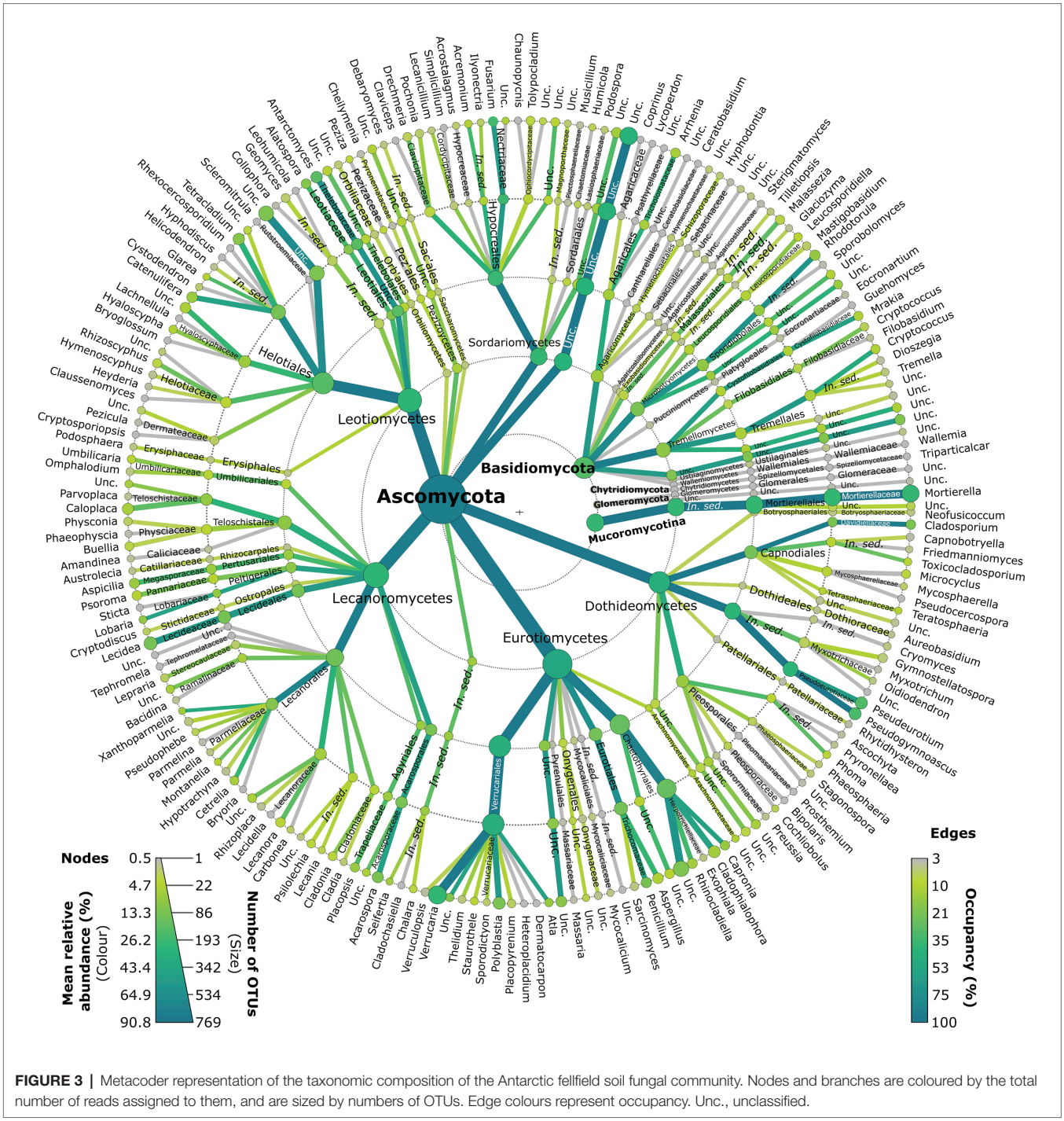

FIGURE 3 | Metacoder representation of the taxonomic composition of the Antarctic fellfield soil fungal community. Nodes and branches are coloured by the total number of reads assigned to them, and are sized by numbers of OTUs. Edge colours represent occupancy. Unc., unclassified.

between the relative abundance of the order and latitude (**Figure 4C**). These fungi, which were primarily *Arrhenia* OTUs (**Supplementary Table S1**), were relatively abundant (4.2–4.8%) in soils at the northern end of the transect sampled from Signy Island and Greenwich Island (60°S and 62°S, respectively) but did not exceed 0.4% abundance in the 27 other soils (r^2 adj. = 58.9%, $F_{1,28}$ = 31.85, p<0.001; **Figure 4C**). Saprotrophic Agaricales OTU richness followed a similar hyperbolic association, with five *Arrhenia* OTUs recorded in soil from Signy Island and 0–2 OTUs of saprotrophic Agaricales recorded in other, more southerly soils (r^2 adj. = 70.9%, $F_{1,28}$ = 23.18, p<0.001; **Figure 4D**).

Yeasts

The relative abundance of yeasts in the total fungal community, and the OTU richness of the growth form, did not vary with latitude (both r^2 adj. = 0.0%, $F_{1,27}$ = 0.07–0.17, both p>0.7; **Supplementary Figure S1**).

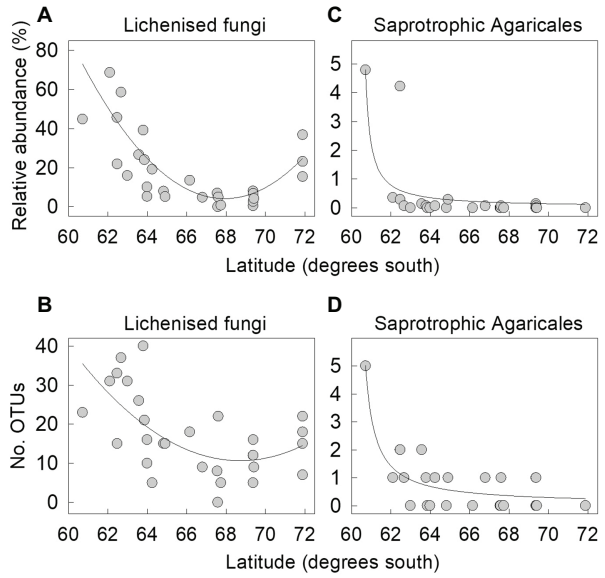

FIGURE 4 | The relative abundances of **(A,C)** lichenised fungi and saprotrophic Agaricales as functions of latitude and the number of OTUs of **(B,D)** lichenised fungi and saprotrophic Agaricales as functions of latitude. Lines show significant first order polynomial **(A,B)** and hyperbolic **(C,D)** fits.

Factors Structuring Guilds and Growth Forms

Lichenised Fungi

Multiple regression models using forward selection indicated that the relative abundance of lichenised fungi in the total fungal community was best predicted by soil Mn concentration, with a positive association between the abundance of the guild and this variable (t = 3.25, p = 0.003; **Figure 5A**). The OTU richness of the lichenised guild was best explained by MASAT, with soil DOC concentration and C:N ratio also predicting the numbers of OTUs of these fungi (**Table 2**). Lichenised fungal OTU richness was positively associated with MASAT (slope = 1.69 species per degree Celsius) and negatively so with DOC concentration (**Figures 5C,D**). PERMANOVA indicated that soil Mn concentration best predicted the composition of the lichenised fungal guild, with MASAT, C:N ratio, and pH value also predicting guild composition (**Table 3**).

Saprotrophic Fungi

The relative abundance of saprotrophic fungi was best predicted by MASAT, with a negative association between the abundance of the guild in the total fungal community and this variable (t = −2.19, p = 0.037; slope = −3.01% per degree Celsius; **Figure 5B**). The OTU richness of the guild was negatively associated with soil Mn concentration (**Table 2**; **Figure 5E**). Its composition was best predicted by dissolved NH_4^+-N concentration, with significant, but weaker, effects of MASAT, pH value, and Mn and dissolved SO_4^{2-} concentrations (**Table 3**).

Yeasts

None of the measured environmental and edaphic factors significantly (p<0.05) predicted the relative abundance of the yeasts in the total fungal community. Multiple regression models indicated that yeast OTU richness was positively associated with soil K concentration (**Table 2**; **Figure 5F**), and PERMANOVA analyses showed that the taxonomic composition of the community was significantly associated with soil C:N ratio (**Table 3**).

DISCUSSION

Maritime Antarctic terrestrial ecosystems underwent significant changes during the second half of the 20th century, with rises in MASAT of 0.13–0.55°C per decade being recorded across the region (Adams et al., 2009). Although this warming trend has since slowed (Turner et al., 2016), temperature increases of 2–4°C are predicted in the region by the end of the 21st century as greenhouse gases continue to accumulate in the atmosphere (Bracegirdle et al., 2008; Bracegirdle and Stephenson, 2012). Building on a previous report predicting that the total species richness of maritime Antarctic soil fungi will increase with rising air temperatures (Newsham et al., 2016), the observations here indicate that increases in MASAT will differentially affect two guilds of fungi inhabiting the fellfield soils of the region, with the lichenised fungal guild likely to show increases in species richness, and the saprotrophic guild potentially showing decreases in its relative abundance, as the region warms. We anticipate that the significant influence of MASAT on the lichenised and saprotrophic fungal guilds reflect not only the positive association between air temperature and soil temperature (Qian et al., 2011; Fang et al., 2019), with consequent effects on soil fungal diversity (Newsham et al., 2016), but are also indicative of the influence of temperature on water availability. Air temperatures in maritime Antarctic terrestrial ecosystems are routinely close to freezing point during summer (Convey et al., 2018), and there is thus a strong positive effect of increasing temperature on the availability of liquid water. Although unlikely to explain the reduced relative abundance of saprotrophs, higher water availability, combined with more frequent rainfall in warmer habitats (Turner et al., 2002), would allow increased productivity and metabolism of lichenised fungi, and permit a switch from survival to growth and dispersal strategies, explaining the positive association between the species richness of the guild and MASAT (Green et al., 2011). Thus, although instantaneous measurements of soil moisture concentration were not a significant predictor in the analyses here, we anticipate that long-term measurements of water availability would have been associated with soil fungal diversity.

Although MASAT was a significant predictor for the richness, relative abundance, and composition of the lichenised and saprotrophic fungal guilds, seven edaphic factors (pH value, C:N ratio, and the concentrations of Mn, K, SO_4^{2-}, DOC, and NH_4^+-N) also correlated with the diversities of the fungal

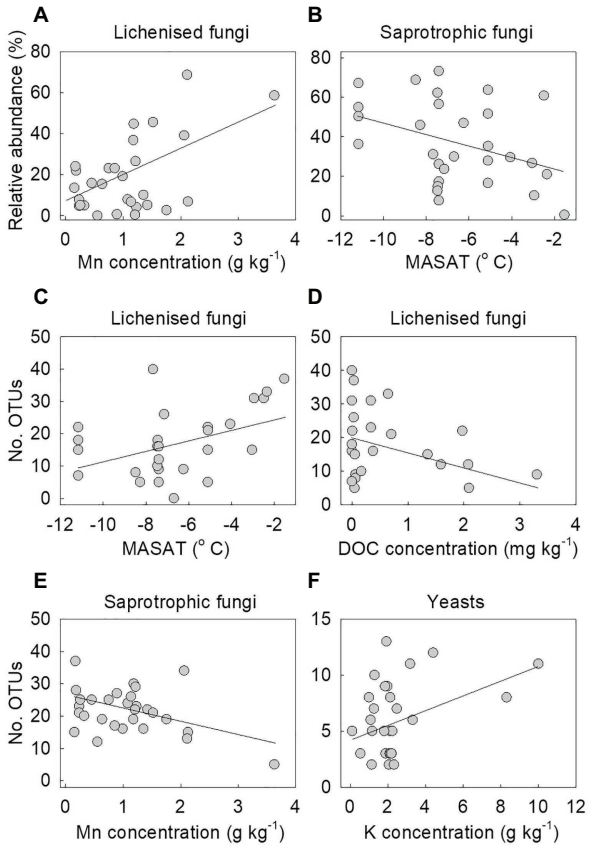

FIGURE 5 | The relative abundances of **(A)** lichenised and **(B)** saprotrophic fungi as functions of soil Mn concentration and mean annual surface air temperature (MASAT), respectively, and the number of OTUs of lichenised fungi as a function of **(C)** MASAT and **(D)** dissolved organic carbon (DOC) concentration, and of **(E)** saprotrophic fungi as a function of Mn concentration and **(F)** yeasts as a function of K concentration. Lines are significant linear fits.

TABLE 2 | Data from multiple regression models using forward selection showing the final model best explaining observed OTU richness within guilds and growth forms of maritime Antarctic soil fungi.

Guild or growth form	Predictors	*t* value	*p*
Lichenised fungi	MASAT	4.87	<0.001
	Dissolved organic C concentration	−3.26	0.001
	C:N ratio	3.34	0.003
Saprotrophic fungi	Mn concentration	−2.31	0.029
Yeasts	K concentration	2.19	0.037

guilds and growth forms studied here. It is important to note that, owing to the correlative nature of the analyses reported here, we cannot be certain of causal relationships between some of the edaphic factors and soil fungal diversity. Notably, the reasons for the relationships between guild diversity and soil Mn concentration, which also partially predicts total soil fungal community composition (Newsham et al., 2016), are

TABLE 3 | Data from permutational multivariate analysis of variance (PERMANOVA) models using forward selection on Hellinger-transformed data showing the factors best explaining the taxonomic composition of guilds and growth forms of maritime Antarctic soil fungi.

Guild or growth form	Predictors	r^2	*F* value	*p*
Lichenised fungi	Mn concentration	12.2	4.36	<0.001
	MASAT	10.4	3.71	<0.001
	C:N ratio	5.2	1.85	0.035
	pH value	5.1	1.84	0.036
Saprotrophic fungi	Dissolved NH_4^+-N concentration	9.1	3.19	<0.001
	MASAT	7.9	2.78	0.004
	pH value	5.5	1.95	0.033
	Mn concentration	5.9	2.09	0.022
	Dissolved SO_4^{2-} concentration	6.4	2.27	0.021
Yeasts	C:N ratio	8.8	2.61	0.005

presently unclear, and changes to the concentrations of this element, along with those of K, SO_4^{2-}, and H^+, seem unlikely in warmer and wetter maritime Antarctic soils. However, changes to soil C:N ratio and concentrations of DOC and NH_4^+-N are plausible as the climate of the region changes. The analyses here indicate that declines in the ratio of C:N in warmer and less arid soils (Callesen et al., 2007), which most probably arise from accelerated C cycling (Swift et al., 1979), will influence the compositions of the yeast community and the lichenised fungal guild, and will offset any increases in the species richness of lichenised fungi resulting from rising air temperatures. The analyses here also indicate that increases in soil DOC and NH_4^+-N concentrations, which can be anticipated as decomposition, and particularly that of amino acids and proteins, accelerates in warmer and less arid maritime Antarctic soils (Kalbitz et al., 2000; Bond-Lamberty and Thomson, 2010; Hill et al., 2011, 2019), will alter the composition of the saprotrophic fungal guild and, as for C:N ratio, offset the increasing species richness of lichenised fungi associated with increasing MASAT.

While previous analyses have indicated that rising air temperature is associated with increased abundances of three OTUs assigned to the Verrucariaceae, and a decrease in a further OTU in the family (Newsham et al., 2016), the data reported here suggest an increase of 1.7 species of all lichenised fungi per degree Celsius rise in MASAT. These were typically mycobionts of saxicolous lichens, such as *Verrucaria*, *Polyblastia*, *Lecidea*, and *Acarospora* (Øvstedal and Smith, 2001). Other studies have also found higher numbers of lichen species in warmer habitats along the Antarctic Peninsula, albeit at higher rates of change, with increases of 24 usually saxicolous species per degree Celsius rise in MASAT (Peat et al., 2007; Green et al., 2011). Given the roles of the lichen symbiosis in cold and arid environments – such as the fixation of C and N from the atmosphere, mineral weathering, and the stabilisation of biological soil crusts (Gold and Bliss, 1995; Pointing and Belnap, 2012; Colesie et al., 2014) – it seems likely that increased species richness of lichenised fungi will

have positive impacts on Antarctic terrestrial ecosystems. However, it is important to note that the studies of Peat et al. (2007) and Green et al. (2011) analyzed records of lichen specimens lodged in herbaria, whereas the study here was based on DNA amplified from soils from which visible lichen thalli were absent, suggesting that maritime Antarctic fellfield soils are rich sources of inoculum for the mycobionts of the saxicolous lichens that are frequent in the region (Øvstedal and Smith, 2001).

Saprotrophic fungi are central to the functioning of all terrestrial ecosystems, owing to their pivotal roles in the decomposition of organic matter and the mineralisation of soil nutrients (Swift et al., 1979). Here, the most widespread saprotroph, recorded in all 29 fellfield soils, was found to be *Pseudogymnoascus roseus*, a fungus that also occurs in both continental Antarctic and high Arctic soils (Zucconi et al., 1996; Bergero et al., 1999; Onofri et al., 2007). Other abundant saprotrophic genera were *Mortierella*, the only representative of the Mucoromycotina recorded here, and a genus that is frequent in cold soils (Onofri et al., 2007; Bridge et al., 2008; Schmidt et al., 2012), along with *Fusarium*, *Pseudeurotium hygrophilum*, *Cladosporium halotolerans*, and *Antarctomyces*, the latter of which was originally described from South Shetland Island soils (Stchigel et al., 2001). The analyses here point to a reduction in the relative abundance of these, and other saprotrophic, fungal taxa as maritime Antarctic soils warm over future decades, with a 3% decrease in the abundance of these fungi in the total community for each degree Celsius rise in MASAT. Given the central role played by saprotrophic fungi in the decomposition of soil organic matter (Waksman, 1931; Lindeberg, 1947; Frankland, 1969), this finding suggests inhibited decay and nutrient cycling in warmer maritime Antarctic soils. However, saprotrophic fungal communities exhibit high levels of functional redundancy, with, for example, a wide range of taxa being capable of simple carbohydrate and cellulose decomposition (Frankland, 1969; Setälä and McLean, 2004). Given a mean of 22 saprotrophic fungal OTUs in each of the soils studied here, it seems unlikely that reductions in the relative abundances of these fungi arising from increases in air temperature of 2–4°C (Bracegirdle et al., 2008; Bracegirdle and Stephenson, 2012) will substantially affect the decomposition process.

Unlike the lichenised and saprotrophic fungal guilds, the yeast growth form, which was dominated by the facultative ascomycetous genera *Capronia*, *Cladophialophora*, and *Rhinocladiella*, and the obligate basidiomycetous genera *Cryptococcus*, *Rhodotorula*, and *Mrakia* – which frequent soils at high latitudes and altitudes (Thomas-Hall et al., 2010; Schmidt et al., 2012; Cox et al., 2016) – was apparently unresponsive to changes in MASAT and the majority of measured edaphic factors. Only soil K concentration and C:N ratio, the latter of which also predicts the composition of yeast communities on other continents (Tedersoo et al., 2014), were significant predictors for the richness and composition of the yeast community. Given the apparent tolerance of the yeast growth form to extreme environments, including both its abundance in soils of the McMurdo Dry Valleys, considered to be some of the most hostile environments for life, and on Mount Howe (87°S), the southernmost mountain on Earth (Atlas et al., 1978; Vishniac, 1996; Fell et al., 2006), increases in yeast abundance in soils at higher latitudes in maritime Antarctica might be expected. However, although such increases are recorded between 69°N and 79°N in the Arctic (Timling et al., 2014), the relative abundance and species richness of yeasts did not vary along the transect studied here.

In contrast to the yeast growth form, the abundance and richness of the lichenised fungal guild varied with latitude. Lichenised fungi accounted for up to 70% of reads from soils at 60–63°S, reflecting the dominance of the symbiosis in all but the wettest habitats of maritime Antarctica (Smith, 2000; Øvstedal and Smith, 2001; Peat et al., 2007), but their abundance and species richness decreased at up to 69°S. This finding contrasts with those of Timling et al. (2014), who showed the frequencies of lichen-forming fungi to increase at higher latitudes in the Arctic. The data here, derived from bare fellfield soils, support the conclusion of Timling et al. (2014) that interactions with higher plants, which are abundant in the Low Arctic and outcompete lichens for light, play an important role in controlling the abundances of lichen-forming fungi in soil. Despite marked decreases in the abundance and richness of lichenised fungi between 60°S and 69°S, subsequent increases in the guild were recorded in soil at Mars Oasis (72°S), suggesting that the oasis, which has a microclimate characterised by midsummer surface soil temperatures of up to 24°C (Convey et al., 2018), may be a favourable habitat not only for soil bacteria and nematodes (Maslen and Convey, 2006; Yergeau et al., 2007b) but also for lichenised fungi as well. Saprotrophic Agaricales similarly declined in relative abundance and richness in soils beyond 63°S, with only two soils at the northern end of the transect generating significant numbers of reads of these taxa. This suggests that the Agaricales, notably species of *Arrhenia*, are poorly adapted to survival in soils at high latitudes, and corroborates field observations that basidiocarps are usually restricted to soils in the South Orkney and South Shetland islands (60–62°S), with very occasional records on the western Antarctic Peninsula to 64–67°S (Pegler et al., 1980; K.K.N., pers. obs.).

In agreement with studies demonstrating that maritime Antarctic soil fungi tend to have bipolar or cosmopolitan distributions (Cox et al., 2016), 16 of the saprotrophic ascomycete genera recorded here were among the 41 genera of fungi found to dominate grassland, shrubland, and forest soils at lower latitudes (Egidi et al., 2019). These fungi were typically free-living saprotrophs with small (length <15 μm; Domsch et al., 2007) conidia, such as *Cladosporium*, *Penicillium*, and *Pseudogymnoascus*, the former of which is capable of intercontinental aerial dispersal to Antarctica (Marshall, 1997). Despite these similarities to soil saprotroph communities at lower latitudes, there are also striking differences between the soil mycoflora of maritime Antarctica and that of other landmasses. Notably, lichenised fungi were abundant in maritime Antarctic fellfield soils, accounting for 19% of all reads in the present study. In contrast, the dominant members of the

soil mycoflora on six other continents reported by Egidi et al. (2019) did not include lichenised taxa. While the Ascomycota was the dominant fungal phylum found in the fellfield soils studied here, with 70% of all reads being assigned to the phylum, just 4% of reads were assigned to the Basidiomycota. Conversely, an assessment of fungal diversity in soils under woody plant species in the Americas, Africa, Asia, Australasia, and Europe found that 31 and 56% of all fungi belonged to the Ascomycota and Basidiomycota, respectively, with 50% of all fungal OTUs being assigned to the Agaricomycetes (Tedersoo et al., 2014). As noted elsewhere (Cox et al., 2016; Newsham et al., 2016), the substantial reduction in the abundance and richness of the Basidiomycota in maritime Antarctic soils is most probably owing to the absence of woody plant species, which routinely form ectomycorrhizas with basidiomycetes, and typically Agaricomycetes, at lower latitudes (Smith and Read, 2008).

In addition to *Mortierella*, other basal fungi were recorded here, with the DNA of Glomeromycota occasionally being amplified from fellfield soils, corroborating previous observations that *Deschampsia antarctica* and *Colobanthus quitensis*, the two native Antarctic higher plant species, form sparse arbuscular mycorrhizas in the maritime Antarctic to 62°S (Upson et al., 2008). A single member of the Spizellomycetales (Chytridiomycota) was also recorded at very low frequencies, corroborating the presence of these motile fungi in southern maritime Antarctic and continental Antarctic soils (Bridge and Newsham, 2009; Dreesens et al., 2014), and those at high altitudes receiving significant amounts of snowfall (Schmidt et al., 2012). Other basal phyla or subphyla, typically animal parasites and anaerobic rumen fungi, such as members of the Kickxellomycotina, Zoopagomycotina, Entomophthoromycotina, and Neocallimastigomycotina, were not recorded in Antarctic soil, most probably reflecting an absence of suitable hosts. Nevertheless, it must be noted that the low abundances of these non-Dikaryotic fungi may reflect primer bias, as the gITS7 primer (Ihrmark et al., 2012) has been demonstrated to have mismatches to early diverging fungal lineages (Tedersoo et al., 2015).

CONCLUSION

The PERMANOVA and multiple regression analyses reported here indicate significant effects of MASAT on the species richness and relative abundance of the lichenised and saprotrophic fungal guilds, suggesting responses of these assemblages to the warming predicted in maritime Antarctica during the 21st century (Bracegirdle et al., 2008; Bracegirdle and Stephenson, 2012). These analyses also indicate that edaphic factors expected to alter in warmer and less arid maritime Antarctic soils, *viz.*, C:N ratio and concentrations of DOC and NH_4^+-N, will influence the responses of these guilds to warming. Contrary to previous research in the Arctic (Timling et al., 2014), the analyses here also show that lichenised fungi decrease in abundance at higher latitudes in maritime Antarctica, with reductions in saprotrophic Agaricales also being recorded in more southerly soils. In contrast with vegetated soils on other continents, lichenised fungal taxa were found to be frequent in fellfield soils, reflecting the abundance of the lichen symbiosis in maritime Antarctica. Despite being based on correlative data, the observations here can be used to formulate testable hypotheses in future studies examining the effects of experimental warming on soil fungal diversity in the maritime Antarctic natural environment.

DATA AVAILABILITY STATEMENT

The datasets presented in this study can be found in the NCBI short read archive (accession code PRJNA282894) and in Dennis et al. (2020) at https://data.bas.ac.uk/full-record.php?id=GB/NERC/BAS/PDC/01402

AUTHOR CONTRIBUTIONS

DH, KN, and PD secured funding and conducted fieldwork. PD generated sequence libraries and soil physicochemical data and, along with MD, analyzed data. KN conceived the study and wrote the manuscript, which was commented on and improved by the other authors. All authors contributed to the article and approved the submitted version.

FUNDING

This work was funded by the Natural Environment Research Council through its Antarctic Funding Initiative scheme (NE/D00893X/1; AFI 7/05) and by the University of Queensland through an Early Career Research Award. The funders had no role in study design, data collection and analysis, decision to publish, or preparation of the manuscript.

ACKNOWLEDGMENTS

Logistical support was provided by the British Antarctic Survey and Royal Navy (HMS *Endurance*). Vito Armando Laudicina, Victoria Ord, Phil Coates, Mike Dunn, Paul Torode, Matt Jobson, Adam Clark, James Wake, Dickie Hall, Gareth Marshall, Peter Fretwell, Magda Biszczuk, Laura Gerrish, and Kate Bazeley provided support and Steve Rushton helped with preliminary data analyses. Two reviewers supplied helpful comments on the manuscript. All are gratefully acknowledged.

SUPPLEMENTARY MATERIAL

The Supplementary Material for this article can be found online at: https://www.frontiersin.org/articles/10.3389/fmicb.2020.615659/full#supplementary-material

REFERENCES

Adams, B., Athern, R., Atkinson, A., Barbante, C., Bargagli, R., Bergstrom, D., et al. (2009). "The instrumental period," in *Antarctic climate change and the environment*. eds. J. Turner, R. A. Bindschadler, P. Convey, G. Di Prisco, E. Fahrbach, J. Gutt, et al. (Cambridge: Scientific Committee on Antarctic Research), 183–298.

Allen, S. E. (1989). *Chemical analysis of ecological materials*. Oxford: Blackwell Scientific Publications.

Archer, S. D. J., Lee, K. C., Caruso, T., Maki, T., Lee, C. K., Cary, S. C., et al. (2019). Airborne microbial transport limitation to isolated Antarctic soil habitats. *Nat. Microbiol.* 4, 925–932. doi: 10.1038/s41564-019-0370-4

Atlas, R. M., DiMenna, M. E., and Cameron, R. E. (1978). "Ecological investigations of yeasts in Antarctic soils" in *Terrestrial biology III. Vol. 30*. ed. B. C. Parker (Washington, DC: Antarctic Research Series, American Geophysical Union), 27–34.

Bahram, M., Hildebrand, F., Forslund, S. K., Anderson, J. L., Soudzilovskaia, N. A., Bodegom, P. M., et al. (2018). Structure and function of the global topsoil microbiome. *Nature* 560, 233–237. doi: 10.1038/s41586-018-0386-6

Bengtsson-Palme, J., Ryberg, M., Hartmann, M., Branco, S., Wang, Z., Godhe, A., et al. (2013). ITSx: improved software detection and extraction of ITS1 and ITS2 from ribosomal ITS sequences of fungi and other eukaryotes for use in environmental sequencing. *Methods Ecol. Evol.* 4, 914–919. doi: 10.1111/2041-210X.12073

Bergero, R., Girlanda, M., Varese, G. C., Intili, D., and Luppi, A. M. (1999). Psychrooligotrophic fungi from Arctic soils of Franz Josef Land. *Polar Biol.* 21, 361–368. doi: 10.1007/s003000050374

Bond-Lamberty, B., and Thomson, A. (2010). Temperature-associated increases in the global soil respiration record. *Nature* 464, 579–582. doi: 10.1038/nature08930

Bracegirdle, T. J., Connolley, W. M., and Turner, J. (2008). Antarctic climate change over the twenty first century. *J. Geophys. Res.* 113:D03103. doi: 10.1029/2007JD008933

Bracegirdle, T. J., and Stephenson, D. (2012). Higher precision estimates of regional polar warming by ensemble regression of climate model projections. *Clim. Dyn.* 39, 2805–2821. doi: 10.1007/s00382-012-1330-3

Bragg, L., Stone, G., Imelfort, M., Hugenholtz, P., and Tyson, G. W. (2012). Fast, accurate error-correction of amplicon pyrosequences using Acacia. *Nat. Methods* 9, 425–426. doi: 10.1038/nmeth.1990

Bridge, P. D., and Newsham, K. K. (2009). Soil fungal community composition at Mars Oasis, a southern maritime Antarctic site, assessed by PCR amplification and cloning. *Fungal Ecol.* 2, 66–74. doi: 10.1016/j.funeco.2008.10.008

Bridge, P. D., Spooner, B. M., and Roberts, P. J. (2008). List of non-lichenised fungi from the Antarctic region. Available at: https://legacy.bas.ac.uk/bas_research/data/access/fungi/ (Accessed October, 2020).

Callesen, I., Raulund-Rasmussen, K., Westman, C. J., and Tau-Strand, L. (2007). Nitrogen pools and C:N ratios in well-drained Nordic forest soils related to climate change and soil texture. *Boreal Environ. Res.* 12, 681–692.

Canini, F., Geml, J., D'Acqui, L. P., Selbmann, L., Onofri, S., Ventura, S., et al. (2020). Exchangeable cations and pH drive diversity and functionality of fungal communities in biological soil crusts from coastal sites of Victoria Land, Antarctica. *Fungal Ecol.* 45:100923. doi: 10.1016/j.funeco.2020.100923

Caporaso, J. G., Kuczynski, J., Stombaugh, J., Bittinger, K., Bushman, F. D., Costello, E. K., et al. (2010). QIIME allows analysis of high-throughput community sequencing data. *Nat. Methods* 7, 335–336. doi: 10.1038/nmeth.f.303

Chan, Y., van Nostrand, J., Zhou, J., Pointing, S. B., and Farrell, R. L. (2013). Functional ecology of an Antarctic dry valley. *Proc. Natl. Acad. Sci. U. S. A.* 110, 8990–8995. doi: 10.1073/pnas.1300643110

Colesie, C., Gommeaux, M., Green, T. G. A., and Büdel, B. (2014). Biological soil crusts in continental Antarctica: Garwood Valley, southern Victoria Land, and Darwin Hill, Darwin Mountains region. *Antarct. Sci.* 26, 115–123. doi: 10.1017/S0954102013000291

Convey, P., Coulson, S. J., Worland, M. R., and Sjöblom, A. (2018). The importance of understanding annual and shorter-term temperature patterns and variation in the surface levels of polar soils for terrestrial biota. *Polar Biol.* 41, 1587–1605. doi: 10.1007/s00300-018-2299-0

Cox, F., Newsham, K. K., Bol, R., Dungait, J. A. J., and Robinson, C. H. (2016). Not poles apart: Antarctic soil fungal communities show similarities to those of the distant Arctic. *Ecol. Lett.* 19, 528–536. doi: 10.1111/ele.12587

Cox, F., Newsham, K. K., and Robinson, C. H. (2019). Endemic and cosmopolitan fungal taxa exhibit differential abundances in total and active communities of Antarctic soils. *Environ. Microbiol.* 21, 1586–1596. doi: 10.1111/1462-2920.14533

Dennis, P. G., Newsham, K. K., and Hopkins, D. W. (2020). Physico-chemical properties of maritime Antarctic fellfield soils collected from along a latitudinal transect between Signy Island (60°S) and south-eastern Alexander Island (72°S) in November 2007–February 2008. Cambridge: UK Polar Data Centre.

Dennis, P. G., Rushton, S. P., Newsham, K. K., Lauducina, V. A., Ord, V. J., Daniell, T. J., et al. (2012). Soil fungal community composition does not alter along a latitudinal gradient through the maritime and sub-Antarctic. *Fungal Ecol.* 5, 403–408. doi: 10.1016/j.funeco.2011.12.002

Domsch, K. H., Gams, W., and Anderson, T. H. (2007). *Compendium of soil fungi. 2nd Edn.* Eching: IHW Verlag.

Dreesens, L. L., Lee, C. K., and Cary, S. C. (2014). The distribution and identity of edaphic fungi in the McMurdo Dry Valleys. *Biology* 3, 466–483. doi: 10.3390/biology3030466

Edgar, R. C. (2010). Search and clustering orders of magnitude faster than BLAST. *Bioinformatics* 26, 2460–2461. doi: 10.1093/bioinformatics/btq461

Egidi, E., Delgado-Baquerizo, M., Plett, J. M., Wang, J., Eldridge, D. J., Bardgett, R. D., et al. (2019). A few ascomycete taxa dominate soil fungal communities worldwide. *Nat. Commun.* 10:2369. doi: 10.1038/s41467-019-10373-z

Fang, X., Luo, S., and Lyu, S. (2019). Observed soil temperature trends associated with climate change in the Tibetan Plateau, 1960–2014. *Theor. Appl. Climatol.* 135, 169–181. doi: 10.1007/s00704-017-2337-9

Fell, J. W., Scorzetti, G., Connell, L., and Craig, S. (2006). Biodiversity of micro-eukaryotes in Antarctic Dry Valley soils with <5% soil moisture. *Soil Biol. Biochem.* 38, 3107–3119. doi: 10.1016/j.soilbio.2006.01.014

Foster, Z., Sharpton, T., and Grunwald, N. (2017). Metacoder: an R package for visualization and manipulation of community taxonomic diversity data. *PLoS Comput. Biol.* 13:e1005404. doi: 10.1371/journal.pcbi.1005404

Frankland, J. C. (1969). Fungal decomposition of bracken petioles. *J. Ecol.* 57, 25–36. doi: 10.2307/2258205

Gold, W. G., and Bliss, L. C. (1995). Water limitations and plant community development in a polar desert. *Ecology* 76, 1558–1568. doi: 10.2307/1938157

Green, T. G. A., Sancho, L. G., Pintado, A., and Schoeter, B. (2011). Functional and spatial pressures on terrestrial vegetation in Antarctica forced by global warming. *Polar Biol.* 34, 1643–1656. doi: 10.1007/s00300-011-1058-2

Hibbett, D. S., Binder, M., Bischoff, J. F., Blackwell, M., Cannon, P. F., Eriksson, O. E., et al. (2007). A higher-level phylogenetic classification of the fungi. *Mycol. Res.* 111, 509–547. doi: 10.1016/j.mycres.2007.03.004

Hill, P. W., Broughton, R., Bougoure, J., Havelange, R., Newsham, K. K., Grant, G., et al. (2019). Angiosperm symbioses with non-mycorrhizal fungal partners enhance N acquisition from ancient organic matter in a warming maritime Antarctic. *Ecol. Lett.* 22, 2111–2119. doi: 10.1111/ele.13399

Hill, P. W., Farrar, J., Roberts, P., Farrell, M., Grant, H., Newsham, K. K., et al. (2011). Vascular plant success in a warming Antarctic may be due to efficient nitrogen acquisition. *Nat. Clim. Chang.* 1, 50–53. doi: 10.1038/nclimate1060

Ihrmark, K., Bödeker, I. T., Martinez-Cruz, K., Friberg, H., Kubartova, A., Schenck, J., et al. (2012). New primers to amplify the fungal ITS2 region—evaluation by 454-sequencing of artificial and natural communities. *FEMS Microbiol. Ecol.* 82, 666–677. doi: 10.1111/j.1574-6941.2012.01437.x

Kalbitz, K., Solinger, S., Park, J. -H., Michalzik, B., and Matzner, E. (2000). Controls on the dynamics of dissolved organic matter in soils: a review. *Soil Sci.* 165, 277–304. doi: 10.1097/00010694-200004000-00001

Kõljalg, U., Nilsson, R. H., Abarenkov, K., Tedersoo, L., Taylor, A. F., Bahram, M., et al. (2013). Towards a unified paradigm for sequence-based identification of fungi. *Mol. Ecol.* 22, 5271–5277. doi: 10.1111/mec.12481

Lawley, B., Ripley, S., Bridge, P., and Convey, P. (2004). Molecular analysis of geographic patterns of eukaryotic diversity in Antarctic soils. *Appl. Environ. Microbiol.* 70, 5963–5972. doi: 10.1128/AEM.70.10.5963-5972.2004

Lindeberg, G. (1947). On the decomposition of lignin and cellulose in litter caused by soil-inhabiting hymenomycetes. *Ark. Bot.* 33A, 1–16.

Margulies, M., Egholm, M., Altman, W. E., Attiya, S., Bader, J. S., Bemben, L. A., et al. (2005). Genome sequencing in microfabricated high-density picolitre reactors. *Nature* 437, 376–380. doi: 10.1038/nature03959

Marshall, W. A. (1997). Seasonality in Antarctic airborne fungal spores. *Appl. Environ. Microbiol.* 63, 2240–2245. doi: 10.1128/AEM.64.3.1167-1167.1998

Maslen, N. R., and Convey, P. (2006). Nematode diversity and distribution in the southern maritime Antarctic—clues to history? *Soil Biol. Biochem.* 38, 3141–3151. doi: 10.1016/j.soilbio.2005.12.007

Newsham, K. K., Hopkins, D. W., Carvalhais, L. C., Fretwell, P. T., Rushton, S. P., O'Donnell, A. G., et al. (2016). Relationship between soil fungal diversity and temperature in the maritime Antarctic. *Nat. Clim. Chang.* 6, 182–186. doi: 10.1038/nclimate2806

Newsham, K. K., Upson, R., and Read, D. J. (2009). Mycorrhizas and dark septate endophytes in polar regions. *Fungal Ecol.* 2, 10–20. doi: 10.1016/j.funeco.2008.10.005

Nguyen, N. H., Song, Z., Bates, S. T., Branco, S., Tedersoo, L., Menke, J., et al. (2016). FUNGuild: an open annotation tool for parsing fungal community datasets by ecological guild. *Fungal Ecol.* 20, 241–248. doi: 10.1016/j.funeco.2015.06.006

Nilsson, R. H., Tedersoo, L., Ryberg, M., Kristiansson, E., Hartmann, M., Unterseher, M., et al. (2015). A comprehensive, automatically updated fungal ITS sequence dataset for reference-based chimera control in environmental sequencing efforts. *Microbes Environ.* 2, 145–150. doi: 10.1264/jsme2.ME14121

Oksanen, J., Blanchet, G., Friendly, M., Kindt, R., Legendre, P., McGlinn, D., et al. (2017). Vegan: community ecology package. R package version 2.4-3. Available at: https://CRAN.R-project.org/package=vegan (Accessed October 2020).

Onofri, S., Zucconi, L., and Tosi, S. (2007). *Continental Antarctic fungi*. Eching: IHW-Verlag.

Øvstedal, D. O., and Smith, R. I. L. (2001). *Lichens of Antarctica and South Georgia: A guide to their identification and ecology*. Cambridge: Cambridge University Press.

Peat, H. J., Clarke, A., and Convey, P. (2007). Diversity and biogeography of the Antarctic flora. *J. Biogeogr.* 34, 132–146. doi: 10.1111/j.1365-2699.2006.01565.x

Pegler, D. N., Spooner, B. M., and Smith, R. I. L. (1980). Higher fungi of Antarctica, the Subantarctic zone and Falkland Islands. *Kew Bull.* 35, 499–562. doi: 10.2307/4110020

Pointing, S. B., and Belnap, J. (2012). Microbial colonisation and controls in dryland ecosystems. *Nat. Rev. Microbiol.* 10, 551–562. doi: 10.1038/nrmicro2831

Qian, B., Gregorich, E. G., Gameda, S., Hopkins, D. W., and Wang, X. L. (2011). Observed soil temperature trends associated with climate change in Canada. *J. Geophys. Res. Atmos.* 116:D02106. doi: 10.1029/2010JD015012

Sannino, C., Borruso, L., Mezzasoma, A., Battistel, D., Zucconi, L., Selbmann, L., et al. (2020). Intra- and inter-cores fungal diversity suggests interconnection of different habitats in an Antarctic frozen lake (Boulder Clay, Northern Victoria Land). *Environ. Microbiol.* 22, 3463–3477. doi: 10.1111/1462-2920.15117

Schmidt, S. K., Naff, C. S., and Lynch, R. C. (2012). Fungal communities at the edge: ecological lessons from high alpine fungi. *Fungal Ecol.* 5, 443–452. doi: 10.1016/j.funeco.2011.10.005

Setälä, H., and McLean, M. A. (2004). Decomposition rate of organic substrates in relation to the species diversity of soil saprophytic fungi. *Oecologia* 139, 98–107. doi: 10.1007/s00442-003-1478-y

Smith, R. I. L. (2000). "Plants of extreme habitats in Antarctica" in *New aspects in cryptogamic research*. eds. B. Schroeter, M. Schlensog and T. G. A. Green (Berlin: Cramer), 405–419.

Smith, S. E., and Read, D. J. (2008). *Mycorrhizal Symbiosis. 3rd Edn.* New York: Academic Press.

Stchigel, A. M., Cano, J., Mac Cormack, W., and Guarro, J. (2001). Antarctomyces psychrotrophicus gen. et sp. nov., a new Ascomycete from Antarctica. *Mycol. Res.* 105, 377–382. doi: 10.1017/S0953756201003379

Swift, M. J., Heal, O. W., and Anderson, J. M. (1979). *Decomposition in terrestrial ecosystems*. Oxford: Blackwell Scientific Publications.

Tedersoo, L., Anslan, S., Bahram, M., Põlme, S., Riit, T., Liiv, I., et al. (2015). Shotgun metagenomes and multiple primer pair-barcode combinations of amplicons reveal biases in metabarcoding analyses of fungi. *MycoKeys* 10, 1–43. doi: 10.3897/mycokeys.10.4852

Tedersoo, L., Bahram, M., Põlme, S., Kõljalg, U., Yorou, N. S., Wijesundera, R., et al. (2014). Global diversity and geography of soil fungi. *Science* 346:1256688. doi: 10.1126/science.1256688

Thomas-Hall, S. R., Turchetti, B., Buzzini, P., Branda, E., Boekhout, T., Theelen, B., et al. (2010). Cold-adapted yeasts from Antarctica and the Italian Alps—description of three novel species: *Mrakia robertii* sp. nov., *Mrakia blollopis* sp. nov. and *Mrakiella niccombsii* sp. nov. *Extremophiles* 14, 47–59. doi: 10.1007/s00792-009-0286-7

Timling, I., Walker, D. A., Nusbaum, C., Lennon, N. J., and Taylor, D. L. (2014). Rich and cold: diversity, distribution and drivers of fungal communities in patterned-ground ecosystems of the North American Arctic. *Mol. Ecol.* 23, 3258–3272. doi: 10.1111/mec.12743

Turner, J., Lachlan-Cope, T. A., Marshall, G. J., Morris, E. M., Mulvaney, R., and Winter, W. (2002). Spatial variability of Antarctic Peninsula net surface mass balance. *J. Geophys. Res.* 107:4173. doi: 10.1029/2001JD000755

Turner, J., Lu, H., White, I., King, J. C., Phillips, T., Hosking, J. S., et al. (2016). Absence of 21st century warming on Antarctic Peninsula consistent with natural variability. *Nature* 535, 411–415. doi: 10.1038/nature18645

Upson, R., Newsham, K. K., and Read, D. J. (2008). Root-fungal associations of *Colobanthus quitensis* and *Deschampsia antarctica* in the Maritime and Subantarctic. *Arct. Antarct. Alp. Res.* 40, 592–599. doi: 10.1657/1523-0430(07-057)[UPSON]2.0.CO;2

Van Lipzig, N. P. M., Van Meijgaard, E., and Oerlemans, J. (1999). Evaluation of a regional atmospheric model using measurements of surface heat exchange processes from a site in Antarctica. *Mon. Weather Rev.* 127, 1994–2011. doi: 10.1175/1520-0493(1999)127<1994:EOARAM>2.0.CO;2

Vishniac, H. S. (1996). Biodiversity of yeasts and filamentous microfungi in terrestrial Antarctic ecosystems. *Biodivers. Conserv.* 5, 1365–1378. doi: 10.1007/BF00051983

Waksman, S. A. (1931). Decomposition of the various chemical constituents etc. of complex plant materials by pure cultures of fungi and bacteria. *Arch. Mikrobiol.* 2, 136–154. doi: 10.1007/BF00446500

White, T. J., Bruns, T., Lee, S., and Taylor, J. (1990). "Amplification and direct sequencing of fungal ribosomal RNA genes for phylogenetics" in *PCR protocols: A guide to methods and applications*. eds. T. White, T. Bruns, S. Lee, J. Taylor, M. Innis, D. Gelfand, et al. (New York: Academic Press), 315–322. doi: 10.1016/b978-0-12-372180-8.50042-1

Yergeau, E., Bokhorst, S., Huiskes, A. H. L., Boschker, H. T. S., Aerts, R., and Kowalchuk, G. A. (2007a). Size and structure of bacterial, fungal and nematode communities along an Antarctic environmental gradient. *FEMS Microbiol. Ecol.* 59, 436–451. doi: 10.1111/j.1574-6941.2006.00200.x

Yergeau, E., Newsham, K. K., Pearce, D. A., and Kowalchuk, G. A. (2007b). Patterns of bacterial diversity across a range of Antarctic terrestrial habitats. *Environ. Microbiol.* 9, 2670–2682. doi: 10.1111/j.1462-2920.2007.01379.x

Zucconi, L., Pagano, S., Fenice, M., Selbmann, L., Tosi, S., and Onofri, S. (1996). Growth temperature preferences of fungal strains from Victoria Land, Antarctica. *Polar Biol.* 16, 53–61. doi: 10.1007/BF01876829

Conflict of Interest: The authors declare that the research was conducted in the absence of any commercial or financial relationships that could be construed as a potential conflict of interest.

frontiers in Microbiology

ORIGINAL RESEARCH
published: 27 January 2021
doi: 10.3389/fmicb.2021.616730

Antarctic Water Tracks: Microbial Community Responses to Variation in Soil Moisture, pH, and Salinity

Scott F. George[1], Noah Fierer[2], Joseph S. Levy[3] and Byron Adams[1,4]*

[1] Department of Biology, Brigham Young University, Provo, UT, United States, [2] Department of Ecology and Evolutionary Biology and Cooperative Institute for Research in Environmental Sciences, University of Colorado Boulder, Boulder, CO, United States, [3] Department of Geology, Colgate University, Hamilton, NY, United States, [4] Monte L. Bean Museum, Brigham Young University, Provo, UT, United States

Ice-free soils in the McMurdo Dry Valleys select for taxa able to cope with challenging environmental conditions, including extreme chemical water activity gradients, freeze-thaw cycling, desiccation, and solar radiation regimes. The low biotic complexity of Dry Valley soils makes them well suited to investigate environmental and spatial influences on bacterial community structure. Water tracks are annually wetted habitats in the cold-arid soils of Antarctica that form briefly each summer with moisture sourced from snow melt, ground ice thaw, and atmospheric deposition via deliquescence and vapor flow into brines. Compared to neighboring arid soils, water tracks are highly saline and relatively moist habitats. They represent a considerable area (~5–10 km^2) of the Dry Valley terrestrial ecosystem, an area that is expected to increase with ongoing climate change. The goal of this study was to determine how variation in the environmental conditions of water tracks influences the composition and diversity of microbial communities. We found significant differences in microbial community composition between on- and off-water track samples, and across two distinct locations. Of the tested environmental variables, soil salinity was the best predictor of community composition, with members of the *Bacteroidetes* phylum being relatively more abundant at higher salinities and the *Actinobacteria* phylum showing the opposite pattern. There was also a significant, inverse relationship between salinity and bacterial diversity. Our results suggest water track formation significantly alters dry soil microbial communities, likely influencing subsequent ecosystem functioning. We highlight how Dry Valley water tracks could be a useful model system for understanding the potential habitability of transiently wetted environments found on the surface of Mars.

Keywords: Antarctica, Mars analog, water tracks, microbial ecology, extremophiles

OPEN ACCESS

Edited by:
Laura Zucconi, University of Tuscia, Italy

Reviewed by:
Fabiana Canini, University of Tuscia, Italy
David A. Lipson, San Diego State University, United States

****Correspondence:***
Scott F. George
scott.f.george@byu.edu

Specialty section:
This article was submitted to Extreme Microbiology, a section of the journal Frontiers in Microbiology

Received: *13 October 2020*
Accepted: *04 January 2021*
Published: *27 January 2021*

Citation:
George SF, Fierer N, Levy JS and Adams B (2021) Antarctic Water Tracks: Microbial Community Responses to Variation in Soil Moisture, pH, and Salinity. Front. Microbiol. 12:616730. doi: 10.3389/fmicb.2021.616730

INTRODUCTION

The abiotic extremes characteristic of the McMurdo Dry Valleys (MDV) region (77–78° S, 160–164° E) (Fountain et al., 1999) select for particular taxa able to cope with the unique environmental conditions (Cary et al., 2010; Doran et al., 2010). The MDV region is a polar desert ecosystem with average air temperatures of −18°C, winter lows of −65°C, and summer temperatures that fluctuate

around 0°C (Doran et al., 2002). Annual precipitation is limited to 3–50 mm (water equivalent) of snow (Fountain et al., 2010), most of which sublimates before entering a liquid phase (Chinn, 1993), making a vast majority of the terrestrial habitat highly arid. Fast, dry drainage winds descend from the polar plateau with speeds up to 37 m s^{-1}, warming valley floors and lowering relative humidity, resulting in further desiccation of surface soils (Nylen et al., 2004). Soil salinity is extremely variable in coastal MDV, with solute salt concentrations ranging from 0 to 6000 eq m^{-2} from young coastal lowland surfaces to ancient glacial tills further inland (Toner et al., 2013). Biota within this region are also subject to dynamic solar radiation regimes, including 4 months of near or constant darkness (Dana et al., 1998).

The MDV lack vertebrates and vascular plants, with photosynthetic primary productivity limited to patchy distributions of cyanobacteria and algae found in lakes (Vincent et al., 1993), seasonally wetted streams and soils (Hawes and Howard-Williams, 2013; Stanish et al., 2013; Niederberger et al., 2015), and lithic niches (Friedmann and Ocampo, 1976; Friedmann, 1982; Pointing et al., 2009). The low complexity of this desert ecosystem makes it a well-suited natural system to investigate physical and chemical controls on soil microbial communities, with generalized findings that can be applied to other habitats (Van Horn et al., 2013).

Liquid water availability limits biological activity within this habitat where water availability is primarily regulated by low temperatures and limited net snow accumulation. During austral spring and summer, a hydrological continuum forms in MDV soils as differentially warmed soils and spatially heterogeneous snow and ice reservoirs generate different volumes of transient liquid water (Levy, 2015). These wetted soil areas in the cold desert range from those that are spatially extensive and perennial, such as glacier-fed streams and lakes, to those that are meter-scale and episodic and include hyporheic zones (i.e., wetted soils around and under lakes, ponds, and streams) (McKnight et al., 2007; Niederberger et al., 2015; Lee et al., 2018), water tracks (channelized subsurface groundwater flow) (Levy et al., 2011, 2013; Gooseff et al., 2013), and "wet patches" that form via deliquescence when exposed hygroscopic salts in the soil absorb atmospheric water vapor and generate liquid solutions (Seinfeld and Pandis, 2006; Levy et al., 2012).

Remote sensing data suggest that transiently wetted soils, specifically those removed from surface water bodies, occupy ∼5–10 km^2 of the landscape during the seasonal thaw (Langford et al., 2015), a small but significant area that is projected to increase within this region due to ongoing climate change (Fountain et al., 2014). Previous work on water track physical, chemical, and biological processes suggest that water track soils are wetter, saltier, finer-grained, and more organic-matter-rich than adjacent, off-track soils (Levy et al., 2013; Ball and Levy, 2015).

At the surface, Antarctic water tracks are identified as visibly damp (dark) soils which grow downslope each summer with the release of meltwater from snow, glaciers, and ground ice (Harris et al., 2007; Levy et al., 2011). Water track liquids flow within the active layer beneath the soil surface but above the ice table, which is located above permanently frozen soil (Levy et al., 2011). Water track soil moisture and soil salinity are generally 5–10 times higher than other arid desert soils in the Dry Valleys (Gooseff et al., 2013; Levy et al., 2013). Accordingly, water tracks represent a pronounced alteration to the desert ecosystem and their presence may result in important shifts in soil microbial community composition, diversity, and ecosystem functioning.

Water tracks have been proposed as useful model systems for the episodically formed features on Mars termed recurring slope lineae (RSL) (Levy, 2012), which, like water tracks, are dark-toned, meter-scale features that grow downslope for hundreds of meters during seasonal warm periods (McEwen et al., 2011; Stillman et al., 2017). Among other similar characteristics, water tracks possess hygroscopic salts capable of deliquescence (Levy et al., 2011; Gooseff et al., 2013), which may contribute additional soil moisture beyond that derived from meltwater sources alone. Deliquescence has been identified as a mechanism for plausible transient water formations on Mars (Rennó et al., 2009; Smith et al., 2009; Martín-Torres et al., 2015), including RSL (Ojha et al., 2015). However, the role, quantity, or even presence of water in RSL has been challenged (Edwards and Piqueux, 2016; Dundas et al., 2017; Schmidt et al., 2017).

McMurdo Dry Valleys water tracks may be more analogous to transiently wetted habitats found historically on Mars. Over the last ∼3.5 billion years, it appears that surface environments on Mars experienced a series of climate successions from cold and semiarid to ultimately a hyperarid state (e.g., Carr and Head, 2010; Mahaffy et al., 2013). These climatic shifts on Mars would have had a significant impact on the evolution of an early Martian biosphere (Davila and Schulze-Makuch, 2016). It is plausible that early in Mars' history (∼3.5 billion years ago), transiently wetted environments similar to Antarctic water tracks existed at the margins of highlands glaciated regions (Wordsworth, 2016), and if so, they would have represented important niches within the increasingly cold and arid planet.

Previous biological investigations of the Dry Valley water tracks are limited in number and have yet to produce concordant conclusions. In some cases, water track soil moisture enhancement has shown to elevate levels of microbial biomass relative to neighboring dry soils (Van Horn et al., 2013; Chan-Yam et al., 2019), though this increase has not always been observed (Ball and Levy, 2015). Other work suggests water tracks promote microbial activity, as measured by phosphorus depletion (Gooseff et al., 2013), CO_2 fluxes (Ball and Levy, 2015), and *in vitro* microcosm radio-respiration assays (Chan-Yam et al., 2019). However, water track fluids are also highly saline, creating "dead zones" in the polar desert that limit habitability to only the most halotolerant organisms (Ball and Levy, 2015). Isolated "wet patches" can be so saline as to exceed water activity limits for cellular growth and reproduction (Levy et al., 2012; Rummel et al., 2014). An investigation of nematodes, the most abundant metazoan in the Dry Valleys, showed pronounced declines in population numbers when measured within water track soils (Gooseff et al., 2013). Several studies have found microbial communities in transiently wetted soils and water tracks have significantly different compositions compared to neighboring arid soils (Van Horn et al., 2014; Niederberger et al., 2015;

Lee et al., 2018), although these differences has not always been observed (Chan-Yam et al., 2019).

One possible confounding factor that may have affected previous studies is differences in soil age and accumulated soil salinity. In an effort to mitigate this effect, we examined sediment profiles from two proximal locations with similar microclimate conditions, but different soil ages. The Goldman Glacier Basin (GB) water track flows through older, Taylor IV tills (2.1–37 Ma), while Water Track 1 (WT1) in the Lake Hoare basin flows through younger mixed Taylor III/Bonney tills (74–210 ka) (Bockheim et al., 2008).

We set out to identify how variation in the measured physical and chemical environment of water tracks within these two water track systems influence soil microbial community structure and diversity. A total of twenty samples from on- and off-track soils were analyzed to assess abiotic influences on microbial composition and diversity. Soil bacterial biodiversity was assessed using cultivation independent 16S rRNA gene sequencing.

We hypothesized that soil salinity, moisture, and pH are significantly different within water tracks than outside of them, and that these geochemical factors are significantly correlated with microbial community structure and diversity. We also hypothesized that soil microbial community composition is significantly different between on-track and off-track habitats, and between the two tested water track systems in Taylor Valley. Namely, the Goldman Glacier Basin water track, and that of the Lake Hoare Basin, Water Track 1. We further hypothesized that the seasonal formation of water tracks results in significantly higher community diversity, richness, and evenness compared to off-track habitats due to increased water availability. Finally, we hypothesized that soil position (i.e., on-track and off-track), salinity, moisture, pH, and the two different site locations of water track systems are significant explanatory variables for soil microbial community composition.

MATERIALS AND METHODS

Sampling and Soil Geochemistry

Soil samples and pore water were collected from the Lake Hoare and Goldman Glacier Basins of Taylor Valley, Antarctica during the austral summer of 2012–2013. Two separate water track systems within Taylor Valley were selected for analysis, Water Track 1 (77.64°S, 162.94°E) and Goldman Glacier Basin (77.67°S, 162.93°E), which are approximately 3.3 km apart. Sediment and pore water collected from the darkened portions of water tracks are designated here as "on-track," and samples from the adjacent lighter soils are classified as "off-track." Off-track samples were located at least 5 m from the current edge of the water track (Levy et al., 2013). Wet, on-track soils have a typical albedo of 0.15, while the off-track soil albedo is generally 0.22 (Levy et al., 2013), making them readily distinguishable in the field. Samples were collected from the upper 10 cm of the soil horizon using aseptic techniques and were stored in sterile Whirl-Pak bags at −20°C until processing. Latitude and longitude of the collected samples, as well as sample states (i.e., on-track or off-track), were recorded at the time of collection (see **Table 1** for details).

TABLE 1 | Summary of sample abiotic properties.

Sample	On-/off-water track	System	EC (dS/m)	GWC (%)	pH	Latitude	Longitude
1	Off	WT1	0.02	2.03	7.99	−77.6393	162.9406
2	Off	WT1	0.03	2.07	8.43	−77.6428	162.9303
3	Off	GB	0.00	2.48	8.49	−77.6669	162.9250
4	On	GB	0.19	3.47	8.30	−77.6668	162.9258
5	Off	WT1	0.01	1.31	8.33	−77.6326	162.9340
6	On	WT1	0.08	7.57	8.24	−77.6427	162.9300
7	On	WT1	0.05	3.79	8.34	−77.6458	162.9177
8	Off	GB	0.05	1.00	8.40	−77.6690	162.9262
9	On	WT1	0.16	1.51	8.31	−77.6364	162.9354
10	On	WT1	0.07	0.79	8.41	−77.6392	162.9404
11	On	GB	0.47	4.35	8.35	−77.6720	162.9325
12	Off	WT1	0.01	2.63	8.84	−77.6460	162.9182
13	On	WT1	0.05	2.84	8.06	−77.6345	162.9351
14	Off	WT1	0.01	1.66	8.02	−77.6363	162.9359
15	On	GB	0.05	4.98	7.96	−77.6690	162.9256
16	On	GB	0.73	2.18	8.00	−77.6644	162.9253
17	On	WT1	0.25	3.81	8.13	−77.6364	162.9353
18	Off	WT1	0.01	1.31	8.37	−77.6326	162.9340
19	Off	GB	0.01	2.02	–	−77.6721	162.9322
20	Off	GB	0.09	2.34	7.99	−77.6644	162.9266

Gravimetric water content (GWC) was calculated to obtain soil moisture values for each sample. Electrical conductivity (EC), a proxy of salinity, was also measured for each sample. GWC was calculated as the percentage of dry weight of sediment per sample, drying approximately 100 g of soil at 105°C for 24 hours and then reweighing the sample. EC (dS/m) was obtained for each sample using a Decagon Devices 5TE probe. Soil pH was measured in a 1:2 0.01 M $CaCl_2$ solution (Thermo Orion pH Meter Model 410A+, Thermo Electron, Waltham, MA, United States).

DNA Extraction and Taxonomic Profiling

DNA extraction and microbial community analyses were conducted using the cultivation-independent 16S rRNA gene sequencing approach as described in Prober et al. (2015). Total genomic DNA was extracted from each soil sample using the MO BIO's PowerSoil DNA Isolation Kit (MO BIO Laboratories Inc., Carlsbad, CA, United States). For microbial analyses, the V4 hypervariable region of the 16S rRNA gene was PCR amplified using the 515f and 806r primer pair which captures both Bacteria and Archaea. Three PCRs were run per sample, with the amplicons from the replicate reactions pooled. Each primer pair included Illumina adapters and 12-bp error-correcting barcodes unique to each sample (Thompson et al., 2017). After gel visualization to confirm amplification, we used a PicoGreen dsDNA assay to quantify amplicon yields, with the amplicons then pooled together in equimolar concentrations for sequencing on the Illumina MiSeq instrument. DNA sequencing was completed at the University of Colorado Next Generation Sequencing Facility using the 2 × 150 bp paired-end

sequencing chemistry. Four DNA extraction and four no-template PCR "blanks" were included in the run to check for potential contamination.

Sequences were demultiplexed using a custom Python script ('prep_fastq_for_uparse.py'[1]), with the UPARSE pipeline used for quality filtering and phylotype (i.e., operational taxonomic unit) clustering (Edgar, 2013). Quality filtering was conducted using a maximum e-value of 0.5 with paired-end sequences merged prior to downstream processing. Representative sequences from returned phylotypes that were not ≥75% similar to sequences contained in the Greengenes database (McDonald et al., 2012) were removed; afterward, the raw sequences were mapped to phylotypes at a 97% similarity cutoff. Taxonomic classification of each phylotype was determined using the Ribosomal Database Project classifier (Wang et al., 2007) against the Greengenes database with a confidence threshold of 0.5.

Statistical Analyses

To determine soil chemical and physical effects on community structure, statistical tests of inter- and intra-site relationships and differences were undertaken. Accordingly, phylotype data were rarefied in R (R Core Team, 2017) to 11,649 reads per sample with the vegan package (Oksanen et al., 2019) before all diversity analyses. Alpha diversity metrics were calculated using the microbiome package (Lahti and Shetty, 2012), for Pielou's evenness, and the vegan package (Oksanen et al., 2019), for Shannon diversity (H') (**Supplementary Table S1**). Independent *t*-tests of the alpha diversity metrics between on and off-track samples were run in SPSS (IBM, 2016). Phyla relative abundances (**Figure 1** and **Supplementary Table S2**) were calculated with the funrar package (Grenié et al., 2017). Stacked histograms and clustered box plots for phyla relative abundances were generated with SPSS (IBM, 2016).

To test for correlations between community composition and measured soil properties, Mantel tests based on Pearson's product-moment correlations were run for each variable using the vegan package (Oksanen et al., 2019). Hypotheses regarding relationships between soil properties and microbial diversity, richness, and evenness were also explored using Pearson correlation tests. Mann–Whitney U and independent *t*-tests, as appropriate, were used to test significant differences in soil chemical and physical properties between on- and off-track samples.

PERMANOVA tests, with pairwise distances calculated using Bray–Curtis distance, were run in the vegan package (Oksanen et al., 2019) to test for significant differences in soil microbial communities between on-track and off-track samples; WTI and GB systems; on-track communities of GB and on-track communities of WT1; and finally, off-track communities of GB and off-track communities of WT1. A multidimensional scaling (MDS) plot informed by a Bray–Curtis dissimilarity matrix was created in the vegan package (Oksanen et al., 2019) to represent microbial community clustering based on sample type (On/Off-track) and water track system (GB/WT1) within the axes of soil salinity, moisture, and pH.

[1]https://github.com/leffj/helper-code-for-uparse

Redundancy analysis (RDA) with variation partitioning was run using the vegan package (Oksanen et al., 2019) to estimate the percent at which the measured abiotic variables, individually and collectively, explained microbial community composition in the tested soils. ANOVA tests were run on the specific canonical axes produced from the underlying RDAs to see if the explanatory variables were significant in the partition variance.

RESULTS

Soil Properties

The mean on-track soil moisture of the Lake Hoare Basin water tracks was significantly higher than the adjacent off-track soils ($P = 0.03$). Water track soil moisture was, on average, ∼1.9 times higher than neighboring dry soil (3.53–1.89%), ranging from 0.79–7.57% on-track, and 1.00–2.63% off-track (**Table 1**).

On-track soil values were also significantly more saline ($U = 93.5$, $P < 0.001$) than the proximal off-track counterparts. Median salinity on-track was ten times higher than off-track (0.12 dS/m compared to 0.01 dS/m). The range of on-track salinities were more variable (0.05 dS/m to 0.73 dS/m) than off-track salinities, which were consistently low across the tested samples (0.00 dS/m to 0.09 dS/m).

Soil pH was fairly uniform across all samples, with no significant difference in the mean pH between on-track and off-track soils (8.21 and 8.32, respectively) ($P = 0.31$) (**Table 1**). There was no apparent correlation between any of the measured abiotic variables, namely: moisture and pH [$r(19) = -0.16$, $P = 0.52$], pH and salinity [$r(19) = -0.25$, $P = 0.30$], and salinity and moisture [$r(20) = 0.52$, $P = 0.15$].

Microbial Communities

Across all samples, we detected a total of 1457 unique phylotypes after rarefaction, with the number of phylotypes per sample ranging from 182 to 713 (**Supplementary Table S1**). Eight archaeal phylotypes, not included in analyses here, were identified as belonging to two phyla, and represented <0.23% of the sequences. On-track samples had higher average numbers of phylotypes (420 phylotypes per sample ±56) compared to off-track samples (392 ± 32), though this was not significant ($P > 0.7$). There was also no significant difference in average Shannon diversity ($P > 0.4$) between on-track (4.13 ± 0.23) and off-track (4.37 ± 0.12) samples. Pielou's evenness was not significantly different on- or off-track ($P > 0.1$), although it was higher off-track than on-track (0.74 ± 0.01, 0.69 ± 0.03).

The majority of recovered microbial communities were comprised of a handful of phyla (**Figure 1** and **Supplementary Table S2**), particularly *Actinobacteri*a, which was the most abundant phylum detected in soils both on and off water tracks (27.6% and 48% of reads, respectively). Other abundant phyla on and off water tracks included *Proteobacteria* (23.8%, 10.6%), *Bacteroidetes* (17.4%, 4.8%) *Gemmatimonadetes* (10.4%, 4.4%) and *Acidobacteria* (8.5%, 16.8%). The relative abundance of these five phyla, from the 25 phyla identified, accounted for 87.7% of all communities on-track and 84.5% of those off-track (**Supplementary Table S2**). For some phyla, the intra-sample

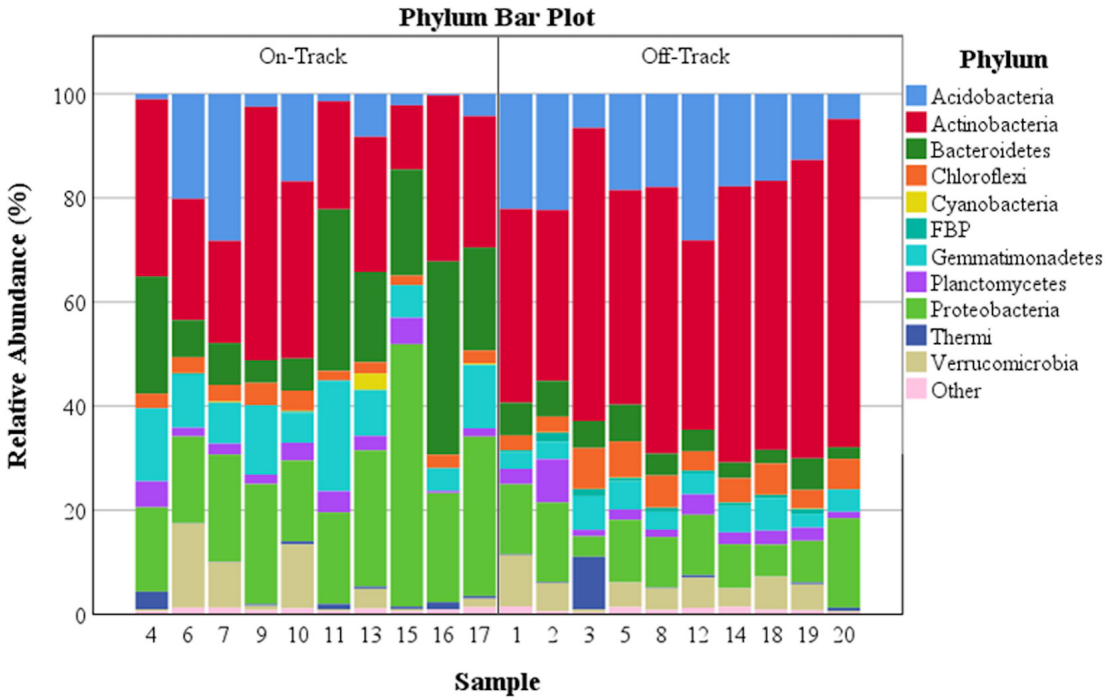

FIGURE 1 | The percent relative abundance of major soil bacterial taxa across all samples. Phyla with a relative abundance >0.39% either on or off water tracks are identified.

(e.g., on-track versus on-track) variation in relative abundances was considerable (**Figure 2**).

We observed a high degree of variation in the composition of bacterial communities, with community composition patterns correlated with select physiochemical properties and spatial scale (**Figure 3**). On-track microbial communities were significantly different than those off-track (PERMANOVA R^2 = 0.203, $P < 0.001$). Microbial communities between the GB and WTI water track systems were also significantly different (PERMANOVA R^2 = 0.156, P = 0.004). Finally, comparisons of intra-track types between systems, namely on-track to on-track and off-track to off-track soils between GB and WT1, showed significant differences in microbial communities (PERMANOVA R^2 = 0.33, P = 0.01, PERMANOVA R^2 = 0.208, P = 0.03, respectively). On-track communities in the MDS plot were distinctly clustered with each other, as were off-track communities and assemblages based on system (GB/WT1) (**Figure 3**).

A Mantel statistic based on Pearson's correlation showed a statistically significant relationship between soil salinity and community composition [$r(20)$ = 0.41, P = 0.005]. However, a Mantel test exploring possible correlations between soil moisture and microbial community composition was not significant [$r(20)$ = 0.20, P = 0.065], as was the relationship between pH and community composition [$r(19)$ = −0.04, P = 0.58]. Salinity was the only environmental variable that was significantly correlated with microbial diversity (H') [$r(20)$ = −0.537, P = 0.02], richness [$r(20)$ = −0.45, P = 0.045], and evenness (H') [$r(20)$ = −0.48, P = 0.03]. In all instances, as salinity increased these diversity metrics declined.

Redundancy analysis with variance partitioning showed highly similar patterns with the Mantel tests. Specifically, RDA with variance partitioning estimated that collectively, sample location in regard to water tracks (On/Off-Track), soil salinity, and the water track system location (WT1/GB) were significant explanatory variables for 22.7% of the tested soils' microbial community composition (ANOVA, P = 0.002). Sample location (On/Off-Track) explained 5.8% of the variation in community composition conditioned on the other variables included in the model (ANOVA, P = 0.03). For soil salinity, this was 7.7% (ANOVA, P = 0.046), and for system location, it was 6.7% (ANOVA, P = 0.02). The canonical axes of soil moisture and pH were not significant explanatory variables in structuring the tested microbial communities (ANOVA, P = 0.38, P = 0.58, respectively).

DISCUSSION

The annual formation of water tracks in this polar desert ecosystem represents a significant alteration in this relatively low-complexity terrestrial landscape. Similar to other observations (Gooseff et al., 2013; Levy et al., 2013), our tested average water track salinity was an order of magnitude and significantly higher than adjacent 'non-water track' soils. The observed differences in community composition were most strongly associated with

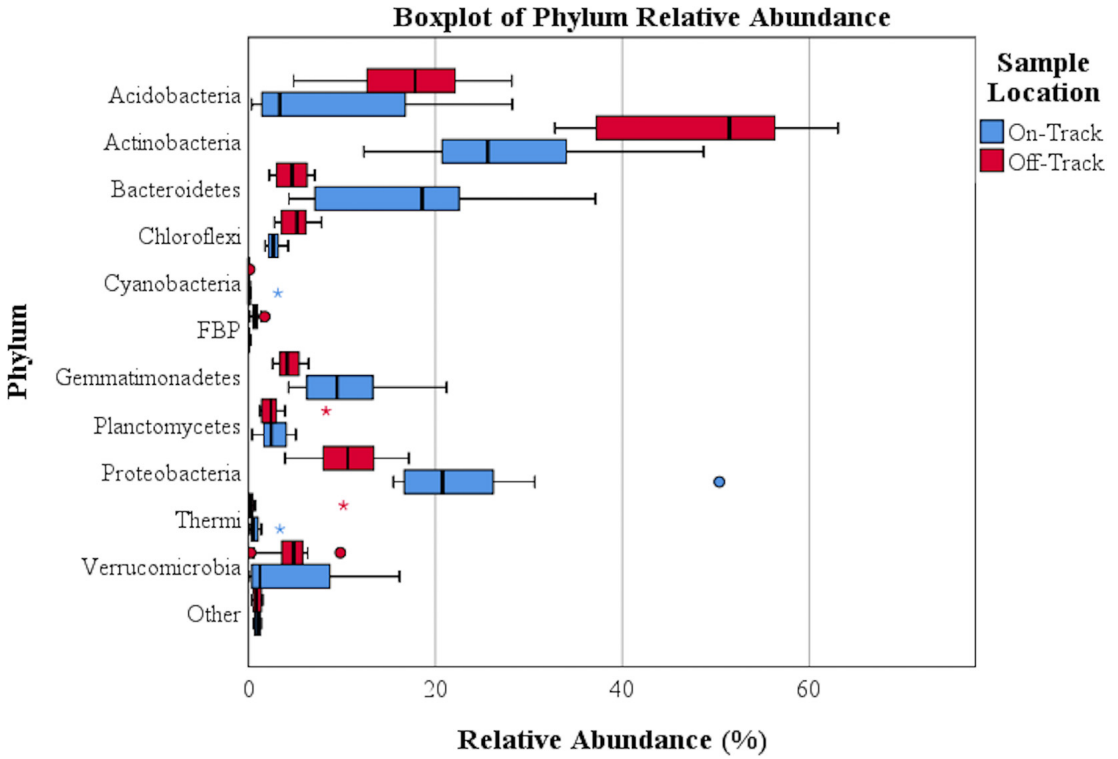

FIGURE 2 | A boxplot of bacterial relative abundance on and off the tested water tracks. Asterisks represent extreme outliers; solid circles represent standard outliers. Phyla with a relative abundance >0.39% either on or off water tracks are identified.

differences in soil salinity (**Figure 3**), a pattern that is in agreement with previous studies (Lee et al., 2012; Van Horn et al., 2013). As salinity increased, the relative abundance of *Bacteroidetes* increased considerably, with observed decreases in *Actinobacteria,* suggesting a shift toward a more halotolerant community. No correlations were found among soil salinity, pH, and moisture.

We observed no significant differences in average diversity, richness, or evenness between on-track and off-track soils, in spite of nearly twofold increases in soil moisture and tenfold increases in salinity when on track. However, soil salinity was significantly correlated with diversity, richness and evenness, and in all cases the relationship was negative. Similar significant soil salinity relationships with microbial diversity (Zeglin et al., 2011; Van Horn et al., 2014) have been observed elsewhere in the Dry Valleys. Salinity measured by Zeglin et al. (2011) was largely within the range measured in our study. Salinity measured by Van Horn et al. (2014) reached levels several orders of magnitude above ours, yet the same relationship was exhibited. Our findings suggest that MDV soil microbial richness is sensitive to even moderate changes in salinity, with higher soil salinities associated with less diverse bacterial communities.

Soil salinity can have a pronounced direct and indirect affect in shaping microbial communities and their ecological responses (Rietz and Haynes, 2003; Lozupone and Knight, 2007; Rath and Rousk, 2015; O'Brien et al., 2019; Rath et al., 2019). Salt-affected soils generally show decreases in microbial respiration (Sardinha et al., 2003; Yuan et al., 2007), biomass (Rietz and Haynes, 2003; Yuan et al., 2007), and extracellular enzymatic activity (Rietz and Haynes, 2003; Ghollarata and Raiesi, 2007). In more extreme cases, as demonstrated in aquatic habitats, elevated salt concentrations can prevent metabolic activity (Oren, 2013) and inhibit life via denaturing of biological macromolecules (Hallsworth et al., 2007). However, microbial communities within salt-affected areas should exhibit adaptive and taxonomic responses if the salinity is elevated to meaningful ecological levels (Rath and Rousk, 2015; Gunde-Cimerman et al., 2018; O'Brien et al., 2019), which may alter at least some ecosystem functions (Kimbrel et al., 2018; Rath et al., 2019).

The absence we observed of statistically significant correlations between water content and community composition in the MDV was also observed in several, though not all, sites sampled by Van Horn et al., 2013. Chan-Yam et al. (2019) similarly found no significant correlation between community composition and soil moisture content from their MDV soil investigations. However, our MDS plot strongly hints that water content, which can be seasonally dynamic, may play an important role in community structure.

Soil pH has been shown to have a strong influence on bacterial community structure at the continental scale (Fierer and Jackson, 2006; Lauber et al., 2009). Regional analyses looking at the influence of soil pH on microbial communities in Antarctica are in agreement with these large-scale studies (Smith et al., 2010;

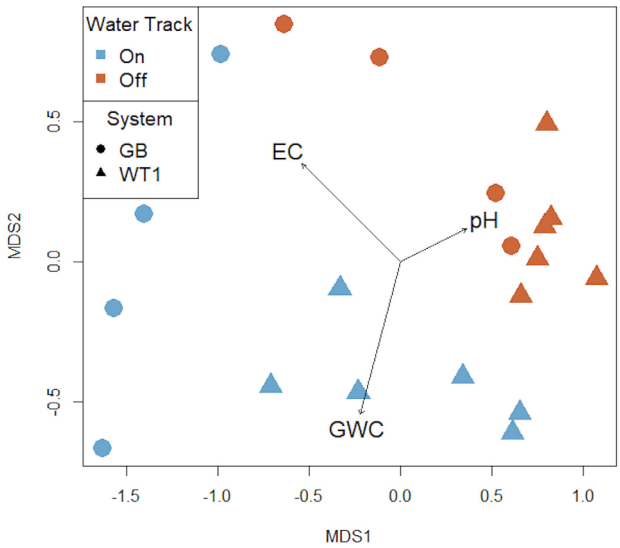

FIGURE 3 | Multidimensional scaling (MDS) plot of soil microbial community composition. Water tracks (blue) harbor significantly different bacterial communities from those collected off-track (red) (PERMANOVA R^2 = 0.203, P = 0.001). Other significant differences include water track system, namely the Goldman Glacier Basin (GB) and Water Track 1 (WT1) (PERMANOVA R^2 = 0.156, P = 0.004); on- versus on-track soil communities between GB and WT1 (PERMANOVA R^2 = 0.33, P = 0.01); and off- versus off-track soils communities between GB and WT1 (PERMANOVA R^2 = 0.208, P = 0.033). The black vectors represent measured environmental parameters (pH, EC = electrical conductivity, GWC = gravimetric water content) that fit into the ordination space. R^2 = 0.995. Stress score = 0.068 in two dimensions.

Van Horn et al., 2013), as are some localized studies (Van Horn et al., 2013; Chan-Yam et al., 2019). However, other localized Dry Valley investigations failed to find soil pH as a significant factor in community partitioning (Lee et al., 2018), or being correlated with diversity metrics (Zeglin et al., 2011). Soil pH from our study was reasonably constrained across all collected samples (**Table 1**), which may be one reason we did not identify significant relationships between it and microbial community composition, diversity, richness or evenness.

The off-track samples had communities dominated by the phyla *Acidobacteria, Actinobacteria, Proteobacteria,* and to a lesser extent *Bacteroidetes, Chloroflexi, Gemmatimonadetes, Verrucomicrobia,* and *Planctomycetes* (**Figure 1** and **Supplementary Table S2**). The dominance of these particular phyla within arid MDV soil communities are concordant with previous studies, especially for the phyla *Acidobacteria* and *Actinobacteria* (Pointing et al., 2009; Zeglin et al., 2011; Lee et al., 2012; Niederberger et al., 2015). The phyla *Acidobacteria* and *Actinobacteria* have also been found to be among the most abundant taxa in the extremely arid and significantly warmer soils of the Atacama Desert in Chile (Crits-Christoph et al., 2013).

On-track soil samples were composed largely of the phyla *Acidobacteria, Actinobacteria, Bacteroidetes, Gemmatimonadetes,* and *Proteobacteria*. *Acidobacteria* and *Actinobacteria* were the two most dominant phyla off-track, but their abundances dropped nearly in half within water track samples (**Figure 1** and **Supplementary Table S2**). *Bacteroidetes, Gemmatimonadetes,* and *Proteobacteria* saw dramatic increases in their relative abundances within water track soils.

Other investigations regarding phyla in transiently wetted Dry Valley soils observed similar trends, with the phyla *Proteobacteria* (Stanish et al., 2013; Niederberger et al., 2015) and *Bacteroidetes* (Zeglin et al., 2011) as the dominant members in wetter soils.

Several genera were found to be closely related to known extremophilic and extremotolerant taxa. Members from the genus *Gillisia* (phylum Bacteroidetes) were notably abundant in on-track samples. Closely related psychrophilic isolates from this genus were also found in Antarctic Lake Fryxell of Taylor Valley (Van Trappen et al., 2004), within soils from an Antarctic valley further south (Niederberger et al., 2015), and in Antarctic maritime environments (Bowman and Nichols, 2005). Phylotypes from the genus *Rubrobacter* (phylum Actinobacteria) were present in every sample, a genus which includes isolates which have been shown to exhibit resistance to ionizing radiation (Rainey et al., 2005) (Ferreira et al., 1999).

The genus *Modestobacter* (phylum Actinobacteria) was also detected, which has been isolated from the hyperarid Atacama Desert soils of Chile (Busarakam et al., 2016) and from the nearby Asgard Range of Antarctica (Mevs et al., 2000). A phylotype from genus *Truepera* (phylum Thermi) was also characterized. *Truepera* has been found in the ephemeral Lake Lucero playa of New Mexico, United States (Sirisena et al., 2018), an episodically wetted environment which shifts between a freshwater habitat and a hypersaline dry desert. Isolates from the genus *Truepera* have also shown to be highly resistant to ionizing radiation (Albuquerque et al., 2005). *Pseudoxanthomonas* and *Sphingomonas* (Phylum Proteobacteria) were present, genera which have been cultured from both saline and freshwater lakes in the Transantarctic Mountains and Shackleton Range of Antarctica (Peeters et al., 2011). The identification of phylotypes closely related to known psychrophilic, halotolerant, and ionizing-radiation-resistant isolates suggests, though does not confirm, adaptations found within the sampled microbial communities.

Other possible explanatory variables in shaping MDV soil microbial structure and diversity are the legacy influences associated with long-term water track presence. Within our study at least one water track system, Water Track 1, has persisted in a remarkably similar form and shape since at least 1911. This valuable information was preserved by photographic evidence gathered during Robert Falcon Scott's *Terra Nova* Expedition, evidence which has been compared with present-day imagery (Levy et al., 2013). Temporal legacies associated with long-term water track presence may therefore be reasonably important in shaping microbial communities of water tracks, though this is challenging to test. A possible approach could include a time series investigation of newly forming water tracks that are now entering historically dry soils (Fountain et al., 2014).

Water tracks within the MDV region represent a small, though important, area of the cold-arid desert that is anticipated

to expand with ongoing climate change. Our investigation found significant differences between microbial communities on- and off-water track samples and at different water track system locations. Of the tested variables, we found salinity to be the best predictor of microbial community composition, with *Bacteroidetes* concentrated at higher levels of salinity and *Actinobacteria* in low-saline soils. The microbial communities appeared to be sensitive to even moderate variations in salinity. Increases in salinity significantly correlated with decreases in microbial diversity, richness and evenness. There were no significant differences for microbial diversity, richness, or evenness on- and off-track. Soil moisture in this study was significantly higher within water track samples, yet it was not meaningfully correlated with community composition or diversity. Our research suggests this low complexity environment has complex abiotic and spatial influences upon microbial communities. Results from this study indicate water track formation significantly alters the arid soil microbial community composition in Antarctica soils, and therefore, possibly ecosystem functions. Water tracks may also serve as useful models for transiently wetted habitats that may have existed, or exist, on Mars surface.

DATA AVAILABILITY STATEMENT

The authors acknowledge that the data presented in this study must be deposited and made publicly available in an acceptable repository, prior to publication. Frontiers cannot accept a manuscript that does not adhere to our open data policies. The data presented in this study are deposited in the Environmental Data Initiative (EDI) Repository at https://doi.org/10.6073/pasta/a98c5ce00cc51d5424b07aebcfcf9f74 (George et al., 2020).

AUTHOR CONTRIBUTIONS

NF and JL conceived and designed the experiment. JL carried out the field work, with sample processing by JL and SG. SG analyzed the data. SG, NF, JL, and BA wrote the manuscript. All authors contributed to the article and approved the submitted version.

FUNDING

This study was funded by the United States Antarctic Program and the National Science Foundation with the grants NSF-1341629, NSF-1847067, and OPP-1637708 for Long Term Ecological Research.

ACKNOWLEDGMENTS

We thank the considerable logistical support provided by the United States Antarctic Program and the National Science Foundation in the form of grants NSF-1341629, NSF-1847067, and OPP-1637708 for Long Term Ecological Research. We also thank Trevor Williams, Nick Dragone, and Angela Oliverio for their valuable assistance on this project.

SUPPLEMENTARY MATERIAL

The Supplementary Material for this article can be found online at: https://www.frontiersin.org/articles/10.3389/fmicb.2021.616730/full#supplementary-material

REFERENCES

Albuquerque, L., Simões, C., Nobre, M. F., Pino, N. M., Battista, J. R., Silva, M. T., et al. (2005). *Truepera radiovictrix* gen. nov., sp. nov., a new radiation resistant species and the proposal of *Trueperaceae* fam. nov. *FEMS Microbiol. Lett.* 247, 161–169. doi: 10.1016/j.femsle.2005.05.002

Ball, B. A., and Levy, J. (2015). The role of water tracks in altering biotic and abiotic soil properties and processes in a polar desert in Antarctica. *J. Geophys. Res.* 120, 270–279. doi: 10.1002/2014JG002856

Bockheim, J. G., Prentice, M. L., and McLeod, M. (2008). Distribution of glacial deposits, soils, and permafrost in Taylor Valley, Antarctica. *Arctic Antarct. Alpine Res.* 40, 279–286. doi: 10.1657/1523-1430

Bowman, J. P., and Nichols, D. S. (2005). Novel members of the family Flavobacteriaceae from Antarctic maritime habitats including *Subsaximicrobium wynnwilliamsii* gen. nov., sp. nov., *Subsaximicrobium saxinquilinus* sp. nov., *Subsaxibacter broadyi* gen. nov., sp. nov., *Lacinutrix copepodicola* gen. *Intern. J. Syst. Evol. Microbiol.* 55, 1471–1486. doi: 10.1099/ijs.0.63527-63520

Busarakam, K., Bull, A. T., Trujillo, M. E., Riesco, R., Sangal, V., van Wezel, G. P., et al. (2016). *Modestobacter caceresii* sp. nov., novel *Actinobacteria* with an insight into their adaptive mechanisms for survival in extreme hyper-arid Atacama Desert soils. *Syst. Appl. Microbiol.* 39, 243–251. doi: 10.1016/j.syapm.2016.03.007

Carr, M. H., and Head, J. W. (2010). Geologic history of Mars. *Earth Planet. Sci. Lett.* 294, 185–203. doi: 10.1016/j.epsl.2009.06.042

Cary, S. C., McDonald, I. R., Barrett, J. E., and Cowan, D. A. (2010). On the rocks: the microbiology of Antarctic dry valley soils. *Nat. Rev. Microbiol.* 8, 129–138. doi: 10.1038/nrmicro2281

Chan-Yam, K., Goordial, J., Greer, C., Davila, A., McKay, C. P., and Whyte, L. G. (2019). Microbial activity and habitability of an Antarctic dry valley water track. *Astrobiology* 19, 757–770. doi: 10.1089/ast.2018.1884

Chinn, T. J. (1993). "Physical hydrology of the Dry Valley lakes," in *Antarctic Research Series: Physical and Biogeochemical Processes in Antarctic Lakeseds*, eds W. J. Green and E. I. Friedmann (Washington, DC: American Geophysical Union), 1–51. doi: 10.1029/ar059p0001

Crits-Christoph, A., Robinson, C. K., Barnum, T., Fricke, W. F., Davila, A. F., Jedynak, B., et al. (2013). Colonization patterns of soil microbial communities in the Atacama Desert. *Microbiome* 1, 28–28. doi: 10.1186/2049-2618-1-28

Dana, G. L., Wharton, R. A., and Ralph, D. A. (1998). *Solar Radiation in the Mcmurdo Dry Valleys, Antarctica*. Washington, DC: American Geophysical Union.

Davila, A. F., and Schulze-Makuch, D. (2016). The last possible outposts for life on Mars. *Astrobiology* 16, 159–168. doi: 10.1089/ast.2015.1380

Doran, P. T., Lyons, W. B., and McKnight, D. M. (2010). *Life in Antarctic Deserts and Other Cold Environments*. Cambridge: Cambridge University Press.

Doran, P. T., McKay, C. P., Clow, G. D., Dana, G. L., Fountain, A. G., Nylen, T., et al. (2002). Valley floor climate observations from the McMurdo Dry Valleys, Antarctica, 1986-2000. *J. Geophys. Res. Atmos.* 107, 1–12. doi: 10.1029/2001JD002045

Dundas, C. M., McEwen, A. S., Chojnacki, M., Milazzo, M. P., Byrne, S., McElwaine, J. N., et al. (2017). Granular flows at recurring slope lineae on

Mars indicate a limited role for liquid water. *Nat. Geosci.* 10, 903–907. doi: 10.1038/s41561-017-0012-15

Edgar, R. C. (2013). UPARSE: highly accurate OTU sequences from microbial amplicon reads. *Nat. Methods* 10, 996–998. doi: 10.1038/nmeth.2604

Edwards, C. S., and Piqueux, S. (2016). The water content of recurring slope lineae on Mars. *Geophys. Res. Lett.* 43, 8912–8919. doi: 10.1002/2016GL070179

Ferreira, A. C., Nobre, M. F., Moore, E., Rainey, F. A., Battista, J. R., and Da Costa, M. S. (1999). Characterization and radiation resistance of new isolates of *Rubrobacter radiotolerans* and *Rubrobacter xylanophilus*. *Extremophiles* 3, 235–238. doi: 10.1007/s007920050121

Fierer, N., and Jackson, R. B. (2006). The diversity and biogeography of soil bacterial communities. *Proc. Natl. Acad. Sci. U.S.A.* 103, 626–631. doi: 10.1073/pnas.0507535103

Fountain, A. G., Levy, J. S., Gooseff, M. N., and Van Horn, D. (2014). The McMurdo Dry Valleys: a landscape on the threshold of change. *Geomorphology* 225, 25–35. doi: 10.1016/j.geomorph.2014.03.044

Fountain, A. G., Lyons, W. B., Burkins, M. B., Dana, G. L., Peter, T., Lewis, K. J., et al. (1999). Physical controls on the Taylor Valley ecosystem, Antarctica. *Bioscience* 49, 961–971. doi: 10.1525/bisi.1999.49.12.961

Fountain, A. G., Nylen, T. H., Monaghan, A., Basagic, H. J., and Bromwich, D. (2010). Snow in the McMurdo Dry Valleys, Antarctica. *Intern. J. Climatol.* 30, 633–642. doi: 10.1002/joc.1933

Friedmann, E. I. (1982). Endolithic microorganisms in the Antarctic cold desert. *Science* 215, 1045–1053. doi: 10.1126/science.215.4536.1045

Friedmann, E. I., and Ocampo, R. (1976). Endolithic blue-green algae in the Dry Valleys: primary producers in the Antarctic Desert ecosystem. *Science* 193, 1247–1249. doi: 10.1126/science.193.4259.1247

George, S., Fierer, N., Levy, J., and Adams, B. J. (2020). Operational taxonomic unit (OTU) table characterizing water track and adjacent soil microbial communities in Taylor Valley, Antarctica during the 2012-13 austral summer. *Environ. Data Initiat.* 1:74.

Ghollarata, M., and Raiesi, F. (2007). The adverse effects of soil salinization on the growth of *Trifolium alexandrinum* L. and associated microbial and biochemical properties in a soil from Iran. *Soil Biol. Biochem.* 39, 1699–1702. doi: 10.1016/j.soilbio.2007.01.024

Gooseff, M. N., Barrett, J. E., and Levy, J. S. (2013). Shallow groundwater systems in a polar desert, McMurdo Dry Valleys, Antarctica. *Hydrogeol. J.* 21, 171–183. doi: 10.1007/s10040-012-0926-923

Grenié, M., Denelle, P., Tucker, C. M., Munoz, F., and Violle, C. (2017). funrar: an R package to characterize functional rarity. *Divers. Distribut.* 23, 1365–1371. doi: 10.1111/ddi.12629

Gunde-Cimerman, N., Plemenitaš, A., and Oren, A. (2018). Strategies of adaptation of microorganisms of the three domains of life to high salt concentrations. *FEMS Microbiol. Rev.* 42, 353–375. doi: 10.1093/femsre/fuy009

Hallsworth, J. E., Yakimov, M. M., Golyshin, P. N., Gillion, J. L. M., D'Auria, G., De Lima Alves, F., et al. (2007). Limits of life in MgCl2-containing environments: chaotropicity defines the window. *Environ. Microbiol.* 9, 801–813. doi: 10.1111/j.1462-2920.2006.01212.x

Harris, K. J., Carey, A. E., Lyons, W. B., Welch, K. A., and Fountain, A. G. (2007). Solute and isotope geochemistry of subsurface ice melt seeps in Taylor Valley, Antarctica. *Bull. Geol. Soc. Am.* 119, 548–555. doi: 10.1130/B25913.1

Hawes, I., and Howard-Williams, C. (2013). "Primary production processes in streams of the McMurdo Dry Valleys, Antarctica," in *Ecosystem Dynamics in a Polar Desert: The Mcmurdo Dry Valleys, Antarctica*, ed. J. C. Priscu (Washington, DC: American Geophysical Union), 129–140. doi: 10.1029/ar072p0129

IBM (2016). *IBM SPSS Statistics for Windows*. Armonk, NY: IBM Corp.

Kimbrel, J. A., Ballor, N., Wu, Y. W., David, M. M., Hazen, T. C., Simmons, B. A., et al. (2018). Microbial community structure and functional potential along a hypersaline gradient. *Front. Microbiol.* 9:1492. doi: 10.3389/fmicb.2018.01492

Lahti, L., and Shetty, S. (2012). *microbiome R Package*.

Langford, Z. L., Gooseff, M. N., and Lampkin, D. J. (2015). Spatiotemporal dynamics of wetted soils across a polar desert landscape. *Antarct. Sci.* 27, 197–209. doi: 10.1017/S0954102014000601

Lauber, C. L., Hamady, M., Knight, R., and Fierer, N. (2009). Pyrosequencing-based assessment of soil pH as a predictor of soil bacterial community structure at the continental scale. *Appl. Environ. Microbiol.* 75, 5111–5120. doi: 10.1128/AEM.00335-339

Lee, C. K., Barbier, B. A., Bottos, E. M., McDonald, I. R., and Cary, S. C. (2012). The inter-valley soil comparative survey: the ecology of dry valley edaphic microbial communities. *ISME J.* 6, 1046–1057. doi: 10.1038/ismej.2011.170

Lee, K. C., Caruso, T., Archer, S. D. J., Gillman, L. N., Lau, M. C. Y., Craig Cary, S., et al. (2018). Stochastic and deterministic effects of a moisture gradient on soil microbial communities in the McMurdo dry valleys of Antarctica. *Front. Microbiol.* 9:2619. doi: 10.3389/fmicb.2018.02619

Levy, J. (2012). Hydrological characteristics of recurrent slope lineae on Mars: evidence for liquid flow through regolith and comparisons with Antarctic terrestrial analogs. *Icarus* 219, 1–4. doi: 10.1016/j.icarus.2012.02.016

Levy, J. (2015). A hydrological continuum in permafrost environments: the morphological signatures of melt-driven hydrology on Earth and Mars. *Geomorphology* 240, 70–82. doi: 10.1016/j.geomorph.2014.02.033

Levy, J. S., Fountain, A. G., Gooseff, M. N., Barrett, J. E., Vantreese, R., Welch, K. A., et al. (2013). Water track modification of soil ecosystems in the Lake Hoare basin, Taylor Valley, Antarctica. *Antarct. Sci.* 26, 153–162. doi: 10.1017/S095410201300045X

Levy, J. S., Fountain, A. G., Gooseff, M. N., Welch, K. A., and Lyons, W. B. (2011). Water tracks and permafrost in Taylor Valley, Antarctica: extensive and shallow groundwater connectivity in a cold desert ecosystem. *Bull. Geol. Soc. Am.* 123, 2295–2311. doi: 10.1130/B30436.1

Levy, J. S., Fountain, A. G., Welch, K. A., and Lyons, W. B. (2012). Hypersaline "wet patches" in Taylor Valley, Antarctica. *Geophys. Res. Lett.* 39, 1–5. doi: 10.1029/2012GL050898

Lozupone, C. A., and Knight, R. (2007). Global patterns in bacterial diversity. *Proc. Natl. Acad. Sci. U.S.A.* 104, 11436–11440. doi: 10.1073/pnas.0611525104

Mahaffy, P. R., Webster, C. R., Atreya, S. K., Franz, H., Wong, M., Conrad, P. G., et al. (2013). Abundance and isotopic composition of gases in the martian atmosphere from the Curiosity rover. *Science* 341, 263–266. doi: 10.1126/science.1237966

Martín-Torres, F. J., Zorzano, M.-P., Valentín-Serrano, P., Harri, A.-M., Genzer, M., Kemppinen, O., et al. (2015). Transient liquid water and water activity at Gale crater on Mars. *Nat. Geosci.* 8, 357–361. doi: 10.1038/ngeo2412

McDonald, D., Price, M. N., Goodrich, J., Nawrocki, E. P., Desantis, T. Z., Probst, A., et al. (2012). An improved Greengenes taxonomy with explicit ranks for ecological and evolutionary analyses of bacteria and archaea. *ISME J.* 6, 610–618. doi: 10.1038/ismej.2011.139

McEwen, A. S., Ojha, L., Dundas, C. M., Mattson, S. S., Byrne, S., Wray, J. J., et al. (2011). Seasonal flows on warm Martian slopes. *Science* 333, 740–743. doi: 10.1126/science.1204816

McKnight, D. M., Tate, C. M., Andrews, E. D., Niyogi, D. K., Cozzetto, K., Welch, K., et al. (2007). Reactivation of a cryptobiotic stream ecosystem in the McMurdo Dry Valleys, Antarctica: a long-term geomorphological experiment. *Geomorphology* 89, 186–204. doi: 10.1016/j.geomorph.2006.07.025

Mevs, U., Stackebrandt, E., Schumann, P., Gallikowski, C. A., and Hirsch, P. (2000). *Modestobacter multiseptatus* gen. nov., sp. nov., a budding actinomycete from soils of the Asgard Range (Transantarctic Mountains). *Intern. J. Syst. Evol. Microbiol.* 50, 337–346. doi: 10.1099/00207713-50-1-337

Niederberger, T. D., Sohm, J. A., Gunderson, T. E., Parker, A. E., Tirindelli, J., Capone, D. G., et al. (2015). Microbial community composition of transiently wetted Antarctic Dry Valley soils. *Front. Microbiol.* 6:9. doi: 10.3389/fmicb.2015.00009

Nylen, T. H., Fountain, A. G., and Doran, P. T. (2004). Climatology of katabatic winds in the McMurdo Dry Valleys, southern Victoria Land, Antarctica. *J. Geophys. Res. D Atmos.* 109, 1–9. doi: 10.1029/2003jd003937

O'Brien, F. J. M., Almaraz, M., Foster, M. A., Hill, A. F., Huber, D. P., King, E. K., et al. (2019). Soil salinity and pH drive soil bacterial community composition and diversity along a lateritic slope in the Avon river critical zone observatory, Western Australia. *Front. Microbiol.* 10:1486. doi: 10.3389/fmicb.2019.01486

Ojha, L., Wilhelm, M. B., Murchie, S. L., McEwen, A. S., Wray, J. J., Hanley, J., et al. (2015). Spectral evidence for hydrated salts in recurring slope lineae on Mars. *Nat. Geosci.* 8, 829–832. doi: 10.1038/ngeo2546

Oksanen, J., Blanchet, F. G., Friendly, M., Kindt, R., Legendre, P., McGlinn, D., et al. (2019). *vegan: Community Ecology Package*.

Oren, A. (2013). "Life in magnesium- and calcium-rich hypersaline environments: Salt stress by chaotropic ions," in *Polyextremophiles. Cellular Origin, Life in Extreme Habitats and Astrobiology*, eds J. Seckbach, A. Oren, and H. Stan-Lotter (Dordrecht: Springer), 215–232. doi: 10.1007/978-94-007-6488-0_8

Peeters, K., Hodgson, D. A., Convey, P., and Willems, A. (2011). Culturable diversity of heterotrophic bacteria in Forlidas Pond (Pensacola Mountains) and Lundström Lake (Shackleton Range), Antarctica. *Microb. Ecol.* 62, 399–413. doi: 10.1007/s00248-011-9842-7

Pointing, S. B., Chan, Y., Lacap, D. C., and Lau, M. C. Y. (2009). Highly specialized microbial diversity in hyper-arid polar desert. *Proc. Natl. Acad. Sci. U.S.A.* 106, 19964–19969. doi: 10.1073/pnas.0908274106

Prober, S. M., Leff, J. W., Bates, S. T., Borer, E. T., Firn, J., Harpole, W. S., et al. (2015). Plant diversity predicts beta but not alpha diversity of soil microbes across grasslands worldwide. *Ecol. Lett.* 18, 85–95. doi: 10.1111/ele.12381

R Core Team (2017). *R: A Language and Environment for Statistical Computing*. Vienna: R Foundation for Statistical Computing.

Rainey, F. A., Ray, K., Ferreira, M., Gatz, B. Z., Nobre, M. F., Bagaley, D., et al. (2005). Extensive diversity of ionizing-radiation-resistant bacteria recovered from Sonoran Desert soil and description of nine new species of the genus *Deinococcus* obtained from a single soil sample. *Appl. Environ. Microbiol.* 71, 5225–5235. doi: 10.1128/AEM.71.9.5225-5235.2005

Rath, K. M., Fierer, N., Murphy, D. V., and Rousk, J. (2019). Linking bacterial community composition to soil salinity along environmental gradients. *ISME J.* 13, 836–846. doi: 10.1038/s41396-018-0313-318

Rath, K. M., and Rousk, J. (2015). Salt effects on the soil microbial decomposer community and their role in organic carbon cycling: a review. *Soil Biol. Biochem.* 81, 108–123. doi: 10.1016/j.soilbio.2014.11.001

Rennó, N. O., Bos, B. J., Catling, D., Clark, B. C., Drube, L., Fisher, D., et al. (2009). Possible physical and thermodynamical evidence for liquid water at the Phoenix landing site. *J. Geophys. Res.* 114:E00E03326. doi: 10.1029/2009JE003362

Rietz, D. N., and Haynes, R. J. (2003). Effects of irrigation-induced salinity and sodicity on soil microbial activity. *Soil Biol. Biochem.* 35, 845–854. doi: 10.1016/S0038-0717(03)00125-121

Rummel, J. D., Beaty, D. W., Jones, M. A., Bakermans, C., Barlow, N. G., Boston, P. J., et al. (2014). A new analysis of Mars "Special Regions": findings of the second MEPAG special regions science analysis group (SR-SAG2). *Astrobiology* 14, 887–968. doi: 10.1089/ast.2014.1227

Sardinha, M., Müller, T., Schmeisky, H., and Joergensen, R. G. (2003). Microbial performance in soils along a salinity gradient under acidic conditions. *Appl. Soil Ecol.* 23, 237–244. doi: 10.1016/S0929-1393(03)00027-21

Schmidt, F., Andrieu, F., Costard, F., Kocifaj, M., and Meresescu, A. G. (2017). Formation of recurring slope lineae on Mars by rarefied gas-triggered granular flows. *Nat. Geosci.* 10, 270–273. doi: 10.1038/ngeo2917

Seinfeld, J. H., and Pandis, S. N. (2006). *Atmospheric Chemistry and Physics: From Air Pollution to Climate Change*. New Jersey: John Wiley & Sons, Ltd.

Sirisena, K. A., Ramirez, S., Steele, A., and Glamoclija, M. (2018). Microbial diversity of hypersaline sediments from Lake Lucero playa in White sands national monument, New Mexico, USA. *Microb. Ecol.* 76, 404–418. doi: 10.1007/s00248-018-1142-z

Smith, J. L., Barrett, J. E., Tusnády, G., Rejtö, L., and Cary, S. C. (2010). Resolving environmental drivers of microbial community structure in Antarctic soils. *Antarct. Sci.* 22, 673–680. doi: 10.1017/S0954102010000763

Smith, P. H., Tamppari, L. K., Arvidson, R. E., Bass, D., Blaney, D., Boynton, W. V., et al. (2009). H_2O at the phoenix landing site. *Science* 325, 58–61. doi: 10.1126/science.1172339

Stanish, L. F., O'Neill, S. P., Gonzalez, A., Legg, T. M., Knelman, J., McKnight, D. M., et al. (2013). Bacteria and diatom co-occurrence patterns in microbial mats from polar desert streams. *Environ. Microbiol.* 15, 1115–1131. doi: 10.1111/j.1462-2920.2012.02872.x

Stillman, D. E., Michaels, T. I., and Grimm, R. E. (2017). Characteristics of the numerous and widespread recurring slope lineae (RSL) in Valles Marineris, Mars. *Icarus* 285, 195–210. doi: 10.1016/j.icarus.2016.10.025

Thompson, L. R., Sanders, J. G., McDonald, D., Amir, A., Ladau, J., Locey, K. J., et al. (2017). A communal catalogue reveals Earth's multiscale microbial diversity. *Nature* 551, 457–463. doi: 10.1038/nature24621

Toner, J. D., Sletten, R. S., and Prentice, M. L. (2013). Soluble salt accumulations in Taylor Valley, Antarctica: implications for paleolakes and Ross Sea Ice Sheet dynamics. *J. Geophys. Res.* 118, 198–215. doi: 10.1029/2012JF002467

Van Horn, D. J., Okie, J. G., Buelow, H. N., Gooseff, M. N., Barrett, J. E., and Takacs-Vesbach, C. D. (2014). Soil microbial responses to increased moisture and organic resources along a salinity gradient in a polar desert. *Appl. Environ. Microbiol.* 80, 3034–3043. doi: 10.1128/AEM.03414-3413

Van Horn, D. J., Van Horn, M. L., Barrett, J. E., Gooseff, M. N., Altrichter, A. E., Geyer, K. M., et al. (2013). Factors controlling soil microbial biomass and bacterial diversity and community composition in a cold desert ecosystem: role of geographic scale. *PLoS One* 8:e066103. doi: 10.1371/journal.pone.0066103

Van Trappen, S., Vandecandelaere, I., Mergaert, J., and Swings, J. (2004). *Gillisia limnaea* gen. nov., sp. nov., a new member of the family *Flavobacteriaceae* isolated from a microbial mat in Lake Fryxell, Antartica. *Intern. J. Syst. Evol. Microbiol.* 54, 445–448. doi: 10.1099/ijs.0.02922-2920

Vincent, W. F., Downes, M. T., Castenholz, R. W., and Howard-Williams, C. (1993). Community structure and pigment organisation of cyanobacteria-dominated microbial mats in antarctica. *Eur. J. Phycol.* 28, 213–221. doi: 10.1080/09670269300650321

Wang, Q., Garrity, G. M., Tiedje, J. M., and Cole, J. R. (2007). Naïve Bayesian classifier for rapid assignment of rRNA sequences into the new bacterial taxonomy. *Appl. Environ. Microbiol.* 73, 5261–5267. doi: 10.1128/AEM.00062-67

Wordsworth, R. D. (2016). "The climate of early Mars," in *Annual Review of Earth and Planetary Sciences*, Vol. 44, eds R. Jeanloz and K. H. Freeman (Palo Alto: Annual Reviews), 381–408.

Yuan, B. C., Li, Z. Z., Liu, H., Gao, M., and Zhang, Y. Y. (2007). Microbial biomass and activity in salt affected soils under arid conditions. *Appl. Soil Ecol.* 35, 319–328. doi: 10.1016/j.apsoil.2006.07.004

Zeglin, L. H., Dahm, C. N., Barrett, J. E., Gooseff, M. N., Fitpatrick, S. K., and Takacs-Vesbach, C. D. (2011). Bacterial community structure along moisture gradients in the parafluvial sediments of two ephemeral desert streams. *Microb. Ecol.* 61, 543–556. doi: 10.1007/s00248-010-9782-9787

Conflict of Interest: The authors declare that the research was conducted in the absence of any commercial or financial relationships that could be construed as a potential conflict of interest.

frontiers in Microbiology

ORIGINAL RESEARCH
published: 16 February 2021
doi: 10.3389/fmicb.2021.628792

Heterogeneity of Microbial Communities in Soils From the Antarctic Peninsula Region

*Pablo Almela[1], Ana Justel[2] and Antonio Quesada[1]**

[1] Department of Biology, Universidad Autónoma de Madrid, Madrid, Spain, [2] Department of Mathematics, Universidad Autónoma de Madrid, Madrid, Spain

Ice-free areas represent less than 1% of the Antarctic surface. However, climate change models predict a significant increase in temperatures in the coming decades, triggering a relevant reduction of the ice-covered surface. Microorganisms, adapted to the extreme and fluctuating conditions, are the dominant biota. In this article we analyze the diversity and composition of soil bacterial communities in 52 soil samples on three scales: (i) fine scale, where we compare the differences in the microbial community between top-stratum soils (0–2 cm) and deeper-stratum soils (5–10 cm) at the same sampling point; (ii) medium scale, in which we compare the composition of the microbial community of top-stratum soils from different sampling points within the same sampling location; and (iii) coarse scale, where we compare communities between comparable ecosystems located hundreds of kilometers apart along the Antarctic Peninsula. The results suggest that in ice-free soils exposed for longer periods of time (millennia) microbial communities are significantly different along the soil profiles. However, in recently (decades) deglaciated soils the communities are not different along the soil profile. Furthermore, the microbial communities found in soils at the different sampling locations show a high degree of heterogeneity, with a relevant proportion of unique amplicon sequence variants (ASV) that appeared mainly in low abundance, and only at a single sampling location. The Core90 community, defined as the ASVs shared by 90% of the soils from the 4 sampling locations, was composed of 26 ASVs, representing a small percentage of the total sequences. Nevertheless, the taxonomic composition of the Core80 (ASVs shared by 80% of sampling points per location) of the different sampling locations, was very similar, as they were mostly defined by 20 common taxa, representing up to 75.7% of the sequences of the Core80 communities, suggesting a greater homogeneity of soil bacterial taxa among distant locations.

Keywords: microorgamisms, soil, distribution, heterogeneity, homogeneity, Antarctica

OPEN ACCESS

Edited by:
Laura Zucconi,
University of Tuscia, Italy

Reviewed by:
Angelina Lo Giudice,
National Research Council (CNR), Italy
Kevin Newsham,
Natural Environment Research Council, United Kingdom

****Correspondence:***
Antonio Quesada
antonio.quesada@uam.es

Specialty section:
This article was submitted to Extreme Microbiology, a section of the journal Frontiers in Microbiology

Received: *12 November 2020*
Accepted: *28 January 2021*
Published: *16 February 2021*

Citation:
Almela P, Justel A and Quesada A (2021) Heterogeneity of Microbial Communities in Soils From the Antarctic Peninsula Region. Front. Microbiol. 12:628792. doi: 10.3389/fmicb.2021.628792

INTRODUCTION

Ice-free areas in Antarctica comprise less than 1% of the continent (Cowan, 2014; Burton-Johnson et al., 2016), constituting extremely cold and arid distant and isolated patches within a matrix of ice. These areas, which are not permanently covered by snow or ice, considered oases in the middle of a desert, are of an enormous ecological relevance, since are home to most of the continent's biodiversity.

Antarctica is warming. Although the rate of warming in maritime Antarctica seems to be slowing down (Turner et al., 2016), Rignot et al. (2019) has determined an ice mass loss of billions of tons per year, for the period 1979 to 2017, in all regions of the continent due to climate change. The Antarctic Peninsula region has had the largest warming of any other terrestrial environment in the southern hemisphere in recent decades (Siegert et al., 2019). The predictions for the end of the century suggest a 25% increase of new ice-free areas in Antarctica, with more than 85% emerging in the North Antarctic Peninsula bioregion (Lee et al., 2017).

These ice-free areas have been exposed for a variable time span, being subjected to glacier retreats and advances. Thus, some areas have been only recently deglaciated and exposed for some decades, as Clark Nunatak (Oliva and Ruiz-Fernández, 2017), while others have been mostly deglaciated for millennia, as Byers Peninsula (Livingston Island, Antarctic Peninsula region) (Oliva et al., 2016). They include islands, nunataks (exposed mountain tops), cliffs, plateaus, ice-free valleys and scree slopes, among others. In any of its forms, these ecosystems are governed by low temperatures, wide temperature fluctuations, low nutrient status, low water availability, high incident radiation, and high levels of physical disturbance (e.g., glaciofluvial activity, frost weathering and cryoturbation). These extreme conditions preclude the establishment of larger organisms (macrobes), resulting in environments dominated by microorganisms (Hughes et al., 2015). Therefore, they constitute a perfect scenario for the study of distribution establishment and ecological functioning of soil microbial communities.

Although new 'omics' techniques have contributed greatly to a better understanding of communities inhabiting soils (Smith et al., 2006; Krauze et al., 2020), this knowledge is quite fragmented, and results obtained from different studies are hardly comparable among them to obtain a clear idea about the distribution of microbial communities in polar regions. It is well known in other latitudes that the microbial communities are different along the soil profiles, with relevant heterogeneity in the distribution of the soil microorganisms in the same biotope (Frey et al., 2013). The highest abundance and diversity of microorganisms that inhabit soils are located in the most superficial centimeters (Brown and Jumpponen, 2014). Previous studies have examined the effects of depth on Antarctic soil bacterial communities (Herbold et al., 2014). Nevertheless, this heterogeneous distribution of the microbial communities has not been as widely studied on a wide geographical scale (Horrocks et al., 2020), where cryoturbation and other physical process can alter the biotope.

In this paper we analyze the composition of the soil bacteria at three different scales, in order to determine at what level of sampling we were able to identify heterogeneity between ecologically comparable soils. At the fine scale, we compare the microbial community differences between the top-stratum soil (tss) and deeper-stratum soils (dss) at exactly the same sampling point at two sampling locations. In the medium scale, we study the heterogeneity of bacterial communities in top stratum soils at a local scale, comparing the diversity and structure of the communities obtained in sectors within the same geographical location. Finally, in the coarse scale we compare communities from the top stratum soils among sampling locations located in a wide range in the Antarctic Peninsula region.

Our main working hypothesis is that in extreme ecosystems, such as Antarctic soils, in which environmental constraints are the limiting factors, some microorganisms with better survival strategies and better dispersal mechanisms, will occur in those communities without reference to geographical distribution, or local minor aspects. Therefore, microbial communities will present common taxa in ecologically comparable ecosystems even at wide geographical scale.

MATERIALS AND METHODS

Study Area

The study area included four locations along the Antarctic Peninsula (**Figure 1A**). These areas were selected based on their ecological similarity, remaining ice-free during the summer and vegetation free and free of megafauna disturbances, to the best of our knowledge (**Supplementary Plate 1**). The physical and chemical characteristics of the soil were similar among locations (**Supplementary Table 1**), with values of Total Organic Matter (TOM) and C/N ranging between 0.2–0.3%(p/p) and 3.8–5, respectively. The apparent density of soils showed equal values for all locations (1.6 g/cm^3), and the soil texture classification was determined as 'sandy loam' and 'loamy sand.' The pH values showed variations that ranged between 4.6 and 7.9.

There are evidences indicating that the four sampling locations were ice covered for different time periods (from millennia to decades), following next gradient from the oldest to the most recent: Byers Plateau, Elephant Point, Clark Nunatak, and Biscoe Point.

Three sampling locations were located in Livingston Island, the second largest island in the South Shetland archipelago: Byers Plateau, Clark Nunatak and Elephant point. Byers Peninsula, located at the western end of Livingston Island, is one of the largest ice-free areas in the Antarctic Peninsula and the largest in the South Shetland Islands. The coast itself and the ice margin of Rotch Dome glacier form a clearly defined and visually obvious boundary with the island, of approximately 60 km^2. The retreat of Rotch Dome glacier predated 8.3 cal. ky in the westernmost third of the peninsula as a response to warmer climate conditions in the Antarctic Peninsula region during the Early Holocene, and continued eastwards, becoming ice-free the easternmost area probably before 1.8 cal. Ky (Oliva et al., 2016). Today the Rotch Dome sits in contact with the moraine in the central plateau, therefore not being associated to a recent process of glacial retreat. Soils from Byers Plateau (62°38′S, 60°58′W, **Supplementary Table 2**) were collected from an area of the plateau bordering the Rotch dome glacier front and moving away up to 500 m (**Figure 1B**).

Clark Nunatak is a rocky peak located in the SE corner of Byers Peninsula, surrounded by the Rotch Dome glacier. It is estimated that the glacier has retreated from the moraine limits

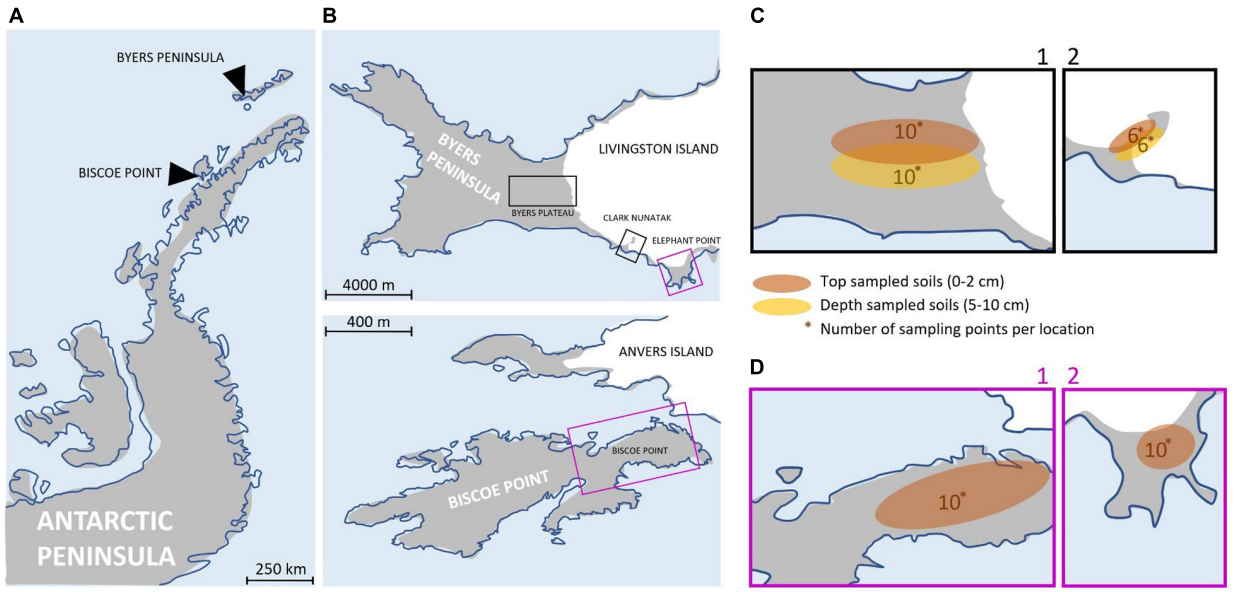

FIGURE 1 | (A) Map of the Antarctic Peninsula. **(B)** Maps showing the 4 sampling locations at Byers Peninsula and Elephant Point in Livingston island (South Shetland Islands) and Biscoe Point (Anvers Island). The sampling locations have been highlighted by squares of different colors, depending on whether the samplings were of top-stratum soils (0–2 cm; purple square) or top- and depper-stratum soils (0–2 cm/5–10 cm; black square). **(C)** Local-scale sampling locations where top- and depper-stratum soils samples were collected: Plateau (C1) and Nunatak (C2). The numbers indicate the samples that were collected. **(D)** Local-scale sampling locations where top-stratum soil samples were collected: Biscoe (D1) and Elephant (D2). The numbers indicate the samples that were collected.

very recently, probably after 1950 (Oliva and Ruiz-Fernández, 2017; Palacios et al., 2020). For this reason, it is not until 2002 when the Antarctic Treaty Consultative Meeting (ATCM) included it within ASPA 126, since in previous versions the small ice-free ground surface did not exist. Samples from Nunatak (62°40′S, 60°54′W, **Supplementary Table 2**) were collected from an area bordering the Rotch Dome glacier front and moving away up to 200 m (**Figure 1B**). Elephant Point (E) is an ice-free peninsula of 1.16 km^2 in the SW of Livingston Island. It is limited by the Rotch Dome glacier in the north and the sea encircling the rest of its margins. In this area there is evidence of glacial retreat, which has been accelerated over the last decades in response to the recent warming detected in the Antarctic Peninsula region (Steig et al., 2009; Thomas et al., 2009). It is estimated that 17% of the total land surface exposed today in Elephant Point appeared between 1956 and 2010 (Oliva and Ruiz-Fernández, 2015). Soil samples from Elephant Point (62°40′S, 60°51′W, **Supplementary Table 2**) were collected from an area bordering the Rotch Dome glacier front and moving away up to 300 m (**Figure 1B**).

The fourth sampling location was at Biscoe Point, an area of 0.59 km^2 located near the south-west coast of Anvers Island, in the Palmer Archipelago. Until recently, Biscoe Point formed a peninsula joined to Anvers Island by an ice ramp extending from the adjacent glacier. The ice ramp disappeared as the glacier retreated at least between 1985 and 2004 (ATCM XIII, 1985; ATCM, 2004), and a narrow sea channel now separates Anvers Island from the island on which Biscoe Point lies (ATCM, 2014). Soil samples from Biscoe (64°48′S, 63°46′W, **Supplementary Table 2**) were collected from the area closest to the glacier front, now on Anvers Island, and moving away up to 400 m (**Figure 1B**).

Sampling

Samplings were conducted during two different Antarctic campaigns: February 2018 in Plateau and Nunatak (**Figure 1C**) and January 2019 in Biscoe and Elephant (**Figure 1D**). The sampling points were fixed previously to the field campaign to collect in each location two samples from each of the 5 sectors (from I to V) in Plateau, Elephant and Biscoe, and 3 sectors (from I to III) in Nunatak (**Supplementary Table 2**), in order to test the potential heterogeneity due to patchy distribution of bacterial soil communities.

At each sampling point, we obtained samples comprised of 3 subsamples collected within at approx. 1 m distance of top-stratum soils (0–2 cm) to avoid the vertical heterogeneity in microbial communities attributable to soil horizon development, as recommended by Sigler et al. (2002) and Rime et al. (2015). It is in these first few centimeters that factors such as light, among others, could be critical for the C input in the ecosystem, and conditioning the composition of the communities. The soils considered into this study do not have another organic C input than microbial primary production (i.e., photosynthesis), since there are no plants and animal debris cannot reach the sites, besides the aerial transportation and eventual birds droppings. Additionally, in order to test the fine scale homogeneity due to the soil horizons development, deeper-stratum soil (5–10 cm) were collected in each sampling point of Plateau and Nunatak.

All soil samples were placed in sterile 50 ml Falcon® tubes and frozen at −20°C for shipment and storage until processing in the laboratory. Every sample was obtained directly with the plastic tubes without any tool to avoid potential contamination.

DNA Extraction, Sequencing and Taxonomical Assignment

Total genomic DNA extraction was performed independently from the 4 different sampling locations and for soil strata, using the PowerSoil DNA Isolation Kit (MO BIO Laboratories, Inc.) according to standard procedures. DNA concentrations were determined in a NanoDrop ND 1000 spectrophotometer (Thermo Fisher Scientific™). The 16S rRNA gene was amplified by PCR using barcoded primers set 341F (5′- CCT AYGGGRBGCASCAG -3′) and 806R (5′- GGACTACNNGGG TATCTAAT -3′) targeting the V3–V4 hypervariable regions (Otani et al., 2014). This universal primer set is for bacterial community and the archaeal community was not included in the study. The pool of samples with the prepared libraries was sequenced by Illumina MiSeq platform. The sequencing was performed in two cycles, in the first cycle the Plateau and Nunatak samples were included, and in the second cycle the Elephant and Biscoe samples.

Microbiome 16S rRNA gene diversity was assessed with QIIME v2-2019.4 (Bolyen et al., 2019). Briefly, cleaned and trimmed paired reads were filtered and denoised using DADA2 plug-in (Callahan et al., 2016). For chimera identification, 250.000 training sequences were used. Identified amplicon sequence variants (ASVs) were aligned using MAFFT (Katoh et al., 2002) and further processed to construct a phylogeny with fasttree2 (Price et al., 2010). Taxonomy was assigned to ASVs using the q2-feature-classifier (Bokulich et al., 2018) and blasted against the SILVA v132 99% 16S sequence database (Quast et al., 2012). Taxonomical assignation was carried out at the same time with all samples after the bioinformatics took place.

Sequences generated by this study were deposited to GenBank under the BioProject accession number PRJNA678471.

Statistical Analysis

Some summary statistics of the ASVs obtained in each sampling location were calculated to obtain 'Total ASV' (total quantity), 'Different ASV', 'Predominant ASV' (more than 1000 copies per sampling location) and 'Unique ASV' (present in a sampling location and absent in the others). Also, ASVs were binned into 'core community' (highly persistent) if present in 90% (referred to as the Core90) or 80% (Core80) of soil samples. The Core90 community analysis was carried out for Plateau, Nunatak, Elephant and Biscoe sampling locations together. The Core80 community analysis was performed for the 4 sampling locations separately, thus obtaining the 'core community' of each location (if present in 80% of sampling points of a sampling location). The data obtained from each Core80, and their taxonomic assignments, were jointly compared between the 4 locations to determine their distributions. Results are shown in **Table 2**.

Alpha diversity indices (Richness and Shannon Index) and their rarefaction curves were estimated using the plugin q2-diversity (running 10 iterations and 1000 sequence steps up to the maximum number of sequences per sample). The lowest sample-specific sequencing depth (104777) were used to compensate for the variation in read numbers. Beta diversity was assessed using Bray-Curtis dissimilarities between the community compositions of the sampling sites.

We have proposed different experimental design models, depending on the scale, for analyzing the influence of the depth, sector or location factors on the diversity:

- At the fine scale, we adjusted two balanced block experimental design models in which the factor was the soil depth, and the block was the sampling point. One with data from 2 soil depths at 10 sampling points in Plateau, and the other with data from 2 soil depths at 6 sampling points in Nunatak.
- At the medium scale, we adjusted four balanced one-factor experimental design models, one for each location (Plateau, Nunatak, Elephant, and Biscoe), in which the sector was the factor. Each model was fitted with data from two top-stratum soils of each of the sectors into which the sampling locations were divided.
- At the coarse scale, we adjusted a one-factor experimental design model, in which the factor was the location, with the data from all the top-stratum soils collected at the four locations.

We tested the homogeneity of alpha diversity indices between the two soil horizons, within site locations, and between locations, using one- and two-way ANOVA tests. To make the same comparisons using the information provided by the Bray-Curtis dissimilarity matrices, we used permutational multivariate analysis of variance tests (PERMANOVA). Differences are considered statistically significant if p-value < 0.05. When any of the hypothesis of equality of means is rejected, the corresponding multiple comparisons are made with Bonferroni correction with overall significance level $\alpha = 0.05$.

Plots of the two principal components of PCoA were used to visualized proximity in the community composition among samples. A heatmap of two-way cluster using Bray-Curtis dissimilarities was used to visualize the relative abundances of bacteria in Core80 of Plateau, Nunatak, Elephant and Biscoe. The heatmap was based on the predominant ASVs ($\geq$1000 copies) present in any of the Core80.

Data visualization, alpha and beta diversity comparisons and multivariate statistics were performed using the R environment with the vegan (Oksanen et al., 2015) and ggplot packages.

RESULTS

Diversity and Microbial Community at Different Soil Strata (Fine Scale)

Our sampling design focuses first on identifying the differences between the bacterial community in the two soil-strata defined at two sampling locations (Plateau and Nunatak). The alpha diversity indices have shown a markedly different pattern

between the sampling locations (**Figure 2A**). At the sampling location Nunatak, there were no significant differences between the means of the Richness (1328 and 1238 for tss and dss, respectively) and Shannon indices (8.5 and 8.1 for tss and dss, respectively) in the communities found at the two soil-strata (**Table 1**). On the contrary, the means of both alpha diversity indices were significantly different at Plateau sampling location. The mean Richness in tss was 1729 (SD = 422), higher than in dss, where it was 1512 (SD = 373). The mean of Shannon index in tss was 9.4 (SD = 0.6), also higher than in dss, where it was 8.9 (SD = 0.6). Similar behavior was observed in the bacterial community composition. The PERMANOVA tests (**Table 1**) showed that there were significant differences between tss and dss communities in Plateau ($p = 0.007$), while the differences were not significant in the soil profile at Nunatak ($p = 0.814$).

The differences between tss and dss community structures were smaller at Nunatak than at Plateau. The PCoA plot (**Figure 2B**) illustrates these two different results, showing closer similarity between samples in the same sampling point in the case of Nunatak. In Plateau, samples from the same sampling point are as similar as those from different sampling points at the same or different depths points.

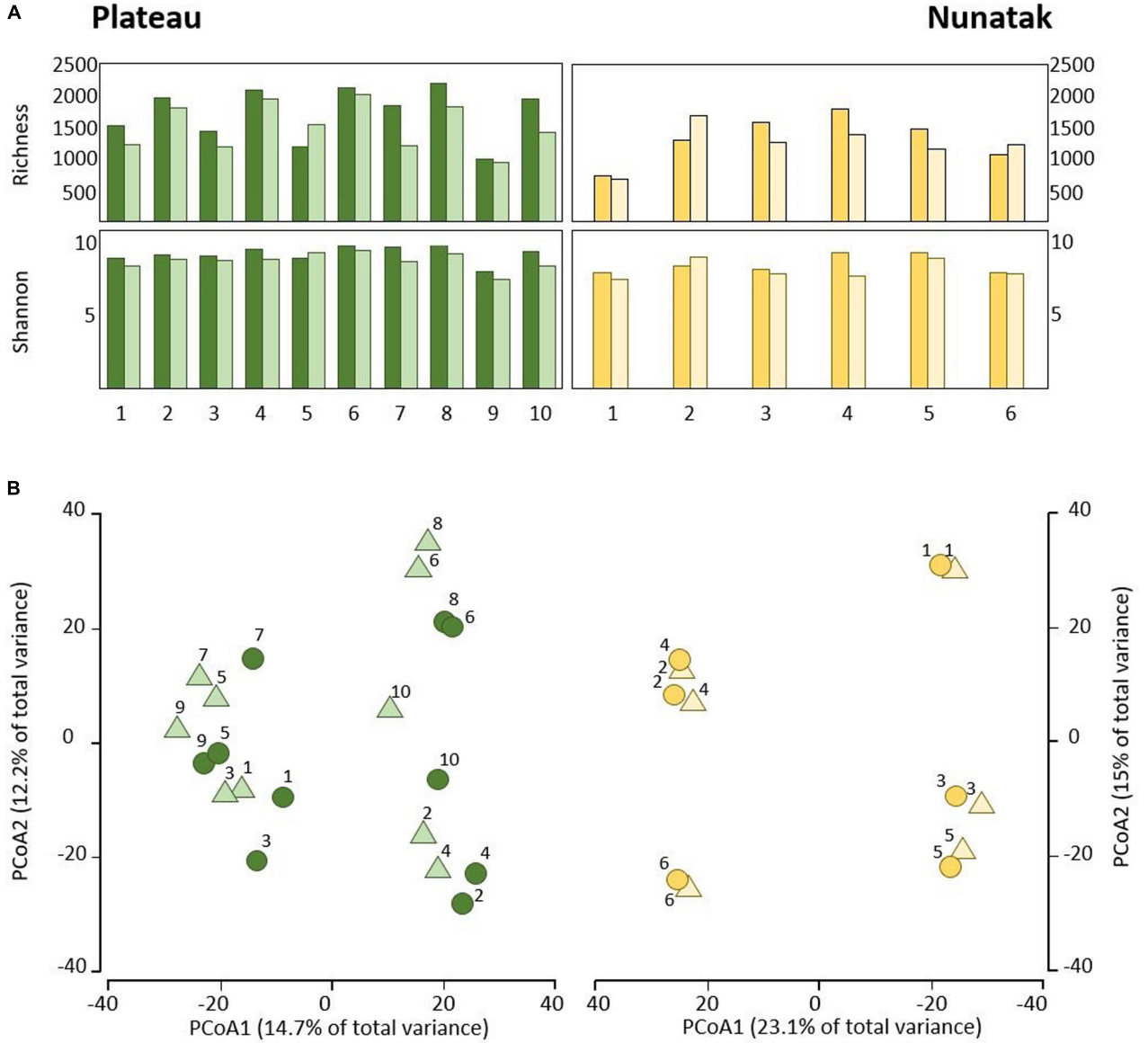

FIGURE 2 | (A) Alpha diversity indices of the bacterial community of top-stratum soils (0–2 cm; dark colored plots) and deeper-stratum soils (5–10 cm; light colored plots) from Plateau and Nunatak. **(B)** Principal coordinate analysis (PCoA) of the bacterial community composition of top-stratum soils (0–2 cm; dark colored dots) and deeper-stratum soils (5–10 cm; light colored triangles) from Plateau and Nunatak. The principal coordinate analysis are based on Bray-Curtis dissimilarity matrices between the microbiome profiles. Distances between symbols on the ordination plot reflect relative dissimilarities in community structures. The variation in microbial community structures explained by each PCoA axis is given in parentheses.

TABLE 1 | *p*-values of the ANOVA and PERMANOVA (Permutational Multivariate Analysis of Variance) tests for comparisons of richness and diversity, and composition of the bacterial community, respectively, among surface soil samples at different areas in each location (Plateau, Nunatak, Elephant, and Biscoe).

Scale	Description of the samples	Richness	Diversity	Community	ANOVA/ Permanova	Sample size
Fine	Top-stratum soils (0–2 cm) and deeper-stratum soils (5–10 cm) from Plateau	**0.034**	**0.005**	**0.007**	Two-way	10 pairs
Fine	Top-stratum soils (0–2 cm) and deeper-stratum soils (5–10 cm) from Nunatak	0.517	0.259	0.815	Two-way	6 pairs
Medium	top-stratum soils (0–2 cm) from Plateau	0.753	0.452	0.657	One-way	2 samples for 5 areas
Medium	top-stratum soils (0–2 cm) from Nunatak	0.205	0.832	0.800	One-way	2 samples for 3 areas
Medium	top-stratum soils (0–2 cm) from Elephant	0.990	0.590	**0.012**	One-way	2 samples for 5 areas
Medium	top-stratum soils (0–2 cm) from Biscoe	0.208	0.149	0.380	One-way	2 samples for 5 areas
Coarse	Top-stratum soils (0–2 cm) from Plateau (P), Nunatak (N), Elephant (E), and Biscoe (B)	0.099	**0.003**	**0.000**	One-way	10 samples of P, 6 of N, 10 of E, 10 of B

Diversity and Composition of Prokaryotic Communities Within the Different Sampling Locations (Medium Scale)

The bacterial communities from top-stratum soils from Plateau, Nunatak, Elephant and Biscoe locations were analyzed independently for each sampling location. There were not significant differences in terms of richness, diversity and community structure (**Table 1**). ANOVA and PERMANOVA tests showed no significant evidence of within location heterogeneity when comparing the different sampling sectors, with the glacial front of each site as a reference point, considered in Plateau, Nunatak and Biscoe. In location Elephant there were no significant differences between the sampled sectors in terms of richness and diversity; although a significant evidence of heterogeneity (PERMANOVA test $p = 0.012$) was observed in the structure of the prokaryotic communities among the sampled sectors.

Bacterial Community Diversity, Richness and Structure at Different Locations (Coarse Scale)

From the results obtained in the medium scale, we can consider all the sampling sites within the same location as a representative sample of its soil microbial community. Comparing the four locations, we observe that median of ASVs richness and diversity was the highest in the Plateau samples and lowest in the Nunatak ones (**Figure 3A**). ANOVA and PERMANOVA tests (**Table 1**) indicated that both the diversity and composition of the bacterial community were different between locations, while there were no significantly clear differences between the means of Richness. For the Shannon index, the Bonferroni multiple comparison tests showed that there were only significant differences between the Plateau mean and the Elephant and Biscoe means. There was no significant evidence of heterogeneity in the comparisons among Nunatak, Elephant and Biscoe, neither between Plateau and Elephant (**Figure 3A**).

The differences in the bacterial communities measured with the Bray-Curtis dissimilarity are represented in the plot of the two main principal coordinates obtained in a PCoA **(Figure 3B**). Ordinations based on this metric demonstrated a clear separation of bacterial communities among the sampling locations, except for the bacterial community from Nunatak which was slightly intermixed with Plateau and midway toward the other two communities, Biscoe and Elephant.

Description of Microbial Communities and Similarities in Communities Among Sampling Locations

The description of the communities found in the different sampling locations is illustrated in **Figure 4**. In Plateau the highest number of different ASV was found, which was almost 2-fold higher than the community from Nunatak location (11566 and 6366 ASVs for Plateau and Nunatak, respectively), with the lowest amount of different ASVs. At Plateau location only 0.6% of the different ASVs (70 ASVs) were found predominant with more than 1000 copies and represented over 41% of the total ASVs, indicating that a low number of different sequences represented a large proportion of the community found at this location. Moreover, at Plateau location 11% of the total sequences were found only at this sampling location (unique ASVs) and reached 68.9% of the different sequences. Most of those unique sequences are found in low abundance, thus, only 2.7% of the total sequences were unique and predominant (over 100 copies) representing 1.7% of the different ASVs. A very similar pattern was found in the other locations, where the number of predominant ASVs (more than 1000 copies) reached 44, 45.7 and 52% of the total ASVs for Nunatak, Elephant and Biscoe, respectively. These predominant sequences were composed of few different ASVs, representing 0.8, 1.8, and 2% of the total different ASVs for Nunatak, Elephant, and Biscoe. In addition, 5.3, 10.9 and 9.9% of the total ASVs found in Nunatak, Elephant and Biscoe were classified as unique ASVs, representing 48, 54.9 and 55.9% of the diversity of the different ASVs determined in each location.

Core Community

The microbial Core90 analysis revealed that 26 ASVs were found in at least 90% of the total sampling points from all locations (**Figure 4**). These results indicated that the soil bacterial communities at the highest level of taxonomic resolution were apparently not homogeneous between the 4 sampling locations. This 'core community' represented a low proportion of ASVs from total ASVs sequenced.

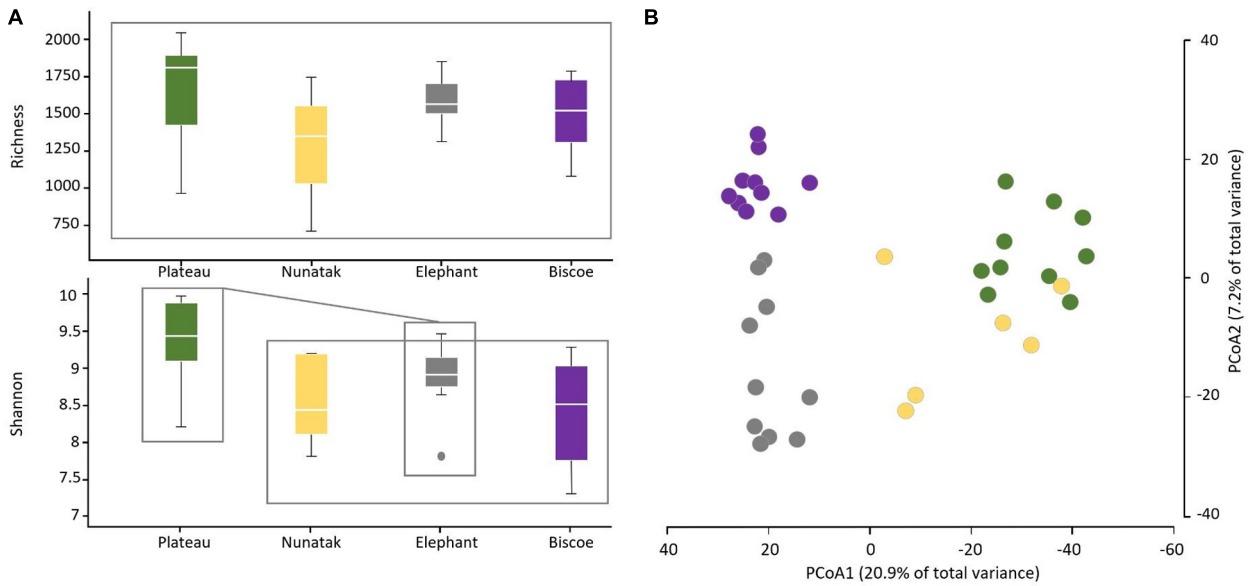

FIGURE 3 | (A) Boxplots of the alpha diversity indices of the bacterial community composition of top-stratum soils (0–2 cm) for each of the sampling locations included in this study. **(B)** Principal coordinate analysis (PCoA) of the bacterial community composition of top-stratum soils (0–2 cm) from the samplings. The principal coordinate analysis is based on Bray-Curtis dissimilarity matrix. Distances between symbols on the ordination plot reflect relative dissimilarities in community structures. The variation in microbial community structures explained by each PCoA axis is given in parentheses.

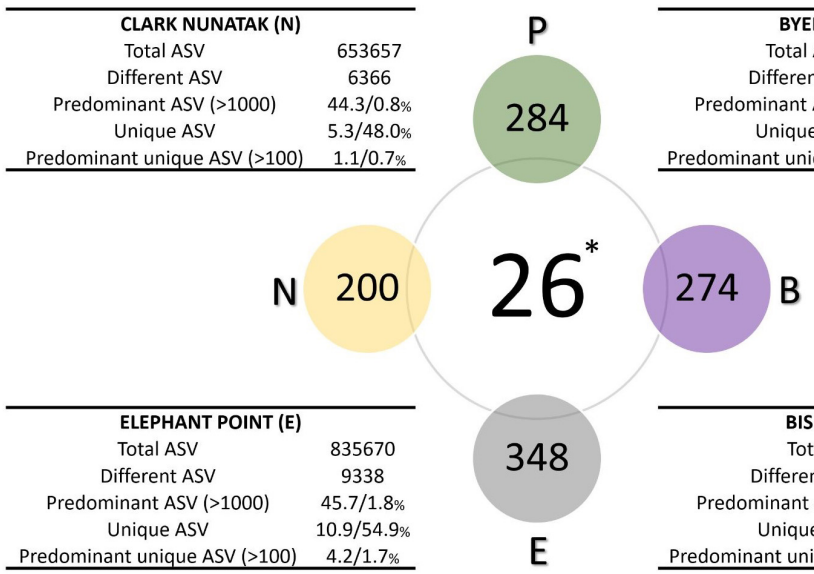

CLARK NUNATAK (N)	
Total ASV	653657
Different ASV	6366
Predominant ASV (>1000)	44.3/0.8%
Unique ASV	5.3/48.0%
Predominant unique ASV (>100)	1.1/0.7%

BYERS PLATEAU (P)	
Total ASV	1148861
Different ASV	11566
Predominant ASV (>1000)	41.4/0.6%
Unique ASV	11.0/68.9%
Predominant unique ASV (>100)	2.7/1.7%

ELEPHANT POINT (E)	
Total ASV	835670
Different ASV	9338
Predominant ASV (>1000)	45.7/1.8%
Unique ASV	10.9/54.9%
Predominant unique ASV (>100)	4.2/1.7%

BISCOE POINT (B)	
Total	890643
Different ASV	8570
Predominant ASV (>1000)	52.4/2.0%
Unique ASV	9.9/55.9%
Predominant unique ASV (>100)	3.4/1.7%

FIGURE 4 | Diagram comparing the bacterial core communities. Colored spheres indicate the number of ASVs in at least 80% of top-stratum soils (core80) of each sampling location, while the central sphere (*) indicates the Core90 (90% of all the top-stratum soils). For each location, in the tables are shown the number of total and different ASV of the bacterial community, and the percentages of the predominant ASV (at least 1000 copies), the unique ASV at each location (not present in other sampling areas), and the percentage of the predominant unique ASV (at least 100 copies), according to total and different ASV, respectively.

The 'Core80' was analyzed for Plateau, Nunatak, Elephant, and Biscoe, to describe its local composition and relative abundances (**Figure 4**). Thus, 284 ASVs in Plateau, 200 ASVs in Nunatak, and 348 and 274 ASVs in Elephant and Biscoe, respectively, were revealed. A PCoA plot, based on Bray-Curtis dissimilarity, was generated (**Figure 5B**) to visualize the proximities between the sampling points when considering only the ASVs found in any of the Core80. Results showed that ASVs from the four Core80 bacterial communities are well separated, except for one sample from Nunatak that is closer to some samples from Plateau than to the rest. A Heatmap (**Figure 5A**) was used to visualize the relative abundance of predominant ASVs (≥1000 copies) from

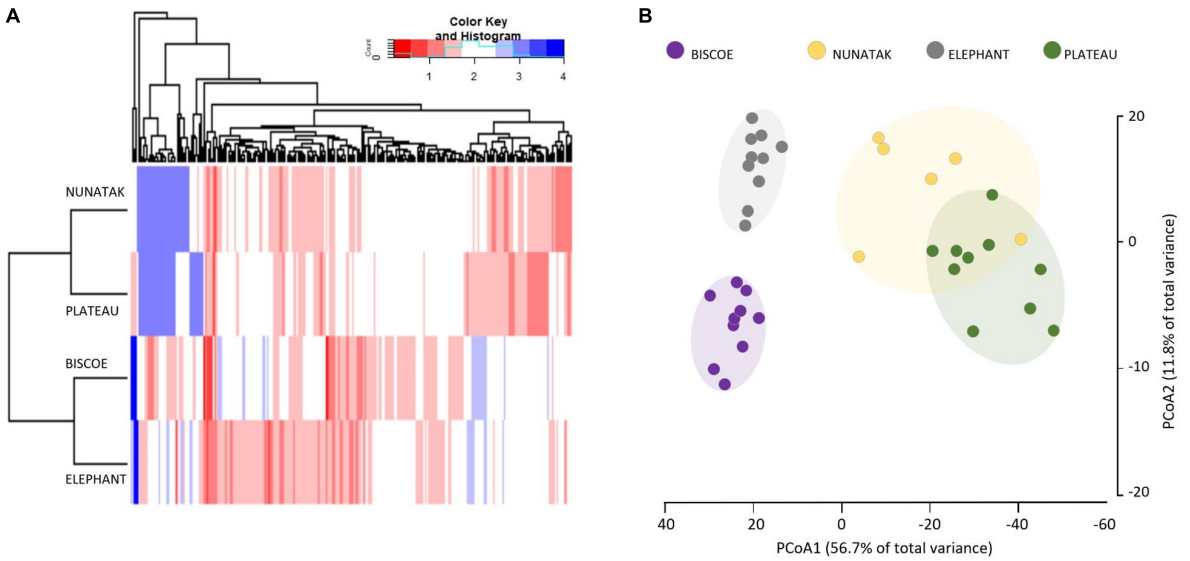

FIGURE 5 | (A) Heatmap of two-way cluster analysis performed on most abundant Core80 bacterial community (only ASVs > 1000 copies) of all top-stratum sample soils from Plateau, Nunatak, Elephant and Biscoe, using Bray-Curtis dissimilarities. The color intensity in the cluster dendrogram correspond to the abundance of normalized reads. **(B)** Principal coordinate analysis (PCoA) for all the sampling points when considering only the ASVs in any of the Core80. The principal coordinate analysis is based on the Bray-Curtis dissimilarity matrix. Distances between symbols on the ordination plot reflect relative dissimilarities in community structures. The variation in microbial community structures explained by each PCoA axis is given in parentheses.

Core80, regardless of taxonomic assignment. Results revealed that Plateau and Nunatak clustered together and separately from Elephant and Biscoe, that also clustered together, suggesting that core communities from those locations have more in common than the other locations.

The Core80 communities were also explored in detail in terms of taxonomic assignment. Family level was considered appropriate because of taxonomic resolution and ecological relevance for most of the bacterial groups. At this taxonomic level (or similar) the core communities were represented by a much lower number of identities, which ranged from 25 to 28. The ASVs included in those groups represented between 77.1 and 85.4% of the total sequences within the Core80 community. The most part (20) of the identities were found in all the core communities and represented up to 75.7% of the total ASVs in the Core80. These 20 groups belonged in the majority to Actinobacteria (8) and Proteobacteria (6), but Acidobacteria, Gemmatobacteria, Bacteriodetes, Cyanobacteria, and Chloroflexi were also represented (**Table 2**).

DISCUSSION

Microorganisms are the dominant biota and play a key role in the ecology of Antarctic terrestrial ecosystems (Cowan, 2014). Investigating the distribution of microbial diversity is essential to understanding ecological functioning of these ecosystems. The purpose of our analysis is to investigate the heterogeneity of the microbial community inhabiting ecologically comparable soils (no vegetation in the proximity of the sampling site, no megafauna presence, similar microtopographic characteristics, granulometry, etc.) in the Antarctic Peninsula. This work considers different scales, starting at the fine scale, in which we compare, at the closest sampling locations (Plateau and Nunatak), the microbial community differences between the top-stratum (tss) and deeper-stratum soils (dss) at exactly the same sampling point. The medium scale brings into comparison the top-stratum communities found within the same sampling location (e.g., Plateau). Finally, the coarse scale compares the top stratum communities found among the four sampling locations (Plateau, Biscoe, Nunatak and Elephant) with diverse geographical distance.

The study revealed that comparisons of bacterial communities from different soil strata at Plateau resulted in low P-values (P = 0.007), indicating significant differences among the soil-strata, and therefore a non-homogeneous and differentiated distribution according to a vertical profile. Conversely, bacterial populations from Nunatak have shown a vertical homogeneity of their communities. These differences in the homogeneity of distribution among soil strata in the two locations are attributable to the length of the ice-free period, since ecologically the sampling locations are comparable. Oliva et al. (2016) have dated areas close to the soils studied in Byers Peninsula in thousands of years, while the soil samples from Nunatak Clark have only been ice-free in summer for a few decades from the present. As described by Barrett et al. (2006), vertical distributions of the soil microbiomes would be related to the variation in soil properties. Niederberger et al. (2008) showed how the highest microbial diversity in Antarctic soils was related with the highest levels of organic matter, while Chu et al. (2016) also related it to the N available in the different soil layers of the Tibetan Plateau. Such large temporal differences among Plateau and Nunatak should

TABLE 2 | Taxonomy summary of the dominant bacteria in Core80 analysis of the sampling locations.

Taxa	Plateau	Nunatak	Elephant	Biscoe
	% Core80	% Core80	% Core80	% Core80
Hydrogenophilaceae (Thiobacillus)	–	–	1.7	0.4
Iamiaceae (Iamia)	0.7	0.4	1.4	0.7
Tenderiaceae (Tenderia)	–	1.2	7.1	0.2
Pseudanabaenaceae (Pseudanabaena)	–	4.1	0.8	0.3
Phormidiaceae (Tychonema)	–	0.0	6.7	10.9
Intrasporangiacea (Oryzihumus)	11.8	9.9	3.6	1.2
Gaiellales	14.4	2.4	2.5	1.6
Chitinophagaceae (Chitinophaga)	7.1	5.3	5.0	7.4
Gemmatimonadetes (Gemmatimonas)	12.0	21.9	3.2	4.9
Chthoniobacteraceae (Udaeobacter)	7.0	0.5	–	–
Actinobacteria (MB-A2-108)	2.8	0.7	–	–
ilumatobacter (Ilumatobacter)	3.1	2.4	4.2	4.5
Frankiales	2.5	0.6	2.3	2.4
Chloroflexi- KD4	2.2	1.9	1.8	1.2
Pyrinomonadaceae (RB-41)	1.8	0.1	–	–
Sphingomonadaceae (Sphingomonas)	4.4	12.3	13.2	17.9
IMCC26256 (Ferrimicrobium)	2.1	0.8	0.1	–
Nocardioidaceae (Nocardioides)	1.5	1.1	4.7	2.6
Xanthomonadaceae (Lysobacter)	1.4	7.2	5.0	7.4
Rubrobacteria	1.4	0.1	1.4	2.3
Solibacteraceae (Bryobacter)	1.3	0.2	0.6	0.4
Blastocatellaceae (JGI 0001001-H03)	1.8	0.6	0.7	3.0
Burkholderiaceae (Burkholderia-Caballeronia-Paraburkholderia)	1.6	3.2	4.3	5.2
Holophagae	1.0	0.3	0.2	0.4
Rhodobacteraceae	0.0	0.2	0.7	1.4
Rhizobiales + Xanthobacteraceae	1.4	1.0	1.3	1.3
Hymenobacteraceae (Hymenobacter)	0.0	0.0	1.5	1.0
Rhodanobacteraceae (Rhodanobacter)	0.4	0.9	0.7	1.0
Nitrosomonadaceae (Nitrosomonas)	1.0	1.5	1.1	0.0
Acetobacteraceae	0.7	0.4	0.2	0.0
Micrococcaceae	0.7	3.4	1.0	1.5
Total%	86.0	84.8	77.1	81.0

The total number of sequences belonging to the Ce80 communities ranged from 120209 in Nunatak to 500390 in Biscoe.

differentiate both locations in terms of soil properties established along the vertical profile. Therefore, the relative homogeneity in Nunatak among their prokaryotic communities would be related to the uniform characteristics of the soils, both in surface and depth. The opposite is shown in Plateau, where the microbial activity, over time, would have contributed by modifying the characteristics of the soil. Shannon diversity analysis indicated significant differences in microbial diversity between soil strata in Plateau (9.4 tss and 8.9 dss) and did not indicate relevant differences in Nunatak (8.5 tss and 8.1 dss). For both locations, bacterial communities in top-stratum soils have shown greater richness and diversity values than those from the deeper-stratum soils. Therefore, our results are similar to those reported from other Antarctic soils (Aislabie et al., 2006; Bajerski and Wagner, 2013), showing that the highest abundance and diversity of soil microorganisms are located in the most superficial centimeters.

Previous studies have shown high levels of spatial heterogeneity in prokaryote biodiversity across terrestrial environments in Antarctica (Barrett et al., 2006; Chong et al., 2010). This spatial heterogeneity is generated by physicochemical and trophic variations acting at all spatial scales. However, our results with the top-stratum soils of each sampling location showed no significant evidence of within locations heterogeneity, both for alpha diversity and community composition. The diversity of prokaryotes is sensitive to local environmental conditions such as the availability of water and nutrients (Barrett et al., 2006; Chong et al., 2010) and soil heterogeneity is expected in small spatial scales (Fraschetti et al., 2005). However, our data, from samples taken from carefully chosen ecologically comparable sites and locations, offer another view about the microbial compositions of soils at different scales of analysis. When all sequences from the sampling sites are analyzed jointly, data points from the same locations are closer supporting the heterogeneous distribution of the microbial communities. Differences in bacterial communities measured with Bray-Curtis provide insight into differences in community

composition among samples, with the advantage of being based on ASV counts, regardless of taxonomic assignment as maximum sequencing resolution. The results showed that the bacterial communities from soils are again grouped by locations, suggesting that inter-site variations are greater than intra-site variations. Therefore, geological variables (i.e., spatial distance, climate conditions, geological features and historical context) are also of influence on microbial communities. These results are similar with previous studies such as that of Yergeau et al. (2007), which have reported significant differences in bacterial diversity in Antarctica on a continental scale.

Description of microbial communities from ASVs allows a different perspective of its composition, being able to analyze sequences with the maximum potential resolution, and with no risk of introducing deviations due to the taxonomic reference (Callahan et al., 2016). However, one of the costs of this method leads to a possible loss of real sequences that would be present at very low levels. Our data indicate that a large proportion of the different sequences are unique. The amount of these unique ASVs assigned to each location is high, ranging from 5.3 to 11% of the total sequences, having a key role in the heterogeneity of the communities. However, clustering thresholds greater than 97% identity can lead to an overestimation of the rare biosphere present in the samples (Kunin et al., 2010). Most of these unique ASVs are in low abundance but represent between 48% and 69% of the different sequences. At the moment, the ecological role of that rare biosphere is not well understood, but frequently neglected.

Analyses based on the core communities allow us to know the specific weight of those groups shared between different samples. The core at maximum resolution for the 4 sampling locations (Core90) makes up a common bacterial community in 90% of sampled soils, of 26 ASVs which do not dominate the set sequences. These data, similar to those obtained in previous studies of core communities from different Antarctic environments (Murray et al., 2020), show that at least a few dozen sequences are identical between ice-free areas separated by hundreds of kilometers along the Antarctic Peninsula. The possibilities of dispersal of microorganisms are numerous, ranging from air transport (Archer et al., 2019; King-Miaow et al., 2019; Cao et al., 2020) and ocean currents (Fraser et al., 2018), to the anthropogenic activities (Kirtsideli et al., 2018). The dispersal capabilities of bacteria are evidenced in Antarctica showing that identical sequences are found in relatively distant regions. However, the ASVs heterogeneity between locations in the Core80 community is significant. Although the sampling locations Plateau, Nunatak and Elephant are located at the same island with a maximum distance of 10 km, bacterial community from location Elephant, located at more than 300 km away from location Biscoe, is more similar to that one than to the closer ones.

The previous analyses used ASVs as an expression of diversity, without considering the taxonomic assignment of those sequences. However, when the taxonomy is the purpose, it is necessary to find a balance between the genotypic diversity and the functional diversity, making in this case relevant to reduce the taxonomic resolution for the analyses. The detailed taxonomic assignment of the Core80 communities indicated that a small number of taxa, at Family level, conformed the bacterial core communities (less than 30 taxa) of each location. On average, these groups represented over 82% of the sequences forming those core communities. In fact, 20 of those identities were present at all sampling locations and can be considered cosmopolitan taxa in this region and represented up to 75.7% of the total sequences found at the Core80 community. Soils from extreme Antarctic environments present severely limited terrestrial productivity and, consequently, soil organic matter concentrations are very low (Burkins et al., 2001). Nutrient inputs in these ecosystems have been attributed to aerial deposition (Reynolds et al., 2001), abiotic processes driven by temperature changes (Parsons et al., 2004), and microbial activity (Cary et al., 2010). The presence of phototrophic bacterial families in the Core80 community suggests its key role in carbon and energy input to the ecosystem. Therefore, *Pseudanabaena* and *Tychonema* could be involved in the CO_2 photoassimilation and the fixation of N_2, as observed in high-elevated 'barren' soils from other latitudes (Freeman et al., 2009). The presence of Chloroflexi could also be related to the CO_2 uptake. Cyanobacteria and Chloroflexi can utilize different portions of the radiation spectrum for photosynthesis (Ley et al., 2006) and would be photosynthetically active at different microtopographic positions. The presence of *Thiobacillus* is also relevant, since all species described are obligate autotrophs (Boden, 2017), allowing an alternative energy input to the ecosystem. However, the metabolic diversity of the Core80 community does not only include autotrophic bacteria. In fact, 16 of these 20 common taxa belonged to Proteobacteria and Actinobacteria phyla, typically described for glacier retreat areas (Brown and Jumpponen, 2014). Proteobacteria is a major player in soil microbial communities around the globe, due to its high metabolic versatility. This phylum, and especially *Burkholderia*, acquires a key role in organic matter decomposition processes in Arctic soils (Tao et al., 2020), and its prevalence is related with increased soil carbon turnover upon warming in Antarctic soils (Thomson et al., 2010; Yergeau et al., 2012). Likewise, Actinobacteria groups are able to decompose organic matter, including recalcitrant polymers (Větrovský et al., 2014). Therefore, most of the Core80 described for the 4 sampling locations would be associated to processes of degradation of recalcitrant organic matter, not accessible to other microorganisms (Hawes, 2008), with a probably key role in the subsequent colonization of these oligotrophic soils.

Our results indicate that the same functional taxa (with the taxonomical resolution used in this work) are inhabiting the ecologically comparable soils sampled in this study in the Antarctic Peninsula region, regardless of the potentially different environmental constraints and independently of their geographical proximity, or duration of the ice-free period. This is consistent with previous reports from Antarctic soils, where higher levels of similarity were observed between locations with similar physico-chemical characteristics (Chong et al., 2010). Considering that the ice-free condition was acquired at different time scales at the different locations (millennia at Byers Peninsula Plateau, and few decades at Biscoe Point), it can be assumed that these taxa are first, highly transportable (most likely by the wind) and second, highly versatile. These characteristics confer

those taxa a pioneer status in Antarctic soils, relating to potential colonizers in the new deglaciated soils subjected to global change, due to a wider range of stress tolerance strategies than other microorganisms (Sigler et al., 2002; Sigler and Zeyer, 2004). However, its presence in soils of such different ages, suggests that primary succession processes, in extreme ecosystems, could have an indeterminate duration.

Certainly, every sampling location, besides the central core community showed a unique fingerprint in terms of the microbial community inhabiting those soils. For instance, Biscoe showed a high diversity and abundance of Cyanobacteria which was obviously absent from other locations such as Plateau, while *Chthoniobacteraceae* were conspicuously abundant in Plateau (6.95% of the total sequences in that core community) and absent or very scarce in the other locations. We suggest that those particularities are due to local environmental characteristics as higher humidity, or different mineral composition, or even to stochastic processes for the distribution that are out of the scope of this work.

CONCLUSION

In conclusion, our work is a contribution to understanding the distribution and dispersal characteristics of the microbial communities inhabiting Antarctic soils. While the heterogeneity of microbial communities can reach high levels in the soil profiles in older soils, this heterogeneity is clearer at geographical scales. However, only 20 common taxonomic groups formed the highest proportion of the ASVs sequenced from the Core80 communities, and most likely conform the Antarctic bare soil bacterial community identity. The potential metabolic diversity of the Core80 community could be linked to all the fundamental metabolic activities required for the acquisition and recycling of organic C, which would justify its presence in all the sampling locations studied.

DATA AVAILABILITY STATEMENT

The datasets presented in this study can be found in online repositories. The names of the repository/repositories and accession number(s) can be found below: BioProject ID PRJNA678471.

AUTHOR CONTRIBUTIONS

PA wrote the initial manuscript. All authors designed the experiments, collected the samples, analyzed the experimental data, and contributed to elaborate the final manuscript.

FUNDING

This work was supported by the Spanish Agencia Estatal de Investigación (AEI) and Fondo Europeo de Desarrollo Regional (FEDER), Grants CTM2016-79741-R and PCIN-2016-001. PA was supported by a FPI-contract fellowship (BES-2017-080558) from MINECO.

ACKNOWLEDGMENTS

The authors are grateful to the members of field teams from MICROAIRPOLAR projects Sergi González and David Velázquez, Unidad Técnica Marina (UTM), Navy crew of BIO Hespérides and B/O Sarmiento de Gamboa. The authors acknowledge the computer resources, technical expertise and assistance provided by the Centro de Computación Científica at the Universidad Autónoma de Madrid (CCC-UAM). Special thanks to Pedro Mustieles for his dedication. The authors are grateful to the two reviewers and the editors for their assistance in improving the manuscript.

SUPPLEMENTARY MATERIAL

The Supplementary Material for this article can be found online at: https://www.frontiersin.org/articles/10.3389/fmicb.2021.628792/full#supplementary-material

Supplementary Plate 1 | Wide angle and detail picture of every soil sampled at Antarctic Peninsula region. **(A)** Byers Peninsula Plateau. **(B)** Nunatak. **(C)** Elephant Point (Livingston Is.). **(D)** Biscoe Point.

Supplementary Table 1 | Soil physical and chemical characteristics from the 4 sampling locations. The values represent the mean of all sample points analyzed.

Supplementary Table 2 | Coordinates of the 4 sampling locations along the Antarctic Peninsula. The Area refers to the clusters of the samples considering the glacier front as a reference point, with (I) being the closest to it.

REFERENCES

Aislabie, J. M., Chhour, K., Saul, D. J., Miyauchi, S., Ayton, J., Paetzold, R. F., et al. (2006). Dominant bacteria in soils of Marble point and Wright valley, Victoria land, Antarctica. *Soil Biol. Biochem.* 38, 3041–3056. doi: 10.1016/j.soilbio.2006.02.018

Archer, S. D., Lee, K. C., Caruso, T., Maki, T., Lee, C. K., Cary, S. C., et al. (2019). Airborne microbial transport limitation to isolated Antarctic soil habitats. *Nat. Microbiol.* 4, 925–932. doi: 10.1038/s41564-019-0370-4

ATCM (2004). Management Plan for Antarctic Specially Protected Area (ASPA) No. 139 Biscoe Point, Anvers Island, Palmer Archipelago.

ATCM (2014). Management Plan for Antarctic Specially Protected Area (ASPA) No. 139 Biscoe Point, Anvers Island, Palmer Archipelago.

ATCM XIII (1985). RE XIII-8 Management Plan for SSSI 20 Biscoe Point, Anvers Island, Palmer Archipelago.

Bajerski, F., and Wagner, D. (2013). Bacterial succession in Antarctic soils of two glacier forefields on Larsemann Hills, East Antarctica. *FEMS Microbiol. Ecol.* 85, 128–142. doi: 10.1111/1574-6941.12105

Barrett, J. E., Virginia, R. A., Hopkins, D. W., Aislabie, J., Bargagli, R., Bockheim, J. G., et al. (2006). Terrestrial ecosystem processes of Victoria Land, Antarctica. *Soil Biol. Biochem.* 38, 3019–3034. doi: 10.1016/j.soilbio.2006.04.041

Boden, R. (2017). 115 years of sulfur microbiology. *FEMS Microbiol. Lett.* 364:fnx043.

Bokulich, N. A., Kaehler, B. D., Rideout, J. R., Dillon, M., Bolyen, E., Knight, R., et al. (2018). Optimizing taxonomic classification of marker-gene amplicon sequences with QIIME 2′s q2-feature-classifier plugin. *Microbiome* 6:90.

Bolyen, E., Rideout, J. R., Dillon, M. R., Bokulich, N. A., Abnet, C. C., Al-Ghalith, G. A., et al. (2019). Reproducible, interactive, scalable and extensible microbiome data science using QIIME 2. *Nat. Biotechnol.* 37, 852–857. doi: 10.1038/s41587-019-0209-9

Brown, S. P., and Jumpponen, A. (2014). Contrasting primary successional trajectories of fungi and bacteria in retreating glacier soils. *Mol. Ecol.* 23, 481–497. doi: 10.1111/mec.12487

Burkins, M. B., Virginia, R. A., and Wall, D. H. (2001). Organic carbon cycling in Taylor Valley, Antarctica: quantifying soil reservoirs and soil respiration. *Glob. Chang. Biol.* 7, 113–125. doi: 10.1046/j.1365-2486.2001.00393.x

Burton-Johnson, A., Black, M., Fretwell, P., and Kaluza-Gilbert, J. (2016). An automated methodology for differentiating rock from snow, clouds and sea in Antarctica from Landsat 8 imagery: a new rock outcrop map and area estimation for the entire Antarctic continent. *Cryosphere* 10, 1665–1677. doi: 10.5194/tc-10-1665-2016

Callahan, B. J., McMurdie, P. J., Rosen, M. J., Han, A. W., Johnson, A. J. A., and Holmes, S. P. (2016). DADA2: high-resolution sample inference from Illumina amplicon data. *Nat. Methods* 13, 581–583. doi: 10.1038/nmeth.3869

Cao, Y., Yu, X., Ju, F., Zhan, H., Jiang, B., Kang, H., et al. (2020). Airborne bacterial community diversity, source and function along the Antarctic Coast. *Sci. Total Environ.* 2020:142700. doi: 10.1016/j.scitotenv.2020.142700

Cary, S. C., McDonald, I. R., Barrett, J. E., and Cowan, D. A. (2010). On the rocks: the microbiology of Antarctic dry valley soils. *Nat. Rev. Microbiol.* 8, 129–138. doi: 10.1038/nrmicro2281

Chong, C. W., Pearce, D. A., Convey, P., Tan, G. A., Wong, R. C., and Tan, I. K. (2010). High levels of spatial heterogeneity in the biodiversity of soil prokaryotes on Signy Island, Antarctica. *Soil Biol. Biochem.* 42, 601–610. doi: 10.1016/j.soilbio.2009.12.009

Chu, H., Sun, H., Tripathi, B. M., Adams, J. M., Huang, R., Zhang, Y., et al. (2016). Bacterial community dissimilarity between the surface and subsurface soils equals horizontal differences over several kilometers in the western Tibetan Plateau. *Environ. Microbiol.* 18, 1523–1533. doi: 10.1111/1462-2920.13236

Cowan, D. A. (2014). *Antarctic Terrestrial Microbiology: Physical and Biological Properties of Antarctic Soils*. New York, NY: Springer.

Fraschetti, S., Terlizzi, A., and Benedetti-Cecchi, L. (2005). Patterns of distribution of marine assemblages from rocky shores: evidence of relevant scales of variation. *Mar. Ecol. Prog. Ser.* 296, 13–29. doi: 10.3354/meps296013

Fraser, C. I, Morrison, A. K., Hogg, A. M., Macaya, E. C., van Sebille, E., Ryan, P. G., et al. (2018). Antarctica's ecological isolation will be broken by storm-driven dispersal and warming. *Nat. Clim. Chang.* 8, 704–708. doi: 10.1038/s41558-018-0209-7

Freeman, K. R., Pescador, M. Y., Reed, S. C., Costello, E. K., Robeson, M. S., and Schmidt, S. K. (2009). Soil CO_2 flux and photoautotrophic community composition in high-elevation,'barren'soil. *Environ. Microbiol.* 11, 674–686. doi: 10.1111/j.1462-2920.2008.01844.x

Frey, B., Bühler, L., Schmutz, S., Zumsteg, A., and Furrer, G. (2013). Molecular characterization of phototrophic microorganisms in the forefield of a receding glacier in the Swiss Alps. *Environ. Res. Lett.* 8, 704–708. doi: 10.1088/1748-9326/8/1/015033

Hawes, T. C. (2008). Aeolian fallout on recently deglaciated terrain in the high Arctic. *Polar Biol.* 31:295301. doi: 10.1007/s00300-007-0357-0

Herbold, C. W., Lee, C. K., McDonald, I. R., and Cary, S. C. (2014). Evidence of global-scale aeolian dispersal and endemism in isolated geothermal microbial communities of Antarctica. *Nat. Commun.* 5:3875. doi: 10.1038/ncomms4875

Horrocks, C. A., Newsham, K. K., Cox, F., Garnett, M. H., Robinson, C. H., and Dungait, J. A. J. (2020). Predicting climate change impacts on maritime Antarctic soils: a space-for-time substitution study. *Soil Biol. Biochem.* 141:107682. doi: 10.1016/j.soilbio.2019.107682

Hughes, K. A., Cowan, D. A., and Wilmotte, A. (2015). Protection of Antarctic microbial communities-'out of sight, out of mind'. *Front. Microbiol.* 6:151. doi: 10.3389/fmicb.2015.00151

Katoh, K., Misawa, K., Kuma, K. I., and Miyata, T. (2002). MAFFT: a novel method for rapid multiple sequence alignment based on fast Fourier transform. *Nucleic Acids Res.* 30, 3059–3066. doi: 10.1093/nar/gkf436

King-Miaow, K., Lee, K., Maki, T., LaCap-Bugler, D., and Archer, S. D. J. (2019). "Airborne microorganisms in Antarctica: transport, survival and establishment," in *The Ecological Role of Micro-Organisms in the Antarctic Environment*, ed. S. Castro-Sowinski (Cham: Springer), 163–196. doi: 10.1007/978-3-030-02786-5_8

Kirtsideli, I. Y., Vlasov, D. Y., Novozhilov, Y. K., Abakumov, E. V., and Barantsevich, E. P. (2018). Assessment of anthropogenic influence on antarctic mycobiota in areas of Russian polar stations. *Contemp. Probl. Ecol.* 11, 449–457. doi: 10.1134/S1995425518050074

Krauze, P., Wagner, D., Spinola, D. N., and Kühn, P. (2020). Influence of microorganisms on initial soil formation along a glacier forefield on King George Island, maritime Antarctica. *Biogeosci. Discuss.* [Preprint], doi: 10.5194/bg-2020-203

Kunin, V., Engelbrektson, A., Ochman, H., and Hugenholtz, P. (2010). Wrinkles in the rare biosphere: pyrosequencing errors can lead to artificial inflation of diversity estimates. *Environ. Microbiol.* 12, 118–123. doi: 10.1111/j.1462-2920.2009.02051.x

Lee, J. R., Raymond, B., Bracegirdle, T. J., Chadès, I., Fuller, R. A., Shaw, J. D., et al. (2017). Climate change drives expansion of Antarctic ice-free habitat. *Nature* 547, 49–54. doi: 10.1038/nature22996

Ley, R. E., Harris, J. K., Wilcox, J., Spear, J. R., Miller, S. R., Bebout, B. M., et al. (2006). Unexpected diversity and complexity of the Guerrero Negro hypersaline microbial mat. *Appl. Environ. Microbiol.* 72, 3685–3695. doi: 10.1128/AEM.72.5.3685-3695.2006

Murray, A. E., Avalon, N. E., Bishop, L., Davenport, K. W., Delage, E., Dichosa, A. E., et al. (2020). Uncovering the core microbiome and distribution of palmerolide in synoicum adareanum across the Anvers Island Archipelago, Antarctica. *Mar. Drugs* 18:60298. doi: 10.3390/md18060298

Niederberger, T. D., McDonald, I. R., Hacker, A. L., Soo, R. M., Barrett, J. E., Wall, D. H., et al. (2008). Microbial community composition in soils of Northern Victoria Land, Antarctica. *Environ. Microbiol.* 10, 1713–1724. doi: 10.1111/j.1462-2920.2008.01593.x

Oksanen, J., Blanchet, F. G., Kindt, R., Legendre, P., Minchin, P. R., O'Hara, R. B., et al. (2015). Vegan: community ecology package. R package vegan, version 2.2-1. *Worl. Agro. Cent* 3, 7–81.

Oliva, M., Antoniades, D., Giralt, S., Granados, I., Pla-Rabes, S., Toro, M., et al. (2016). The Holocene deglaciation of the Byers Peninsula (Livingston Island, Antarctica) based on the dating of lake sedimentary records. *Geomorphology* 261, 89–102. doi: 10.1016/j.geomorph.2016.02.029

Oliva, M., and Ruiz-Fernández, J. (2015). Coupling patterns between para-glacial and permafrost degradation responses in Antarctica. *Earth Surf. Process. Landforms* 40, 1227–1238. doi: 10.1002/esp.3716

Oliva, M., and Ruiz-Fernández, J. (2017). Geomorphological processes and frozen ground conditions in elephant point (Livingston Island, South Shetland Islands, Antarctica). *Geomorphology* 293, 368–379. doi: 10.1016/j.geomorph.2016.01.020

Otani, S., Mikaelyan, A., Nobre, T., Hansen, L. H., Koné, N. G. A., Sørensen, S. J., et al. (2014). Identifying the core microbial community in the gut of fungus-growing termites. *Mol. Ecol.* 23, 4631–4644. doi: 10.1111/mec.12874

Palacios, D., Ruiz-Fernández, J., Oliva, M., Andrés, N., Fernández-Fernández, J. M., Schimmelpfennig, I., et al. (2020). Timing of formation of neoglacial landforms in the South Shetland Islands (*Antarctic Peninsula*): regional and global implications. *Quat. Sci. Rev.* 234, 106248. doi: 10.1016/j.quascirev.2020.106248

Parsons, A. N., Barrett, J. E., Wall, D. H., and Virginia, R. A. (2004). Soil carbon dioxide flux in Antarctic dry valley ecosystems. *Ecosystems* 7, 286–295. doi: 10.1007/s10021-003-0132-1

Price, M. N., Dehal, P. S., and Arkin, A. P. (2010). FastTree 2-approximately maximum-likelihood trees for large alignments. *PLoS One* 5:e9490. doi: 10.1371/journal.pone.0009490

Quast, C., Pruesse, E., Yilmaz, P., Gerken, J., Schweer, T., Yarza, P., et al. (2012). The SILVA ribosomal RNA gene database project: improved data processing and web-based tools. *Nucleic Acids Res.* 41:gks1219. doi: 10.1093/nar/gks1219

Reynolds, R., Belnap, J., Reheis, M., Lamothe, P., and Luiszer, F. (2001). Aeolian dust in Colorado Plateau soils: nutrient inputs and recent change in source. *Proc. Natl. Acad. Sci. U.S.A.* 98, 7123–7127. doi: 10.1073/pnas.121094298

Rignot, E., Mouginot, J., Scheuchl, B., van den Broeke, M., van Wessem, M. J., and Morlighem, M. (2019). Four decades of Antarctic Ice Sheet mass balance from 1979-2017. *Proc. Natl. Acad. Sci. U.S.A.* 116, 1095–1103. doi: 10.1073/pnas.1812883116

Rime, T., Hartmann, M., Brunner, I., Widmer, F., Zeyer, J., and Frey, B. (2015). Vertical distribution of the soil microbiota along a successional gradient in a glacier forefield. *Mol. Ecol.* 24, 1091–1108. doi: 10.1111/mec.13051

Siegert, M. J., Rumble, J., Atkinson, A., Rogelj, J., Edwards, T., Davies, B. J., et al. (2019). The Antarctic Peninsula under a 1.5 C global warming scenario. *Front. Environ. Sci.* 7:102. doi: 10.3389/fenvs.2019.00102

Sigler, W. V., Crivii, S., and Zeyer, J. (2002). Bacterial succession in glacial forefield soils characterized by community structure, activity and opportunistic growth dynamics. *Microb. Ecol.* 44, 306–316. doi: 10.1007/s00248-002-2025-9

Sigler, W. V., and Zeyer, J. (2004). Colony-forming analysis of bacterial community succession in deglaciated soils indicates pioneer stress-tolerant opportunists. *Microb. Ecol.* 48, 316–323. doi: 10.1007/s00248-003-0189-6

Smith, J. J., Tow, L. A., Stafford, W., Cary, C., and Cowan, D. A. (2006). Bacterial diversity in three different Antarctic cold desert mineral soils. *Microb. Ecol.* 51, 413–421. doi: 10.1007/s00248-006-9022-3

Steig, E. J., Schneider, D. P., Rutherford, S. D., Mann, M. E., Comiso, J. C., and Shindell, D. T. (2009). Warming of the Antarctic ice-sheet surface since the 1957 International Geophysical Year. *Nature* 457, 459–462. doi: 10.1038/nature07669

Tao, X., Feng, J., Yang, Y., Wang, G., Tian, R., Fan, F., et al. (2020). Winter warming in Alaska accelerates lignin decomposition contributed by *Proteobacteria*. *Microbiome* 8:84. doi: 10.1186/s40168-020-00838-5

Thomas, E. R., Dennis, P. F., Bracegirdle, T. J., and Franzke, C. (2009). Ice core evidence for significant 100-year regional warming on the Antarctic Peninsula. *Geophys. Res. Lett.* 36:L2070. doi: 10.1029/2009GL040104

Thomson, B. C., Ostle, N., McNamara, N., Bailey, M. J., Whiteley, A. S., and Griffiths, R. I. (2010). Vegetation affects the relative abundances of dominant soil bacterial taxa and soil respiration rates in an upland grassland soil. *Microb. Ecol.* 59, 335–343. doi: 10.1007/s00248-009-9575-z

Turner, J., Lu, H., White, I., King, J. C., Phillips, T., Hosking, J. S., et al. (2016). Absence of 21st century warming on Antarctic Peninsula consistent with natural variability. *Nature* 535, 411–415. doi: 10.1038/nature18645

Větrovský, T., Steffen, K. T., and Baldrian, P. (2014). Potential of cometabolic transformation of polysaccharides and lignin in lignocellulose by soil Actinobacteria. *PLoS One* 9:e89108. doi: 10.1371/journal.pone.0089108

Yergeau, E., Bokhorst, S., Kang, S., Zhou, J., Greer, C. W., Aerts, R., et al. (2012). Shifts in soil microorganisms in response to warming are consistent across a range of Antarctic environments. *ISME J.* 6, 692–702. doi: 10.1038/ismej.2011.124

Yergeau, E., Newsham, K. K., Pearce, D. A., and Kowalchuk, G. A. (2007). Patterns of bacterial diversity across a range of Antarctic terrestrial habitats. *Environ. Microbiol.* 9, 2670–2682. doi: 10.1111/j.1462-2920.2007.01379.x

Conflict of Interest: The authors declare that the research was conducted in the absence of any commercial or financial relationships that could be construed as a potential conflict of interest.

frontiers in Microbiology

ORIGINAL RESEARCH
published: 12 March 2021
doi: 10.3389/fmicb.2021.628746

Tundra Type Drives Distinct Trajectories of Functional and Taxonomic Composition of Arctic Fungal Communities in Response to Climate Change – Results From Long-Term Experimental Summer Warming and Increased Snow Depth

József Geml[1,2]*, *Luis N. Morgado*[2,3] *and Tatiana A. Semenova-Nelsen*[2]

[1]*MTA-EKE Lendület Environmental Microbiome Research Group, Eszterházy Károly University, Eger, Hungary,* [2]*Naturalis Biodiversity Center, Leiden, Netherlands,* [3]*Department of Biosciences, University of Oslo, Oslo, Norway*

OPEN ACCESS

Edited by:
Pietro Buzzini, University of Perugia, Italy

Reviewed by:
Minna Männistö, Natural Resources Institute Finland (Luke), Finland
Luiz H. Rosa, Federal University of Minas Gerais, Brazil
Ursula Peintner, University of Innsbruck, Austria

***Correspondence:**
József Geml
jozsef.geml@gmail.com

Specialty section:
This article was submitted to Extreme Microbiology, a section of the journal Frontiers in Microbiology

Received: *12 November 2020*
Accepted: *18 February 2021*
Published: *12 March 2021*

Citation:
Geml J, Morgado LN and Semenova-Nelsen TA (2021) Tundra Type Drives Distinct Trajectories of Functional and Taxonomic Composition of Arctic Fungal Communities in Response to Climate Change – Results From Long-Term Experimental Summer Warming and Increased Snow Depth. Front. Microbiol. 12:628746. doi: 10.3389/fmicb.2021.628746

The arctic tundra is undergoing climate-driven changes and there are serious concerns related to the future of arctic biodiversity and altered ecological processes under possible climate change scenarios. Arctic land surface temperatures and precipitation are predicted to increase further, likely causing major transformation in terrestrial ecosystems. As a response to increasing temperatures, shifts in vegetation and soil fungal communities have already been observed. Little is known, however, how long-term experimental warming coupled with increased snow depth influence the trajectories of soil fungal communities in different tundra types. We compared edaphic variables and fungal community composition in experimental plots simulating the expected increase in summer warming and winter snow depth, based on DNA metabarcoding data. Fungal communities in the sampled dry and moist acidic tundra communities differed greatly, with tundra type explaining ca. one-third of compositional variation. Furthermore, dry and moist tundra appear to have different trajectories in response to climate change. Specifically, while both warming and increased snow depth had significant effects on fungal community composition and edaphic variables in dry tundra, the effect of increased snow was greater. However, in moist tundra, fungal communities mainly were affected by summer warming, while increased snow depth had a smaller effect and only on some functional groups. In dry tundra, microorganisms generally are limited by moisture in the summer and extremely low temperatures in winter, which is in agreement with the stronger effect of increased snow depth relative to warming. On the contrary, moist tundra soils generally are saturated with water, remain cold year-round and show relatively small seasonal fluctuations in temperature. The greater observed effect of warming on fungi in moist tundra may be explained by the narrower temperature optimum compared to those in dry tundra.

Keywords: climate change, fungal ecology, International Tundra Experiment, metabarcoding, tundra

INTRODUCTION

The arctic tundra is being transformed by a wide range of climate-driven processes and there are serious concerns related to the future of arctic biodiversity because of the threats represented by climate change (Wookey, 2007). In addition to the profound consequences for arctic biota, nutrient cycling in the Arctic is of paramount importance for global change (Tarnocai et al., 2009). The arctic tundra occupies an area of 8 million km^2 and stores a great portion of the Earth's soil carbon (C) that is critically important in global C cycles and climate feedback (Callaghan et al., 2004; Tarnocai et al., 2009).

The arctic tundra is considered a maritime biome, because of approximately 80% of its area being located within 100 km of a coastline (Walker et al., 2005) and because arctic sea surface and sea ice cover temperature have been shown to be closely linked to adjacent land surface temperature, precipitation, and primary productivity (Bhatt et al., 2010). Due to retreating sea ice, arctic land surface temperatures have increased and will continue to increase, causing major changes in terrestrial ecosystems (Kaufman et al., 2009). Furthermore, pronounced increase in arctic precipitation is predicted due to increased local surface evaporation of the Arctic Ocean, as well as greater moisture inflow from lower latitudes (Kattsov and Walsh, 2000; Stocker et al., 2013; Bintaja and Selten, 2014). Because most of the precipitation falls as snow, deeper snow is expected in many parts of the Arctic (Bintaja and Selten, 2014).

Warming-induced changes have already been observed in terrestrial arctic ecosystems, including higher microbial activity and resulting increased plant nitrogen (N) availability (Chapin, 1983; Aerts, 2006), faster C turnover in soils (Hobbie and Chapin, 1998; Shaver et al., 2006), and compositional shifts in land surface vegetation (Chapin et al., 1995; Bret-Harte et al., 2002). For example, shrub cover and abundance has increased, which is expected to have positive feedbacks on ecosystem change and greater climate forcing (Sturm et al., 2001). Greater shrub size leads to increased local accumulation of snow in winter, resulting in increased soil insulation, higher winter and spring soil temperatures, and higher rates nutrient mineralization, with positive feedback on shrub growth and expansion (Sturm et al., 2005). Moreover, the expansion of shrubs lowers surface albedo and increases regional summer temperatures, providing another positive feedback to warming (Chapin et al., 2005).

Fungi play key functional roles in terrestrial arctic ecosystems as mutualistic symbionts, pathogens, and decomposers. The vast majority of arctic plants are highly dependent on associations with mycorrhizal fungi for survival in these nutrient-limited environments (Hobbie et al., 2009; Bjorbækmo et al., 2010). Moreover, non-mycorrhizal root endophytic fungi are ubiquitous in arctic-alpine plants (Newsham et al., 2009), their diversity, identity, and ecological roles are scarcely known. Because many fungi of various functional guilds directly interact with plants in a variety of manners, fungi are expected to play important roles in climate-driven changes in arctic vegetation.

Soil fungi are known to respond strongly to warming and elevated nutrient levels (Clemmensen et al., 2006). While vascular plant species diversity is strongly influenced by summer temperatures, soil temperature may be important as a determining factor of soil fungal diversity, particularly in winter, when most fungal metabolic activity takes place (Nemergut et al., 2005). As such, snow depth (the thickness of the insulating layer) and its spatial distribution are expected influence soil fungal communities at small spatial scales. In this study, we analyzed DNA metabarcoding data generated from long-term (18 years) experimental plots simulating climate change in the Alaska Arctic. We compared community composition of soil-borne fungi across sampling plots with (1) ambient and experimentally increased summer air and near-surface soil temperature; (2) ambient and experimentally increased snow depth; and with (3) combined treatment of increased summer warming and increased snow depth in dry heath and moist tussock tundra. We aimed to answer (1) how composition of fungal functional groups change in response to long-term increase in winter snow depth, summer temperature, and their combination; and (2) whether there are differences in responses between dry and moist tundra.

MATERIALS AND METHODS

Study Site and Experimental Design

The sampling was conducted at the International Tundra Experiment (ITEX) long-term research site in the Toolik Lake region in the northern foothills of the Brooks Range, AK, United States (68°37'N, 149°32'W; 760 m above sea level; Walker et al., 1999; Welker et al., 2000; Pattison and Welker, 2014). The region belongs to the bioclimatic subzone E that is the warmest subzone of the arctic tundra, where mean July temperatures ranges from 9 to 12°C and annual precipitation ranges from 200 to 400 mm, of which ca. 50% falls as snow (Walker et al., 2005). The two main vegetation types of the sampled site are dry acidic heath tundra, characterized by *Dryas octopetala*, *Salix polaris*, *Vaccinium* species, and fruticose lichens, and moist acidic tussock tundra, dominated by *Betula nana*, *Salix pulchra* species, the sedge *Eriophorum vaginatum*, and several peat moss species (*Sphagnum* spp.). Detailed descriptions of the plant communities can be found in Walker et al. (1999).

As a part of ITEX network, hexagonal open top chambers (OTCs) and the snow fences were established in 1994, in both the dry (D) and moist (M) tundra, to increase summer air and upper soil temperature and winter snow depth, respectively (Welker et al., 2000). The OTCs, made of translucent fiberglass, have a 1 m^2 surface area and they increase the summer air and upper soil temperature by a mean daily average of 1.5–2°C measured at 15 cm height and 5 cm depth, respectively (Marion et al., 1997; Jones et al., 1998; Walker et al., 1999). Since 1994, the OTCs were set up every year when 50% of the ground area of the plot became snow-free (late May or early June) and were removed at the end of August or early September, based on the ITEX protocol (Welker et al., 1997). Snow fences, 2.8 m tall and 60 m long, were erected to create a ca. 60-m leeward snow drift with multiple snow depth zones. The soil

sampling was focused on the intermediate zone near the center of the experimental setup, corresponding to ca. 1–1.5 m winter snow depth. The average winter soil temperatures 2 cm below the surface were −2.9°C (±0.2) and −4.7°C (±0.2) in the increased snow depth plots and in the control plots with ambient snow depth, respectively (Pattison and Welker, 2014). The lowest soil temperatures recorded for the snow fence plots were ca −7°C vs. ca. −35°C observed for the control plots (Walker et al., 1999; Schimel et al., 2004). Changes in abiotic factors resulting from the increased snow depth have led to marked increases in aboveground plant biomass as well as compositional shifts in vegetation, as described in detail in Walker et al. (1999, 2006), Wahren et al. (2005), Welker et al. (2005), Mercado-Diaz (2011), and Pattison and Welker (2014).

Data Generation

Soil sampling was done in July, 2012, as described by Morgado et al. (2015, 2016) and Semenova et al. (2015, 2016). In each tundra type, we sampled five replicate plots in the summer warming (W) and increased snow depth (S) treatments, their combination (SW) as well as in the control (C) plots, located adjacent to the experimental treatments. In each replicate plot, five soil cores of 2 cm diameter and 20 cm depth were taken. Both organic and mineral layers were included in the soil cores, while coarse litter, moss, gravel, and coarse roots were removed. Soil cores from each replicate plot were thoroughly mixed and kept frozen until lyophilization. In total, 200 soil cores across 40 plots were sampled.

We extracted DNA from soil samples using Macherey-Nagel NucleoSpin Soil kit (Macherey-Nagel Gmbh and Co., Düren, Germany) with SL2 lysis buffer, which is more suitable for soils rich in organic matter. We used approximately 0.5 ml (ca. 0.2–0.5 g) of soil for DNA extraction and the volume of elution buffer was set to 30 µl. DNA extraction was carried out twice for each sample. The remaining parts of the lyophilized samples were used for soil chemical analyses to measure pH, electrical conductivity (EC) following protocols described in Sparks et al. (1996), and total C and N contents, using vario MAX cube CNS analyzer (Elementar Analysensysteme GmbH, Germany) based on the manufacturer's protocol.

The PCR and sequencing protocols were as in Geml et al. (2015, 2016), described here briefly. Forward primer fITS7 (Ihrmark et al., 2012) and reverse sample-specific primer ITS4 (White et al., 1990) were used to amplify the ITS2 rDNA region (ca. 250 bp). The ITS4 primer was labeled with sample-specific Multiplex Identification DNA-tags. We used the following PCR protocol for all samples and for the positive and negative controls: one cycle of 95°C for 5 min, and then 25 cycles of 95°C for 20 s, 56°C for 30 s, and 72°C for 1.5 min, ending with one cycle of 72°C for 7 min. DNA concentrations of the PCR products were checked using QIAxcel Advanced System (QIAGEN). Emulsion PCR and Ion Torrent sequencing was carried out at the Naturalis Biodiversity Center with Ion 318TM Chip. The PGM was programmed to split the obtained reads in 40 files, corresponding to the samples, according to MID tags attached to the reverse primer.

Bioinformatic Analyses

The initial clean-up of the raw sequence data was carried out using the online platform Galaxy,[1] in which the sequences were sorted according to samples, and adapters (identification tags) and primers were removed. The poor-quality ends were trimmed off with Geneious Pro 5.6.1 (BioMatters, New Zealand), based on 0.02 error probability limit. Quality filtering was done using USEARCH v.8.0 (Edgar, 2010) by truncating all sequences to 200 bp and discarding sequences with expected error > 1. High-quality sequences that passed quality filtering were grouped into operational taxonomic units (OTUs) at 97% sequence similarity with USEARCH, with putatively chimeric sequences discarded. Pairwise similarity searches against the latest USEARCH/UTAX version (8.2) of the curated UNITE fungal ITS sequence database containing identified fungal sequences (Kõljalg et al., 2013) were used for taxonomic classification and to assign OTUs groups to Species Hypothesis groups. We excluded global singletons and OTUs with <80% similarity to a fungal sequence in UNITE. The resulting final dataset contained 4,405 OTUs and 1,941,539 high-quality sequences. We assigned OTUs to functional groups following Tedersoo et al. (2014), supplemented by information regarding the isolation source of curated reference sequences in UNITE. This Targeted Locus Study project has been deposited at DDBJ/EMBL/GenBank under the accession KEOG00000000. The version described in this paper is the first version, KEOG01000000.

Statistical Analyses

Unless otherwise noted, all statistical analyses were done in R (R Core Team, 2013). The fungal community matrix was normalized (rarefied) by random subsampling to the smallest library size (16,482 reads) on a per-sample basis using the *vegan* package (Oksanen et al., 2012). We excluded OTUs that were found in only one sample, resulting in a matrix containing 2,520 OTUs present in at least two samples, which was the basis for further analyses.

We statistically compared OTU richness and relative abundance of fungal functional groups among the samples with ANOVA and Tukey's HSD test and presented these graphically as boxplots with *ggplot2* (Wickham, 2016). Compositional differences among samples were visualized using non-metric multidimensional scaling (NMDS) in *vegan* with Bray-Curtis distance measure on the Hellinger-transformed matrix. We performed PerMANOVA (adonis) with 9,999 permutations to estimate the amount of variation explained by the tundra type and the experimental manipulations of summer warming and increased snow depth in a combined model. The combined warming and increased snow depth treatments were assigned to both experimental manipulation types. The distribution of fungal OTUs among

[1]https://main.g2.bx.psu.edu/root

tundra types and treatments was visualized in a network with *sna* (Butts, 2008).

RESULTS

Patterns of Fungal Richness and Abundance and Edaphic Variables

We detected 484 fungal genera among the matching taxa, of which 320 belonged to Ascomycota, 158 to Basidiomycota, and the rest to more early-diverging fungal lineages. Because the taxonomic groups present at the sampling sites have been discussed in detail by Morgado et al. (2015, 2016) and Semenova et al. (2015, 2016), we only present a brief list of the most diverse genera in the complete dataset. The five most OTU-rich genera included *Cladophialophora* (53 OTUs), *Archaeorhizomyces* (36), *Pezoloma* (34), *Meliniomyces* (30) and *Hyaloscypha* (27) in Ascomycota and *Serendipita* (80), *Cortinarius* (69), *Tomentella* (53), *Inocybe* (43), and *Mycena* (29) in Basidiomycota. Of the non-Dikarya genera, Mortierella (47) was by far the most diverse. Total fungal richness was similar in all dry tundra sites, with a non-significant increase in S and SW treatments relative to the control, while all experimental manipulations resulted in a clear decrease in fungal richness in the moist tundra, although only the combined SW treatment was statistically different from the control (**Figure 1**). With respect to functionality, 1,186 of 2,520 OTUs present in at least two samples were assigned to functional groups. Significant differences in richness among treatments were observed in four of the six functional groups analyzed (**Figure 1**). Richness of ectomycorrhizal (ECM) fungi was significantly higher in control than any of the treatment plots in moist tundra. The second highest richness was found in the dry tundra control plots, but it was not significantly different from any of the experimental treatments. In plant pathogenic fungi, highest richness was observed in the S and SW treatments, although only the latter differed significantly from the control. No statistical differences were observed in the moist tundra for the same functional group. Conversely, root-associated non-mycorrhizal fungi showed highest richness in moist control plots and decreased in all treatment plots, with significant difference observed between control and the SW and S treatments, while richness values were uniformly low for all treatments in the dry tundra. Saprotrophic fungal richness was highest in the dry S treatment, with no statistical differences among the other treatments (**Figure 1**).

With respect to proportional abundance, four out of six functional groups exhibited significant differences, with the important differences that although litter and wood decomposers did not differ in proportional abundance among tundra types and treatments, they showed the strongest changes in proportional abundance (**Figure 2**). The abundance of litter fungi consistently increased in the snow addition plots in dry and moist tundra, with the strongest increase observed in the latter, particularly in the SW treatment. Conversely, experimental manipulations seemed to have stronger effects on wood decomposers in the dry tundra, with a significant increase in richness observed in the SW treatment relative to the control. Even though S and SW treatments resulted in higher observed richness in the moist tundra as well, the difference from the control was not significant. In ECM fungi, the only significant differences were observed between the high value of proportional abundance observed in the dry W and the low values in the dry S and moist W and SW treatments. In generalist saprotrophs, the moist W and SW showed the highest proportional abundance, with the W being statistically different from the control (**Figure 2**).

Of the five edaphic variables tested (pH, EC, C and N content, and C/N ratio), only pH and C/N ratio differed among the experimental treatments (**Figure 3**). In both tundra types, soil pH was lower under increased snow depth than in the control, although the difference mostly remained non-significant. The pattern of C/N ratio was practically opposite of the trend observed for pH. These changes were greater in the dry tundra than in the moist, primarily under increased snow depth in the dry tundra, that had the lowest pH and the highest C/N ratio values among all treatments.

Comparing Fungal Community Composition Among Tundra Types and Treatments

PerMANOVA revealed that tundra type was by far the strongest driver for the structuring of fungal communities, explaining between 21 and 42% of the variation in community composition of the various functional groups when considering all sites (**Supplementary Table S1**). Therefore, additional PerMANOVA analyses were carried out for all functional groups to evaluate the effects of treatment on compositional variation separately in the dry and moist tundra. In dry tundra, the effects of experimental increase in snow depth, soil pH, and EC, and to a smaller extent warming and soil N content, tended to explain the greatest variation in community structure, but substantial differences were observed among the functional groups (**Supplementary Table S1**). Wood decomposer fungi differed most from the above general trend: C/N ratio was the most influential to their community composition, followed by pH and warming treatment, with increased snow depth having non-significant contribution to explained variance. In moist tundra, the contribution of warming was significant for most functional groups, except ECM fungi and wood decomposers. The effect of increased snow depth generally was weaker, with significant treatment effect on community composition being observed only in ECM and other root-associated fungi in the moist tundra. Of the edaphic variables, EC explained surprisingly large fractions of the variation in community composition in ECM, litter decomposer and generalist saprotrophic fungi (all above 10%).The effect of soil pH was only significant in ECM and other root-associated fungi.

Non-metric multidimensional scaling plots of the selected functional groups of fungi confirmed the dominant contribution of tundra type to community structure as detailed above (**Figure 4**). However, network graphs of all

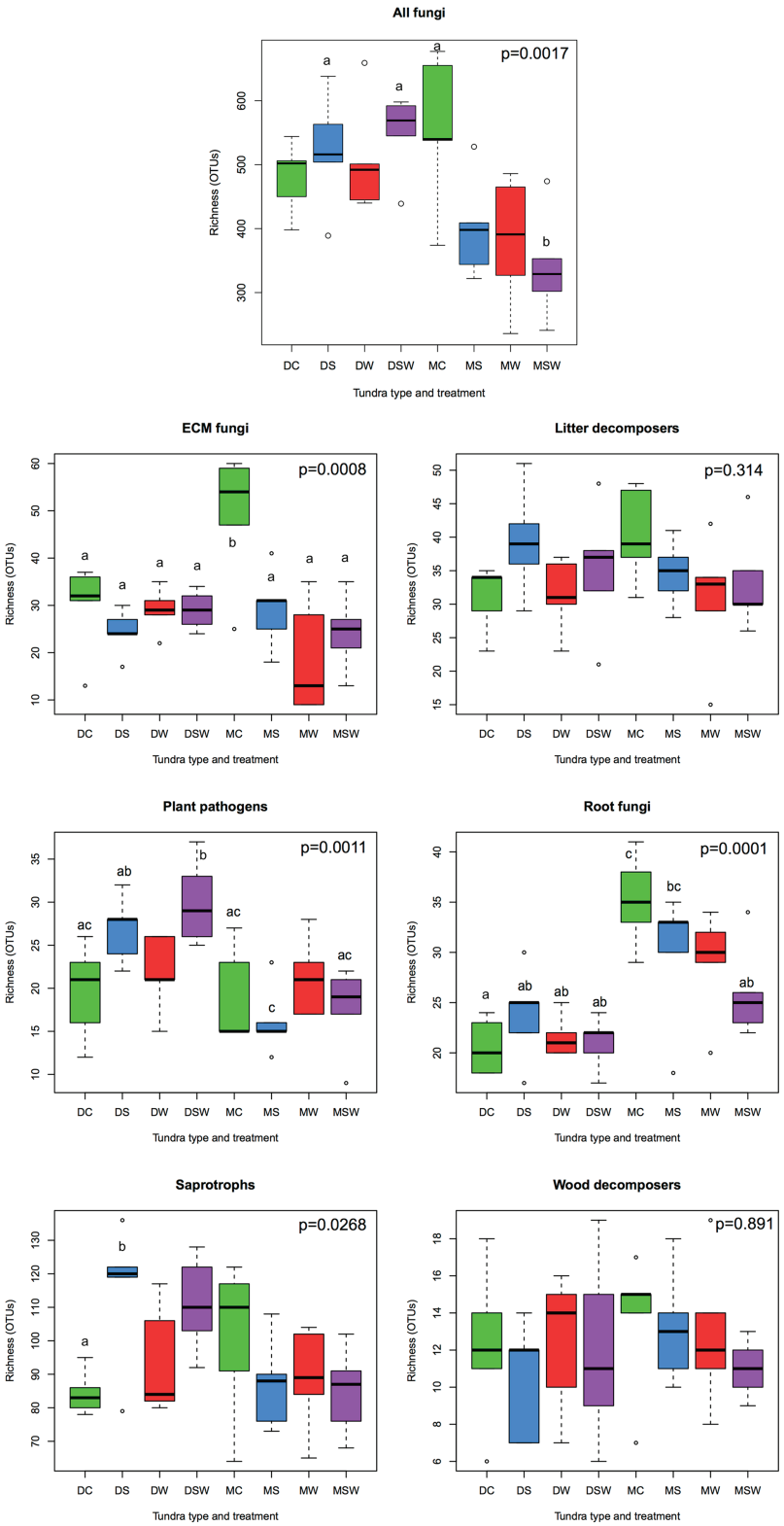

FIGURE 1 | Comparisons of richness of functional groups of arctic fungi across dry and moist tundra and experimental treatments. Means were compared using ANOVA and Tukey's HSD tests, with letters denote significant differences. D, dry tundra; M, moist tundra; W, summer warming; S, increased winter snow depth; WS, combined summer warming and increased snow depth treatments.

fungi showed that a substantial proportion of OTUs from different functional groups were shared between dry and moist tundra and among treatments (**Figure 5**). In addition, each treatment contained unique OTUs, particularly the control plots contained many OTUs that were absent from the treatment plots. The network of ECM fungal OTUs showed that the /tomentella-thelephora, /cortinarius, and /russula-lactarius lineages dominated the ECM community. Although these lineages had many OTUs restricted to either dry or moist tundra, OTUs that occurred in both tundra

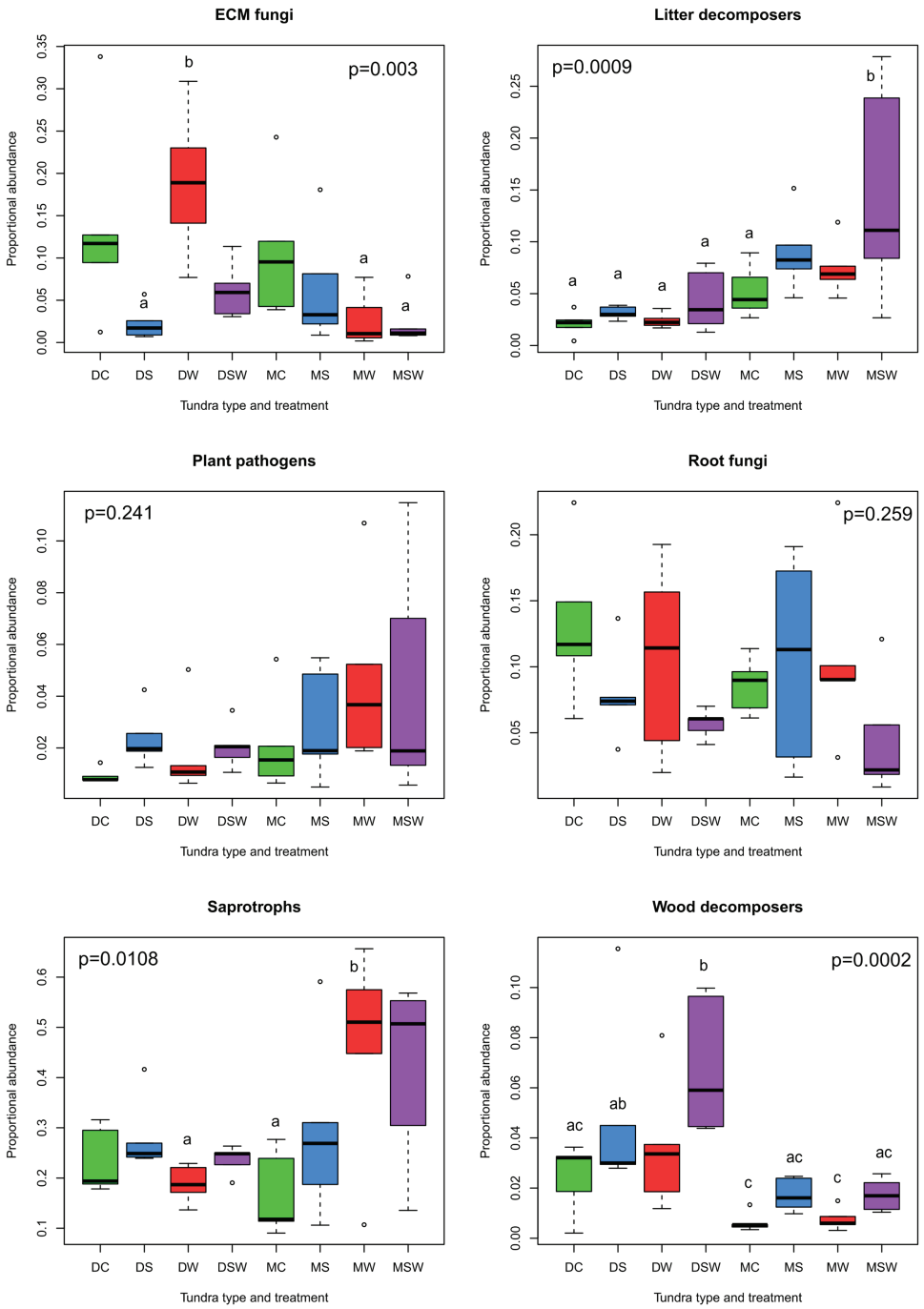

FIGURE 2 | Comparisons of proportional abundance of functional groups of arctic fungi across dry and moist tundra and experimental treatments. Means were compared using ANOVA and Tukey's HSD tests, with letters denote significant differences. D, dry tundra; M, moist tundra; W, summer warming; S, increased winter snow depth; WS, combined summer warming and increased snow depth treatments.

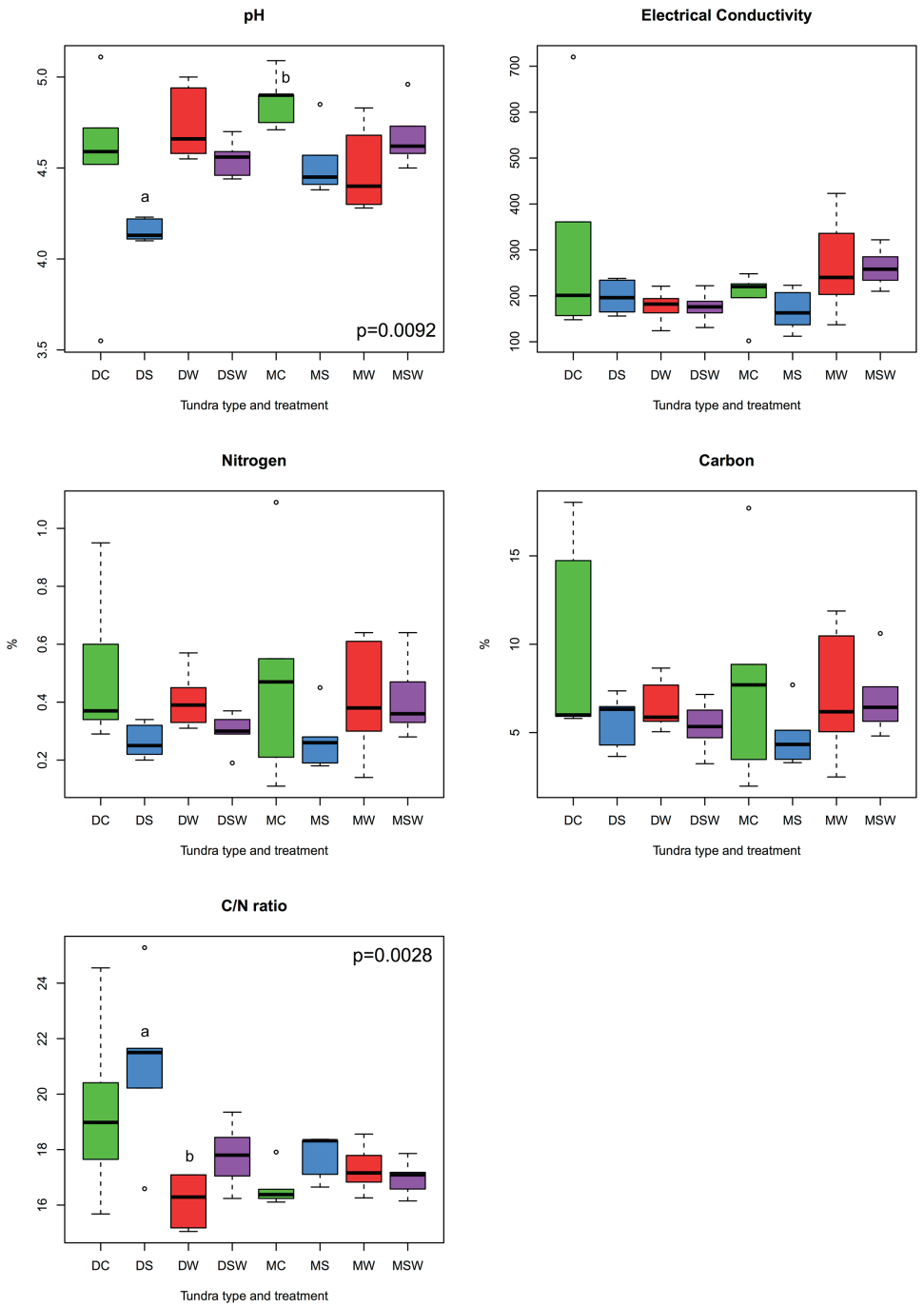

FIGURE 3 | Comparisons of measured edaphic variables across dry and moist tundra and experimental treatments. Means were compared using ANOVA and Tukey's HSD tests, with letters denote significant differences. D, dry tundra; M, moist tundra; W, summer warming; S, increased winter snow depth; WS, combined summer warming and increased snow depth treatments.

types came overwhelmingly from these lineages. OTUs in the/inocybe lineage, which is among the most diverse and widespread lineages of arctic fungi (Geml et al., 2012b), appeared to be more restricted to a certain tundra type (**Figure 5**).

DISCUSSION

This study provides insights into the compositional dynamics of arctic fungi, highlighting their diversity, abundance, and distribution in dry and moist acidic tundra and their possible

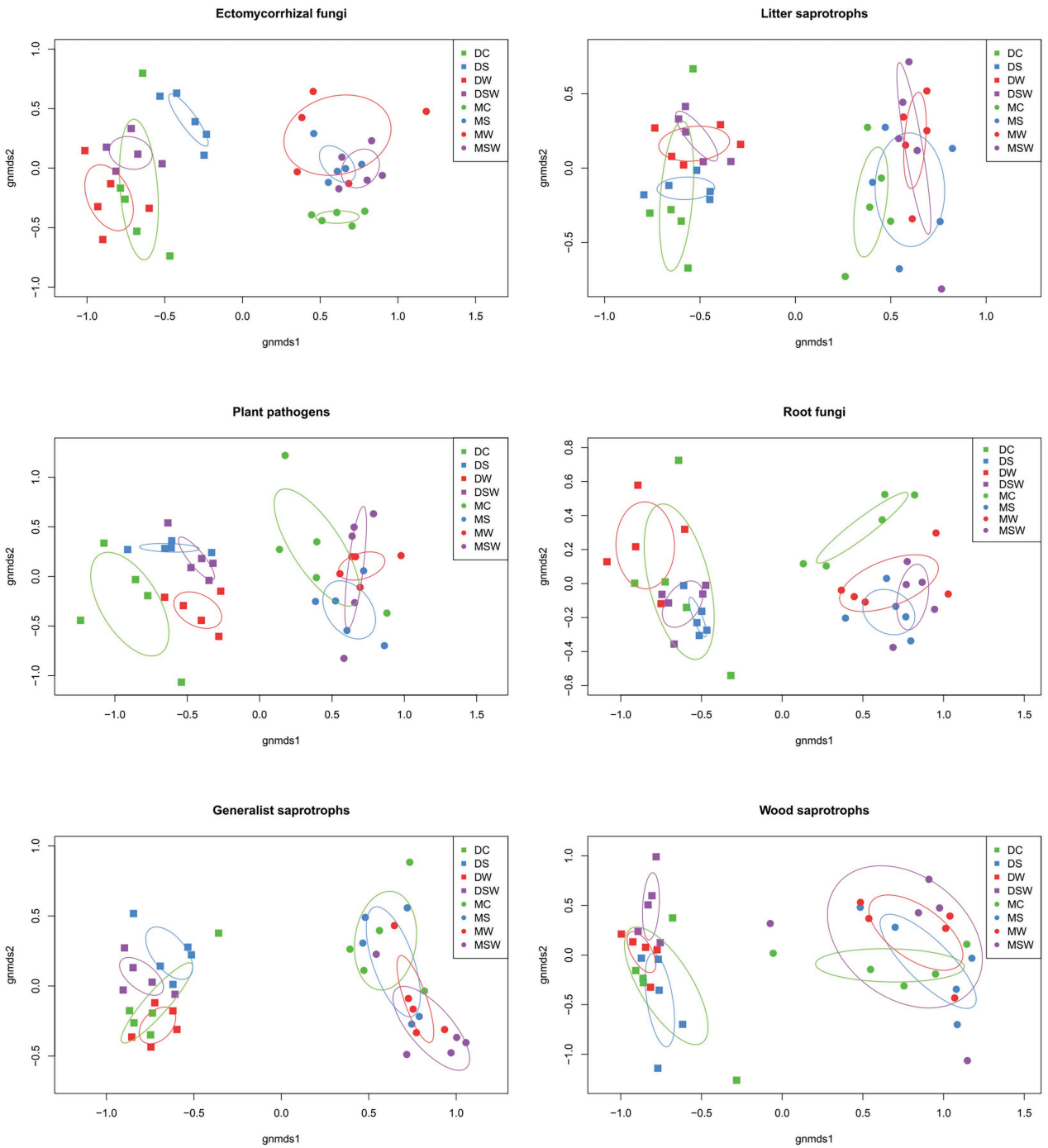

FIGURE 4 | Non-metric multidimensional scaling (NMDS) ordination plots of the six most diverse functional groups of arctic fungi based on Hellinger-transformed data. For each treatment, circles indicate the SD. D, dry tundra; M, moist tundra; W, summer warming; S, increased winter snow depth; WS, combined summer warming and increased snow depth treatments.

responses to warming and increased winter precipitation. The deep sequence data presented here, coupled with the measured edaphic variables, clearly show that (1) arctic fungal community composition at the selected sites is determined principally by tundra type; (2) experimental warming and increased snow depth have different effects edaphic variables and fungal communities on dry vs. moist tundra; (3) a substantial proportion of the effects of summer warming and increased winter snow depth on fungal communities likely is mediated through changes in edaphic conditions, and that (4) there are important differences

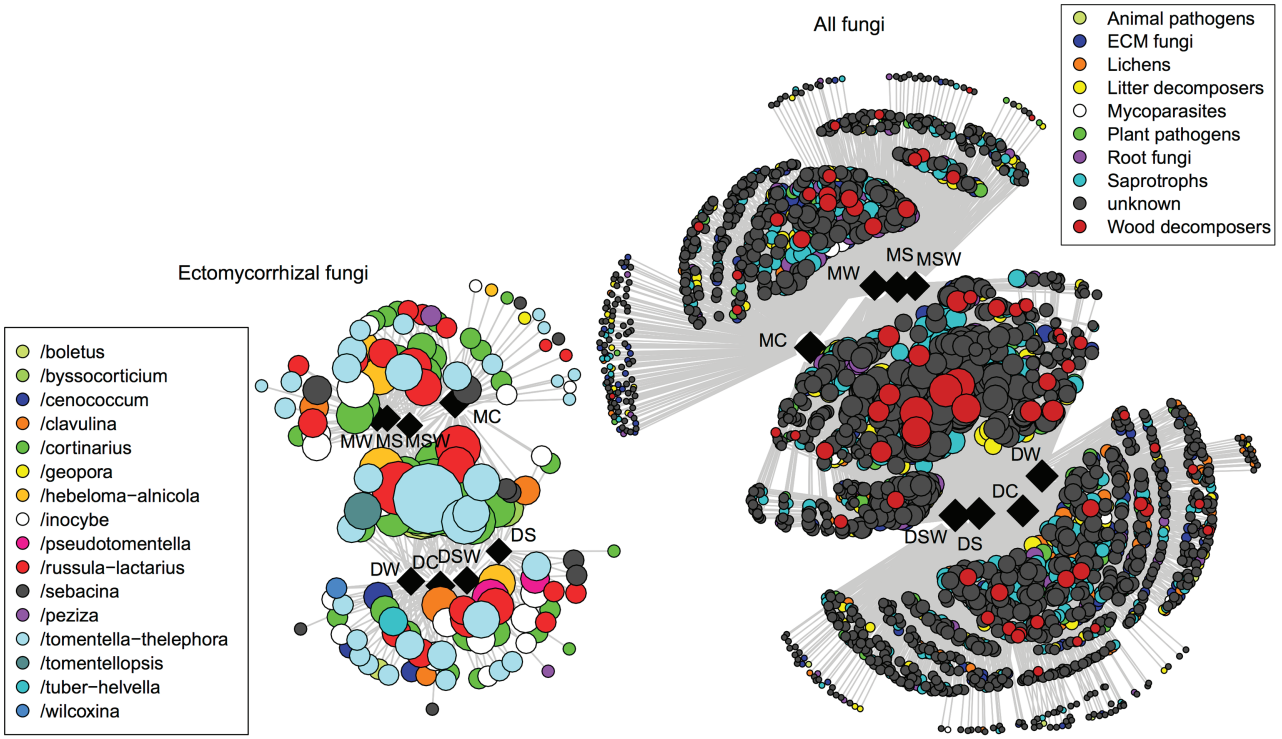

FIGURE 5 | Distribution of operational taxonomic units (OTUs) of ectomycorrhizal and all fungi as visualized by network analysis for the different tundra types and experimental treatments. Squares and circles indicate sample categories and OTUs, respectively. Circles representing OTUs are connected with straight lines to samples (squares) they occur in. Centrally located OTUs are shared among multiple treatments and/or tundra types. Circle size is proportional to the number of samples (in respective habitats and/or treatments) the OTU is present in.

among functional groups of fungi in how they respond to increases in summer temperatures, snow depth, and related alterations in soil chemistry.

Despite the spatial proximity of the dry and moist tundra plots (<500 m), the overwhelming compositional differences in fungi suggest that many fungi appear to be sensitive to the differences in hydrology and vegetation between these tundra types. However, it is worth to note that a relatively large fraction of the fungal community is shared between the dry and moist tundra and among various treatments. It is plausible that climate change and related changes in abiotic factors will favor these fungi with apparently wide niche breadth as opposed to those with narrower observed niche breadth that are restricted to a certain habitat, particularly to the control sites. Because dispersal generally is not considered a limiting factor in arctic fungi (Geml, 2011; Geml et al., 2012a,b), it is presumed that, other than stochastic factors related to "founder effects," environmental filtering drives fungal community composition in the sampling area. Landscape-scale studies on the compositional dynamics of arctic fungi among several tundra habitats spanning moisture and acidity gradients are needed to learn more about fungal niches in the Arctic.

In addition to the differences in fungal species pools in dry and moist acidic tundra at the sampling sites, there were also distinct responses of the dry and moist tundra fungal communities to experimental warming and increase in snow depth. This suggests that species pool and pre-disturbance environmental factors, such as site hydrology and resulting differences in vegetation structure, likely drive response trajectories of fungal communities, similar to what has been reported for plants as well (Walker et al., 2006; Mercado-Diaz, 2011; Pattison and Welker, 2014). For example, the strong responses in fungal communities to warming in the moist tundra are in agreement with more pronounced plant community responses in the moist than in the dry tundra, although it is unclear to what extent compositional shifts in fungal communities drive vegetation shifts or are driven by them. In addition, differential fungal responses to warming in the dry and moist tundra likely are related to differences in natural temperature fluctuations in the dry and moist tundra. Moist tundra soils generally experience less temperature variation due to higher water content and a dense peat moss layer that buffers changes in air and surface temperature. In dry tundra, where vegetation cover generally is below 50% and soils are relatively dry, the ca. 2°C warming during the summer may represent a negligible change relative to the high variation in temperatures experienced under normal circumstances. With respect to increased snow depth, it is important to note that greater snow depth increases winter soil temperature as well as soil moisture, particularly in early summer, and these effects cannot be decoupled.

The strong effect of available moisture on fungal growth has repeatedly been shown in dry tundra (Jones et al., 1998; Schimel et al., 2004; Wahren et al., 2005; Mercado-Diaz, 2011). Therefore, the stronger response by the community of the dry heath tundra may partly be explained by partially alleviating water stress in this habitat. In addition, the edaphic data presented here indicate that of all treatments, S treatment plots in the dry tundra differ most from the rest in soil pH and C/N ratio. More precisely, these plots have the most acidic soils that contain the most decay-resistant organic matter. The fact that the richness of generalist saprotrophs was the highest in this treatment, but not their relative abundance, may indicate that the low nutrient levels favor a high diversity of relatively slow-growing saprotrophic fungi. Moist tundra soils are mostly saturated by water throughout the growing season and winter snow cover is deeper and more homogenous than in the dry tundra community, where soils tend to have little or no snow cover and low moisture content, resulting in very cold temperatures and frequent desiccations. It is noteworthy that, particularly in the dry tundra, the compositional effects of the combined SW treatment resulted in communities that appeared to be intermediate between those of S or W only, as suggested by the NMDS results. Similarly, opposite trends in S and W treatment were also observed to some extent in richness and in soil pH and C/N ratio, though they remained mostly non-significant. This suggests that in the dry tundra, these S and W treatments may have divergent effects on the fungal communities, possibly because they alter soil moisture and soil chemical processes in opposite directions.

ECM and non-mycorrhizal root fungi appear to be most diverse in the moist tundra, but their high richness is not coupled with high overall abundance. Their decreasing trends in richness and abundance and the strong compositional shifts in the moist tundra treatment plots, suggest that the altered abiotic conditions, and possibly the resulting differences in vegetation, are no longer suitable for many root-associated fungi that normally inhabit moist acidic tussock tundra. This is surprising, because ECM fungal richness and abundance generally correlate with host plant abundance (Tedersoo et al., 2014) and higher density and biomass of ECM shrubs were reported in increased snow depth plots in both tundra types (Mercado-Diaz, 2011; Pattison and Welker, 2014). Differences in nutrient scavenging capabilities among ECM fungal species under the altered conditions may explain some of the observed patterns, as changes in plant community and N dynamics had been reported to be more strongly affected by the increased snow depth in the moist than in the dry tundra (Schimel et al., 2004; Wahren et al., 2005; Mercado-Diaz, 2011). For example, presenting data from the S and W plots analyzed here, Morgado et al. (2015, 2016) argued that ECM fungi with exploration types adapted to labile N uptake generally showed decreasing richness under increased snow depth, while the richness of ECM fungi with exploration types adapted to acquire recalcitrant soil N were not affected by increased snow depth. Although Morgado et al. (2015, 2016) did not analyze data from the combined SW plots that are presented here, their observations, coupled with the higher C/N values observed here suggest that the capability of acquiring recalcitrant N may represent an important environmental filter for ECM fungi under increased snow depth and appear to be explain partly the lower richness and abundance of ECM fungi. Alternatively, it could partly be caused by the water-logged, likely anaerobic conditions in the SW plots in the summer (József Geml, pers. obs.). The findings presented here show that the above differences likely are at fine taxonomic scales, i.e., at species level, as most ECM genera included numerous OTUs that were specific to a habitat and others that were shared among tundra types and treatments, indicating that in most genera comprise species that represent a wide spectrum of ecological preferences and niche breadths. It is well-known that ECM fungi compete with saprotrophic fungi for water and nutrients (Orwin et al., 2011) and the decline in ECM fungi, the increased abundance of decomposers, and higher rates of decomposition with increasing summer and winter soil temperatures (as discussed below), may result in decreased C sinks in tundra soils, as plants in cold climates are known to transfer up to 50–70% of their C uptake directly to ECM fungal mycelia (Clemmensen et al., 2013).

The increased relative abundance of decomposers of litter and wood in the snow addition treatments (S and SW) in moist and dry tundra, respectively, may be related to the abilities of these fungi to take advantage of more available substrate as well as more favorable conditions for enzymatic degradation. Increased quantities of litter and woody debris resulting from the greater above-ground biomass of shrubs and graminoids have been reported for these plots with increased snow depths as well as with summer warming (Hollister et al., 2005; Wahren et al., 2005; Mercado-Diaz, 2011; Semenova et al., 2015) and microbial decomposition rates have been found to be greater (Sistla et al., 2013). Saprotrophic fungal activity generally is correlated with decomposition rates and CO_2 flux between the terrestrial and atmospheric pools. Therefore, an increased abundance of saprotrophic fungi may increase fungal enzymatic activity in soils, with higher rates of C mineralization and greater CO_2 emission to the atmosphere (Guhr et al., 2015). The greater aboveground plant biomass of the moist tundra treatment plots also is in agreement with the higher proportional abundance of plant pathogenic fungi that could benefit from greater host biomass. Greater snow depth increases winter soil temperature, which is expected to have positive effects on microbial decomposition. The increased abundance of generalist saprotrophs in the increased snow depth and warming plots provides further support for this idea. Overall, the observed changes in richness and abundance decomposer and other saptrophic fungi provides proof for the conceptual framework that increased snow depth provides greater soil insulation, resulting in higher winter and spring-time soil temperatures, and increased rates of nutrient mineralization. This, in turn, favors shrub growth and expansion, which leads to decreased albedo, increased snow trapping, and enhanced CO_2 release to the atmosphere, providing positive feedback to climate change.

CONCLUSION

Fungi play numerous ecological roles of key importance and are involved in a complex array of interactions with

other organisms that are still poorly known. We observed greater treatment effect on edaphic variables in dry tundra than in the moist that suggest that dry tundra may be more responsive to climate change, particularly increased winter snow depth. Climate-driven fungal community dynamics and changes in richness and abundance of functional guilds will likely have a wide range of consequences. While the currently prevailing view is that altered plant community composition drives fungal community change in the Arctic, it seems that fungal community composition may change more rapidly and independently of plant communities and that fungi may be particularly well-suited to monitor early responses to environmental changes. It is possible that, in response to experimental manipulations simulating predicted changes in climate, functional groups fungi in our dataset declined or increased under due to alterations in communities of other organismal groups which were not investigated here and with which they could have mutualistic or competitive interactions. Because of the scarcity of information on other components of soil biodiversity in the Arctic in general and at the sampling site in particular, it is difficult to assess the extent to which fungal responses to the above-mentioned manipulations are the results of abiotic factors vs. biotic interactions. Future studies on inter-kingdom interactions, e.g., among fungi, bacteria, myxomycetes and soil invertebrates, are needed to gain a more complete understanding of soil biota and its resilience to climate change.

DATA AVAILABILITY STATEMENT

The datasets presented in this study can be found in online repositories. The names of the repository/repositories and accession number(s) can be found at: https://www.ncbi.nlm.nih.gov/genbank/, KEOG01000000.

AUTHOR CONTRIBUTIONS

JG designed the research and selected sampling sites. JG, LM, and TS-N performed the fieldwork, labwork, and the initial bioinformatics. JG completed the bioinformatics and the statistical analyses, to which LM contributed R scripts. JG wrote the first draft of the paper and all authors contributed to the revisions of the manuscript that resulted in the first submitted version.

FUNDING

Financial support for the research presented in this manuscript was provided by the NWO-ALW Open Program research grant (821.01.016) to JG and by the Naturalis Biodiversity Center to all authors. JG gratefully acknowledges support by the Lendület Program (award no. 96049) of the Hungarian Academy of Sciences and the Eötvös Loránd Research Network.

ACKNOWLEDGMENTS

We thank the staff of the Toolik Lake Field Station for logistical support, Elza Duijm and Marcel Eurlings (Naturalis) for help with the Ion Torrent sequencing, Todd O'Hara and Perry S. Barboza (University of Alaska Fairbanks) for providing equipment and assistance to lyophilize the soil samples, and Miklós Gulyás (Department of Soil Sciences, Hungarian University of Agricultural and Life Sciences) for help with the soil chemical analyses.

SUPPLEMENTARY MATERIAL

The Supplementary Material for this article can be found online at: https://www.frontiersin.org/articles/10.3389/fmicb.2021.628746/full#supplementary-material

REFERENCES

Aerts, R. (2006). The freezer defrosting: global warming and litter decomposition rates in cold biomes. *J. Ecol.* 94, 712–724. doi: 10.1111/j.1365-2745.2006.01142.x

Bhatt, U. S., Walker, D. A., Raynolds, M. K., Comiso, J. C., Epstein, H. E., Jia, G., et al. (2010). Circumpolar arctic tundra vegetation change is linked to sea ice decline. *Earth Interact.* 14, 1–20. doi: 10.1175/2010EI315.1

Bintaja, R., and Selten, F. M. (2014). Future increases in arctic precipitation linked to local evaporation and sea-ice retreat. *Nature* 509, 479–482. doi: 10.1038/nature13259

Bjorbækmo, M. F. M., Carlsen, T., Brysting, A., Vrålstad, T., Høiland, K., Ugland, K. I., et al. (2010). High diversity of root associated fungi in both alpine and arctic *Dryas octopetala*. *BMC Plant Biol.* 10:244. doi: 10.1186/1471-2229-10-244

Bret-Harte, M. S., Shaver, G. R., and Chapin, F. S. (2002). Primary and secondary stem growth in arctic shrubs: implications for community response to environmental change. *J. Ecol.* 90, 251–267. doi: 10.1046/j.1365-2745.2001.00657.x

Butts, C. T. (2008). Social network analysis with *sna*. *J. Stat. Softw.* 24, 1–51. doi: 10.18637/jss.v024.i06

Callaghan, T. V., Björn, L. O., Chernov, Y., Chapin, T., Christensen, T. R., Huntley, B., et al. (2004). Biodiversity, distributions and adaptations of arctic species in the context of environmental change. *Ambio* 33, 404–417. doi: 10.1579/0044-7447-33.7.404

Chapin, F. S. III. (1983). Direct and indirect effects of temperature on Arctic plants. *Polar Biol.* 2, 47–52. doi: 10.1007/BF00258285

Chapin, F. S. I. I. I., Shaver, G. R., Giblin, A. E., Nadelhoffer, K. J., and Laundre, J. A. (1995). Response of arctic tundra to experimental and observed changes in climate. *Ecology* 76, 694–711. doi: 10.2307/1939337

Chapin, F. S. I. I. I., Sturm, M., Serreze, M. C., and McFadden, J. P. (2005). Role of land surface changes in Arctic summer warming. *Science* 310, 657–660. doi: 10.1126/science.1117368

Clemmensen, K. E., Michelsen, A., Jonasson, S., and Shaver, G. R. (2006). Increased ectomycorrhizal fungal abundance after long-term fertilization and warming of two Arctic tundra ecosystems. *New Phytol.* 171, 391–404. doi: 10.1111/j.1469-8137.2006.01778.x

Clemmensen, K. E., Ovaskainen, A. B. O., Dahlberg, A., Ekblad, A., Wallander, H., Stenlid, J., et al. (2013). Roots and associated fungi drive long-term carbon sequestration in boreal forest. *Science* 339:1615. doi: 10.1126/science.1231923

Edgar, R. C. (2010). Search and clustering orders of magnitude faster than BLAST. *Bioinformatics* 26, 2460–2461. doi: 10.1093/bioinformatics/btq461

Geml, J. (2011). "Coalescent analyses reveal contrasting patterns of inter-continental gene flow in arctic-alpine and boreal-temperate fungi" in

Biogeography of microscopic organisms – Is everything small everywhere? ed. D. Fontaneto (Cambridge: Cambridge University Press), 177–190.

Geml, J., Kauff, F., Brochmann, C., Lutzoni, F., Laursen, G. A., Redhead, S. A., et al. (2012a). Frequent circumpolar and rare transequatorial dispersals in the lichenised agaric genus *Lichenomphalia* (Hygrophoraceae, Basidiomycota). *Fung. Biol.* 116, 388–400. doi: 10.1016/j.funbio.2011.12.009

Geml, J., Morgado, L. N., Semenova, T. A., Welker, J. M., Walker, M. D., and Smets, E. (2015). Long-term warming alters richness and composition of taxonomic and functional groups of arctic fungi. *FEMS Microbiol. Ecol.* 91:fiv095. doi: 10.1093/femsec/fiv095

Geml, J., Semenova, T. A., Morgado, L. N., and Welker, J. M. (2016). Changes in composition and abundance of functional groups of arctic fungi in response to long-term summer warming. *Biol. Lett.* 12:20160503. doi: 10.1098/rsbl.2016.0503

Geml, J., Timling, I., Robinson, C. H., Lennon, N., Nusbaum, H. C., Brochmann, C., et al. (2012b). An arctic community of symbiotic fungi assembled by long-distance dispersers: phylogenetic diversity of ectomycorrhizal basidiomycetes in Svalbard based on soil and sporocarp DNA. *J. Biogeogr.* 39, 74–88. doi: 10.1111/J.1365-2699.2011.02588.X

Guhr, A., Borken, W., Spohn, M., and Matzner, E. (2015). Redistribution of soil water by a saprotrophic fungus enhances carbon mineralization. *PNAS* 112, 14647–14651. doi: 10.1073/pnas.1514435112

Hobbie, S. E., and Chapin, F. S. I. I. I. (1998). The response of tundra plant biomass, above-ground production, nitrogen, and CO_2 flux to experimental warming. *Ecology* 79, 1526–1544. doi: 10.1890/0012-9658(1998)079[1526:TROTPB]2.0.CO;2

Hobbie, J. E., Hobbie, E. A., Drossman, H., Conte, M. H., Weber, J. C., Shamhart, J., et al. (2009). Mycorrhizal fungi supply nitrogen to host plants in Arctic tundra and boreal forests: ^{15}N is the key signal. *Can. J. Microbiol.* 55, 84–94. doi: 10.1139/W08-127

Hollister, R. D., Webber, P. J., and Bay, C. (2005). Plant response to temperature in northern Alaska: implications for predicting vegetation change. *Ecology* 86, 1562–1570. doi: 10.1890/04-0520

Ihrmark, K., Bödeker, I. T. M., Cruz-Martinez, K., Friberg, H., Kubartova, A., Schenck, J., et al. (2012). New primers to amplify the fungal ITS2 region – evaluation by 454-sequencing of artificial and natural communities. *FEMS Microbiol. Ecol.* 82, 666–677. doi: 10.1111/j.1574-6941.2012.01437.x

Jones, M. H., Fahnestock, J. T., Walker, D. A., Walker, M. D., and Welker, J. M. (1998). Carbon dioxide fluxes in moist and dry arctic tundra during the snow-free season: responses to increases in summer temperature and winter snow accumulation. *Arct. Antarct. Alp.* 30, 373–380. doi: 10.2307/1552009

Kattsov, V. M., and Walsh, J. E. (2000). Twentieth-century trends of Arctic precipitation from observational data and a climate model simulation. *J. Clim.* 13, 1362–1370. doi: 10.1175/1520-0442(2000)013<1362:TCTOAP>2.0.CO;2

Kaufman, D. S., Schneider, D. P., McKay, M. P., Ammann, C. M., Bradley, R. S., Briffa, K. R., et al. (2009). Recent warming reverses long-term Arctic cooling. *Science* 325, 1236–1239. doi: 10.1126/science.1173983

Kõljalg, U., Nilsson, R. H., Abarenkov, K., Tedersoo, L., Taylor, A. F. S., Bahram, M., et al. (2013). Towards a unified paradigm for sequence-based identification of Fungi. *Mol. Ecol.* 22, 5271–5277. doi: 10.1111/mec.12481

Marion, G. M., Henry, G. H. R., Freckman, D. W., Johnstone, J., Jones, G., Jones, M. H., et al. (1997). Open-top designs for manipulating field temperature in high-latitude ecosystems. *Glob. Chang. Biol.* 3, 20–32. doi: 10.1111/j.1365-2486.1997.gcb136.x

Mercado-Diaz, J. (2011). Changes in composition and structure of plant communities in the Alaskan Arctic Tundra after 14 years of experimental warming and snow manipulation. MS Thesis, University of Porto Rico.

Morgado, L. N., Semenova, T. A., Welker, J. M., Walker, M. D., Smets, E., and Geml, J. (2015). Summer temperature increase has distinct effect on the ectomycorrhizal fungal communities of moist tussock and dry tundra in Arctic Alaska. *Glob. Chang. Biol.* 21, 959–972. doi: 10.1111/gcb.12716

Morgado, L. N., Semenova, T. A., Welker, J. M., Walker, M. D., Smets, E., and Geml, J. (2016). Long-term increase in snow depth leads to compositional changes in arctic ectomycorrhizal fungal communities. *Glob. Chang. Biol.* 22, 3080–3096. doi: 10.1111/gcb.13294

Nemergut, D. R., Costello, E. K., Meyer, A. F., Pescador, M. Y., Weintraub, M. N., and Schmidt, S. K. (2005). Structure and function of alpine and arctic soil microbial communities. *Res. Microbiol.* 156, 775–784. doi: 10.1016/j.resmic.2005.03.004

Newsham, K. K., Upson, R., and Read, D. J. (2009). Mycorrhizas and dark septate root endophytes in polar regions. *Fungal Ecol.* 2, 10–20. doi: 10.1016/j.funeco.2008.10.005

Oksanen, J., Blanchett, F. G., Kindt, R., Legendre, P., Minchin, P. R, O'Hara, B, et al. (2012) Vegan: community Ecology Package. R Package 2.0.3.

Orwin, K. H., Kirschbaum, M. U. F., St John, M. G., and Dickie, I. A. (2011). Organic nutrient uptake by mycorrhizal fungi enhances ecosystem carbon storage: a model-based assessment. *Ecol. Lett.* 14, 493–502. doi: 10.1111/j.1461-0248.2011.01611.x

Pattison, R. R., and Welker, J. M. (2014). Differential ecophysiological response of deciduous shrubs and a graminoid to long-term experimental snow reduction and addition in moist tundra, northern Alaska. *Oecologia* 174, 339–350. doi: 10.1007/s00442-013-2777-6

R Core Team (2013). R: a language and environment for statistical computing. R Foundation for Statistical Computing, Vienna, Austria. Available at: http://www.R-project.org/ (Accessed September 15, 2020).

Schimel, J. P., Bilbrough, C., and Welker, J. M. (2004). Increased snow depth affects microbial activity and nitrogen mineralization in two arctic tundra communities. *Soil Biol. Biochem.* 36, 217–227. doi: 10.1016/j.soilbio.2003.09.008

Semenova, T. A., Morgado, L. N., Welker, J. M., Walker, M. D., Smets, E., and Geml, J. (2015). Long-term experimental warming alters community composition of ascomycetes in Alaskan moist and dry arctic tundra. *Mol. Ecol.* 24, 424–437. doi: 10.1111/mec.13045

Semenova, T. A., Morgado, L. N., Welker, J. M., Walker, M. D., Smets, E., and Geml, J. (2016). Compositional and functional shifts in arctic fungal communities in response to experimentally increased snow depth. *Soil Biol. Biochem.* 100, 201–209. doi: 10.1016/j.soilbio.2016.06.001

Shaver, G. R., Giblin, A. E., Nadelhoffer, K. J., Thieler, K. K., Downs, M. R., Laundre, J. A., et al. (2006). Carbon turnover in Alaskan tundra soils: effects of organic matter quality, temperature, moisture and fertilizer. *J. Ecol.* 94, 740–753. doi: 10.1111/j.1365-2745.2006.01139.x

Sistla, S. A., Moore, J. C., Simpson, R. T., Gough, L., Shaver, G. R., and Schimel, J. P. (2013). Long-term warming restructures Arctic tundra without changing net soil carbon storage. *Nature* 497, 615–618. doi: 10.1038/nature12129

Sparks, D. L., Page, A. L., Helmke, P. A., and Loeppert, R. H. (1996). *Methods of soil analysis part 3 – Chemical methods. Soil Society of America Book Series*. Madison, Wisconsin, U.S.A.: American Society of Agronomy, Inc.

Stocker, T. F., Qin, D., Plattner, G. K., Tignor, M., Allen, S. K., Boschung, J., et al. (2013). Climate Change 2013: The Physical Science Basis. Contribution of Working Group I to the Fifth Assessment Report of the Intergovernmental Panel on Climate Change. Cambridge, UK, Cambridge University Press, 1535.

Sturm, M., Racine, C. R., and Tape, K. (2001). Increasing shrub abundance in the Arctic. *Nature* 411, 546–547. doi: 10.1038/35079180

Sturm, M., Schimel, J., Michelson, G., Welker, J. M., Oberbauer, S. F., Liston, G. E., et al. (2005). Winter biological processes could help convert arctic tundra to shrubland. *Bioscience* 55, 17–26. doi: 10.1641/0006-3568(2005)055[0017:WBPCHC]2.0.CO;2

Tarnocai, C., Canadell, J. G., Schuur, E. A. G., Kuhry, P., Mazhitova, G., and Zimov, S. (2009). Soil organic carbon pools in the northern circumpolar permafrost region. *Glob. Biogeochem. Cycles* 23:2. doi: 10.1029/2008GB003327

Tedersoo, L., Bahram, M., Põlme, S., Kõljalg, U., Yorou, N. S., and Wijesundera, R. (2014). Global diversity and geography of soil fungi. *Science* 28:6213. doi: 10.1126/science.1256688

Wahren, C. H. A., Walker, M. D., and Bret-Harte, M. S. (2005). Vegetation responses in Alaskan arctic tundra after 8 years of a summer warming and winter snow manipulation experiment. *Glob. Chang. Biol.* 11, 537–552. doi: 10.1111/j.1365-2486.2005.00927.x

Walker, D. A., Raynolds, M. K., Daniëls, F. J. A., Robinson, C. H., and Wookey, P. A. (2005). The circumpolar Arctic vegetation map. *J. Veg. Sci.* 16, 267–282. doi: 10.1111/j.1654-1103.2005.tb02365.x

Walker, M. D., Wahren, H. C., Hollister, R. D., Henry, G. H. R., Ahlquist, L. E., Alatalo, J. M., et al. (2006). Plant community responses to experimental warming across the tundra biome. *Proc. Natl. Acad. Sci. USA.* 103, 1342–1346. doi: 10.1073/pnas.0503198103

Walker, M. D., Walker, D. A., Welker, J. M., Arft, A. M., Bardsley, T., Brooks, P. D., et al. (1999). Long-term experimental manipulation of winter snow regime and summer temperature in arctic and alpine tundra. *Hydrol. Process.* 13,

2315–2330. doi: 10.1002/(SICI)1099-1085(199910)13:14/15<2315::AID-HYP888>3.0.CO;2-A

Welker, J. M., Fahnestock, J. T., and Jones, M. H. (2000). Annual CO_2 flux from dry and moist acidic tundra: field responses to increases in summer temperature and winter snow depth. *Clim. Chang.* 44, 139–150. doi: 10.1023/A:1005555012742

Welker, J. M., Fahnestock, J. T., Sullivan, P. F., and Chimner, R. A. (2005). Leaf mineral nutrition of arctic plants in response to long-term warming and deeper snow in N. Alaska. *Oikos* 109, 167–177. doi: 10.1111/j.0030-1299.2005.13264.x

Welker, J. M., Molau, U., Parsons, A. N., Robinson, C. H., and Wookey, P. A. (1997). Response of *Dryas octopetala* to ITEX manipulations: a synthesis with circumpolar comparisons. *Glob. Chang. Biol.* 3, 61–73. doi: 10.1111/j.1365-2486.1997.gcb143.x

White, T. J., Bruns, T., Lee, S., Taylor, J. W., Innis, M. A., Gelfand, D. H., et al. (1990). "Amplification and direct sequencing of fungal ribosomal RNA for phylogenetics" in *PCR protocols: A guide to methods and applications*. eds. M. A. Innis, D. H. Gelfand, J. J. Sninsky and T. J. White (San Diego: Academic Press), 315–321.

Wickham, H. (2016). *ggplot2: Elegant graphics for data analysis*. New York: Springer-Verlag.

Wookey, P. A. (2007). Climate change and biodiversity in the Arctic – Nordic perspectives. *Polar Res.* 26, 96–103. doi: 10.1111/j.1751-8369.2007.00035.x

Conflict of Interest: The authors declare that the research was conducted in the absence of any commercial or financial relationships that could be construed as a potential conflict of interest.

frontiers in Microbiology

ORIGINAL RESEARCH
published: 10 June 2021
doi: 10.3389/fmicb.2021.654135

Gullies and Moraines Are Islands of Biodiversity in an Arid, Mountain Landscape, Asgard Range, Antarctica

Adam J. Solon[1†], Claire Mastrangelo[2], Lara Vimercati[1], Pacifica Sommers[1], John L. Darcy[3], Eli M. S. Gendron[4], Dorota L. Porazinska[4] and S. K. Schmidt[1†]*

[1] Department of Ecology and Evolutionary Biology, University of Colorado, Boulder, Boulder, CO, United States, [2] School of Public Health, University of California, Berkeley, Berkeley, CA, United States, [3] Division of Biomedical Informatics and Personalized Medicine, University of Colorado-Anschutz Medical Campus, Denver, CO, United States, [4] Department of Entomology and Nematology, University of Florida, Gainesville, FL, United States

OPEN ACCESS

Edited by:
Laura Zucconi,
University of Tuscia, Italy

Reviewed by:
Charles K. Lee,
University of Waikato, New Zealand
Wei Li,
Lawrence Livermore National Laboratory, United States Department of Energy (DOE), United States
Giora Jehiel Kidron,
Hebrew University of Jerusalem, Israel

***Correspondence:**
S. K. Schmidt
steve.schmidt@colorado.edu

[†] These authors have contributed equally to this work

Specialty section:
This article was submitted to Extreme Microbiology, a section of the journal Frontiers in Microbiology

Received: 15 January 2021
Accepted: 04 May 2021
Published: 10 June 2021

Citation:
Solon AJ, Mastrangelo C, Vimercati L, Sommers P, Darcy JL, Gendron EMS, Porazinska DL and Schmidt SK (2021) Gullies and Moraines Are Islands of Biodiversity in an Arid, Mountain Landscape, Asgard Range, Antarctica. Front. Microbiol. 12:654135. doi: 10.3389/fmicb.2021.654135

Cold, dry, and nutrient-poor, the McMurdo Dry Valleys of Antarctica are among the most extreme terrestrial environments on Earth. Numerous studies have described microbial communities of low elevation soils and streams below glaciers, while less is known about microbial communities in higher elevation soils above glaciers. We characterized microbial life in four landscape features (habitats) of a mountain in Taylor Valley. These habitats varied significantly in soil moisture and include moist soils of a (1) lateral glacial moraine, (2) gully that terminates at the moraine, and very dry soils on (3) a southeastern slope and (4) dry sites near the gully. Using rRNA gene PCR amplicon sequencing of Bacteria and Archaea (16S SSU) and eukaryotes (18S SSU), we found that all habitat types harbored significantly different bacterial and eukaryotic communities and that these differences were most apparent when comparing habitats that had macroscopically visible soil crusts (gully and moraine) to habitats with no visible crusts (near gully and slope). These differences were driven by a relative predominance of Actinobacteria and a *Colpodella* sp. in non-crust habitats, and by phototrophic bacteria and eukaryotes (e.g., a moss) and predators (e.g., tardigrades) in habitats with biological soil crusts (gully and moraine). The gully and moraine also had significantly higher 16S and 18S ESV richness than the other two habitat types. We further found that many of the phototrophic bacteria and eukaryotes of the gully and moraine share high sequence identity with phototrophs from moist and wet areas elsewhere in the Dry Valleys and other cold desert ecosystems. These include a Moss (*Bryum* sp.), several algae (e.g., a *Chlorococcum* sp.) and cyanobacteria (e.g., *Nostoc* and *Phormidium* spp.). Overall, the results reported here broaden the diversity of habitat types that have been studied in the Dry Valleys of Antarctica and suggest future avenues of research to more definitively understand the biogeography and factors controlling microbial diversity in this unique ecosystem.

Keywords: cold deserts, gullies, microbial oases, extremophiles, biological soil crusts, *Bryum*, cryobiosphere

INTRODUCTION

In the cold, nutrient-poor, and hyper-arid McMurdo Dry Valleys (MDV) of Antarctica, water availability serves as a primary factor governing the persistence and distribution of life (Kennedy, 1993). Climate, generally understood as long-term records of air temperature and precipitation, determines water availability on a regional scale, whereas variations in terrain (e.g., slope, aspect, shade, and soil conditions) determine water availability on a local level. Evaluating how differences in mountain terrain (habitats) influence microbial community structure and diversity in the MDV will provide a better understanding of microbial biogeography and connectivity between mountain slopes and the glaciers, lakes, and soils in valleys below.

Within the MDV, there are three geomorphic zones that are determined by interactions between climate conditions and landforms. These zones are defined by summertime mean air temperature and relative humidity as well as prevailing winds and precipitation and include the coastal thaw zone (CTZ), the inland mixed zone (IMZ), and the stable upland zone (SUZ) (Fountain et al., 2014). These zones correspond with elevation above sea level and distance from the coast. For example, in Taylor Valley, the warmest and wettest zone, the CTZ, is found dozens of kilometers from the coast at low elevations and the colder and drier IMZ is found a few kilometers from the coast at higher elevations. The SUZ, the coldest and driest zone, occurs in the highest elevations and valleys farthest from the coast. In addition, the zones correspond with differences in geologic histories (Bockheim et al., 2008), parent material and stages of weathering (Hall et al., 2000; Bockheim, 2002), and soil chemistries (Bockheim, 1997). These four factors create physical environments distinct from one another that govern moisture availability (Campbell et al., 1998). Previous work at lower elevations in the MDV indicates water is a primary limiting factor for life (Gooseff et al., 2003; Lee et al., 2018) and there is evidence of a lower soil moisture limit for eukaryotic phototrophy (Fell et al., 2006). Soil water content is also the primary factor controlling other microbial functions (Barrett et al., 2006; Ball et al., 2009; Niederberger et al., 2019) and moss photosynthesis in the MDV (Pannewitz et al., 2005). On a broader scale soil moisture affects biological soil crust formation in other cold deserts (Costello et al., 2009; Solon et al., 2018), and even in hot deserts like the Negev Desert (Kidron and Benenson, 2014; Hagemann et al., 2017).

While numerous studies have described microbial communities of the CTZ (Van Horn et al., 2016; Feeser et al., 2018) and SUZ (Wood et al., 2008; Goordial et al., 2016), less is known of microbes in the intermediate elevation sites of the IMZ. Existing studies that include life from the IMZ focus exclusively on bacterial endoliths (Archer et al., 2017), soil yeasts (Connell et al., 2008), or micro-eukaryotes (Fell et al., 2006), or include a single terrain feature (Smith et al., 2006; Lee et al., 2012). One mountain chain within the Transantarctic, the Asgard Range, establishes the northern border of Taylor Valley and is representative of the IMZ in the valley. As part of a larger study of factors contributing to the assembly of microbial communities in cryoconite holes on Canada Glacier and other glaciers in Taylor Valley (cf. Sommers et al., 2019a,b,c), the four mountain habitats discussed in the present study were identified as possible sources of inoculum for the cryoconite holes found on Canada Glacier below.

To our knowledge no previous studies have sampled all domains of soil biota across a range of habitats found within one mountain landscape of the IMZ of Taylor Valley. We identified four habitats with different gravimetric soil moisture levels: moister soils of a (1) lateral glacial moraine (henceforth, moraine), (2) gully (gully), and drier soils of a (3) southeastern slope (slope) and (4) alongside the gully (near gully). Our study addresses the following questions: How different are microbial communities among these habitats? Do the habitats with higher soil moisture support more diverse communities? Are phototrophs of the IMZ also found in lower elevations of the MDV or other cold deserts? By incorporating the full spectrum of life found in each habitat (Bacteria, Archaea, and eukaryotes) as well as identifying habitat-specific community compositions and individual organisms most associated with those habitats, we used a natural experiment to explore how the variation of terrain within a geomorphic zone governs soil moisture and influences microbial community structure in the IMZ of the MDV and identified potential connections with microbial communities of cryoconite holes on the glaciers below.

MATERIALS AND METHODS

Site Description

The McMurdo Dry Valleys (MDV) are ∼4,800 km^2 of mostly ice-free expanse and are the largest ice-free area of Antarctica. Located in Southern Victoria Land between the East Antarctica Ice Sheet and the Ross Sea, this cold desert environment is the product of multiple physical factors, one of which is the presence of the Transantarctic Mountains which extend across most of the continent and divide the East and West Antarctica Ice Sheets. One of these ranges, the Asgard, separates Taylor Valley from Wright Valley to the north. Taylor Valley was first explored during the 1907 British Antarctic Expedition and in recent decades has seen an enhanced focus of scientific investigation since the establishment of the McMurdo Long-Term Ecological Research (LTER) site in 1993.

Of the three geomorphic zones in the MDV most studies in Taylor Valley take place in the lower elevation coastal thaw zone (CTZ), defined by mean summer air temperatures > −5°C and a wet-active layer of permafrost. However, the higher elevations in the valley, in the Asgard Mountains and Kukri Hills, which form the southern edge of Taylor Valley, exist in the inland mixed zone (IMZ). The IMZ is defined by an isotherm of mean summer air temperature between −5 and −10°C and a dry active layer (Fountain et al., 2014). For this study we selected a mountain in the Asgard Range that rises above the Lake Hoare field camp and Canada Glacier- 77°36′36.71″ S, 162°50′07.32″ E, 1,180 m a.s.l (**Figure 1**).

The first habitat is representative of most of the Asgard mountains and is located on the rocky, barren, southeastern slope, which we refer to as "slope." The second and third habitats

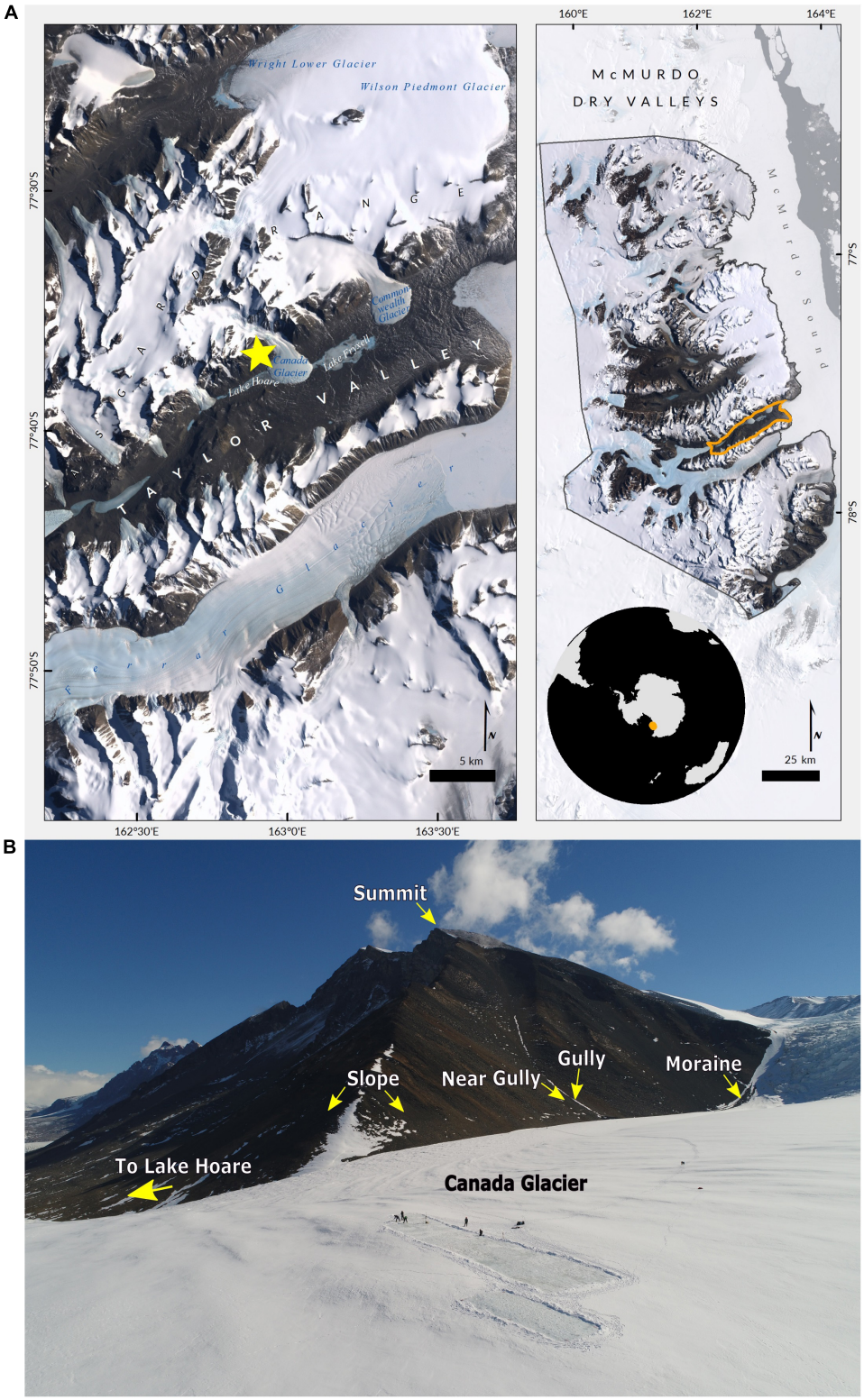

FIGURE 1 | Research site. **(A)** Satellite map of the McMurdo Dry Valleys (right) and Taylor Valley Valley (left). The yellow star identifies the location of the area sampled within the Asgard Range (images: Cathleen Torres Parisian, Polar Geospatial Center). **(B)** View from drone taken above Canada Glacier with arrows pointing to the habitats sampled in this study, and other key landmarks (photo: Brendan Hodge, UNAVCO).

are defined by inside and 10m outside of a gully that runs vertically down the mountain's east side, which we, respectively, call "gully" and "near gully." The fourth habitat is a lateral moraine that runs along the western edge of the glacier and eastern slope of the mountain, which we term "moraine." It is noteworthy that the gully runs perpendicular to the moraine and intersects it. Each habitat offered a different combination of terrain- slope, aspect, and other geologic and geographic features- but we were especially interested in the differences of gravimetric soil moisture that are present in this hyper-arid mountain landscape. While gravimetric soil moisture is limited to the amount of water at a single point in time, and not a full indicator of water availability, this metric has been used in previous studies of life in the dry valleys (Barrett et al., 2006; Ball et al., 2009; Niederberger et al., 2019). Additionally, biological soil crusts were seen in the gully and moraine and are referred to as crust habitats, whereas no soil crusts were observed in the near gully and slope and are referred to as non-crust habitats. Photos of habitats and additional sample information are included as supplemental materials (**Supplementary Material 1** and **Supplementary Table 1**).

Soil Collection

Mineral soils were collected over two field seasons using sterile technique with an ethanol-cleaned stainless-steel spoon from the top 0 to 4 cm of the surface and homogenized in individual, sterile Whirl-Pak® bags. The slope was sampled on 24 Dec 2016 in a lateral transect from 77° 36′ 35.6394″ S, 162° 55′ 29.892″ E (287 m a.s.l.) to 77° 36′ 43.272″ S, 162° 55′ 36.336″ E (256 m a.sl.) for a total of eight samples. The gully and near gully were sampled on 22 Jan 2018 along an elevational gradient from 77° 36′ 29.628″ S, 162° 54′ 22.2012″ E (424 m a.s.l) to 77° 36′ 26.6394″ S, 162° 54′ 48.8412″ E (358 m a.s.l). Samples were collected from both inside the gully, where green and black crusts were occasionally visible, and a corresponding sample 10 m outside the gully for a total twenty-one gully and nine near gully samples. The nine moraine samples were collected on 25 Jan 2018 along an elevational gradient from 77°36′13.50″ S, 162°54′14.26″ E (459 m a.s.l) to 77°36′18.86″ S, 162°54′33.57″ E (402 m a.s.l.) and featured occasional visible crusts. MDV environmental regulations were followed and influenced the locations and limited amounts of sampling. Soil temperatures were recorded in the gully and moraine from 26 November 2018 to 24 January 2019 with HOBO Pendant® Temperature/Light data loggers. Loggers were placed within a few mm of the surface along elevational gradients with 8 loggers in the gully and 4 loggers in the moraine.

Sample Processing, DNA Sequencing, and Bioinformatics

All soils were transported down the mountain and kept frozen in −20°C freezers located at Lake Hoare camp, then flown in coolers to the A.P. Crary Science and Engineering Center at McMurdo Station where they were kept at −70°C. At the end of each season, the samples were shipped at −20°C to Boulder, CO, United States and stored at −70°C until further processing took place. Gravimetric soil moisture was determined by weighing 3 g of soil (wet weight), drying at 100°C for 24 h, and re-weighing the mass again (dry weight). The difference between the two weights was then divided by the dry weight for soil moisture (%). Gravimetric soil moisture determines the water content of soil, although not the overall availability of it seasonally nor at the time of sampling, and has been used as a metric for soil microbial studies in the MDV (Barrett et al., 2006; Fell et al., 2006; Ball et al., 2009; Niederberger et al., 2019). Microinveterbrate counts were conducted following protocols outlined in Porazinska et al. (2018) but which included homogenizing and subsetting soil and storing at 4℃ before sieving and counting. DNA was extracted from 0.3 to 0.45 g/soil using a Qiagen PowerSoil DNA Extraction kits (Qiagen, Hilden, Germany) and the concentration of DNA was quantified with a Qubit fluorometer (Invitrogen Corp., CA, United States). Qubit values in ng/μL were back calculated into ng/g soil. DNA was then amplified in triplicates with Earth Microbiome Project primers for the 16S SSU rRNA gene (515f-806r) and 18S SSU rRNA gene (1391f-EukBr), amplified triplicates pooled and normalized to equimolar concentrations with a SequalPrep Normalization Plate Kit (Invitrogen Corp., CA, United States). Pooled samples were then sequenced at University of Colorado-Boulder BioFrontiers Sequencing Facility on an Illumina MiSeq 2 × 250 bp for 16S SSU amplicons and 2 × 150 bp for 18S SSU amplicons. Raw sequence reads are stored in the NCBI SRA database under BioProject accession number PRJNA721735. All bioinformatics were conducted with either PYTHON (version 2.7) or R (version 3.6.1) programming languages in R Studio (version 1.2.1335). Additional labels and image grouping for figures were conducted in Inkscape[1]. Samples were processed with a template developed by Angela Oliveira and Hannah Holland-Moritz[2] which was modified from the DADA2 tutorial pipeline[3]. This template provides a pipeline where reads are demultiplexed and primers are removed (idemp; cutadapt, version 1.18) (Martin, 2011). Following DADA2 protocols any sequences with an "N," that is undetermined base pairs, were filtered out. Using a graph produced in the DADA2 pipeline of the frequency of each quality score at each base position sequence lengths were trimmed when the average PHRED score dropped below 30. Error rate learning for DADA2 was set to the default minimum number of total bases to use for error rate learning at 1e8. After trimming and filtering exact sequence variants (ESVs) were inferred, forward and reverse reads paired, chimeras removed, and taxonomy assigned ("dada2" package, version 1.6.0; "plotly" package, version 4.9.0). Taxonomy was provided by the SILVA SSU 132 database for both 16S and 18S reads (Quast et al., 2013). For richness estimation samples were pooled before ESVs were inferred. Further processing with "phyloseq" R package (McMurdie and Holmes, 2013) included subsetting data for study-specific samples, removing erroneous domain assignments (e.g., eukaryotes in 16S data) and contamination (e.g., human DNA). Chloroplasts and mitochondria were also removed from the 16S. Finally, samples with very low read counts

[1]https://inkscape.org/

[2]https://github.com/fiererlab/dada2_fiererlab

[3]http://benjjneb.github.io/dada2/tutorial.html

(<1,000) were filtered from the data set ("phyloseq" package, version 1.32.0). The 16S SSU dataset started with 725615 reads and the 18S SSU dataset 502052 reads. After processing the 16S contained 663595 filtered reads and 4340 ESVs across 44 samples and the 18S dataset 499200 filtered reads and 527 ESVs across 32 samples. For richness estimation, the pooled datasets contained 766311 16S reads and 475343 18S reads. After processing the 16S dataset yielded 699606 reads and 4327 ESVs across 44 samples and the 18S dataset 472888 reads and 521 ESVs across 32 samples.

Beta Diversity

The use of DNA-seq data for abundance-related analyses is limited to relative abundances and necessitates data transformations for compositional analyses (Gloor and Reid, 2016; Gloor et al., 2017). To determine differences between communities we transformed the data into Aitchison distances with, first, a zero-replacement function ("zCompositions" package, version 1.3.3–1), and second, center-log ratio (clr) transformation ("compositions" package, version 1.40–3) (Gloor and Reid, 2016). Principal Components Analysis (PCA) ordinations were created ("CoDaSeq" package, version 0.99.6, "ggplot2" package). PERMANOVA was used to test differences among communities by habitat based on centroids of their Aitchison distances. To determine which organisms were most responsible for the differences in the crust and non-crust communities we used the "ALDEx2" package (version 1.20.0). ALDEx2 determines which ESVs are most differentially relatively abundant between two groups by using median center-log ratio values (Fernandes et al., 2013, 2014). We assigned groups based on the presence or absence of crusts in the habitat type. The gully and moraine had crusts and the near gully, and slope did not have crusts. This yielded positive values indicating greater association with the crust communities and negative values more associated with non-crust communities. Additionally, an effect size for each ESV was computed as the difference between two groups divided by the dispersion within each respective group, and significance values were determined with Benjamini-Hochberg corrected *P*-values of Wilcoxon tests. We only report those ESVs that had effect sizes greater than 1, or less than −1, and $p < 0.05$.

Alpha Diversity

For a quantitative estimate of ESV richness we used the "breakaway" package (version 4.7.2) to generate estimates with "breakaway" (Willis and Bunge, 2015) and conduct null hypothesis significance testing with "betta" (Willis et al., 2017). Two sample outliers from the 16S dataset (GB7 and SL5) were removed as those samples provided estimate ranges with negative numbers of ESVs which is not biologically possible (**Supplementary Material 2**). To assess dominant organisms in each habitat, we produced boxplots with the top 10 average ESVs (median) of each habitat using untransformed relative abundances.

RESULTS

Site Characteristics

The most obvious macro-scale differences between the sites we sampled are that the gulley and moraine are areas that accumulate wind-blown snowpack due to local topography (**Figure 1B** and see **Supplementary Figures 1**, **3**, **4**). It is likely that the residual water from this snowpack accumulation accounted for the significantly higher soil moisture levels observed in those two habitats at the time of sampling (Dunn Test: $p < 0.02$) (**Table 1** and **Figure 2**). Likewise, levels of estimated biomass (DNA concentration) and direct microscopic counts of tardigrades and rotifers (but not nematodes) were generally higher in the gulley and on the moraine compared to the drier sites sampled nearby (**Table 2**).

Communities

PCA and PERMANOVA analyses showed significant clustering of communities by habitat type for both 16S and 18S communities (**Figure 3**). The communities in the habitats that contain spatially irregular biological soil crusts (gully and moraine) separated along the *x*-axis from communities that had no visible soil crusts (near gully and slope). These separations were significant for both the 16S (PERMANOVA: $R^2 = 0.28$, $p = 0.001$) and 18S ($R^2 = 0.29$, $p = 0.001$) communities, with *post hoc* pairwise tests confirming significant differences between every habitat pairing (Pairwise PERMANOVA, FDR-adjusted: 16S $p = 0.001$, 18S $p < 0.006$).

Differential relative abundance of ESVs (Fernandes et al., 2014) differed significantly between crust and non-crust communities for both 16S and 18S (**Figure 4**) (Wilcoxon, BH-adjusted: 16S $p < 0.0001$, 18S $p < 0.01$). For the 16S communities, most of the ESVs with greater differential abundance in the non-crust communities were Actinobacteria (7 out of 10 phylotypes),

TABLE 1 | Environmental data by habitat.

Habitat	Elevation[a]	Aspect	Snowbank formation[b]	Soil moisture[c]	Soil temperature[d]
Moraine	407–457	South	Yes	4.18–15.99	Nov (−8.58, 16.5) Dec (−3.85, 17.1) Jan (−2.24, 17.4)
Gully	320–441	East	Yes	1.10–10.96	Nov (−7.66, 27.0) Dec (−4.19, 29.5) Jan (−4.02, 28.6)
Near gully	320–441	East	No	0.00–2.59	n/a
Slope	256–287	East/South	No	0.00–1.62	n/a

[a] *Meters above sea level.*
[b] *Does snowbank accumulation occur over the summer?*
[c] *Gravimetric soil moisture (%) values across samples.*
[d] *Mean minimum and maximum temperatures in degrees Celsius (Nov = Nov 26–30, Dec = Dec 1–31, Jan = Jan 1–24).*

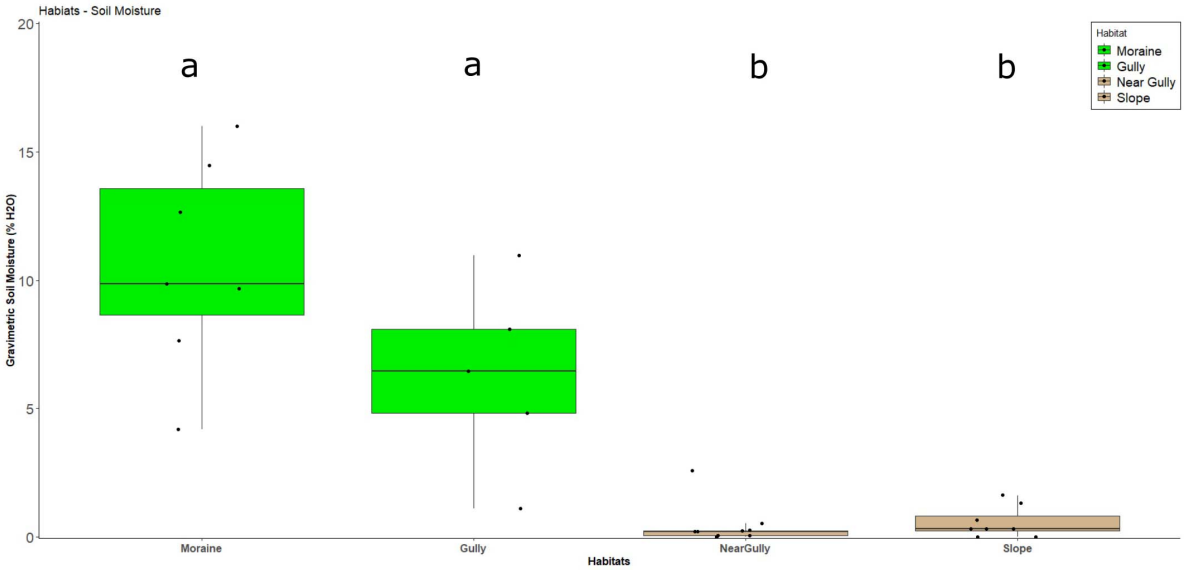

FIGURE 2 | Soil moisture boxplots of gravimetric soil moisture by habitat. Green identifies habitats with crusts. Non-crust habitats are in tan. Each dot is a single sample, the box represents the 25–75% quartile values, and the dark line in the box represents median values of soil moisture. Lower-case letters indicate the presence of statistical difference among habitats as determined by pairwise Dunn tests.

TABLE 2 | Abundance data by habitat.

Habitat	Biocrust	Biomass[a]	Rotifers[b]	Tardigrades[c]	Nematodes[d]
Moraine	Yes	928–14,200	0–7	3–123	0–364
Gully	Yes	3690–400,000+	0–2	8–55	0–10
Near gully	No	1,370–3,060	0–1	0	7–44
Slope	No	103–1,690	n/a	n/a	n/a

[a]*Biomass in ng DNA/g of soil (Qubit Fluorometer).*
[b]*Number of Rotifers, alive or dead, standardized to 20 g dry weight soil.*
[c]*Number of Tardigrades, alive or dead, standardized to 20 g dry weight soil.*
[d]*Number of Nematodes, alive or dead, standardized to 20 g dry weight soil.*

while the crust communities contained a wider diversity of phylotypes, including only 1 Actinobacteria ESV and notably 3 cyanobacteria ESVs among them (**Figure 4A**). The 18S analysis revealed the non-crust communities featured only a single member with higher differential abundance, an Alveolata (*Colpodella* sp.), while the crust communities had many more differentially abundant taxa including a moss (*Bryum* sp.) and higher order predators including a tardigrade, a nematode (*Plectus* sp.), and a rotifer (*Adineta* sp.) (**Figure 4B**).

Richness estimates revealed higher levels of richness in the habitats with prominent soil crusts (gully and moraine) than in the habitats without soil crusts (near gully and slope) for both 16S ($p < 0.003$) and 18S ($p < 0.001$) communities (**Figure 5**). Also, among the non-crust habitats the near gully had significantly greater richness than the slope for both 16S ($p < 0.001$) and 18S ($p < 0.001$) communities.

Organisms

The differences between crust and non-crust microbial communities were even more evident when we examined the predominant organisms across habitat types. The relative abundances of the top 10 16S ESVs indicated that 16S crust communities were dominated by phototrophic Bacteria, whereas the nearby drier habitats had no phototrophs among the top-10 phylotypes (**Figure 6**). The Cyanobacteria in crust habitats included ESVs that most closely matched *Nostoc*, *Phormidium*, *Tychonema,* and *Phormidesmis*. In contrast, although eukaryotic phototrophs were present in the top 10 ESVs in all habitats, they were less abundant in the drier habitats (**Figure 7**). The most abundant 18S ESV in crust habitats was a moss (*Bryum* sp.) that shares 100% sequence identity with a moss previously described from the Dry Valleys (Seppelt et al., 2010). In addition, two genera of green algae from the class Chlorophyceae were also present (*Chlorococcum* in the gully and moraine, and *Paulschulzia* in the gully).

DISCUSSION

How Different Are Microbial Communities Among Habitats?

We characterized microbial communities from mineral soils of four landscape features (habitats) and found that all habitats supported significantly different microbial communities (16S, $p = 0.001$; 18S, $p < 0.006$), although there was a notable separation between moist habitats with biological soil crusts (gully and moraine) and dry habitats with no crusts (near gully and slope) (**Figure 3**). These findings highlight the extent of environmental heterogeneity across this mountain landscape. These habitats were only a few hundred meters apart sharing similar elevations, parent material, geologic history, and climate (Bockheim, 2002; Fountain et al., 2014) and yet differences in habitat influenced

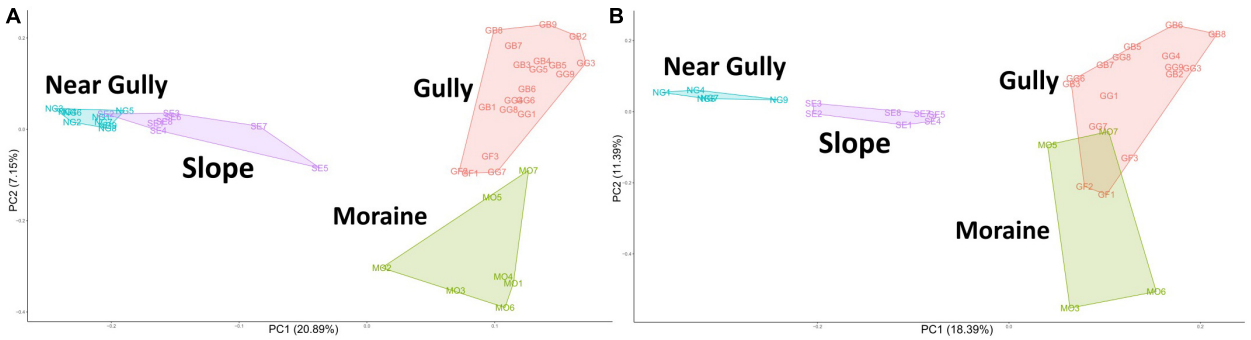

FIGURE 3 | Principal components analysis (PCA) plot of Aitchison distances with polygons capturing all samples from within a habitat. **(A)** 16S, **(B)** 18S. Pairwise PERMANOVA significance test revealed the centroid of each habitat as significantly different from all other habitats for both the bacterial and eukaryotic communities (16S $p = 0.001$; 18S $p < 0.006$).

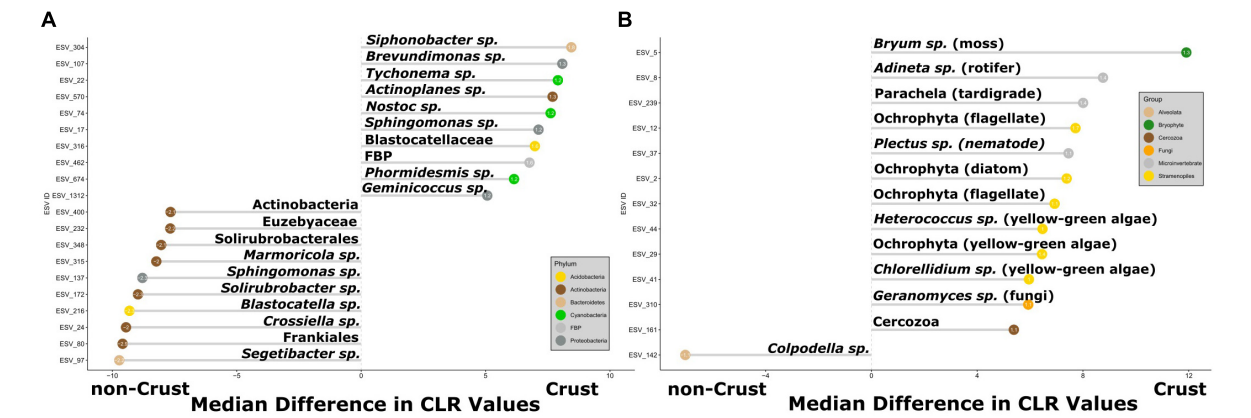

FIGURE 4 | Organisms with the greatest differential relative abundances between samples from crust communities and those from non-crust communities **(A)** 16S, and **(B)** 18S. The *x*-axis displays the difference in median center-log ratio (CLR) transformed abundances and only ESVs with effect sizes > 1 or < –1 and *p*-values < 0.05 are displayed. The value inside the dot is the effect size. The positive values indicate ESVs in crusts and negative values indicate ESVs in non-crusts. Each ESV is labeled with the lowest taxonomic assignment from the SILVA 132 or NCBI GenBank databases. The colored dots refer to bacterial phyla or higher-level taxonomic grouping for Eukaryotes.

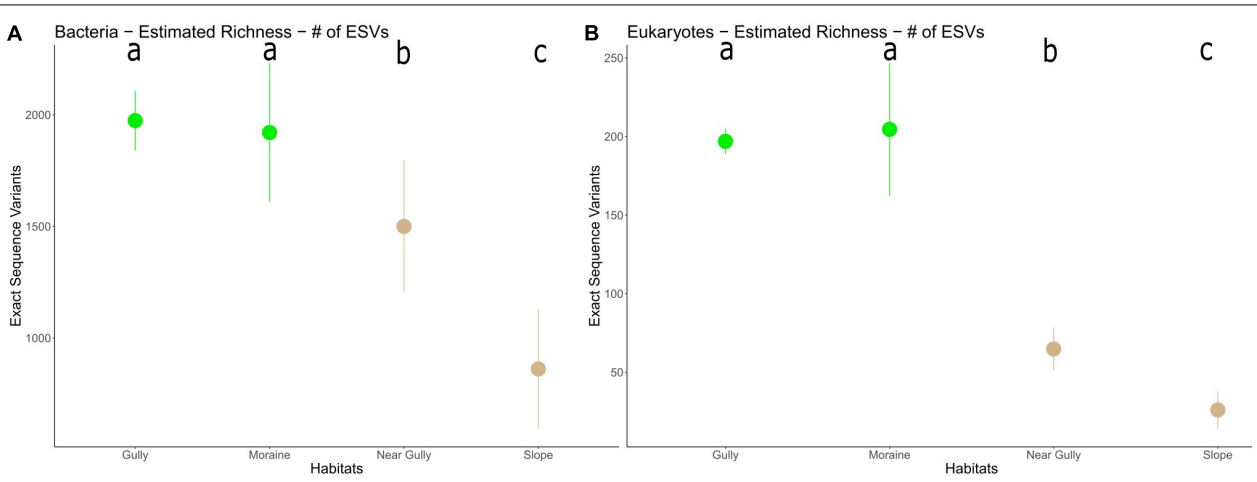

FIGURE 5 | Microbial ESV richness in each habitat **(A)** 16S and **(B)** 18S. The dots represent the mean richness in each habitat with error bars indicating 95% CI. Lower case letters indicate significant differences among habitats ($p < 0.003$).

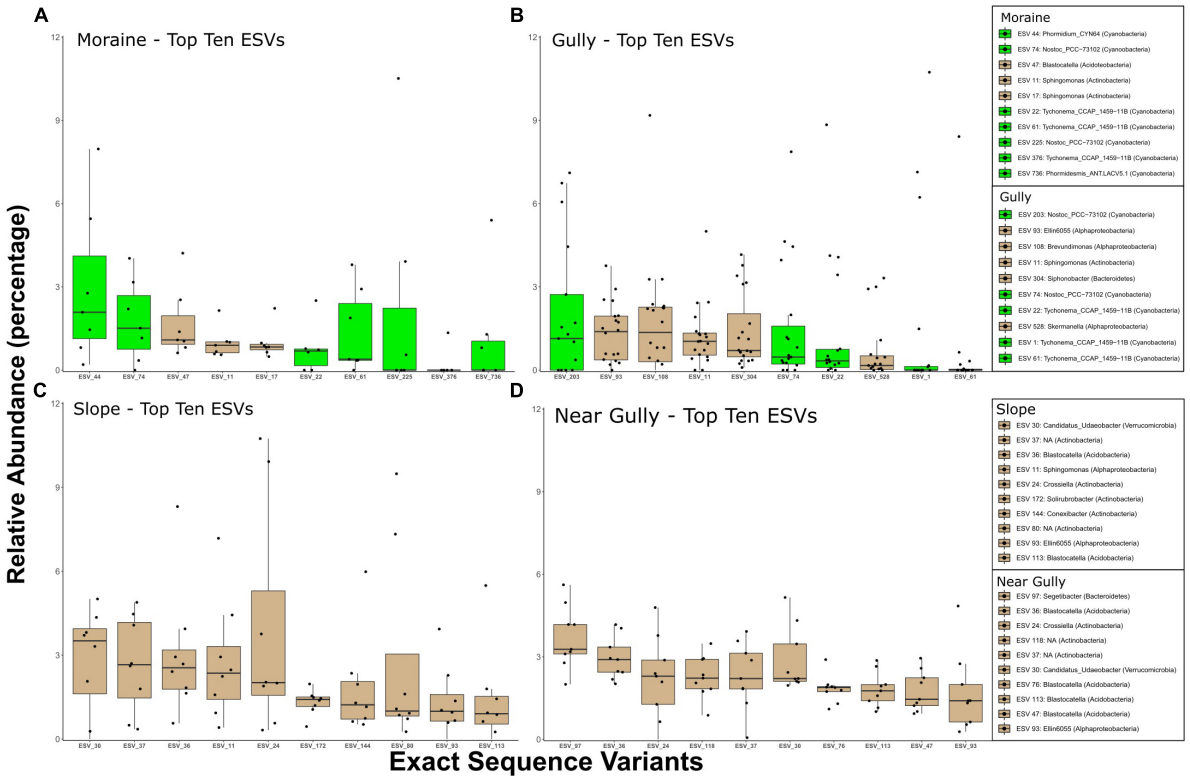

FIGURE 6 | Top 10 16S ESVs from each habitat. **(A)** moraine, **(B)** gully, **(C)** slope, and **(D)** near gully. Boxplots are ordered by the median relative abundance of untransformed DNA-seq data and colored according to inferred energy-carbon acquisition-photoautotrophs (green) and chemoheterotrophs (tan).

not only differences in soil moisture but more importantly for this study, the presence or absence of biological soil crusts. Similar findings have been noted in ice-free desert soils of the Larsemann Hills and Bunger Hills regions of the continent, were physiochemical factors (moisture and organic matter) and the presence of crusts/mats (e.g., phototrophs) influenced bacterial community structure (Kudinova et al., 2020).

Given that crust vs. non-crust communities significantly separated on the main PCA axis (**Figure 3**), we carried out a differential relative abundance analysis (Fernandes et al., 2014) to examine which organisms contributed the most to this separation. For Bacteria, a wide variety of Actinobacteria drove the separation of the non-crust, drier communities, whereas a mix of major bacterial groups (e.g., Cyanobacteria and Proteobacteria) drove the separation of the crust communities (**Figure 4A**). These findings agree with previous studies in Taylor Valley in that elevated soil moisture corresponds with higher abundance of Cyanobacteria and reduced soil moisture corresponds with higher abundance of Actinobacteria (Niederberger et al., 2015; Lee et al., 2018; Rego et al., 2019), although Buelow et al. (2016) found a different pattern. A similar general pattern was also observed elsewhere on the continent at high elevations in the Sør Rondane Mountains of Queen Maud Land (Tytgat et al., 2016). Likewise, higher soil moisture was correlated with higher rates of CO_2 and N_2 fixation in *Nostoc*-associated microbial mats in Miers Valley (Sohm et al., 2020). Also, the preponderance of Actinobacteria and the lack of Cyanobacteria in other cold-dry ecosystems outside of Antarctica is well known (e.g., An et al., 2013; Gupta et al., 2015). For example, at extreme high elevation (>6,000 m) sites in the Atacama Desert, Actinobacteria are dominant, and Cyanobacteria are undetectable except near sources of water (Costello et al., 2009; Solon et al., 2018).

The eukaryotic taxa contributing to the separation of crust and non-crust communities were taxa associated with the crust habitats including a common moss (a *Bryum* species), a few Xanthophyceae (e.g., *Heterococcus* sp. and *Chlorellidium* sp.), a variety of other potentially photosynthetic Ochrophyta, a diversity of predators (nematodes, rotifers, and tardigrades), and a fungus (*Geranomyces* sp.) (**Figure 4B**). The Ochrophyta, a phylum of Stramenopiles, which include the class Xanthophyceae (yellow-green algae), represent an exceptionally diverse group of protists with both photosynthetic and non-photosynthetic members (Cavalier-Smith and Chao, 2006; Yang et al., 2012). Much is still to be learned about this clade and the results herein suggest they are worthy of more intensive investigation in the MDV. The nematode *Plectus* and the rotifer *Adineta* are commonly found in wetter areas of the MDV which includes areas with crusts (Porazinska et al., 2002; Fontaneto et al., 2015). Consistent with the relative abundance analyses, our microinvertebrate count data (**Table 2**) revealed higher abundances of rotifers and *Plectus* in the moist gully and

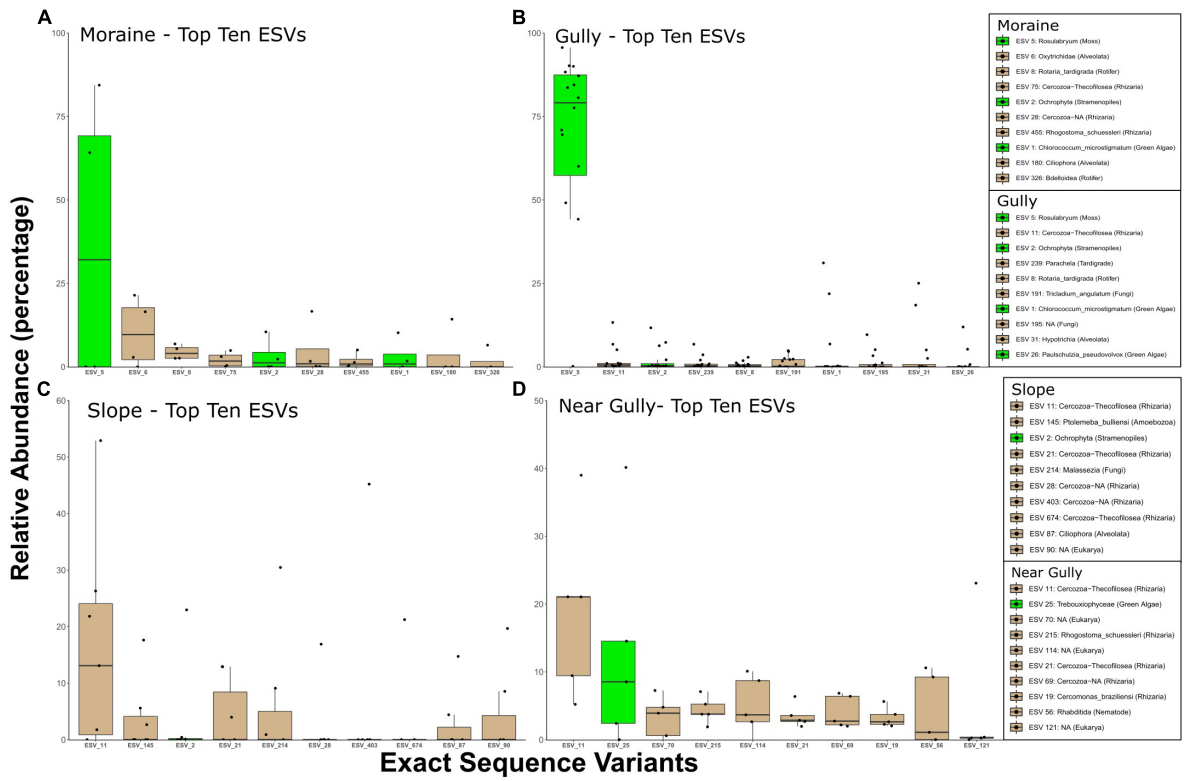

FIGURE 7 | Top 10 18S ESVs from each habitat **(A)** moraine, **(B)** gully, **(C)** slope, and **(D)** near gully. Boxplots are ordered by the median relative abundance of untransformed DNA-seq data and colored according to inferred energy-carbon acquisition- photoautotrophs (green) and chemoheterotrophs (tan).

moraine while *Scottnema* was the most abundant nematode in the dry near gully (**Table 2** and **Supplementary Table 1**). Additionally, no tardigrades were observed in the dry near gully while being present in each gully and moraine sample (**Table 2**). In contrast, only one phylotype, a *Colpodella* sp., showed significant differential relative abundance in the non-crust community (**Figure 4B**). *Colpodella* species have been previously identified in Taylor Valley soils with moderately low moisture levels of 3.1–4.9% (Fell et al., 2006) and are known as generalist predators of algae, ciliates and other protozoa (Olmo et al., 2011; Heidelberg et al., 2013; Sam-Yellowe et al., 2019). It may be that their generalist lifestyle allows them to be intermittently active during rare periods of higher soil moisture, utilizing any form of available prey.

Do Habitats With Higher Soil Moisture Support More Diverse Communities?

Higher richness was found in the moister crust habitats (gully and moraine) than the drier non-crust habitats (near gully and slope) for both 16S ($p < 0.003$) and 18S ($p < 0.001$) (**Figure 5**). However, between the dry non-crust habitats, the near gully had significantly greater richness than the slope for both 16S ($p < 0.001$) and 18S ($p < 0.001$). The influence of soil moisture on microbial richness in the MDV varies depending on the valley and habitat type. For example, no correlation between sediment water content and bacterial richness was found in Wright Valley along moisture gradients perpendicular to the Onyx River (Zeglin et al., 2011). However, a correlation between community composition and sediment water content was present. Conductivity (as a proxy for salinity) was suggested as the primary factor controlling richness in those sediments. Higher salinity in Pearce Valley soils also seemed to play a role in microbial richness but not on community composition (Chan-Yam et al., 2019). In Miers Valley soils, both effects were observed with bacterial richness positively correlated with soil water content and negatively correlated with soil conductivity (Bottos et al., 2020).

Are Phototrophs of the IMZ Also Found in Lower Elevations of the MDV or Other Cold Deserts?

Perhaps the most important finding of this study in terms of organismic diversity is the identity of both bacterial and eukaryotic phototrophs. In this regard we wanted to know if these phototrophs are endemic to the IMZ or if they are similar to phylotypes found elsewhere in Taylor Valley and other cold deserts. The most conspicuous phototroph was a moss that dominated (in relative abundance) the crusts of the gully (79% of sequences) and the moraine (32%) but not the non-crust communities (**Figure 7**). This moss also had the greatest difference in relative abundance for all eukaryotes between crust

and non-crust communities (**Figure 4B**). The identity of the moss was the same in both the gully and moraine habitats (ESV 5). The 100% match of the moss to a putative *Bryum* species (NCBI acc # KT343959) from Botany Bay on the nearby coast (Seppelt et al., 2010), and to an environmental sequence (acc # HM490232) from hypolithic communities in the Miers Valley (Khan et al., 2011) suggests it is likely not endemic to the IMZ but may be endemic to Antarctica. Although it is not possible to determine the exact species identity of this moss using only short-read 18S sequences, this finding points to future work using a variety of genes to examine the biogeography of this and related mosses in Antarctica and across the cryobiosphere.

Like the moss, other abundant eukaryotic phototrophs in the crust communities also showed high 18S sequences similarity to previously studied phototrophs in Antarctica and other cold ecosystems. For example, an abundant phylotype in the gully and moraine (ESV 1) is a *Chlorococcum* sp. (formerly *Pleurastrum*, Kawasaki et al., 2015) that shares 100% identity with isolates from several sites in Antarctica (De Wever et al., 2009), including two isolates (acc# FJ946903, FJ946905) from Lake Fryxell and an isolate (acc# FJ946902) from Ace Lake (over 2,500 km from the Dry Valleys). At an even broader geographic scale, it shares over 99% identity with many environmental sequences from peri-glacial sediments in the high Himalayas (e.g., HQ188976, Schmidt et al., 2011) and from the debris-covered Toklat Glacier in central Alaska (e.g., KM870774, Schmidt and Darcy, 2015) indicating that this group (formerly the "CP-clade") has broad geographical distribution in the cryosphere as discussed previously by Schmidt et al. (2011) and Sommers et al. (2019a). Given that phylotypes in this group have been isolated from Antarctic lakes, cryoconite holes, and peri-glacial soils throughout the world, it is currently unclear if they are functional components of the terrestrial sites in the Dry Valleys, or if they are dormant organisms deposited there from nearby lakes such as Lake Fryxell. Given that they are more abundant in wetter sites in the present study and that they dominate soils that are not near lakes in the Himalayas and Alaska, it is likely that they are functioning components of soil crust communities in the Dry Valleys, but much more work is needed on these abundant soil algae.

Despite differences in relative abundance of eukaryotic phototrophs between crust and non-crust habitats, it is important to note that phototrophic phylotypes were among the top 10 18S phylotypes in all habitats. For example, the dry near gully had a relatively abundant phylotype (ESV 25) in the Trebouxiophyceae (**Figure 7**) which was 100% identical to sequences (e.g., acc.# LC487925) of lithic crustose lichen photobionts in Queen Maud Land, Antarctica and other locations (Sweden, acc.# MH807084 and Germany, acc. # MH807084). Though lichen diversity in Taylor Valley is comparable to other ice-free areas of the Ross Sea region (Colesie et al., 2014); they exist in a narrow zone with regards to snow accumulation. Too much or too little snow and they are not able to survive (Green et al., 2012) and are generally found only in higher elevations of the IMZ. The dry slope also had a potential phototroph (ESV 2) in its top 10, a diatom of the Ochrophyta phylum of Stramenopiles that are incredibly diverse (Raven and Giordano, 2017; Varela et al., 2017), including some non-photosynthetic species (Kamikawa et al., 2017).

In contrast to the eukaryotic phototrophs, bacterial phototrophs were more restricted to the wetter crust habitats (**Figure 6**) similar to patterns observed in soils near MDV lakes, ponds, and streams (Zeglin et al., 2009; Niederberger et al., 2015; Van Horn et al., 2016). *Nostoc* phylotypes were the most and second most abundant ESVs in the gully and moraine habitats, respectively (**Figure 6**) agreeing with previous studies showing that Nostocales are found almost exclusively in moister soils of the Taylor Valley (Buelow et al., 2016) where they are likely important nitrogen fixers (Coyne et al., 2020). The most abundant phylotype in the gully (ESV_203) was a 100% match across our relatively short reads (253 bp) to several *Nostoc* sequences, including one (accession # MN243125, Jung et al., 2019) from a biological soil crust in the high Arctic (Ny-Alesund, Spitsbergen). Longer sequence reads and a more polyphasic approach would be needed to assess the biogeography of these and other phototrophs discussed here, but these results have revealed interesting organisms for future in-depth study. Likewise, the most abundant phylotype on the moraine (ESV_44) was a *Phormidium* with a 100% match for many sequences from mats of Lake Fryxell down valley from our study sites (e.g., AY151763, Taton et al., 2003), and a 99.2% match to sequences from a high-elevation site in the Himalayas (e.g., HQ188993, Schmidt et al., 2011). Also, in the top 10 phylotypes of the moraine was a strain of *Phormidesmis* sp. (ESV 736), a genus known to be associated with glacial environments and microbial mats near both poles (Raabova et al., 2019). Given its ability to produce exopolysaccharides (EPS), it is well suited for living under polar conditions (Christmas et al., 2016).

As mentioned above, the drier, non-crust sites of the near gully and slope were mostly dominated by members of the Actinobacteria and Acidobacteria (**Figure 6**). Actinobacteria are common in dry soils in the MDV regardless of geomorphic zone (Pointing et al., 2009; Lee et al., 2012; Van Goethem et al., 2016) and are ubiquitous in cold deserts across the Earth (An et al., 2013; Gupta et al., 2015). The most abundant actinobacterium belonged to the genus *Crossiella* that has been identified in Saharan dust in the Alps and may be snowpack colonizers (Chuvochina et al., 2011). While Actino- and Acidobacteria generally dominated the dry soils, the most abundant bacterium in the near gully was *Segetibacter* sp., a member of the Bacteroidetes. *Segetibacter* spp. have been found in soils elsewhere on the continent (Kudinova et al., 2020) and in high elevations throughout the world (Solon et al., 2018; Vimercati et al., 2019a; Aszalós et al., 2020) and are found in snowpack (Maccario et al., 2019).

Among the most abundant Acidobacteria in both the near gully and slope was *Blastocatella* spp. One of the more abundant *Blastocatella* phylotypes (ESV 47), however, was also present in moist soils of the moraine. Phylotypes similar to *Blastocatella* were previously reported from other high elevation ecosystems, including lake sediments from Ojos Del Salado in the Andes (acc.# LN929609, Aszalós et al., 2020).

The most cosmopolitan genus across all four habitats was *Sphingomonas* (Alphaproteobacteria). Previous studies in the

MDV have also uncovered *Sphingomonas* species in a variety of habitats ranging from the mats and moats of lakes (Brambilla et al., 2001; Van Trappen et al., 2002) to lithic environments (Gunnigle et al., 2015). A strain of *Sphingomonas sediminicola* collected from tundra soil on Svalbard in the Arctic circle (acc.# MH929654) provided the closest match (100%) to sequences of *Sphingomonas* species in our soils. The genus is known for being cosmopolitan and its EPS production and biodegradative abilities make it ecologically versatile (Baraniecki et al., 2002; Asaf et al., 2020) perhaps explaining its widespread occurrence in our study.

Broader Relevance of This Study

The initial impetus for this study was to explore the mountain slopes above Canada Glacier for possible sources of inoculum for cryoconite holes on Canada Glacier and other glaciers in the MDV. Many of the more abundant cyanobacterial genera found in the crust communities (e.g., *Nostoc*, *Phormidium, Phormidesmis*) were also found to be abundant in cryoconite holes on glaciers of Taylor Valley (Porazinska et al., 2004; Sommers et al., 2019a). Likewise, *Chlorococcum* sp., the most abundant algal phylotype in crusts was also the most common alga in cryoconite holes of the valley (Sommers et al., 2019a). This link is also seen with heterotrophic bacterial genera common in our soils (e.g., *Sphingomonas*, *Blastocatella*) that were also found in high relative abundance in cryoconite holes across Taylor Valley (Sommers et al., 2020). Although an in-depth analysis of the comparisons between terrestrial mountain habitats and cryoconite hole sediments is beyond the scope of this paper, more investigation into whether high-elevation soils are the main source of inoculum for cryoconite holes is warranted.

CONCLUSION

The data presented here indicate the gully and moraine habitats are acting as islands of biodiversity in this dry, windswept environment. Both habitats accumulate excess snow compared to the surrounding landscape (see **Supplementary Figures 1, 3, 4**) and had higher soil water content (**Figure 2**). Positive effects of increased snow accumulation on soil water content and microinvertebrate population size has been documented in lower elevations of the MDV (Gooseff et al., 2003; Ayres et al., 2010) and studies of other cold, dry environments show topographic features that promote snow accumulation (i.e., depressions and ridgelines) serve as hotspots of microbial diversity and functioning across otherwise barren high-elevation landscapes (e.g., Costello et al., 2009; Solon et al., 2018; Vimercati et al., 2019b). A similar effect is also seen in hot deserts where increased water accumulation strongly influences microbial and crust diversity (Kidron et al., 2000; Kidron and Benenson, 2014; Hagemann et al., 2017). However, to our knowledge there has been no previous work examining the microbial diversity of gullies in the MDV despite recent attention focused on these landscape features by geomorphologists (Dickson and Head, 2009; Levy et al., 2009; Dickson et al., 2019). Likewise, lateral and medial moraines have received very little attention as possible oases for life (Mapelli et al., 2011; Darcy et al., 2017) or as sources of cryoconite (Franzetti et al., 2017), but the present study indicates that they may be important hotspots of microbial diversity and activity in glacial and periglacial environments. Obviously, much more work is needed to fully understand how topographic features lead to enhanced microbial activity and functioning across extreme high-elevation landscapes.

DATA AVAILABILITY STATEMENT

The data presented in the study are deposited in the NCBI BioProject database under accession number PRJNA721735. The data is publicly available at the following link: https://www.ncbi.nlm.nih.gov/bioproject/721735.

AUTHOR CONTRIBUTIONS

SS acquired funding for the study. AS, PS, LV, JD, DP, and SS contributed to the design of the study and conducted the field sampling. DP processed and counted the microinvertebrates. EG, LV, and CM processed samples for sequencing and gravimetric soil moisture. AS, CM, and EG performed data analysis. AS wrote the first draft of the manuscript. SS wrote sections of the manuscript. AS and SS contributed equally to the final manuscript. All authors contributed to manuscript revision and approved the submitted version.

FUNDING

This research was funded by the National Science Foundation (grant no. 1443578). Publication of this article was funded by the University of Colorado Boulder Libraries Open Access Fund.

ACKNOWLEDGMENTS

We thank the United States Antarctic Program for logistical, field, and lab support during our time in Antarctica, Brendan Hodge and Thomas Nylen for UNAVCO drone support and soil sampling, Cathleen Torres Parisian and the Polar Geospatial Center for creation of the map in figure one, Jessica Henley and Noah Fierer's laboratory for rRNA gene amplification and library preparation, and the University of Colorado BioFrontiers Next-Gen Sequencing Core Facility for Ilumina MiSeq sequencing. We also appreciate the helpful comments of the three reviewers. Additionally, we thank the University of Colorado Boulder Libraries Open Access Fund for funding this publication.

SUPPLEMENTARY MATERIAL

The Supplementary Material for this article can be found online at: https://www.frontiersin.org/articles/10.3389/fmicb.2021.654135/full#supplementary-material

REFERENCES

An, S., Couteau, C., Luo, F., Neveu, J., and DuBow, M. S. (2013). Bacterial diversity of surface sand samples from the Gobi and Taklamaken deserts. *Microb. Ecol.* 66, 850–860. doi: 10.1007/s00248-013-0276-2

Archer, S. D., de los Ríos, A., Lee, K. C., Niederberger, T. S., Cary, S. C., Coyne, K. J., et al. (2017). Endolithic microbial diversity in sandstone and granite from the McMurdo dry valleys, Antarctica. *Polar Biol.* 40, 997–1006. doi: 10.1007/s00300-016-2024-9

Asaf, S., Numan, M., Khan, A. L., and Al-Harrasi, A. (2020). *Sphingomonas*: from diversity and genomics to functional role in environmental remediation and plant growth. *Crit. Rev. Biotechnol.* 40, 138–152. doi: 10.1080/07388551.2019.1709793

Aszalós, J. M., Szabó, A., Megyes, M., Anda, D., Nagy, B., and Borsodi, A. K. (2020). Bacterial diversity of a high-altitude permafrost thaw pond located on Ojos del Salado (Dry Andes, Altiplano-Atacama region). *Astrobiology* 20, 754–765. doi: 10.1089/ast.2018.2012

Ayres, E., Nkem, J. N., Wall, D. H., Adams, B. J., Barrett, J. E., Simmons, B. L., et al. (2010). Experimentally increased snow accumulation alters soil moisture and animal community structure in a polar desert. *Polar Biol.* 33, 897–907. doi: 10.1007/s00300-010-0766-3

Ball, B. A., Virginia, R. A., Barrett, J. E., Parsons, A. N., and Wall, D. H. (2009). Interactions between physical and biotic factors influence CO2 flux in Antarctic dry valley soils. *Soil Biol. Biochem.* 41, 1510–1517. doi: 10.1016/j.soilbio.2009.04.011

Baraniecki, C. A., Aislabie, J., and Foght, J. M. (2002). Characterization of *Sphingomonas* sp. Ant 17, an aromatic hydrocarbon-degrading bacterium isolated from Antarctic soil. *Microb. Ecol.* 43, 44–54. doi: 10.1007/s00248-001-1019-3

Barrett, J. E., Virginia, R. A., Hopkins, D. W., Aislabie, J., Bargagli, R., Bockheim, J., et al. (2006). Terrestrial ecosystem processes of Victoria land, Antarctica. *Soil Biol. Biochem.* 38, 3019–3034. doi: 10.1016/j.soilbio.2006.04.041

Bockheim, J. G. (1997). Properties and classification of cold desert soils from Antarctica. *Soil Sci. Soc. Am. J.* 61, 224–231. doi: 10.2136/sssaj1997.03615995006100010031x

Bockheim, J. G. (2002). Landform and soil development in the McMurdo dry valleys, Antarctica: a regional synthesis. *Arct. Antarct. Alp. Res.* 34, 308–317. doi: 10.1080/15230430.2002.12003499

Bockheim, J. G., Prentice, M. L., and McLeod, M. (2008). Distribution of glacial deposits, soils, and permafrost in Taylor Valley, Antarctica. *Arct. Antarct. Alp. Res.* 40, 279–286. doi: 10.1657/1523-0430(06-057)[bockheim]2.0.co;2

Bottos, E. M., Laughlin, D. C., Herbold, C. W., Lee, C. K., McDonald, I. R., and Cary, S. C. (2020). Abiotic factors influence patterns of bacterial diversity and community composition in the dry valleys of Antarctica. *FEMS Microb. Ecol.* 96:fiaa042.

Brambilla, E., Hippe, H., Hagelstein, A., Tindall, B. J., and Stackebrandt, E. (2001). 16S rDNA diversity of cultured and uncultured prokaryotes of a mat sample from Lake Fryxell, McMurdo dry valleys, Antarctica. *Extremophiles* 5, 23–33. doi: 10.1007/s007920000169

Buelow, H. N., Winter, A. S., Van Horn, D. J., Barrett, J. E., Gooseff, M. N., Schwartz, E., et al. (2016). Microbial community responses to increased water and organic matter in the arid soils of the McMurdo dry valleys, Antarctica. *Front. Microbiol.* 7:1040. doi: 10.3389/fmicb.2016.01040

Campbell, I. B., Clairidge, G. G. C., Campbell, D. I., and Balks, M. R. (1998). "The Soil Environment of the McMurdo dry valleys, Antarctica," in *Ecosystem Dynamics in a Polar Desert: the McMurdo Dry Valleys, Antarctica*, ed. J. C. Priscu (Washington, DC: American Geophysical Union), 297–322. doi: 10.1029/ar072p0297

Cavalier-Smith, T., and Chao, E. E. (2006). Phylogeny and megasystematics of phagotrophic heterokonts (kingdom Chromista). *J. Mol. Evol.* 62, 388–420. doi: 10.1007/s00239-004-0353-8

Chan-Yam, K., Goordial, J., Greer, C., Davila, A., McKay, C. P., and Whyte, L. G. (2019). Microbial activity and habitability of an Antarctic dry valley water track. *Astrobiology* 19, 757–770. doi: 10.1089/ast.2018.1884

Christmas, N. A., Barker, G., Anesio, A. M., and Sánchez-Baracaldo, P. (2016). Genomic mechanisms for cold tolerance and production of exopolysaccharides in the Arctic cyanobacterium *Phormidesmis priestleyi* BC1401. *BMC Genomics* 17:533. doi: 10.1186/s12864-016-2846-4

Chuvochina, M. S., Alekhina, I. A., Normand, P., Petit, J. R., and Bulat, S. A. (2011). Three events of Saharan dust deposition on the Mont Blanc glacier associated with different snow-colonizing bacterial phylotypes. *Microbiology* 80, 125–131. doi: 10.1134/s0026261711010061

Colesie, C., Green, T. G. A., Türk, R., Hogg, I. D., Sancho, L. G., and Büdel, B. (2014). Terrestrial biodiversity along the Ross Sea coastline, Antarctica: lack of a latitudinal gradient and potential limits of bioclimatic modeling. *Polar Biol.* 37, 1197–1208.

Connell, L., Redman, R., Craig, S., Scorzetti, G., Iszard, M., and Rodriguez, R. (2008). Diversity of soil yeasts isolated from South Victoria Land, Antarctica. *Microb. Ecol.* 56, 448–459. doi: 10.1007/s00248-008-9363-1

Costello, E. K., Halloy, S. R. P., Reed, S. C., Sowell, P., and Schmidt, S. K. (2009). Fumarole-supported islands of biodiversity within a hyperarid, high-elevation landscape on Socompa Volcano, Puna de Atacama, Andes. *Appl. Environ. Microbiol.* 75, 735–747. doi: 10.1128/aem.01469-08

Coyne, K. J., Parker, A. E., Lee, C. K., Sohm, J. A., Kalmbach, A., Gunderson, T., et al. (2020). The distribution and relative ecological roles of autotrophic and heterotrophic diazotrophs in the McMurdo dry valleys, Antarctica. *FEMS Microbiol. Ecol.* 96, fiaa010.

Darcy, J. L., King, A. J., Gendron, E. M. S., and Schmidt, S. K. (2017). Spatial autocorrelation of microbial communities atop a debris-covered glacier is evidence of a supraglacial chronosequence. *FEMS Microbiol. Ecol.* 93. doi: 10.1093/femsec/fix095

De Wever, A., Leliaert, F., Verleyen, E., Vanormelingen, P., Van der Gucht, K., Hodgson, D. A., et al. (2009). Hidden levels of phylodiversity in Antarctic green algae: further evidence for the existence of glacial refugia. *Proc. R. Soc. B Biol. Sci.* 276, 3591–3599. doi: 10.1098/rspb.2009.0994

Dickson, J. L., and Head, J. W. (2009). The formation and evolution of youthful gullies on Mars: gullies as the late-stage phase of Mars' most recent ice age. *Icarus* 204, 63–86. doi: 10.1016/j.icarus.2009.06.018

Dickson, J. L., Head, J. W., Levy, J. S., Morgan, G. A., and Marchant, D. R. (2019). Gully formation in the McMurdo dry valleys, Antarctica: multiple sources of water, temporal sequence and relative importance in gully erosion and deposition processes. *Geol. Soc. Lond. Spec. Pub.* 467, 289–314. doi: 10.1144/sp467.4

Feeser, K. L., Van Horn, D. J., Buelow, H. N., Colman, D. R., McHugh, T. A., Okie, J. G., et al. (2018). Local and regional scale heterogeneity drive bacterial community diversity and composition in a polar desert. *Front. Microbiol.* 9:1928. doi: 10.3389/fmicb.2018.01928

Fell, J. W., Scorzetti, G., Connell, L., and Craig, S. (2006). Biodiversity of micro-eukaryotes in Antarctic dry valley soils with < <5% soil moisture. *Soil Biol. Biochem.* 38, 3107–3119. doi: 10.1016/j.soilbio.2006.01.014

Fernandes, A. D., Macklaim, J. M., Linn, T. G., Reid, G., and Gloor, G. B. (2013). ANOVA-like differential gene expression analysis of single-organism and meta-RNA-seq. *PLoS One* 8:e67019. doi: 10.1371/journal.pone.0067019

Fernandes, A. D., Reid, J. N., Macklaim, J. M., McMurrough, T. A., Edgell, D. R., and Gloor, G. B. (2014). Unifying the analysis of high-throughput sequencing datasets: characterizing RNA-seq, 16S rRNA gene sequencing and selective growth experiments by compositional data analysis. *Microbiome* 2:15. doi: 10.1186/2049-2618-2-15

Fontaneto, D., Iakovenko, N., and De Smet, W. H. (2015). Diversity gradients of rotifer species richness in Antarctica. *Hydrobiologia* 761, 235–248. doi: 10.1007/s10750-015-2258-5

Fountain, A. G., Levy, J. S., Gooseff, M. N., and Van Horn, D. (2014). The McMurdo dry valleys: a landscape on the threshold of change. *Geomorphology* 225, 25–35. doi: 10.1016/j.geomorph.2014.03.044

Franzetti, A., Navarra, F., Tagliaferri, I., Gandolfi, I., Bestetti, G., Minora, U., et al. (2017). Potential sources of bacteria colonizing the cryoconite of an Alpine glacier. *PLoS One* 12:e0174786. doi: 10.1371/journal.pone.0174786

Gloor, G. B., Macklaim, J. M., Pawlowsky-Glahn, V., and Egozcue, J. J. (2017). Microbiome datasets are compositional: and this is not optional. *Front. Microbiol.* 8:2224. doi: 10.3389/fmicb.2017.02224

Gloor, G. B., and Reid, G. (2016). Compositional analysis: a valid approach to analyze microbiome high-throughput sequencing data. *Can. J. Microbiol.* 62, 692–703. doi: 10.1139/cjm-2015-0821

Goordial, J., Davila, A., Lacelle, D., Pollard, W., Marinova, M. M., Greer, C. W., et al. (2016). Nearing the cold-arid limits of microbial life in permafrost of an

upper dry valley, Antarctica. *ISME J.* 10, 1613–1624. doi: 10.1038/ismej.2015.239

Gooseff, M. N., Barrett, J. E., Doran, P. T., Fountain, A. G., Lyons, W. B., Parsons, A. N., et al. (2003). Snow-patch influence on soil biogeochemical processes and invertebrate distribution in the McMurdo dry valleys, Antarctica. *Arct. Antarct. Alp. Res.* 35, 91–99. doi: 10.1657/1523-0430(2003)035[0091:spiosb]2.0.co;2

Green, T. A., Brabyn, L., Beard, C., and Sancho, L. G. (2012). Extremely low lichen growth rates in Taylor Valley, Dry Valleys, continental Antarctica. *Polar Biol.* 35, 535–541. doi: 10.1007/s00300-011-1098-7

Gunnigle, E., Ramond, J. B., Guerrero, L. D., Makhalanyane, T. P., and Cowan, D. A. (2015). Draft genomic DNA sequence of the multi-resistant *Sphingomonas* sp. strain AntH11 isolated from an Antarctic hypolith. *FEMS Microbiol. Lett.* 362:fnv037.

Gupta, P., Sangwan, N., Lal, R., and Vakhlu, J. (2015). Bacterial diversity of Drass, cold desert in Western Himalaya, and its comparison with Antarctic and Arctic. *Arch. Microbiol.* 197, 851–860. doi: 10.1007/s00203-015-1121-4

Hagemann, M., Henneberg, M., Felde, V. J., Berkowicz, S. M., Raanan, H., Pade, N., et al. (2017). Cyanobacterial populations in biological soil crusts of the northwest Negev Desert, Israel—effects of local conditions and disturbance. *FEMS Microbiol. Ecol.* 93:fiw228. doi: 10.1093/femsec/fiw228

Hall, B. L., Denton, G. H., and Hendy, C. H. (2000). Evidence from Taylor Valley for a grounded ice sheet in the Ross Sea, Antarctica. *Geogr. Ann. Ser. Phys. Geogr.* 82, 275–303. doi: 10.1111/1468-0459.00126

Heidelberg, K. B., Nelson, W. C., Holm, J. B., Eisenkolb, N., Andrade, K., and Emerson, J. B. (2013). Characterization of eukaryotic microbial diversity in hypersaline Lake Tyrrell, Australia. *Front. Microbiol.* 4:115. doi: 10.3389/fmicb.2013.00115

Jung, P., Briegel-Williams, L., Schermer, M., and Budel, B. (2019). Strong in combination: polyphasic approach enhances arguments for cold-assigned cyanobacterial endemism. *MicrobiologyOpen* 8:e00729. doi: 10.1002/mbo3.729

Kamikawa, R., Moog, D., Zauner, S., Tanifuji, G., Ishida, K.-I., Miyashita, H. et al. (2017). A non-photosynthetic diatom reveals early steps of reductive evolution in plastids. *Mol. Biol. Evol.* 34, 2355–2366.

Kawasaki, Y., Nakada, T., and Tomita, M. (2015). Taxonomic revision of oil−producing green algae, Chlorococcum oleofaciens (Volvocales, Chlorophyceae), and its relatives. *J. Phycol.* 51, 1000–1016. doi: 10.1111/jpy.12343

Kennedy, A. D. (1993). Water as a limiting factor in the Antarctic terrestrial environment: a biogeographical synthesis. *Arct. Alp. Res.* 254, 308–315. doi: 10.2307/1551914

Khan, N., Tuffin, M., Stafford, W., Cary, C., Lacap, D. C., Pointing, S. B., et al. (2011). Hypolithic microbial communities of quartz rocks from Miers Valley, McMurdo dry valleys, Antarctica. *Polar Biol.* 34, 1657–1668. doi: 10.1007/s00300-011-1061-7

Kidron, G. J., Barzilay, E., and Sachs, E. (2000). Microclimate control upon sand microbiotic crusts, western Negev Desert, Israel. *Geomorphology* 36, 1–18. doi: 10.1016/s0169-555x(00)00043-x

Kidron, G. J., and Benenson, I. (2014). Biocrusts serve as biomarkers for the upper 30 cm soil water content. *J. Hydrol.* 509, 398–405. doi: 10.1016/j.jhydrol.2013.11.041

Kudinova, A. G., Petrova, M. A., Dolgikh, A. V., Soina, V. S., Lysak, L. V., and Maslova, O. A. (2020). Taxonomic diversity of Bacteria and their filterable forms in the soils of Eastern Antarctica (Larsemann Hills and Bunger Hills). *Microbiology.* 89, 574–584. doi: 10.1134/s0026261720050136

Lee, C. K., Barbier, B. A., Bottos, E. M., McDonald, I. R., and Cary, S. C. (2012). The inter-valley soil comparative survey: the ecology of dry valley edaphic microbial communities. *ISME J.* 6, 1046–1057. doi: 10.1038/ismej.2011.170

Lee, K. C., Caruso, T., Archer, S. D., Gillman, L. N., Lau, M. C. Y., Cary, S. C., et al. (2018). Stochastic and deterministic effects of a moisture gradient on soil microbial communities in the McMurdo dry valleys of Antarctica. *Front. Microbiol.* 9:2619. doi: 10.3389/fmicb.2018.02619

Levy, J. S., Head, J. W., Marchant, D. R., Dickson, J. L., and Morgan, G. A. (2009). Geologically recent gully–polygon relationships on Mars: Insights from the Antarctic dry valleys on the roles of permafrost, microclimates, and water sources for surface flow. *Icarus* 201, 113–126. doi: 10.1016/j.icarus.2008.12.043

Maccario, L., Carpenter, S. D., Deming, J. W., Vogel, T. M., and Larose, C. (2019). Sources and selection of snow-specific microbial communities in a Greenlandic sea ice snow cover. *Sci. Rep.* 9, 1–14.

Mapelli, F., Marasco, R., Rizzi, A., Baldi, F., Ventura, S., Daffonchio, D., et al. (2011). Bacterial communities involved in soil formation and plant establishment triggered by pyrite bioweathering on Arctic moraines. *Microb. Ecol.* 61, 438–447. doi: 10.1007/s00248-010-9758-7

Martin, M. (2011). Cutadapt removes adapter sequences from high-throughput sequencing reads. *EMBnet J.* 17, 10–12. doi: 10.14806/ej.17.1.200

McMurdie, P. J., and Holmes, S. (2013). Phyloseq: an R package for reproducible interactive analysis and graphics of microbiome census data. *PloS One* 8:e61217. doi: 10.1371/journal.pone.0061217

Niederberger, T. D., Bottos, E. M., Sohm, J. A., Gunderson, T., Parker, A., Coyne, K. J., et al. (2019). Rapid microbial dynamics in response to an induced wetting event in Antarctic Dry Valley soils. *Front. Microbiol.* 10:621. doi: 10.3389/fmicb.2019.00621

Niederberger, T. D., Sohm, J. A., Gunderson, T. E., Parker, A. E., Tirindelli, J., Capone, D. G., et al. (2015). Microbial community composition of transiently wetted Antarctic dry valley soils. *Front. Microbiol.* 6:9. doi: 10.3389/fmicb.2015.00009

Olmo, J. L., Esteban, G. F., and Finlay, B. J. (2011). New records of the ectoparasitic flagellate *Colpodella gonderi* on non-Colpoda ciliates. *Int. Microbiol.* 14, 207–211.

Pannewitz, S., Green, T. G. A., Maysek, K., Schlensog, M., Seppelt, R., Sancho, L. G., et al. (2005). Photosynthetic responses of three common mosses from continental Antarctica. *Antarct. Sci.* 17, 341–352. doi: 10.1017/s0954102005002774

Pointing, S. B., Chan, Y., Lacap, D. C., Lau, M. C., Jurgens, J. A., and Farrell, R. L. (2009). Highly specialized microbial diversity in hyper-arid polar desert. *Proc. Natl. Acad. Sci. U.S.A.* 106, 19964–19969. doi: 10.1073/pnas.0908274106

Porazinska, D. L., Farrer, E. C., Spasojevic, M. J., de Mesquita, B., Sartwell, S. A., Smith, J. G., et al. (2018). Plant diversity and density predict belowground diversity and function in an early successional alpine ecosystem. *Ecology* 99, 1942–1952. doi: 10.1002/ecy.2420

Porazinska, D. L., Fountain, A. G., Nylen, T. H., Tranter, M., Virginia, R. A., and Wall, D. H. (2004). The biodiversity and biogeochemistry of cryoconite holes from McMurdo dry valley glaciers. *Arct. Antarct. Alp. Res.* 36, 84–91. doi: 10.1657/1523-0430(2004)036[0084:tbaboc]2.0.co;2

Porazinska, D. L., Wall, D. H., and Virginia, R. A. (2002). Population age structure of nematodes in the Antarctic dry valleys: perspectives on time, space, and habitat suitability. *Arct. Antarct. Alp. Res.* 34, 159–168. doi: 10.1080/15230430.2002.12003480

Quast, C., Pruesse, E., Yilmaz, P., Gerken, J., Schweer, T., Yarza, P., et al. (2013). The SILVA ribosomal RNA gene database project: improved data processing and web-based tools. *Nuclic Acids Res.* 41, D590–D596.

Raabova, L., Kovacik, L., Elster, J., and Strunecky, O. (2019). Review of the genus *Phormidesmis* (cyanobacteria) based on environmental, morphological, and molecular data with description of a new genus *Leptodesmis*. *Phytotaxa* 395, 1–16. doi: 10.11646/phytotaxa.395.1.1

Raven, J. A. and Giordano, M. (2017). Acquisition and metabolism of carbon in the Ochrophyta other than diatoms. *Proc. R. Soc. B.* 372:20160400.

Rego, A., Raio, F., Martins, T. P., Ribeiro, H., Sousa, A. G. G., Séneca, J., et al. (2019). Actinobacteria and cyanobacteria diversity in terrestrial Antarctic microenvironments evaluated by culture-dependent and independent methods. *Front. Microbiol.* 10:1018. doi: 10.3389/fmicb.2019.01018

Sam-Yellowe, T. Y., Yadavalli, R., Fujioka, H., Peterson, J. W., and Drazba, J. A. (2019). RhopH3, rhoptry gene conserved in the free-living alveolate flagellate *Colpodella* sp. (Apicomplexa). *Euro. J. Protistol.* 71:125637. doi: 10.1016/j.ejop.2019.125637

Schmidt, S. K., and Darcy, J. L. (2015). Phylogeography of ulotrichalean soil algae from extreme high-altitude and high-latitude ecosystems. *Polar Biol.* 38, 689–697. doi: 10.1007/s00300-014-1631-6

Schmidt, S. K., Lynch, R., King, A. J., Karki, D., Robeson, M. S., Nagy, L., et al. (2011). Phylogeography of microbial phototrophs in the dry valleys of the high Himalayas and Antarctica. *Proc. R. Soc. B.* 278, 702–708. doi: 10.1098/rspb.2010.1254

Seppelt, R. D., Türk, R., Green, T. A., Moser, G., Pannewitz, S., Sancho, L. G., et al. (2010). Lichen and moss communities of Botany Bay, Granite Harbour, Ross Sea, Antarctica. *Antarct. Sci.* 22:691. doi: 10.1017/s0954102010000568

Smith, J. J., Tow, L. A., Stafford, W., Cary, C., and Cowan, D. A. (2006). Bacterial diversity in three different Antarctic cold desert mineral soils. *Microb. Ecol.* 51, 413–421. doi: 10.1007/s00248-006-9022-3

Sohm, J., Niederberger, T., Parker, A., Tirindelli, J., Gunderson, T., Cary, S. C., et al. (2020). Microbial mats of the McMurdo dry valleys, Antarctica: oases of biological activity in a very cold desert. *Front. Microbiol.* 11:537960. doi: 10.3389/fmicb.2020.537960

Solon, A. J., Vimercati, L., Darcy, J. L., Arán, P., Porazinska, D., Dorador, C., et al. (2018). Microbial communities of high-elevation fumaroles, penitentes and dry tephra "soils" of the Puna de Atacama Volcanic Zone. *Microb. Ecol.* 76, 340–351. doi: 10.1007/s00248-017-1129-1

Sommers, P., Darcy, J. L., Porazinska, D. L., Gendron, E. M. S., Fountain, A. G., Zamora, F., et al. (2019a). Comparison of microbial communities in the sediments and water columns of frozen cryoconite holes in the McMurdo dry valleys, Antarctica. *Front. Microbiol.* 10:65. doi: 10.3389/fmicb.2019.00065

Sommers, P., Fontenele, R. S., Kringen, T., Kraberger, S., Porazinska, D. L., Darcy, J. L., et al. (2019b). Single-stranded DNA viruses in Antarctic cryoconite holes. *Viruses* 11:1022. doi: 10.3390/v11111022

Sommers, P., Porazinska, D. L., Darcy, J. L., Gendron, E. M. S., Vimercati, L., Solon, A. J., et al. (2020). Microbial species–area relationships in Antarctic cryoconite holes depend on productivity. *Microorganisms* 8:1747. doi: 10.3390/microorganisms8111747

Sommers, P., Porazinska, D. L., Darcy, J. L., Zamora, F., Fountain, A., and Schmidt, S. K. (2019c). Experimental cryoconite holes as mesocosms for studying community ecology. *Polar Biol.* 42, 1973–1984. doi: 10.1007/s00300-019-02572-7

Taton, A., Grubisic, S., Brambilla, E., De Wit, R., and Wilmotte, A. (2003). Cyanobacterial diversity in natural and artificial microbial mats of Lake Fryxell (McMurdo dry valleys, Antarctica): a morphological and molecular approach. *Appl. Environ. Microbiol.* 69, 5157–5169. doi: 10.1128/aem.69.9.5157-5169.2003

Tytgat, B., Verleyen, E., Sweetlove, M., D'hondt, S., Clercx, P., Van Ranst, E., et al. (2016). Bacterial community composition in relation to bedrock type and macrobiota in soils from the Sør Rondane Mountains, East Antarctica. *FEMS Microbiol. Ecol.* 92:fiw126. doi: 10.1093/femsec/fiw126

Van Goethem, M. W., Makhalanyane, T. P., Valverde, A., Cary, S. C., and Cowan, D. A. (2016). Characterization of bacterial communities in lithobionts and soil niches from Victoria Valley, Antarctica. *FEMS Microbiol. Ecol.* 92:fiw051. doi: 10.1093/femsec/fiw051

Van Horn, D. J., Wolf, C. R., Colman, D. R., Jiang, X., Kohler, T. J., McKnight, D. M., et al. (2016). Patterns of bacterial biodiversity in the glacial meltwater streams of the McMurdo dry valleys, Antarctica. *FEMS Microbiol. Ecol.* 92:fiw148. doi: 10.1093/femsec/fiw148

Van Trappen, S., Mergaert, J., Van Eygen, S., Dawyndt, P., Cnockaert, M. C., and Swings, J. (2002). Diversity of 746 heterotrophic bacteria isolated from microbial mats from ten Antarctic lakes. *Syst. Appl. Microbiol.* 25, 603–610. doi: 10.1078/07232020260517742

Varela, D. A., Hernríquez, L. A., Fernández, P. A., Leal, P., Harnández-Gonález, M. C., Figueroa, F. L. et al. (2018). Photosynthesis and nitrogen uptake of the giant kelp Macrocystis pyrifera (Ochrophyta) grown close to salmon farms. *Mar. Environ. Res.* 135, 93–102.

Vimercati, L., Darcy, J. L., and Schmidt, S. K. (2019a). The disappearing periglacial ecosystem atop Mt. Kilimanjaro supports both cosmopolitan and endemic microbial communities. *Sci. Rep.* 9, 1–14.

Vimercati, L., Solon, A. J., Krinsky, A., Arán, P., Porazinska, D. L., Darcy, J. L., et al. (2019b). Nieves penitentes are a new habitat for snow algae in one of the most extreme high-elevation environments on Earth. *Arct. Antarct. Alp. Res.* 51, 190–200. doi: 10.1080/15230430.2019.1618115

Willis, A., and Bunge, J. (2015). Estimating diversity via frequency ratios. *Biometrics* 71, 1042–1049. doi: 10.1111/biom.12332

Willis, A., Bunge, J., and Whitman, T. (2017). Improved detection of changes in species richness in high-diversity microbial communities. *J. R. Stat. Soc. Ser. C (Appl. Stat.)* 66, 963–977. doi: 10.1111/rssc.12206

Wood, S. A., Rueckert, A., Cowan, D. A., and Cary, S. C. (2008). Sources of edaphic cyanobacterial diversity in the Dry Valleys of Eastern Antarctica. *ISME J.* 2, 308–320. doi: 10.1038/ismej.2007.104

Yang, E. C., Boo, G. H., Kim, H. J., Cho, S. M., Boo, S. M., Andersen, R. A., et al. (2012). Supermatrix data highlight the phylogenetic relationships of photosynthetic stramenopiles. *Protist* 163, 217–231. doi: 10.1016/j.protis.2011.08.001

Zeglin, L. H., Dahm, C. N., Barrett, J. E., Gooseff, M. N., Fitpatrick, S. K., and Takacs-Vesbach, C. D. (2011). Bacterial community structure along moisture gradients in the parafluvial sediments of two ephemeral desert streams. *Microb. Ecol.* 61, 543–556. doi: 10.1007/s00248-010-9782-7

Zeglin, L. H., Sinsabaugh, R. L., Barrett, J. E., Gooseff, M. N., and Takacs-Vesbach, C. D. (2009). Landscape distribution of microbial activity in the McMurdo dry valleys: linked biotic processes, hydrology, and geochemistry in a cold desert ecosystem. *Ecosystems* 12, 562–573. doi: 10.1007/s10021-009-9242-8

Conflict of Interest: The authors declare that the research was conducted in the absence of any commercial or financial relationships that could be construed as a potential conflict of interest.

Advantages of publishing in Frontiers

OPEN ACCESS
Articles are free to read for greatest visibility and readership

FAST PUBLICATION
Around 90 days from submission to decision

HIGH QUALITY PEER-REVIEW
Rigorous, collaborative, and constructive peer-review

TRANSPARENT PEER-REVIEW
Editors and reviewers acknowledged by name on published articles

Frontiers
Avenue du Tribunal-Fédéral 34
1005 Lausanne | Switzerland

Visit us: www.frontiersin.org
Contact us: frontiersin.org/about/contact

REPRODUCIBILITY OF RESEARCH
Support open data and methods to enhance research reproducibility

DIGITAL PUBLISHING
Articles designed for optimal readership across devices

FOLLOW US
@frontiersin

IMPACT METRICS
Advanced article metrics track visibility across digital media

EXTENSIVE PROMOTION
Marketing and promotion of impactful research

LOOP RESEARCH NETWORK
Our network increases your article's readership